UNCLASSIFIED

AD NUMBER

ADB024657

NEW LIMITATION CHANGE

TO

Approved for public release, distribution unlimited

FROM

Distribution authorized to U.S. Gov't. agencies only; Test and Evaluation; JAN 1974. Other requests shall be referred to U.S. Army Engineer Waterways Experiment Station, Vicksburg, MS.

AUTHORITY

WES letter dtd 17 Jul 1978

THIS PAGE IS UNCLASSIFIED

AD B024657

AD No.
DDC FILE COPY

TECHNICAL REPORT N-764

CRATERING BY EXPLOSIONS: A COMPENDIUM AND AN ANALYSIS

by

A. D. Rooke, Jr., B. L. Carter, L. K. Davis

Destroy this report when no longer needed. Do not return
it to the originator.

The findings in this report are not to be construed as an official
Department of the Army position unless so designated
by other authorized documents.

REPRODUCTION QUALITY NOTICE

This document is the best quality available. The copy furnished to DTIC contained pages that may have the following quality problems:

- Pages smaller or larger than normal.
- Pages with background color or light colored printing.
- Pages with small type or poor printing; and or
- Pages with continuous tone material or color photographs.

Due to various output media available these conditions may or may not cause poor legibility in the microfiche or hardcopy output you receive.

☐ If this block is checked, the copy furnished to DTIC contained pages with color printing, that when reproduced in Black and White, may change detail of the original copy.

ACCESSION for
NTIS White Section
DDC Buff Section
UNANNOUNCED
JUSTIFICATION
BY
DISTRIBUTION/AVAILABILITY CODES
Dist. AVAIL. and/or SPECIAL
B

TECHNICAL REPORT N-74-1

CRATERING BY EXPLOSIONS: A COMPENDIUM AND AN ANALYSIS

by

A. D. Rooke, Jr., B. L. Carnes, L. K. Davis

DDC
RECEIVED
FEB 6 1978
D

January 1974

Sponsored by Office, Chief of Engineers, U. S. Army
Project 4A062118A880, Task 04

Conducted by U. S. Army Engineer Waterways Experiment Station
Weapons Effects Laboratory
Vicksburg, Mississippi

ARMY MRC VICKSBURG,MISS

Distribution limited to U. S. Government agencies only; test and evaluation; January 1974.
Other requests for this document must be referred to U. S. Army Engineer Waterways Experiment Station.

ABSTRACT

Cratering programs and data resulting from numerous single-charge explosion tests are summarized and compiled in tabular form. Analyses are performed on these data to provide means of predicting basic cratering parameters. Prediction equations were developed by use of the method of least squares. Means of updating these tabulations and analyses on a regular basis by automatic data processing are discussed.

Data are grouped so as to account for the factors which primarily affect crater size and shape: yield, burst geometry, and cratered medium. The influence of other conditions, such as soil moisture, layered media, etc., is also considered. Emphasis is on single-charge, dry-land experiments, which best permit isolation of the factors contributing to the basic parameters. However, effects of environmental influences, unusual charge geometries, and other factors significantly affecting craters are also briefly considered. Similarly, basic ejecta information is included.

Trends in crater dimensions are shown by means of graphs normalized to charge sizes commensurable to large chemical and small nuclear yields. Scaling as a prediction tool is discussed.

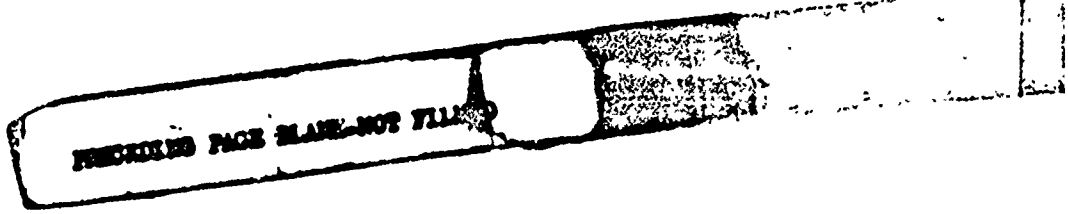

PREFACE

This report deals with cratering from explosive charges. It is intended to compile in tabular form all single-charge cratering data suitable for analysis, taken from numerous test programs conducted in a variety of media, and it includes a somewhat abbreviated empirical analysis of these data. The study was conducted for the Office, Chief of Engineers, Department of the Army, under Task 04, Project No. 4A062118A880, by the U. S. Army Engineer Waterways Experiment Station (WES) during the period January 1970 through April 1971. The research was under the general supervision of Mr. G. L. Arbuthnot, Jr., Chief, Weapons Effects Laboratory, and Mr. J. N. Strange, Chief, Engineering Research Branch, and under the direct supervision of Mr. A. D. Rooke, Jr., Chief, Earth Kinetics Section. This report was prepared by Messrs. Rooke, B. L. Carnes, and L. K. Davis. Assistance in the search for data and in the bibliographical compilation was given by Mr. J. A. Conway; Mr. S. B. Price assisted in preparation of the graphs. Assemblage, typing, and proofing of the report draft were by Miss Virginia Mason and Mrs. Dean McAlpin. Additionally, special assistance in certain subject areas was provided as follows: crater ejecta - Mr. J. W. Meyer; charge stemming - SP5 H. L. Knudson; and crater-cavity formation - 1LT H. D. Hardcastle.

A previous WES compendium on cratering was used as the primary source of cratering data prior to 1960, and a previous analysis of crater data served as a guideline for this analysis. The usefulness of these research efforts in preparing this report is gratefully acknowledged.

COL Levi A. Brown, CE, BG Ernest D. Peixotto, CE, and COL G. H. Hilt, CE, were Directors of the WES during the preparation of this report, and Mr. F. R. Brown was Technical Director.

CONTENTS

ABSTRACT---- 3

PREFACE---- 4

NOTATIONS, ABBREVIATIONS, AND DEFINITIONS---- 9

CONVERSION FACTORS, BRITISH TO METRIC UNITS OF MEASUREMENT---- 13

CHAPTER 1 INTRODUCTION---- 14

1.1 Background---- 14
1.2 Purpose---- 15
1.3 Scope---- 16

CHAPTER 2 SYNOPSIS OF CRATERING RESEARCH EFFORTS---- 20

2.1 HE Test Programs: Prior to 1962---- 20
2.2 HE Test Programs: 1962 and After---- 21
2.3 Nuclear Tests---- 25
2.3.1 Pacific Test Programs---- 25
2.3.2 NTS Test Programs---- 25
2.4 Plowshare Experiments---- 26
2.5 USSR Cratering Experiments---- 29
2.6 Summary---- 29

CHAPTER 3 CRATERING DATA---- 31

3.1 Description of Data---- 31
3.2 Explosives Characteristics---- 31
3.3 Data Presentation---- 32
3.4 Subsurface Deformation---- 34

CHAPTER 4 ANALYSIS OF DATA TRENDS---- 37

4.1 Crater Size and Shape---- 37
4.2 Cratering Mechanisms---- 37
4.3 Scaling Considerations---- 40
4.3.1 Scaling as a Prediction Tool---- 40
4.3.2 Linear Scaling Relations---- 41
4.3.3 Volumetric Scaling Relations---- 42
4.3.4 Depth-of-Burial Scaling---- 42

CHAPTER 5 CRATER EJECTA---- 63

5.1 Composition and Origin---- 63
5.2 Descriptive Parameters---- 64
5.2.1 Crater Lip---- 64
5.2.2 Discrete Ejecta Field---- 65

CHAPTER 6 EFFECTS OF VARIATION IN SHOT GEOMETRIES---- 73

6.1 Multiple-Explosion Arrays---- 73
6.1.1 Row Craters---- 73
6.1.2 Other Multiple-Explosion Arrays---- 74
6.2 Charge Stemming---- 74

6.3 Underwater Cratering---------- 75
6.4 Deeply Buried Explosions---------- 75
6.5 Bomb/Shell Craters---------- 77
6.6 Successive Shots on a Vertical Axis---------- 78

CHAPTER 7 ENVIRONMENTAL INFLUENCES---------- 87

7.1 Sloping Topography---------- 87
7.2 Layered Systems---------- 88
7.2.1 Water Tables---------- 88
7.2.2 Bedrock---------- 88
7.2.3 Rock Bedding/Jointing---------- 88
7.3 Snow and Ice---------- 89

CHAPTER 8 SUMMARY AND RECOMMENDATIONS---------- 92

8.1 Summary---------- 92
8.2 Recommendations---------- 92

APPENDIX A TABULATION OF CRATER DATA---------- 94

APPENDIX B GRAPHICAL PRESENTATION OF CRATER DATA---------- 129

APPENDIX C BIBLIOGRAPHY---------- 315

APPENDIX D COMPUTER PROGRAM FOR CRATER DATA---------- 331

REFERENCES---------- 339

TABLES

3.1 Comparison of Explosive Cratering Efficiency with That of TNT---------- 36
A.1 Crater Data for Basalt and Granite---------- 100
A.2 Crater Data for Sandstone---------- 103
A.3 Crater Data for Shale, Tuff, and Frozen Ground---------- 106
A.4 Crater Data for Dry Clay---------- 110
A.5 Crater Data for Moist Clay---------- 111
A.6 Crater Data for Wet Clay---------- 113
A.7 Crater Data for Moist Loess and Moist Lacustrine Silt---------- 116
A.8 Crater Data for Moist Silty Clay---------- 118
A.9 Crater Data for Dry-to-Moist Sandy Silty Clay---------- 119
A.10 Crater Data for Dry Desert Alluvium---------- 121
A.11 Crater Data for Moist Sandy Silt---------- 123
A.12 Crater Data for Dry-to-Moist Sand---------- 124
A.13 Crater Data for Wet Sand---------- 126
A.14 Crater Data for Hemispherical Charges---------- 128
D.1 Computer Program for Crater Data---------- 332

FIGURES

1.1 Aerial view of a typical crater formed by a low-yield nuclear device at near-optimum depth of burial in basalt--- 18
1.2 Typical half-crater profile and nomenclature for a buried charge---------- 19
2.1 Illustrated history of major blast- and shock-effects tests---------- 30

4.1 Apparent crater dimensions for 1-ton TNT spheres in basalt and granite---------- 44
4.2 True crater dimensions for 1-ton TNT spheres in sandstone-- 45
4.3 Apparent crater dimensions for 1-ton TNT spheres in shale, tuff, and frozen ground---------- 46
4.4 Apparent crater dimensions for 1-ton TNT spheres in moist clay---------- 47
4.5 Apparent crater dimensions for 1-ton TNT spheres in dry clay---------- 48
4.6 Apparent crater dimensions for 1-ton TNT spheres in moist loess and moist lacustrine silt---------- 49
4.7 Apparent crater dimensions for 1-ton TNT spheres in dry desert alluvium---------- 50
4.8 Apparent crater dimensions for 1-ton TNT spheres in dry-to-moist sand---------- 51
4.9 Apparent crater dimensions for 1-ton TNT spheres in wet sand---------- 52
4.10 Composite graph for apparent crater radius for 1-ton TNT spheres---------- 53
4.11 Composite graph for apparent crater depth for 1-ton TNT spheres---------- 54
4.12 Composite graph for apparent crater lip height for 1-ton TNT spheres---------- 55
4.13 Apparent crater dimensions for 1-kt charges in desert alluvium---------- 56
4.14 True crater dimensions for 1-kt charges in desert alluvium---------- 56
4.15 Apparent crater dimensions for 1-kt charges in rock-------- 57
4.16 True crater dimensions for 1-kt charges in rock---------- 57
4.17 Apparent crater dimensions for 1-kt charges in moist clay-- 58
4.18 Composite graph for apparent crater radius for 1-kt charges---------- 58
4.19 Composite graph for apparent crater depth for 1-kt charges---------- 59
4.20 Apparent crater dimensions versus charge yield, showing the variation of scaling exponent with charge yield-------- 60
4.21 Charge yields scaled to various powers---------- 61
4.22 Crater shapes as affected by burst geometries---------- 62
5.1 Throwout of ejecta by a low-yield cratering explosion at near-optimum depth of burial---------- 66
5.2 Ejection process for a buried explosion---------- 67
5.3 Ejection process for a near-surface explosion---------- 68
5.4 Ejecta origins and relative ranges for HE detonations------ 69
5.5 Fraction of total ejecta volume as a function of range from GZ---------- 70
5.6 Dimensionless plot of ejecta mass density as a function of range expressed as multiples of the apparent crater radius---------- 71
5.7 Maximum missile range for buried charges---------- 72

6.1	Project Dugout, a row crater 135 feet wide, 35 feet deep, and 285 feet long, formed by the detonation of five 20-ton HE charges at near-optimum DOB----------	79
6.2	Enhancement of single-charge apparent crater dimensions in a row crater as a function of charge spacing at optimum DOB in soil----------	80
6.3	Increase in HE crater dimensions as functions of stemming and DOB----------	81
6.4	Apparent dimensions of underwater craters from 1-ton charges fired at the earth-water interface in a variety of fine-grained materials----------	82
6.5	Adiabatic expansion coefficient α as a function of medium's moisture content----------	83
6.6	Apparent crater dimensions for deeply buried bomb explosions----------	84
6.7	Increase in apparent crater dimensions for nail-driving experiments----------	85
6.8	Increase in true crater dimensions for nail-driving experiments----------	86
7.1	Crater and crater lip formed in sloping terrain-------	90
7.2	Crater dimensions for surface detonations in snow and ice----------	91
B.1-B.9	Dimensions of craters in basalt and granite----------	130
B.10-B.15	Dimensions of craters in sandstone----------	148
B.16-B.23	Dimensions of craters in shale, tuff, and frozen ground----------	160
B.24-B.33	Dimensions of craters in dry clay----------	176
B.34-B.39	Dimensions of craters in moist clay----------	196
B.40-B.46	Dimensions of craters in wet clay----------	208
B.47-B.54	Dimensions of craters in moist loess and moist lacustrine silt----------	222
B.55-B.58	Dimensions of craters in moist silty clay----------	238
B.59-B.61	Dimensions of craters in dry-to-moist sandy silty clay----------	246
B.62-B.68	Dimensions of craters in desert alluvium----------	252
B.69-B.74	Dimensions of craters in moist sandy silt----------	266
B.75-B.82	Dimensions of craters in dry-to-moist sand----------	278
B.83-B.92	Dimensions of craters in wet sand----------	294
B.93	Apparent crater radius and depth versus charge yield for hemispherical charges in sandy silty clay---------	314

NOTATIONS, ABBREVIATIONS, AND DEFINITIONS

Notations

C	An observed cavity proportionality constant
d	Crater depth (general)
d_a	Depth of apparent crater at ground zero
d_d	Depth to limit of plastic deformation at ground zero
d_r	Depth to limit of rupture zone at ground zero
d_t	Depth of true crater at ground zero
e	A factor which represents the enhancement of crater dimensions in multiple explosions
h	Height of apparent crater lip
k	A constant used in scaling relations
K	A constant representing the fraction of ejecta volume contributing to the formation of the crater lip
L	The length of a row crater
n	Crater scaling exponent
N	The number of charges in a row shot. Shot number in successive charges fired on a common vertical axis
r	Crater radius (general)
r_a	Radius of apparent crater
r_c	Radius of true crater cavity
r_{ch}	Radius of charge
r_d	Radius to outer limit of plastic deformation
r_e	Radius to outer limit of ejecta
r_h	Radius to maximum lip height
r_l	Radius to outer limit of apparent lip
r_r	Radius to outer limit of apparent rupture
r_t	Radius of true crater
r_u	Radius to point of maximum upthrust
R	Range (distance) from ground zero
s	Charge spacing in a row shot
u	Height of upthrust
v	Crater volume (general)
v_a	Volume of apparent crater

V_c	Volume of crater due to compression (compaction)
V_{dis}	Preshot volume of material dissociated by the explosion
V_e	Volume of ejecta
V_{exp}	Volume of joint expansion
V_f	Volume of crater due to plastic flowage of the medium
V_{fb}	Volume of fallback
V_l	Volume of crater lip
V_t	Volume of true crater
V_u	Volume of upthrust
V_r	Void ratio
W	Charge weight
Z	Scaled depth or height of burst (negative if DOB)
α	An exponent based on the adiabatic (γ gas) expansion coefficient
γ	Unit weight of the cratered medium
δ	Areal density of ejecta
ν	Dynamic viscosity of the cratered medium
ρ	Density of the cratered medium
σ	Compressive, shear, and tensile strengths or elastic properties of the cratered medium

Abbreviations

AN	Ammonium nitrate
ANFO	Ammonium nitrate/fuel oil
DOB	Depth of burst (to center of gravity of charge) below original ground
GZ	Ground zero, the hypocenter or epicenter of the burst
HE	High explosive
HOB	Height of burst (to center of gravity of charge) above original ground
kt	Kiloton
Mt	Megaton
NE	Nuclear explosive
NM	Nitromethane
TNT	Trinitrotoluene

Common dimensional abbreviations are used in accordance with "Weapon Test Reports Preparation Manual"; DASA-26, September 1966; Defense Atomic Support Agency, Washington, D. C.

Additional abbreviations are used in Chapters 1 and 2 to designate agencies, and in Appendix A to identify explosion-effects tests and programs. All such abbreviations are identified where used.

Definitions

Apparent crater	The visible crater, bounded at the top by the original ground surface elevation
Crater lip	The region of continuous ejecta surrounding a crater
Ejecta	Earth material permanently ejected from the crater void by the explosion
Fallback	Material, dissociated by the explosion, which has fallen back within the true crater void
Multiple explosion	The detonation of two or more charges with sufficient simultaneity and proximity to cause interaction in crater formation
Nail driving	A blasting technique using successive explosions on a vertical axis, with each charge being emplaced in the center of the crater of the preceding shot
Optimum DOB	The depth of burst at which the largest desired crater dimension occurs
Row crater	A crater or channel formed by the detonation of charges emplaced in a row-shot geometry
Row shot	A multiple explosion with the charges emplaced in a linear array
Rupture zone	Material below and beyond the true crater which has sustained significant physical damage (fracturing, crushing, shearing, etc.) as a result of the explosion
Stemming	(verb) The backfilling of the charge emplacement hole of an underground charge; (noun) backfill material
Surface tangent (above and below)	A charge geometry with the surface of the spherical charge tangent to the ground surface. (Above indicates the charge is resting on the ground and below indicates the charge is buried one charge radius)

True crater	The boundary of the crater representing the limit of dissociation of the medium by the explosion (the crater prior to fallback)
True surface burst	A charge geometry with the center of gravity of the charge at the ground surface
Upthrust	Material that has been permanently displaced above the original ground surface, but not dissociated

CONVERSION FACTORS, BRITISH TO METRIC UNITS OF MEASUREMENT

British units of measurement used in this report can be converted to metric units as follows:

Multiply	By	To Obtain
feet	0.3048	meters
square feet	0.09290	square meters
cubic feet	0.02832	cubic meters
pounds	0.4536	kilograms
short tons	0.9072	metric tons
pounds per cubic foot	16.02	kilograms per cubic meter

CHAPTER 1

INTRODUCTION

1.1 BACKGROUND

The importance of explosive cratering was greatly increased when, through the advent of nuclear weapons, it became possible to release instantaneously enormous amounts of energy from essentially a point source. Certainly the best method to establish the effects of nuclear explosives (NE) is through full-scale testing. However, because of the hazards involved and the restrictions imposed by international treaties, not to mention costs, full-scale testing is presently impractical. Often, the best method to approximate nuclear explosives or weapons effects is through chemical or high-explosive (HE) testing, despite difficulties in scaling HE results to NE charge yields.

Scaling difficulties, which have absorbed much of the research effort in this field, stem primarily from a lack of definitive information regarding the relative importance of various crater-forming mechanisms and the physical factors bearing on these mechanisms, as well as from similarity violations which inevitably occur in this type of experimentation. They are compounded by basic differences in energy release and partitioning between HE and NE charges. However, by considering these facts and weighing the scaled HE data against the actual NE data that are available, the former can be useful in predicting the effects of nuclear devices or weapons, particularly when the nuclear yields in question are below the megaton level.

Future weapons-effects research will undoubtedly involve the application of near-surface or below-surface HE and NE detonations. A knowledge of the effects of cratering and its associated debris-ejection mechanism will be a prerequisite to any such application. The crater, its surrounding zones of subsurface deformation, and the ejecta field represent varying degrees of damage or possible damage to structures located therein (Figures 1.1 and 1.2). Moreover, the size of the crater produced in such an explosion is an indicator of the total energy coupled into

the medium; therefore, the prediction of crater parameters is of major concern in weapons employment. Crater size has also been shown to be useful in normalizing other explosion effects phenomena, e.g., ground motion.

The military applications of cratering research include the capability of weapons to damage or destroy hardened defense installations, to create obstacles or barriers in various situations, or to provide expedient means of excavation. The civil applications are mostly involved with excavations of canals, harbors, etc., river diversion or damming, underground stimulation of mineral production, underground storage, etc.

1.2 PURPOSE

In the past, efforts to analyze and correlate cratering data have met with considerable difficulty because of the large number of reports in which the data are presented, and because of the fact that cratering data are often secondary to the main purpose of the research. The compendium of 1960 (Reference 1) and analysis of 1961 (Reference 2) alleviated this situation; however, much cratering research has been done since that time, and a fresh look at the problem of tabulation, correlation, and analysis is in order.

The purpose of this report is to compile and analyze all available, useful cratering data (both HE and NE) in one report, and to present it in such a manner that it will serve as a guide both for cratering applications and for planning future cratering research. It is intended that the compilation be in such form as to permit continuous updating as additional cratering experiments are performed. The data are grouped to permit isolation and quantification of factors which significantly influence crater size and shape. These include charge yield, shot geometry, and properties of the cratered medium, as well as other factors that are less dominant in their influence on the cratering process. The purpose of the analysis is to provide prediction techniques so that all important cratering phenomena can be predicted with a reasonable degree of accuracy.

It is also the purpose of this compendium to present all important aspects of cratering phenomenology. True crater dimensions (see Figure 1.2) are important as the limit of dissociation of the medium; it is unlikely that any structure can survive within this boundary. Both true and apparent crater volumes are important from the standpoint of excavation, and apparent crater lip height and the interior angle of slope are considerations in the creation of crater barriers and the slope stability of the crater walls. Also important in the design of hardened structures are the limits of subsurface deformation surrounding a crater. Few observations are available on these limits, but they are summarized in Chapter 3.

1.3 SCOPE

Although this report is intended to describe cratering phenomena in general, it has been necessary to limit the contents in some cases. Thus, single-charge craters produced in conditions of uncomplicated media and on more or less level topography are considered at length, while multiple-charge arrays and craters occurring under less usual geometric or environmental conditions are examined only briefly. It has also been necessary to restrict the lower limit of charge size to 1 pound.[1] Successful experiments with smaller charges have been conducted, but too often cratering results are open to question, due primarily to difficulties in scaling medium properties so as to be suitable to such small yields. Data from shaped charges have also been omitted, since their use is highly specialized. Cratering data in certain unusual media or conditions (e.g. snow and ice, earth-water interfaces) are considered only briefly in this report, but bibliographical references for these experiments are included. The same is true for craters formed by unstemmed or partially stemmed charges. In such cases, previous U. S. Army Engineer Waterways Experiment Station (WES) reports are

[1] A table of factors for converting British units of measurement to metric units is presented on page 12.

cited which provide compendia of these data.

A further limitation in content results from a self-imposed requirement that this publication be unclassified, making it available to the maximum number of users. However, while classified data are excluded per se, they have been included in the construction of the cratering curves and the empirical expressions derived therefrom.

In order to bring the compendium to a conclusion, it was necessary to establish a cutoff date for consideration of new test results. This was set as the end of calendar year 1970. Important tests have taken place since that time, and these will hopefully be included in future updating of this report.

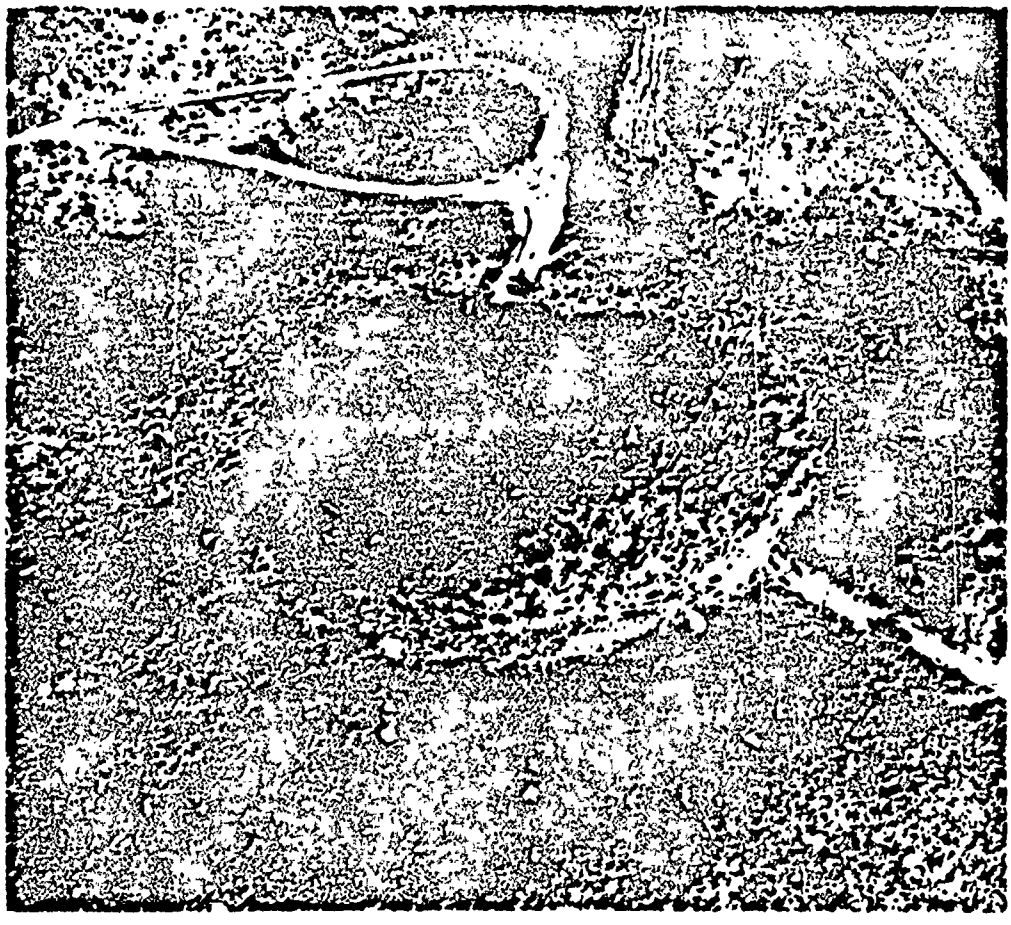

(Courtesy of Lawrence Radiation Laboratory and U. S. Atomic Energy Commission)

Figure 1.1 Aerial view of a typical crater formed by a low-yield nuclear device at near-optimum depth of burial in basalt (Event Danny Boy). Note the size of boulders in the crater and crater lip as compared to the vehicle (arrow).

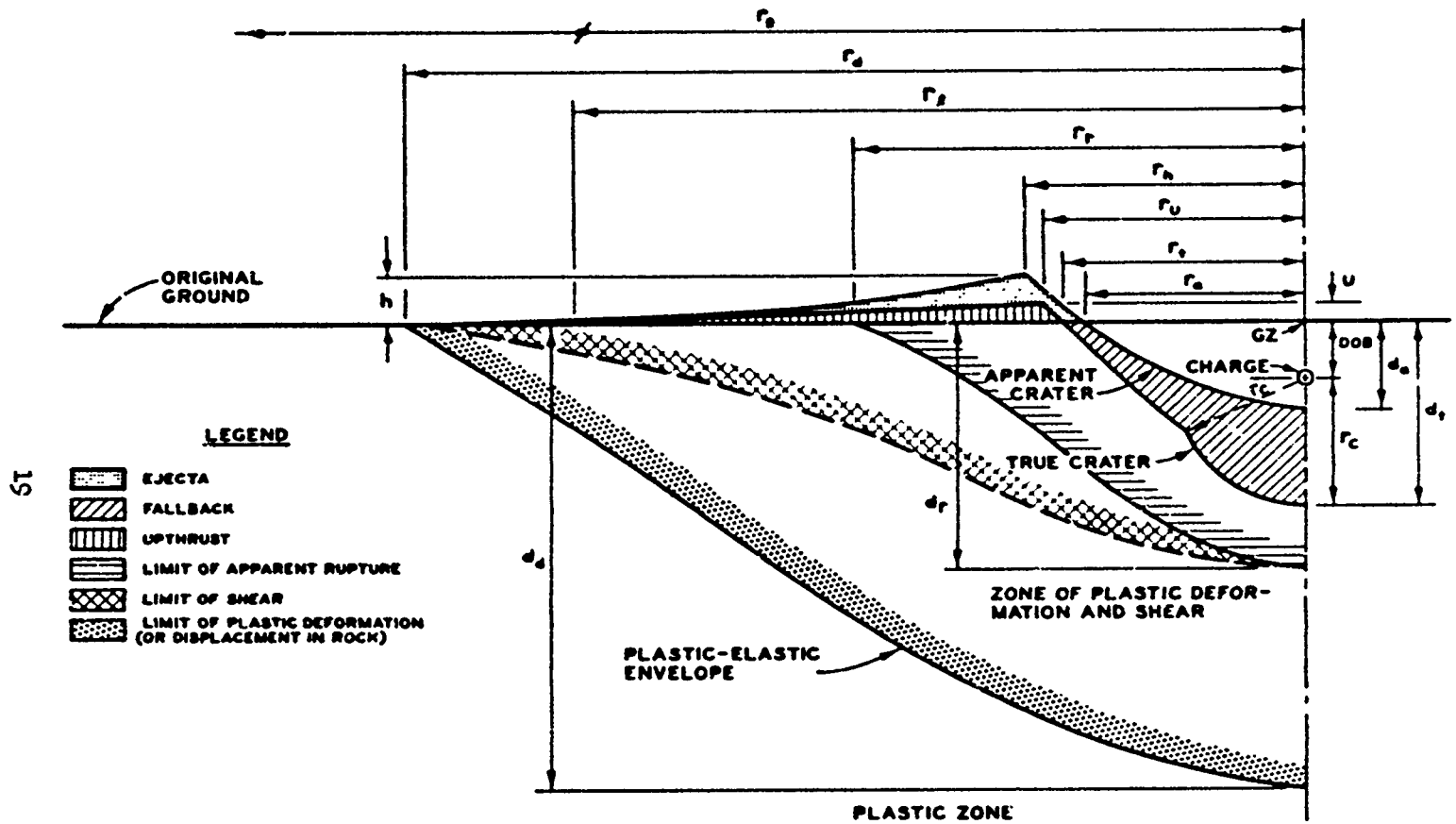

Figure 1.2 Typical half-crater profile and nomenclature for a buried charge. Profiles and dimensions are symmetrical about the centerline. Various radial and depth dimensions are indicated by r and d, respectively. For explanation of terms, see pages 9 through 1'. A crater formed by a near-surface explosion is similar in profile, but usually without a distinct cavity radius r_c.

CHAPTER 2

SYNOPSIS OF CRATERING RESEARCH EFFORTS

2.1 HE TEST PROGRAMS: PRIOR TO 1962

The first significant efforts to investigate the phenomena of cratering from explosives appear to have originated during World War II. Both the U. S. War Department and the Ministry of Home Security in England conducted investigations in which various types of American, British, and German bombs were statically detonated in different types of soil. An early study involving the modeling of large-scale cratering effects by using small-scale charges was conducted by the U. S. Army Ballistic Research Laboratories to estimate the amount of material required to fill bomb craters. References for these and other tests summarized in this chapter are contained in the Bibliography (Appendix C).

Near the end of World War II, the Underground Explosion Test (UET) program was conceived to study design criteria for underground structures to resist the effects of underground explosions. The size of the largest test charge detonated in the program, 320,000 pounds,[1] indicates that the possibility of attack by a nuclear weapon was now also considered as a threat. The UET program was conducted in two major phases: a preliminary program of detonations in rock by the Colorado School of Mines in 1948-49, and a more extensive program by Engineering Research Associates, Inc., from 1949 through 1951. Although several series of tests were fired for crater investigations alone, the majority of the tests involved target structures in earth and tunnels in rock.

A second major test program initiated by the postwar interest in protection against bombing attacks was the Isthmian Canal Studies (ICS) conducted in 1947. This program was conducted by the Canal Zone Division of the Army Corps of Engineers, and involved the study of cratering

---

[1] Unless otherwise specified, charge weights are given in terms of trinitrotoluene (TNT) or its energy equivalent.

damage and the initiation of slope failures from bomb explosions in the embankments adjacent to the Panama Canal. TNT charges ranging from 8 to 200 pounds were fired in five different media representative of the soil and rock types along the canal route.

The first nuclear test series at the Nevada Test Site (NTS) in which cratering was studied per se was Operation Jangle. The operation required a limited HE test series to permit some reasonable basis for predicting the nuclear test phenomena that were to be measured. The Jangle-HE series was conducted in the fall of 1951, and involved four shots: three 2,560-pound charges and a 20-ton event. Three of the HE spheres were tangent to the surface (above and below), and the fourth was shallowly buried. An additional objective of these tests was to relate the results of the UET program, conducted at Dugway, Utah, to the soil characteristics of the desert alluvium at NTS.

Project Mole was an HE program consisting of four test series: two in a sand-gravel medium, one in dry clay, and one in moist clay. All charges were 256-pound TNT spheres, with charge positions ranging from 6 feet above to 6 feet below the ground surface. The purpose of Project Mole was to investigate the relations between charge position and soil type and to study the effects of underground explosions. The program was conducted by the Stanford Research Institute for the Army Corps of Engineers in 1952-54.

A number of studies were conducted at WES during the period 1957-60 to investigate various phenomena associated with cratering. Among these were investigations of the effects of different types of charge stemming (backfill of the charge-emplacement hole), the effects of a shallow soil-rock interface below the explosion area, and the formation of craters in loess and clay. Charge weights in these tests ranged from 1/8 to 256 pounds.

2.2 HE TEST PROGRAMS: 1962 AND AFTER

In 1962, the entire complexion of testing programs involving large, crater-forming explosions changed. Part of the change was due to a redirection of cratering research in support of the newly initiated

Plowshare Program to utilize nuclear explosives for peaceful purposes (discussed in Section 2.4), but the increased intensity of testing efforts was in larger part due to the end of the first moratorium on atmospheric nuclear testing in 1961 and the consequent resumption of nuclear testing by the U. S. early in 1962. The most important cratering experiments conducted during this period are illustrated in Figure 2.1. Nuclear cratering tests were conducted at NTS from March through July 1962. After a six-month pause, an additional series of experiments, named Ferris Wheel, was planned for early 1963 to directly compare the cratering efficiencies of nuclear and TNT explosives of equal yield. The advent of the second moratorium on nuclear testing came within a few weeks of the execution of Ferris Wheel, however, and the program was cancelled.

The Flat Top Series utilized two of the experimental arrays that were emplaced in Frenchmen Flat at NTS for the Ferris Wheel Series. Event II was a 20-ton, half-buried, spherical TNT charge as originally planned for Ferris Wheel, while Event III involved the substitution of an identical 20-ton TNT charge for the originally planned nuclear device. A third event, Flat Top I, was added to the series to compare the craters formed in playa silt by Events II and III with a crater formed by an identical 20-ton charge in limestone. The entire program was sponsored and directed by the Defense Atomic Support Agency, now the Defense Nuclear Agency (DNA).

The Air Vent Series was sponsored by DNA and conducted in 1963-64 by the Sandia Corporation to provide a tie-in between the Flat Top crater results in playa and previous large HE cratering tests fired at deeper depths of burst (DOB) in NTS desert alluvium. The Air Vent Series was composed of three phases: Phase I was a single 20-ton TNT sphere detonated at a DOB of 17 feet, Phase II was a series of twenty 256-pound spherical TNT charges fired at a wide range of DOB, and Phase III was a series of nine TNT charges of 64, 1,000, and 6,000 pounds, all fired as true surface bursts (center of gravity at ground surface).

The Multiple Threat Cratering Experiment (MTCE) was sponsored by

DNA and conducted by the Boeing Company under the supervision of the Air Force Weapons Laboratory at the U. S. Army Yakima Firing Range, Washington, in 1965. The purposes were to investigate the effects of detonating successive charges along a single vertical axis, and to study the influence of the charge shape on the crater and ejecta from near-surface explosions. The MTCE tests consisted of eighteen 4,000-pound charges and two 16,000-pound TNT charges, with one each of the two sizes being hemispherical and the remainder spherical. Nine of the spherical 4,000-pound charges were "nail-driving" shots (i.e., the charge was detonated in the crater of a preceding detonation), four were true surface events, three were surface-tangent above the surface, and one was surface-tangent below the surface. The second 16,000-pound charge was a true surface detonation. All events were fired in a weak basalt.

Additional nail-driving experiments were conducted in small-scale experiments in 1963-64, prior to the MTCE tests. A single series of 64-pound TNT charges was fired in desert alluvium in a Sandia Corporation test program, while 4- and 21-pound TNT charges were fired in a sandy-clayey silt by WES.

Operation Sailor Hat was a series of three 500-ton, hemispherical charges detonated on the surface of a basalt medium on Kahoolawe Island, Hawaii, in 1965. Crater measurements were only made for the first event, since the latter two events were decoupled from the basalt by placing the charges on artificial fill materials. Sailor Hat was conducted by the Navy, under the sponsorship of DNA, to test the response of ships (anchored offshore) to airblast loadings.

The Mine Shaft Series was conducted in 1968-69 on a granite medium near Cedar City, Utah. These tests were sponsored by DNA and conducted by WES to develop data on the effects of near-surface explosions over a hard rock medium. The main events were preceded by ten 1,000-pound calibration shots fired at different heights of burst (HOB) very near the air-rock interface. The Mine Shaft I Series involved two 100-ton spherical TNT charges: Mine Under at an HOB of two charge radii (or $2r_{ch}$) and Mine Ore at an HOB of $0.9r_{ch}$. The Mine Shaft II Series

consisted of the 100-ton Mineral Rock Event, a duplicate of Mine Ore, and the Mineral Lode Event, a 16-ton spherical charge of ammonium nitrate slurry detonated at a DOB of 100 feet.

Cratering experiments were conducted at the Canadian Defence Research Board's Suffield Experimental Station (SES, later designated the Defence Research Establishment, Suffield, or DRES) at Ralston, Alberta, from 1958 to 1970. Both the Watching Hill and Drowning Ford test ranges at DRES consist of glacial till, a heterogeneous mixture of clay, silt, gravel, and fine sand strata. An early test series involved the detonation of 74 TNT charges ranging in weight from 8 to 10,065 pounds, in both spherical and hemispherical charge shapes. The spherical charges were fired in both half-buried and surface-tangent geometries, while the hemispherical charges were all resting on the surface. From 1959 through 1963, six additional detonations of large, hemispherical TNT charges occurred at DRES, with charge weights ranging from 5 to 100 tons. In 1964, a 500-ton hemispherical charge was detonated on the surface for the Snowball Event. As with other tests involving hemispherical charges, airblast measurements primarily dictated shot geometry.

The Distant Plain Series was conducted in 1966-67 at DRES as a part of the Quadrapartite[2] program to develop improved methods for simulating and predicting the effects of nuclear explosions. Six of the Distant Plain Events produced craters: Events 1A, 3, 5, and 6A were 20-ton spherical TNT charges, with the first fired at an HOB of 29 feet, the second and third half-buried, and the last placed tangent to the surface; Event 4 was a 50-ton hemispherical charge detonated on the ground surface in a forest near Hinton, Alberta; and Event 6 was a 100-ton spherical charge in a surface-tangent geometry.

Two recent tests were made at DRES, both 500-ton spherical charges fired surface-tangent. The Prairie Flat Event occurred in 1968 and the Dial Pack Event in 1970.

---

[2] A cooperative effort for blast-effects research between the U. S., Great Britain, Canada, and Australia. Prior to the inclusion of Australia, it was known as the Tripartite program.

2.3 NUCLEAR TESTS

2.3.1 Pacific Test Programs. The testing of nuclear devices for weapons development began at the Pacific Test Range almost immediately after World War II. Of the many tests conducted, only a few produced measurable craters (i.e., the major portion of the crater being contained in a land area), and relatively few of those craters were adequately measured. Ten of the Pacific tests produced craters whose measurements were recorded. All were fired at either the Bikini or Eniwetok Atolls, where the soil medium is described as coral sand underlain with intermittent beds of hard coral and cemented rubble.

The Mike Event of Operation Ivy in 1952 was the first test of a thermonuclear weapon. The 10.4-Mt device was fired at a height of 35 feet above the island surface. Five more high-yield devices, ranging from 1.3 to 15 Mt, were detonated: Bravo, Zuni, and Tewa at Bikini and Koa and Oak at Eniwetok. Tewa and Oak were both detonated on barges floating in shallow water. The Koon Event was a 110-kt detonation at Bikini, while Lacrosse, Seminole, and Cactus were 40-, 14-, and 18-kt yields, respectively, at Eniwetok. Seminole was detonated inside a tank of water.

2.3.2 NTS Test Programs. The first nuclear cratering experiments conducted at the NTS were the Jangle-S and Jangle-U Events of Operation Plumbob in 1957. Both were 1.2-kt yields, fired in desert alluvium--Jangle-S at an HOB of 3.5 feet and Jangle-J at a DOB of 17 feet. The Teapot Ess Event followed in 1955, and was detonated still deeper in alluvium at 67 feet. In 1958, the Neptune Event was fired inside a chamber 100 feet beneath a sloping mountainside, in a volcanic tuff medium. The Neptune device had a yield of 0.115 kt.

No nuclear cratering tests were conducted during the first moratorium on nuclear testing from 1959 through 1961. After the resumption of testing by the USSR in 1961, the 0.42-kt Danny Boy Event was fired in March 1962, at a DOB of 110 feet in a basalt mesa at NTS. Danny Boy was soon followed by Small Boy, a low airburst[3] over playa, and the

[3] Classified yields are omitted.

Little Feller I and Little Feller II Events, all in desert alluvium. Johnie Boy was a near-surface detonation, while the Little Feller Events were both small weapons fired at low HOB's. Except for the Plowshare Program, no further nuclear cratering tests were scheduled until the Ferris Wheel Events of February 1963, which were cancelled due to the commencement of the second moratorium on nuclear testing.

2.4 PLOWSHARE EXPERIMENTS

The Plowshare Program was inaugurated by the U. S. Atomic Energy Commission (AEC) in 1957 to develop peaceful applications of nuclear explosive energy. The most immediately obvious application was, of course, earthmoving by explosive cratering. The first actual planned use of nuclear cratering for constructive purposes was the excavation of a harbor on the coast of Alaska. This experiment, nicknamed Project Chariot, was to proof-test the feasibility of nuclear excavation in the early 1960's. Unfortunately, the project was soon postponed, then eventually cancelled. Among the planned or proposed projects for nuclear excavation were (1) the excavation of a railroad pass through a mountain ridge in California, (2) the construction of a portion of a canal connecting the Tennessee and Tombigbee Rivers, (3) the blasting of a harbor at Cape Keraudren, Australia, and (4) a sea-level canal through or near the Isthmus of Panama. As of this writing, the use of nuclear explosions as a means of producing excavations has been indefinitely postponed as either unjustifiable, uneconomical, or unpopular from an environmental and/or political viewpoint.

The most ambitious concept for nuclear excavation was the construction of a new, sea-level "Panama" Canal. This project afforded the primary stimulus for extensive research in the field of cratering technology supported by the AEC for the past decade under the Plowshare Program. Much of the testing was done in desert alluvium at NTS because of its availability and the economic advantages of support at NTS, but many of media later selected for cratering experiments were chosen due to their similarity to the soil and rock indigenous to the Panamanian Isthmus.

The first significant cratering experiment under the Plowshare

Program was Project Stagecoach which included three separate detonations of 20-ton spherical TNT charges at DOB's of 17, 34, and 80 feet. The tests were conducted in desert alluvium at NTS in March 1960. One of the chief objectives of Stagecoach was to determine if cube-root scaling was actually valid for HE crater formation in desert alluvium. Sandia Corporation was primarily responsible for the conduct of this experiment and the next two which followed it.

Project Buckboard was a similar test series fired in basalt at the NTS to provide basic information on the formation of craters in a hard rock environment. This series, conducted in 1960, consisted of ten 1,000-pound cast TNT charges fired at DOB's ranging from 5 to 25 feet in 5-foot intervals, followed by three 40,000-pound spherical TNT charges fired at DOB's of 26, 43, and 60 feet.

Project Scooter was a 500-ton spherical TNT charge fired at a DOB of 125 feet in desert alluvium at NTS in October 1960. This test, the final in the Sandia series, was designed to extend knowledge of the mechanics of crater formation into yields near the kiloton regime.

The Sedan Event was the largest explosive cratering experiment ever conducted by the U. S. The 100-kt device was detonated in 1962 at a DOB of 635 feet in the desert alluvium at NTS. The main purpose of the experiment was to extend empirically based cratering theory to large yields representative of those that would be employed in an actual large-scale construction project under the Plowshare Program. Equally important was the evaluation of the physical hazards, particularly radiation, that could be expected from such employment. The Lawrence Radiation Laboratory, now the Lawrence Livermore Laboratory (LLL) at Livermore, California, had primary responsibility for the Sedan experiment.

In late 1962, the Nuclear Cratering Group, now the WES Explosive Excavation Research Laboratory (EERL), was created as an organization under the U. S. Army Corps of Engineers to have direct responsibility for supervising experimental research on the use of nuclear explosions for civil construction purposes. The first test program under the supervision of EERL was Pre-Buggy I, conducted in desert alluvium at NTS in the winter of 1962-63 to develop design criteria for a future

large-scale nuclear row-charge cratering experiment. Pre-Buggy I was, in turn, partially designed from data acquired in an earlier, smaller scale row experiment called Project Rowboat (by LLL). Six single-charge tests were fired to determine optimum DOB, followed by four 5-charge row events to determine the most desirable charge spacing for the creation of row craters or channels. Each charge was a 1,000-pound sphere of a liquid explosive, nitromethane (NM).[4] The Pre-Buggy II Series was fired several months later, and consisted of six row shots in which charge spacings, DOB, and stemming were further varied.

The Pre-Schooner Series was executed by EERL in February 1964 in basalt on the Buckboard Mesa at NTS. Four shots of 20 tons of NM each were fired at DOB's ranging from 42 to 66 feet. These were soon followed by the Dugout Event, a row-charge crater shot in basalt consisting of five 20-ton NM charges. In December of 1964, a low-yield (85-ton) nuclear cratering event named Sulky was detonated in the basalt at Buckboard Mesa. The DOB of 90 feet was slightly greater than optimum in an attempt to contain a greater percentage of radioactivity. The Pre-Schooner II Event was an 85-ton charge of NM fired in rhyolite in southwestern Idaho in September 1965.

The Palanquin Event was a 4.3-kt nuclear cratering experiment in a rhyolitic rock at NTS, fired at a DOB of 280 feet, in April 1965. A second nuclear cratering experiment in rhyolite, the 2.3-kt Cabriolet Event, was fired in January 1968. The largest cratering shot in rock was the 35-kt Schooner Event, fired in tuff at NTS in December 1968. In 1969 the Buggy Event, a nuclear row charge consisting of five 1.1-kt devices, was detonated in basalt at NTS.

An extensive program of testing known as Pre-Gondola was also conducted by EERL in a wet clay-shale medium at Ft. Peck Reservoir, Montana, from October 1966 to October 1968. Charge weights ranged from very small (less than 10 pounds) to 40 tons, in both single-charge crater tests and various row-charge tests. Most of these experiments employed NM as the explosive, although some tests used an ammonium nitrate slurry.

---

[4] Explosive equivalences in terms of cratering efficiency are considered in Chapter 3.

Concurrent with their larger scale experiments, EERL carried out an extended series of single- and row-charge studies using 1-pound charges in a closely controlled sand medium, under the name Project Zulu.

An additional program of multiple-charge cratering research, using relatively small HE charges, has been conducted at Sandia for the last decade under sponsorship of the Plowshare Program. Most of these studies have been concerned with the cratering effects of multiple charges detonated simultaneously or in a particular sequence, such as adjacent rows of charges fired in sequence, square arrays of charges fired simultaneously, or vertical arrays of charges. Virtually all of these tests were conducted in desert alluvium near Albuquerque, New Mexico.

2.5 USSR CRATERING EXPERIMENTS

In recent years, an ambitious program of civil cratering applications has been undertaken in Russia, generally paralleling the U. S. Plowshare Program. At this writing, 11 nuclear projects have been carried out, as described in Reference 3. Since reported results are incomplete, these tests are, with one exception, not included in this report. Reports of these projects make interesting reading, however, and they are listed in Appendix C.

2.6 SUMMARY

The foregoing synopsis, which lists only major recent cratering experimentation (illustrated in Figure 2.1), indicates the accumulation of a wealth of crater data, much of it in the past decade. To the casual reader, it might appear that sufficient testing has been accomplished to answer virtually all questions pertaining to this subject; unfortunately, this is not the case. Cratering phenomena are so complex, and cratering applications are so varied, that much yet remains to be done. In the chapters that follow, an attempt will be made to define basic crater parameters, drawing on all applicable data available to the authors, and methods of applying this information will be discussed. In the process, areas of insufficient data will be pointed out.

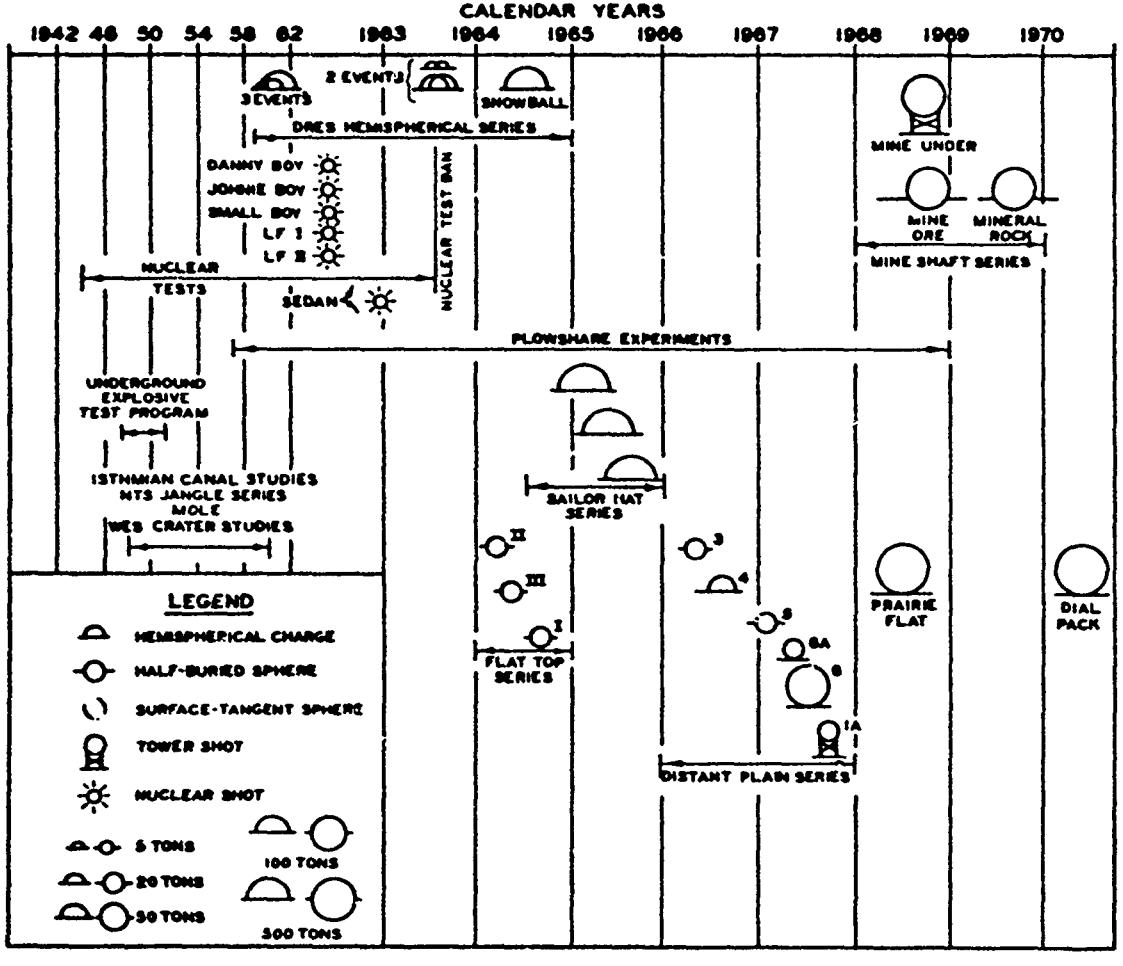

Figure 2.1 Illustrated history of major blast- and shock-effects tests.

CHAPTER 3

CRATERING DATA

3.1 DESCRIPTION OF DATA

The size and shape of an explosively generated crater are dependent upon many different factors. The areas of influence are divided into two main categories: environmental parameters and explosive parameters. The environmental parameters include the density, composition, and strength of the medium in which the crater is formed, the material's moisture content, the jointing or layering of the medium, and, for the sake of completeness, the atmospheric conditions at the time of detonation. Explosive parameters include the quantity and type of explosive used, the geometry of the charge, the method of charge emplacement, and the position of the charge relative to the air-medium interface, (in every case, a complete detonation of the charge is assumed). The actions and interactions of these independent variables on crater formation are complex, and only the major influencing factors are examined in this report. These major factors form the basis upon which the data tables (Appendix A) are subdivided. Within the appropriate subdivisions, data on crater sizes and shapes are included.

The tables are as complete as is possible in a mass compilation of this sort. If all variables have tabulated values for any particular shot, the crater can be essentially reconstructed. For example, by using the available apparent crater depth, radius, lip height, and angle of slope in connection with a crater shape code, a typical crater profile can be drawn.

3.2 EXPLOSIVES CHARACTERISTICS

Approximately 10 different kinds of explosive have been widely used for different test programs, depending upon the requirements of the test and/or the convenient availability of various explosive types. For this report, all explosives are converted to an equivalent TNT yield; each equivalent TNT weight is assumed to be a sphere of cast explosive.

The explosives that have been most commonly used for cratering research are TNT, NM, ammonium nitrate/fuel oil mixtures (ANFO), and ammonium nitrate (AN) slurries. TNT has been selected as the basic explosive due to its widespread use in the past, a result of the fact that it is readily available (to military users); it can be cast in any size and shape, and it is a relatively insensitive explosive and thus safe to handle. NM is a liquid; actually, it is classed as a solvent rather than an explosive. It has been widely used in Plowshare cratering experiments due to the fact that a large volume of NM (up to 100 tons has been used) can be poured into an underground emplacement chamber through small-diameter fill pipes from the surface, thus greatly simplifying the problem of charge emplacement for large, deeply buried shots. ANFO has been used for many years for cratering. It is classed as a blasting agent, and can be mixed on-site prior to placement in its cavity or container. AN slurry has been used increasingly in recent years, since it is also classed as a blasting agent and can be pumped into deeply buried charge emplacement chambers; its higher viscosity in most instances eliminates the need for extensive lining of the chamber to prevent leakage.

Unfortunately, very few data exist that permit performance comparisons of the crater-forming abilities of different types of chemical explosives as compared to the base explosive TNT. In the absence of more definitive research on cratering performance, a list of common explosives and their TNT equivalents has been compiled from References 1 and 10 and is presented as Table 3.1. Table 3.1 does not take into account the effects of different soils or rocks on cratering.

3.3 DATA PRESENTATION

All crater data available to the authors and falling within the scope of this report are presented in Appendix A, Tables A.1 through A.14. The data tables are subdivided into three major parts. First, they are separated according to type of medium, since crater size is strongly dependent on strength of the material cratered. Second, the shots in each medium are grouped according to water content because of

the variation in medium strength and shock-propagation characteristics with change in water content. For example, all crater data for sand are further subdivided into wet, dry-to-moist, and dry sands. The third data group consists of 10 categories of scaled depths (heights) of burst, since differences in charge positioning affect energy partitioning into the medium. For specifying the charge position, cube-root scaling has been used. Thus, depth or height of the charge position is divided by the cube root of charge weight, permitting the grouping of explosion events of different yields. Selection of this cube-root scaling exponent is further discussed in Chapter 4. Note that the categorical divisions are uneven; they have been selected to identify HOB/DOB at which critical changes in crater dimensions and/or crater scaling "laws" can be expected.

A special data group which stands apart from the regular, spherical-charge cratering tests, but which is properly included in a cratering guide such as this, is that of the hemispherical-charge data contained in Table A.14. All available cratering data for this charge geometry, which is frequently encountered in connection with airblast measurements, are included in this table.

The data in Tables A.1 through A.13 are graphically presented in Appendix B, Figures B.1 through B.92; Figure B.93 is a graphical representation of the hemispherical-charge data from Table A.14. Data are fitted by the method of least squares to provide empirical equations. Each equation is based on a minimum of two data points representing a minimum range in charge yields $\geq 2/3$ of a logarithmic cycle. In addition, no curve with a slope $1.5 < \frac{dy}{dx} < 0$ was considered. Each curve was drawn from 1 pound on the abscissa to a point slightly beyond the largest yield for which data were available.

The computer program used to separate, analyze, and plot the data is shown in Appendix D. Explanations necessary to the use of the crater-data tables precede the tables. Note especially that only HOB is listed; a negative number denotes a buried charge geometry (DOB).

3.4 SUBSURFACE DEFORMATION

As shown in Figure 1.2, extensive permanent subsurface deformation accompanies a large crater. The outer limit of this deformation, too indistinct for precise measurement, marks the boundary at which the transient stresses (compressive, tensile, or shear) imposed by the explosion shock wave exceed the respective medium strengths. Beyond this boundary, the medium responds elastically.

Subsurface deformation may be divided into two general zones: rupture and plastic deformation. The rupture zone is so named because of the extensive crushing and cracking which it contains, while the plastic zone exhibits a smoother flowage of the medium (in soil), often unnoticeable unless special methods, such as preemplaced colored sand columns, are used to detect such movement. In the upper portion of the plastic zone, a shearing action often occurs by slippage along horizontal planes of weakness. In rock, the plastic zone is nonexistent or insignificant, but permanent displacement occurs by the closing or opening of joints. In rock as well as many soils, boundaries of the individual zones of deformation are irregular and indistinct.

Relatively few observations are available for definition of subsurface deformation zones, especially for large explosions. Summarized in the following tabulation, in terms of true crater radius r_t and depth d_t or cavity radius r_c, are "rule-of-thumb" limits of these zones in soil and rock:

Type of Failure	Shot Geometry			
	Near-Surface		Deeply Buried	
	Horizontal Limit	Vertical Limit	Horizontal Limit	Vertical Limit
	For Soil			
Rupture	$2r_t$	$1.5d_t$	$2r_t$	$1.5d_t$ [a]
Plastic	$6r_t$	$3.0d_t$	$4r_t$	--[b]
	(Continued)			

[a] Where d_t = DOB + r_c. [b] Insufficient data.

Type of Failure	Shot Geometry			
	Near-Surface		Deeply Buried	
	Horizontal Limit	Vertical Limit	Horizontal Limit	Vertical Limit
	For Rock			
Rupture	$2r_t$	$3.0d_t$	$2r_t$	$2.0d_t$ [a]
Displacement	$4r_t$	$4.0d_t$	--[b]	--[b]

[a] Where $d_t = DOB + r_c$.

[b] Insufficient data.

Dimensions of cavity radius r_c are discussed in Section 6.4.

Plastic deformations or displacements are intended to include only those which are definitely measurable. In general, movement of the medium close to the charge is radially outward, or away from the explosion. There is often a vertical component to such movement, usually upward for surface and buried charges (upthrust) and downward for above-surface geometries. Farther from the charge, permanent displacement toward GZ has frequently been observed. Some surface rotation (in the horizontal plane) is usually observed on survey monuments that were permanently displaced by an explosion, but no pattern of rotation is discernible. Relaxation of the deformed medium has also been observed to occur over a period of several days, while a condition of equilibrium is established among pore and/or joint pressures and the crater void itself. Relaxation is manifested by a small but measurable movement of the compacted medium toward GZ.

TABLE 3.1 COMPARISON OF EXPLOSIVE CRATERING EFFICIENCY WITH THAT OF TNT (REFERENCES 1 AND 10)

To determine relative cratering efficiency (TNT), multiply weight of explosive charge by conversion factor.

Explosive	Conversion Factor
TNT[a]	1.00
Amatol	0.94
Dynamite (40%)	0.68
Pentolite	1.23
C-4, C-3	1.34
Ammonium Nitrate	1.00
Nitromethane	1.10

[a] TNT explosive energy $\approx 10^9$ calories/ton heat of detonation $\approx 10^{12}$ calories/kt.

CHAPTER 4

ANALYSIS OF DATA TRENDS

4.1 CRATER SIZE AND SHAPE

The logarithmic graphs of Appendix B are summarized in Figures 4.1 through 4.19. Figures 4.1 through 4.9 are constructed to show crater dimensions at the 1-ton yield (weight) level in terms of TNT equivalence for those media for which sufficient data exist and for the range of HOB/DOB available. For this yield, crater radius, depth. and lip height may be read directly from the curves; for other yields, the graphs may be entered with scaled HOB or DOB, and dimensions may be scaled to the appropriate charge weight using the nearest value of the scaling exponent shown or an interpolated value. Section 4.3 discusses scaling in more detail. Figures 4.10, 4.11, and 4.12 each show the variation of a single crater dimension for the same charge weight with different media. This makes possible an estimate of crater dimensions for those media for which insufficient data exist to support a separate curve.

Figures 4.13 through 4.19 show crater dimensions for the 1-kt yield level. It will be noted that fewer data are available for this yield, a problem which worsens rapidly as yield increases. No attempt is made in this study to illustrate crater dimensions above the 1-kt level; the general trends in yield scaling exponents for crater radius and depth from small to very large yields are illustrated, however, in Figure 4.20. Scaled values for yields of interest may be approximated by the use of Figure 4.21.

An illustration of the general shapes of craters for charges of all sizes and for geometries ranging from low airbursts to containment depths, at which subsidence craters may be formed, is shown in Figure 4.22. Details of crater nomenclature were shown in Figure 1.2. Deeply buried explosions are discussed in more detail in Section 6.4.

4.2 CRATERING MECHANISMS

An understanding of the mechanics of crater formation aids in

predicting (or explaining) the size and shape of the crater void and the volume of material ejected from it. In addition to the three primary cratering variables (charge yield, shot geometry, and characteristics of the cratered medium), there are three basic mechanisms which govern the formation of HE craters: material ejection, compaction, and plastic flowage. For practical purposes, the same may be said of nuclear craters, since the volume of material involved in the fourth mechanism--vaporization--is generally regarded as being insignificant.

One method of defining the importance of different cratering mechanisms is through their contributions to crater volume. A number of volumetric parameters for craters have been isolated and defined. For craters in soil, the following relations are valid:

$$V_t = V_{dis} + V_c + V_f \tag{4.1}$$

$$V_{dis} = \frac{\gamma_1}{\gamma_o}(V_e + V_{fb}) \tag{4.2}$$

$$V_{fb} = V_t - V_a \tag{4.3}$$

$$V_\ell = KV_e + V_u \tag{4.4}$$

$$V_u = V_f \tag{4.5}$$

Where:
- V_t = volume of true crater
- V_{dis} = volume (preshot) of material dissociated by the explosion
- V_c = volume of crater due to compression (compaction)
- V_f = volume of crater due to plastic flowage of the medium
- γ_o, γ_1 = preshot (in situ) and postshot unit weights of cratered material, respectively
- V_e = volume of ejecta
- V_{fb} = volume of fallback
- V_a = volume of apparent crater
- V_ℓ = total volume of crater lip
- K = a constant representing the fraction of ejecta volume contributing to the formation of the crater lip

V_u = volume of upthrust region

Equations 4.1 through 4.5 permit assessment of the contributions of various cratering mechanisms to total crater volume. Similar relations have been developed on the basis of mass (Reference 4). These same equations (4.1 through 4.5) are equally applicable in rock, except that the plastic flowage term for this medium is negligible; therefore, Equation 4.5 does not apply. Upthrusting of the lip region does occur, however, by upward displacement of rock strata (buried shots) and expansion of joints by rebound action in near-surface shots. A similar action has been noted beneath the rock craters for near-surface geometries. When this occurs,

$$V_t = V_{dis} - V_{exp} \tag{4.6}$$

where V_{exp} = net volume of joint expansion.

Reference 5 examines in detail the dimensional analyses which serve as background to scaling relations. Selecting from the listed properties of medium variables those which are probable primary contributors to the three basic mechanisms, the following tabulation can be made:

Cratering Mechanism	Contributing Properties of the Medium
Material Ejection	σ
Compaction	σ, v_r
Plastic Flow	σ, ν

Where: σ = compression, shear, and tensile strengths or elastic properties $ML^{-1}T^{-2}$ in units of mass-length-time

v_r = void ratio, dimensionless

ν = dynamic viscosity, $ML^{-1}T^{-1}$

4.3 SCALING CONSIDERATIONS

4.3.1 Scaling as a Prediction Tool. A primary purpose of the graphs in Appendix B is the development of exponents to permit prediction of crater size. Generally referred to as "scaling," this is a mathematical exercise of the form

$$r, d, v = kW^n \tag{4.7}$$

Where: r = crater radius (apparent or true)

d = crater depth

v = crater volume

k = a constant numerically equal to the graphical intercept at W = 1

W = charge weight (TNT equivalent)

n = the scaling exponent (slope of logarithmic graph)

A related procedure can be employed when crater dimensions from a similar experiment are available and when n is known or can be approximated. Thus,

$$\frac{r_1, d_1, v_1}{W_1^n} = \frac{r_2, d_2, v_2}{W_2^n} \tag{4.8}$$

where the subscripts 1 and 2 refer to two different cratering events, the results of which are known for one or the other. The foregoing equations have been used extensively.

An alternative method, now under development, is computer simulation of cratering processes. A thorough discussion of this technique is beyond the scope of this report; briefly, it utilizes a numerical computer routine such as a finite element program to simulate the effects of a detonation upon a medium of known physical properties. The results can be graphed to illustrate crater formation at any stage (as a function of time). Obviously, a detailed knowledge of both the explosive and the medium characteristics is prerequisite. While this method has contributed greatly to the science of cratering, it will probably never replace scaling as a rapid means of crater prediction.

4.3.2 Linear Scaling Relations. Reference 5 develops four scaling rules governing crater radius and depth dimensions. Each rule is predicated upon certain assumptions, some controversial. Three of these rules result in the generally well-known cube-root scaling ($W^{1/3}$); the fourth rule, based on energy-gravity scaling (charge energy and gravitational acceleration g are considered when forming the dimensional terms, but with g and the medium density ρ held constant), results in fourth-root scaling of linear dimensions. In all cases, experimental similarity--to include scaling of material properties--is necessary for unqualified application of the rules. In practice, similarity requirements are seldom (if ever) met, and violation of these requirements generally results in larger crater dimensions for increased charge sizes than would be predicted by formal scaling rules. Thus, observations of crater data frequently show $n > 1/3$, especially for low yields. By the same token, where experiment shows $n < 1/3$, the influence of energy-gravity scaling considerations may be suspected. Since empirical exponents for linear crater dimensions show a general decrease with increasing charge yield (Figure 4.20), it seems likely that energy release rather than charge mass or weight becomes increasingly important in the larger yields. It can be seen from the foregoing discussion that predictions which span a wide difference in charge yields may be subject to the conflicting influences of similarity violations and energy-gravity considerations.

As explosion yield increases, and one moves out of the HE domain and into the NE domain, basic differences in scaling behavior between the two must be considered. HE occupies some finite volume and generates its own explosion gases, while NE is essentially a point source of thermal energy which vaporizes the adjacent material, thereby generating gases. Thus, differences in energy partitioning and coupling into the cratered medium almost surely cause differences in the means by which the craters are formed and in the scaling factors applied to them. Experience shows that HE craters are larger than those for comparable NE yields.

It seems probable that no single scaling exponent will ever

suffice to precisely predict any crater dimension except under closely controlled conditions and for a limited range of charge yields. This is probably true in homogeneous media, not to mention real-world soils, where layering and inhomogeneities abound. It is for this reason that empirical approaches to crater scaling are so generally used. Analyses presented in this report show that scaling exponents for linear crater dimensions fall roughly between 0.20 and 0.40 for spherical charges; however, higher values have been observed for scaling crater depths from hemispherical charges in plastic soil.

Presumably, scaling of crater ejecta field dimensions could be accomplished in a manner similar to that discussed here. As with crater formation, attempts are under way to describe ejecta deposition by computer simulation, as well as by analysis of experimental data. Thus far, rather tenuous scaling exponents in the range of $0.3 \geq n \geq 0.17$ have been developed from the latter, with the larger exponent applying to surface geometries. Empirical scaling exponents for ejecta ranges are further discussed in Chapter 5.

4.3.3 Volumetric Scaling Relations. For most of the geometric shapes which best describe craters (e.g., paraboloid, hyperboloid), volume is proportional to r^2. It is frequently assumed that

$$\left(W^{n_1}\right)_d \left(W^{2n_2}\right)_r = \left(W^{n_1+2n_2}\right)_v = \left(W^{n_3}\right)_v \qquad (4.9)$$

where n_1, n_2, and n_3 represent the scaling exponents for depth, radius, and volume, respectively. Intuitively, it would seem that $n_3 \leq 1.0$, although apparent violations have frequently been noted. Development of scaling relations for crater volumes, in addition to the problems outlined above, is plagued by difficulties in obtaining good volume measurements. Volumes given in the literature, especially those obtained prior to 1960, are oftentimes based on one or two radial surveys and are therefore not as accurate as those developed from aerial stereophotography or from a number of radial surveys.

4.3.4 Depth-of-Burial Scaling. Cube-root (mass or mass-gravity) scaling is used in this report for charge DOB, a common approach. Two

alternatives are also found in other studies:

1. If the appropriate scaling exponent is known or assumed beforehand, it can also be applied to DOB scaling.

2. An iterative approach can be used in which yield is held constant and an exponent is found which best matches both crater dimension and DOB (Reference 6).

Generally, all three methods produce satisfactory data fits; some advantage may be noted in the last method where data are grouped to facilitate its use. This was not always the case in this study, however. A primary purpose of this report was to develop and illustrate dimension scaling relations; hence the choice of cube-root DOB scaling.

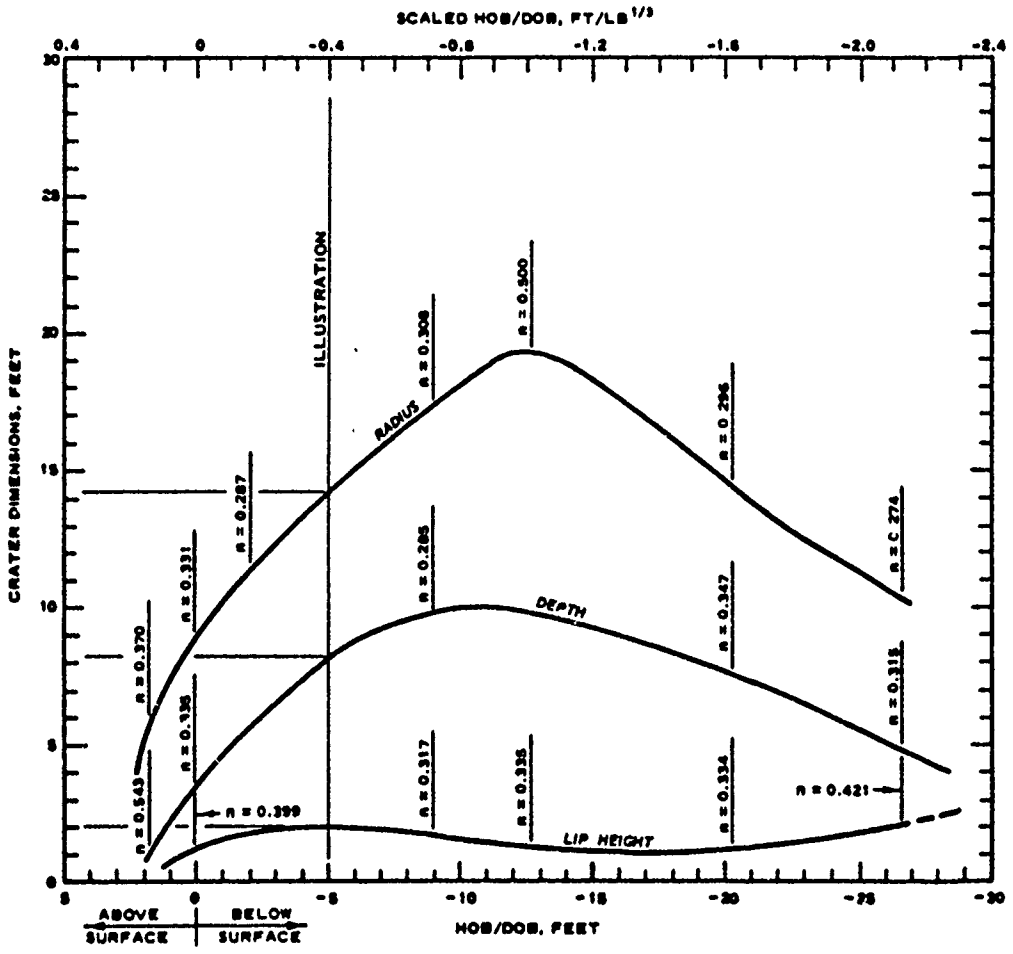

Figure 4.1 Apparent crater dimensions for 1-ton TNT spheres in basalt and granite. Example: For a 2-ton detonation in granite at a DOB of 6.3 feet, find scaled DOB = $6.3/(4{,}000)^{1/3} = 0.4$ ft/lb$^{1/3}$. From the graph, the dimensions for a 1-ton charge at the same scaled DOB are (see illustration): $r_a = 14$ feet, $d_a = 8$ feet, $h = 2$ feet. By interpolation, scaling exponents are approximately 0.297, 0.308, and 0.354, respectively. Thus, scaled dimensions are as follows:

$$r_a = 14\left(\frac{4{,}000}{2{,}000}\right)^{0.297} = 17.2 \text{ feet}; \quad d_a = 8\left(\frac{4{,}000}{2{,}000}\right)^{0.308} = 9.9 \text{ feet};$$

$$h = 2\left(\frac{4{,}000}{2{,}000}\right)^{0.354} = 2.5 \text{ feet}.$$

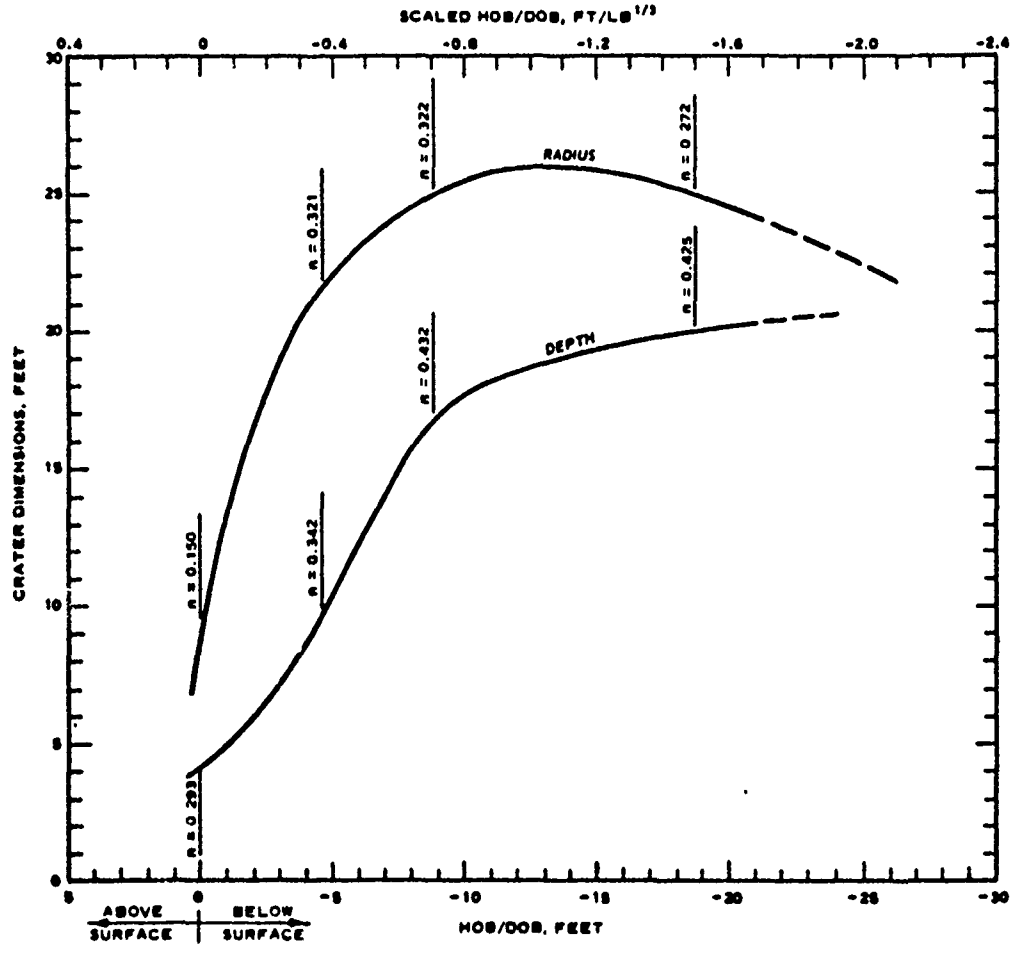

Figure 4.2 True crater dimensions for 1-ton TNT spheres in sandstone.

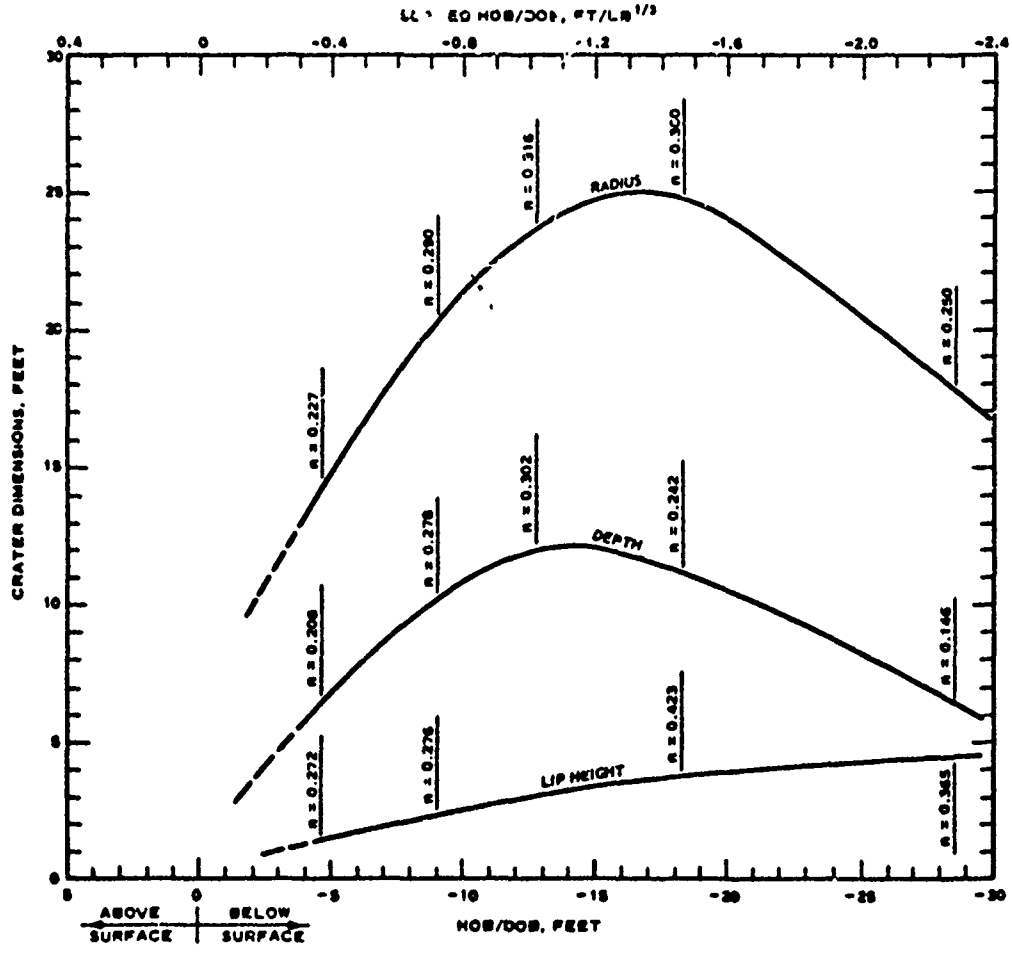

Figure 4.3 Apparent crater dimensions for 1-ton TNT spheres in shale, tuff, and frozen ground.

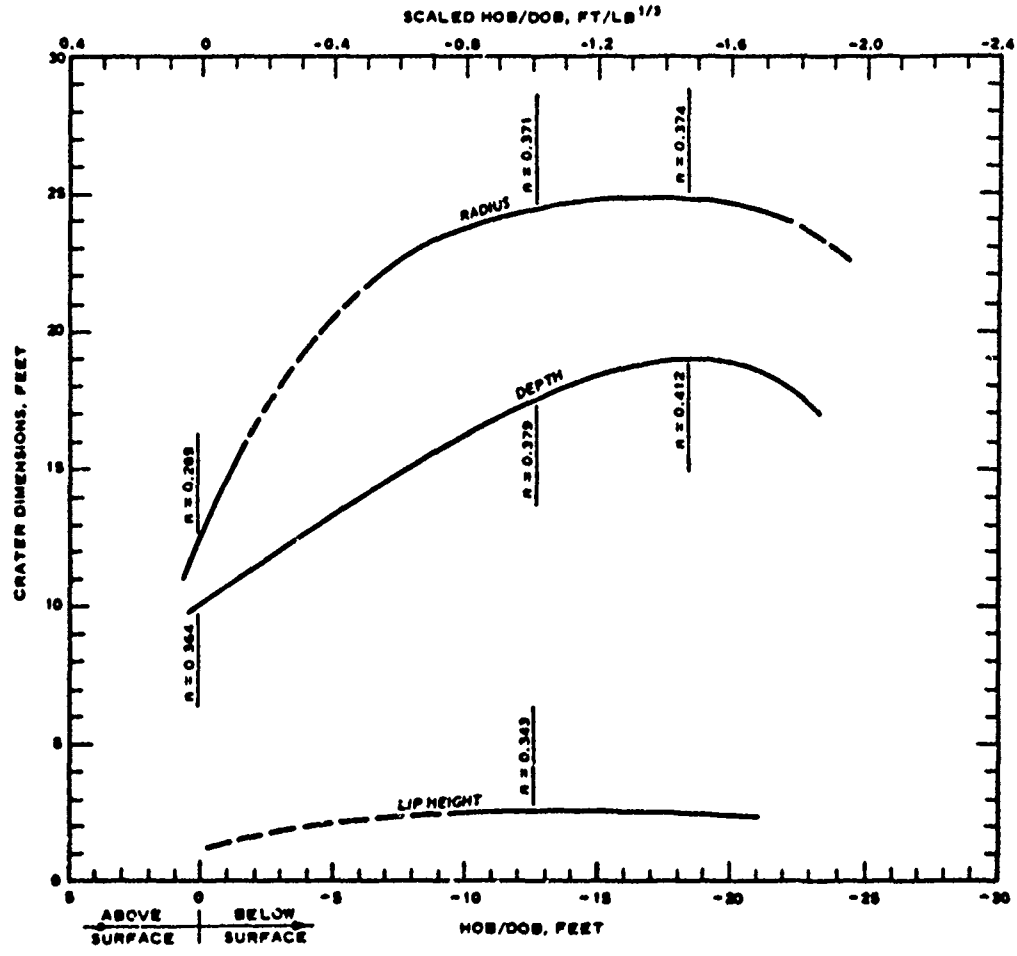

Figure 4.4 Apparent crater dimensions for 1-ton TNT spheres in moist clay.

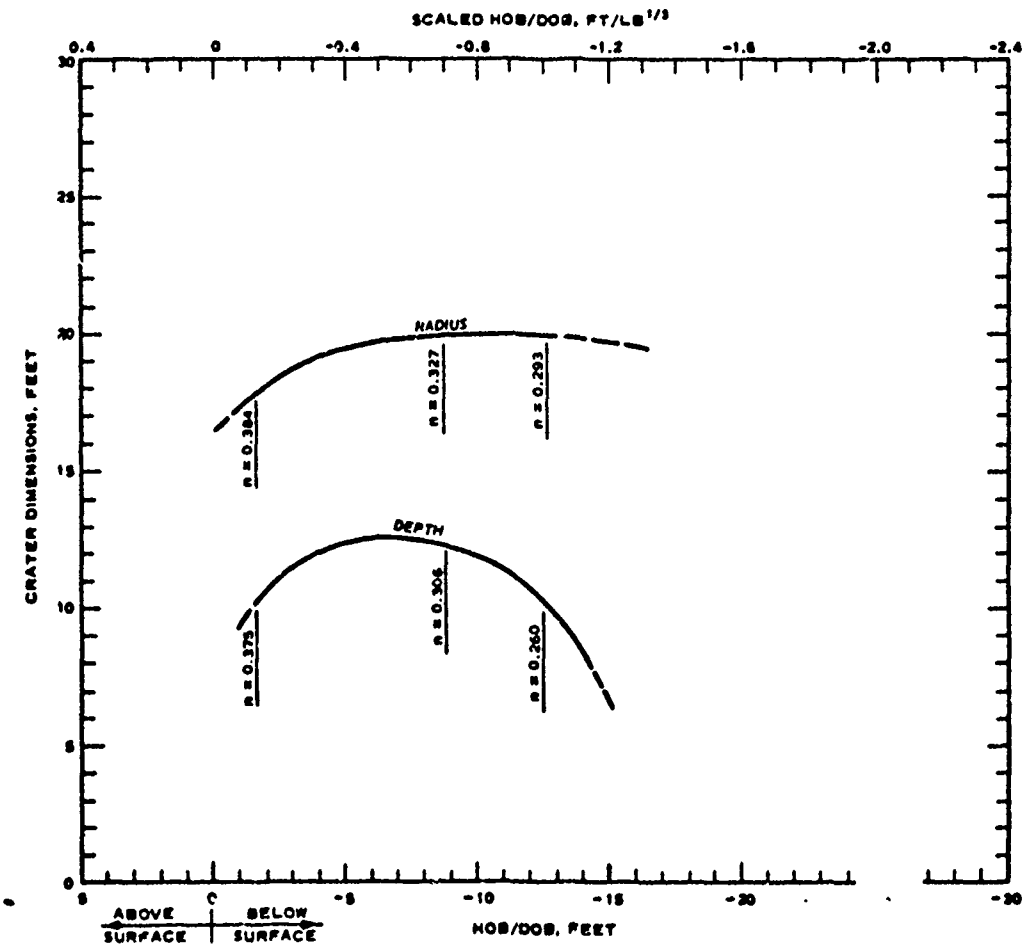

Figure 4.5 Apparent crater dimensions for 1-ton TNT spheres in dry clay.

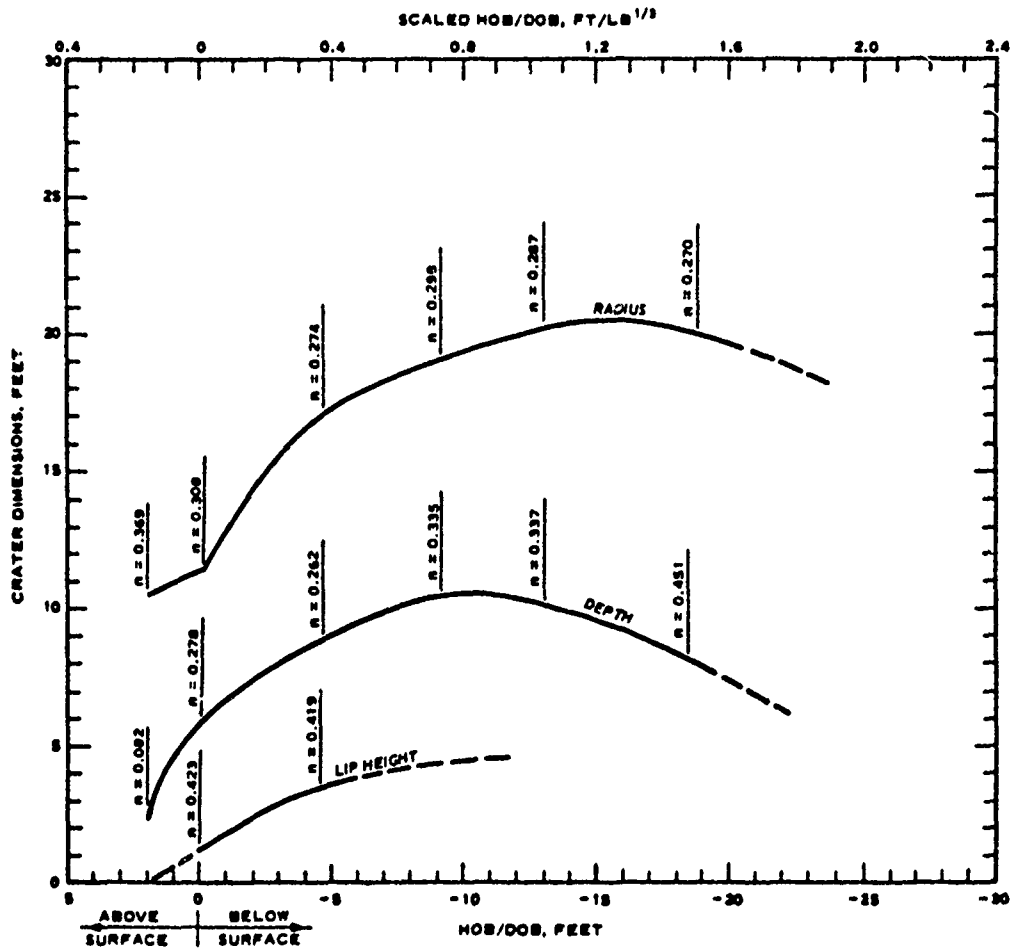

Figure 4.6 Apparent crater dimensions for 1-ton TNT spheres in moist loess and moist lacustrine silt.

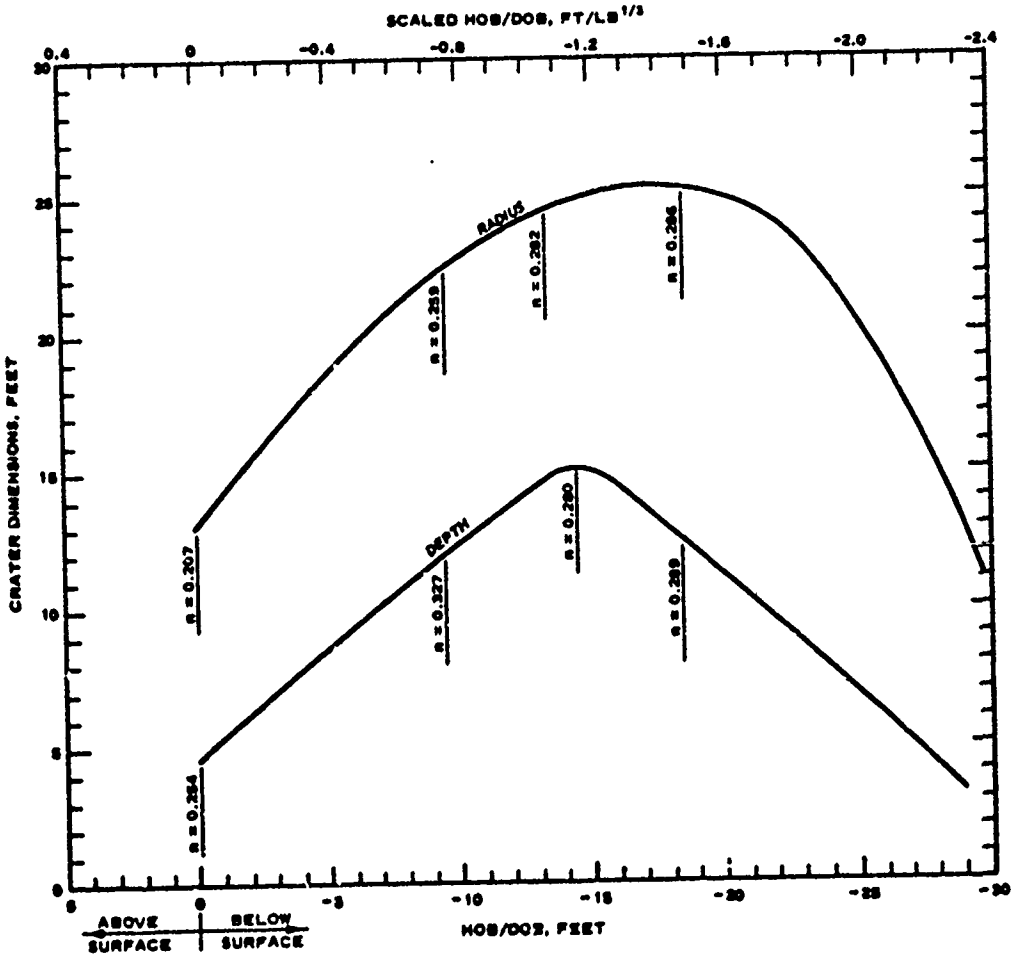

Figure 4.7 Apparent crater dimensions for 1-ton TNT spheres in dry desert alluvium.

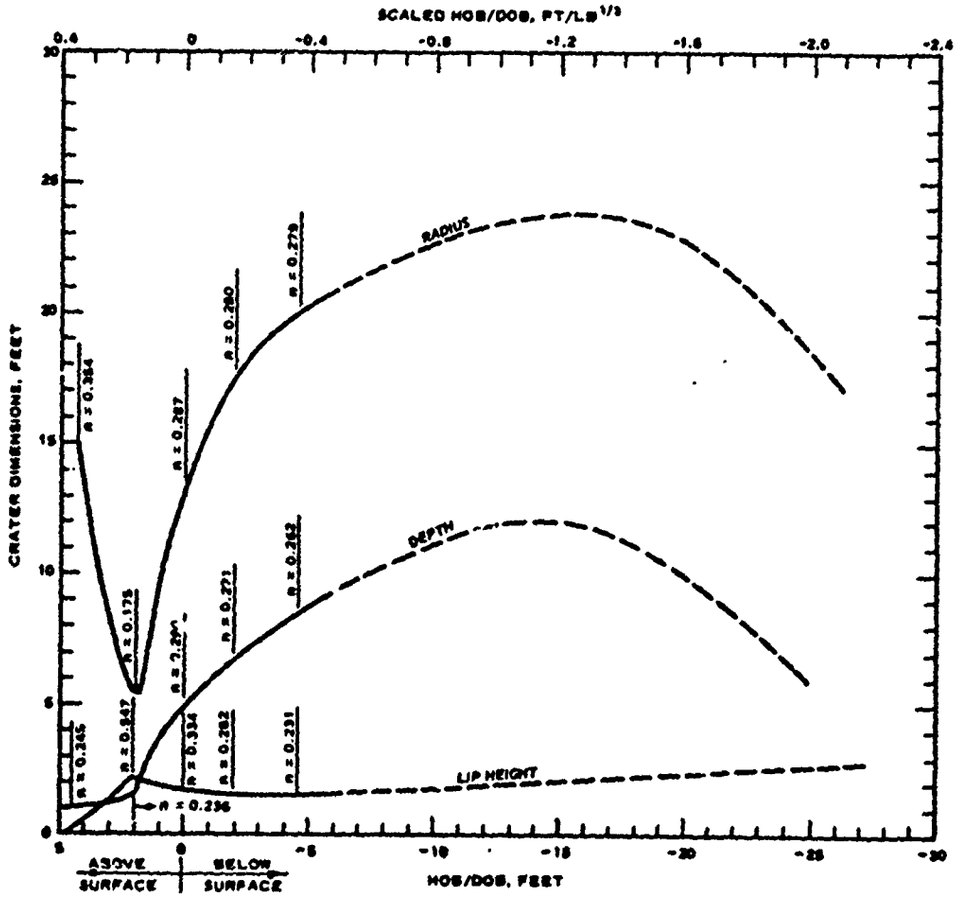

Figure 4.8 Apparent crater dimensions for 1-ton TNT spheres in dry-to-moist sand.

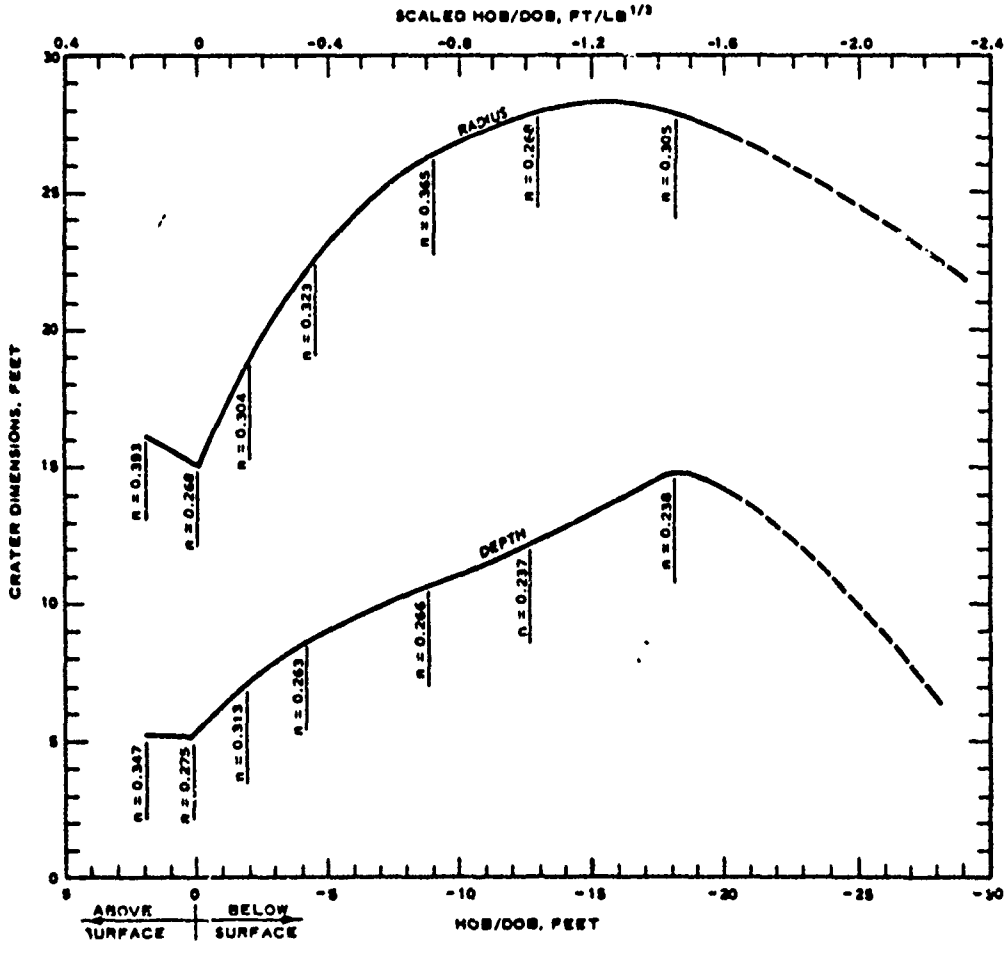

Figure 4.9 Apparent crater dimensions for 1-ton TNT spheres in wet sand.

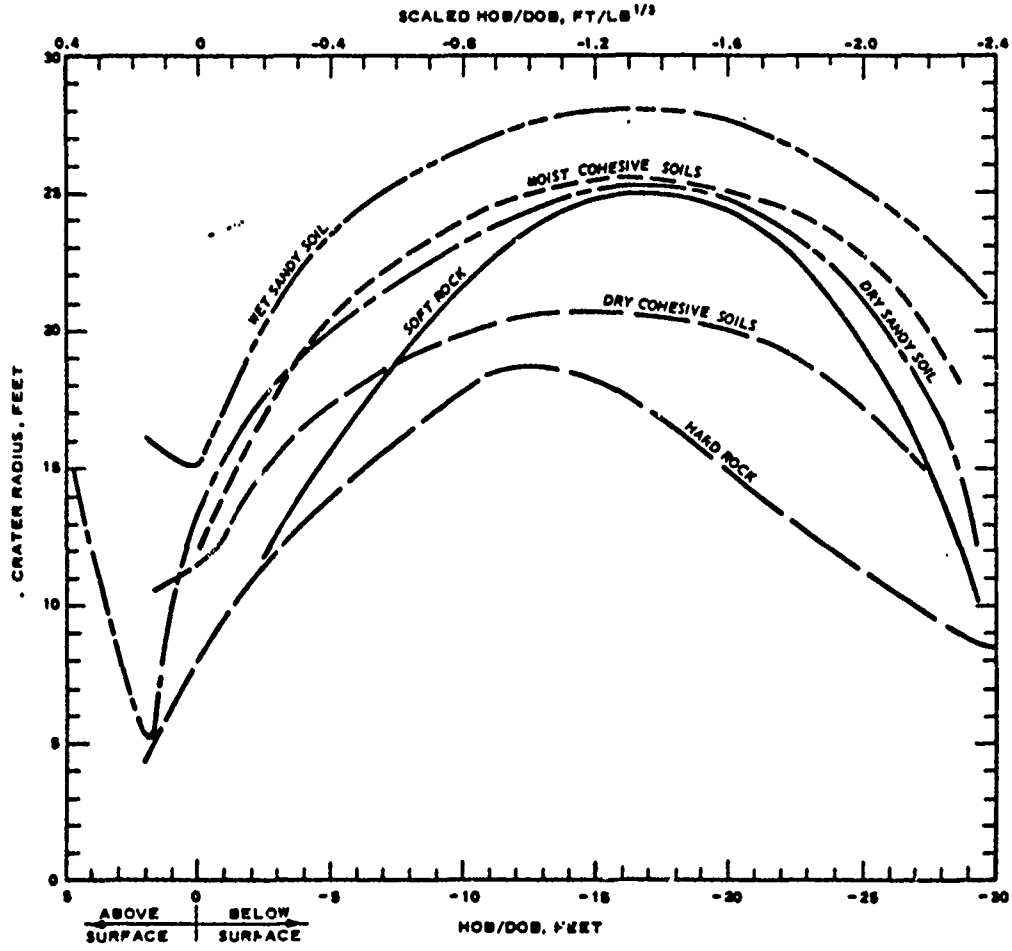

Figure 4.10 Composite graph for apparent crater radius for 1-ton TNT spheres.

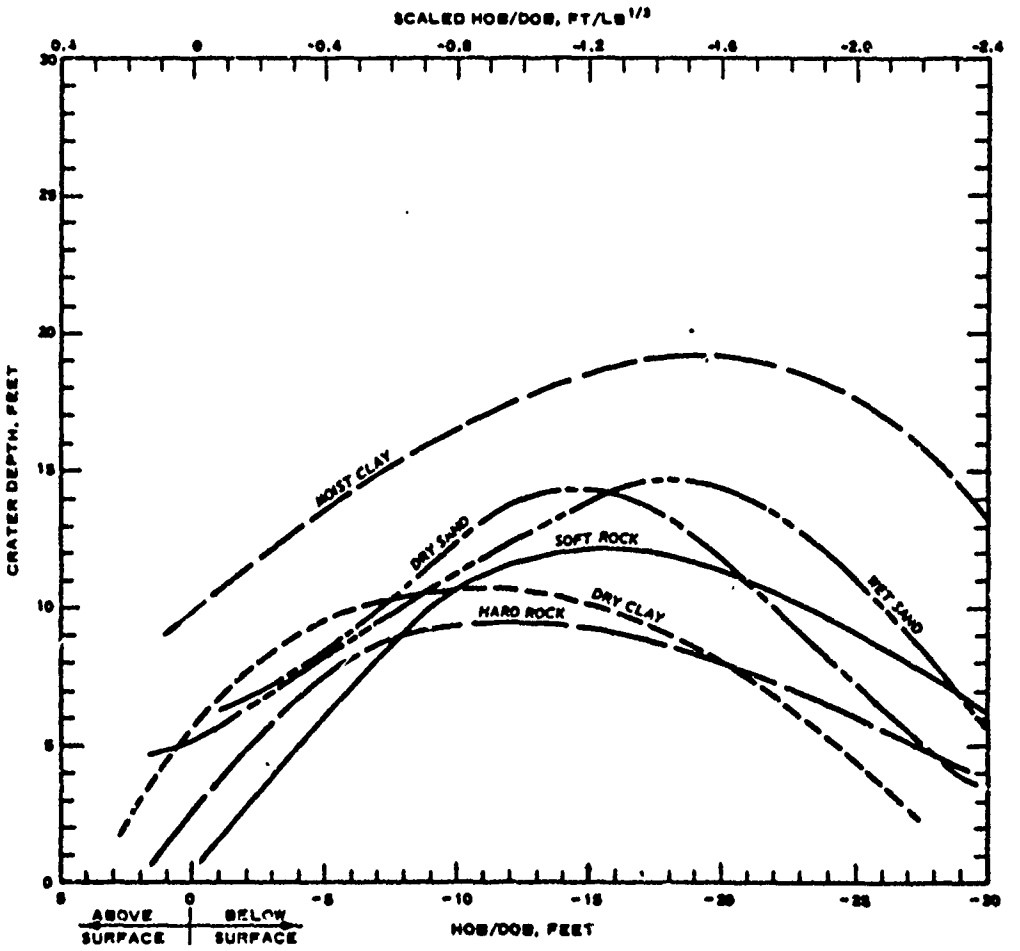

Figure 4.11 Composite graph for apparent crater depth for 1-ton TNT spheres.

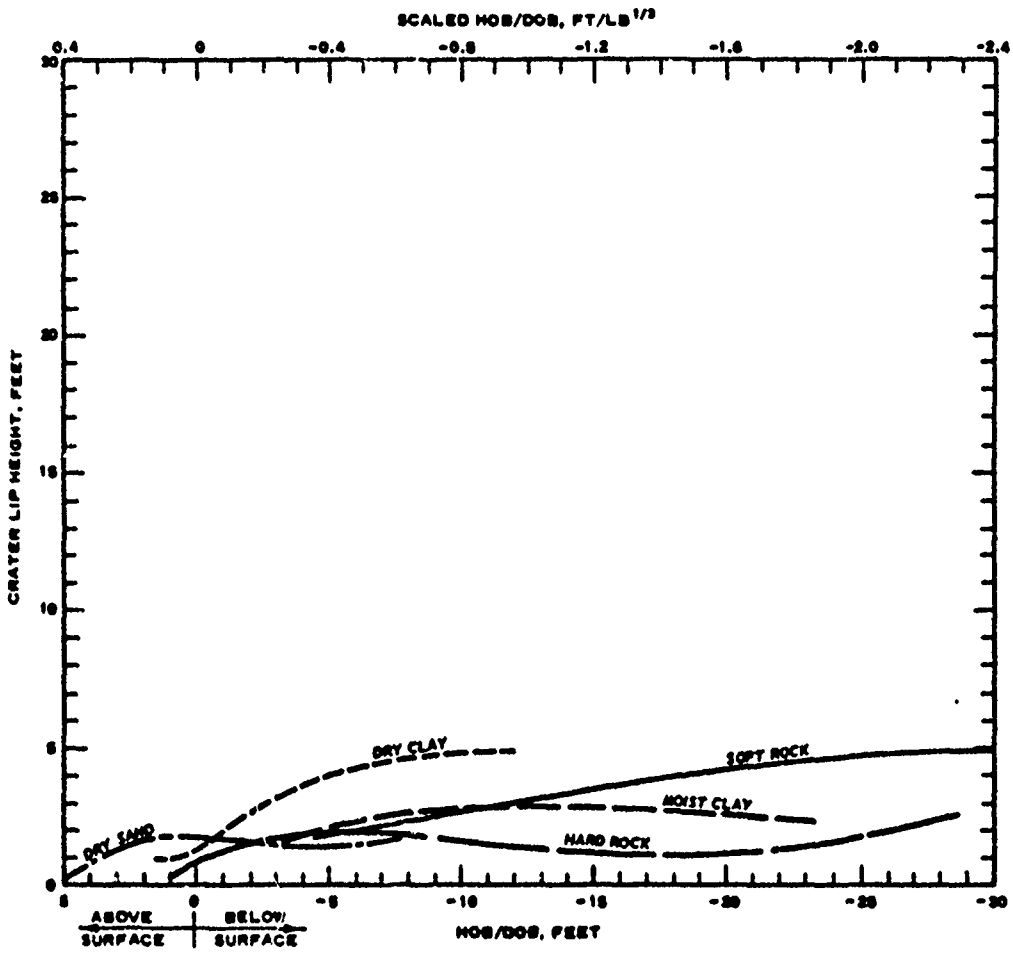

Figure 4.12 Composite graph for apparent crater lip height for 1-ton TNT spheres.

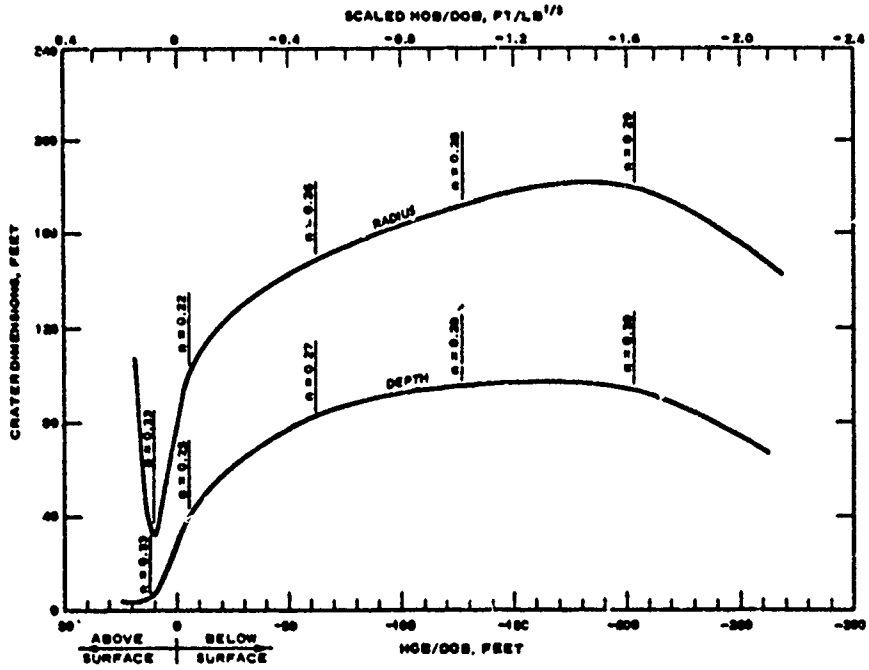

Figure 4.13 Apparent crater dimensions for 1-kt charges in desert alluvium.

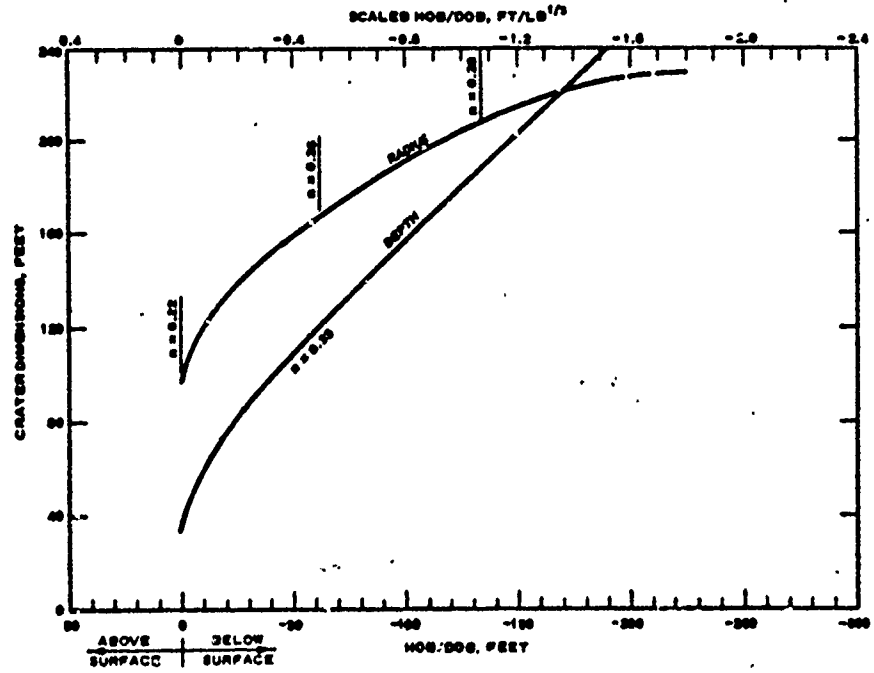

Figure 4.14 True crater dimensions for 1-kt charges in desert alluvium.

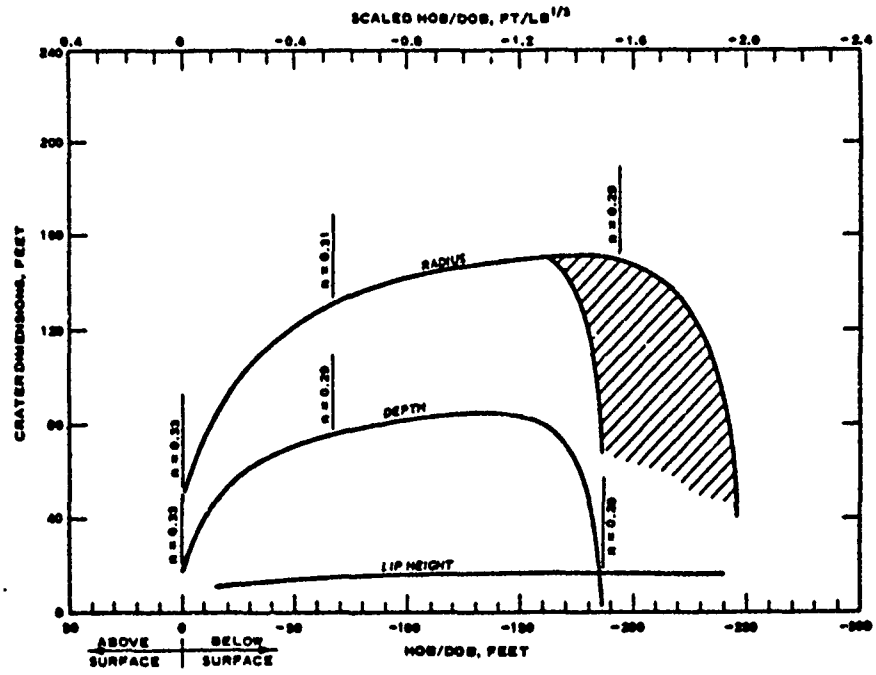

Figure 4.15 Apparent crater dimensions for 1-kt charges in rock. Cross-hatched area shows region in which uncertain results are obtained, depending upon strength and composition of rock.

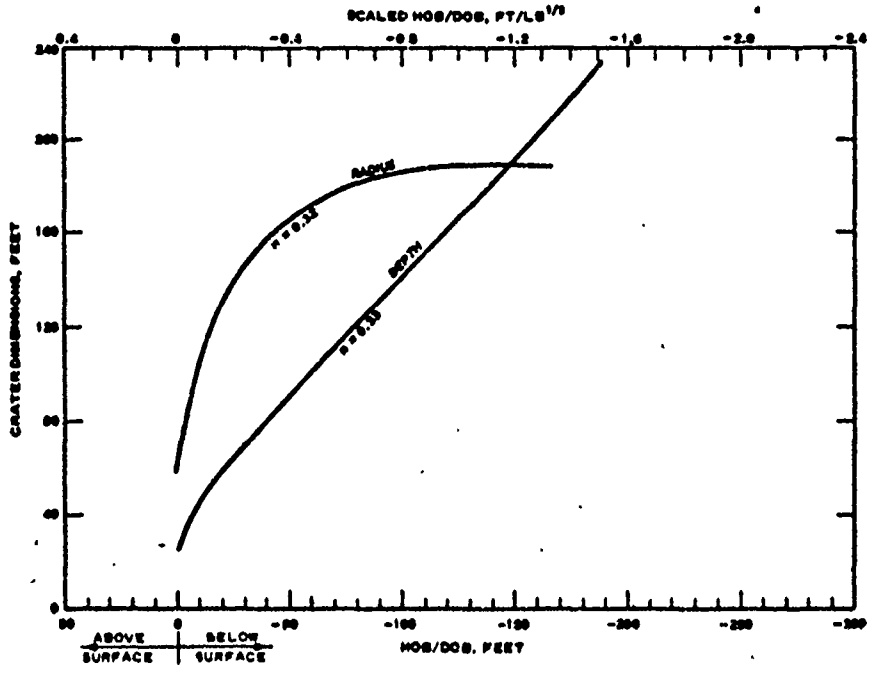

Figure 4.16 True crater dimensions for 1-kt charges in rock.

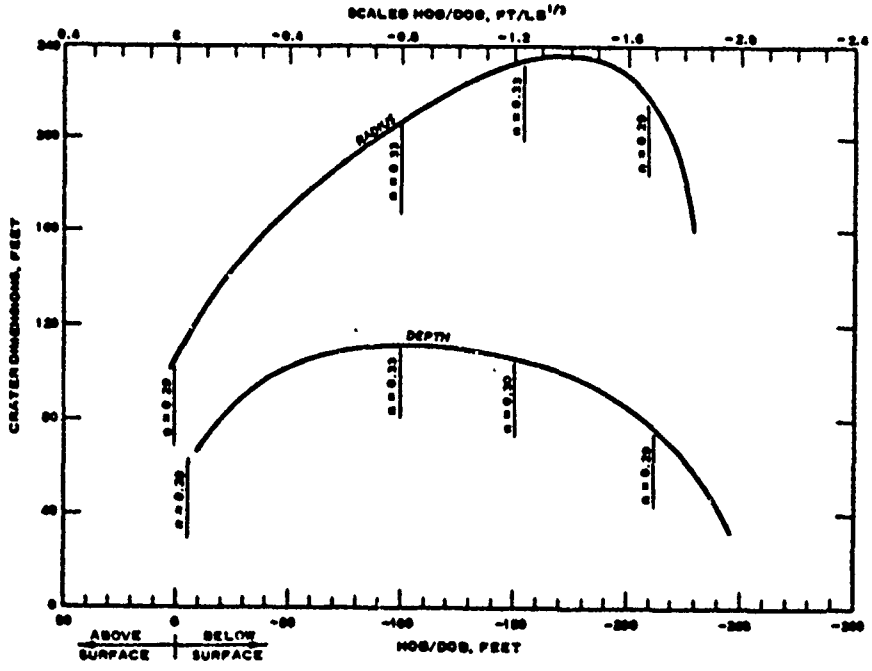

Figure 4.17 Apparent crater dimensions for 1-kt charges in moist clay.

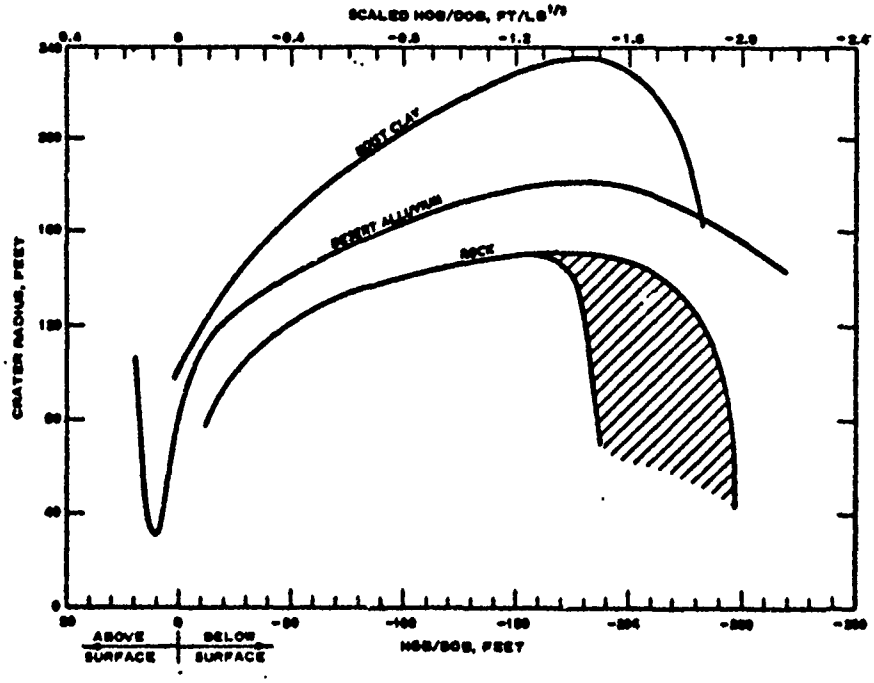

Figure 4.18 Composite graph for apparent crater radius for 1-kt charges.

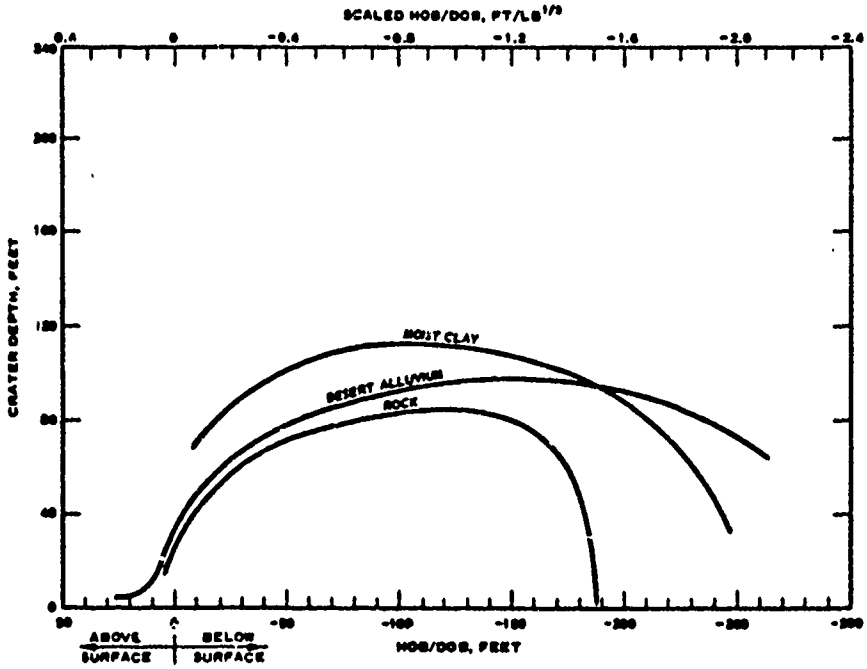

Figure 4.19 Composite graph for apparent crater depth for 1-kt charges.

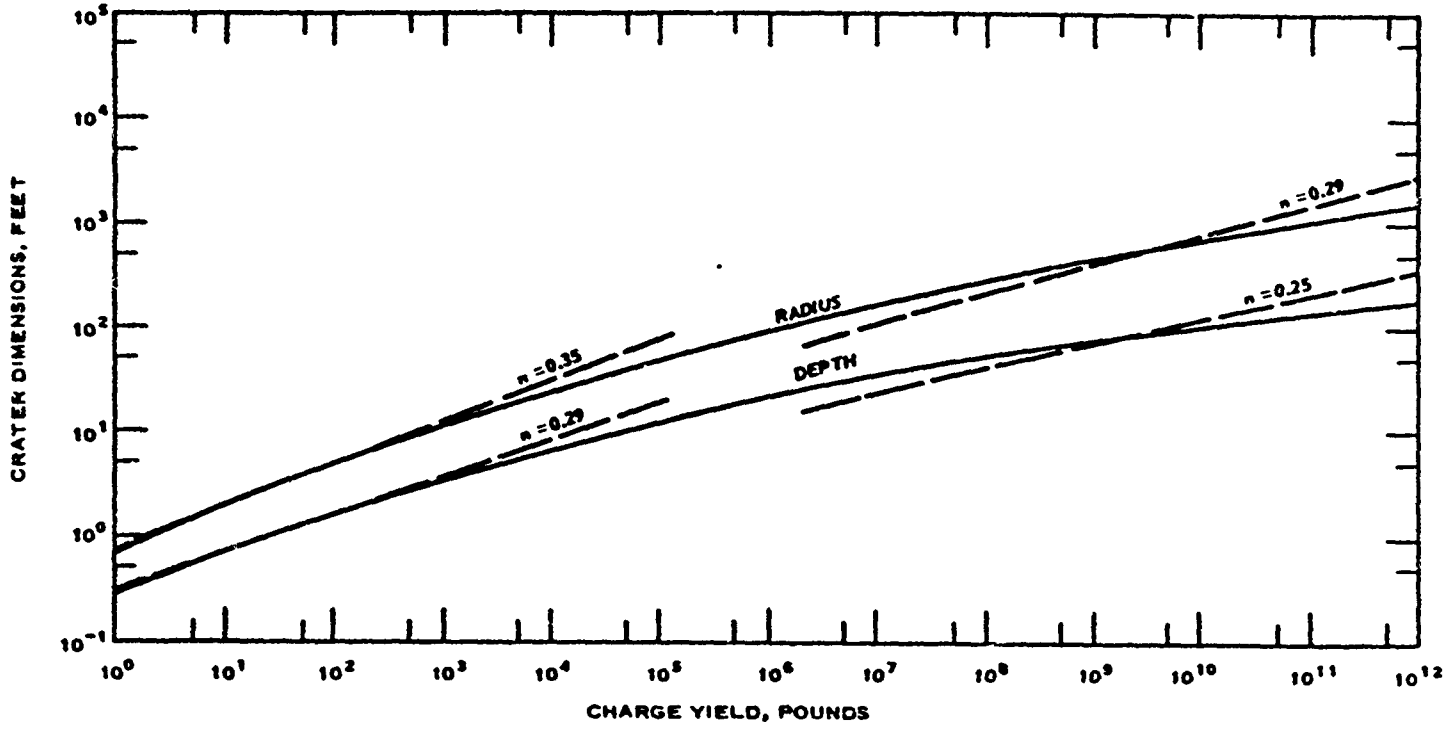

Figure 4.20 Apparent crater dimensions versus charge yield, showing the variation of scaling exponent with charge yield.

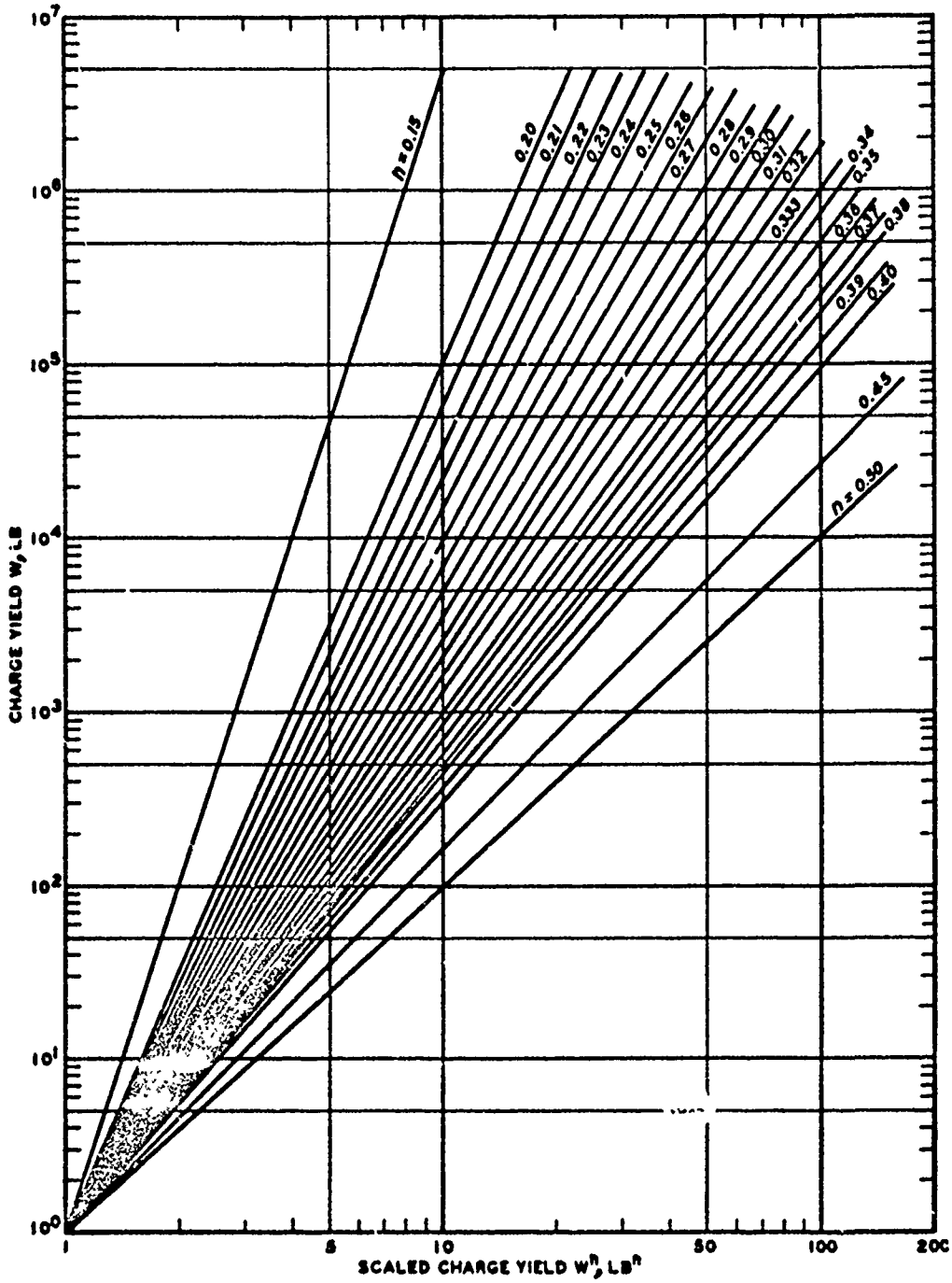

Figure 4.21 Charge yields scaled to various powers.

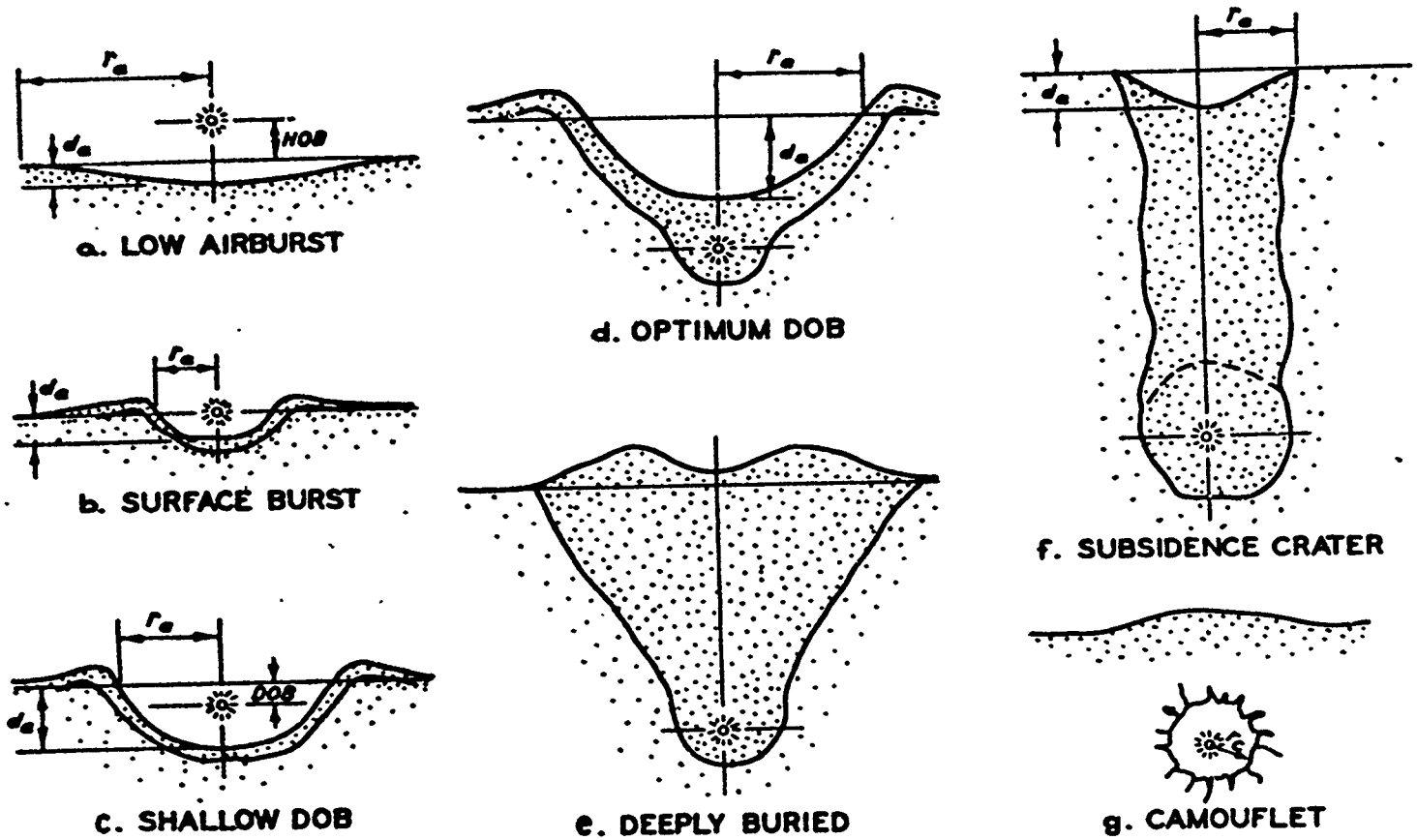

Figure 4.22 Crater shapes as affected by burst geometries.

CHAPTER 5

CRATER EJECTA

Although not a primary consideration in this report, the ejection mechanism is sufficiently important in the formation of a crater to warrant explanation. A complete treatment is properly the subject of a separate study; for this, the reader is referred to the Bibliography. The following paragraphs are intended to provide a general appreciation of this phenomenon.

5.1 COMPOSITION AND ORIGIN

Crater ejecta consists of that portion of the soil or rock debris thrown beyond the boundaries of the apparent crater by an explosion (Figure 5.1). Together with the fallback, which lies between the true and apparent crater boundaries, it comprises all material completely dissociated from the parent medium by the explosion. It may represent a significant hazard at considerable distances from the crater.

In a buried explosion, ejecta mainly originates in the dome of earth material which is forced upward by the expanding gas bubble. As the dome disintegrates and gas venting occurs (Figure 5.2), discrete particles of ejected material enter a trajectory which is, except for very small, windborne particles, essentially ballistic. For near-surface explosions, where the fireball obscures the cratered region, the mechanics of ejection are not so well known. Observations of near-surface explosions show an early, fast-moving corona of material ejected from a position near the charge and at a steep angle to the ground surface. The ejection process is, however, known to take place over a longer period of time and to include lower exit angles.

Material fractured by the compressive stress wave may be dislodged and ejected by the explosion gases, as visualized in Figure 5.3. However, attempts to predict ejecta ranges by consideration of shock-front conditions and by calculation from early trajectory parameters have been unsatisfactory. It appears that additional experimental observations will be necessary for this purpose.

Theoretical studies indicate that in large near-surface detonations, ejecta particles of considerable size may be captured by the thermal updrafts and lofted into high, nonballistic trajectories. Figure 5.4 illustrates origins and relative ranges for general cases of HE charge geometries, as determined from field observations.

5.2 DESCRIPTIVE PARAMETERS

The ejecta field is divided into two zones: (1) the crater lip (the continuous ejecta surrounding the apparent crater), and (2) the discontinuous ejecta, comprising the discrete natural missiles falling beyond the crater lip.

The principal parameters used to describe the ejecta are the average lip crest height (h) (Figure 1.2); the radial extent of the crater lip (r_ℓ) from GZ; the depth of deposition, ejecta mass density, and missile size/distribution defined as functions of radial distance from GZ; and the maximum missile range (r_e). The principal variables which control the ejecta parameters are the shot yield and geometry and the physical nature of the earth medium.

5.2.1 Crater Lip. The amount and extent of the continuously deposited ejecta in the crater lip are determined primarily by the shot yield and geometry. The radial extent of the crater lip will usually vary from about 2 to 4 apparent crater radii. The maximum depth of ejecta in the lip occurs at or near the lip crest, and its height above original ground can be estimated as about one-fourth to one-third the apparent crater depth for near-surface bursts. For deeper bursts, the lip height is usually one-fifth to one-fourth the apparent crater depth. The depth of ejecta will decrease rapidly in an exponential fashion as the distance from GZ increases. In general, the volume of ejecta deposited within the crater lip varies from about 40 percent to over 90 percent of the total, the latter figure representing near-optimum DOB's in cohesive media. Deeper bursts may, of course, result in a lip containing all of the ejected material, surrounding an apparent crater of insignificant size (Figure 4.22e). Figure 5.5 illustrates the fraction of total deposition with range from GZ.

5.2.2 Discrete Ejecta Field. The discontinuous ejecta beyond the crater lip is usually described by areal mass density (e.g., pounds of ejecta per square foot) and a numerical density (number of missiles per square foot). Both parameters decrease exponentially as distance from GZ increases, and a wide circumferential variation is usual, which is mainly the result of medium inhomogeneities. Figure 5.6 provides a means of predicting ejecta areal density for a given explosion. Predictions obtained from these curves should be considered only as first-order approximations, as deviation can be caused by variations in shot geometry, earth media characteristics, and the asymmetry of the ejecta field itself.

Ejecta missile size and quantity, both in the crater lip and in the discontinuous portion of the ejecta field, depend primarily on the characteristics of the earth medium. For example, the cohesiveness of a soil with a high clay content often results in missiles of substantial size, while a noncohesive material such as sand will produce almost no missiles of significant size. Explosions in glacial tills will produce a large number of long-range missiles. In rock, the spacing of joints is a controlling factor in determining missile size. At this writing, means of predicting natural missile-size distribution, either analytically or empirically, are considered too tentative for inclusion in a report of this nature.

For buried charges, maximum missile range is approximately proportional to $W^{1/6}$, and is shown graphically as a function of DOB in Figure 5.7 (from Reference 7). Surface or near-surface, aboveground bursts produce maximum missile ranges which more nearly scale as $W^{0.3}$. It has been observed that, for near-surface HE geometries, the periphery of the ejecta field consists of predominantly small ($\leq$1 pound) particles.

Finally, the reader is cautioned that the figures of this chapter are primarily qualitative, showing trends and very rough values for ejecta parameters. No attempt should be made to extract from them detailed quantitative information.

Figure 5.1 Throwout of ejecta by a low-yield cratering explosion at near-optimum depth of burial.

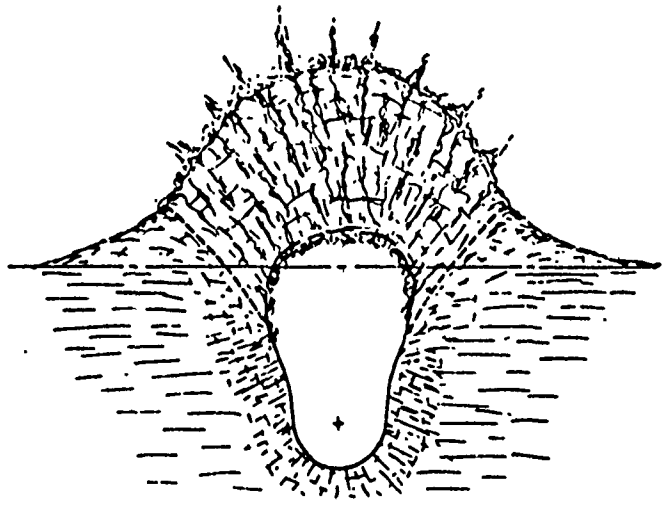

a. Cavity and dome immediately prior to venting.

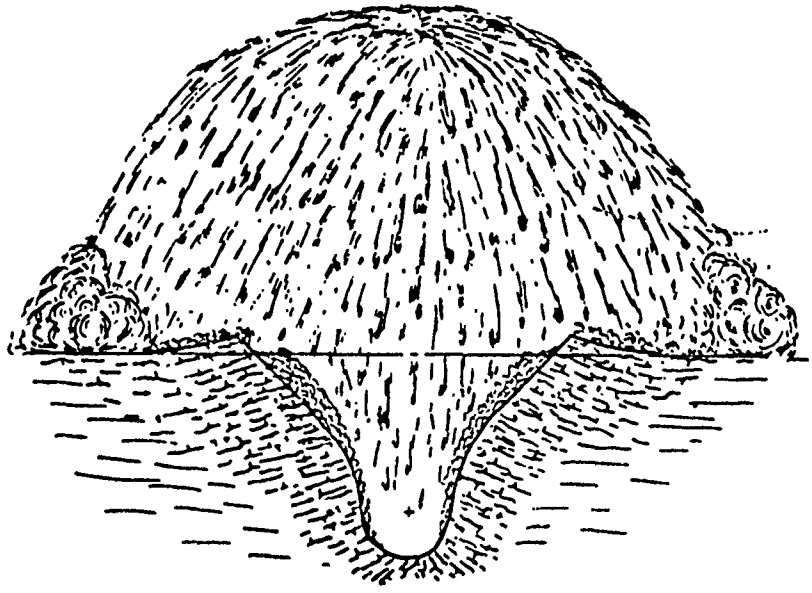

b. Venting and ejection of in situ material.

Figure 5.2 Ejection process for a buried explosion.

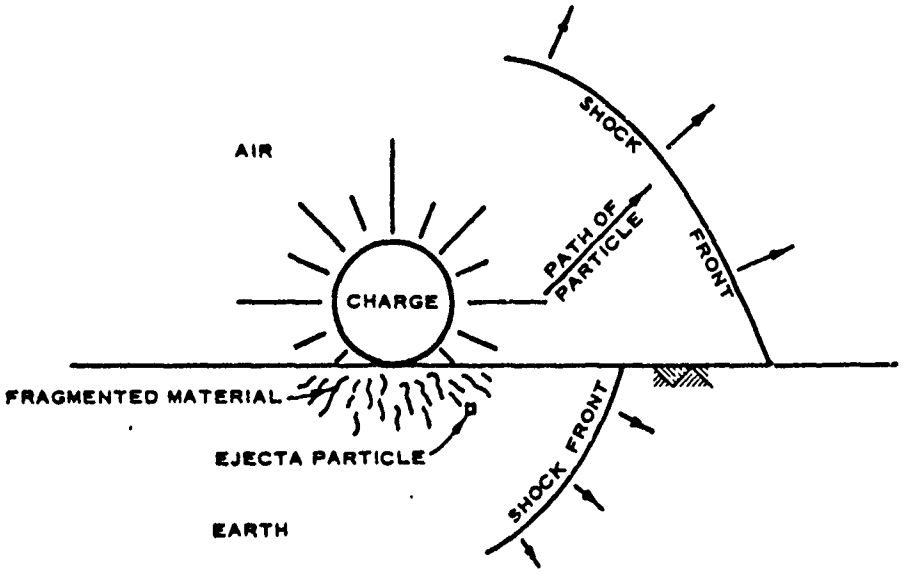

Figure 5.3 Ejection process for a near-surface explosion.

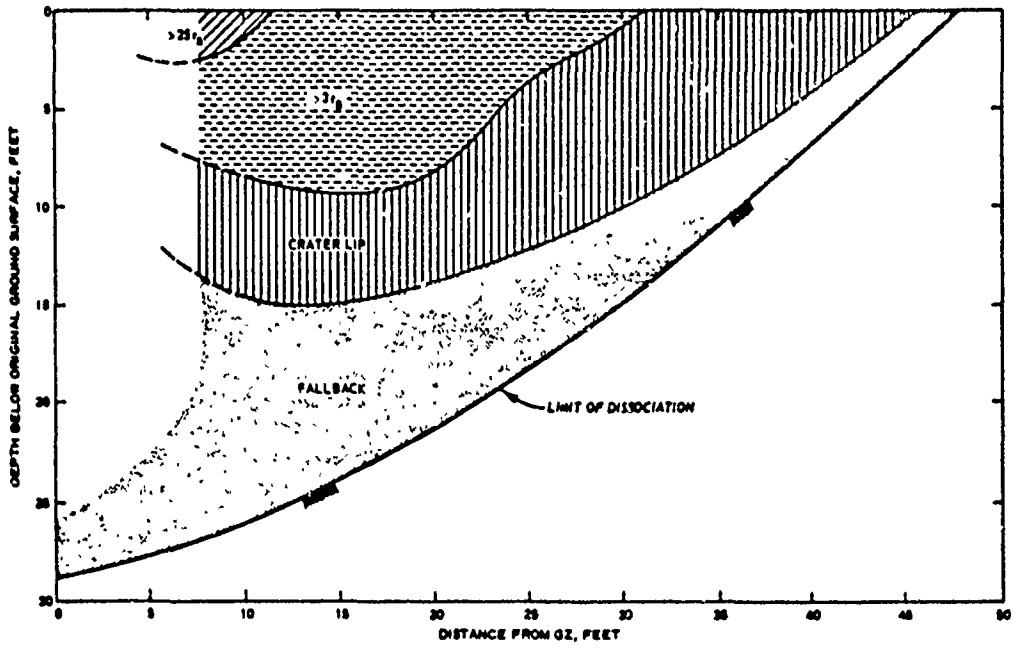

a. Buried detonation (20 tons)

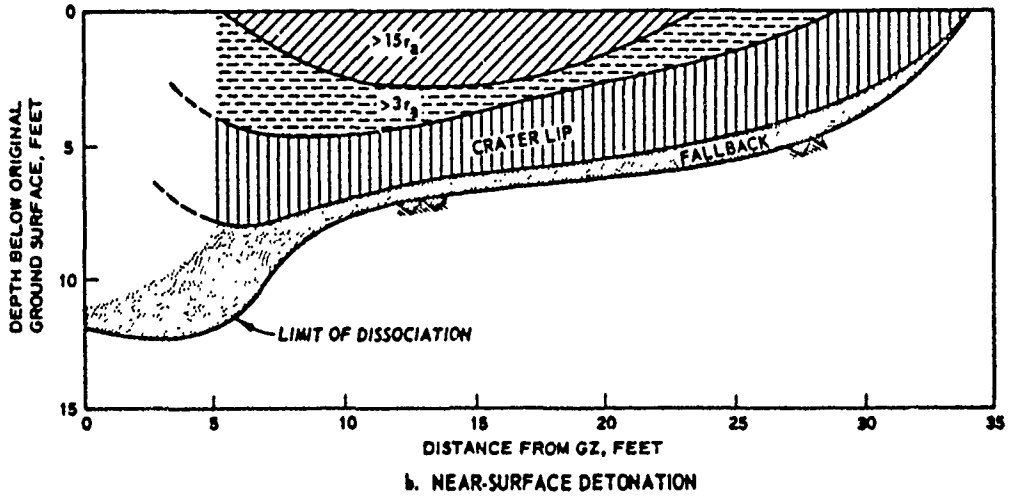

b. Near-surface detonation (100 tons)

Figure 5.4 Ejecta origins and relative ranges for HE detonations.

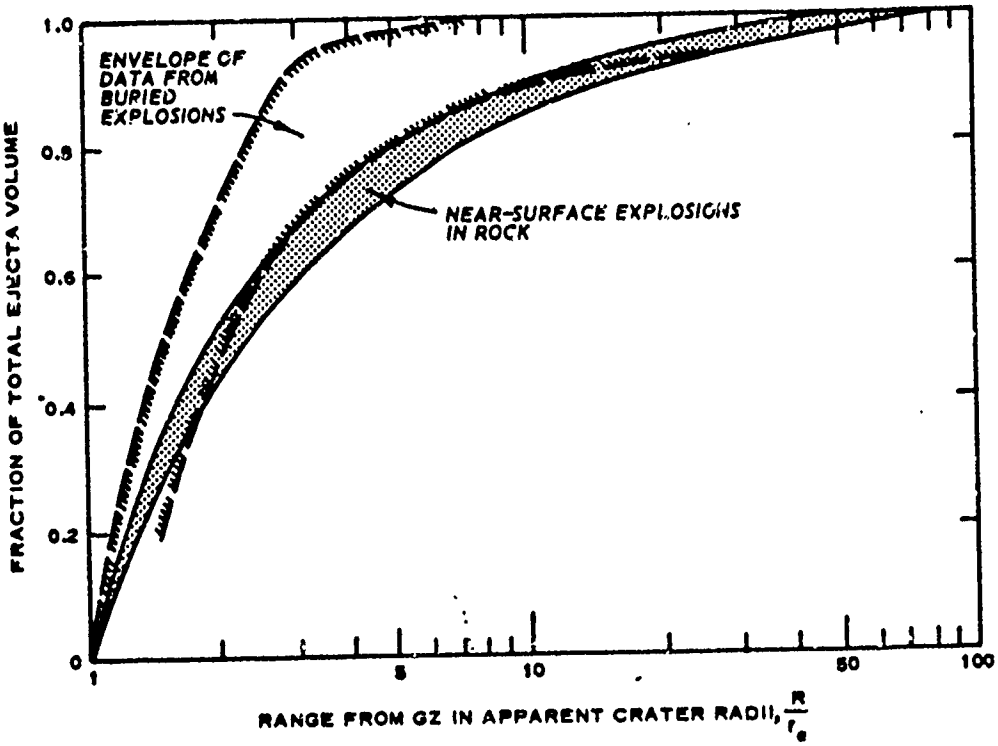

Figure 5.5 Fraction of total ejecta volume as a function of range from GZ.

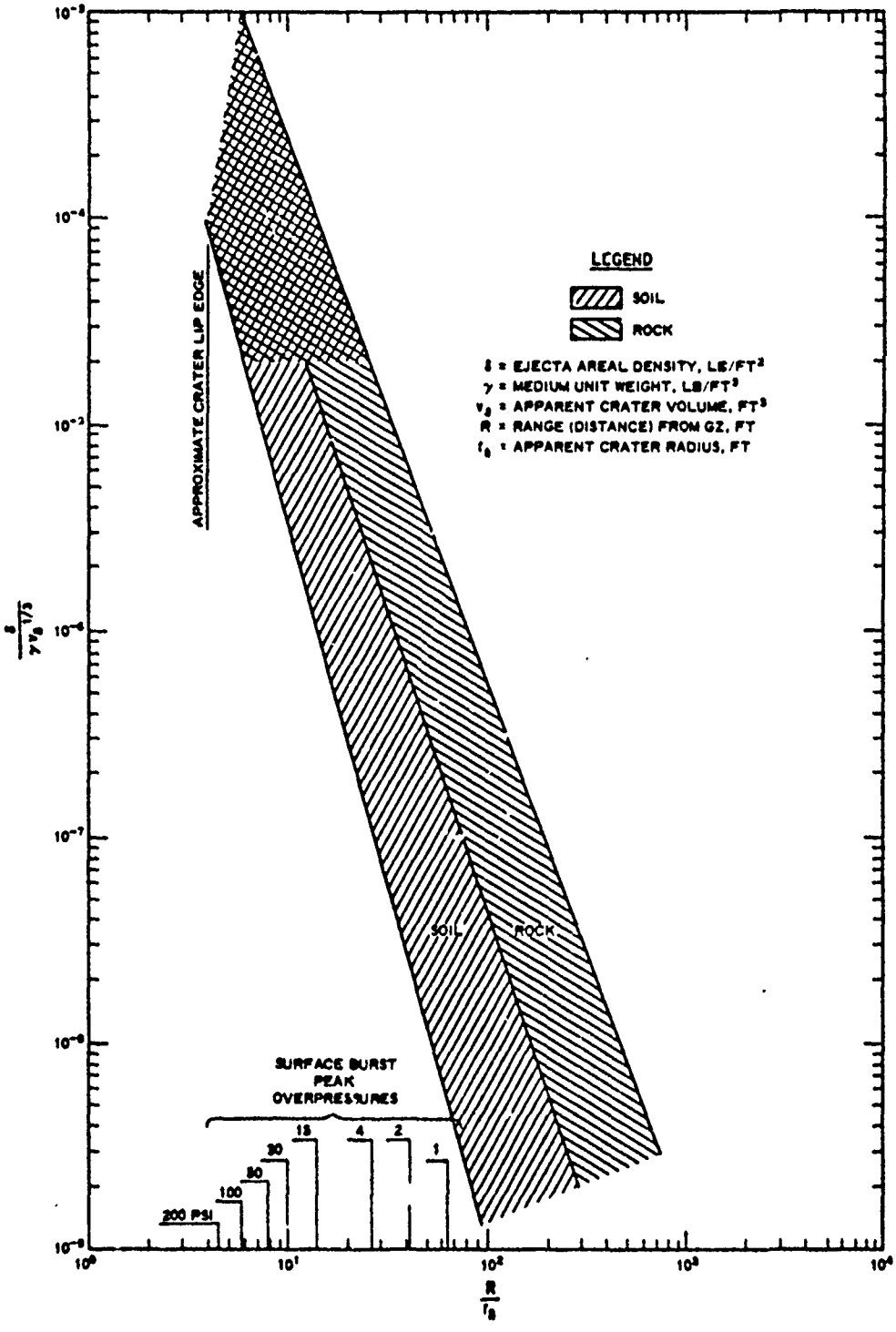

Figure 5.6 Dimensionless plot of ejecta mass density as a function of range expressed as multiples of the apparent crater radius.

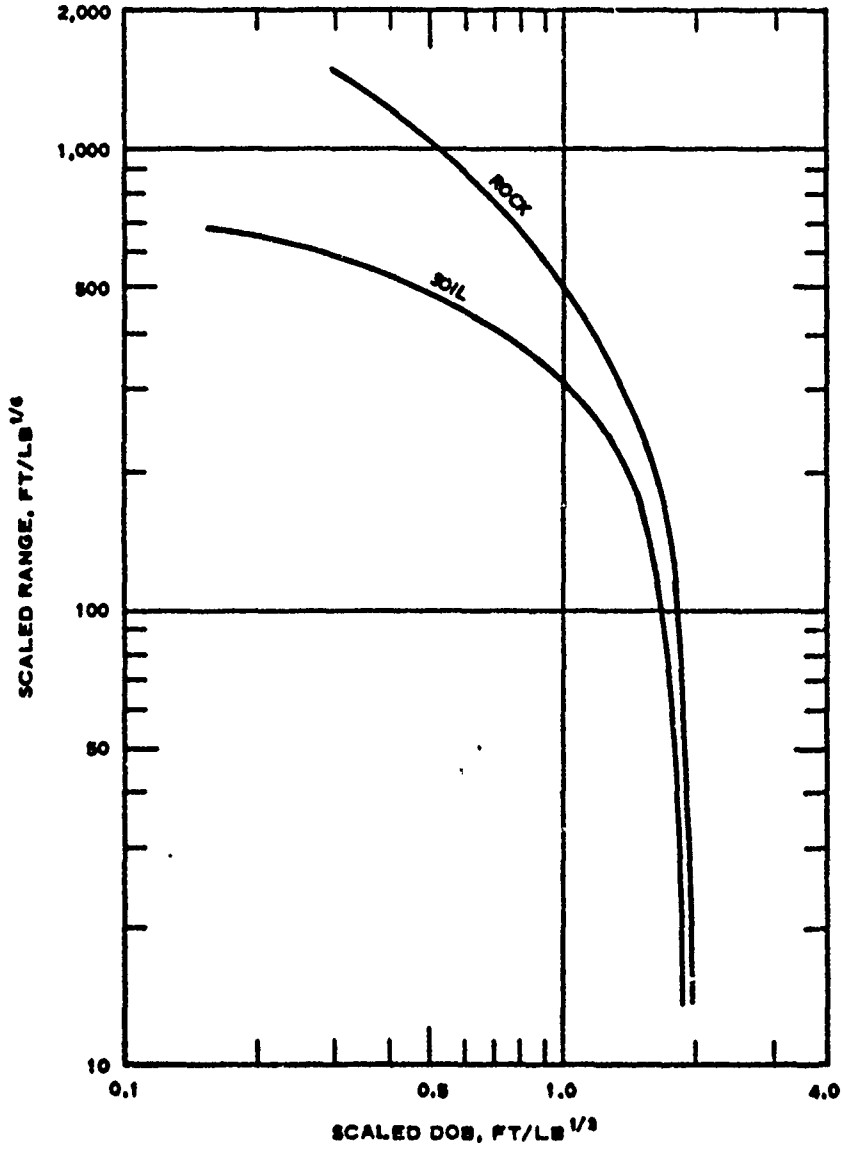

Figure 5.7 Maximum missile range for buried charges.

CHAPTER 6

EFFECTS OF VARIATION IN SHOT GEOMETRIES

6.1 MULTIPLE-EXPLOSION ARRAYS

Weapons or munitions may be detonated in close proximity to one another for the purpose of creating military obstacles or for excavation purposes (Figure 6.1). When the detonations are simultaneous and sufficiently close to permit interaction between charges, the shot geometry is herein termed "multiple explosion." A linear array of this nature is termed a "row shot," and the resulting crater is referred to as a "row crater" or a "channel." The channel may also result from two or more connecting row shots. The row-shot geometry has been the object of widespread research, due to its numerous possible military and civil applications. Multiple-explosion arrays may also be tailored to other, less common purposes, however, and may be nonlinear and/or detonated in varying sequences. A portion of the Bibliography is devoted to this general cratering application.

6.1.1 Row Craters. In addition to the cratering variables discussed in Chapters 3 and 4, row shots are dependent upon the spacing between charges and the degree of simultaneity of detonation. Significant departure from detonation simultaneity may degrade row-charge crater dimensions. Close spacings of charges (less than 1.4 single-charge crater radii) enhance both crater radius and depth, as compared to single craters at the same scaled DOB. Figure 6.2 shows the enhancement of single-charge crater dimensions obtained by reducing the spacing between charges in a row charge at optimum DOB. As the charge spacing decreases, the optimum DOB for each charge must be increased by the enhancement factor. The length L of a row crater can be found from the equation

$$L = s(N - 1) + 2r_a \qquad (6.1)$$

Where: N = the number of charges in the row

s = charge spacing

Spacings of about $3r_a$ in soil and up to $4r_a$ in rock may produce satisfactory linear obstacles, since the crater lip is part of the obstacle.

6.1.2 Other Multiple-Explosion Arrays. As explained in Chapter 2, a variety of geometries has been studied, mostly in granular soil, for specific applications of multiple-explosion arrays. These have included nonlinear arrays, adjacent row shots fired simultaneously and in varying sequences, and "multiple-pass" geometries, wherein row charges are fired beneath channels created by preceding row shots. The applications include explosively formed earth dams, overburden removal, and the shaping of row-shot channels to certain specifications. Since these applications are quite specialized, no attempt will be made in this report to discuss them further. Those having such an interest should consult the Bibliography.

6.2 CHARGE STEMMING

"Stemming" refers to the backfilling of material in the charge-emplacement hole. Ideally, charges should be completely stemmed and tamped to a density equal to that of the parent material to insure that the explosive provides the maximum in cratering performance. There are, however, occasional requirements, mostly military, that stemming be reduced or that its emplacement and removal be expedited. Thus, some attention has been given to the effects on crater dimensions of various sizes of emplacement holes with different depths of stemming and with different stemming materials, including water. Based on HE experiments, it has been concluded that stemming does little to increase crater diameter, which is generally the dimension of greatest military importance. Stemming of about one-half the emplacement-hole depth (50 percent stemming) provides most of the crater depth which would be expected from a fully stemmed charge. Water appears to be an efficient stemming material. Figure 6.3 illustrates the small-scale experimental results, as compiled in Reference 8.

6.3 UNDERWATER CRATERING

A limited amount of experimentation has been devoted to cratering underwater. With one exception known to the authors, all such experiments within the time frame of consideration in this report have involved charges resting on or only partially buried beneath the earth-water interface. The exception is Project Tugboat (by EERL), for which both small and large HE tests of buried charges have been conducted. The goal of this study is a light-draft harbor at Kawaihae on the island of Hawaii.

Reference 9, which is included in the Bibliography on this subject, is in itself a compendium on underwater cratering preceding Tugboat. Data from a number of tests are compiled, interpreted, and analyzed in this reference. In addition to single charges, limited data are included on row and "nail-driving" detonations (see Section 6.6). The data from the single-charge experiments are included in Figure 6.4, scaled to the 1-ton yield level. In general, both row and nail-driving experience parallels that for land craters, with allowances made for differences in single-charge crater shapes and sizes.

Two additional 5-ton TNT charges fired at Mono Lake, California, in 1966 resulted in underwater mounds rather than craters. Due to the anomalous, unexplained results, these shots were not included in Reference 9. Also, a small quantity of old, formerly classified data has recently been located, and this may be included in future analyses.

6.4 DEEPLY BURIED EXPLOSIONS

The cratering effects of explosive charges buried deeper than optimum DOB are illustrated in Appendix A and in Figures 4.1 through 4.19. A continued increase in DOB will result in a smaller apparent crater, although true crater dimensions will continue to increase. At some DOB, the apparent crater will cease to be evident, or may (especially in cohesive material) result in a mound due to heaving and/or bulking action. Essentially, this is the containment DOB. Below this depth, a camouflet, or underground cavity, is formed. The true crater no longer intersects the surface, but is coincident with the camouflet, with concentric zones

of deformation. These conditions are illustrated in Figure 4.22.

Approximate containment depths may be extrapolated from the figures of Chapter 4 in terms of $DOB/W^{1/3}$. The depth of containment was reported in Reference 2 as about 3.5 $ft/lb^{1/3}$. Cavity radii are approximately 1.2 $ft/lb^{1/3}$ for HE charges, or about 47 $ft/kt^{1/3}$ for NE, as taken from reports on a number of nuclear experiments. For HE, an empirical equation which considers DOB is

$$r_c \approx \frac{1.25W^{2/3}}{DOB} \qquad (6.2)\ \text{(Reference 10)}$$

More accurate calculations for NE, which take into account the effects of medium properties and DOB, provide the equation

$$r_c = C\,\frac{W^{1/3}}{(\rho Z)^{\alpha}} \qquad (6.3)\ \text{(Reference 11)}$$

Where: C = an observed cavity proportionality constant

α = an exponent based on the adiabatic (gas) expansion coefficient

Other terms are as previously defined in the text or Figure 1.2. The explosion gases are, of course, formed by vaporization of the medium. Figure 6.5 shows values of α as a function of water content, and assumed values of α, ρ, and C are shown below for several rock media.

Medium	α	ρ	C
		gm/cm^3	
Granite	0.324	2.7	103
Tuff	0.292	1.9	97
Alluvium	0.296	1.9	89
Salt	0.311	2.3	96
Dolomite	0.329	2.3	89

To use Equation 6.3, enter W in kilotons and Z in meters; cavity radius r_c will be found in meters.

In desert alluvium, subsidence craters have been experienced for large yields fired below containment depths. This action, which may take place over several days, results from the subsidence of overlying soil into the cavity formed by the explosion. Characteristically, these craters are wide and shallow. In view of the uncertainties associated with their formation, no prediction techniques appear applicable.

6.5 BOMB/SHELL CRATERS

As indicated in Chapter 2, cratering by conventional bombs has long been of interest to the military. Recently, limited cratering tests have been conducted with artillery and mortar shells in connection with the design of protective structures. It does not appear sufficient to predict bomb/shell crater dimensions from those formed by bare charges equivalent in yield to the bomb or shell filler material, even though it may be argued that explosive energy lost in rupturing the case is regained in kinetic energy of the fragments. The explosive filler material is usually cast in a cylindrical configuration, and detonation is usually initiated in the nose or tail of the warhead; these considerations also fail to answer completely the questions raised over differences in craters.

The limited study which has been done on this subject indicates that deeply buried bombs produce craters smaller in radius but larger in depth than do comparable bare charges. There do not seem to be sufficient data on shallowly buried bombs to permit conclusions. Experience with mortar and artillery shells, which contain a proportionately heavier casing, indicates that near-surface (fuze quick) bursts form craters which are somewhat larger than those of bare charges. Unfortunately, a complete resolution of the problem is hampered by lack of definitive test data. Figure 6.6 shows general bomb-data trends, and may be compared with spherical-charge curves in Appendix B.

6.6 SUCCESSIVE SHOTS ON A VERTICAL AXIS

Some interest has been shown in the craters produced by a series of surface or near-surface explosions, each detonation (after the first) occurring in the center of the crater left by the preceding shot. This technique, known as nail driving, may represent a means of attacking deeply buried, hardened structures. The results of several experiments conducted in granular and clayey soils and in competent rock are shown by envelopes of data in Figures 6.7 and 6.8. Although there is considerable scatter in the data, the envelopes approximate the expected increases in crater dimensions, and also show the general differences to be expected in soil and rock.

(Courtesy of Lawrence Radiation Laboratory and U. S. Atomic Energy Commission)

Figure 6.1 Project Dugout, a row crater 135 feet wide, 35 feet deep, and 285 feet long, formed by the detonation of five 20-ton HE charges at near-optimum DOB.

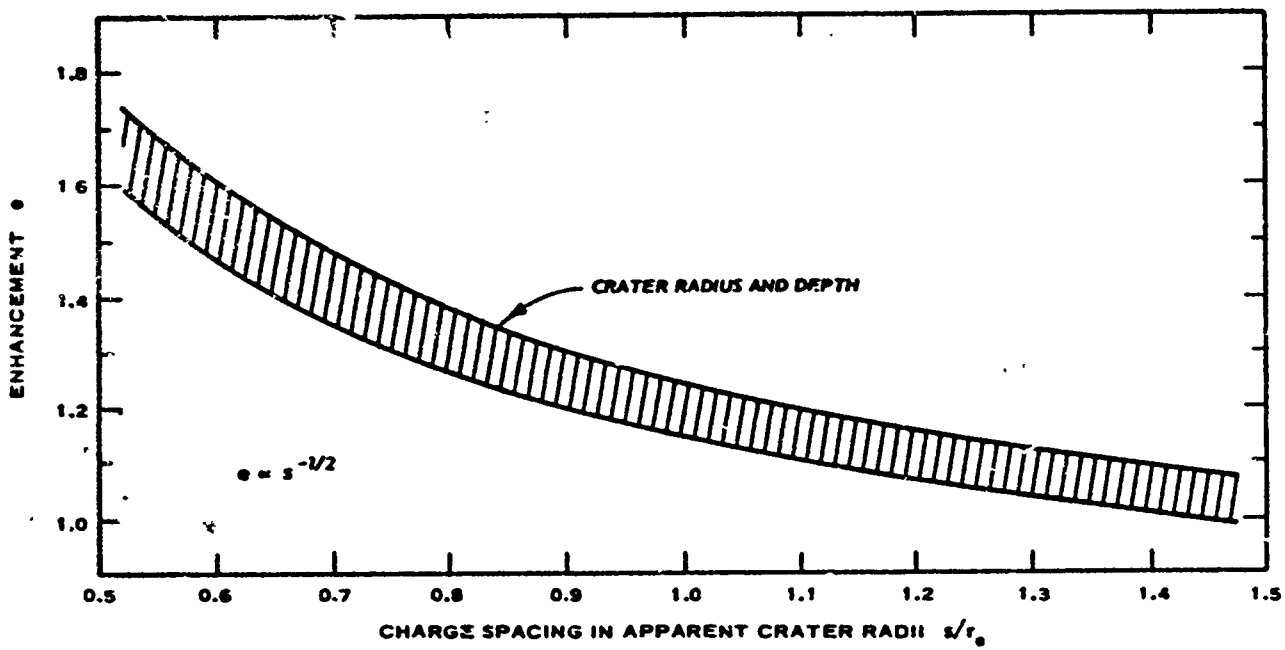

Figure 6.2 Enhancement of single-charge apparent crater dimensions in a row crater as a function of charge spacing at optimum DOB in soil (Reference 12). Hatchured area shows approximate variation in data.

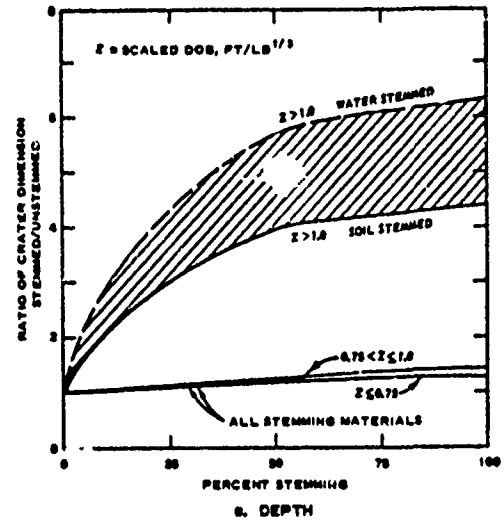

a. DEPTH

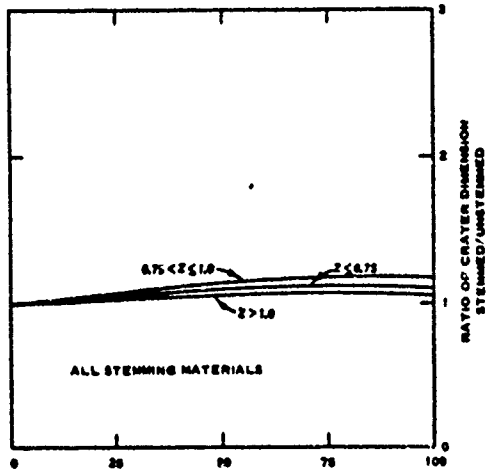

b. DIAMETER

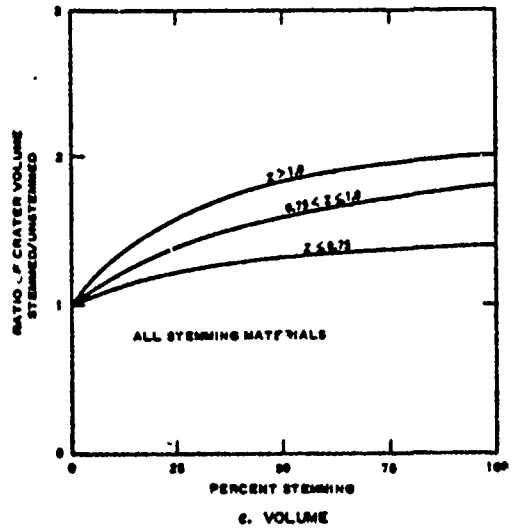

c. VOLUME

Figure 6.3 Increase in HE crater dimensions as functions of stemming and DOB.

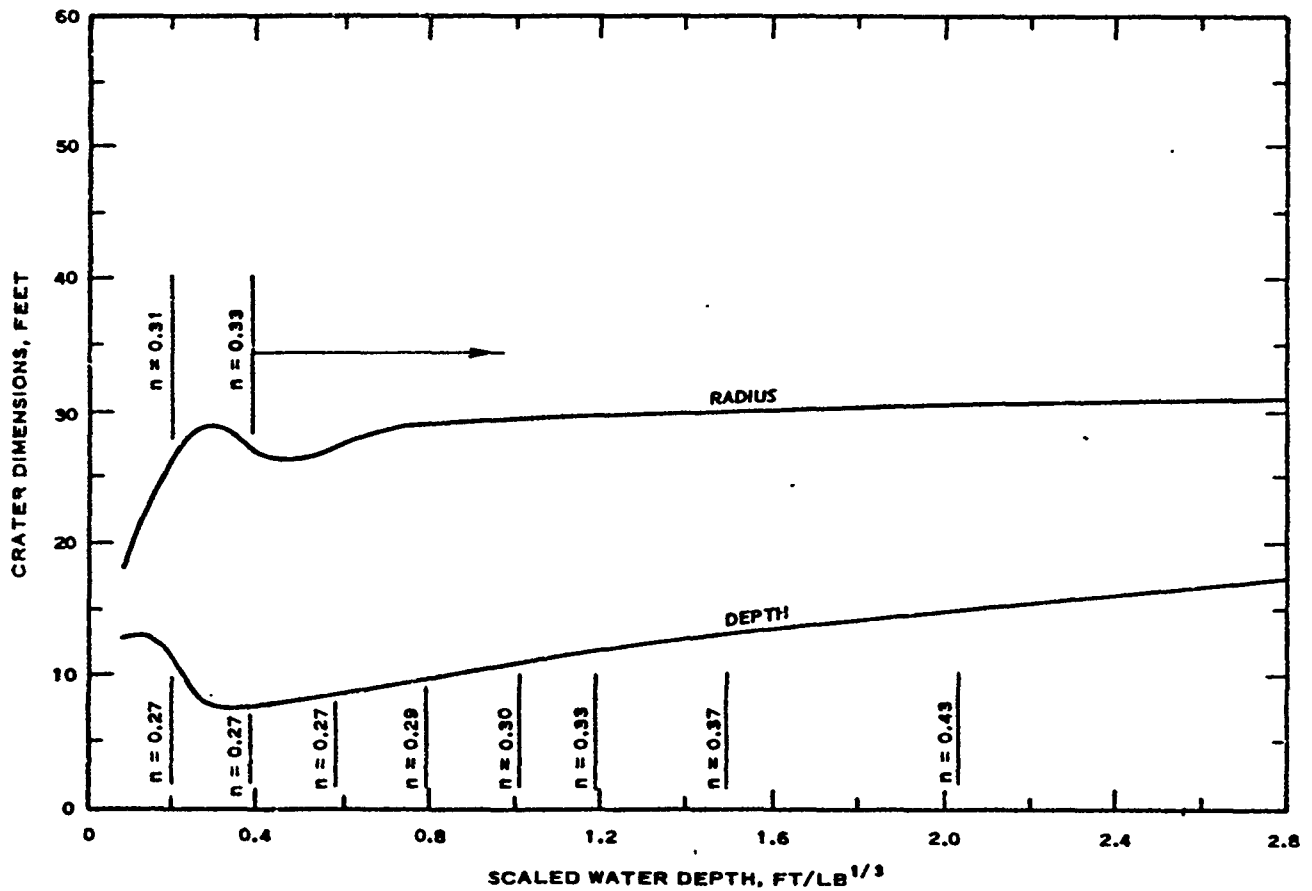

Figure 6.4 Apparent dimensions of underwater craters from 1-ton charges fired at the earth-water interface in a variety of fine-grained materials. Anomalous appearance of curves in very shallow water (left side of graph) is attributed to washback effect, in which ejected material is carried back into crater.

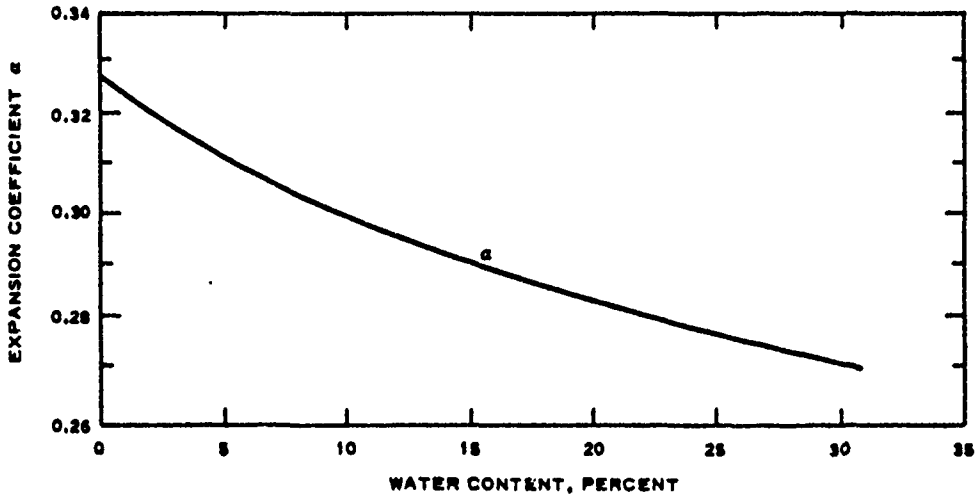

Figure 6.5 Adiabatic expansion coefficient α as a function of medium's moisture content (Reference 11).

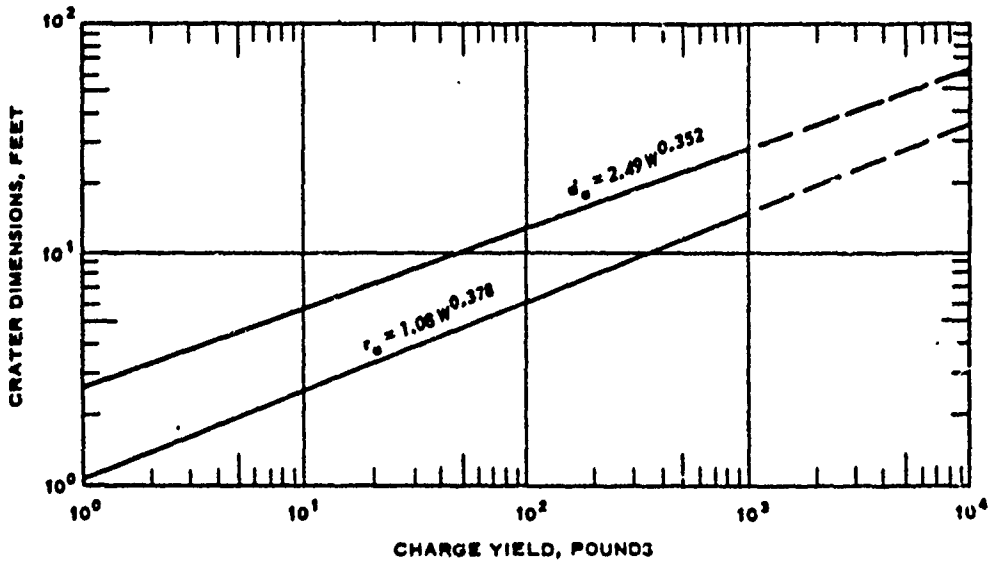

Figure 6.6 Apparent crater dimensions for deeply buried bomb explosions.

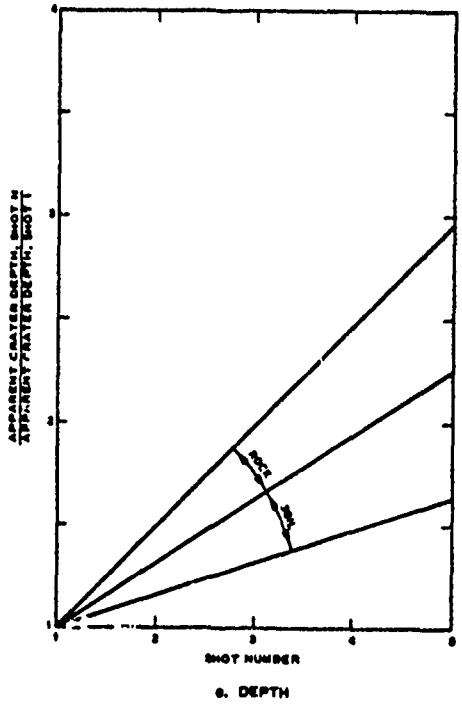

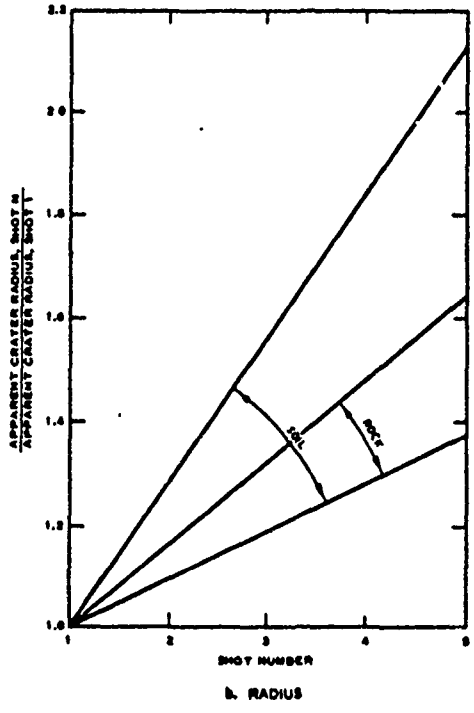

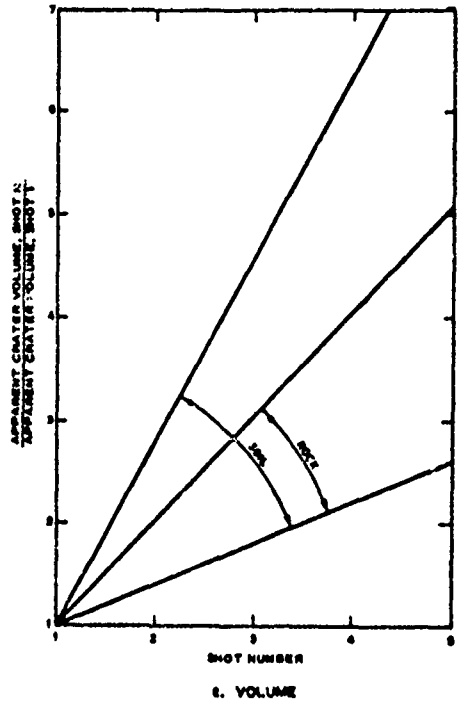

Figure 6.7 Increase in apparent crater dimensions for nail-driving experiments.

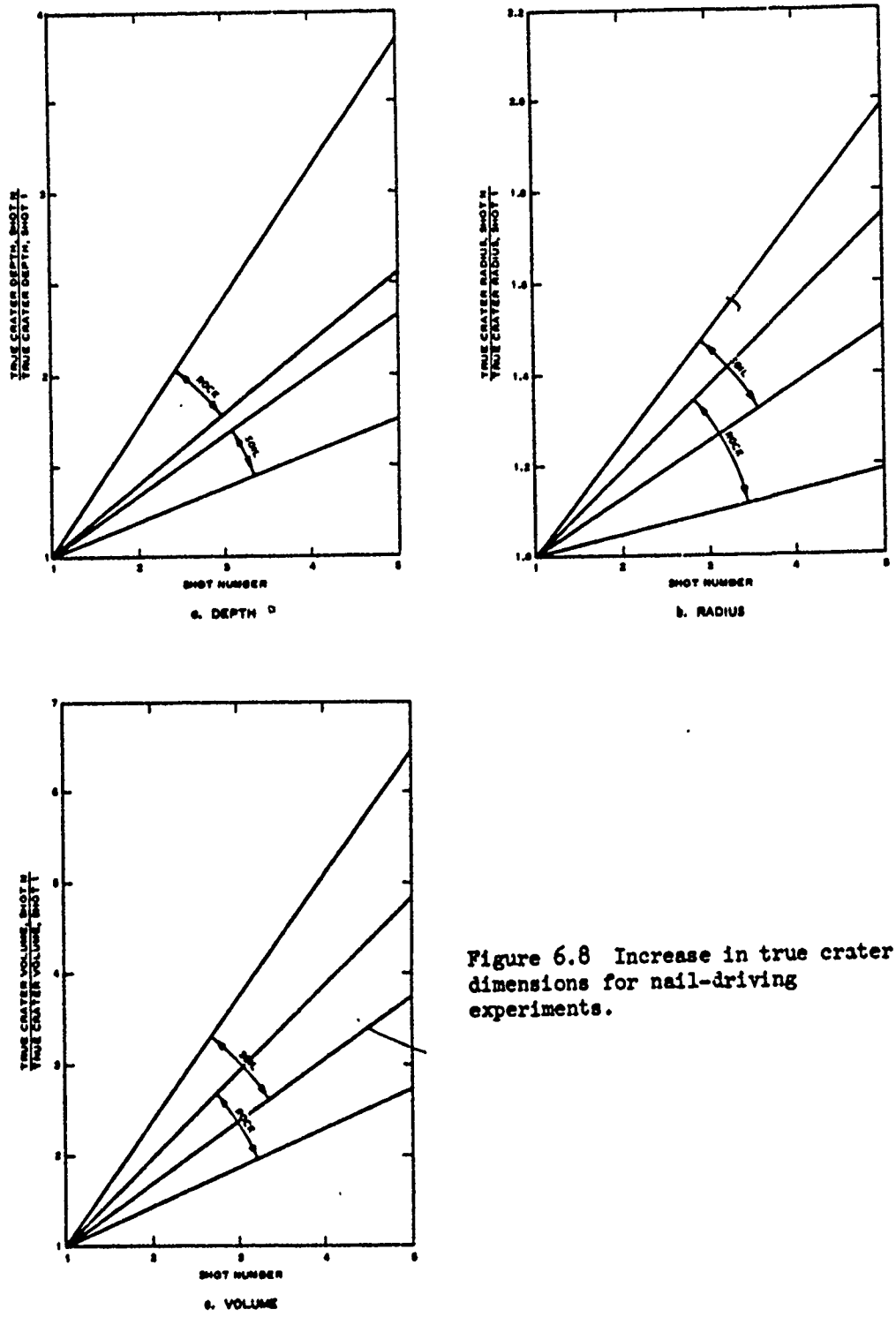

Figure 6.8 Increase in true crater dimensions for nail-driving experiments.

CHAPTER 7

ENVIRONMENTAL INFLUENCES

The graphs in Appendix B and Chapter 4 are based primarily on tests conducted in relatively homogeneous, isotropic media. In many situations, however, it may be necessary to detonate explosives in a medium containing some environmental anomaly, such as a water table at a shallow depth, a layering of one type of soil over another, parallel planes of distinct jointing in rock, or a steeply sloping ground surface. All of these factors can influence the formation of a crater and, in some cases, radically change its size or characteristics.

7.1 SLOPING TOPOGRAPHY

Terrain slopes of about 5 degrees or greater will affect crater formation for a surface explosion, the venting process for a buried explosion, and ejecta distribution in any case. For gentle slopes, the total volumetric effects will be about the same as for craters on level ground, but the resulting crater will be asymmetrical, wider up-slope and with a larger lip down-slope (Figure 7.1). For the field of discrete ejecta particles, greater maximum ranges will occur down-slope, assuming that the wind is not a significant factor.

Limited small-scale cratering experiments have been conducted in moist, sandy soil and in desert alluvium on slopes ranging from 40 degrees to vertical wedges, the latter representing the extreme in sloping topography. For charges buried on severe but nonvertical slopes, with DOB measured from the sloping surface and with the vertical depth of overburden being greater than containment depth, crater dimensions decrease with increasing slope. Optimum vertical DOB and optimum distance from the free, vertical face of a wedge appear roughly the same, and perhaps larger by about one-third than optimum DOB on level terrain. For this geometry, ejecta distribution is preponderantly directed toward the free face, with about three-fourths of the total ejecta mass falling in this direction when DOB is optimum for crater volume. The disparity in ejecta distribution increases with further increase in DOB.

7.2 LAYERED SYSTEMS

7.2.1 Water Tables. Based upon HE experiments, a subsurface water table in a soil medium will begin to influence the size and shape of the crater when its depth below the surface is equal to or less than three-fourths the predicted apparent crater radius. Its effect is to flatten and widen the crater. As the water table depth decreases, its effect becomes more evident; for a water table depth of one-fourth to one-fifth the original predicted crater radius, the final radius may be as much as 50 percent greater than and the depth as little as one-third that of the original predicted value.

7.2.2 Bedrock. The influence of a bedrock layer below a soil medium is similar to that of a water table, though somewhat less pronounced. For HE explosions at the surface, the bedrock layer may increase the crater radius slightly (5-10 percent), and may decrease the final depth by as much as one-third when the overburden layer is as shallow as one-fourth the predicted apparent crater radius.

7.2.3 Rock Bedding/Jointing. For low-yield NE and high-yield HE explosions at or very near the surface, the bedding or jointing planes in rock can influence the shape of the crater produced, as well as the direction of the ejection process. The formation of the crater will tend to follow the direction of the predominant joints, thus increasing the crater radius by as much as one-third in the direction parallel to the joints, or decreasing it by as much as one-third normal to the joints. The magnitude of the crater depth is usually not affected significantly, but the deepest point may be shifted to one side of the crater. As yield or DOB is increased, the influence of rock jointing is reduced.

The dip of bedding planes will influence energy propagation, causing the maximum crater depth to be offset in the down-dip direction. Little overall effect is noted in regard to crater radius, but differences in ejection angles cause the maximum lip height and ejecta radius to occur down-dip.

7.3 SNOW AND ICE

Measured craters in snow or ice are a rarity, and for this reason are presented separate from the more general data of Appendix B and Chapter 4. A few craters have been recorded for surface HE explosions in snow/ice; these are larger than craters in soil, and are characteristically wide and flat. Figure 7.2 shows trends in crater size and shape for a surface-burst geometry in this medium.

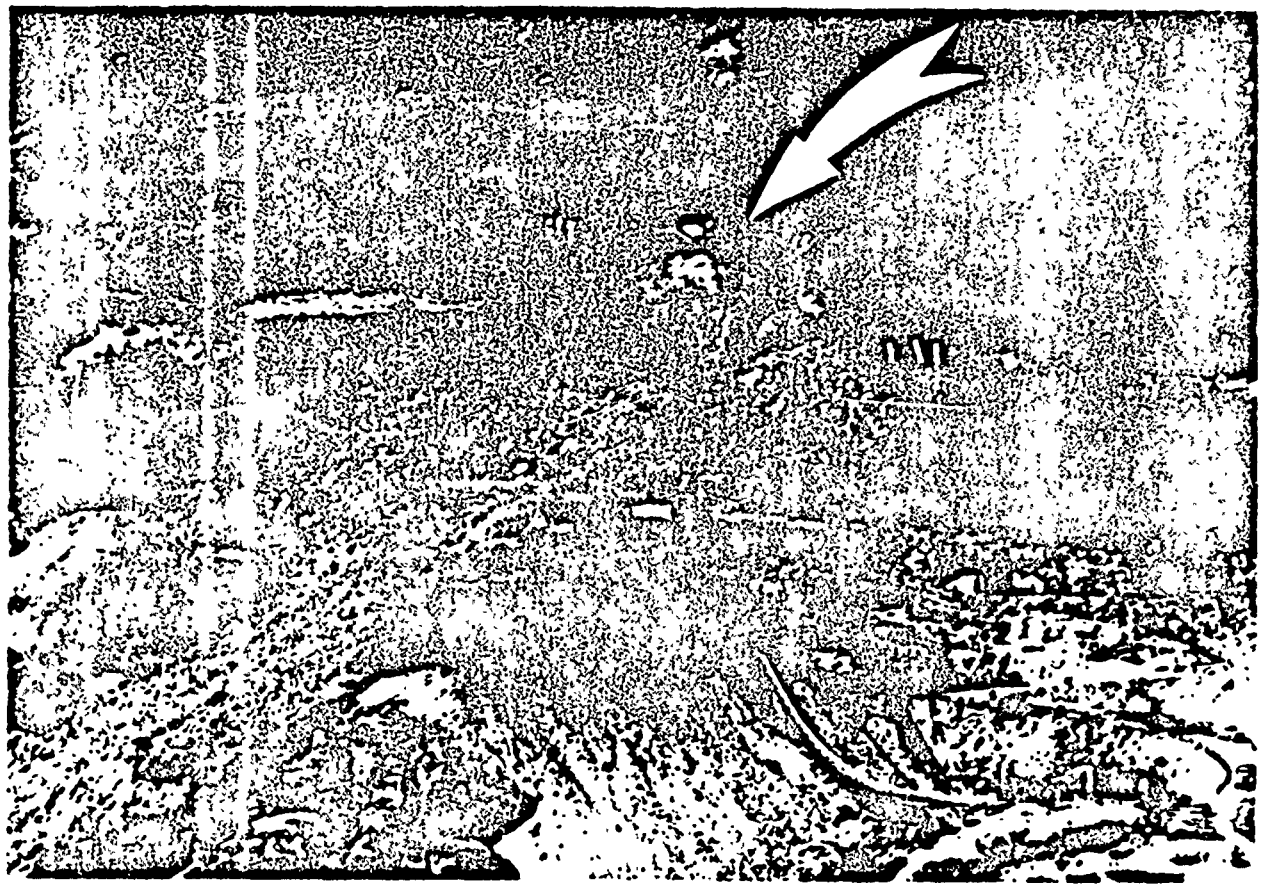

(Courtesy of Lawrence Radiation Laboratory and U. S. Atomic Energy Commission)

Figure 7.1 Crater (arrow) and crater lip formed in sloping terrain.

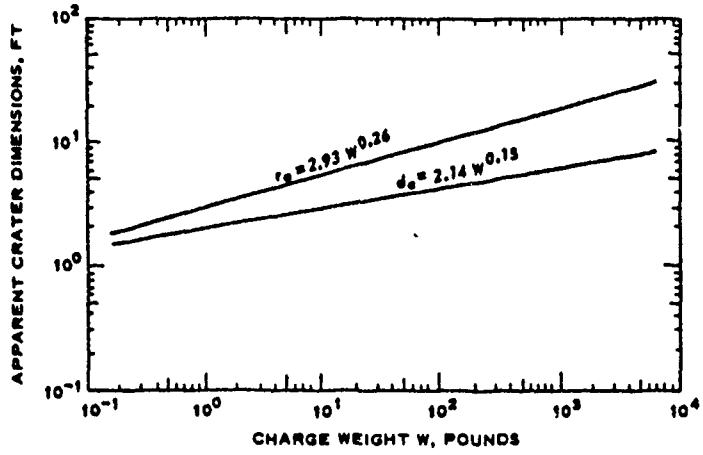

a. APPARENT CRATER RADIUS AND DEPTH

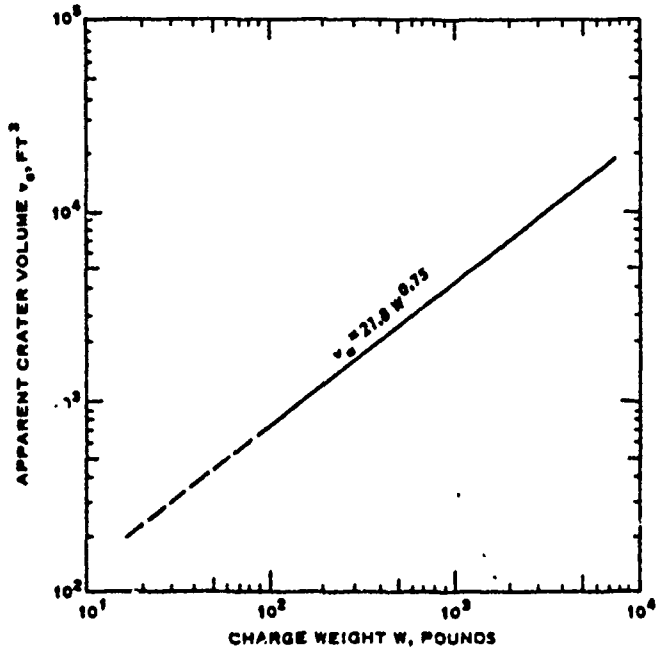

b. APPARENT CRATER VOLUME

Figure 7.2 Crater dimensions for surface detonations in snow and ice.

CHAPTER 8

SUMMARY AND RECOMMENDATIONS

8.1 SUMMARY

The foregoing chapters have presented a brief history of cratering research and a compilation of HE and NE crater data. An attempt has been made to sort these data in such a fashion as to identify the significant variables affecting crater size, and an analysis has been conducted to provide the tools necessary for crater predictions. Variations in crater shapes and sizes due to departures from the usual test geometries or to unusual environmental conditions have been discussed. Phenomena associated with debris ejection from the crater have also been examined briefly. The result is a series of graphs from which crater parameters may be read directly (Appendix B) or from which data trends can be identified (Chapters 4 and 5), and to which certain judgment factors can be applied for practical usage.

8.2 RECOMMENDATIONS

The report has been prepared in a manner to facilitate the addition of crater data by the user. It is recommended that a formal updating be accomplished on a periodic basis--say, biennially or triennially--to insure maximum use of new data as it becomes available. With the data retrieval and computerized plotting system which has been established, this could be done without great effort. For the more specialized crater applications (e.g., multiple-charge arrays, cratering on slopes), such a periodic updating would help fill serious gaps in the existing data. To aid in updating, users are urged to submit suggestions and corrections which they feel are appropriate.

A crater/ejecta study should be a part of every experimental plan, and especially so for tests involving NE ~ large HE yields. In the past, where this has been overlooked or neglected, the result has been the loss of data needed at some later time. In general, the area in which crater data are most needed is that of large yields in clays and

silts and mixtures thereof which probably represent the major portion of the earth's soils. More information is needed on cratering in layered systems, also, to insure proper application of available data to practical problems. True crater dimensions and zones of subsurface deformation, often omitted from explosion test research, should be measured wherever possible. These data are important not only in the prediction of damage to underground structures, but also in the formulation of volumetric and mass-balance equations, as well as in formulating expressions for basic cratering mechanisms. Accurate volumetric data, particularly of true craters, are valuable for normalizing certain other energy input phenomena, e.g. ground motion, cratering efficiency, etc. Finally, every available opportunity to study the phenomenon of crater ejecta should be explcited, since it is the damage mechanism in cratering which is potentially the most far reaching. Considerable research is needed to accurately quantify the parameters discussed in Chapter 5.

APPENDIX A

TABULATION OF CRATER DATA

This appendix contains the data tabulation (Tables A.1 through A.14) introduced in Section 3.3. All but Table A.14 are reproductions of computer printouts, the program for which is contained in Appendix D. Explanatory material, also included in the program, is reproduced below.

IDENTIFICATION OF CODES AND VARIABLES

STC	Operation Stagecoach
RRV	Railroad Vulnerability Program
SES	Cratering by Ground Burst at Suffield Experimental Station
SCH	Project Schooner
PB	Project Pre-Buggy
AV	Air Vent Cratering Series
MS C	Mine Shaft - Calibration Cratering Series
MS I-MO	Mine Shaft I - Mine Ore
MS I-MU	Mine Shaft I - Mine Under
MS II-MR	Mine Shaft II - Mineral Rock
BKBD	Operation Buckboard
SC II	Sandia Corporation Cratering Series II
SC I	Sandia Corporation Cratering Series I
MTCE	Multiple Threat Cratering Experiment
DB	Project Danny Boy
DP	Operation Distant Plain
TPOTS	Teapot Ess
PAL	Palanquin
FT	Flat Top
STAMS	Simulation Tests of Artillery and Mortar Shell Explosions
J,JS,JU	Operation Jangle
CSM	Colorado School of Mines, Underground Explosion Test Program
UETP	Underground Explosion Test Program
USSC	Cratering in Sand from Spherical Charges

EUE	Effects of Underground Explosions
FCBT	Fort Churchill Blast Tests
MOLE	Small Explosion Tests, Project Mole
CESBC	Cratering Effects of Surface and Buried HE Charges
CDS	Cratering in Dry Sand
ESRIC	Effects of a Soil-Rock Interface on Cratering
SEU	Effects of Stemming on Underground Explosions
SE	Stemming Effects for Certain HE Charges
PCE	Energy Partitioning for Partially Confined Explosions
ICSBA	Cratering Tests in Basalt - Inter-Oceanic Canal Study
ICSCC	Cratering Tests in Cucaracha Culebra - Inter-Oceanic Canal Study
ICSGS	Cratering Tests in Gatun Sandstone - Inter-Oceanic Canal Study
ICSMM	Cratering Tests in Marine Muck - Inter-Oceanic Canal Study
ICSRC	Cratering Tests in Residual Clay - Inter-Oceanic Canal Study
FICS	Investigation of Charge Shape at Ft. Churchill
SRI	Crater Study, Operation Castle, Stanford Research Institute
ANC	Ammonium Nitrate Cratering
RUS	Russian Nuclear Event
PG	Project Pre-Gondola
NEP	Project Neptune
TRIN	Project Trinidad
JJ	WES Stemming Series
PF	Operation Prairie Flat
SEDAN	Operation Sedan
SL	Sandia Laboratories Series
ZUL	Project Zulu
DIAL	Operation Dial Pack

MEDIUM CODE

Concrete or Grout	0
Hard Rock-Granite, Basalt, Limestone, Etc.	1
Soft Rock-Sandstone, Etc.	2
Very Soft Rock or Very Hard Soil - Shale, Tuff, Frozen Soil	3
Clay	4
Silty Clay	6
Loess and Lacustrine Silt	5
Silt, Sand, and Clay	7
Silty Sand and Desert Alluvium	8
Sand	9

MOISTURE CODE

Completely Dry	0
Very Dry	1
Dry	2
Slightly Moist	3
Moist	4
Very Moist	5
Slightly Wet	6
Wet	7
Very Wet	8
Saturated	9

EXPLOSIVE CODE

Nuclear	0
TNT	1
C-4, C-3	2
Pentolite	3
Ammonium Nitrate - Slurry or Grains	4

Nitromethane. 5
Dynamite. 6
Amatol. 7
C-3 and Tetrytal. 8

CRATER SHAPE CODE

0-Unknown

(Continued)

CRATER SHAPE CODE (Continued)

1-STANDARD

2-HYPERBOLIC

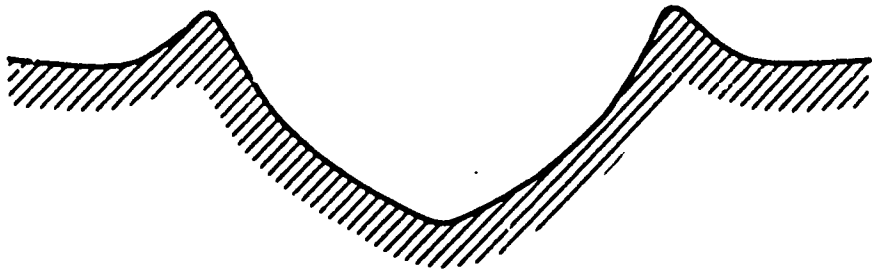

3-SHALLOW PARABOLA

4-SOMBRERO

5-LONGHORN

(Continued)

CRATER SHAPE CODE (Concluded)

6-PAN

7-CONE

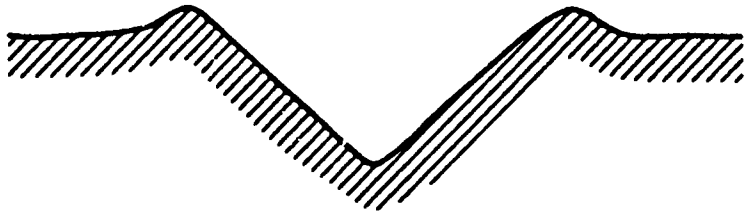

8-HALF-EGG OFFSET

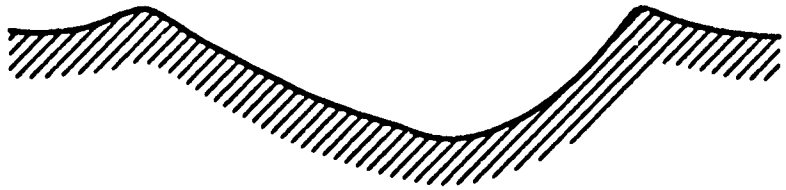

9-MOUND

TABLE A.1 CRATER DATA FOR BASALT AND GRANITE

Shot Identification	Bibliography Number	Charge Yield (TNT-Equivalent)	Type of Explosive	Moisture Code	Medium Code	Height of Burst	Scaled Height of Burst $\bar{z}$	Apparent Crater Radius r_a	Apparent Crater Depth d_a	Apparent Crater Lip Height h	Volume of Apparent Crater v_a	True Crater Radius r_t	True Crater Depth d_t	Volume of True Crater v_t	Angle of Crater Slope	Crater Shape Code
		pounds				feet	$ft/lb^{1/3}$	feet	feet	feet	ft^3	feet	feet	ft^3	degrees	
Scaled Height of Burst Greater Than +0.40, Category 1:																
								No Data available								
Scaled Height of Burst Less Than +0.40 and Greater Than +0.20, Category 2:																
HUSH-402	58	32	1	1	1	2.50	0.37	1.2	--	--	--	--	--	--	--	0
Scaled Height of Burst Less Than +0.20 and Greater Than +0.05, Category 3:																
HICE 371	17h	4,000	1	1	1	2.20	0.14	3.7	1.0	0.5	37	--	--	--	--	0
HICE 372A	17h	4,000	1	1	1	2.20	0.14	6.8	1.4	0.9	139	--	--	--	--	0
HICE 372A	17h	4,000	1	1	1	2.20	0.14	4.5	0.9	0.3	35	--	--	--	--	0
HE C 04	41	1,000	1	1	1	1.38	0.13	3.5	0.9	--	--	3.3	1.1	--	--	0
HE C 08	41	1,000	1	1	1	1.21	0.12	4.5	0.9	--	--	4.3	1.5	--	--	0
HE C 05	41	1,000	1	1	1	1.75	0.18	--	--	--	--	2.3	0.1	--	--	0
HE C 06	41	1,000	1	1	1	0.96	0.09	5.0	0.2	--	--	5.2	2.0	--	--	0
HE C 06	41	1,000	1	1	1	1.21	0.12	3.9	0.6	--	--	3.9	1.1	--	--	0
HE C 10	41	1,000	1	1	1	1.68	0.15	2.7	0.1	--	--	2.8	0.8	--	--	0
HE-HD	42	200,000	1	1	1	7.10	0.12	29.0	9.9	2.8	9,800	29.0	11.5	11,000	--	0
HE-HE	43	200,000	1	1	1	7.10	0.12	31.5	9.5	--	8,100	35.5	14.0	15,000	--	0
Scaled Height of Burst Less Than +0.05 and Greater Than -0.05, Category 4:																
ICHA-1A	30	35	1	1	1	0.00	0.00	2.0	0.7	0.2	6	3.1	1.6	29	--	0
ICHA-15A	30	300	1	1	1	0.00	0.00	4.6	1.6	--	49	7.1	3.3	273	--	0
ICHA-16A	30	300	1	1	1	0.00	0.00	4.3	1.2	--	43	7.1	2.6	201	--	0
HICE 81 C1	17h	4,000	1	1	1	0.00	0.00	12.1	3.4	1.2	733	16.0	5.3	2,300	--	0
HICE 82A	17h	4,000	1	1	1	0.00	0.00	10.7	3.9	1.4	672	--	--	--	--	0
HICE 83A	17h	4,000	1	1	1	0.00	0.00	11.4	4.0	1.7	893	--	--	--	--	0
HICE 84A	17h	4,000	1	1	1	0.00	0.00	10.4	3.1	1.4	625	--	--	--	--	0
HICE 1A	17h	16,000	1	1	1	0.00	0.00	18.7	5.4	1.8	3,672	23.5	9.1	7,587	--	0
HUSH-408	58	320	1	1	1	0.00	0.00	--	--	--	--	8.4	1.7	169	--	0
PT 1	53	60,000	1	1	1	0.00	0.00	27.0	9.5	3.6	9,990	38.3	10.8	38,300	--	0
HE C 09	41	1,000	1	1	1	0.00	0.00	5.4	1.7	--	--	8.2	3.7	--	--	0
Scaled Height of Burst Less Than -0.05 and Greater Than -0.20, Category 5:																
HICE C2	17h	4,000	1	1	1	-2.20	-0.14	14.0	4.6	1.3	1,500	--	--	--	--	0
HE C 07	41	1,000	1	1	1	-0.50	-0.05	9.4	0.9	--	--	11.1	4.1	--	--	0
Scaled Height of Burst Less Than -0.20 and Greater Than -0.50, Category 6:																
ICHA-17A	30	700	1	1	1	-1.80	-0.21	9.9	1.3	--	43	7.9	3.2	363	--	0
ICHA-18A	30	700	1	1	1	-1.70	-0.21	9.7	1.1	--	31	7.5	4.0	379	--	0
BASH 9	7	1,000	1	1	1	-4.80	-0.68	15.0	7.5	--	1,800	--	--	--	--	0
BASH 10	7	1,000	1	1	1	-4.80	-0.68	14.8	7.0	--	2,660	--	--	--	--	0
CHE II B-9	61	2,460	8	1	1	-1.17	-0.30	--	--	--	--	27.7	9.9	3,199	--	0
CHE II B-1	61	1,080	1	1	1	-3.31	-0.32	--	--	--	--	16.7	6.8	[illegible]	--	0
HUSH-403	58	320	1	1	1	-2.50	-0.37	--	--	--	--	9.7	2.4	[illegible]	--	0
HUSH-407	58	320	1	1	1	-2.50	-0.37	--	--	--	--	14.4	5.3	2,500	--	0
HUSH-411	58	320	1	1	1	-2.50	-0.37	--	--	--	--	13.4	5.0	1,450	--	0
HUSH-408	58	320	1	1	1	-2.50	-0.37	--	--	--	--	14.0	6.6	1,460	--	0
HUSH-409	58	8,160	1	1	1	-5.00	-0.37	--	--	--	--	25.2	10.2	12,320	--	0
HUSH-413	58	8,160	1	1	1	-5.00	-0.37	--	--	--	--	23.1	8.7	8,680	--	0
HUSH-3GE	58	320	1	1	1	-2.50	-0.37	--	--	--	--	8.3	3.9	414	--	0

(Continued)

TABLE A.1 (CONTINUED)

Shot Identification	Bibliography Number	Charge Yield (TNT-Equivalent)	Type of Explosive	Moisture Code	Medium Code	Height of Burst	Scaled Height of Burst $\bar{z}$	Apparent Crater Radius r_a	Apparent Crater Depth d_a	Apparent Crater Lip Height h	Volume of Apparent Crater v_a	True Crater Radius r_t	True Crater Depth d_t	Volume of True Crater v_t	Angle of Crater Slope	Crater Shape Code
		pounds				feet	$ft/lb^{1/3}$	feet	feet	feet	ft^3	feet	feet	ft^3	degrees	
Scaled Height of Burst Less Than -0.90 and Greater Than -0.90, Category 7:																
ICBA-13	20	75	1	1	1	-1.50	-0.51	4.6	1.0	0.3	36	6.0	1.4	104	71	3
MAD 11	7	60,000	1	1	1	-25.50	-0.75	44.7	24.9	3.0	94,200	--	--	--	71	3
CHE 17 C-2	61	320	2	1	1	-4.17	-0.61	--	--	--	--	10.0	5.9	1,261	71	
UNTF-60A	58	320	1	1	1	-5.08	-0.73	--	--	--	--	10.5	3.6	1,236	71	
CHE 11 C-1	61	70.5	1	1	1	-3.46	-0.68	--	--	--	--	8.1	2.4	169	71	
CHE 9-15A	61	100	1	1	1	-3.98	-0.84	--	--	--	--	6.6	4.1	197	71	0
Scaled Height of Burst Less Than -0.90 and Greater Than -1.10, Category 8:																
ICBA-08	20	75	1	1	1	-4.36	-0.95	3.4	0.7	0.4	34	9.9	5.2	478	71	
ICBA-09	20	35	1	1	1	-3.36	-1.03	2.4	1.2	0.3	11	5.3	4.9	178	71	
MAD 6	7	1,000	1	1	1	-9.40	-0.96	10.7	6.4	--	2,000	--	--	--	71	
MAD 9	7	1,000	1	1	1	-9.00	-0.92	12.1	5.8	--	900	--	--	--	71	
CHE A-08	61	9.69	1	1	1	-1.98	-0.93	--	--	--	--	2.6	0.7	5	71	
CHE C-15	61	70.12	1	1	1	-4.12	-1.00	--	--	--	--	11.4	4.3	548	71	
CHE C-16	61	14.18	1	1	1	-2.65	-1.10	--	--	--	--	4.2	2.2	40	71	
UNTF-1.1	58	320	1	1	1	-6.66	-0.96	--	--	--	--	11.2	9.1	2,966	71	
Scaled Height of Burst Less Than -1.10 and Greater Than -2.00, Category 9:																
ICBA-03	20	75	1	1	1	-4.00	-1.42	6.9	3.4	0.4	21	11.8	7.5	1,165	71	
ICBA-01	20	8	1	1	1	-3.36	-1.50	3.2	1.1	0.3	35	8.5	3.8	345	71	
ICBA-06	20	35	1	1	1	-4.36	-1.34	2.9	0.8	0.3	17	7.9	3.4	270	71	
MAD 2	7	1,000	1	1	1	-18.80	-1.89	14.6	1.6	--	65	--	--	--	71	
MAD 3	7	1,000	1	1	1	-14.70	-1.47	15.6	9.2	--	1,800	--	--	--	71	
MAD 7	7	1,000	1	1	1	-18.60	-1.86	12.7	3.8	--	694	--	--	--	71	
MAD 8	7	1,000	1	1	1	-14.70	-1.47	16.9	8.8	--	3,500	--	--	--	71	
MAD 12	7	65,000	1	1	1	-42.73	-1.25	97.0	36.7	3.0	135,000	--	--	--	71	
MAD 13	7	65,000	1	1	1	-48.30	-1.72	96.8	18.2	3.0	23,200	--	--	--	71	
10	39	80,000	0	1	1	-110.00	-1.16	158.2	62.3	25.0	1,500,000	138.2	146.0	1,917,200	71	3
CHE C-10	61	70.12	1	1	1	-4.08	-1.11	--	--	--	--	9.9	4.2	320	71	
CHE C-01	61	10	2	1	1	-2.65	-1.11	--	--	--	--	4.8	3.0	137	71	
CHE 9-22	61	320	2	1	1	-7.10	-1.13	--	--	--	--	16.2	7.5	2,549	71	
CHE C-20	61	1.5	2	1	1	-1.33	-1.15	--	--	--	--	10.5	5.9	684	71	
CHE A-07	61	1.69	1	1	1	-1.46	-1.26	--	--	--	--	2.5	1.3	9	71	
CHE A-04	61	2.2	2	1	1	-1.63	-1.31	--	--	--	--	2.7	1.1	9	71	
CHE C-17	61	70.18	1	1	1	-3.66	-1.25	--	--	--	--	6.8	2.3	114	71	
CHE 9-16	61	50	2	1	1	-3.71	-1.71	--	--	--	--	9.0	3.6	324	71	
CHE A-12	61	18	2	1	1	-3.29	-1.48	--	--	--	--	8.1	2.8	179	71	
CHE 7-15-4	61	3	2	1	1	-1.98	-1.78	--	--	--	--	10.3	3.0	321	71	
CHE A-14	61	4.5	2	1	1	-2.18	-1.32	--	--	--	--	3.5	1.6	21	71	
CHE 9-21	61	214	2	1	1	-8.15	-1.96	--	--	--	--	11.9	8.1	1,206	71	
CHE A-16	61	8.1	2	1	1	-2.80	-1.57	--	--	--	--	6.6	2.7	156	71	
CHE A-11	61	10.13	1	1	1	-3.20	-1.48	--	--	--	--	6.5	1.6	91	71	
CHE C-18	61	80.18	1	1	1	-5.08	-1.48	--	--	--	--	7.3	2.9	169	71	
CHE A-03	61	20	2	1	1	-4.04	-1.49	--	--	--	--	9.3	3.0	194	71	
CHE C-07	61	45	2	1	1	-5.34	-1.50	--	--	--	--	7.5	2.8	169	71	
CHE A-17	61	1.18	1	1	1	-1.60	-1.54	--	--	--	--	4.1	0.6	22	71	
CHE A-15-4	61	4.5	2	1	1	-2.59	-1.57	--	--	--	--	6.2	2.2	96	71	
CHE A-15	61	7	2	1	1	-3.00	-1.57	--	--	--	--	6.8	1.8	86	71	
CHE A-10	61	1.18	1	1	1	-1.68	-1.62	--	--	--	--	1.7	0.5	2	71	
CHE C-02	61	10	2	1	1	-3.55	-1.65	--	--	--	--	6.3	1.7	78	71	
CHE 9-13	61	65	2	1	1	-6.95	-1.66	--	--	--	--	8.6	4.0	313	71	
CHE C-09	61	35.18	1	1	1	-5.01	-1.71	--	--	--	--	6.7	3.6	173	71	
CHE A-13	61	2.6	2	1	1	-2.42	-1.76	--	--	--	--	1.0	0.5	1	71	

(Continued)

TABLE A.1 (CONCLUDED)

Shot Identification	Bibliography Number	Charge Yield (TNT-Equivalent)	Type of Explosive	Moisture Code	Medium Code	Height of Burst	Scaled Height of Burst $\bar{z}$	Apparent Crater Radius $\bar{r}_a$	Apparent Crater Depth $\bar{d}_a$	Apparent Crater Lip Height $\bar{h}$	Volume of Apparent Crater $\bar{v}_a$	True Crater Radius $\bar{r}_t$	True Crater Depth $\bar{d}_t$	Volume of True Crater $\bar{v}_t$	Angle of Crater Slope	Crater Shape Code
		pounds				feet	ft/lb$^{1/3}$	feet	feet	feet	ft^3	feet	feet	ft^3	degrees	
Scaled Height of Burst Less Than -1.10 and Greater Than -2.00, Category 9 (Continued):																
CHE B-05	61	14	2	1	1	-4.75	-1.78	--	--	--	--	5.6	2.0	K	--	
CHE A-02	61	1	2	1	1	-1.19	-1.19	--	--	--	--	2.1	1.0	17	--	
HE7-605	48	500	1	1	1	-11.46	-1.09	--	--	--	--	17.1	6.1	2,390	--	
CHE A-37	61	5	2	1	1	-1.98	-1.98	--	--	--	--	3.5	1.2	16	--	
CHE A-11-A	61	1.5	2	1	1	-1.54	-1.47	--	--	--	--	2.9	1.0	9	--	
PAL	46	8,600,000	0	2	2	-290.00	-1.37	119.1	78.8	21.2	1,350,000	--	--	--	35	9
Scaled Height of Burst Less Than -2.00, Category 10:																
ICEBA-06	20	25	1	1	1	-6.01	-2.05	6.6	2.9	0.1	98	7.4	7.3	371	--	0
ICEBA-12	20	200	1	1	1	-12.30	-2.55	9.4	4.0	1.3	567	--	--	--	--	0
ICEBA-05	20	25	1	1	1	-7.46	-2.56	0.0	0.0	0.8	0	9.5	8.5	637	--	0
ICEBA-11	20	25	1	1	1	-12.46	-2.56	0.0	0.0	0.8	0	--	--	--	--	0
ICEBA-07	20	25	1	1	1	-9.00	-2.08	9.5	8.3	0.4	14	4.7	9.5	153	--	0
ICEBA-08	20	8	1	1	1	-7.08	-2.50	7.9	1.0	0.5	15	5.6	7.7	213	--	0
ICEBA-10	20	25	1	1	1	-10.55	-2.49	1.9	0.6	0.3	2	9.7	11.7	196	--	0
MIDI 6	7	1,000	1	1	1	-39.00	-2.82	6.1	9.2	--	195	--	--	--	--	0
CHE B-16	61	99	2	1	1	-4.88	-2.01	--	--	--	--	4.4	3.5	263	--	0
CHE A-36-A	61	3.13	2	1	1	-3.34	-2.38	--	--	--	--	6.5	1.6	71	--	0
CHE A-29	61	3.13	2	1	1	-3.34	-2.08	--	--	--	--	3.8	2.0	73	--	0
CHE C-03	61	10	2	1	1	-4.90	-2.09	--	--	--	--	6.7	2.4	154	--	0
CHE A-10	61	4.13	2	1	1	-3.73	-2.20	--	--	--	--	4.6	2.7	97	--	0
CHE A-38	61	3.75	2	1	1	-3.56	-2.29	--	--	--	--	5.4	2.7	85	--	0
CHE A-35	61	3	2	1	1	-3.37	-2.34	--	--	--	--	3.8	1.2	19	--	0
CHE B-08	61	7.12	2	1	1	-4.96	-2.38	--	--	--	--	1.6	1.8	3	--	0
CHE B-17	61	23.81	2	1	1	-6.86	-2.36	--	--	--	--	7.7	2.9	181	--	0
CHE B-19-A	61	25	2	1	1	-6.92	-2.45	--	--	--	--	6.1	1.8	7	--	0
HE7-613	48	500	1	1	1	-17.08	-2.63	--	--	--	--	13.2	7.6	2,0	--	0
CHE C-04	61	10	2	1	1	-5.52	-2.56	--	--	--	--	3.8	1.9	19	--	0
CHE B-06	61	7	2	1	1	-4.98	-2.59	--	--	--	--	4.6	1.7	38	--	0
CHE A-12	61	1.1	2	1	1	-2.69	-2.61	--	--	--	--	0.2	0.1	0	--	0
CHE A-39	61	3.63	2	1	1	-3.73	-2.70	--	--	--	--	3.4	0.4	6	--	0
CHE B-20	61	15	2	1	1	-5.48	-2.97	--	--	--	--	6.7	1.8	7	--	0
CHE B-12	61	15.12	2	1	1	-7.17	-2.90	--	--	--	--	3.8	0.9	17	--	0
CHE A-30	61	9	2	1	1	-3.70	-2.96	--	--	--	--	2.1	0.1	1	--	0
CHE C-09	61	10	2	1	1	-4.42	-3.03	--	--	--	--	3.6	0.8	11	--	0
CHE B-08	61	5.3	2	1	1	-4.33	-3.16	--	--	--	--	2.9	0.4	7	--	0
CHE B-18	61	11.38	2	1	1	-4.98	-3.17	--	--	--	--	4.6	1.2	30	--	0
CHE B-09	61	4	2	1	1	-3.14	-3.34	--	--	--	--	4.3	1.4	53	--	0
CHE C-12	61	70	2	1	1	-13.36	-3.28	--	--	--	--	7.7	1.5	7	--	0
CHE B-05	61	3.25	2	1	1	-4.30	-3.31	--	--	--	--	5.4	1.4	58	--	0
CHE A-32	61	1.13	2	1	1	-3.46	-3.41	--	--	--	--	0.2	0.2	0	--	0
CHE B-07	61	2.5	2	1	1	-4.34	-3.43	--	--	--	--	2.8	0.8	7	--	0
HE7-606	48	500	1	1	1	-24.00	-3.66	--	--	--	--	1.2	2.0	857	--	0
CHE C-08	61	7.5	2	1	1	-7.25	-3.70	--	--	--	--	2.5	0.5	4	--	0
CHE C-14	61	50.12	1	1	1	-11.7	-3.76	--	--	--	--	2.3	1.6	10	--	0
CHE A-31	61	1	2	1	1	-3.49	-3.52	--	--	--	--	0.6	0.1	0	--	0
CHE B-01	61	2.13	1	1	1	-4.20	-4.34	--	--	--	--	0.2	0.2	0	--	0
CHE B-11	61	4.63	1	1	1	-4.88	-4.10	--	--	--	--	0.3	0.3	0	--	0
CHE HE-1-C	61	26.2	2	1	1	-10.21	-4.13	--	--	--	--	1.1	0.4	1	--	0

(3 of 3 sheets)

TABLE A.2 CRATER DATA FOR SANDSTONE

Shot Identification	Bibliography Number	Charge Yield (TNT-Equivalent)	Type of Explosive	Moisture Code	Medium Code	Height of Burst	Scaled Height of Burst Z	Apparent Crater Radius r_a	Apparent Crater Depth d_a	Apparent Crater Lip Height h	Volume of Apparent Crater v_a	True Crater Radius r_t	True Crater Depth d_t	Volume of True Crater v_t	Angle of Crater Slope	Crater Shape Code
		pounds				feet	$ft/lb^{1/3}$	feet	feet	feet	ft^3	feet	feet	ft^3	degrees	
Scaled Height of Burst Greater Than +0.50, Category 1:																
							No Data Available									
Scaled Height of Burst Less Than +0.50 and Greater Than +0.20, Category 2:																
							No Data Available									
Scaled Height of Burst Less Than +0.20 and Greater Than +0.05, Category 3:																
							No Data Available									
Scaled Height of Burst Less Than +0.05 and Greater Than -0.05, Category 4:																
ICRDB-16	22	25	1	1	2	0.00	0.00	3.4	0.8	0.1	19	3.8	1.1	31	--	0
UETP-802	59	320	1	1	2	0.00	0.00	--	--	--	--	5.6	2.3	169	--	0
Scaled Height of Burst Less Than -0.05 and Greater Than -0.20, Category 5:																
							No Data Available									
Scaled Height of Burst Less Than -0.20 and Greater Than -0.50, Category 6:																
CRN E-02	61	2,560	2	1	2	-4.71	-0.94	--	--	--	--	23.4	9.0	5,148	--	0
CRN B-01	61	1,080	2	1	2	-3.60	-0.95	--	--	--	--	13.1	8	1,518	--	0
UETP-803	59	320	1	1	2	-2.50	-0.37	--	--	--	--	11.6	4.	810	--	0
UETP-807	59	320	1	1	2	-2.50	-0.37	--	--	--	--	14.3	5.1	1,460	--	0
UETP-808	59	320	1	1	2	-2.50	-0.37	--	--	--	--	13.1	5.6	1,020	--	0
UETP-818	59	320	1	1	2	-2.50	-0.37	--	--	--	--	17.5	6.0	1,820	--	0
UETP-819	59	320	1	1	2	-2.50	-0.37	--	--	--	--	15.6	6.5	1,440	--	0
UETP-809	59	1,080	1	1	2	-3.75	-0.37	--	--	--	--	19.0	8.6	3,530	--	0
UETP-810	59	2,560	1	1	2	-5.00	-0.37	--	--	--	--	32.6	9.7	8,650	--	0
UETP-811	59	2,560	1	1	2	-5.00	-0.37	--	--	--	--	25.1	10.5	7,050	--	0
UETP-812	59	2,560	1	1	2	-5.00	-0.37	--	--	--	--	23.3	11.0	6,880	--	0
UETP-813	59	10,000	1	1	2	-7.90	-0.37	--	--	--	--	39.4	16.1	22,000	--	0
UETP-814	59	40,000	1	1	2	-12.50	-0.37	--	--	--	--	56.5	26.9	108,000	--	0
UETP-815	59	40,000	1	1	2	-12.50	-0.37	--	--	--	--	70.5	26.9	125,000	--	0
UETP-816	59	40,000	1	1	2	-12.50	-0.37	--	--	--	--	53.6	27.5	106,000	--	0
UETP-817	59	320,000	1	1	2	-25.00	-0.37	--	--	--	--	94.8	47.0	512,000	--	0
CRN C-02	61	320	1	1	2	-2.96	-0.43	--	--	--	--	11.9	7.1	1,057	--	0
ICSDB-11	22	8	1	1	2	-1.00	-0.50	3.5	1.3	0.1	25	5.0	1.7	73	--	0
CRN A-08	61	125	2	1	2	-1.48	-0.30	--	--	--	--	2.8	1.1	9	--	0
Scaled Height of Burst Less Than -0.50 and Greater Than -0.90, Category 7:																
ICSDB-09	22	25	1	1	2	-1.50	-0.51	5.1	2.2	0.2	88	5.5	2.7	140	--	0
ICSCC-01	21	25	1	1	2	-1.50	-0.51	6.0	2.2	0.6	127	6.7	3.0	237	--	0
UETP-804	59	320	1	1	2	-5.00	-0.73	--	--	--	--	14.0	7.6	1,440	--	0

(Continued)

TABLE A.2 (CONTINUED)

Shot Identification	Bibliography Number	Charge Yield (TNT-Equivalent)	Type of Explosive	Moisture Code	Medium Code	Height of Burst	Scaled Height of Burst Z	Apparent Crater Radius r_a	Apparent Crater Depth d_a	Apparent Crater Lip Height h	Volume of Apparent Crater v_a	True Crater Radius r_t	True Crater Depth d_t	Volume of True Crater v_t	Angle of Crater Slope	Crater Shape Code
		pounds				feet	$ft/lb^{1/3}$	feet	feet	feet	ft^3	feet	feet	ft^3	degrees	
Scaled Height of Burst Less Than -0.50 and Greater Than -0.90, Catetory 7 (Continued):																
CRH B-14	61	104	1	1	2	-3.40	-0.74	--	--	--	--	11.5	5.6	788	--	0
CRH A-16	61	2	2	1	2	-1.04	-0.83	--	--	--	--	2.5	0.8	5	--	0
CRH A-12	61	2.25	2	1	2	-1.12	-0.85	--	--	--	--	3.6	1.1	15	--	0
Scaled Height of Burst Less Than -0.90 and Greater Than -1.10, Category 8:																
CRH C-01	61	70	1	1	2	-3.84	-0.93	--	--	--	--	8.8	5.9	485	--	0
ICSGE-06	22	75	1	1	2	-4.00	-0.95	8.4	4.5	0.4	429	11.9	9.3	2,234	--	0
ICSGE-14	22	85	1	1	2	-3.00	-1.03	4.9	1.3	0.2	40	6.5	4.7	342	--	0
Scaled Height of Burst Less Than -1.10 and Greater Than -2.00, Category 9:																
CRH A-42	61	10	2	1	2	-2.38	-1.10	--	--	--	--	4.8	1.6	39	--	0
CRH A-14	61	1.62	2	1	2	-1.34	-1.14	--	--	--	--	2.6	1.4	10	--	0
CRH C-01	61	10	2	1	2	-2.50	-1.16	--	--	--	--	5.1	2.5	68	--	0
CRH A-29	61	9.5	2	1	2	-2.50	-1.18	--	--	--	--	4.0	2.0	33	--	0
CRH A-17	61	4.25	2	1	2	-2.00	-1.23	--	--	--	--	3.2	1.5	16	--	0
CRH A-18	61	4.25	2	1	2	-2.00	-1.23	--	--	--	--	4.6	2.1	49	--	0
CRH A-39	61	9	2	1	2	-2.70	-1.30	--	--	--	--	4.9	2.5	62	--	0
CRH A-04	61	1.5	2	1	2	-1.51	-1.32	--	--	--	--	2.8	2.9	12	--	0
ICSGE-08	22	8	1	1	2	-3.00	-1.50	3.8	1.7	0.2	60	6.5	5.0	384	--	0
ICSGE-13	22	25	1	1	2	-4.50	-1.54	3.0	1.4	0.3	80	7.9	5.7	595	--	0
CRH B-08	61	18.38	2	1	2	-4.14	-1.57	--	--	--	--	10.1	3.8	407	--	0
CRH A-36	61	6	2	1	2	-2.80	-1.60	--	--	--	--	5.8	2.6	89	--	0
CRH A-24	61	3	2	1	2	-2.32	-1.61	--	--	--	--	5.0	1.4	37	--	0
CRH C-02	61	10	2	1	1	-3.50	-1.62	--	--	--	--	6.0	3.2	122	--	0
CRH C-02A	61	10	2	1	2	-3.50	-1.62	--	--	--	--	9.7	4.6	155	--	0
CRH B-HX3	61	10	2	1	2	-3.50	-1.62	--	--	--	--	5.1	2.3	64	--	0
CRH A-37	61	4.62	1	1	2	-2.75	-1.65	--	--	--	--	4.0	1.9	32	--	0
CRH A-26	61	6	2	1	2	-3.15	-1.73	--	--	--	--	6.1	2.3	98	--	0
CRH B-10	61	14	2	1	2	-4.30	-1.78	--	--	--	--	8.9	3.4	224	--	0
CRH A-35	61	4.12	1	1	2	-2.87	-1.79	--	--	--	--	4.0	2.3	39	--	0
WSTF-80:	59	320	1	1	2	-12.40	-1.83	--	--	--	--	9.3	14.9	1,190	--	0
CRH B-19	61	38.12	1	1	2	-6.20	-1.84	--	--	--	--	6.4	5.4	232	--	0
CRH D-05	61	8.38	1	1	2	-4.00	-1.97	--	--	--	--	9.3	2.8	252	--	0
CRH C-06	61	21	2	1	2	-5.45	-1.98	--	--	--	--	6.2	2.3	93	--	0
ICSGE-10	22	200	1	1	2	-11.60	-1.98	5.0	1.2	0.5	189	16.3	13.8	6,001	--	0
Scaled Height of Burst Less Than -2.00, Category 10:																
ICSGE-12	22	25	1	1	2	-6.00	-2.05	4.6	1.4	0.3	78	10.9	7.4	1,487	--	0
CRH C-01	61	10	2	1	2	-4.50	-2.09	--	--	--	--	6.0	1.8	66	--	0
CRH A-22	61	1.5	2	1	2	-2.41	-2.11	--	--	--	--	3.2	1.2	13	--	0
CRH A-20	61	1.56	2	1	2	-2.38	-2.05	--	--	--	--	3.5	1.2	15	--	0
CRH A-45	61	1.42	1	1	2	-2.50	-2.22	--	--	--	--	1.5	0.6	1	--	0

(Continued)

TABLE A.9 (CONCLUDED)

Shot Identification	Bibliography Number	Charge Yield (TNT-Equivalent)	Type of Explosive	Moisture Code	Medium Code	Height of Burst	Scaled Height of Burst Z	Apparent Crater Radius r_a	Apparent Crater Depth d_a	Apparent Crater Lip Height h	Volume of Apparent Crater v_a	True Crater Radius r_t	True Crater Depth d_t	Volume of True Crater v_t	Angle of Crater Slope	Crater Shape Code
		pounds				feet	$ft/lb^{1/3}$	feet	feet	feet	ft^3	feet	feet	ft^3	degrees	
Scaled Height of Burst Less Than -2.00, Category 10 (Continued):																
CRH A-40	61	2.75	1	1	2	-3.21	-2.09	--	--	--	--	3.3	1.0	11	--	0
CRH C-09	61	12.12	1	1	2	-5.31	-2.31	--	--	--	--	6.0	1.8	69	--	0
CRH A-19	61	1.2	2	1	2	-2.50	-2.35	--	--	--	--	2.4	1.0	6	--	0
CRH A-30	61	3.20	2	1	2	-3.40	-2.36	--	--	--	--	2.7	1.2	9	--	0
CRH A-21	61	1.4	2	1	2	-2.66	-2.38	--	--	--	--	2.6	0.9	6	--	0
CRH A-32	61	3	2	1	2	-3.33	-2.45	--	--	--	--	3.0	1.2	12	--	0
CRH A-47	61	6.5	2	1	2	-4.60	-2.46	--	--	--	--	4.1	1.4	25	--	0
CRH B-17	61	17.62	1	1	2	-6.42	-2.47	--	--	--	--	8.5	2.3	177	--	0
CRH B-18	61	12.75	1	1	2	-5.75	-2.46	--	--	--	--	5.2	2.4	70	--	0
CRH A-50	61	4.62	1	1	2	-4.15	-2.49	--	--	--	--	2.5	0.7	4	--	0
ICSAB-03	22	8	1	1	2	-5.00	-2.50	4.2	0.9	0.4	24	7.9	5.6	631	--	0
ICSCC-03	21	8	1	1	2	-5.00	-2.50	4.8	1.6	0.6	56	6.6	6.5	407	--	0
CRH A-33	61	2.8	2	1	2	-3.55	-2.52	--	--	--	--	3.2	1.0	11	--	0
CRH C-06	61	10	2	1	2	-5.50	-2.55	--	--	--	--	4.8	1.9	46	--	0
ICSC4-01	22	25	1	1	2	-7.50	-2.56	1.1	0.4	0.4	9	11.5	9.1	2,327	--	0
CRH B-01	61	6	2	1	2	-4.73	-2.61	--	--	--	--	3.5	2.0	25	--	0
CRH A-49	61	4.5	2	1	2	-4.85	-2.64	--	--	--	--	1.1	0.7	1	--	0
ICSAB-04	22	75	1	1	2	-12.00	-2.85	0.5	1.0	1.3	1	16.3	12.8	5,900	--	0
CRH C-07	61	8.12	1	1	2	-5.80	-2.89	--	--	--	--	1.9	0.8	3	--	0
CRH C-13	61	70	2	1	2	-12.27	-2.98	--	--	--	--	13.0	5.7	1,016	--	0
CRH B-16	61	10.62	1	1	2	-6.62	-3.01	--	--	--	--	3.7	2.3	33	--	0
CRH B-20	61	12	2	1	2	-6.91	-3.02	--	--	--	--	5.2	2.2	63	--	0
ICSAB-07	22	35	1	1	2	-9.00	-3.08	0.0	0.0	0.8	0	13.2	10.7	3,078	--	0
CRH B-11	61	11	2	1	2	-6.85	-3.08	--	--	--	--	2.0	0.6	3	--	0
CRH C-10	61	6	2	1	2	-6.17	-3.40	--	--	--	--	2.0	0.8	3	--	0
ICSAB-05	22	8	1	1	2	-7.00	-3.50	--	--	0.2	0	3.1	8.6	35	--	0
ICSAB-08	22	9	1	1	2	-10.50	-3.59	--	--	0.4	0	9.5	12.0	1,209	--	0
CRH C-11	61	33.62	1	1	2	-11.99	-3.70	--	--	--	--	2.6	0.7	3	--	0
CRH C-14	61	35	2	1	2	-12.62	-3.80	--	--	--	--	1.9	1.6	6	--	0

TABLE A.3 CRATER DATA FOR BASALT, TUFF, AND ALLUVIUM GROUND

Shot Identification	Drilling-Log Number	Charge Yield (TNT-Equivalent)[1]	Type of Explosive	Moisture Code	Medium Code	Height of Burst	Scaled Height of Burst $\frac{Z}{W^{1/3}}$	Apparent Crater Radius r_a	Apparent Crater Depth d_a	Apparent Crater Lip Height h	Volume of Apparent Crater V_a	True Crater Radius r_t	True Crater Depth d_t	Volume of True Crater V_t	Angle of Crater Slope	Crater Shape Code
		pounds				feet	ft/lb$^{1/3}$	feet	feet	ft	ft^3	feet	feet	ft^3	degrees	
Scaled Height of Burst Greater Than +0.50, Category 1:																
								[2] Data Available								
Scaled Height of Burst Less Than +0.50 and Greater Than +0.20, Category 2:																
								[2] Data Available								
Scaled Height of Burst Less Than +0.20 and Greater Than +0.05, Category 3:																
SHB-4J	66	1.2AC	1	A	3	1.77	0.77	3.5	1.9	--	--	--	--		--	
Scaled Height of Burst Less Than +0.05 and Greater Than +0.0, Category 4:																
ICCCC-0A	21	25	1	1	3	0.10	0.05	[illegible]	[illegible]	[illegible]	38	[illegible]	2.4	[illegible]	--	[illegible]
ICCCC-1B	21	50	1	1	3	0.10	0.05	[illegible]	[illegible]	[illegible]	29	[illegible]	1.4	[illegible]	--	[illegible]
ICBCC-1C	21	50	1	1	3	0.10	0.05	[illegible]	[illegible]	[illegible]	[illegible]	[illegible]	[illegible]	[illegible]	--	[illegible]
Scaled Height of Burst Less Than +0.05 and Greater Than +0.20, Category 5:																
ICBCC-A	21	50	1	1	3	+0.40	+0.16	7.2	2.6	--		7.6	3.0	333	--	[illegible]
Scaled Height of Burst Less Than +0.20 and Greater Than +0.50, Category 6:																
ICBCC-07	21	8	1	1	3	+1.00	+0.40		1.8	0.3	[illegible]	[illegible]	0.9	143	--	[illegible]
PCPT-10J	178	19.61	2	A	3	+1.04	+0.39	[illegible]	2.2	--	[illegible]	--	--	--	--	[illegible]
RAE-1	88	280,000,000	0	0	3	+147.0	+0.26	203.4	65.6	24.9	3,[illegible]	--	--	--	--	[illegible]
Scaled Height of Burst Less Than +0.50 and Greater Than +0.80, Category 7:																
ICBCC-09	21	25	1	1	3	+1.50	+0.61	[illegible]	[illegible]	[illegible]	156	[illegible]	[illegible]	[illegible]	--	[illegible]
BCH	44	70,000,000	0	1	3	+355.00	+0.86	[illegible]	[illegible]	[illegible]	61,6[illegible]	--	--	--	--	[illegible]
PCPT-12A	178	19.51	2	A	3	+1.53	+0.47	[illegible]	[illegible]	--	[illegible]	--	--	--	--	[illegible]
FICB-01	62	1.26	3	A	3	+1.30	+0.47	2.7	2.6	--	[illegible]	--	--	--	--	[illegible]
FICB-08	62	1.26	3	A	3	+1.70	+0.67	3.0	2.4	--	[illegible]	--	--	--	--	[illegible]
FICB-03	62	1.26	3	A	3	+1.30	+0.67	3.2	2.6	--	[illegible]	--	--	--	--	[illegible]
FICB-04	62	1.26	3	A	3	+1.30	+0.67	3.1	2.6	--	[illegible]	--	--	--	--	[illegible]
FICB-05	62	1.26	3	A	3	+1.30	+0.67	2.9	2.2	--	[illegible]	--	--	--	--	[illegible]
FICB-06	62	1.26	3	A	3	+1.00	+0.67	2.7	1.7	--	[illegible]	--	--	--	--	[illegible]
FICB-07	62	1.26	3	A	3	+1.30	+0.67	3.5	1.4	--	[illegible]	--	--	--	--	[illegible]
FICB-08	62	1.26	3	A	3	+1.30	+0.67	3.3	1.7	--	[illegible]	--	--	--	--	[illegible]
FICB-09	62	1.26	3	A	3	+1.30	+0.67	2.9	1.2	--	[illegible]	--	--	--	--	[illegible]
FICB-10	62	1.26	3	A	3	+1.30	+0.67	3.7	1.7	--	[illegible]	--	--	--	--	[illegible]
FICB-11	62	1.26	3	A	3	+1.30	+0.67	3.1	1.9	--	[illegible]	--	--	--	--	[illegible]
FICB-12	62	1.26	3	A	3	+1.30	+0.67	3.4	1.9	--	[illegible]	--	--	--	--	[illegible]
FICB-13	62	1.26	3	A	3	+1.00	+0.67	3.1	1.4	--	[illegible]	--	--	--	--	[illegible]
FICB-1A	62	1.26	3	A	3	+1.00	+0.67	3.7	1.8	--	[illegible]	--	--	--	--	[illegible]
FICB-10B	62	2.62	2	A	3	+1.04	+0.72	4.0	1.9	--	[illegible]	--	--	--	--	[illegible]
PCPT-09A	178	1	2	A	3	+0.73	+0.73	2.1	1.7	--	[illegible]	--	--	--	--	[illegible]
PCPT-10J	178	19.39	2	A	3	+2.09	+1.47	[illegible]	3.7	--	[illegible]	--	--	--	--	[illegible]
PCPT-07A	178	4.9	2	A	3	+1.47	+0.89	[illegible]	2.6	--	[illegible]	--	--	--	--	[illegible]
Scaled Height of Burst Less Than +0.80 and Greater Than +1.10, Category 8:																
ICBCC-0A	21	6	1	1	3	+2.00	+1.00	[illegible]	2.0	0.2	[illegible]	[illegible]	[illegible]	157	--	[illegible]
PCPT-06J	178	1.19	2	A	3	+1.02	+0.38	2.9	1.6	--	[illegible]	--	--	--	--	[illegible]

(Continued)

(1 of 4 sheets)

TABLE A.3 (CONTINUED)

Shot Identification	Pitllogrity Number	Charge Yield (TNT-Equivalent)	Type of Explosive	Moisture Code	Medium Code	Height of Burst	Scaled Height of Burst Z	Apparent Crater Radius r_a	Apparent Crater Depth d_a	Apparent Crater Lip Height h	Volume of Apparent Crater v_a	True Crater Radius r_t	True Crater Depth d_t	Volume of True Crater v_t	Angle of Crater Slope	Crater Shape Code
		pounds				feet	$ft/lb^{1/3}$	feet	feet	feet	ft^3	feet	feet	ft^3	degrees	
Scaled Height of Burst Less Than -0.90 and Greater Than -1.10, Category 8 (Continued):																
FCPT-106	178	19.12	2	4	3	-2.68	-0.98	9.9	2.2	--	175	--	--	--	--	
FICE-15	62	9.26	3	4	3	-1.52	-1.01	4.8	2.2	--	18	--	--	--	--	
FICE-16	62	9.26	3	4	3	-1.50	-1.01	3.6	2.1	--	17	--	--	--	--	
FICE-17	62	9.26	3	4	3	-1.47	-1.01	3.6	1.8	--	22	--	--	--	--	
FICE-18	62	9.26	3	4	3	-1.50	-1.01	3.0	2.4	--	19	--	--	--	--	
FICE-19	62	9.26	3	4	3	-1.46	-1.01	3.3	2.3	--	23	--	--	--	--	
FICE-20	62	9.26	3	4	3	-1.46	-1.01	3.1	2.1	--	21	--	--	--	--	
FICE-21	62	9.26	3	4	3	-1.50	-1.01	3.4	2.0	--	20	--	--	--	--	
FICE-22	62	9.26	3	4	3	-1.50	-1.01	4.3	2.2	--	43	--	--	--	--	
FICE-23	62	9.26	3	4	3	-1.50	-1.01	2.9	2.4	--	17	--	--	--	--	
FICE-24	62	9.26	3	4	3	-1.76	-1.01	3.4	1.7	--	12	--	--	--	--	
FICE-25	62	9.26	3	4	3	-1.42	-1.01	2.8	2.1	--	11	--	--	--	--	
FICE-26	62	9.26	3	4	3	-1.45	-1.01	2.7	2.3	--	20	--	--	--	--	
FICE-27	62	9.26	3	4	3	-1.50	-1.01	2.6	1.9	--	15	--	--	--	--	
FICE-28	62	9.26	3	4	3	-1.50	-1.01	2.7	1.8	--	16	--	--	--	--	
Scaled Height of Burst Less Than -1.10 and Greater Than -2.00, Category 9:																
ICECC-03	21	8	1	1	3	-3.00	-1.50	4.9	2.4	0.2	39	6.2	4.5	1[illegible]	--	
ICECC-02	21	25	1	1	3	-3.60	-1.84	6.8	2.5	0.7	47[illegible]	9.9	7.3	[illegible]	--	
ICECC-10	21	25	1	1	3	-3.60	-1.84	6.5	3.2	0.8	66[illegible]	10.6	6.8	[illegible]	--	
ICECC-02	21	8	1	1	3	-3.00	-1.50	6.2	2.5	0.6	138	9.6	5.6	3[illegible]	--	
FCPT-095	178	1	2	4	3	-1.34	-1.34	2.5	1.7	--	12	--	--	--	--	
FCPT-064-R	178	8	2	4	3	-1.55	-1.35	3.3	2.1	--	20	--	--	--	--	
FCPT-065	178	1.99	2	4	3	-1.48	-1.38	2.3	2.1	--	11	--	--	--	--	
FCPT-108	178	19.59	2	4	3	-1.93	-1.35	4.8	3.1	--	37[illegible]	--	--	--	--	
FCPT-096	178	[illegible]	2	4	3	-1.35	-1.35	2.5	1.7	--	9	--	--	--	--	
FCPT-065	178	1.99	2	4	3	-1.77	-1.41	2.7	2.5	--	21	--	--	--	--	
FICE-29	62	9.26	3	4	3	-2.04	-1.35	4.0	2.3	--	36	--	--	--	--	
FICE-30	62	9.26	3	4	3	-2.00	-1.35	3.3	2.2	--	26	--	--	--	--	
FICE-31	62	9.26	3	4	3	-2.00	-1.35	3.5	2.4	--	27	--	--	--	--	
FICE-32	62	9.26	3	4	3	-2.00	-1.35	4.0	1.9	--	36	--	--	--	--	
FICE-33	62	9.26	3	4	3	-2.00	-1.35	3.1	1.9	--	30	--	--	--	--	
FICE-34	62	9.26	3	4	3	-2.00	-1.35	3.3	2.1	--	29	--	--	--	--	
FICE-35	62	9.26	3	4	3	-2.00	-1.35	3.4	2.3	--	27	--	--	--	--	
FICE-36	62	9.26	3	4	3	-2.04	-1.35	3.3	2.[illegible]	--	2[illegible]	--	--	--	--	
FICE-37	62	9.26	3	4	3	-2.00	-1.35	3.4	1.7	--	18	--	--	--	--	
FICE-38	62	9.26	3	4	3	-2.00	-1.35	3.4	1.9	--	24	--	--	--	--	
FICE-39	62	9.26	3	4	3	-2.00	-1.35	3.4	1.7	--	21	--	--	--	--	
FICE-40	62	9.26	3	4	3	-2.00	-1.35	3.2	2.2	--	28	--	--	--	--	
FICE-41	62	9.26	3	4	3	-2.00	-1.35	3.4	1.7	--	21	--	--	--	--	
FICE-42	62	9.26	3	4	3	-2.00	-1.35	3.1	1.7	--	18	--	--	--	--	
FICE-108	62	2.65	2	4	3	-2.00	-1.35	3.7	2.4	--	29	--	--	--	--	
FCPT-109	178	19.68	2	4	3	-2.04	-1.36	6.4	3.4	--	77	--	--	--	--	
FCPT-076	178	4.58	2	4	3	-2.[illegible]	-1.32	4.[illegible]	3.5	--	5[illegible]	--	--	--	--	
FCPT-066	178	1.99	2	4	3	-1.98	-1.36	3.3	2.8	--	2[illegible]	--	--	--	--	
FCPT-110	178	19.88	2	4	3	-2.68	-1.69	7.1	3.9	--	34[illegible]	--	--	--	--	
FCPT-067-R	178	2	2	4	3	-2.21	-1.75	3.8	2.9	--	37	--	--	--	--	
FICE-43	62	9.26	3	4	3	-2.5[illegible]	-1.69	3.3	2.1	--	21	--	--	--	--	
FICE-44	62	9.26	3	4	3	-2.55	-1.74	3.6	2.1	--	1[illegible]	--	--	--	--	
FICE-45	62	9.26	3	4	3	-2.[illegible]	-1.69	3.7	1.7	--	20	--	--	--	--	
FICE-46	62	9.26	3	4	3	-2.90	-1.69	3.7	2.3	--	30	--	--	--	--	
FICE-47	62	9.26	3	4	3	-2.50	-1.69	4.8	3.1	--	39	--	--	--	--	

(Continued)

(2 of 4 sheets)

TABLE A.3 (CONTINUED)

Shot Identification	Bibliography Number	Charge Yield (TNT-Equivalent)	Type of Explosive	Moisture Code	Medium Code	Height of Burst	Scaled Height of Burst $\bar{z}$	Apparent Crater Radius r_a	Apparent Crater Depth d_a	Apparent Crater Lip Height h	Volume of Apparent Crater v_a	True Crater Radius r_t	True Crater Depth d_t	Volume of True Crater v_t	Angle of Crater Slope	Crater Shape Code
		pounds				feet	$ft/lb^{1/3}$	feet	feet	feet	ft^3	feet	feet	ft^3	degrees	
Scaled Height of Burst Less Than -1.10 and Greater Than -2.00, Category 9 (Continued):																
PICE-48	62	1.26	3	4	3	-2.50	-1.69	3.7	2.5	--	56	--	--	--	--	0
PICE-49	62	1.26	3	4	3	-2.50	-1.69	4.2	2.7	--	65	--	--	--	--	0
PICE-50	62	1.26	3	4	3	-2.50	-1.69	5.0	2.9	--	99	--	--	--	--	0
PICE-51	62	1.26	3	4	3	-2.50	-1.69	4.1	2.6	--	56	--	--	--	--	0
PICE-52	62	1.26	3	4	3	-2.50	-1.69	4.5	2.9	--	76	--	--	--	--	0
PICE-53	62	1.26	3	4	3	-2.50	-1.69	5.1	3.2	--	107	--	--	--	--	0
PICE-54	62	1.26	3	4	3	-2.50	-1.69	3.9	3.3	--	94	--	--	--	--	0
PICE-55	62	1.26	3	4	3	-2.50	-1.69	4.0	3.3	--	66	--	--	--	--	0
PICE-56	62	1.26	3	4	3	-2.50	-1.69	4.2	3.6	--	51	--	--	--	--	0
PCRT-097	178	1	2	4	3	-1.81	-1.81	2.9	2.3	--	33	--	--	--	--	0
PCRT-067	178	1.99	2	4	3	-2.29	-1.82	3.8	2.7	--	33	--	--	--	--	0
PCRT-111	178	19.87	2	4	3	-5.01	-1.85	6.9	6.4	--	459	--	--	--	--	0
PCRT-077	178	1.05	2	4	3	-3.06	-1.98	4.9	3.7	--	73	--	--	--	--	0
PCRT-066-R	178	2	2	4	3	-2.65	-1.94	3.9	3.1	--	49	--	--	--	--	0
PCRT-068	178	1.99	2	4	3	-2.49	-1.98	3.1	3.0	--	28	--	--	--	--	0
PI SC-2	66	1,000	5	2	3	-15.80	-1.58	27.3	12.5	3.1	--	--	--	--	--	0
PI SC-4	66	1,000	5	2	3	-12.20	-1.22	24.5	13.0	3.8	--	--	--	--	--	0
PI A	66	50,000	5	2	3	-52.70	-1.94	76.1	32.1	13.9	835,300	--	--	--	--	0
PI B	66	50,000	5	2	3	-46.22	-1.35	78.5	29.5	13.7	841,260	--	--	--	--	0
PI C	66	50,000	5	2	3	-42.50	-1.24	80.4	32.6	14.5	877,550	--	--	--	--	0
PI D	66	50,000	5	2	3	-56.90	-1.66	65.1	25.2	13.0	133,880	--	--	--	--	0
MEP	82	230,000	0	1	3	-100.00	-1.63	100.0	37.0	--	994,200	--	--	--	--	0
TRIN 91	8	2,000	4	4	3	-15.50	-1.23	16.9	7.9	--	--	--	--	--	--	0
TRIN 92	8	2,000	4	4	3	-18.00	-1.43	20.0	11.5	--	--	--	--	--	--	0
TRIN 93	8	2,000	4	4	3	-19.50	-1.55	24.0	6.5	--	--	--	--	--	--	0
TRIN 94	8	2,000	4	4	3	-16.00	-1.27	23.6	12.6	--	--	--	--	--	--	0
TRIN 95	8	2,000	4	4	3	-18.50	-1.47	23.2	13.0	--	--	--	--	--	--	0
TRIN 96	8	2,000	4	4	3	-21.00	-1.67	21.8	11.5	--	--	--	--	--	--	0
TRIN 97	8	2,000	4	4	3	-22.50	-1.79	20.0	6.0	--	--	--	--	--	--	0
Scaled Height of Burst Less Than -2.00, Category 10:																
ICHCC-11	21	200	1	1	3	-12.00	-2.09	12.9	4.3	2.1	1,253	17.6	15.5	8,413	--	0
ICHCC-12	21	8	1	1	3	-5.00	-2.50	5.0	1.7	0.6	76	6.3	6.1	332	--	0
ICHCC-01	21	25	1	1	3	-7.50	-2.56	6.2	1.5	0.8	122	8.0	10.7	1,066	--	0
ICHCC-12	21	75	1	1	3	-12.00	-2.85	9.9	2.3	1.6	481	13.0	--	--	--	0
ICHCC-02	21	8	1	1	3	-6.00	-3.00	6.1	2.8	0.7	182	7.8	5.6	497	--	0
ICHCC-09	21	8	1	1	3	-7.00	-3.50	4.1	1.2	0.8	28	5.6	7.9	316	--	0
PCRT-112	178	19.95	2	4	3	-9.55	-2.05	9.3	6.7	--	647	--	--	--	--	0
PCRT-078	178	4.81	2	4	3	-3.56	-2.11	6.3	2.7	--	69	--	--	--	--	0
PICE-57	62	1.26	3	4	3	-3.00	-2.08	4.8	4.0	--	110	--	--	--	--	0
PICE-58	62	1.26	3	4	3	-3.00	-2.08	5.9	4.4	--	123	--	--	--	--	0
PICE-59	62	1.26	3	4	3	-3.00	-2.08	4.7	3.3	--	76	--	--	--	--	0
PICE-60	62	1.26	3	4	3	-3.00	-2.08	4.5	3.4	--	65	--	--	--	--	0
PICE-61	62	1.26	3	4	3	-3.00	-2.08	5.4	3.6	--	93	--	--	--	--	0
PICE-62	62	1.26	3	4	3	-3.00	-2.08	4.8	3.9	--	123	--	--	--	--	0
PICE-63	62	1.26	3	4	3	-3.00	-2.08	5.4	3.5	--	80	--	--	--	--	0
PICE-64	62	1.26	3	4	3	-3.00	-2.08	5.9	3.7	--	94	--	--	--	--	0
PICE-65	62	1.26	3	4	3	-3.00	-2.08	5.1	3.1	--	58	--	--	--	--	0
PICE-66	62	1.26	3	4	3	-3.00	-2.08	5.8	3.5	--	82	--	--	--	--	0
PICE-68	62	1.26	3	4	3	-3.00	-2.08	4.9	3.5	--	66	--	--	--	--	0
PICE-69	62	1.26	3	4	3	-3.00	-2.08	6.0	3.1	--	77	--	--	--	--	0

(Continued)

TABLE A.3 (CONCLUDED)

Shot Identification	Bibliography Number	Charge Yield (TNT-Equivalent)	Type of Explosive	Moisture Code	Medium Code	Height of Burst	Scaled Height of Burst $\bar{z}$	Apparent Crater Radius r_a	Apparent Crater Depth d_a	Apparent Crater Lip Height h	Volume of Apparent Crater V_a	True Crater Radius r_t	True Crater Depth d_t	Volume of True Crater V_t	Angle of Crater Slope	Crater Shape Code
		pounds				feet	$ft/lb^{1/3}$	feet	feet	feet	ft^3	feet	feet	ft^3	degrees	
Scaled Height of Burst Less Than -2.00, Category 10 (Continued):																
PICE-70	60	3.86	3	4	3	-3.00	-2.08	6.8	3.9	--	111	--	--	--	--	0
PICE-110	62	2.65	2	4	3	-3.00	-2.17	4.9	2.7	--	43	--	--	--	--	0
PCNT-069	178	1.99	2	4	3	-2.77	-2.20	4.5	2.1	--	45	--	--	--	--	0
PCNT-113	178	19.98	2	4	3	-4.[illegible]	-2.22	2.2	--	--	--	--	--	--	--	--
PCNT-068	178	1	2	4	3	-2.[illegible]	-2.24	2.0	2.8	--	1	--	--	--	--	0
PCNT-070	178	1.99	2	4	3	-2.99	-2.39	2.3	1.4	--	5	--	--	--	--	0
PCNT-071	178	1.99	2	4	3	-3.15	-2.50	4.4	2.3	--	45	--	--	--	--	0
PCNT-069	178	1	2	4	3	-2.56	-2.56	1.6	1.1	--	1	--	--	--	--	0
PICE-71	62	3.86	3	4	3	-3.40	-2.58	4.7	2.1	--	28	--	--	--	--	0
PICE-72	62	3.86	3	4	3	-3.50	-2.66	5.8	3.7	--	63	--	--	--	--	0
PICE-73	62	3.86	3	4	3	-3.60	-2.74	4.1	3.5	--	[illegible]	--	--	--	--	0
PICE-74	62	3.86	3	4	3	-3.50	-2.66	6.5	4.0	--	[illegible]	--	--	--	--	0
PICE-75	62	3.86	3	4	3	-3.50	-2.66	4.9	3.0	--	58	--	--	--	--	0
PICE-81	62	3.86	3	4	3	-3.50	-2.66	4.0	1.2	--	16	--	--	--	--	0
PCNT-080	178	8.98	2	4	3	-4.34	-2.67	3.0	1.3	--	11	--	--	--	--	0
PCNT-100	178	1	2	4	3	-2.79	-2.79	0.6	3.4	--	0	--	--	--	--	0
PCNT-072	178	1.99	2	4	3	-3.53	-2.81	0.8	--	--	--	--	--	--	--	0
PCNT-101	178	1	2	4	3	-2.95	-2.84	1.8	3.4	--	3	--	--	--	--	0
PICE-68	62	3.86	3	4	3	-4.00	-2.97	5.0	2.8	--	55	--	--	--	--	0
PICE-93	62	3.86	3	4	3	-4.00	-2.70	3.1	1.7	--	16	--	--	--	--	0
PICE-112	62	2.65	2	4	3	-4.00	-2.89	4.1	0.9	--	6	--	--	--	--	0
PCNT-102	178	1	2	4	3	-3.36	-3.36	0.7	--	--	--	--	--	--	--	0
PC DC-3	65	1,000	5	2	3	-23.30	-6.33	14.2	3.4	5.3	--	--	--	--	--	0

(4 of 4 sheets)

TABLE A.4 CRATER DATA FOR DRY CLAY

Shot Identification	Bibliography Number	Charge Yield (TNT-Equivalent)	Type of Explosive	Moisture Code	Medium Code	Height of Burst	Scaled Height of Burst $\bar{Z}$	Apparent Crater Radius R_a	Apparent Crater Depth D_a	Apparent Crater Lip Height h	Volume of Apparent Crater V_a	True Crater Radius R_t	True Crater Depth D_t	Volume of True Crater V_t	Angle of Crater Slope	Crater Shape Code
		pounds				feet	$ft/lb^{1/3}$	feet	feet	feet	ft^3	feet	feet	ft^3	degrees	
Scaled Height of Burst Greater Than +0.50, Category 1:																
UET-301	60	380	1	2	4	3.50	0.51	2.5	1.0	--	--	2.5	1.0	--	[illegible]	[illegible]
Scaled Height of Burst Less Than +0.50 and Greater Than +0.20, Category 2:																
MOLE-111	44	256	1	2	4	1.65	0.26	--	-		--	--	--	750	--	0
Scaled Height of Burst Less Than +0.20 and Greater Than +0.05, Category 3:																
MOLE-104	45	256	1	2	4	0.83	0.13	5.4	1.4	0.4	60	--	--	490	26	3
Scaled Height of Burst Less Than +0.05 and Greater Than -0.05, Category 4:																
MOLE-107	45	256	1	2	4	0.00	0.00	6.6	3.9	1.	232	--	--	1,[illegible]	42	3
UET-302	60	380	1	2	4	0.00	0.00	7.2	4.0	--	360	9.7	5.3	600	24	3
Scaled Height of Burst Less Than -0.05 and Greater Than -0.20, Category 5:																
UET-303	60	380	1	2	4	-1.30	-0.19	9.0	5.5	--	600	13.5	7.0	2,300	38	0
UET-308	60	2,560	1	2	4	-2.60	-0.19	20.0	12.0	--	9,600	24.5	13.5	10,000	51	0
Scaled Height of Burst Less Than -0.20 and Greater Than -0.50, Category 6:																
MOLE-106	45	256	1	2	4	-1.65	-0.26	9.1	6.2	0.7	538	--	--	3,560	31	3
Scaled Height of Burst Less Than -0.50 and Greater Than -0.90, Category 7:																
MOLE-102	45	256	1	2	4	-3.15	-0.50	10.2	6.4	0.6	410	--	--	3,120	[illegible]	[illegible]
MOLE-102A	45	256	1	2	4	-3.15	-0.50	9.6	5.3	0.9	445	--	--	4,470	[illegible]	[illegible]
UET-316	60	110	1	2	4	-2.65	-0.51	7.0	4.0	--	360	--	--	--	[illegible]	[illegible]
UET-306	60	380	1	2	4	-3.50	-0.51	10.5	6.0	--	920	13.7	10.0	3,120	[illegible]	[illegible]
UET-310	60	380	1	2	4	-3.50	-0.51	11.0	7.0	--	600	14.5	10.0	2,500	[illegible]	[illegible]
UET-313	60	380	1	2	4	-3.50	-0.51	12.7	8.0	--	1,530	15.2	9.4	3,000	[illegible]	[illegible]
UET-309	60	2,560	1	2	4	-7.00	-0.51	21.4	15.5	--	7,800	29.5	17.4	19,000	[illegible]	[illegible]
UET-312	60	2,560	1	2	4	-7.00	-0.51	24.0	15.0	--	13,000	30.4	19.0	24,000	[illegible]	[illegible]
UET-317	60	2,560	1	2	4	-7.00	-0.51	23.0	15.5	--	11,000	27.5	17.0	14,000	[illegible]	[illegible]
UET-319	60	2,560	1	2	4	-7.00	-0.51	23.0	13.5	--	7,[illegible]30	25.0	17.0	17,000	[illegible]	[illegible]
UET-311	60	40,000	1	2	4	-17.50	-0.51	64.0	42.0	--	190,000	78.0	47.0	[illegible]0,000	[illegible]	[illegible]
UET-318	60	380,000	1	2	4	-35.00	-0.51	120.0	60.0	--	1,100,000	130.0	77.0	1,[illegible]00,000	[illegible]	[illegible]
RAW-59	53	378	1	2	4	-4.50	-0.62	20.0	9.3	--	--	--	--	--	[illegible]	[illegible]
Scaled Height of Burst Less Than -0.90 and Greater Than -1.10, Category 8:																
UET-311	60	8	1	2	4	-8.00	-1.00	4.0	2.5	--	16	9.5	5.0	250	[illegible]	[illegible]
MOLE-101	45	256	1	2	4	-6.35	-1.00	10.5	5.4	1.2	742	--	--	4,[illegible]20	[illegible]	[illegible]
MOLE-105	45	256	1	2	4	-6.35	-1.00	10.9	5.8	1.6	857	--	--	5,[illegible]40	[illegible]	[illegible]
UET-305	60	380	1	2	4	-7.00	-1.02	11.7	7.0	--	1,300	14.5	11.5	4,000	[illegible]	[illegible]
UET-ETHEY	60	380	1	2	4	-7.00	-1.02	12.5	7.0	--	1,330	15.0	10.5	3,500	41	0
Scaled Height of Burst Less Than -1.10 and Greater Than -2.00, Category 9:																
UET-314	60	8	1	2	4	-8.50	-1.25	3.0	1.0	--	86	6.5	4.7	230	42	0
RAW-55	53	378	1	2	4	-8.40	-1.16	21.2	8.8	--	--	--	--	--	--	--
RAW-62	53	378	1	2	4	-8.50	-1.15	20.5	11.1	--	--	--	--	--	--	--
RAW-60	53	378	1	2	4	-8.70	-1.20	19.9	7.8	--	--	--	--	--	--	--
RAW-5C	53	378	1	2	4	-9.00	-1.24	18.2	9.0	--	--	--	--	--	--	--
Scaled Height o. Burst Less Than -2.00, Category 10.																
UET-315	60	380	1	2	4	-14.00	-2.05	15.0	1.0	--	236	20.0	14.0	9,300	16	0
UET-307	60	380	1	2	4	-21.00	-3.07	10.0	1.0	--	100	15.5	26.[illegible]	9,[illegible]00	20	0

TABLE 4.5 CRATER DATA FOR NOISE CLAY

Shot Identification	Bibliography Number	Charge Yield (TNT-Equivalent)	Type of Explosive	Moisture Code	Medium Code	Height of Burst	Scaled Height of Burst $\bar{z}$	Apparent Crater Radius r_a	Apparent Crater Depth d_a	Apparent Crater Lip Height h	Volume of Apparent Crater V_a	True Crater Radius r_t	True Crater Depth d_t	Volume of True Crater V_t	Angle of Crater Slope	Crater Shape Code
		pounds				feet	$ft/lb^{1/3}$	feet	feet	feet	ft^3	feet	feet	ft^3	degrees	
Scaled Height of Burst Greater Than +0.50, Category 1:																
							No Data Available									
Scaled Height of Burst Less Than +0.50 and Greater Than +0.20, Category 2:																
							No Data Available									
Scaled Height of Burst Less Than +0.20 and Greater Than +0.05, Category 3:																
							No Data Available									
Scaled Height of Burst Less Than +0.05 and Greater Than -0.05, Category 4:																
CHINC-57	11	1	2	b	b	0.00	0.00	1.5	0.6	0.0	2	1.5	0.9	2	23	c
LCSSC-6	24	85	1	b	b	0.00	0.00	3.8	2.1	--	33	4.9	2.5	64	24	c
Scaled Height of Burst Less Than -0.05 and Greater Than -0.20, Category 5:																
							No Data Available									
Scaled Height of Burst Less Than -0.20 and Greater Than -0.50, Category 6:																
PCE-EL-31	166	36.8	6	b	b	-1.50	-0.45	6.0	3.8	0.4	175	7.0	5.4	394	51	c
PCE-EL-32[a]	166	36.8	6	b	b	-1.50	-0.45	6.0	3.6	0.4	170	7.0	5.3	374	51	c
PCE-EL-34	166	36.8	6	b	b	-1.50	-0.45	6.7	3.8	0.5	199	7.9	5.7	467	51	c
PCE-EL-35[a]	166	36.8	6	b	b	-1.50	-0.45	6.6	4.0	0.5	226	7.9	5.4	433	51	c
PCE-EL-36	166	36.8	6	b	b	-1.50	-0.45	7.0	4.6	0.5	289	8.0	6.1	626	51	c
PCE-EL-37[a]	166	36.8	6	b	b	-1.50	-0.45	6.5	4.0	0.6	226	7.0	5.3	358	54	c
PCE-EL-38	166	36.8	6	b	b	-1.50	-0.45	7.0	4.4	0.4	277	7.5	5.8	459	51	c
PCE-EL-39[a]	166	36.8	6	b	b	-1.50	-0.45	6.4	4.1	0.6	216	6.5	5.6	320	51	c
PCE-EL-40	166	36.8	6	b	b	-1.50	-0.45	6.5	3.8	0.6	199	6.5	5.6	309	51	c
PCE-EL-41[a]	166	36.8	6	b	b	-1.50	-0.45	6.2	3.6	0.4	162	6.5	5.0	334	54	c
PCE-EL-47	166	36.8	6	b	b	-1.50	-0.45	7.6	4.3	0.9	365	8.0	5.7	527	51	c
PCE-EL-10	166	27	2	b	b	-1.50	-0.50	6.6	4.5	0.5	292	6.6	5.4	365	58	c
PCE-EL-11[a]	166	27	2	b	b	-1.50	-0.50	6.5	4.3	0.5	274	6.9	5.8	437	57	c
PCE-EL-15	166	27	2	b	b	-1.50	-0.50	6.4	4.6	0.4	287	7.0	5.9	467	61	c
PCE-EL-16[a]	166	27	2	b	b	-1.50	-0.50	5.4	3.2	0.2	126	6.0	5.0	213	51	c
PCE-EL-20	166	27	2	b	b	-1.50	-0.50	6.8	4.0	0.4	213	7.5	5.5	344	58	c
PCE-EL-21[a]	166	27	2	b	b	-1.50	-0.50	6.7	4.0	0.5	229	--	--	--	54	c
PCE-EL-33	166	27	2	b	b	-1.50	-0.50	6.1	4.2	0.5	196	6.5	5.4	374	54	c
Scaled Height of Burst Less Than -0.50 and Greater Than -0.90, Category 7:																
TCSSC-1	24	25	1	b	b	-1.50	-0.91	5.7	2.9	--	94	6.4	4.2	154	45	c
SE-A-1[a]	165	27	2	b	b	-2.25	-0.75	6.5	3.2	0.6	152	7.5	5.5	378	51	c
SE-A-2[a]	165	27	2	b	b	-2.25	-0.75	6.0	3.4	0.6	160	7.5	5.4	414	61	c
SE-A-3	165	27	2	b	b	-2.25	-0.75	6.5	3.7	0.6	227	7.5	5.6	501	61	c
SE-A-4	165	27	2	b	b	-2.25	-0.75	6.0	3.1	0.7	147	6.5	5.2	326	65	c
Scaled Height of Burst Less Than -0.90 and Greater Than -1.10, Category 8:																
SEU S-22[a]	162	36.8	6	b	b	-3.00	-0.90	7.5	3.8	0.5	373	8.5	6.6	654	58	c
SEU S-23[a]	162	36.8	6	b	b	-3.00	-0.90	7.5	4.0	0.6	395	8.0	6.5	510	72	c

(Continued)

[a] Unstemmed.

TABLE A.5 (CONCLUDED)

Shot Identification	Bibliography Number	Charge Yield (TNT-Equivalent)	Type of Explosive	Moisture Code	Medium Code	Height of Burst	Scaled Height of Burst Z	Apparent Crater Radius r_a	Apparent Crater Depth d_a	Apparent Crater Lip Height h	Volume of Apparent Crater v_a	True Crater Radius r_t	True Crater Depth d_t	Volume of True Crater v_t	Angle of Crater Slope	Crater Shape Code
		pounds				feet	$ft/lb^{1/3}$	feet	feet	feet	ft^3	feet	feet	ft^3	degrees	
Scaled Height of Burst Less Than -0.90 and Greater Than -1.10, Category 8 (Continued):																
[illegible]	162	[illegible]	6	4	4	-3.00	-0.90	7.5	4.0	0.5	338	8.0	6.6	530	[illegible]	0
[illegible]	162	[illegible]	6	4	4	-3.00	-0.90	8.5	4.9	0.6	458	9.0	6.7	716	[illegible]	0
[illegible]	162	[illegible]	6	4	4	-3.00	-0.90	8.9	4.9	0.7	535	9.0	6.9	731	[illegible]	0
[illegible]	162	[illegible]	6	4	4	-3.00	-0.90	7.5	5.0	0.5	503	8.5	6.7	693	[illegible]	0
[illegible]	162	[illegible]	6	4	4	-3.00	-0.90	8.0	5.6	0.6	674	9.0	6.7	737	[illegible]	0
[illegible]	162	[illegible]	6	4	4	-3.00	-0.90	8.5	5.1	0.5	681	9.0	6.9	768	[illegible]	0
CHINC-36	11	1	2	4	4	-1.00	-1.00	2.3	1.3	0.2	3	2.3	2.0	14	[illegible]	8
PCE-EI-8	166	27	2	4	4	-3.00	-1.00	6.6	3.4	0.4	182	--	--	--	[illegible]	0
PCE-EI-9	166	27	2	4	4	-3.00	-1.00	6.1	3.0	0.5	327	6.9	6.8	388	[illegible]	0
PCE-EI-12[a]	166	27	2	4	4	-3.00	-1.00	6.0	2.7	0.4	176	6.0	5.9	250	[illegible]	0
PCE-EI-13	166	27	2	4	4	-3.00	-1.00	6.7	4.4	0.4	372	7.5	6.6	455	[illegible]	0
PCE-EI-14[a]	166	27	2	4	4	-3.00	-1.00	6.6	3.3	0.2	150	7.0	6.1	378	[illegible]	0
PCE-EI-17[a]	166	27	2	4	4	-3.00	-1.00	4.8	2.9	0.3	115	6.0	6.2	346	[illegible]	0
PCE-EI-18	166	27	2	4	4	-3.00	-1.00	7.3	4.3	0.7	288	7.9	7.1	554	[illegible]	[illegible]
PCE-EI-19[a]	166	27	2	4	4	-3.00	-1.00	6.1	3.4	0.5	178	7.0	6.4	347	[illegible]	0
PCE-EI-20[a]	166	27	2	4	4	-3.00	-1.00	6.0	3.3	0.6	166	7.7	6.3	318	[illegible]	0
PCE-EI-23	166	27	2	4	4	-3.00	-1.00	6.7	3.9	0.5	230	7.0	6.6	373	[illegible]	0
PCE-EI-24[a]	166	27	2	4	4	-3.00	-1.00	5.3	2.2	0.5	80	6.0	6.0	317	[illegible]	[illegible]
[illegible]	162	27	2	4	4	-3.00	-1.00	6.0	2.2	0.6	104	6.7	5.4	[illegible]	[illegible]	[illegible]
[illegible]	162	27	2	4	4	-3.00	-1.00	5.8	2.7	0.5	128	6.8	5.6	296	[illegible]	0
[illegible]	162	27	2	4	4	-3.00	-1.00	5.7	2.9	0.6	127	6.3	5.6	288	[illegible]	0
[illegible]	162	27	2	4	4	-3.00	-1.00	6.7	3.2	0.7	156	8.0	6.2	451	[illegible]	0
[illegible]	162	27	2	4	4	-3.00	-1.00	7.0	3.3	0.6	213	8.0	6.3	536	[illegible]	0
[illegible]	162	27	2	4	4	-3.00	-1.00	6.6	2.8	0.7	169	7.3	6.2	369	[illegible]	0
[illegible]	162	27	2	4	4	-3.00	-1.00	6.5	3.0	0.8	178	7.5	6.0	413	[illegible]	0
[illegible]	162	27	2	4	4	-3.00	-1.00	6.5	3.1	0.6	152	7.5	6.2	459	[illegible]	0
[illegible]	162	27	2	4	4	-3.00	-1.00	6.7	3.4	0.6	151	7.1	6.3	398	[illegible]	0
[illegible]	162	27	2	4	4	-3.00	-1.00	7.0	3.9	0.4	234	8.0	6.0	456	[illegible]	0
[illegible]	162	27	2	4	4	-3.00	-1.00	7.0	4.7	0.5	288	7.5	6.2	450	[illegible]	0
[illegible]	162	27	2	4	4	-3.00	-1.00	6.9	4.0	0.5	223	7.9	6.2	460	[illegible]	0
[illegible]	162	27	2	4	4	-3.00	-1.00	7.0	4.1	0.6	244	7.5	6.1	422	[illegible]	0
[illegible]	162	27	2	4	4	-3.00	-1.00	6.5	4.0	0.7	230	7.0	6.1	379	[illegible]	0
ICSNC-5	36	200	1	4	4	-2.00	-1.03	10.9	9.4	--	3,550	--	--	--	[illegible]	0
Scaled Height of Burst Less Than -1.10 and Greater Than -2.00, Category 9:																
ICSNC-7	36	35	1	4	4	-4.50	-1.54	7.3	3.2	--	213	9.8	7.2	1,410	[illegible]	0
ICSNC-4	36	75	1	4	4	-5.00	-1.50	10.9	5.0	--	747	--	--	--	[illegible]	0
Scaled Height of Burst Less Than -2.00, Category 10:																
ICSNC-3	36	8	1	4	4	-5.00	-2.50	4.3	1.7	--	46	5.4	4.3	233	[illegible]	0
ICSNC-2	36	75	1	4	4	-12.00	-2.85	12.3	1.[illegible]	--	376	--	--	--	[illegible]	0
ICSNC-8	36	8	1	4	4	-7.30	-3.50	3.5	2.5	--	56	--	--	--	[illegible]	0

[a] Unstemmed.

[b] One-third stemmed.

[c] Two-thirds stemmed.

TABLE A.6 CRATER DATA FOR WET CLAY

Shot Identification	Bibliography Number	Charge Yield (TNT-Equivalent)	Type of Explosive	Moisture Code	Medium Code	Height of Burst	Scaled Height of Burst Z	Apparent Crater Radius r_a	Apparent Crater Depth d_a	Apparent Crater Lip Height h	Volume of Apparent Crater v_a	True Crater Radius r_t	True Crater Depth d_t	Volume of True Crater v_t	Angle of Crater Slope	Crater Shape Code
		pounds				feet	$ft/lb^{1/3}$	feet	feet	feet	ft^3	feet	feet	ft^3	degrees	
Scaled Height of Burst Greater Than +0.50, Category 1:																
No Data Available																
Scaled Height of Burst Less Than +0.50 and Greater Than +0.20, Category 2:																
No Data Available																
Scaled Height of Burst Less Than +0.20 and Greater Than +0.05, Category 3:																
MOLE-313	11	256	1	7	4	0.83	0.13	6.1	3.4	--	163	--	--	--	38	0
Scaled Height of Burst Less Than +0.05 and Greater Than -0.05, Category 4:																
ICSM-15	23	25	1	7	4	0.00	0.00	5.7	3.9	0.9	217	--	--	--	59	0
ICSM-16 1A	23	50	1	7	4	0.00	0.00	7.2	5.0	--	484	--	--	--	69	0
ICSM-17 2A	23	50	1	7	4	0.00	0.00	7.6	5.0	--	499	--	--	--	74	0
EUE B-62	30	64	1	7	4	0.00	0.00	3.4	--	--	--	--	--	--	--	0
Scaled Height of Burst Less Than -0.05 and Greater Than -0.20, Category 5:																
No Data Available																
Scaled Height of Burst Less Than -0.20 and Greater Than -0.50, Category 6:																
UETP-402	60	320	1	7	4	-2.50	-0.37	18.7	10.0	--	4,100	23.5	--	--	44	0
UETP-404	60	320	1	7	4	-2.50	-0.37	17.5	11.5	--	3,000	24.0	--	--	54	0
UETP-403	60	2,560	1	7	4	-5.00	-0.37	41.7	12.7	--	29,000	45.2	--	--	41	0
ICSM-1	23	8	1	7	4	-1.00	-0.50	5.2	4.3	1.5	232	--	--	--	75	0
MOLE-311	11	256	1	7	4	-3.15	-0.50	15.5	11.2	--	3,147	--	--	--	47	0
MOLE-312	11	256	1	7	4	-3.15	-0.50	17.5	9.1	--	3,345	--	--	--	39	0
Scaled Height of Burst Less Than -0.50 and Greater Than -0.90, Category 7:																
ICSM-05	23	25	1	7	4	-1.50	-0.51	8.9	6.6	1.2	704	--	--	--	49	0
EUE B-60	30	64	1	7	4	-2.10	-0.52	8.0	--	--	--	--	--	--	--	0
EUE B-61	30	64	1	7	4	-2.10	-0.52	8.0	--	--	--	--	--	--	--	0
EUE C-42	30	64	1	7	4	-2.10	-0.52	8.0	--	--	--	--	--	--	--	0
EUE C-43	30	64	1	7	4	-2.10	-0.52	10.0	--	--	--	--	--	--	--	0
Scaled Height of Burst Less Than -0.90 and Greater Than -1.10, Category 8:																
ICSM-12	23	75	1	7	4	-4.00	-0.95	12.6	9.3	2.1	2,030	--	--	--	49	0
ICSM-06	23	25	1	7	4	-3.00	-1.03	9.1	6.6	0.9	876	--	--	--	57	0
EUE B-21	30	64	1	7	4	-4.20	-1.05	10.5	--	--	--	--	--	--	--	0
EUE C-40	30	64	1	7	4	-4.20	-1.05	10.0	--	--	--	--	--	--	--	0
EUE C-41	30	64	1	7	4	-4.20	-1.05	10.0	7.0	--	1,400	13.0	11.5	2,900	42	0
EUE C-44	30	64	1	7	4	-4.20	-1.05	10.0	--	--	--	--	--	--	--	0
EUE C-45	30	64	1	7	4	-4.20	-1.05	9.5	--	--	--	--	--	--	--	0

(Continued)

TABLE A.6 (CONTINUED)

Shot Identification	Bibliography Number	Charge Yield (TNT-Equivalent)	Type of Explosive	Moisture Code	Medium Code	Height of Burst	Scaled Height of Burst Z	Apparent Crater Radius r_a	Apparent Crater Depth d_a	Apparent Crater Lip Height h	Volume of Apparent Crater V_a	True Crater Radius r_t	True Crater Depth d_t	Volume of True Crater V_t	Angle of Crater Slope	Crater Shape Code
		pounds				feet	$ft/lb^{1/3}$	feet	feet	feet	ft^3	feet	feet	ft^3	degrees	
Scaled Height of Burst Less Than -0.90 and Greater Than -1.10, Category 8 (Continued):																
HUE C-46	30	64	1	7	4	-4.20	-1.05	9.5	--	--	--	--	--	--	--	0
HUE C-47	30	64	1	7	4	-4.20	-1.05	9.0	--	--	--	--	--	--	--	0
HUE C-49	30	64	1	7	4	-4.20	-1.05	10.0	--	--	--	--	--	--	--	0
HUE C-98	30	64	1	7	4	-4.20	-1.05	9.0	--	--	--	--	--	--	--	0
HUE C-99	30	64	1	7	4	-4.20	-1.05	9.5	--	--	--	--	--	--	--	0
HUE X-1	30	64	1	7	4	-4.20	-1.05	10.7	--	--	--	--	--	--	--	0
HUE X-5	30	64	1	7	4	-4.20	-1.05	9.9	--	--	--	--	--	--	--	0
HUE X-6	30	64	1	7	4	-4.20	-1.05	11.9	--	--	--	--	--	--	--	0
HUE X-7	30	64	1	7	4	-4.20	-1.05	10.7	--	--	--	--	--	--	--	0
HUE X-8	30	64	1	7	4	-4.20	-1.05	10.3	--	--	--	--	--	--	--	0
HUE X-9	30	64	1	7	4	-4.20	-1.05	9.9	--	--	--	--	--	--	--	0
HUE X-10	30	64	1	7	4	-4.20	-1.05	9.9	--	--	--	--	--	--	--	0
Scaled Height of Burst Less Than -1.10 and Greater Than -2.00, Category 9:																
UETP-405	60	8	1	7	4	-2.50	-1.25	6.0	4.1	--	270	8.0	--	--	51	0
ICSM-02	23	8	1	7	4	-3.00	-1.50	6.6	5.1	1.0	257	--	--	--	41	0
ICSM-07	23	25	1	7	4	-4.50	-1.54	7.7	6.2	2.0	737	--	--	--	101	0
UETP-401	60	8	1	7	4	-2.50	-1.25	7.0	5.0	--	310	10.0	--	--	47	0
HUE B-19	30	64	1	7	4	-6.30	-1.57	11.0	--	--	--	--	--	--	--	0
HUE B-20	30	64	1	7	4	-6.30	-1.57	11.0	--	--	--	--	--	--	--	0
HUE C-34	30	64	1	7	4	-6.30	-1.57	10.0	--	--	--	--	--	--	--	0
HUE C-35	30	64	1	7	4	-6.30	-1.57	10.0	7.0	--	1,360	14.0	11.5	3,600	60	0
HUE X-14	30	64	1	7	4	-6.30	-1.57	7.5	--	--	--	--	--	--	--	0
HUE X-15	30	64	1	7	4	-6.30	-1.57	7.7	--	--	--	--	--	--	--	0
HUE X-16	30	64	1	7	4	-6.30	-1.57	7.2	--	--	--	--	--	--	--	0
HUE X-17	30	64	1	7	4	-6.30	-1.57	9.0	--	--	--	--	--	--	--	0
HUE X-19	30	64	1	7	4	-6.30	-1.57	6.7	--	--	--	--	--	--	--	0
HUE X-20	30	64	1	7	4	-6.30	-1.57	7.8	--	--	--	--	--	--	--	0
HUE X-21	30	64	1	7	4	-6.30	-1.57	6.5	--	--	--	--	--	--	--	0
HUE X-22	30	64	1	7	4	-6.30	-1.57	5.2	--	--	--	--	--	--	--	0
HUE X-23	30	64	1	7	4	-6.30	-1.57	6.5	--	--	--	--	--	--	--	0
HUE B-22	30	64	1	7	4	-6.60	-1.60	10.3	--	--	--	--	--	--	--	0
HUE A-1	30	64	1	7	4	-7.00	-1.75	13.0	--	--	--	--	--	--	--	0
HUE A-3	30	64	1	7	4	-7.50	-1.87	13.6	--	--	--	--	--	--	--	0
PG SC-1	48	1,000	5	7	4	-19.10	-1.91	7.1	2.8	3.7	--	--	--	--	--	0
Scaled Height of Burst Less Than -2.00, Category 10:																
ICSM-8	23	25	1	7	4	-6.00	-2.09	6.5	6.0	2.5	574	--	--	--	74	0
ICSM-14	23	200	1	7	4	-12.00	-2 05	33.1	2.5	0.6	3,410	--	--	--	--	0
HUE A-2	30	64	1	7	4	-8.40	-2.10	12.5	--	--	--	--	--	--	--	0
HUE A-4	30	64	1	7	4	-8.40	-2.10	12.8	--	--	--	--	--	--	--	0
HUE A-5	30	64	1	7	4	-8.40	-2.10	14.2	--	--	--	--	--	--	--	0

(Continued)

TABLE A.6 (CONCLUDED)

Shot Identification	Bibliography Number	Charge Yield (TNT-Equivalent)	Type of Explosive	Moisture Code	Medium Code	Height of Burst	Scaled Height of Burst $\bar{z}$	Apparent Crater Radius r_a	Apparent Crater Depth d_a	Apparent Crater Lip Height h	Volume of Apparent Crater V_a	True Crater Radius r_t	True Crater Depth d_t	Volume of True Crater V_t	Angle of Crater Slope	Crater Shape Code
		pounds				feet	$ft/lb^{1/3}$	feet	feet	feet	ft^3	feet	feet	ft^3	degrees	
Scaled Height of Burst Less Than -2.00, Category 10 (Continued):																
HUE A-6	30	6	1	7	4	-8.40	-2.10	11.8	--	--	--	--	--	--	--	0
HUE A-7	30	6	1	7	4	-8.40	-2.10	12.0	--	--	--	--	--	--	--	0
HUE A-8	30	6	1	7	4	-8.40	-2.10	10.0	--	--	--	--	--	--	--	0
HUE A-9	30	6	1	7	4	-8.40	-2.10	12.0	--	--	--	--	--	--	--	0
HUE A-10	30	6	1	7	4	-8.40	-2.10	11.5	--	--	--	--	--	--	--	0
HUE A-24	30	6	1	7	4	-8.40	-2.10	12.0	--	--	--	--	--	--	--	0
HUE A-25	30	6	1	7	4	-8.40	-2.10	11.2	--	--	--	--	--	--	--	0
HUE B-16	30	6	1	7	4	-8.40	-2.10	11.5	--	--	--	--	--	--	--	0
HUE B-18	30	6	1	7	4	-8.40	-2.10	10.0	--	--	--	--	--	--	--	0
HUE B-27	30	6	1	7	4	-8.40	-2.10	10.5	--	--	--	--	--	--	--	0
HUE C-32	30	6	1	7	4	-8.40	-2.10	11.0	--	--	--	--	--	--	--	0
HUE C-33	30	6	1	7	4	-8.40	-2.10	12.6	--	--	--	--	--	--	--	0
HUE C-36	30	6	1	7	4	-8.40	-2.10	11.0	--	--	--	--	--	--	--	0
HUE C-37	30	6	1	7	4	-8.40	-2.10	12.5	5.8	--	900	14.2	14.3	3,800	64	0
HUE C-50	30	6	1	7	4	-8.40	-2.10	9.5	--	--	--	--	--	--	--	0
HUE C-51	30	6	1	7	4	-8.40	-2.10	11.0	--	--	--	--	--	--	--	0
HUE C-56	30	6	1	7	4	-8.40	-2.10	10.0	--	--	--	--	--	--	--	0
HUE C-57	30	6	1	7	4	-8.40	-2.10	9.5	--	--	--	--	--	--	--	0
ICHM-3	23	5	1	7	4	-5.00	-2.50	8.9	1.6	0.4	163	--	--	--	--	0
ICHM-9	23	25	1	7	4	-7.50	-2.96	11.0	3.0	1.0	446	--	--	--	--	0
ICHM-13	23	73	1	7	4	-12.00	-2.85	19.5	2.6	0.9	1,310	--	--	--	--	0
HUE C-29	30	6	1	7	4	-11.60	-2.60	10.5	--	--	--	--	--	--	--	0
ICHM-10	23	25	1	7	4	-9.00	-3.08	11.8	2.0	1.0	402	--	--	--	--	0
HUE B-14	30	6	1	7	4	-12.60	-3.15	10.0	--	--	--	--	--	--	--	0
HUE B-15	30	6	1	7	4	-12.60	-3.15	10.0	--	--	--	--	--	--	--	0
HUE B-17	30	6	1	7	4	-12.60	-3.15	8.5	--	--	--	--	--	--	--	0
HUE B-26	30	6	1	7	4	-12.60	-3.15	9.8	--	--	--	--	--	--	--	0
HUE C-28	30	6	1	7	4	-12.60	-3.15	8.0	--	--	--	--	--	--	--	0
HUE C-38	30	6	1	7	4	-12.60	-3.15	9.0	--	--	--	--	--	--	--	0
HUE C-39	30	6	1	7	4	-12.60	-3.15	9.5	3.1	--	470	12.0	16.4	3,400	--	0
HUE C-52	30	6	1	7	4	-12.60	-3.15	9.5	--	--	--	--	--	--	--	0
HUE C-53	30	6	1	7	4	-12.60	-3.15	8.5	--	--	--	--	--	--	--	0
HUE C-54	30	6	1	7	4	-12.60	-3.15	8.0	--	--	--	--	--	--	--	0
HUE C-55	30	6	1	7	4	-12.60	-3.15	9.0	--	--	--	--	--	--	--	0
ICHM-4	23	5	1	7	4	-7.00	-3.50	4.5	3.1	1.5	138	--	--	--	79	0
HUE B-11	30	6	1	7	4	-14.30	-3.57	4.9	--	--	--	--	--	--	--	0
ICHM-11	23	25	1	7	4	-10.50	-3.59	11.3	2.9	1.5	291	--	--	--	--	0
HUE B-12	30	6	1	7	4	-16.80	-4.20	4.0	--	--	--	--	--	--	--	0
HUE B-13	30	6	1	7	4	-16.80	-4.20	4.4	--	--	--	--	--	--	--	0
HUE C-30	30	6	1	7	4	-16.80	-4.20	4.5	--	--	--	--	--	--	--	0
HUE C-31	30	6	1	7	4	-16.80	-4.20	5.6	--	--	--	--	--	--	--	0

(3 of 3 sheets)

TABLE A.7 CRATER DATA FOR MOIST LOESS AND MOIST LACUSTRINE SILT

Shot Identification	Bibliography Number	Charge Yield (TNT-Equivalent)	Type of Explosive	Moisture Code	Medium Code	Height of Burst	Scaled Height of Burst Z	Apparent Crater Radius r_a	Apparent Crater Depth d_a	Apparent Crater Lip Height h	Volume of Apparent Crater v_a	True Crater Radius r_t	True Crater Depth d_t	Volume of True Crater v_t	Angle of Crater Slope	Crater Shape Code
		pounds				feet	$ft/lb^{1/3}$	feet	feet	feet	ft^3	feet	feet	ft^3	degrees	
Scaled Height of Burst Greater Than +0.50, Category 1:																
							No Data Available									
Scaled Height of Burst Less Than +0.50 and Greater Than +0.20, Category 2:																
							No Data Available									
Scaled Height of Burst Less Than +0.20 and Greater Than +0.05, Category 3:																
AW II 01	5	256	1	3	5	0.86	0.14	3.2	0.8	--	13	4.1	2.5	73	41	4
AHC 1A	6	50	4	4	5	0.52	0.14	3.2	1.8	--	--	3.2	1.8	--	--	3
AHC 2A	6	50	4	4	5	0.52	0.14	2.7	1.9	0.3	--	2.7	1.9	--	--	0
AHC 3A	6	50	1	4	5	0.50	0.14	3.4	2.1	0.2	--	3.6	2.3	--	--	0
AHC 4A	6	50	1	4	5	0.50	0.14	3.2	2.1	0.2	--	3.7	2.2	--	--	0
AHC 5A	6	50	4	4	5	0.60	0.16	2.7	1.5	0.1	--	2.8	1.8	--	--	0
AHC 6A	6	50	4	4	5	0.60	0.16	2.8	1.4	0.2	--	3.4	1.6	--	--	0
Scaled Height of Burst Less Than +0.05 and Greater Than -0.05, Category 4:																
CESDC-19	11	1	2	5	5	0.00	0.00	1.2	0.6	0.0	1	1.2	0.8	1	15	0
CESDC-25	11	1	2	5	5	0.00	0.00	1.2	0.5	0.1	1	1.4	0.5	1	23	0
FT II	33	50,000	1	2	5	0.00	0.00	35.8	11.3	3.9	24,030	38.0	15.3	43,200	--	0
FT III	33	50,000	1	3	5	0.00	0.00	38.8	18.0	5.3	37,800	44.0	23.0	62,1[illegible]	--	0
AW III 02A	5	1,000	1	3	5	0.00	0.00	9.4	4.3	--	442	10.7	6.7	1,007	--	0
AW III 02B	5	1,000	1	3	5	0.00	0.00	10.1	4.5	--	517	11.1	6.3	1,027	--	0
AW III 02C	5	1,000	1	3	5	0.00	0.00	8.9	4.3	--	440	11.1	6.1	1,007	--	0
AW III 03A	5	6,000	1	3	5	0.00	0.00	16.4	6.6	--	2,520	20.0	8.9	4,749	--	0
AW III 03B	5	6,000	1	3	5	0.00	0.00	17.5	6.0	--	2,703	--	--	--	--	0
AW II 02A	5	256	1	3	5	0.00	0.00	5.4	2.4	--	95	6.3	4.3	230	27	1
AW II 02B	5	256	1	3	5	0.00	0.00	5.4	2.4	--	93	--	--	--	--	0
AW III 01A	5	64	1	3	5	0.00	0.00	3.4	1.6	--	24	4.2	2.6	60	--	0
AW III 01B	5	64	1	3	5	0.00	0.00	3.4	1.8	--	26	3.8	2.6	51	--	0
AW III 01C	5	64	1	3	5	0.00	0.00	3.3	1.8	--	23	3.9	2.8	55	--	0
AW III 01D	5	64	1	3	5	0.00	0.00	3.5	1.9	--	28	3.9	2.6	51	--	0
AHC 1B	6	50	4	4	5	0.00	0.00	4.3	2.7	0.4	--	--	--	--	--	0
AHC 2B	6	50	4	4	5	0.00	0.00	4.3	2.8	0.3	--	5.5	3.4	--	--	0
AHC 3B	6	50	4	4	5	0.00	0.00	5.1	2.8	0.5	--	6.2	3.4	--	--	0
AHC 4B	6	50	1	4	5	0.00	0.00	4.4	3.0	0.4	--	6.4	3.2	--	--	0
AHC 5B	6	50	4	4	5	0.00	0.00	4.6	2.9	0.4	--	5.5	3.5	--	--	0
Scaled Height of Burst Less Than -0.05 and Greater Than -0.20, Category 5:																
AW II 03	5	256	1	3	5	-0.87	-0.14	6.7	3.4	--	235	8.3	5.2	387	25	1
AHC 1C	6	50	4	4	5	-0.52	-0.14	6.1	3.6	0.4	--	7.4	4.5	--	--	0
AHC 2C	6	50	4	4	5	-0.52	-0.14	6.2	3.7	0.9	--	6.7	4.3	--	--	0
AHC 3C	6	50	1	4	5	-0.50	-0.14	5.6	3.8	0.4	--	6.4	4.2	--	--	0
AHC 4C	6	50	4	4	5	-0.60	-0.16	6.0	3.4	0.9	--	6.0	4.8	--	--	0
AHC 5C	6	50	4	4	5	-0.60	-0.16	6.3	4.2	0.8	--	7.4	5.0	--	--	0

(Continued)

TABLE A.7 (CONCLUDED)

Shot Identification	Bibliography Number	Charge Yield (TNT-Equivalent)	Type of Explosive	Moisture Code	Medium Code	Height of Burst	Scaled Height of Burst Z	Apparent Crater Radius r_a	Apparent Crater Depth d_a	Apparent Crater Lip Height h	Volume of Apparent Crater V_a	True Crater Radius r_t	True Crater Depth d_t	Volume of True Crater V_t	Angle of Crater Slope	Crater Shape Code
		pounds				feet	$ft/lb^{1/3}$	feet	feet	feet	ft^3	feet	feet	ft^3	degrees	
Scaled Height of Burst Less Than -0.20 and Greater Than -0.90, Category 6:																
CESDC-23	11	1	2	5	5	-0.50	-0.50	2.0	1.2	0.3	4	2.2	1.4	7	21	0
CESDC-27	11	1	2	5	5	-0.50	-0.50	2.0	1.0	0.1	4	2.0	1.5	6	20	0
AV II 04	4	256	1	3	5	-1.59	-0.25	7.6	3.7	--	247	8.5	5.6	490	27	1
ANC 1D	6	50	4	4	5	-1.56	-0.42	7.1	3.7	1.0	--	8.3	4.9	--	--	0
ANC 2D	6	50	4	4	5	-1.68	-0.46	7.3	4.1	0.7	--	8.0	6.0	--	--	0
Scaled Height of Burst Less Than -0.50 and Greater Than -0.90, Category 7:																
AV I 01	5	40,000	1	3	5	-17.19	-0.50	47.6	31.9	--	72,500	50.9	31.8	120,000	--	0
AV II 05A	5	256	1	3	5	-3.19	-0.50	8.8	4.1	--	426	10.0	7.1	920	26	1
AV II 05B	5	256	1	3	5	-3.19	-0.50	8.5	4.3	--	381	--	--	--	--	0
AV II 06	5	256	1	3	5	-4.76	-0.75	9.6	4.6	--	517	11.3	9.3	1,367	25	1
ANC 1E	6	50	4	4	5	-2.60	-0.71	7.5	4.4	0.8	--	9.6	6.0	--	--	0
Scaled Height of Burst Less Than -0.90 and Greater Than -1.10, Category 8:																
CESDC-24	11	1	2	5	5	-1.00	-1.00	2.2	0.7	0.2	6	2.7	2.0	14	30	0
CESDC-26	11	1	2	5	5	-1.00	-1.00	2.2	0.6	0.1	6	2.2	2.1	11	28	0
EUE B-14	30	64	1	5	5	-4.20	-1.05	10.0	--	--	--	--	--	--	--	0
EUE B-13	30	64	1	5	5	-4.20	-1.05	8.0	--	--	--	--	--	--	--	0
EUE C-21	30	64	1	5	5	-4.20	-1.05	9.5	--	--	--	--	--	--	--	0
EUE C-22	30	64	1	5	5	-4.20	-1.05	8.0	--	--	--	--	--	--	--	0
EUE C-24	30	64	1	5	5	-4.20	-1.05	7.5	--	--	--	--	--	--	--	0
EUE C-28	30	64	1	5	5	-4.20	-1.05	6.2	--	--	--	--	--	--	--	0
EUE C-30	30	64	1	5	5	-4.20	-1.05	8.7	--	--	--	--	--	--	--	0
AV II 07A	5	256	1	3	5	-6.35	-1.00	9.8	4.4	--	506	11.2	10.6	1,738	25	1
AV II 07B	5	256	1	3	5	-6.35	-1.00	9.9	4.5	--	544	--	--	--	--	0
Scaled Height of Burst Less Than -1.10 and Greater Than -2.00, Category 9:																
CESDC-22	11	1	1	5	5	-1.50	-1.50	3.2	0.3	0.1	4	3.0	2.5	20	17	0
CESDC-28	11	1	1	5	5	-1.50	-1.50	2.2	0.6	0.1	5	2.5	2.5	17	42	0
EUE B-15	30	64	1	5	5	-6.30	-1.57	9.7	--	--	--	--	--	--	--	0
EUE B-16	30	64	1	5	5	-6.30	-1.57	8.9	--	--	--	--	--	--	--	0
CESDC-18	11	1	1	5	5	-2.00	-2.00	2.2	0.2	0.2	3	2.5	3.0	20	37	0
CESDC-21	11	1	1	5	5	-2.00	-2.00	2.6	0.1	0.1	2	2.7	3.0	20	12	0
AV II 08	5	256	1	3	5	-7.94	-1.25	10.3	4.0	--	483	13.4	12.6	2,533	43	1
AV II 09A	5	256	1	3	5	-9.53	-1.50	11.0	3.6	--	486	14.6	13.9	3,046	16	1
AV II 09B	5	256	1	3	5	-9.53	-1.50	11.0	2.3	--	332	--	--	--	--	0
Scaled Height of Burst Less Than -2.00, Category 10:																
EUE A-7	30	64	1	5	5	-8.40	-2.10	7.5	--	--	--	--	--	--	--	0
EUE B-12	30	64	1	5	5	-8.40	-2.10	9.5	--	--	--	--	--	--	--	0
CESDC-16	11	1	1	5	5	-2.50	-2.50	2.0	0.2	0.1	2	2.5	3.6	21	16	0
CESDC-17	11	1	1	5	5	-2.50	-2.50	1.3	0.4	0.1	1	3.0	3.5	26	28	0

TABLE A.8 CRATER DATA FOR MOIST SILTY CLAY

Shot Identification	Bibliography Number	Charge Yield (T NEquivalent)	Type of Explosive	Moisture Code	Medium Code	Height of Burst	Scaled Height of Burst $\bar{z}$	Apparent Crater Radius r_a	Apparent Crater Depth d_a	Apparent Crater Lip Height h	Volume of Apparent Crater V_a	True Crater Radius r_t	True Crater Depth d_t	Volume of True Crater V_t	Angle of Crater Slope	Crater Shape Code
		pounds				feet	$ft/lb^{1/3}$	feet	feet	feet	ft^3	feet	feet	ft^3	degrees	
Scaled Height of Burst Greater Than +0.50, Category 1:																
PCE E1-51	166	77	2	6	6	1.89	0.62	3.0	0.4	--	4	--	--	--	3	0
PCE E1-52	166	77	2	6	6	1.89	0.62	2.8	0.3	--	2	--	--	--	3	0
PCE E1-53	166	77	2	6	6	1.89	0.62	3.5	0.3	--	5	--	--	--	3	0
Scaled Height of Burst Less Than +0.50 and Greater Than +0.30, Category 2:																
No Data Available																
Scaled Height of Burst Less Than +0.30 and Greater Than +0.05, Category 3:																
No Data Available																
Scaled Height of Burst Less Than +0.05 and Greater Than -0.05, Category 4:																
No Data Available																
Scaled Height of Burst Less Than -0.05 and Greater Than -0.20, Category 5:																
No Data Available																
Scaled Height of Burst Less Than -0.20 and Greater Than -0.50, Category 6:																
PCE E1-48[b]	166	[illegible]	6	6	6	-1.50	-0.45	7.2	3.6	0.8	[illegible]	7.5	3.0	[illegible]	[illegible]	[illegible]
PCE E1-49	166	[illegible]	6	6	6	-1.50	-0.45	8.0	4.5	1.0	[illegible]	8.5	3.2	[illegible]	[illegible]	[illegible]
PCE E1-50	166	[illegible]	6	6	6	-1.50	-0.45	8.3	3.3	1.0	[illegible]	7.0	3.3	[illegible]	[illegible]	[illegible]
PCE E1-58[b]	166	[illegible]	6	6	6	-1.50	-0.45	6.5	3.7	0.6	[illegible]	7.0	4.7	[illegible]	[illegible]	[illegible]
PCE E1-59[b]	166	[illegible]	6	6	6	-1.50	-0.45	6.7	3.6	0.5	[illegible]	7.5	4.8	[illegible]	[illegible]	[illegible]
PCE E1-54	166	[illegible]	2	6	6	-1.50	-0.50	7.5	4.8	1.0	[illegible]	8.5	4.8	[illegible]	[illegible]	[illegible]
PCE E1-55[b]	166	[illegible]	2	6	6	-1.50	-0.50	6.5	3.7	0.8	[illegible]	7.0	3.0	[illegible]	[illegible]	[illegible]
PCE E1-56[b]	166	[illegible]	2	6	6	-1.50	-0.50	7.0	4.0	0.7	[illegible]	8.0	3.7	[illegible]	[illegible]	[illegible]
PCE E1-57	166	[illegible]	2	6	6	-1.50	-0.50	8.2	3.3	0.7	[illegible]	9.0	3.5	[illegible]	[illegible]	[illegible]
Scaled Height of Burst Less Than -0.50 and Greater Than -0.90, Category 7:																
[illegible][a]	161	10	1	6	6	-1.21	-0.[illegible]	3.7	2.2	0.2	[illegible]	7.0	3.1	[illegible]	[illegible]	[illegible]
[illegible]	161	10	1	6	6	-1.64	-0.77	3.8	2.3	0.3	[illegible]	8.5	4.0	[illegible]	[illegible]	[illegible]
[illegible][b]	161	10	1	6	6	-1.48	-0.73	4.1	3.2	0.4	[illegible]	9.0	4.6	[illegible]	[illegible]	[illegible]
[illegible]	161	10	1	6	6	-1.62	-0.77	3.9	2.5	0.3	[illegible]	9.0	3.5	[illegible]	[illegible]	[illegible]
[illegible]	161	10	1	6	6	-1.67	-0.78	3.8	2.5	0.4	[illegible]	8.0	3.1	[illegible]	[illegible]	[illegible]
[illegible][a]	161	10	1	6	6	-1.60	-0.76	4.0	2.7	0.3	[illegible]	8.5	3.5	[illegible]	[illegible]	[illegible]
[illegible]	161	10	1	6	6	-1.63	-0.76	3.8	2.1	0.2	[illegible]	8.0	3.5	[illegible]	[illegible]	[illegible]
[illegible]	161	10	1	6	6	-1.68	-0.78	4.2	2.6	0.3	[illegible]	8.0	3.0	[illegible]	[illegible]	[illegible]
[illegible][a,c]	161	10	1	6	6	-1.65	-0.77	4.2	2.8	0.1	[illegible]	9.0	3.3	[illegible]	[illegible]	[illegible]
[illegible][a]	161	10	1	6	6	-1.65	-0.77	3.6	1.8	0.3	[illegible]	7.5	3.9	[illegible]	[illegible]	[illegible]
Scaled Height of Burst Less Than -0.90 and Greater Than -1.10, Category 8:																
No Data Available																
Scaled Height of Burst Less Than -1.10 and Greater Than -2.00, Category 9:																
[illegible][a]	161	10	1	6	6	-3.17	-1.47	4.3	0.4	0.3	[illegible]	[illegible]	[illegible]	[illegible]	[illegible]	[illegible]
[illegible]	161	10	1	6	6	-3.50	-1.62	5.1	1.9	0.2	[illegible]	9.0	5.7	[illegible]	[illegible]	[illegible]
[illegible]	161	10	1	6	6	-3.71	-1.69	4.8	1.7	0.2	[illegible]	9.0	6.2	[illegible]	[illegible]	[illegible]
[illegible][a]	161	10	1	6	6	-3.29	-1.53	5.1	1.9	0.3	[illegible]	8.5	7.1	[illegible]	[illegible]	[illegible]
[illegible]	161	10	1	6	6	-3.25	-1.51	6.[illegible]	1.5	0.6	[illegible]	7.5	3.9	[illegible]	[illegible]	[illegible]
[illegible][a]	161	10	1	6	6	-3.26	-1.51	4.6	1.6	0.4	[illegible]	[illegible]	[illegible]	[illegible]	[illegible]	[illegible]
[illegible]	161	10	1	6	6	-3.71	-1.69	4.6	1.0	0.4	[illegible]	[illegible]	[illegible]	[illegible]	[illegible]	[illegible]
[illegible]	161	10	1	6	6	-3.13	-1.45	4.3	2.3	0.3	[illegible]	9.0	5.8	[illegible]	[illegible]	[illegible]
[illegible][a,c]	161	10	1	6	6	-3.30	-1.69	4.7	2.6	0.2	[illegible]	9.5	7.6	[illegible]	[illegible]	[illegible]
[illegible][a]	161	10	1	6	6	-3.26	-1.50	5.1	0.0	0.3	[illegible]	8.2	5.8	[illegible]	[illegible]	[illegible]
[illegible][a]	161	10	1	6	6	-3.70	-1.69	3.9	1.6	0.6	[illegible]	9.0	3.7	[illegible]	[illegible]	[illegible]
Scaled Height of Burst Less Than -2.00, Category 10:																
No Data Available																

[a] Unstemmed.

[b] Half-stemmed.

[c] Stemming material was water.

TABLE A.9 CRATER DATA FOR SOIL-TO-ROCK/DRY BASIN ALLUVIAL CLAY

Shot Identification	Sandia Laboratory Number	Charge Yield (TNT-Equivalent)	Type of Explosive	Moisture Code	Medium Code	Height of Burst	Scaled Height of Burst $\bar{z}$	Apparent Crater Radius r_a	Apparent Crater Depth d_a	Apparent Crater Lip Height h	Volume of Apparent Crater v_a	True Crater Radius r_t	True Crater Depth d_t	Volume of True Crater v_t	Angle of Crater Slope	Crater Shape Code
		pounds				feet	$ft/lb^{1/3}$	feet	feet	feet	ft^3	feet	feet	ft^3	degrees	
Scaled Height of Burst Greater Than +0.50, Category 1:																
HP 1A	28	40,000	1	3	7	29.53	0.66	68.9	8.0	--	--	--	--	--	--	0
Scaled Height of Burst Less Than +0.50 and Greater Than +0.30, Category 2:																
No Data Available																
Scaled Height of Burst Less Than +0.30 and Greater Than +0.05, Category 3:																
[redacted]	[redacted]	[redacted]	1	3	7	0.28	0.14	0.8	0.7	[redacted]	[redacted]	[redacted]	[redacted]	[redacted]	[redacted]	0
[redacted]	[redacted]	[redacted]	1	3	7	0.28	0.14	0.8	0.7	[redacted]	[redacted]	[redacted]	[redacted]	[redacted]	[redacted]	0
[redacted]	[redacted]	[redacted]	1	3	7	0.28	0.14	0.8	0.8	[redacted]	[redacted]	[redacted]	[redacted]	[redacted]	[redacted]	0
[redacted]	[redacted]	[redacted]	1	3	7	0.28	0.14	0.8	0.7	[redacted]	[redacted]	[redacted]	[redacted]	[redacted]	[redacted]	0
[redacted]	[redacted]	[redacted]	1	3	7	0.28	0.14	0.8	0.7	[redacted]	[redacted]	[redacted]	[redacted]	[redacted]	[redacted]	0
[redacted]	[redacted]	[redacted]	1	3	7	0.28	0.14	0.8	0.6	[redacted]	[redacted]	[redacted]	[redacted]	[redacted]	[redacted]	0
[redacted]	[redacted]	[redacted]	1	3	7	0.28	0.14	0.8	0.8	[redacted]	[redacted]	[redacted]	[redacted]	[redacted]	[redacted]	0
[redacted]	[redacted]	[redacted]	1	3	7	0.28	0.14	0.8	0.5	[redacted]	[redacted]	[redacted]	[redacted]	[redacted]	[redacted]	0
[redacted]	[redacted]	[redacted]	1	3	7	0.28	0.14	0.7	0.5	[redacted]	[redacted]	[redacted]	[redacted]	[redacted]	[redacted]	0
[redacted]	[redacted]	[redacted]	1	3	7	0.28	0.14	0.8	0.6	[redacted]	[redacted]	[redacted]	[redacted]	[redacted]	[redacted]	0
[redacted]	[redacted]	[redacted]	1	3	7	0.28	0.14	0.8	0.5	[redacted]	[redacted]	[redacted]	[redacted]	[redacted]	[redacted]	0
[redacted]	[redacted]	[redacted]	1	3	7	0.28	0.14	0.8	0.6

TABLE A.9 (CONCLUDED)

Shot Identification	Bibliography Number	Charge Yield (TNT-Equivalent)	Type of Explosive	Moisture Code	Medium Code	Height of Burst	Scaled Height of Burst $\bar{z}$	Apparent Crater Radius r_a	Apparent Crater Depth d_a	Apparent Crater Lip Height h	Volume of Apparent Crater v_a	True Crater Radius r_t	True Crater Depth d_t	Volume of True Crater v_t	Angle of Crater Slope	Crater Shape Code
		pounds				feet	$ft/lb^{1/3}$	feet	feet	feet	ft^3	feet	feet	ft^3	degrees	
Scaled Height of Burst Less Than +0.20 and Greater Than +0.05, Category 3 (Continued):																
SRS-30	16	8	1	3	7	0.12	0.06	0.8	1.5	--	--	--	--	--	--	0
HE 6	28	200,000	1	3	7	7.87	0.13	82.7	14.8	--	--	--	--	--	--	0
HE 6A	28	40,000	1	3	7	4.98	0.14	28.9	16.8	--	--	--	--	--	--	0
PP	47	1,000,000	1	3	7	13.45	0.13	100.1	16.4	--	--	--	--	--	--	0
BIAL	26	1,000,000	1	3	7	13.45	0.13	99.0	13.1	5.0	280,000	155.0	15.0	575,000	--	4
Scaled Height of Burst Less Than +0.05 and Greater Than -0.05, Category 4:																
SRS-11	16	8	1	3	7	0.00	0.00	1.1	0.9	--	--	--	--	--	--	0
SRS-12	16	8	1	3	7	0.00	0.00	1.2	0.6	--	--	--	--	--	--	0
SRS-13	16	8	1	3	7	0.00	0.00	1.1	0.8	--	--	--	--	--	--	0
SRS-14	16	8	1	3	7	0.00	0.00	1.2	0.7	--	--	--	--	--	--	0
SRS-15	16	8	1	3	7	0.00	0.00	1.2	0.9	--	--	--	--	--	--	0
SRS-16	16	8	1	3	7	0.00	0.00	1.2	1.1	--	--	--	--	--	--	0
SRS-17	16	8	1	3	7	0.00	0.00	1.2	0.9	--	--	--	--	--	--	0
SRS-18	16	8	1	3	7	0.00	0.00	1.0	1.0	--	--	--	--	--	--	0
SRS-19	16	8	1	3	7	0.00	0.00	1.4	1.3	--	--	--	--	--	--	0
SRS-20	16	8	1	3	7	0.00	0.00	1.0	1.0	--	--	--	--	--	--	0
SRS-31	16	60	1	3	7	0.00	0.00	2.2	2.0	0.2	--	--	--	--	--	0
SRS-32	16	60	1	3	7	0.00	0.00	2.3	2.3	0.2	--	--	--	--	--	0
SRS-33	16	60	1	3	7	0.00	0.00	2.4	2.1	0.2	--	--	--	--	--	0
SRS-34	16	60	1	3	7	0.00	0.00	2.3	2.4	0.2	--	--	--	--	--	0
SRS-35	16	60	1	3	7	0.00	0.00	2.4	2.4	--	--	--	--	--	--	0
SRS-36	16	60	1	3	7	0.00	0.00	2.8	2.4	0.3	--	--	--	--	--	0
SRS-37	16	60	1	3	7	0.00	0.00	2.9	2.2	0.4	--	--	--	--	--	0
SRS-38	16	60	1	3	7	0.00	0.00	3.1	2.4	0.3	--	--	--	--	--	0
SRS-39	16	60	1	3	7	0.00	0.00	2.4	1.8	0.3	--	--	--	--	--	0
SRS-40	16	60	1	3	7	0.00	0.00	2.4	2.0	--	--	--	--	--	--	0
HE 3	28	40,000	1	3	7	0.00	0.00	33.8	16.0	--	--	--	--	--	29	1
HE 5	28	40,000	1	3	7	0.00	0.00	33.1	14.0	5.0	--	--	--	--	30	1
Scaled Height of Burst Less Than -0.05 and Greater Than -0.20, Category 5:																
							No Data Available									
Scaled Height of Burst Less Than -0.20 and Greater Than -0.50, Category 6:																
							No Data Available									
Scaled Height of Burst Less Than -0.50 and Greater Than -0.90, Category 7:																
							No Data Available									
Scaled Height of Burst Less Than -0.90 and Greater Than -1.10, Category 8:																
							No Data Available									
Scaled Height of Burst Less Than -1.10 and Greater Than -2.00, Category 9:																
							No Data Available									
Scaled Height of Burst Less Than -2.00, Category 10:																
							No Data Available									

TABLE A.10 CRATER DATA FOR DRY DESERT ALLUVIUM

Shot Identification	Bibliography Number	Charge Yield (TNT-Equivalent)	Type of Explosive	Moisture Code	Medium Code	Height of Burst	Scaled Height of Burst Z	Apparent Crater Radius r_a	Apparent Crater Depth d_a	Apparent Crater Lip Height h	Volume of Apparent Crater v_a	True Crater Radius r_t	True Crater Depth d_t	Volume of True Crater v_t	Angle of Crater Slope	Crater Shape Code
		pounds				feet	$ft/lb^{1/3}$	feet	feet	feet	ft^3	feet	feet	ft^3	degrees	
Scaled Height of Burst Greater Than +0.50, Category 1:																
No Data Available																
Scaled Height of Burst Less Than +0.50 and Greater Than +0.20, Category 2:																
No Data Available																
Scaled Height of Burst Less Than +0.20 and Greater Than +0.05, Category 3:																
No Data Available																
Scaled Height of Burst Less Than +0.05 and Greater Than -0.05, Category 4:																
SC II 8-12	31	256	1	1	8	0.00	0.00	8.6	2.5	--	161	--	--	--	--	0
SC II 8-13	31	256	1	1	8	0.00	0.00	8.3	2.6	--	267	--	--	--	--	0
JS	37	2,400,000	0	1	8	3.48	0.03	45.0	19.0	--	49,270	--	--	--	--	0
Scaled Height of Burst Less Than -0.05 and Greater Than -0.20, Category 5:																
JU	37	2,400,000	0	1	8	-17.00	-0.1,	130.0	53.0	--	973,000	--	--	--	--	0
Scaled Height of Burst Less Than -0.20 and Greater Than -0.50, Category 6:																
No Data Available																
Scaled Height of Burst Less Than -0.50 and Greater than -0.90, Category 7:																
STC II	56	40,000	1	1	8	-17.10	-0.50	50.'	23.6	2.5	83,600	--	--	--	32	1
TPOT S	87	2,400,000	0	1	8	-67.00	-0.50	140.0	90.0	--	2,600,000	--	--	--	--	0
Scaled Height of Burst Less Than -0.90 and Greater Than -1.10, Category 8:																
SC I 08	31	256	1	1	8	-6.35	-1.00	13.1	7.3	--	1,489	--	--	--	--	0
STC III	56	40,000	1	1	8	-34.20	-1.00	58.6	29.2	3.0	145,000	--	--	--	31	1
MIDAS	84	200,000,000	0	1	8	-635.00	-1.09	608.0	323.0	--	178,000,000	--	--	--	--	0
Scaled Height of Burst Less Than -1.10 and Greater Than -2.00, Category 9:																
SC I 02	31	256	1	1	8	-9.53	-1.50	15.1	7.9	--	2,146	--	--	--	--	0
SC I 09	31	256	1	1	8	-9.53	-1.50	14.1	7.2	--	1,230	--	--	--	--	0
PB I 01	144	1,103	5	1	8	-15.00	1.45	21.0	9.7	--	6,560	26.0	24.1	17,200	--	0
PB I 02	144	1,112	5	1	8	-16.60	1.60	21.8	9.1	--	7,560	--	--	--	--	0
PB I 03	144	1,112	5	1	8	-18.20	1.75	20.9	7.8	--	5,830	28.0	24.9	20,200	--	0
PB I 04	144	1,110	5	1	8	-19.80	1.91	20.6	9.4	--	6,530	25.0	25.8	19,000	--	0
PB I 06	144	1,117	5	1	8	-19.60	1.88	20.7	8.3	--	6,075	--	--	--	--	0

(Continued)

TABLE A.10 (CONCLUDED)

Shot Identification	Bibliography Number	Charge Yield (TNT-Equivalent)	Type of Explosive	Moisture Code	Medium Code	Height of Burst	Scaled Height of Burst Z	Apparent Crater Radius r_a	Apparent Crater Depth d_a	Apparent Crater Lip Height h	Volume of Apparent Crater v_a	True Crater Radius r_t	True Crater Depth d_t	Volume of True Crater v_t	Angle of Crater Slope	Crater Shape Code
		pounds				feet	$ft/lb^{1/3}$	feet	feet	feet	ft^3	feet	feet	ft^3	degrees	
Scaled Height of Burst Less Than -1.10 and Greater Than -2.00, Category 9 (Continued):																
SCT	55	987,410	1	1	8	-125.00	-1.26	153.8	74.5	8.5	2,660,000	--	--	--	31	6
SL F1	136	64	1	1	8	-6.00	-1.50	9.0	4.5	1.2	517	--	--	--	--	0
SL F2	136	64	1	1	8	-6.00	-1.50	8.8	3.6	0.8	388	--	--	--	--	0
SL FB	136	64	1	1	8	-6.00	-1.50	7.9	2.8	1.3	247	--	--	--	--	0
SL FC	136	64	1	1	8	-6.00	-1.50	8.0	2.6	1.3	303	--	--	--	--	0
SL FD	136	64	1	1	8	-6.00	-1.50	8.3	3.4	1.0	338	--	--	--	--	0
SL 70-2	136	64	1	1	8	-6.00	-1.50	8.1	1.5	2.1	182	--	--	--	--	0
SL 70-3	136	64	1	1	8	-6.00	-1.50	8.2	3.9	1.6	454	--	--	--	--	0
SL 70-4	136	64	1	1	8	-6.00	-1.50	8.2	3.4	0.9	307	--	--	--	--	0
Scaled Height of Burst Less Than -2.00, Category 10:																
SC I 04	31	256	1	1	8	-15.90	-2.50	11.3	1.8	--	368	--	--	--	--	0
SC I 10	31	256	1	1	8	-12.70	-2.00	13.4	4.1	--	1,093	--	--	--	--	0
SC I 11	31	256	1	1	8	-15.90	-2.50	6.5	0.4	--	236	--	--	--	--	0
SC I 12	31	256	1	1	8	-19.05	-3.00	9.4	2.3	--	256	--	--	--	--	0
SC I 15	31	256	1	1	8	-25.40	-4.00	4.2	0.4	--	31	--	--	--	--	0
SC I 16	31	256	1	1	8	-12.70	-2.00	14.2	6.7	--	2,220	--	--	--	--	0
SC I 17	31	256	1	1	8	-19.05	-3.00	5.7	1.7	--	55	--	--	--	--	0
SC II 04	31	256	1	1	8	-25.50	-4.02	2.3	1.1	--	16	--	--	--	--	0
SC II 05	31	256	1	1	8	-23.30	-3.67	3.0	0.3	--	18	--	--	--	--	0
SC II 06	31	256	1	1	8	-22.60	-3.56	4.4	1.0	--	170	--	--	--	--	0
SC II 07	31	256	1	1	8	-19.70	-3.10	8.1	1.0	--	121	--	--	--	--	0
SC II 08	31	256	1	1	8	-19.00	-2.99	10.1	1.6	--	297	--	--	--	--	0
SC II 09	31	256	1	1	8	-16.40	-2.58	14.3	2.6	--	716	--	--	--	--	0
SC II 10	31	256	1	1	8	-16.10	-2.54	14.1	4.5	--	1,077	--	--	--	--	0
SC II 11	31	256	1	1	8	-13.10	-2.06	14.7	5.4	--	1,770	--	--	--	--	0
FIC 1	56	40,000	1	1	8	-80.00	-2.34	57.0	7.9	--	49,000	--	--	--	31	1

TABLE A.11 CRATER DATA FOR HEIST BARREN SILT

Shot Identification	Bibliography Number	Charge Yield (TNT-Equivalent)	Type of Explosive	Moisture Code	Medium Code	Height of Burst	Scaled Height of Burst Z	Apparent Crater Radius r_a	Apparent Crater Depth d_a	Apparent Crater Lip Height h	Volume of Apparent Crater v_a	True Crater Radius r_t	True Crater Depth d_t	Volume of True Crater v_t	Angle of Crater Slope	Crater Shape Code
		pounds				feet	$ft/lb^{1/3}$	feet	feet	feet	ft^3	feet	feet	ft^3	degrees	
Scaled Height of Burst Greater Than +0.50, Category 1:																
No Data Available																
Scaled Height of Burst Less Than +0.50 and Greater Than +0.20, Category 2:																
STANSTO-6	3	4	1	3	8	0.50	0.31	1.9	0.2	--	--	--	--	--	--	5
Scaled Height of Burst Less Than +0.20 and Greater Than +0.05, Category 3:																
STANS 1L	2	16	1	3	6	0.17	0.07	2.7	1.6	--	--	--	--	--	--	0
STANS 1S	2	4	1	3	6	0.11	0.07	1.7	0.6	--	--	--	--	--	--	0
STANSTO-5	3	4	1	3	8	0.17	0.11	1.7	0.5	--	--	--	--	--	--	0
Scaled Height of Burst Less Than +0.05 and Greater Than -0.05, Category 4:																
STANSTO-1	3	4	1	3	8	0.00	0.00	1.8	0.9	--	--	--	--	--	--	0
STANSTO-2	3	4	1	3	8	0.00	0.00	1.7	0.9	--	--	--	--	--	--	0
STANSTO-3	3	4	1	3	8	0.00	0.00	2.0	1.0	--	--	--	--	--	--	0
STANSTO-4	3	4	1	3	8	0.00	0.00	2.2	1.0	--	--	--	--	--	--	0
Scaled Height of Burst Less Than -0.05 and Greater Than -0.20, Category 5:																
No Data Available																
Scaled Height of Burst Less Than -0.20 and Greater Than -0.50, Category 6:																
No Data Available																
Scaled Height of Burst Less Than -0.50 and Greater Than -0.90, Category 7:																
RNV-40	53	270	1	2	8	-5.90	-0.86	17.4	6.0	--	--	--	--	--	--	0
RNV-52	53	540	1	2	8	-7.00	-0.86	20.4	9.2	--	--	--	--	--	--	0
STANS 2L	2	16	1	3	8	-1.73	-0.69	4.7	2.8	--	--	5.2	3.7	--	--	0
Scaled Height of Burst Less Than -0.90 and Greater Than -1.10, Category 8:																
RNV-41	53	540	1	2	8	-8.00	-0.98	21.4	9.1	--	--	--	--	--	--	0
RNV-57	53	540	1	2	8	-8.30	-1.02	19.4	9.3	--	--	--	--	--	--	0
Scaled Height of Burst Less Than -1.10 and Greater Than -2.00, Category 9:																
RNV-48	53	270	1	2	8	-7.80	-1.71	16.9	6.9	--	--	--	--	--	--	0
RNV-53	53	54	1	2	8	-4.70	-1.04	11.0	6.0	--	--	--	--	--	--	0
RNV-54	53	54	1	2	8	-4.70	-1.04	11.3	6.3	--	--	--	--	--	--	0
RNV-55	53	54	1	2	8	-4.70	-1.04	11.0	5.7	--	--	--	--	--	--	0
RNV-56	53	54	1	2	8	-4.70	-1.04	8.0	4.4	--	--	--	--	--	--	0
RNV-44	53	270	1	2	8	-6.00	-1.04	12.7	6.2	--	--	--	--	--	--	0
RNV-49	53	270	1	2	8	-6.00	-1.04	13.3	7.0	--	--	--	--	--	--	0
RNV-39	53	81	1	2	8	-5.40	-1.25	14.7	6.5	--	--	--	--	--	--	0
RNV-47	53	81	1	2	8	-5.40	-1.25	12.2	6.2	--	--	--	--	--	--	0
RNV-63	53	81	1	2	8	-5.40	-1.25	11.8	7.0	--	--	--	--	--	--	0
RNV-46	53	270	1	2	8	-8.90	-1.38	15.9	7.8	--	--	--	--	--	--	0
STANS 2S	2	4	1	3	8	-1.89	-1.19	3.0	1.3	--	--	2.2	1.6	--	--	0
STANS 3L	2	.6	1	3	8	-3.73	-1.48	4.9	2.2	--	--	--	--	--	--	0
Scaled Height of Burst Less Than -2.00, Category 10:																
No Data Available																

TABLE A.12 CRATER DATA FOR DRY-TO-MOIST SAND

Shot Identification	Bibliography Number	Charge Yield (TNT-Equivalent)	Type of Explosive	Moisture Code	Medium Code	Height of Burst	Scaled Height of Burst Z	Apparent Crater Radius r_a	Apparent Crater Depth d_a	Apparent Crater Lip Height h	Volume of Apparent Crater v_a	True Crater Radius r_t	True Crater Depth d_t	Volume of True Crater v_t	Angle of Crater Slope	Crater Shape Code
		pounds				feet	$ft/lb^{1/3}$	feet	feet	feet	ft^3	feet	feet	ft^3	degrees	
Scaled Height of Burst Greater Than +0.50, Category 1:																
CSDC-5C2	13	6.47	3	3	9	1.29	0.69	1.9	0.2	0.1	1	--	--	--	--	0
CSDC-5C1	13	6.48	3	3	9	1.29	0.69	2.0	0.2	0.1	1	--	--	--	--	0
CSDC-1C7	13	1.35	3	3	9	0.75	0.68	1.2	0.2	0.0	0	--	--	--	--	0
CSDC-1C8	13	1.31	3	3	9	0.74	0.68	1.5	0.1	0.0	0	--	--	--	--	0
Scaled Height of Burst Less Than +0.50 and Greater Than +0.20, Category 2:																
CSDC-1C19	13	1.18	3	3	9	0.50	0.47	1.1	0.1	0.0	0	--	--	--	--	0
CSDC-5C3	13	6.43	3	3	9	0.87	0.47	1.8	0.2	0.2	2	--	--	--	--	0
CSDC-5C4	13	6.46	3	3	9	0.87	0.47	1.9	0.2	0.2	1	--	--	--	--	0
CSDC-1C10	13	1.34	3	3	9	0.50	0.45	1.1	0.1	0.0	0	--	--	--	--	0
CSDC-1C9	13	1.35	3	3	9	0.49	0.44	1.3	0.1	0.0	0	--	--	--	--	0
CDS-689	14	4	1	3	9	0.60	0.38	1.8	0.2	0 0	--	--	--	--	14	0
CDS-690	14	4	1	3	9	0.60	0.38	1.8	0.2	0.0	--	--	--	--	13	0
CDS-691	14	4	1	3	9	0.50	0.31	1.7	0.3	0.0	--	--	--	--	14	0
CDS-692	14	4	1	3	9	0.50	0.31	1.7	0.2	0.0	--	--	--	--	14	0
CSDC-1C11	13	1.35	3	3	9	0.25	0.23	1.2	0.2	0.1	0	--	--	--	--	0
CSDC-1C12	13	1.35	3	3	9	0.25	0.23	1.0	0.2	0.1	0	--	--	--	--	0
Scaled Height of Burst Less Than +0.20 and Greater Than +0.05, Category 3:																
CDS-693	14	4	1	3	9	0.30	0.19	1.7	0.3	0.1	--	--	--	--	17	0
CDS-694	14	4	1	3	9	0.30	0.19	1.9	0.3	0.1	--	--	--	--	16	0
J ME-4	39	2,560	1	3	9	2.01	0.15	6.1	1.9	2.8	110	8.0	2.1	180	23	0
CDS-695	14	4	1	3	9	0.20	0.13	2.2	0.5	0.1	--	--	--	--	19	0
CDS-696	14	4	1	3	9	0.20	0.13	2.1	0.6	0.1	--	--	--	--	20	0
Scaled Height of Burst Less Than +0.05 and Greater Than -0.05, Category 4:																
CSDC-1C16	13	1.18	3	3	9	0.00	0.00	1.7	0.5	0.1	2	--	--	--	23	0
CSDC-1C15	13	1.19	3	3	9	0.00	0.00	1.8	0.8	0.2	3	--	--	--	27	0
CSDC-1C14	13	1.20	3	3	9	0.00	0.00	1.7	0.7	0.2	3	--	--	--	28	0
CSDC-1C13	13	1.22	3	3	9	0.00	0.00	1.6	0.5	0.2	2	--	--	--	25	0
CDS-697	14	4	1	3	9	0.00	0.00	2.6	0.9	0.1	--	--	--	--	23	0
CDS-698	14	4	1	3	9	0.00	0.00	2.5	0.8	0.1	--	--	--	--	22	0
CSDC-5C5	13	6.21	3	3	9	0.00	0.00	3.0	0.9	--	10	--	--	--	32	0
ESRIC-1	29	27	2	3	9	0.00	0.00	4.2	1.9	0.4	54	4.5	1.9	61	28	0
ESRIC-2	29	27	2	3	9	0.00	0.00	4.1	2.2	0.5	69	4.6	2.2	73	39	0
ESRIC-10	29	27	2	3	9	0.00	0.00	4.5	2.3	0.4	61	4.5	2.3	78	30	0
ESRIC-11	29	27	2	3	9	0.00	0.00	4.2	2.2	0.5	48	4.3	2.2	53	30	0
ESRIC-3	29	36.8	6	3	9	0.00	0.00	5.0	2.2	0.5	82	5.1	2.2	89	28	0
ESRIC-4	29	36.8	6	3	9	0.00	0.00	5.0	2.1	0.5	72	5.1	2.2	79	32	0
ESRIC-12	29	36.8	6	3	9	0.00	0.00	4.6	2.3	0.6	69	4.7	2.4	73	34	0
ESRIC-13	29	36.8	6	3	9	0.00	0.00	4.9	2.4	0.5	73	4.9	2.4	84	32	0
ESRIC-5	29	256	1	3	9	0.00	0.00	8.5	3.4	0.6	419	8.5	3.6	450	33	0
ESRIC-6	29	256	1	3	9	0.00	0.00	8.6	3.5	0.8	391	8.6	3.5	412	31	0
ESRIC-8	29	256	1	3	9	0.00	0.00	8.7	4.2	0.7	395	--	--	--	27	0
ESRIC-9	29	256	1	3	9	0.00	0.00	9.2	4.4	0.8	539	--	--	--	28	0
ZUL 01	63	1	2	4	9	0.00	0.00	1.3	0.5	--	--	--	--	--	--	0
ZUL 02	63	1	2	4	9	0.00	0.00	1.4	0.5	--	--	--	--	--	--	0
Scaled Height of Burst Less Than -0.05 and Greater Than -0.20, Category 5:																
CDS-699	14	4	1	3	9	-0.21	-0.13	3.0	1.2	0.2	--	--	--	--	26	0
CDS-700	14	4	1	3	9	-0.21	-0.13	3.1	1.2	0.2	--	--	--	--	25	0
J ME-9	38	216	1	3	9	-0.84	-0.14	8.3	3.4	0.7	270	14.7	4.0	1,120	24	0
J ME-9A	38	216	1	3	9	-0.84	-0.14	8.6	3.1	1.0	290	15.0	4.0	1,310	32	0
J ME-1	39	2,560	1	3	9	-2.01	-0.15	18.5	6.7	1.4	2,010	23.0	7.6	4,270	40	0

(Continued)

TABLE A.12 (CONCLUDED)

Shot Identification	Hullograph Number	Charge Yield (TNT-Equivalent)	Type of Explosive	Moisture Code	Medium Code	Height of Burst	Scaled Height of Burst Z	Apparent Crater Radius r_a	Apparent Crater Depth d_a	Apparent Crater Lip Height h	Volume of Apparent Crater V_a	True Crater Radius r_t	True Crater Depth d_t	Volume of True Crater V_t	Angle of Crater Slope	Crater Shape Code
		pounds				feet	ft/lb$^{1/3}$	feet	feet	feet	ft^3	feet	feet	ft^3	degrees	
Scaled Height of Burst Less Than -0.05 and Greater Than -0.20, Category 5 (Continued):																
J ME-2	39	40,000	1	3	9	-4.63	-0.14	39.0	15.0	3.0	37,770	--	--	--	40	0
J ME-8	38	216	3	3	9	-1.08	-0.18	6.7	3.3	1.0	380	16.4	4.3	1,310	35	0
J ME-7	38	2,560	1	3	9	-2.50	-0.18	13.0	6.7	2.0	3,300	32.8	8.6	6,180	35	0
Scaled Height of Burst Less Than -0.20 and Greater Than -0.50, Category 6:																
J ME-6	38	2,560	1	4	9	-3.00	-0.22	19.8	6.1	1.6	3,500	36.3	10.1	8,800	29	0
CHAC-1C17	13	1.14	3	3	9	-0.25	-0.24	2.2	1.0	0.2	8	--	--	--	30	0
CHAC-1C16	13	1.20	3	3	9	-0.25	-0.24	2.3	1.1	0.3	9	--	--	--	33	0
CHE-7C1	14	4	1	3	9	-0.41	-0.26	3.4	1.4	0.3	--	--	--	--	24	0
CHE-7C2	14	4	1	3	9	-0.41	-0.26	3.4	1.4	0.3	--	--	--	--	26	0
J ME-5	38	2,560	1	3	9	-4.00	-0.29	19.4	7.9	1.3	4,000	32.6	9.5	8,700	24	0
CHAC-1C20	13	1.18	3	3	9	-0.50	-0.37	2.3	1.2	0.3	8	--	--	--	31	0
CHAC-1C18	13	1.19	3	3	9	-0.50	-0.47	2.6	1.3	0.2	12	--	--	--	32	0
J ME-10	38	216	1	3	9	-3.00	-0.50	11.3	5.5	0.8	460	18.6	6.3	2,600	40	0
J ME-10P	38	216	3	3	9	-3.00	-0.50	9.6	4.1	1.0	320	16.7	5.5	1,660	40	0
J ME-9	39	2,560	1	3	9	-6.79	-0.50	20.5	10.8	1.2	6,[illegible]40	22.0	11.0	7,580	34	0
ZUL 03	63	1	2	4	9	-0.50	-0.50	2.1	1.0	--	--	--	--	--	--	0
ZUL 04	63	1	2	4	9	-0.50	-0.50	2.3	1.0	--	--	--	--	--	--	0
ZUL 05	63	1	2	4	9	-0.50	-0.50	2.3	1.1	--	--	--	--	--	--	0
Scaled Height of Burst Less Than -0.50 and Greater Than -0.90, Category 7:																
No Data Available																
Scaled Height of Burst Less Than -0.90 and Greater Than -1.10, Category 8:																
CHAC-1C21	13	1.18	3	3	9	-1.00	-0.95	2.9	1.4	0.2	15	--	--	--	35	0
ZUL 06	63	1	2	4	9	-1.00	-1.00	2.6	1.6	--	--	--	--	--	--	0
ZUL 07	63	1	2	4	9	-1.00	-1.00	2.5	1.5	--	--	--	--	--	--	0
ZUL 08	63	1	2	4	9	-1.00	-1.00	2.5	1.5	--	--	--	--	--	--	0
Scaled Height of Burst Less Than -1.10 and Greater Than -2.00, Category 9:																
CHAC-1C22	13	1.16	3	3	9	-1.49	-1.42	2.7	1.5	0.3	5	--	--	--	37	0
CHAC-1C23	13	1.18	3	3	9	-2.01	-1.90	2.4	0.4	0.3	3	--	--	--	--	0
ZUL 09	63	1	2	4	9	-1.50	-1.50	2.6	1.8	--	--	--	--	--	--	0
ZUL 10	63	1	2	4	9	-1.50	-1.50	2.5	1.7	--	--	--	--	--	--	0
ZUL 11	63	1	2	4	9	-1.50	-1.50	2.4	1.7	--	--	--	--	--	--	0
ZUL 12	63	1	2	4	9	-1.75	-1.75	2.5	1.6	--	--	--	--	--	--	0
ZUL 13	63	1	2	4	9	-1.75	-1.75	2.5	1.5	--	--	--	--	--	--	0
ZUL 14	63	1	2	4	9	-2.00	-2.00	2.4	1.3	--	--	--	--	--	--	0
ZUL 15	63	1	2	4	9	-2.00	-2.00	2.4	1.3	--	--	--	--	--	--	0
ZUL 16	63	1	2	4	9	-2.00	-2.00	2.3	1.2	--	--	--	--	--	--	0
ZUL 17	63	1	2	4	9	-2.00	-2.00	2.2	1.2	--	--	--	--	--	--	0
ZUL 18	63	1	2	4	9	-2.00	-2.00	2.2	1.1	--	--	--	--	--	--	0
ZUL 19	63	1	2	4	9	-2.00	-2.00	2.0	1.0	--	--	--	--	--	--	0
Scaled Height of Burst Less Than -2.00, Category 10:																
No Data Available																

TABLE A.13 CRATER DATA FOR WET SAND

Shot Identification	Bibliography Number	Charge Yield (TNT-Equivalent)	Type of Explosive	Moisture Code	Medium Code	Height of Burst	Scaled Height of Burst $\bar{z}$	Apparent Crater Radius r_a	Apparent Crater Depth d_a	Apparent Crater Lip Height h	Volume of Apparent Crater v_a	True Crater Radius r_t	True Crater Depth d_t	Volume of True Crater v_t	Angle of Crater Slope	Crater Shape Code
		pounds				feet	$ft/lb^{1/3}$	feet	feet	feet	ft^3	feet	feet	ft^3	degrees	
Scaled Height of Burst Greater Than +0.50, Category 1:																
UETP-101	60	320	1	7	9	3.50	0.51	4.0	0.5	--	--	4.0	0.5	--	14	0
Scaled Height of Burst Less Than +0.50 and Greater Than +0.20, Category 2:																
CRSC-1A26	13	1.18	3	7	9	0.41	0.39	1.4	0.1	--	--	--	--	--	13	0
CRSC-1A27	13	1.18	3	7	9	0.41	0.39	1.3	0.1	--	--	--	--	--	13	0
CRSC-1A25	13	1.29	3	7	9	0.42	0.39	1.2	0.4	--	--	--	--	--	24	0
Scaled Height of Burst Less Than +0.20 and Greater Than +0.05, Category 3:																
MOLE-207	45	256	1	7	9	0.83	0.13	4.0	1.4	0.5	37	--	--	450	36	0
MOLE-308	45	256	1	7	9	0.80	0.13	8.9	4.0	--	447	--	--	--	47	0
CRSC-5AA1	13	6.47	3	7	9	0.23	0.12	1.8	0.7	--	--	--	--	--	25	0
SRI-1TON	88A	2,000	8	7	9	0.75	0.06	27.5	--	--	--	--	--	--	--	0
SRI-7TON	88A	10,000	8	7	9	1.30	0.06	32.0	--	--	--	--	--	--	--	0
SRI-10TON	88A	20,000	8	7	9	1.63	0.06	37.5	--	--	--	--	--	--	--	0
SRI-15TON	88A	30,000	8	7	9	1.87	0.06	45.5	--	--	--	--	--	--	--	0
SRI-20TON	88A	40,000	8	7	9	2.05	0.06	50.0	--	--	--	--	--	--	--	0
Scaled Height of Burst Less Than +0.05 and Greater Than -0.05, Category 4:																
CRSC-1A16	13	1.29	3	7	9	0.00	0.00	2.1	0.5	--	--	--	--	--	20	0
EGLIC-31	89	27	2	7	9	0.00	0.00	4.4	2.4	0.5	54	--	--	--	30	0
EGLIC-32	89	27	2	7	9	0.00	0.00	4.0	2.2	0.6	47	--	--	--	30	0
MOLE-206	45	256	1	7	9	0.00	0.00	6.3	1.7	0.8	129	--	--	575	37	0
MOLE-307	45	256	1	7	9	0.00	0.00	12.9	4.7	--	1,317	--	--	--	47	0
UETP-102	60	320	1	7	9	0.00	0.00	7.6	2.5	1.0	250	10.7	3.2	520	23	0
Scaled Height of Burst Less Than -0.05 and Greater Than -0.20, Category 5:																
CRSC-1A17	13	1.18	3	7	9	-0.12	-0.11	1.9	0.7	--	--	--	--	--	25	0
CRSC-1A18	13	1.18	3	7	9	-0.12	-0.11	1.9	0.7	--	--	--	--	--	24	0
CRSC-1A19	13	1.29	3	7	9	-0.12	-0.11	2.0	0.8	--	--	--	--	--	25	0
CRSC-5AA2	13	6.54	3	7	9	-0.23	-0.12	3.1	1.4	--	--	--	--	--	27	0
MOLE-205	45	256	1	7	9	-0.83	-0.13	9.0	2.0	0.6	300	--	--	720	38	0
MOLE-306	45	256	1	7	9	-0.80	-0.13	13.1	3.8	--	1,375	--	--	--	58	0
MOLE-403	45	256	1	7	9	-0.83	-0.13	8.3	3.4	1.0	293	--	--	--	33	0
UETP-103	60	320	1	7	9	-1.30	-0.19	10.9	6.0	1.0	720	13.2	7.0	1,400	32	0
UETP-108	60	2,560	1	7	9	-2.60	-0.19	19.0	9.7	--	5,200	27.0	10.5	11,000	30	0
Scaled Height of Burst Less Than -0.20 and Greater Than -0.50, Category 6:																
MOLE-305	45	256	1	7	9	-1.60	-0.25	16.1	6.3	--	2,070	--	--	--	48	0
MOLE-204	45	256	1	7	9	-1.65	-0.26	9.4	2.6	0.4	364	--	--	940	40	0
MOLE-405	45	256	1	7	9	-1.65	-0.26	9.2	4.5	0.8	498	9.3	4.6	626	35	0

(Continued)

TABLE A.13 (CONCLUDED)

Shot Identification	Bibliography Number	Charge Yield (TNT-Equivalent)	Type of Explosive	Moisture Code	Medium Code	Height of Burst	Scaled Height of Burst $\bar{z}$	Apparent Crater Radius r_a	Apparent Crater Depth d_a	Apparent Crater Lip Height h	Volume of Apparent Crater v_a	True Crater Radius r_t	True Crater Depth d_t	Volume of True Crater v_t	Angle of Crater Slope	Crater Shape Code
		pounds				feet	$ft/lb^{1/3}$	feet	feet	feet	ft^3	feet	feet	ft^3	degrees	
Scaled Height of Burst Less Than -0.80 and Greater Than -0.90, Category 6 (Continued):																
CHSC-1A20	13	1.27	3	7	9	-0.49	-0.45	2.3	1.2	--	--	--	--	--	30	0
CHSC-1A22	13	1.29	3	7	9	-0.50	-0.46	2.4	1.2	--	--	--	--	--	30	0
CHSC-1A21	13	1.30	3	7	9	-0.50	-0.46	2.5	1.2	--	--	--	--	--	29	0
MOLE-302	45	256	1	7	9	-3.17	-0.50	20.0	6.2	0.8	3,387	--	--	--	39	0
MOLE-309	45	256	1	7	9	-3.15	-0.50	16.7	6.1	--	2,718	--	--	--	40	0
MOLE-310	45	256	1	7	9	-3.15	-0.50	17.5	5.2	--	2,598	--	--	--	46	0
MOLE-406	45	256	1	7	9	-3.17	-0.50	9.8	4.0	1.2	673	--	--	--	45	0
Scaled Height of Burst Less Than -0.90 and Greater Than -0.90, Category 7:																
MOLE-303	45	256	1	7	9	-3.18	-0.50	8.3	3.9	0.9	356	--	--	920	43	0
MOLE-401	45	256	1	7	9	-3.18	-0.50	10.0	5.5	0.6	824	11.3	6.3	1,182	26	0
UHTF-108	60	320	1	7	9	-3.50	-0.51	12.0	6.5	--	1,300	15.5	7.5	2,600	32	0
UHTF-110	60	320	1	7	9	-3.50	-0.51	13.0	7.5	--	1,600	16.8	8.7	2,800	33	0
UHTF-113	60	320	1	7	9	-3.50	-0.51	14.0	6.7	--	1,900	17.5	7.5	3,000	29	0
UHTF-109	60	2,560	1	7	9	-7.00	-0.51	24.7	8.5	--	8,200	29.7	13.5	14,000	23	0
UHTF-112	60	2,560	1	7	9	-7.00	-0.51	30.0	12.5	--	13,000	34.0	17.5	25,000	26	0
UHTF-115	60	40,000	1	7	9	-17.50	-0.51	75.0	23.0	--	180,000	82.5	30.0	300,000	22	0
MOLE-304	45	256	1	7	9	-4.77	-0.75	19.5	6.6	--	--	--	--	--	44	0
MOLE-402	45	256	1	7	9	-4.77	-0.75	11.0	6.2	1.4	943	12.5	8.2	1,687	35	0
Scaled Height of Burst Less Than -0.90 and Greater Than -1.10, Category 8:																
CHSC-1A24	13	1.29	3	7	9	-1.01	-0.93	3.0	1.8	--	--	--	--	--	34	0
CHSC-1A23	13	1.18	3	7	9	-1.00	-0.95	2.9	1.8	--	--	--	--	--	35	0
MOLE-202	45	256	1	7	9	-6.35	-1.00	11.3	5.5	1.0	1,045	--	--	2,630	40	0
MOLE-212	45	256	1	7	9	-6.35	-1.00	11.7	5.8	1.6	1,207	--	--	4,290	43	0
MOLE-404	45	256	1	7	9	-6.35	-1.00	11.7	6.0	1.9	1,190	14.2	8.4	2,358	42	0
UHTF-105	60	320	1	7	9	-7.00	-1.09	15.5	8.5	--	2,600	18.5	12.5	4,400	32	0
Scaled Height of Burst Less Than -1.10 and Greater Than -2.00, Category 9:																
UHTF-111	60	8	1	7	9	-2.50	-1.25	6.0	4.0	--	140	6.5	5.5	260	37	0
UHTF-114	60	8	1	7	9	-2.50	-1.25	6.0	3.5	--	150	7.5	6.5	510	33	0
UHTF-116	60	320	1	7	9	-8.75	-1.28	18.5	9.0	--	3,500	--	--	--	32	0
Scaled Height of Burst Less Than -2.00, Category 10:																
UHTF-106	60	320	1	7	9	-14.00	-2.05	16.7	4.5	--	1,100	19.5	17.0	6,200	20	0
UHTF-107	60	320	1	7	9	-21.00	-3.07	13.5	3.5	--	790	17.0	23.0	7,300	20	0

TABLE A.14 CRATER DATA FOR HEMISPHERICAL CHARGES

Event	Yield (TNT)	Medium Code	Moisture Code	Apparent Crater			
				Radius	Depth	Lip Height	Volume
	pounds			feet	feet	feet	ft^3
Sandy Silty Clay:							
SES[a] (5-shot series, Fall 1958)	512	7	3	6.2	4.8	1.0	--
	551	7	3	6.1	3.8	0.5	--
	523	7	3	5.8	3.0	0.3	--
	521	7	3	5.8	3.3	0.4	--
	520	7	3	6.2	3.4	0.2	--
SES (Fall 1958)	600	7	3	6.6	3.7	0.5	--
SES (Oct 1959)	10,000	7	3	20.0	12.5	--	--
SES (Aug 1960)	40,000	7	3	36.7	15.1	--	--
SES (Aug 1961)	200,000	7	3	69.9	20.7	--	--
SES (Jul 1963)	40,000	7	3	38.1	21.3	--	--
SES (Aug 1963)	40,000	7	3	40.7	19.7	--	--
SES (Aug 1963)	10,000	7	3	19.7	14.1	--	--
SES (Sep 1963)	10,000	7	3	20.1	14.1	--	--
Snowball	1,000,000	7	3	139.8	13.8	--	580,000
Distant Plain 4	100,000	7	3	40.7	16.4	--	--
Dry Sand:							
White Tribe I-1	11,560	9	1	14.3	6.6	2.1	--
White Tribe I-2	11,560	9	1	20.0	10.3	2.0	--
White Tribe I-3	11,560	9	1	16.0	6.2	2.1	--
White Tribe II-1	11,560	9	1	18.3	8.6	1.8	--
White Tribe II-2	11,560	9	1	17.9	8.3	2.3	--
White Tribe II-3	11,560	9	1	18.0	9.6	2.6	--
White Tribe III-1	11,560	9	1	17.3	6.1	1.5	--
White Tribe III-2	11,560	9	1	15.5	7.5	1.9	--
White Tribe III-3	11,560	9	1	19.1	10.0	1.6	--

[a] Conducted at Suffield Experimental Station (now Defence Research Establishment, Suffield), Alberta, Canada.

APPENDIX B

GRAPHICAL PRESENTATION OF CRATER DATA

The tabular data of Appendix A are contained in graphical form in Figures B.1 through B.93 of this appendix. Essentially, these are least-squares fits of the data, as explained in Section 3.3. Where insufficient data exist to support a curve (actually, a straight-line fit in all but Figure B.93), the available points are shown. Where no data exist for one or two plots in a figure (apparent dimensions, true dimensions, or volumes), the blank graph(s) is (are) included for future entries. This permits the use of a consistent format, with all graphs in a single figure printed and bound for ease in reading.

Where available, classified data have been considered in preparation of the graphs, although not shown here or elsewhere in this report. Existence of such data are noted on the appropriate figures.

The category numbers used in the graphs and in the tables in Appendix A refer to the height-of-burst categories into which the data are divided (as explained in Section 3.3).

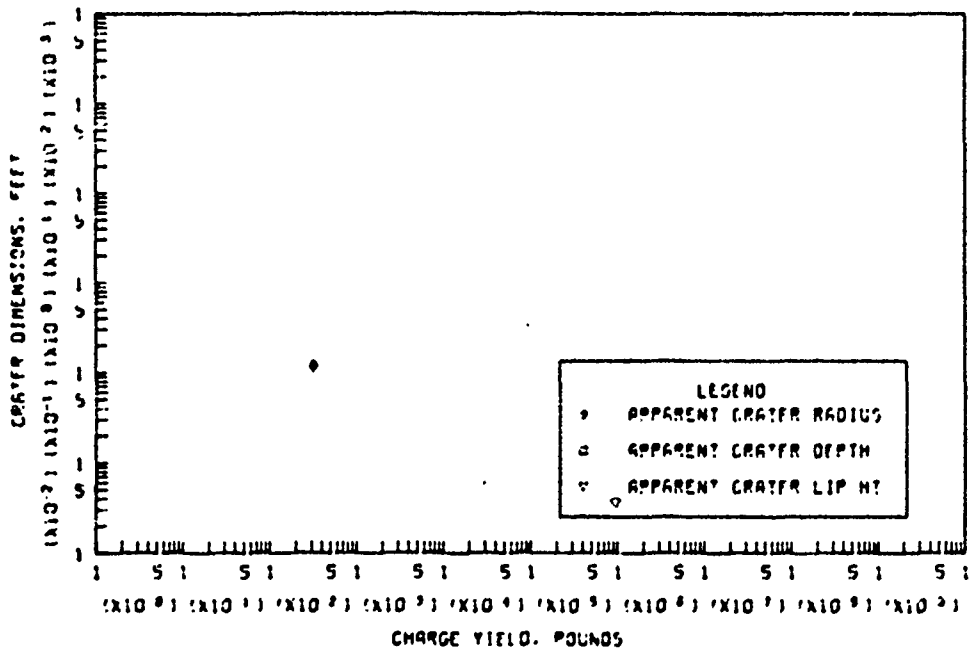

a. APPARENT CRATER DIMENSIONS VERSUS CHARGE YIELD

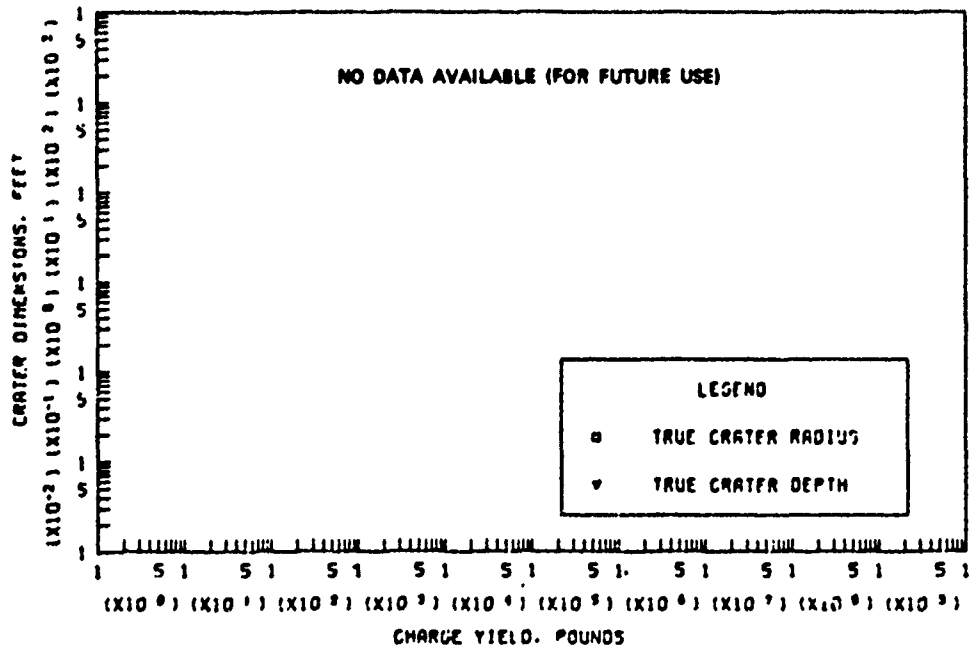

b. TRUE CRATER DIMENSIONS VERSUS CHARGE YIELD

Figure B.1 Dimensions of craters in basalt and granite for $0.20 \leq Z < 0.50$ ft/lb$^{1/3}$, Category 2 (sheet 1 of 2).

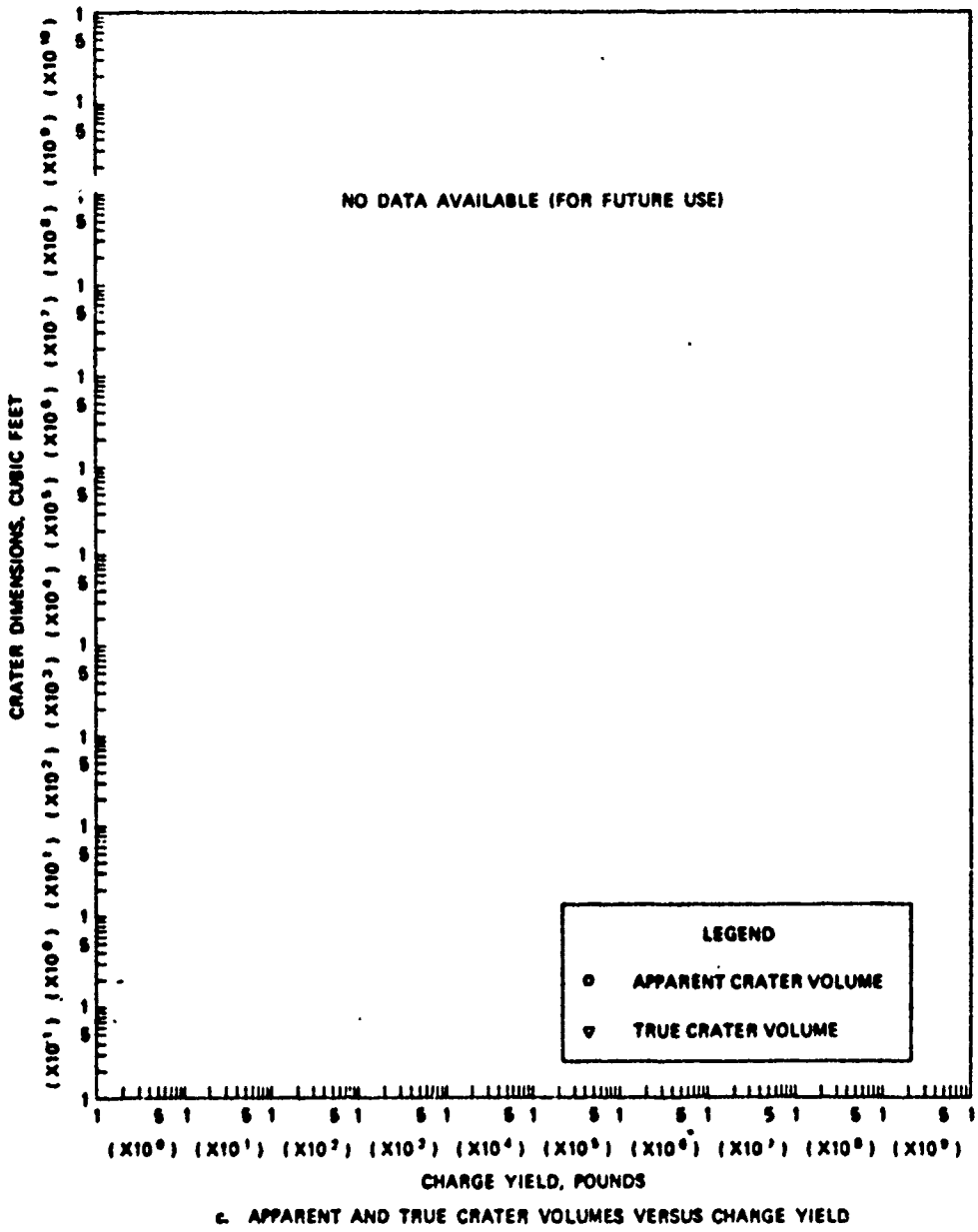

c. APPARENT AND TRUE CRATER VOLUMES VERSUS CHARGE YIELD

Figure B.1 (sheet 2 of 2).

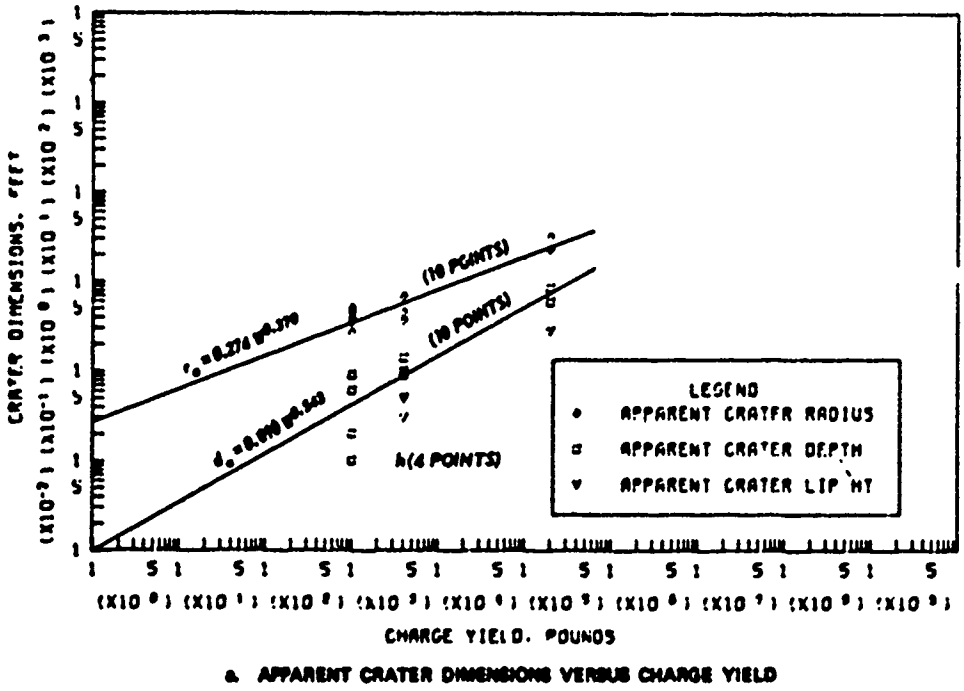

a. APPARENT CRATER DIMENSIONS VERSUS CHARGE YIELD

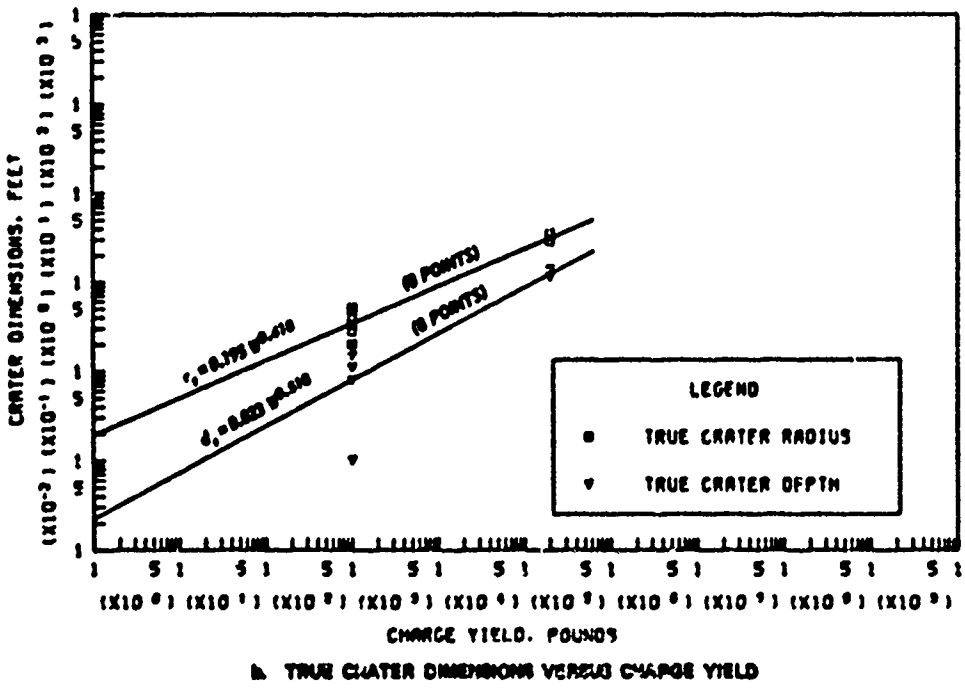

b. TRUE CRATER DIMENSIONS VERSUS CHARGE YIELD

Figure B.2 Dimensions of craters in basalt and granite for $0.05 \leq Z < 0.20$ ft/lb$^{1/3}$, Category 3 (sheet 1 of 2).

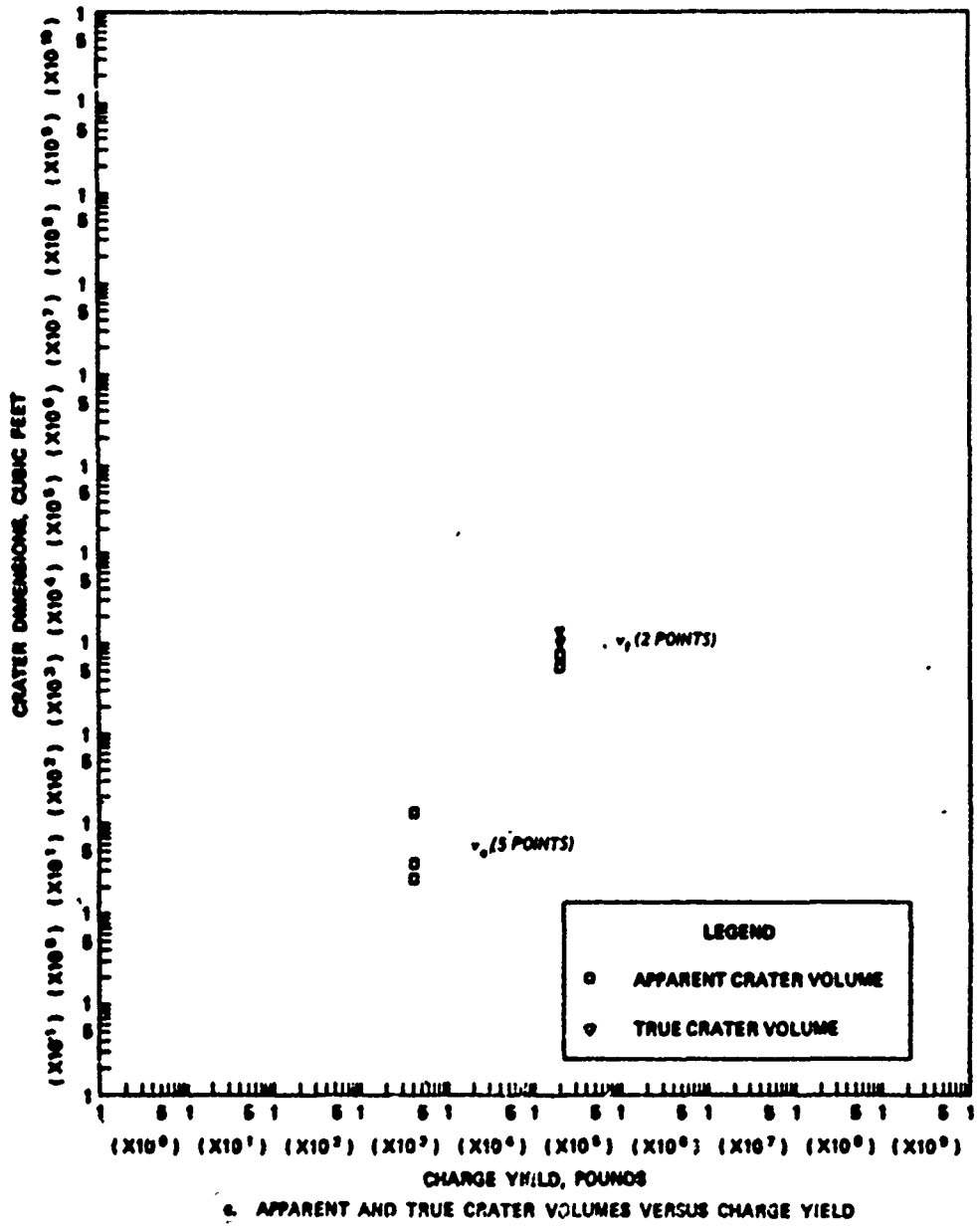

a. APPARENT AND TRUE CRATER VOLUMES VERSUS CHARGE YIELD

Figure B.2 (sheet 2 of 2).

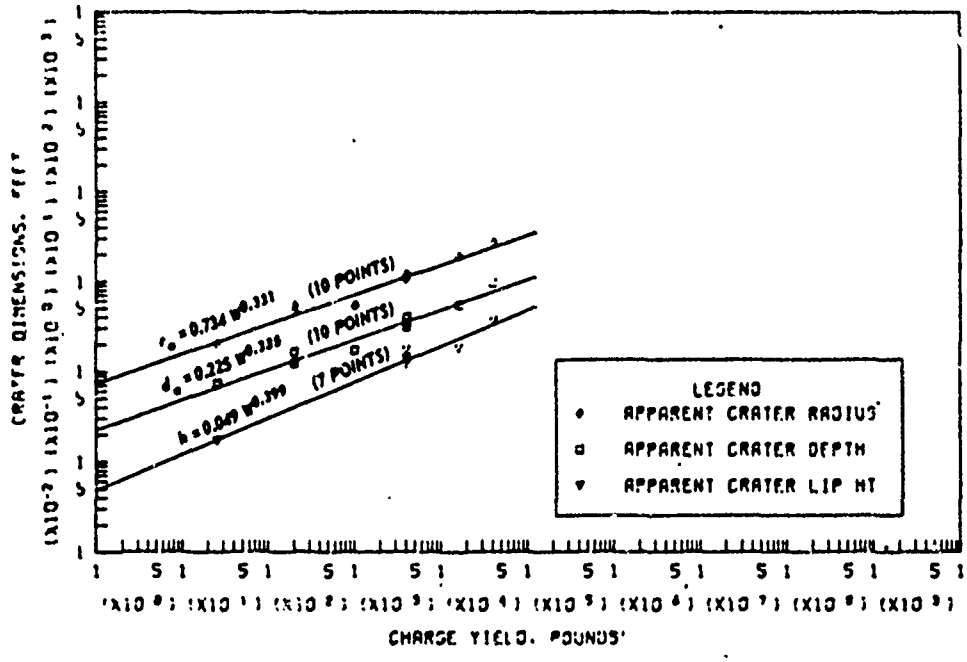

a. APPARENT CRATER DIMENSIONS VERSUS CHARGE YIELD

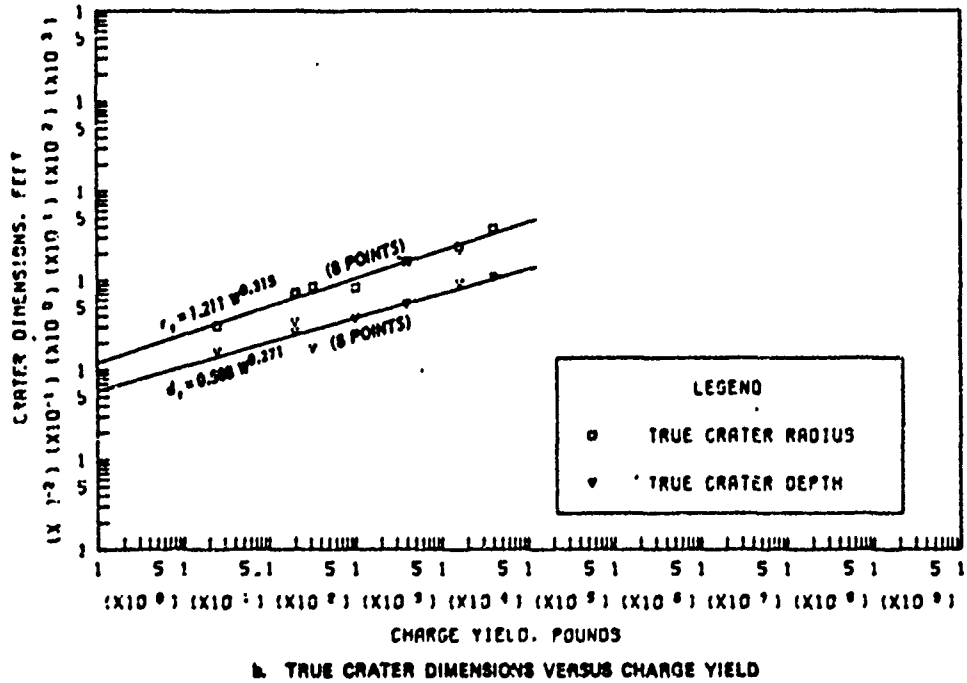

b. TRUE CRATER DIMENSIONS VERSUS CHARGE YIELD

Figure B.3 Dimensions of craters in basalt and granite for $-0.05 \leq Z < 0.05$ ft/lb$^{1/3}$, Category 4 (sheet 1 of 2).

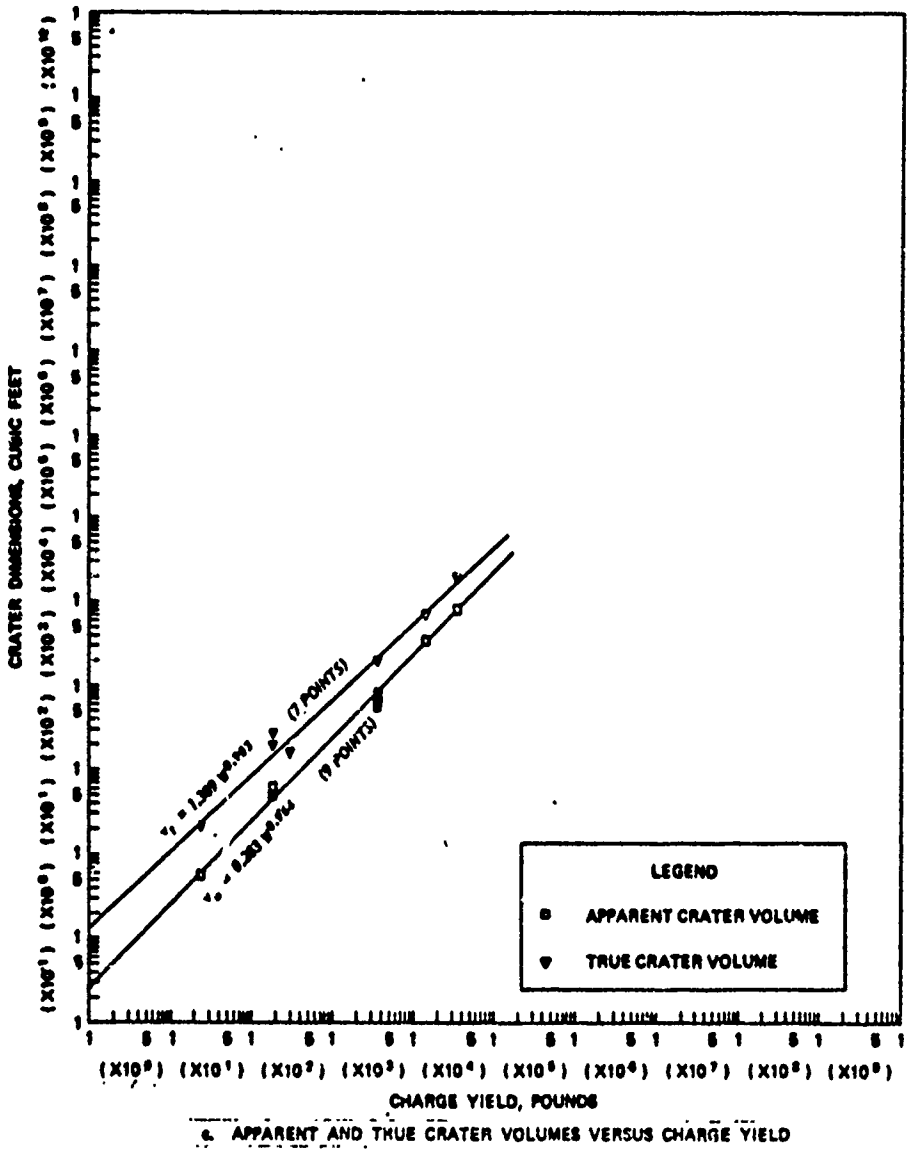

a. APPARENT AND TRUE CRATER VOLUMES VERSUS CHARGE YIELD

Figure B.3 (sheet 2 of 2).

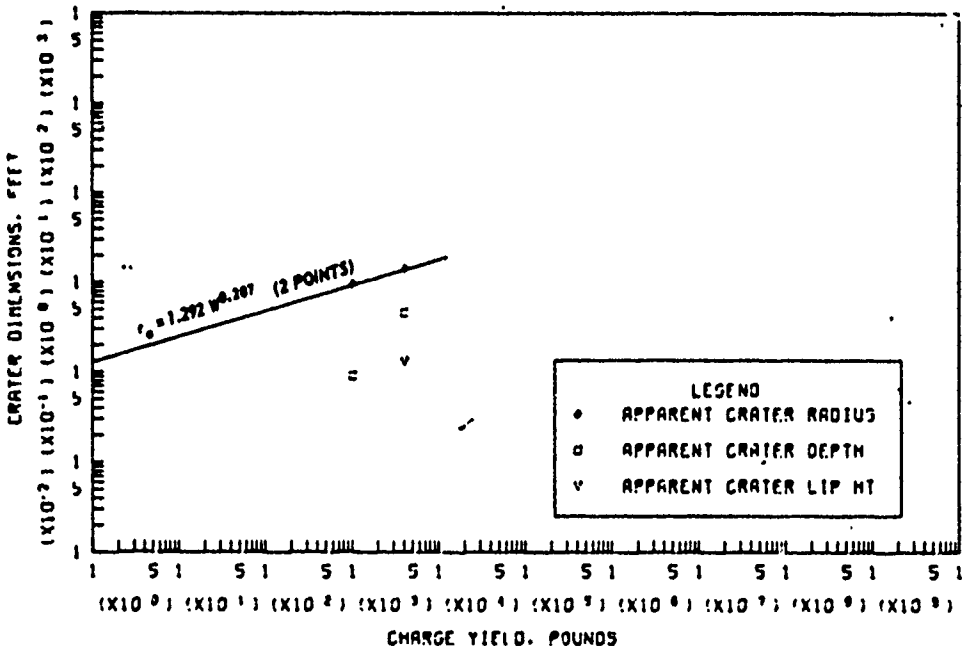

a. APPARENT CRATER DIMENSIONS VERSUS CHARGE YIELD

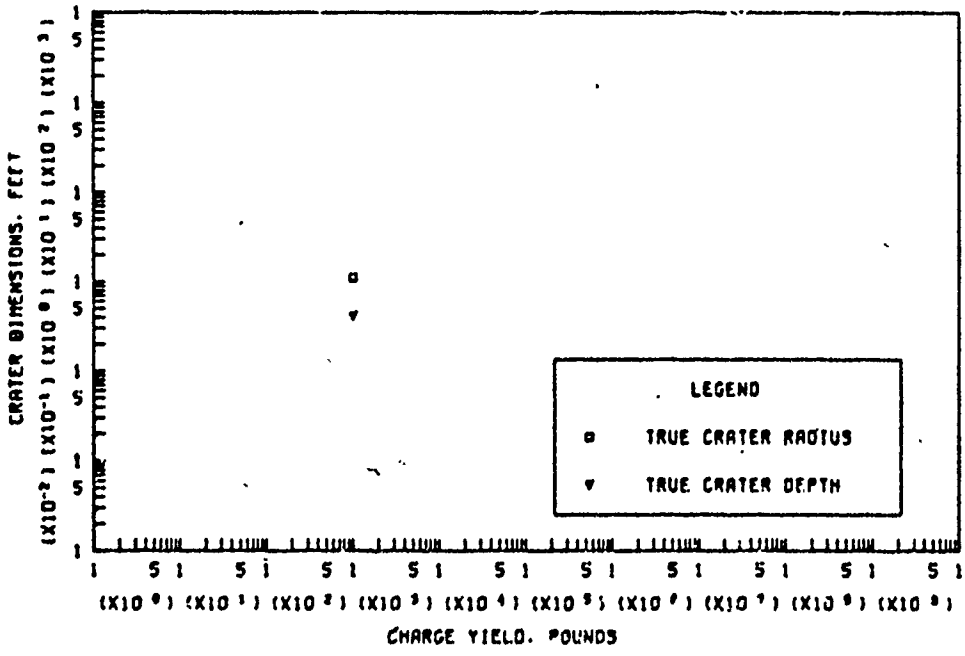

b. TRUE CRATER DIMENSIONS VERSUS CHARGE YIELD

Figure B.4 Dimensions of craters in basalt and granite for $-0.20 \leq Z < -0.05$ ft/lb$^{1/3}$, Category 5 (sheet 1 of 2).

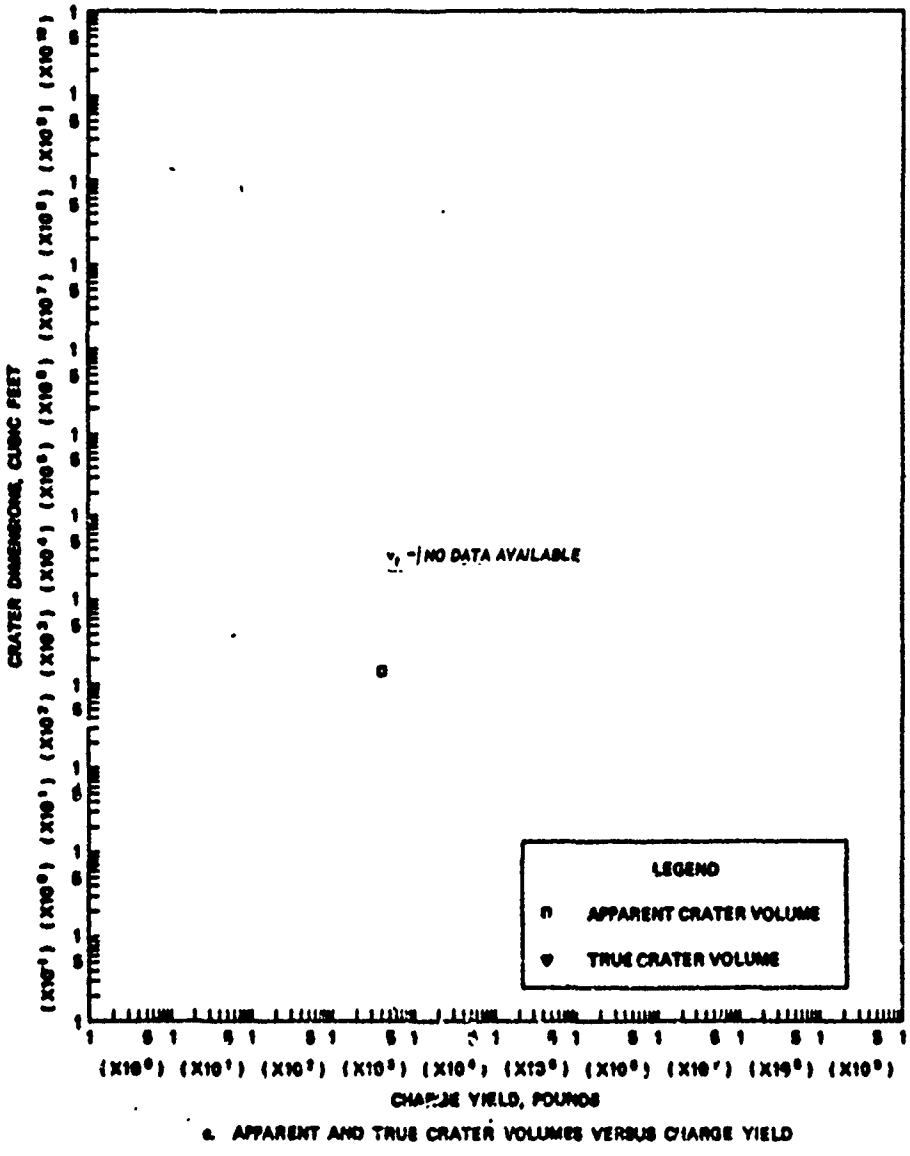

a. APPARENT AND TRUE CRATER VOLUMES VERSUS CHARGE YIELD

Figure B.4 (sheet 2 of 2).

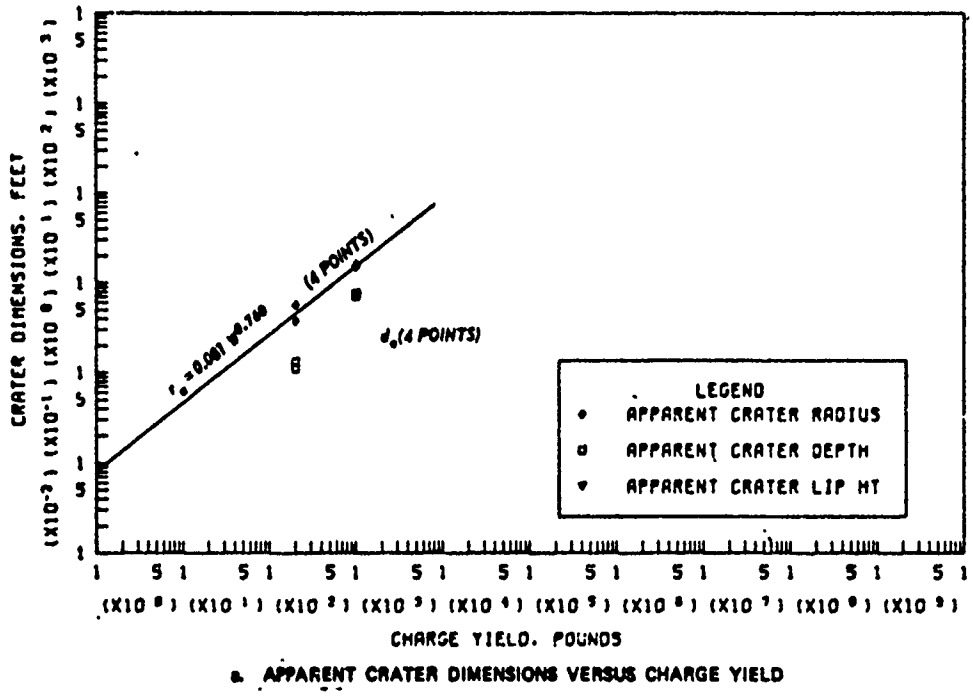

a. APPARENT CRATER DIMENSIONS VERSUS CHARGE YIELD

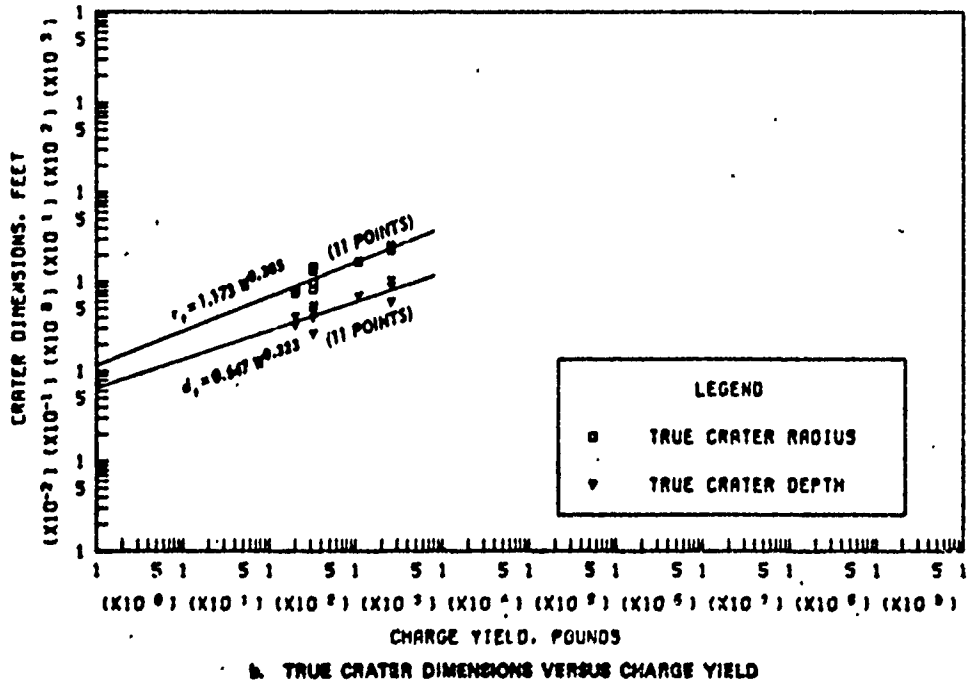

b. TRUE CRATER DIMENSIONS VERSUS CHARGE YIELD

Figure B.5 Dimensions of craters in basalt and granite for $-0.50 \leq Z < -0.20$ ft/lb$^{1/3}$, Category 6 (sheet 1 of 2).

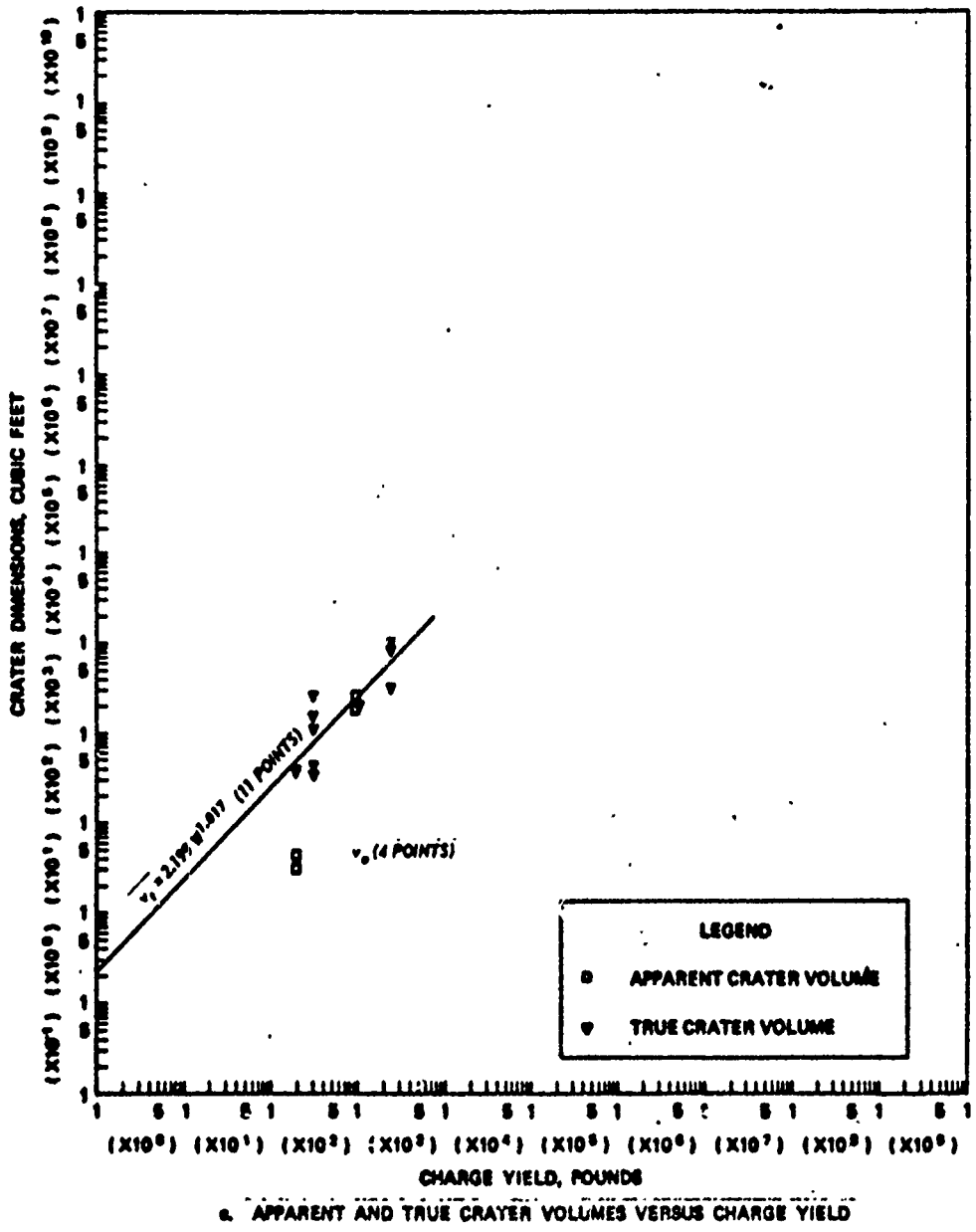

a. APPARENT AND TRUE CRATER VOLUMES VERSUS CHARGE YIELD

Figure B.5 (sheet 2 of 2).

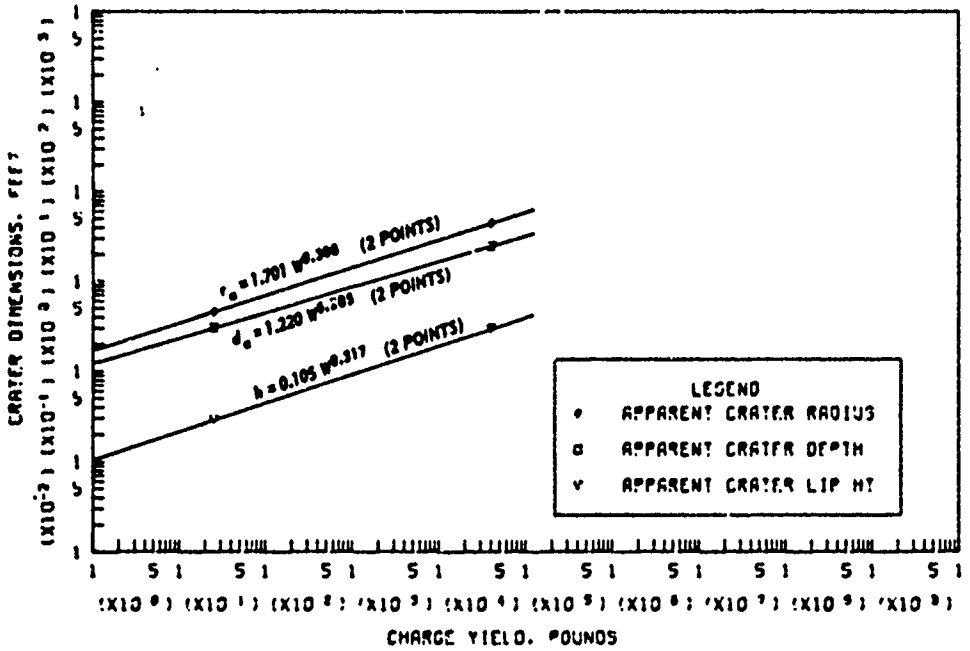

a. APPARENT CRATER DIMENSIONS VERSUS CHARGE YIELD

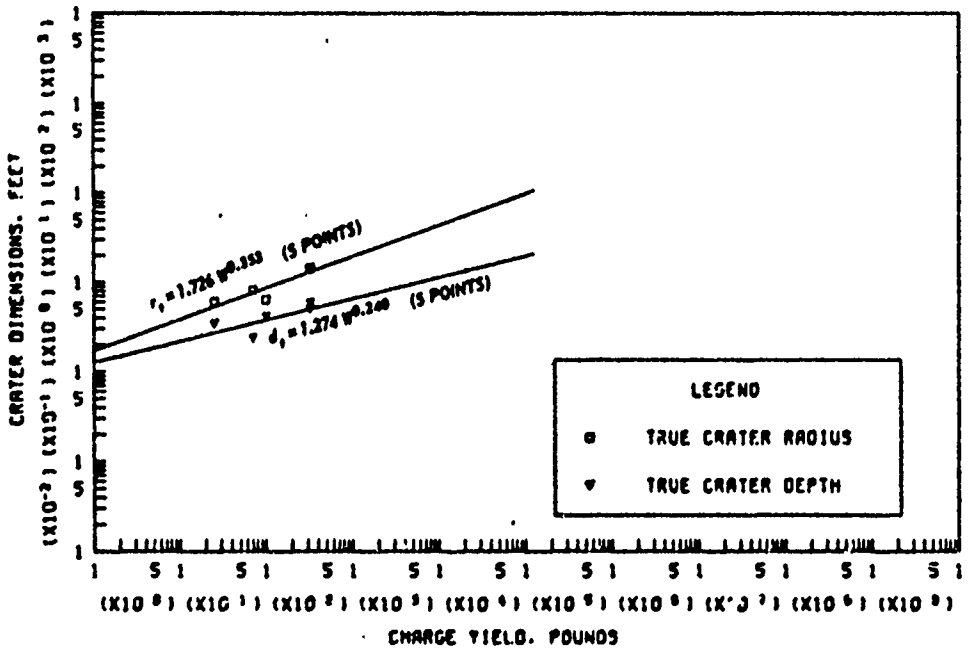

b. TRUE CRATER DIMENSIONS VERSUS CHARGE YIELD

Figure B.6 Dimensions of craters in basalt and granite for $-0.90 \leq Z < -0.50$ ft/lb$^{1/3}$, Category 7 (sheet 1 of 2).

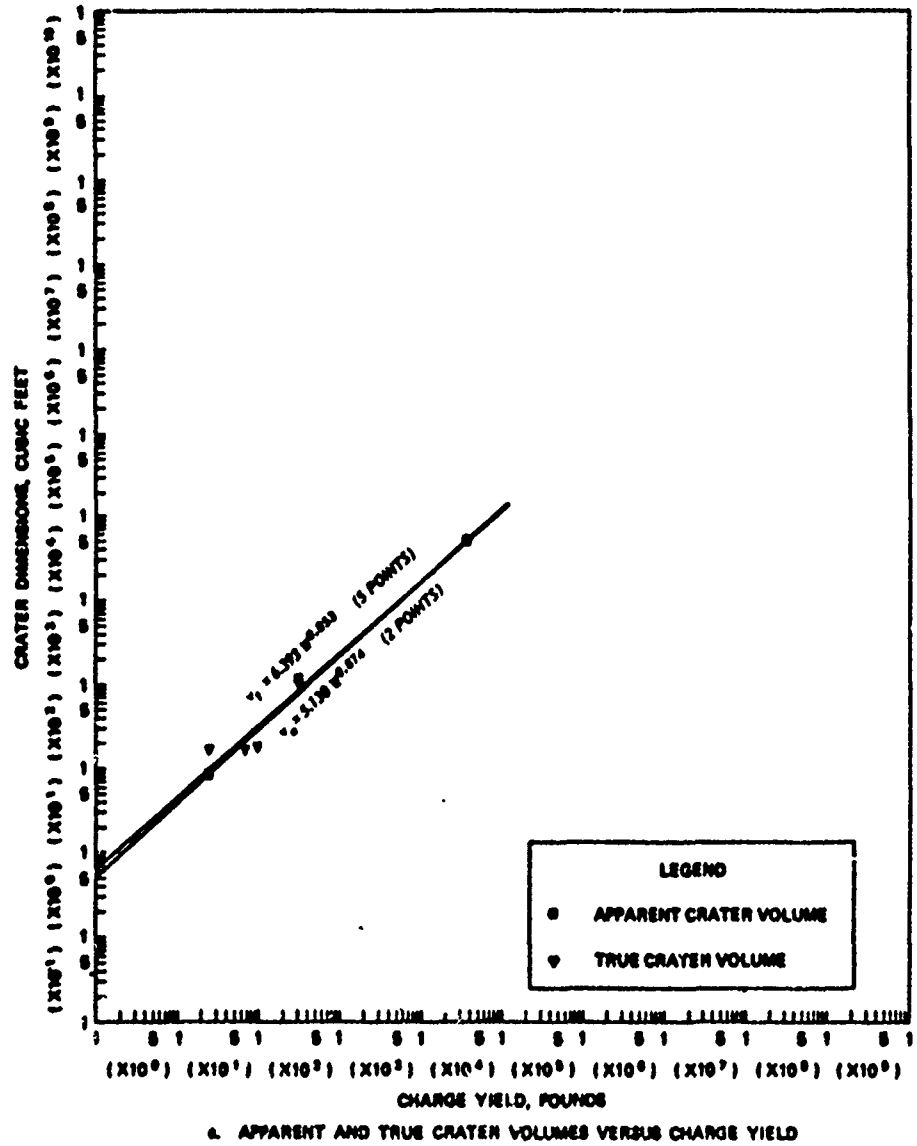

a. APPARENT AND TRUE CRATER VOLUMES VERSUS CHARGE YIELD

Figure B.6 (sheet 2 of 2).

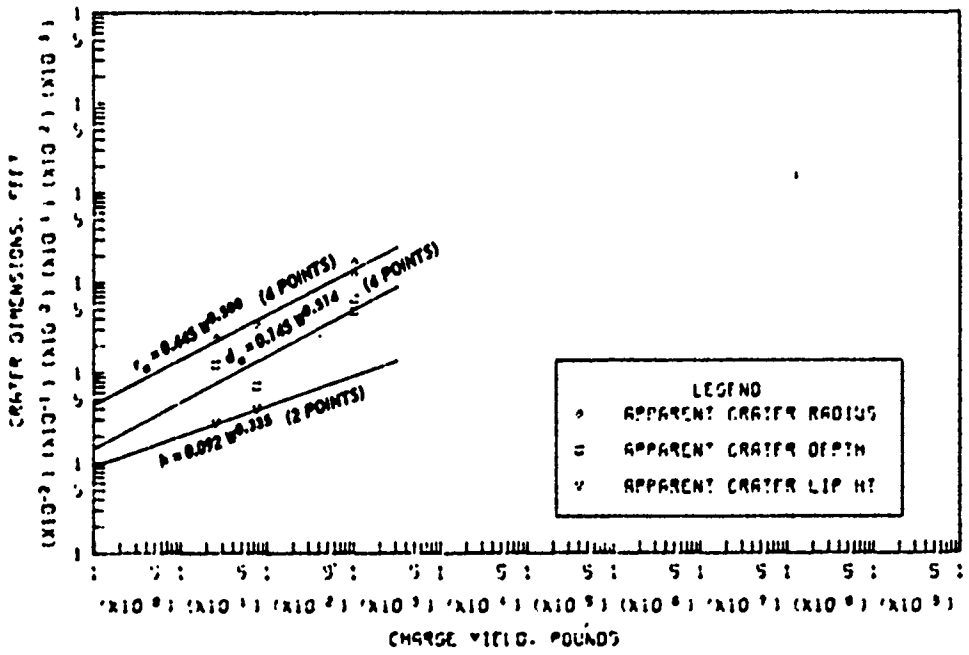

a. APPARENT CRATER DIMENSIONS VERSUS CHARGE YIELD

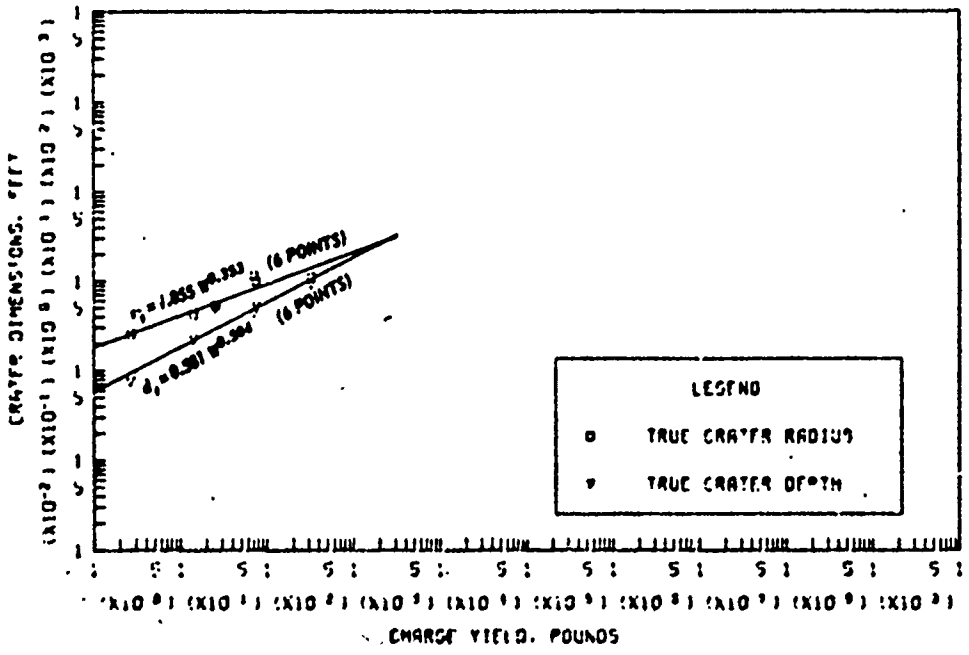

b. TRUE CRATER DIMENSIONS VERSUS CHARGE YIELD

Figure B.7 Dimensions of craters in basalt and granite for $-1.10 \leq Z < -0.90$ ft/lb$^{1/3}$, Category 8 (sheet 1 of 2).

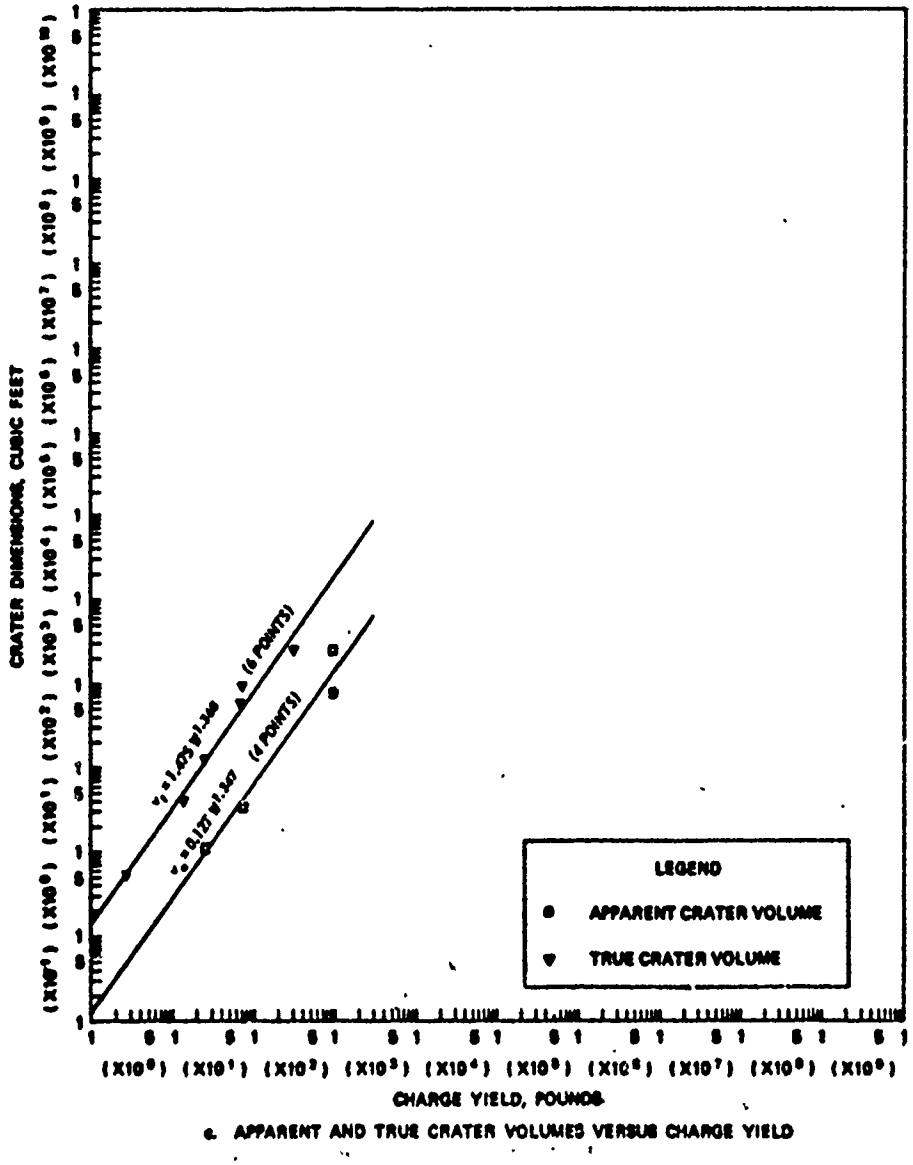

c. APPARENT AND TRUE CRATER VOLUMES VERSUS CHARGE YIELD

Figure 3.7 (sheet 2 of 2).

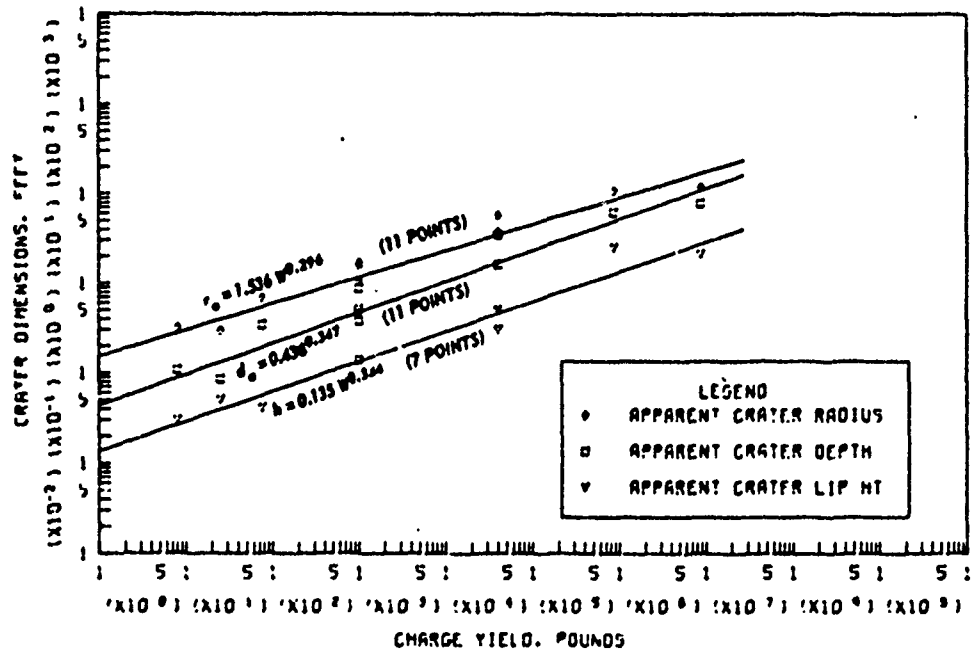

a. APPARENT CRATER DIMENSIONS VERSUS CHARGE YIELD

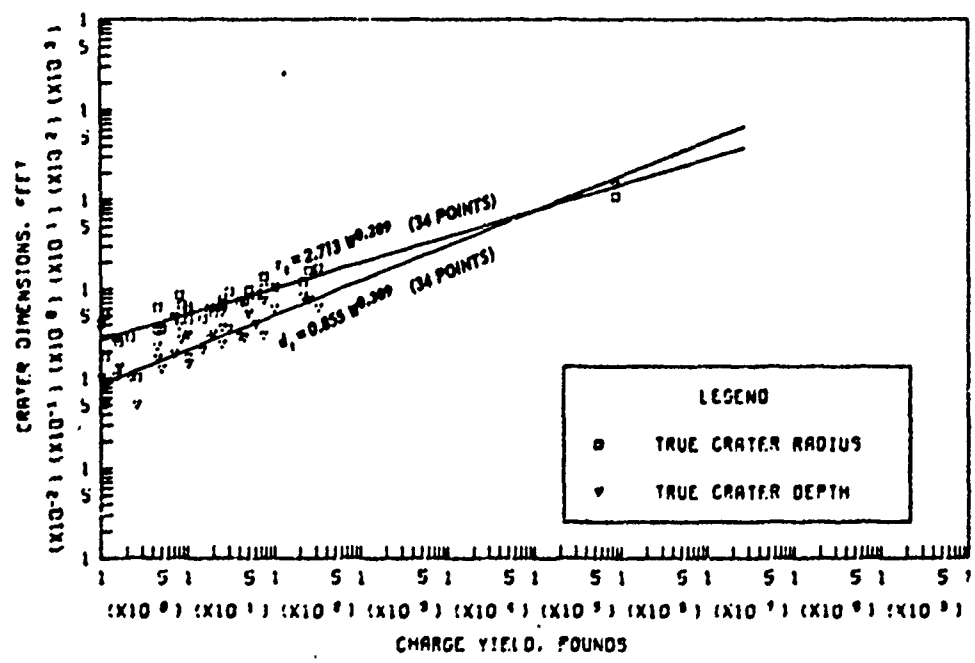

b. TRUE CRATER DIMENSIONS VERSUS CHARGE YIELD

Figure B.8 Dimensions of craters in basalt and granite for $-2.00 \leq Z < -1.10$ ft/lb$^{1/3}$, Category 9 (sheet 1 of 2).

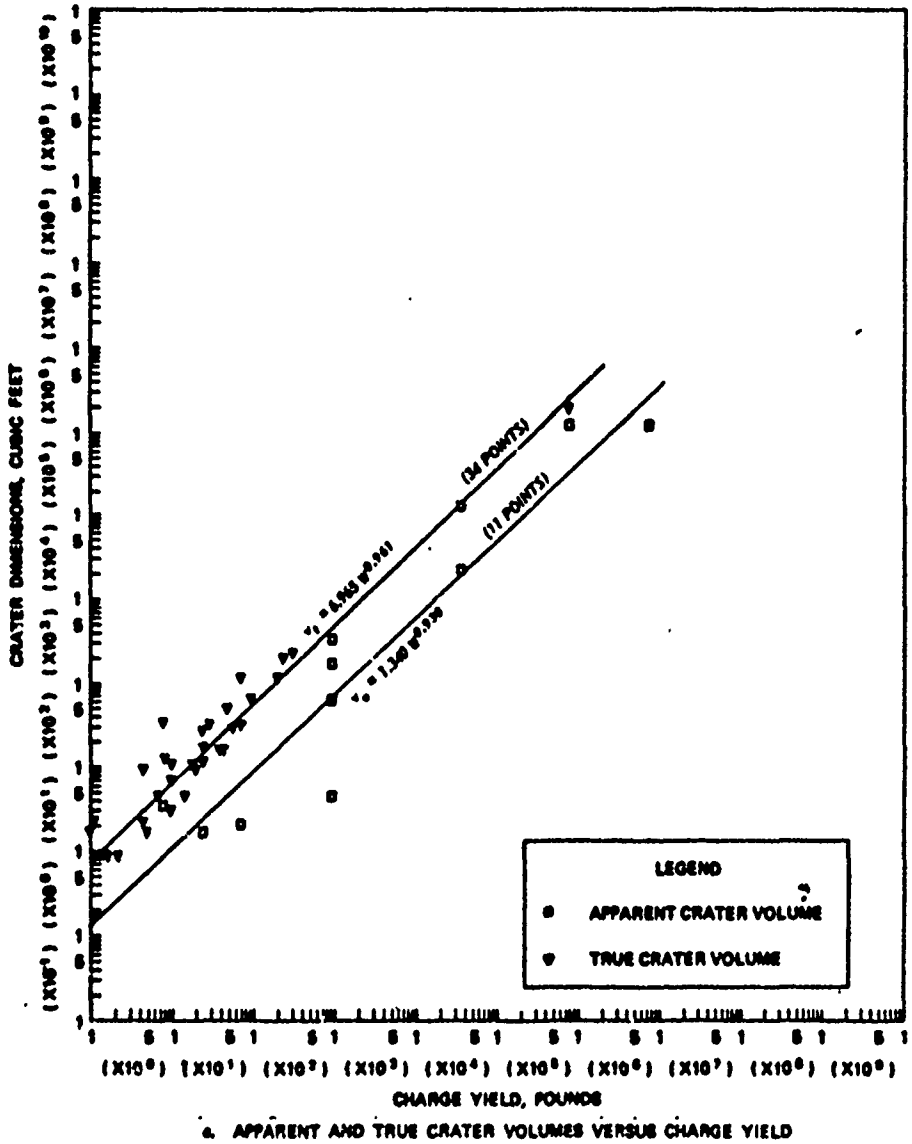

a. APPARENT AND TRUE CRATER VOLUMES VERSUS CHARGE YIELD

Figure B.8 (sheet 2 of 2).

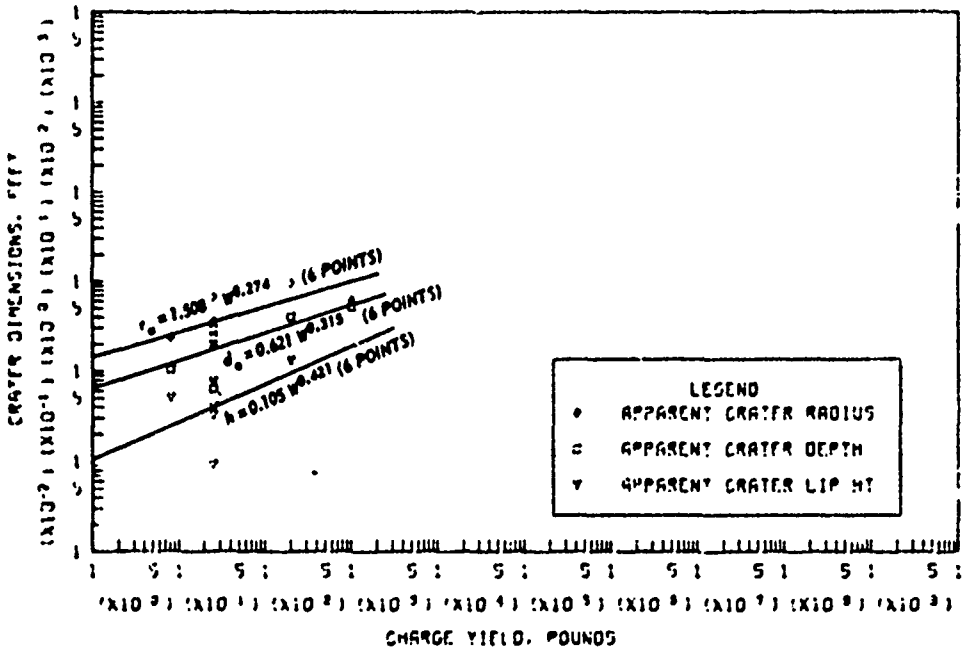

a. APPARENT CRATER DIMENSIONS VERSUS CHARGE YIELD

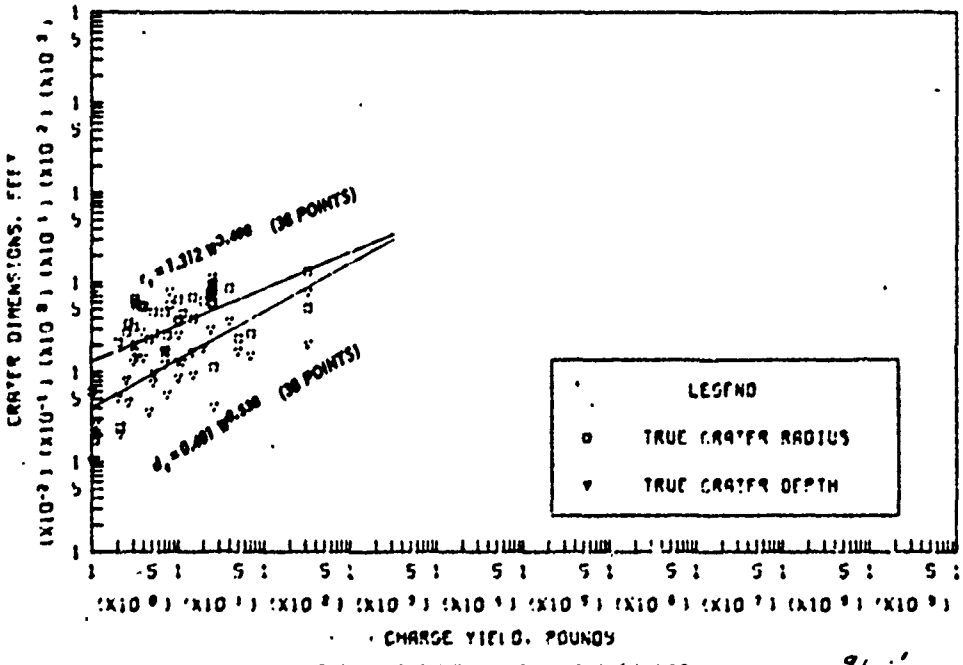

b. TRUE CRATER DIMENSIONS VERSUS CHARGE YIELD

Figure B.9 Dimensions of craters in basalt and granite for $Z < -2.00$ ft/lb$^{1/3}$, Category 10 (sheet 1 of 2).

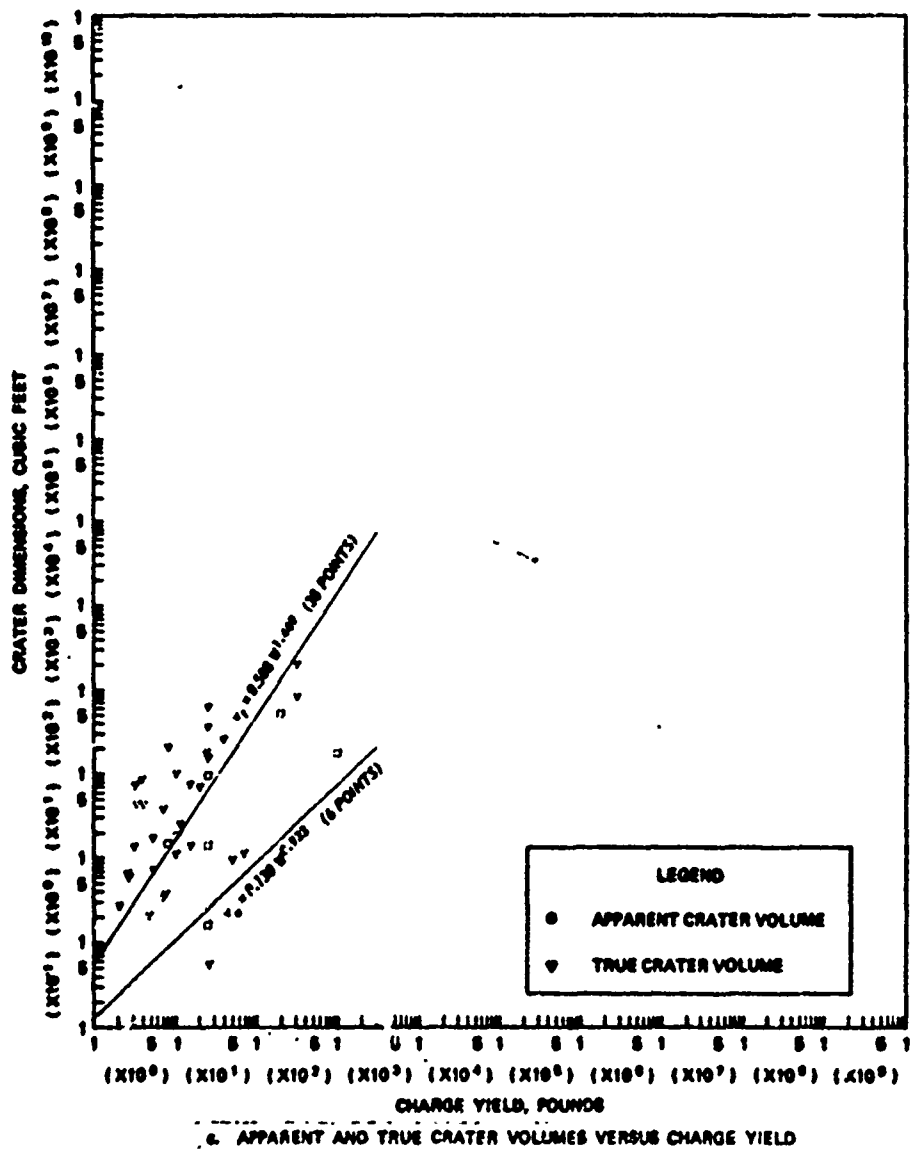

a. APPARENT AND TRUE CRATER VOLUMES VERSUS CHARGE YIELD

Figure B.9 (sheet 2 of 2).

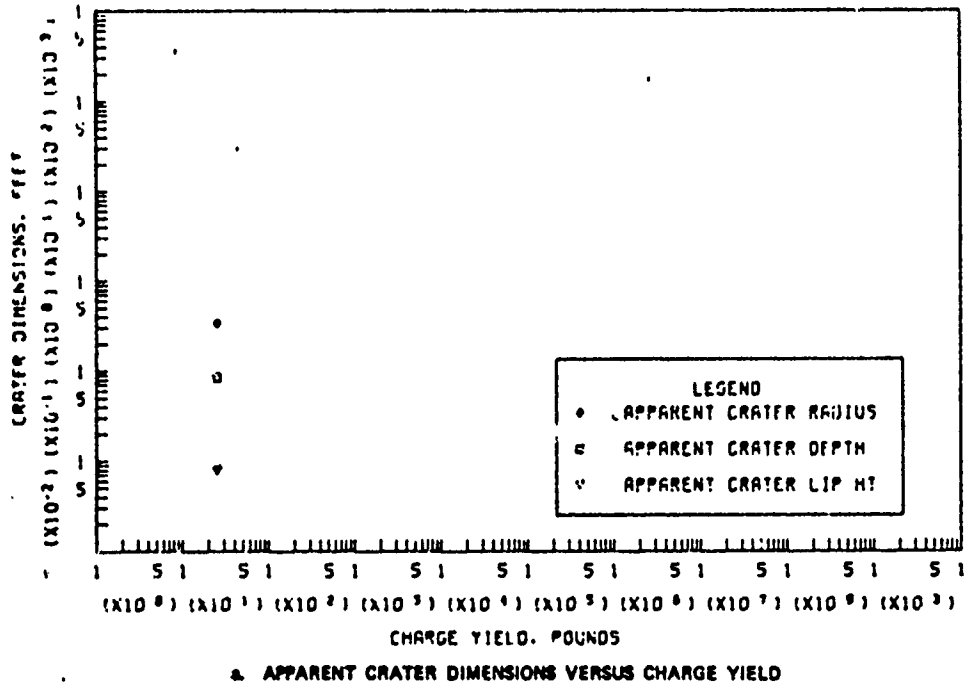

a. APPARENT CRATER DIMENSIONS VERSUS CHARGE YIELD

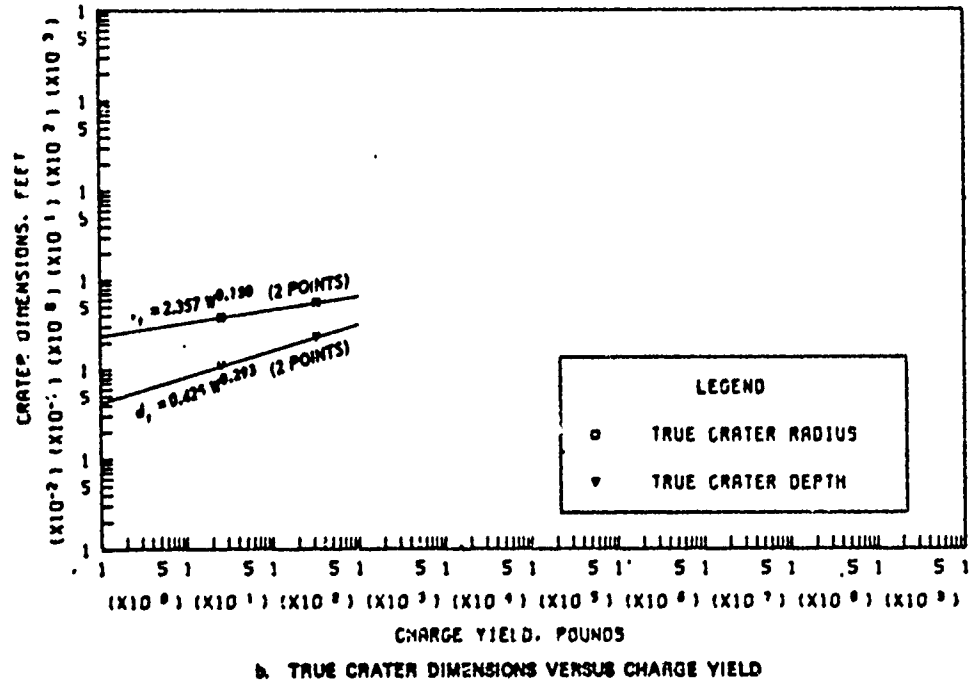

b. TRUE CRATER DIMENSIONS VERSUS CHARGE YIELD

Figure B.10 Dimensions of craters in sandstone for $-0.05 \leq Z < 0.05$ ft/lb$^{1/3}$, Category 4 (sheet 1 of 2).

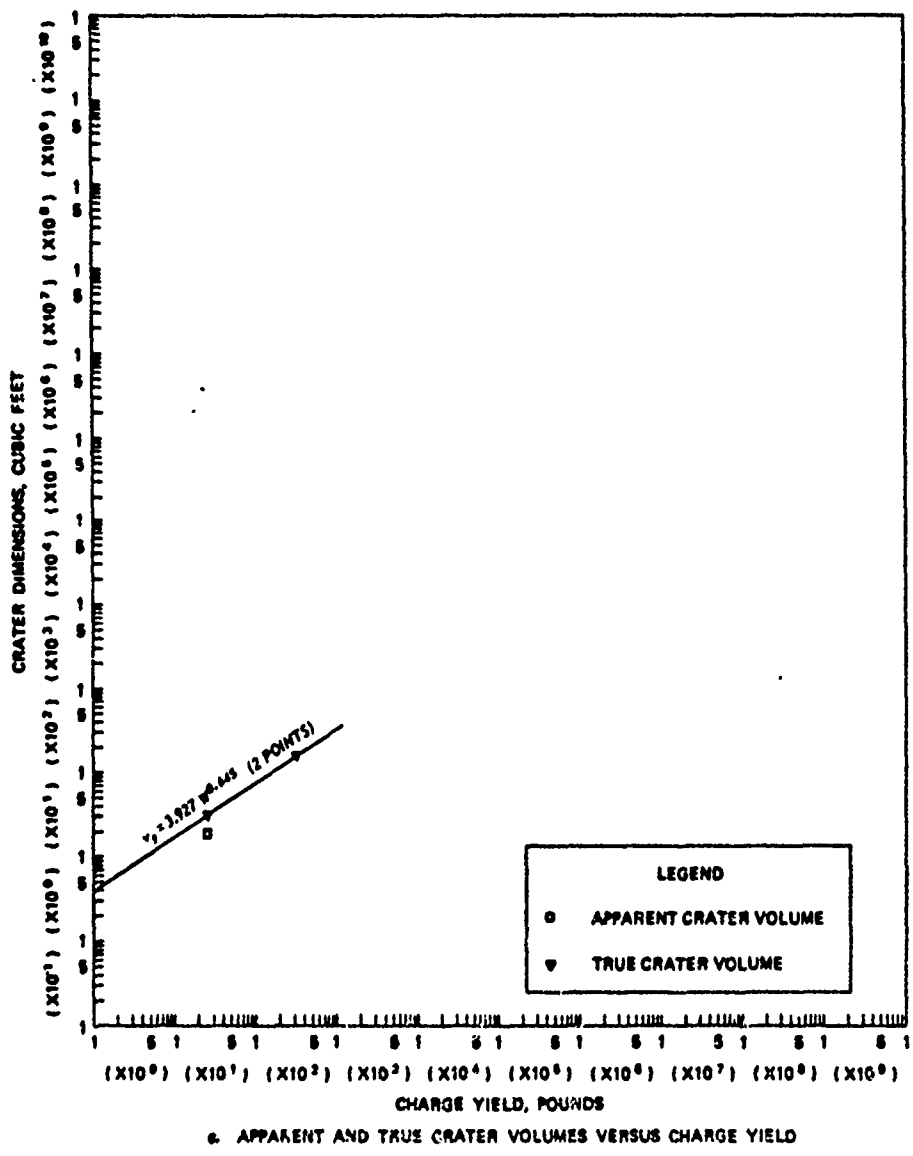

a. APPARENT AND TRUE CRATER VOLUMES VERSUS CHARGE YIELD

Figure B.10 (sheet 2 of 2).

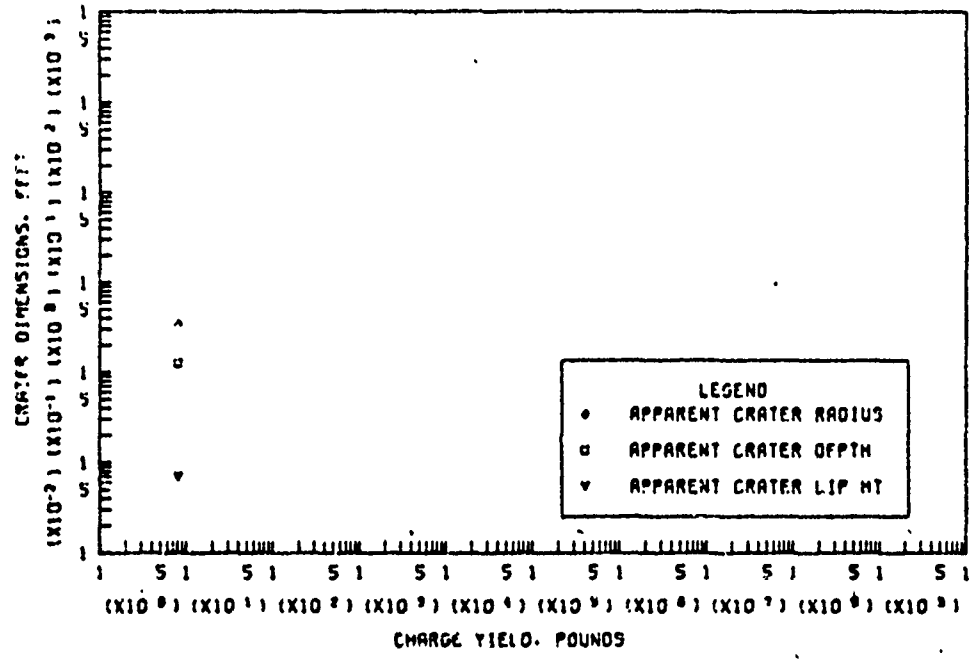

a. APPARENT CRATER DIMENSIONS VERSUS CHARGE YIELD

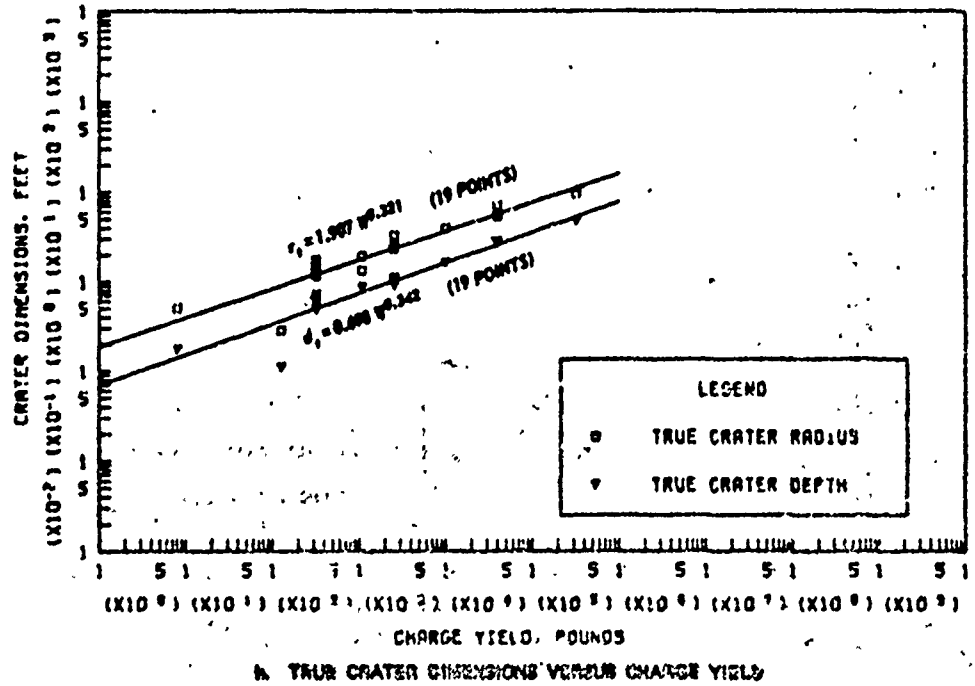

b. TRUE CRATER DIMENSIONS VERSUS CHARGE YIELD

Figure B.11 Dimensions of craters in sandstone for $-0.50 \leq Z < -0.20$ ft/lb$^{1/3}$, Category 6 (sheet 1 of 2).

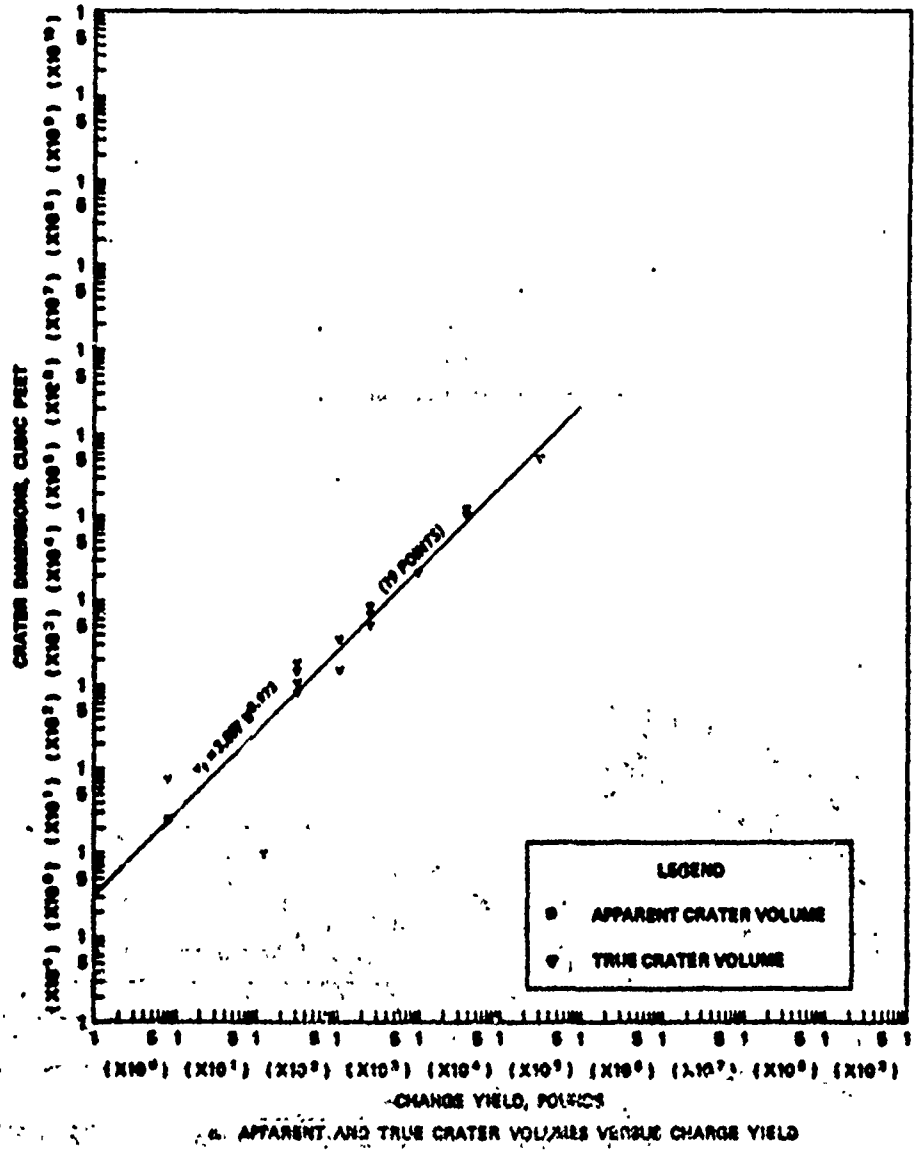

a. APPARENT AND TRUE CRATER VOLUMES VERSUS CHARGE YIELD

Figure E.11 (sheet 2 of 2).

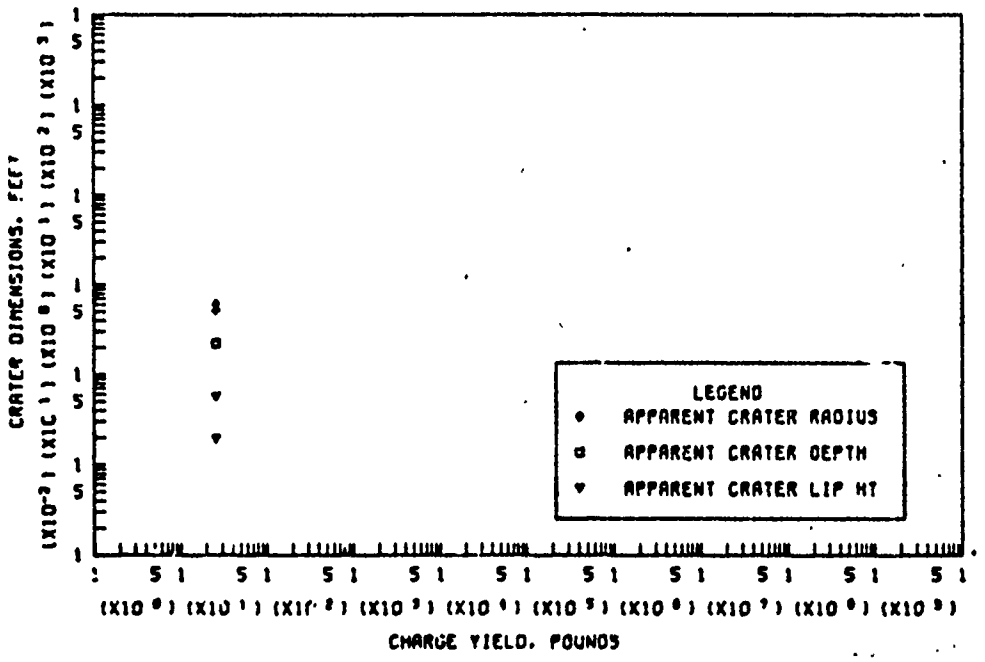

a. APPARENT CRATER DIMENSIONS VERSUS CHARGE YIELD

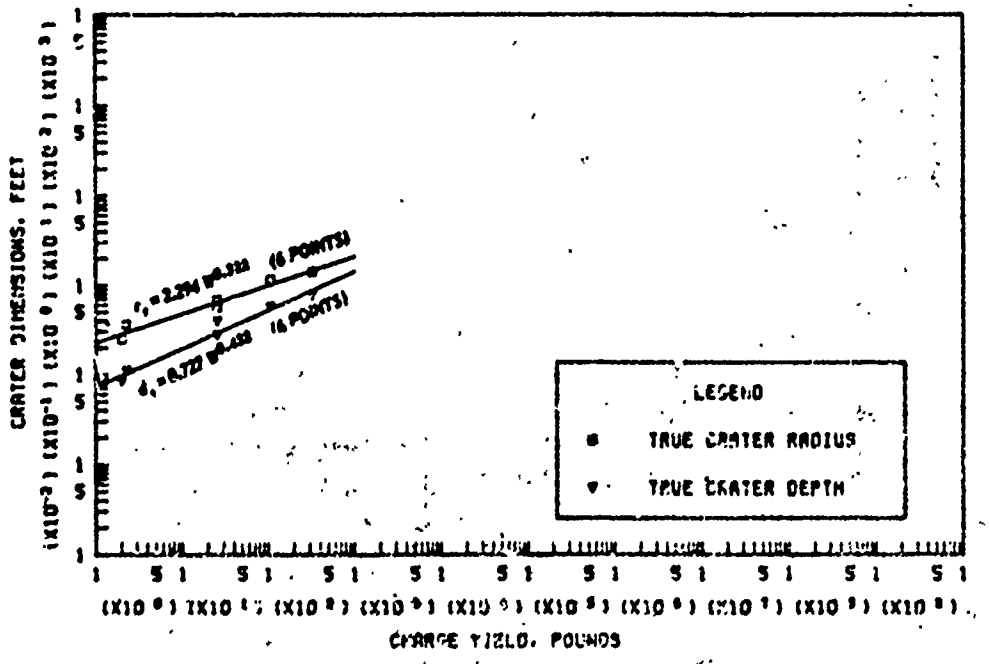

b. TRUE CRATER DIMENSIONS VERSUS CHARGE YIELD

Figure B.12 Dimensions of craters in sandstone for $-0.90 \leq Z < -0.50$ ft/lb$^{1/3}$, Category 7 (sheet 1 of 2).

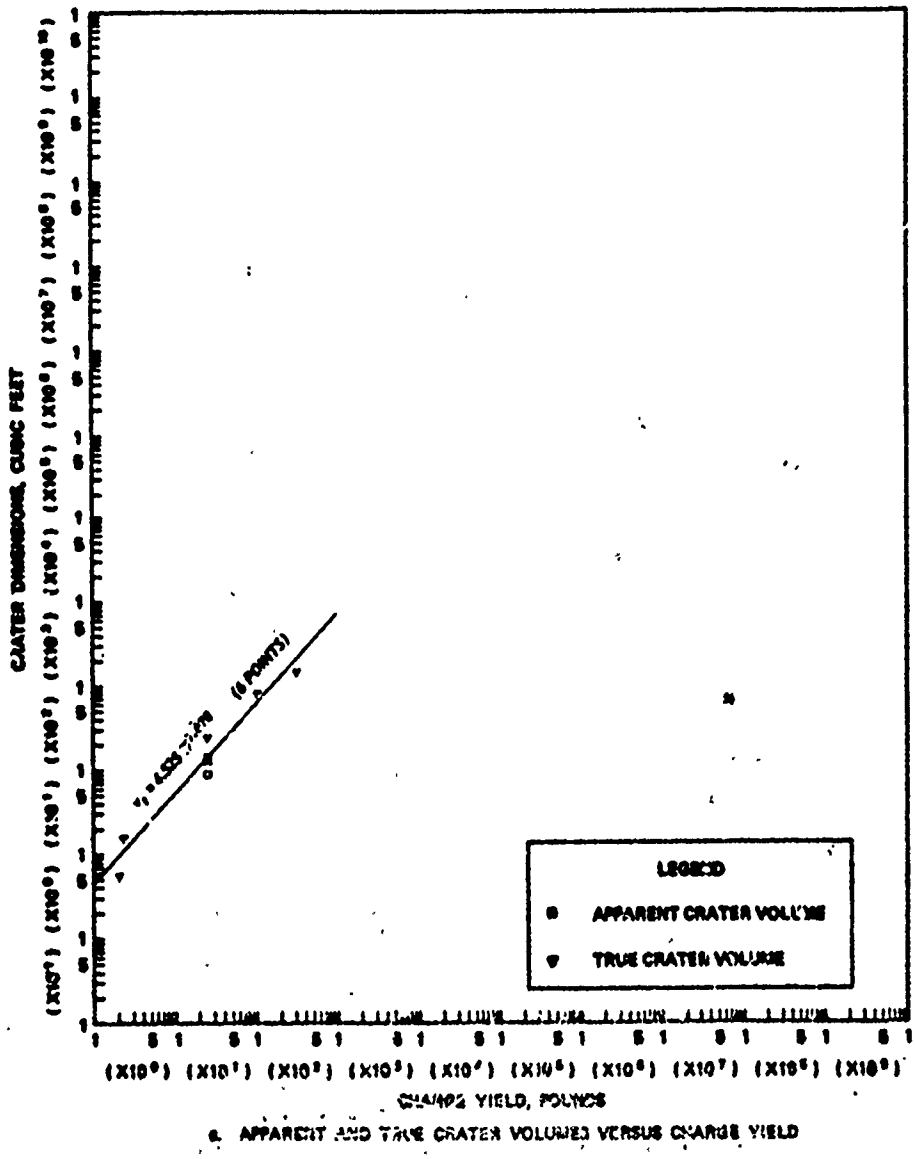

a. APPARENT AND TRUE CRATER VOLUMES VERSUS CHARGE YIELD

Figure B.12 (sheet 2 of 2).

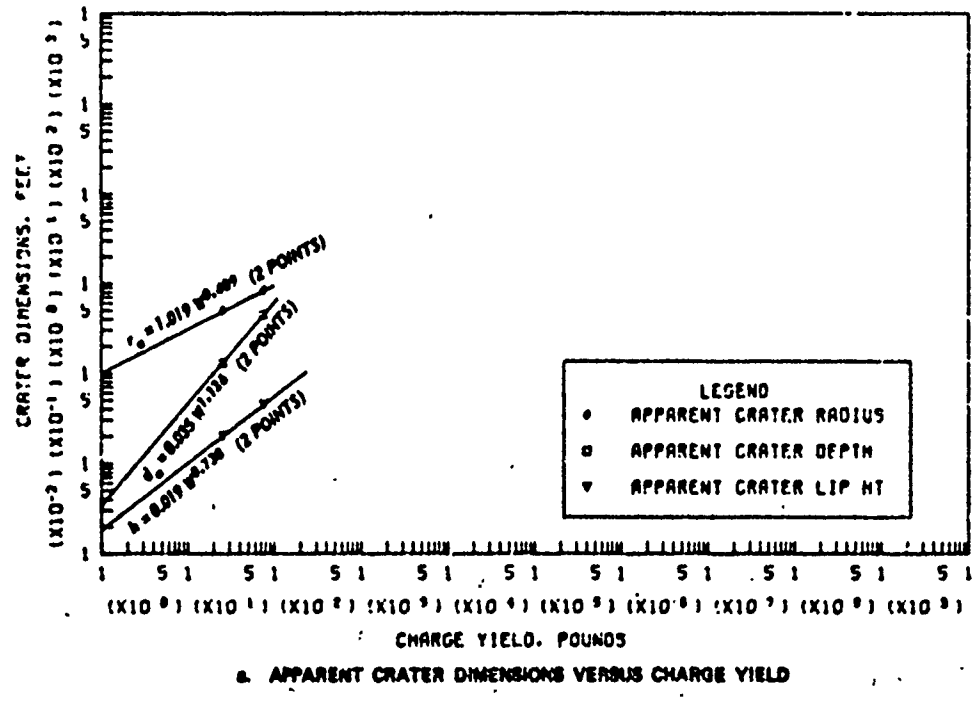

a. APPARENT CRATER DIMENSIONS VERSUS CHARGE YIELD

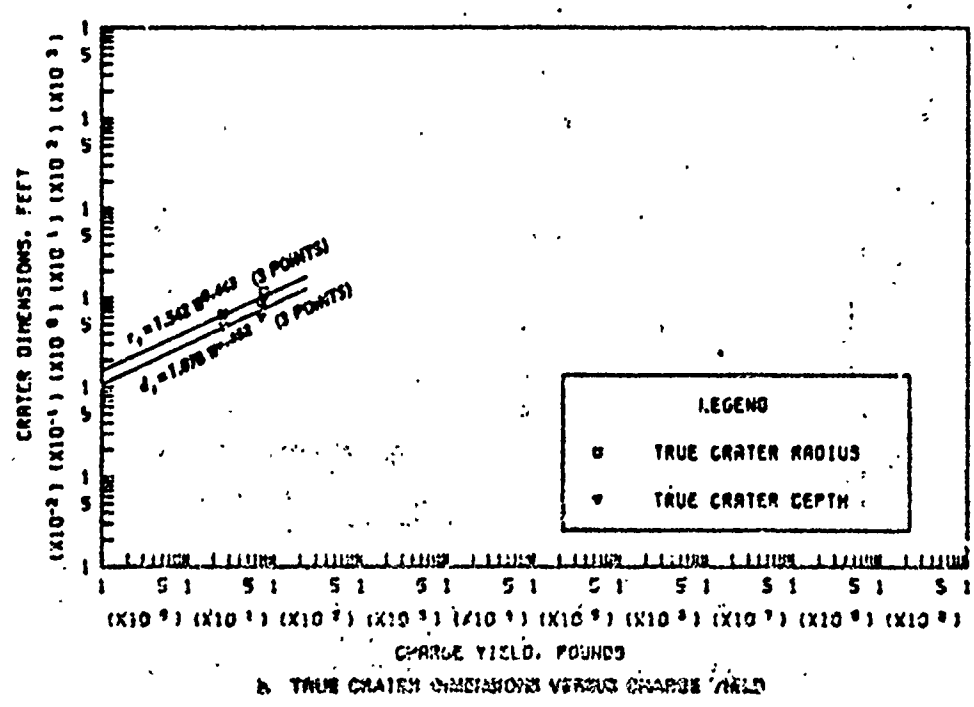

b. TRUE CRATER DIMENSIONS VERSUS CHARGE YIELD

Figure B.13 Dimensions of craters in sandstone for $-1.10 \leq \gamma < -0.90$ ft/lb$^{1/3}$, Category 8 (sheet 1 of 2).

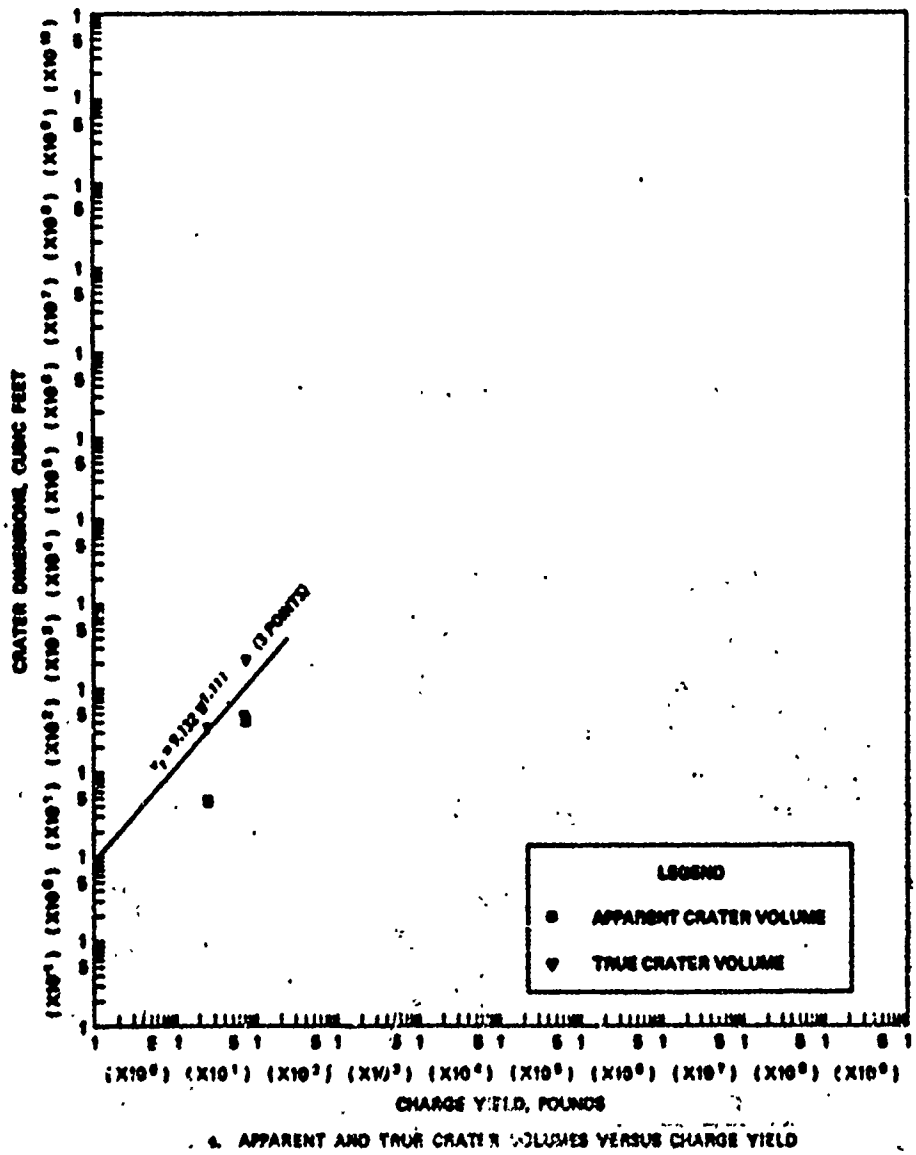

a. APPARENT AND TRUE CRATER VOLUMES VERSUS CHARGE YIELD

Figure B.13 (sheet 2 of 2).

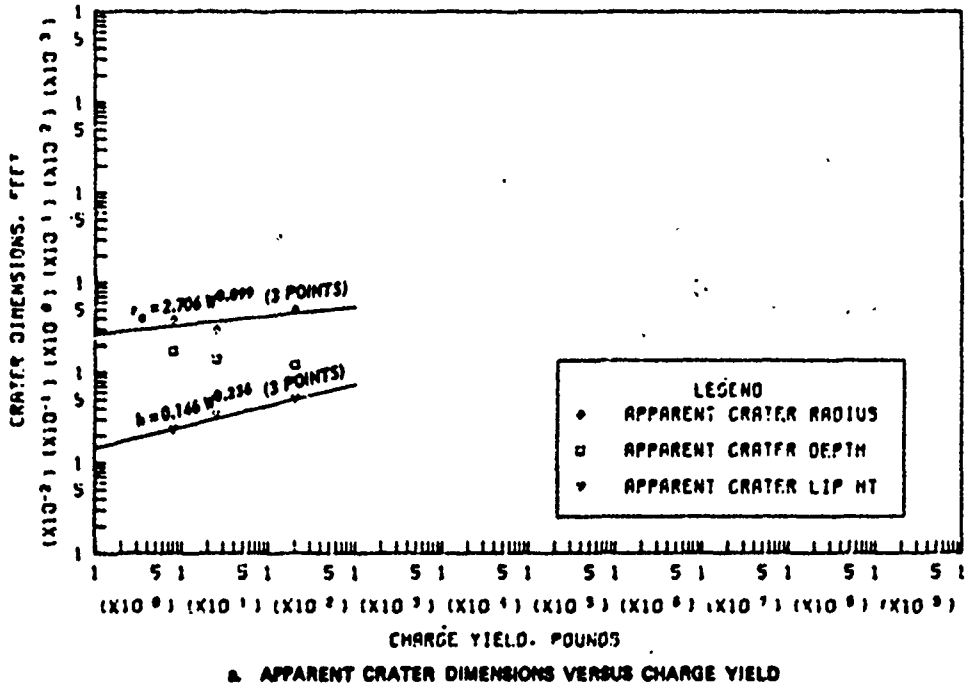

a. APPARENT CRATER DIMENSIONS VERSUS CHARGE YIELD

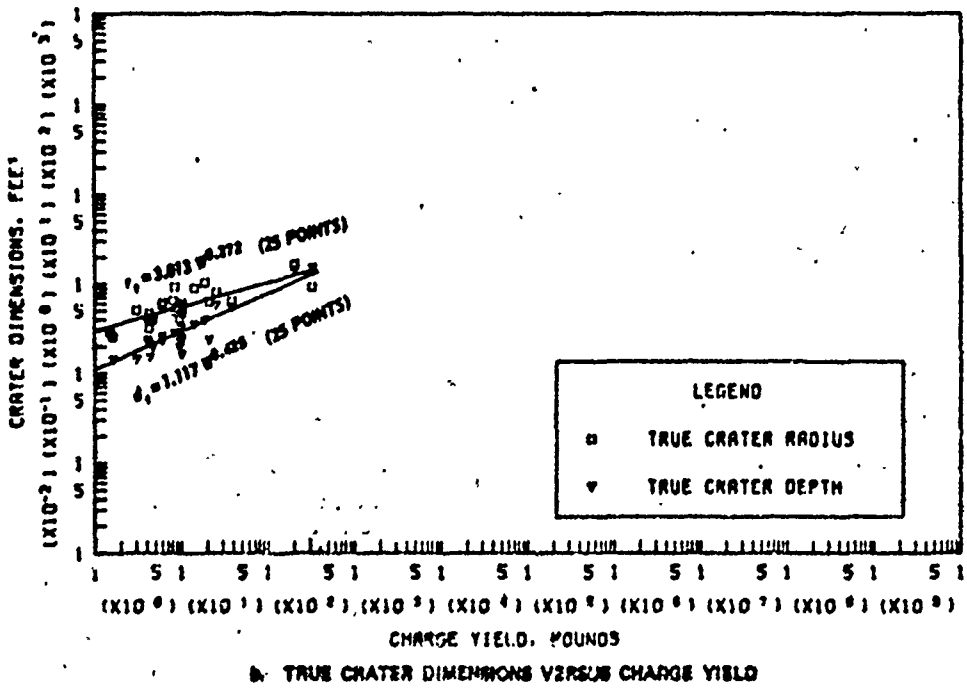

b. TRUE CRATER DIMENSIONS VERSUS CHARGE YIELD

Figure B.14 Dimensions of craters in sandstone for $-2.00 \leq Z < -1.10$ ft/lb$^{1/3}$, Category 9 (sheet 1 of 2).

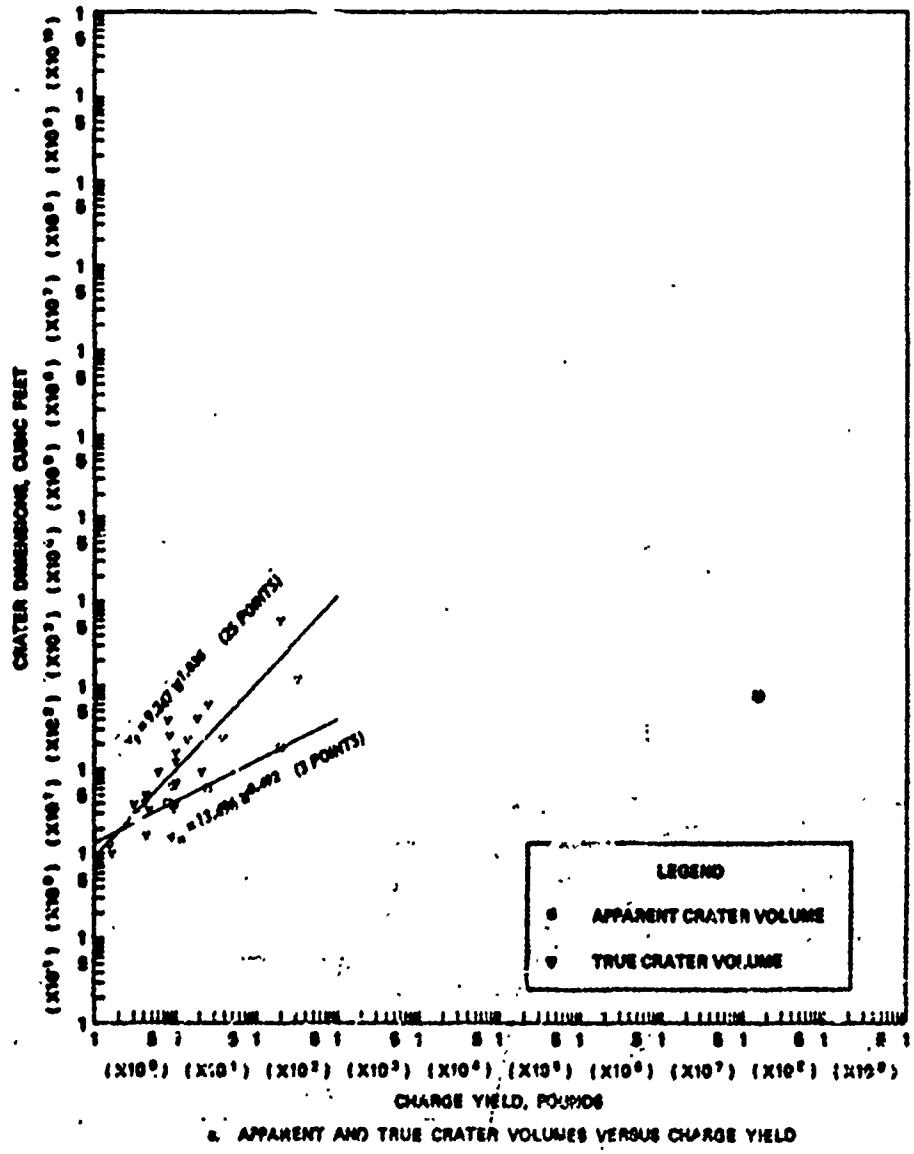

a. APPARENT AND TRUE CRATER VOLUMES VERSUS CHARGE YIELD

Figure B.14 (sheet 2 of 2).

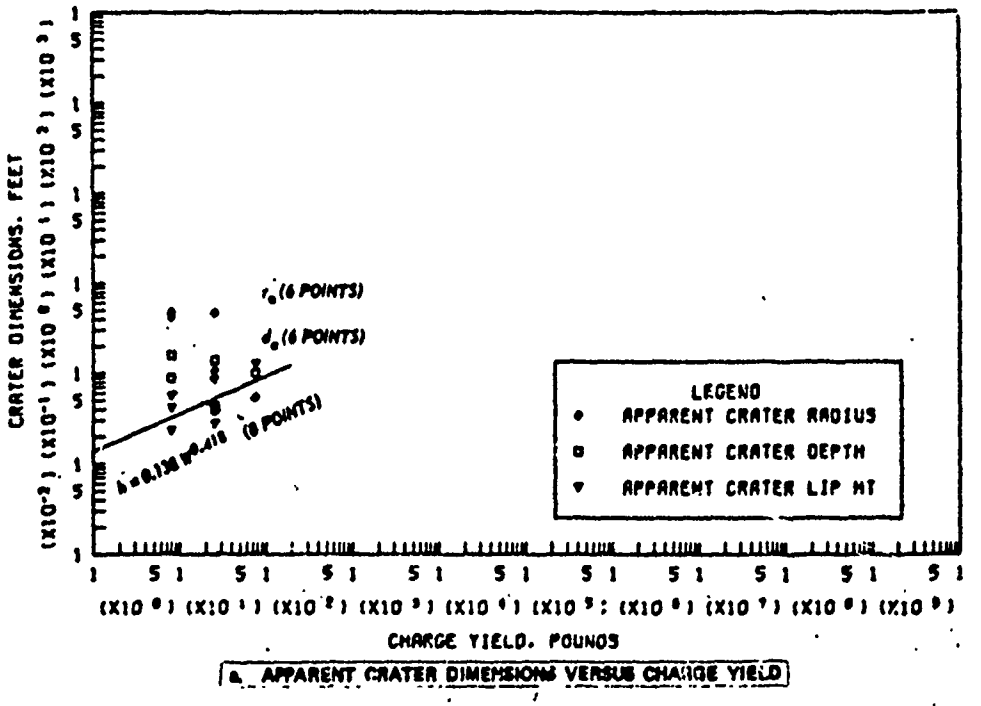

a. APPARENT CRATER DIMENSIONS VERSUS CHARGE YIELD

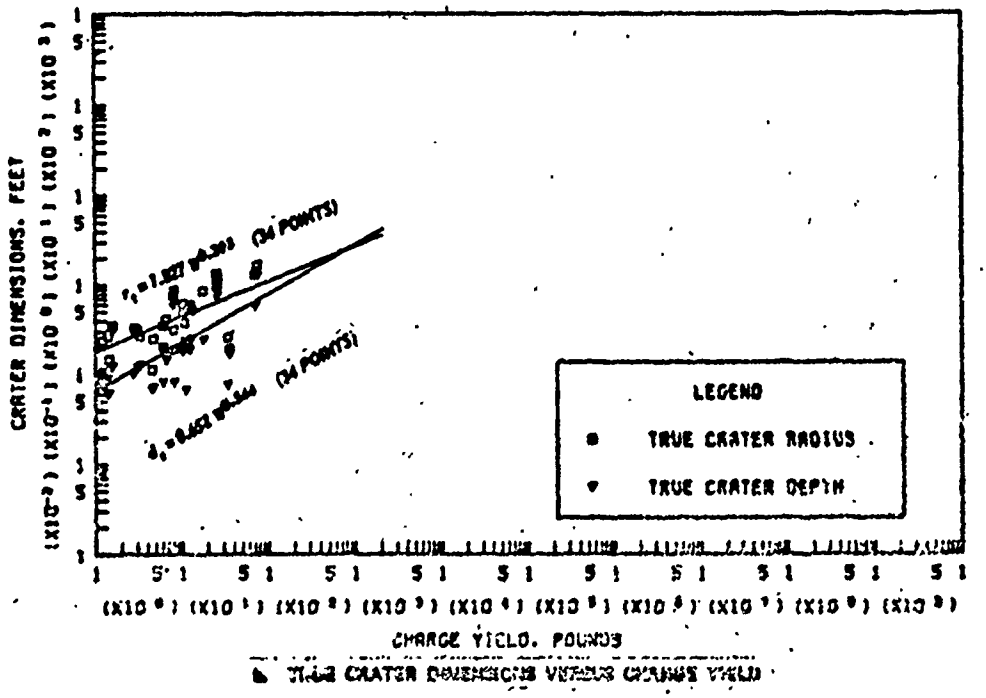

b. TRUE CRATER DIMENSIONS VERSUS CHARGE YIELD

Figure B.15 Dimensions of craters in sandstone for $Z < -2.00$ ft/lb$^{1/3}$, Category 10 (sheet 1 of 2).

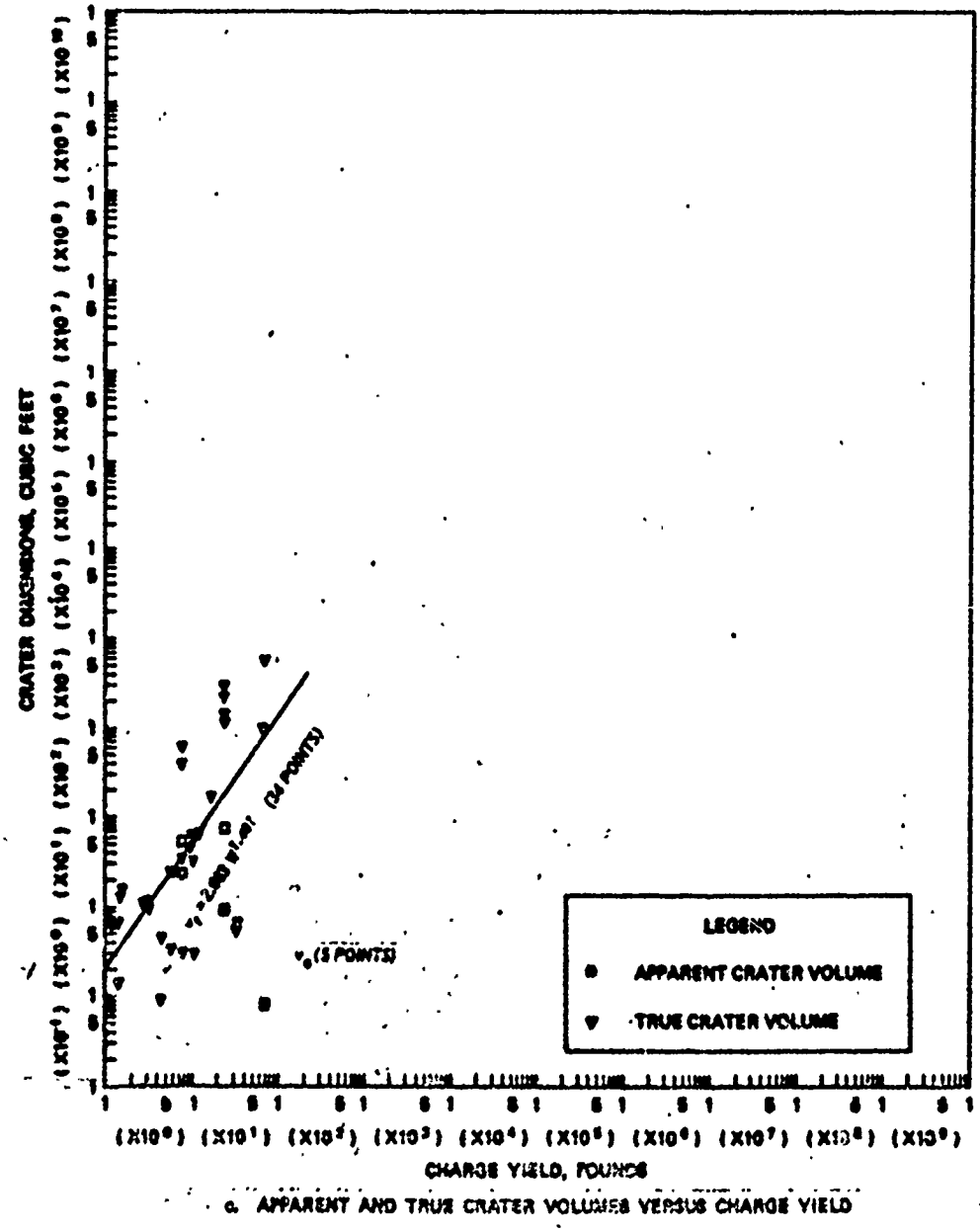

a. APPARENT AND TRUE CRATER VOLUMES VERSUS CHARGE YIELD

Figure B.15 (sheet 2 of 2).

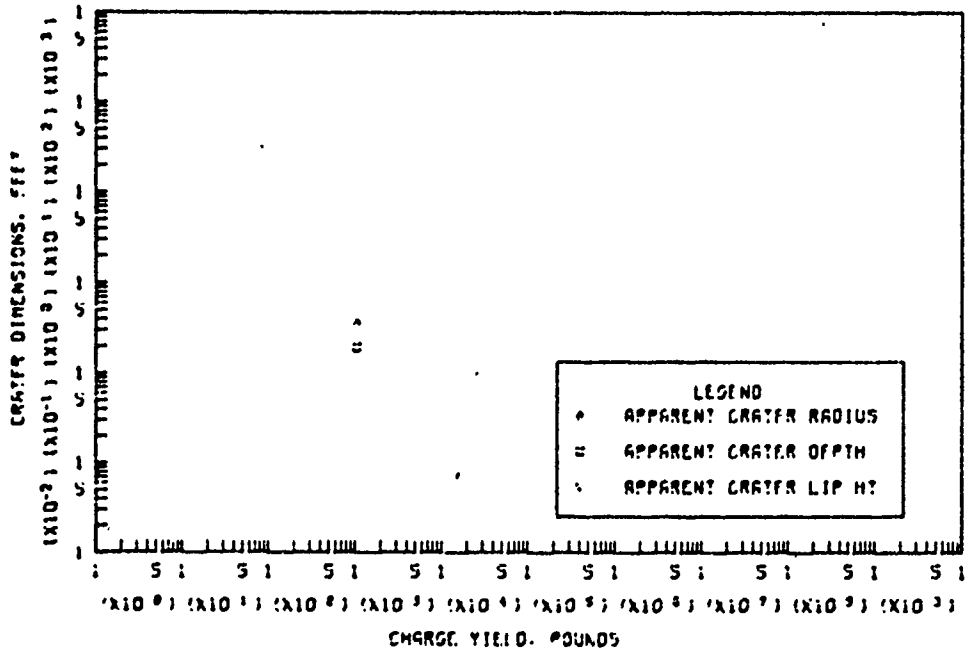

a. APPARENT CRATER DIMENSIONS VERSUS CHARGE YIELD

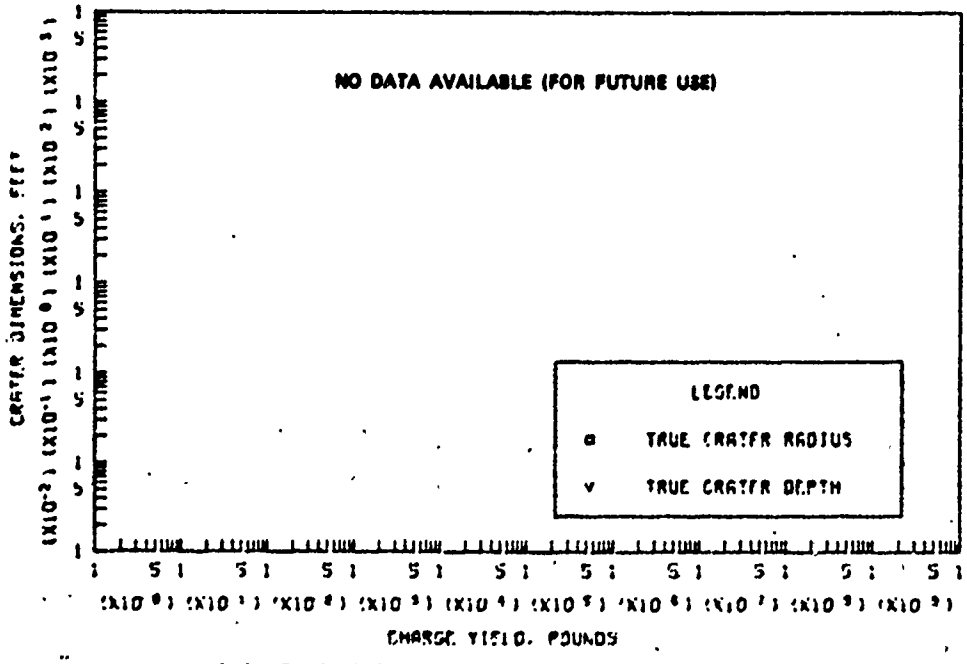

b. TRUE CRATER DIMENSIONS VERSUS CHARGE YIELD

Figure B.16 Dimensions of craters in shale, tuff, and frozen ground for $0.05 \leq Z < 0.20$ ft/lb$^{1/3}$, Category 3 (sheet 1 of 2).

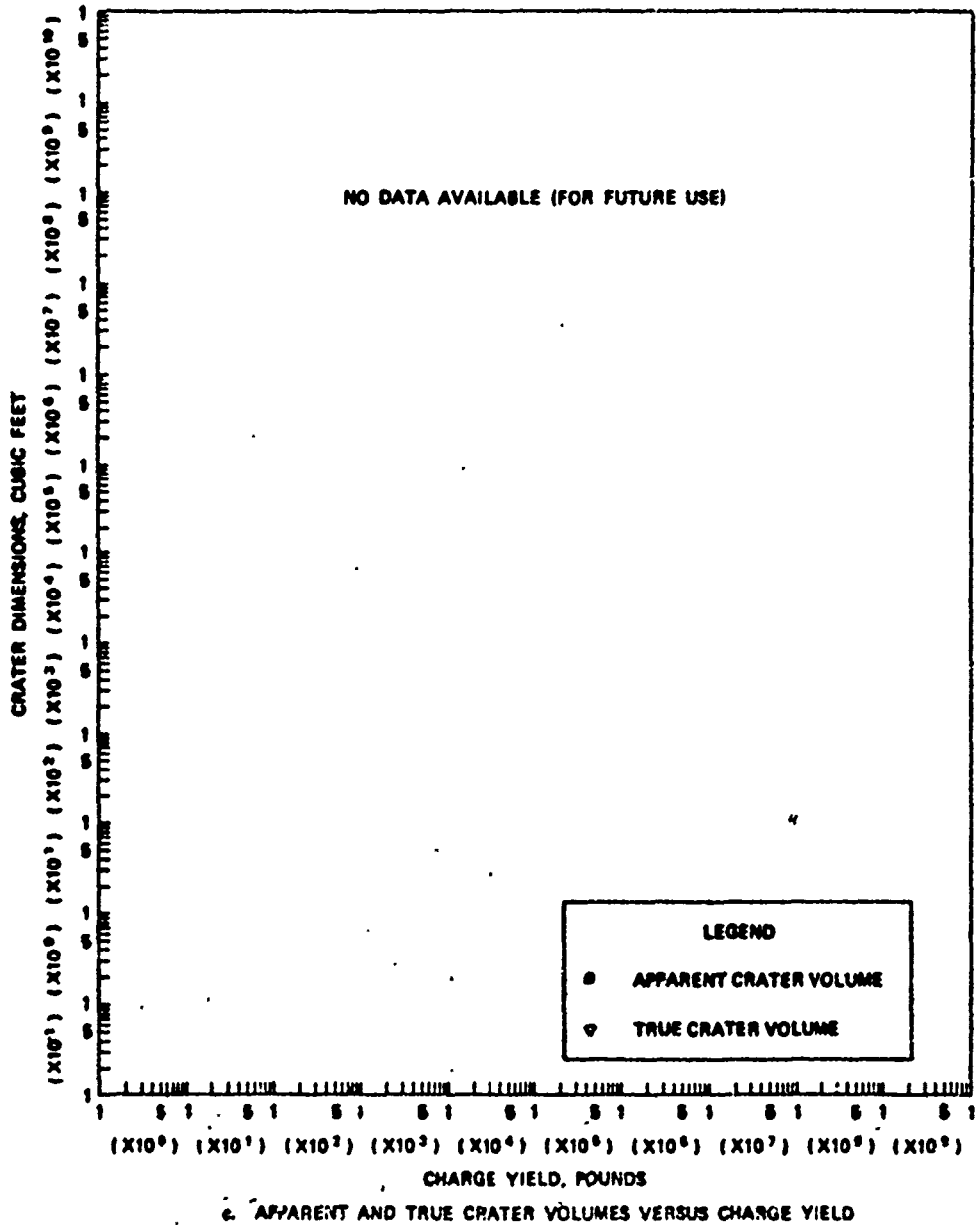

c. APPARENT AND TRUE CRATER VOLUMES VERSUS CHARGE YIELD

Figure B.16 (sheet 2 of 2).

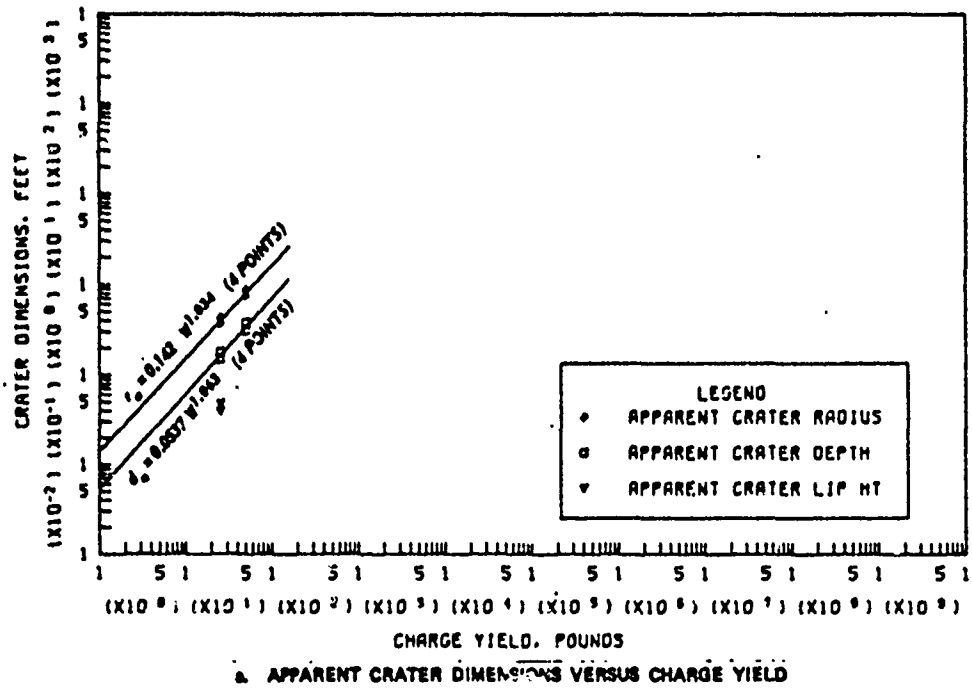

a. APPARENT CRATER DIMENSIONS VERSUS CHARGE YIELD

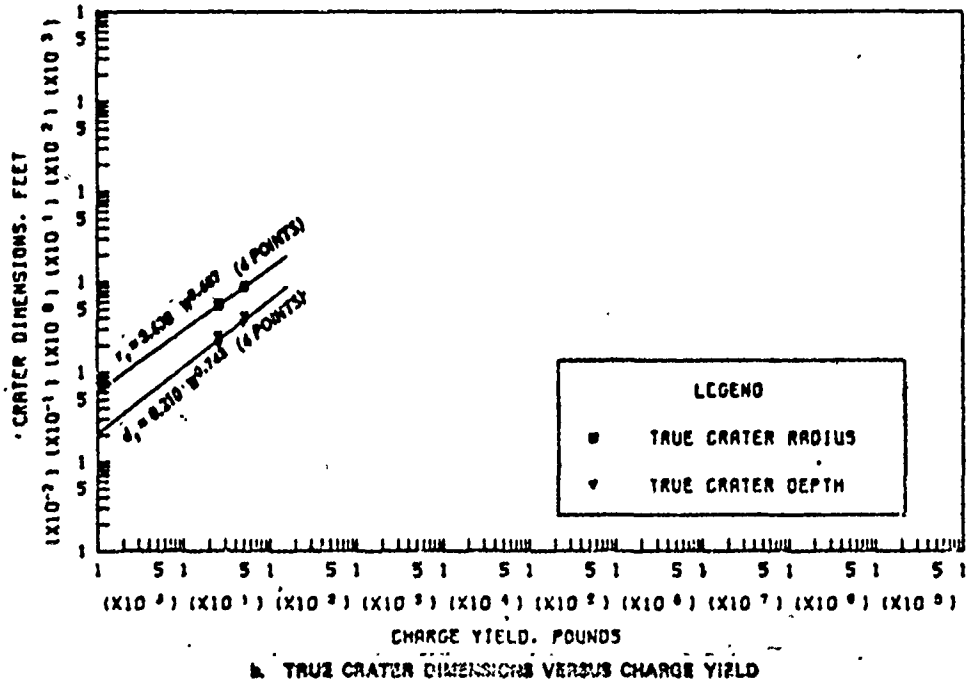

b. TRUE CRATER DIMENSIONS VERSUS CHARGE YIELD

Figure B.17 Dimensions of craters in shale, tuff, and frozen ground for $-0.05 \leq Z < 0.05$ ft/lb$^{1/3}$, Category 4 (sheet 1 of 2).

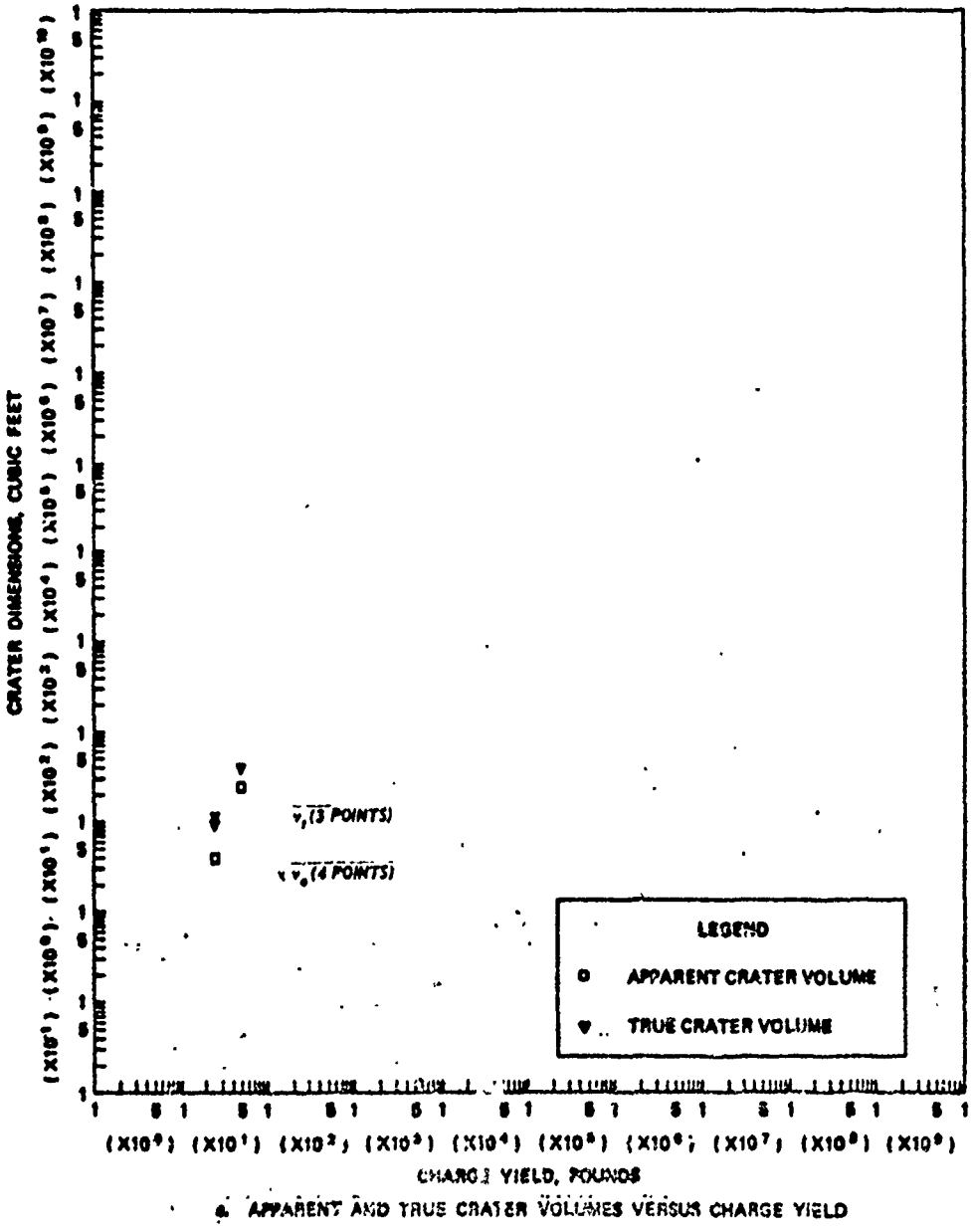

Figure 3.17 (sheet 2 of 2).

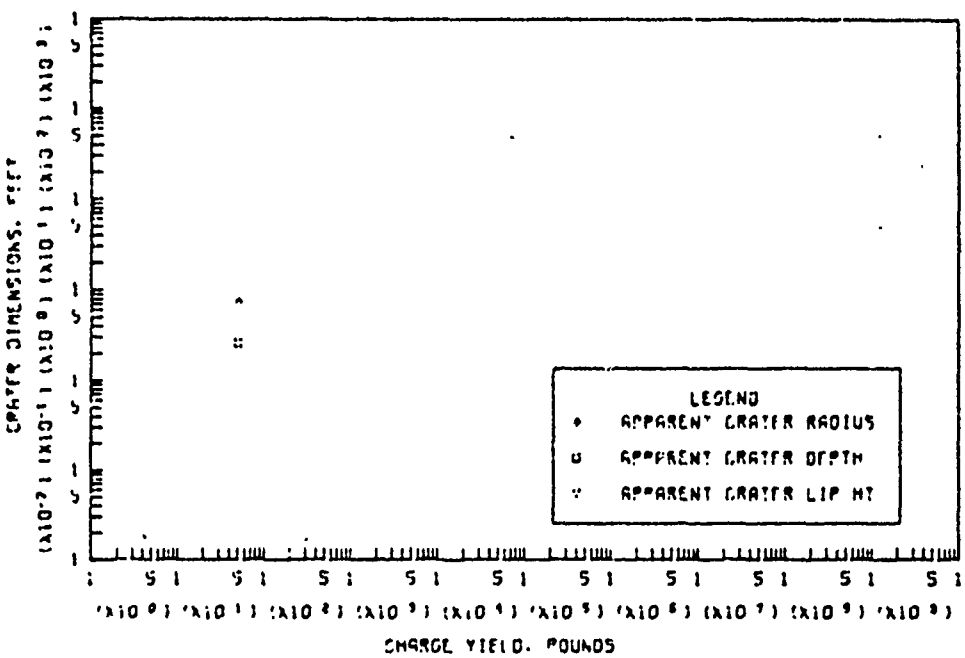

a. APPARENT CRATER DIMENSIONS VERSUS CHARGE YIELD

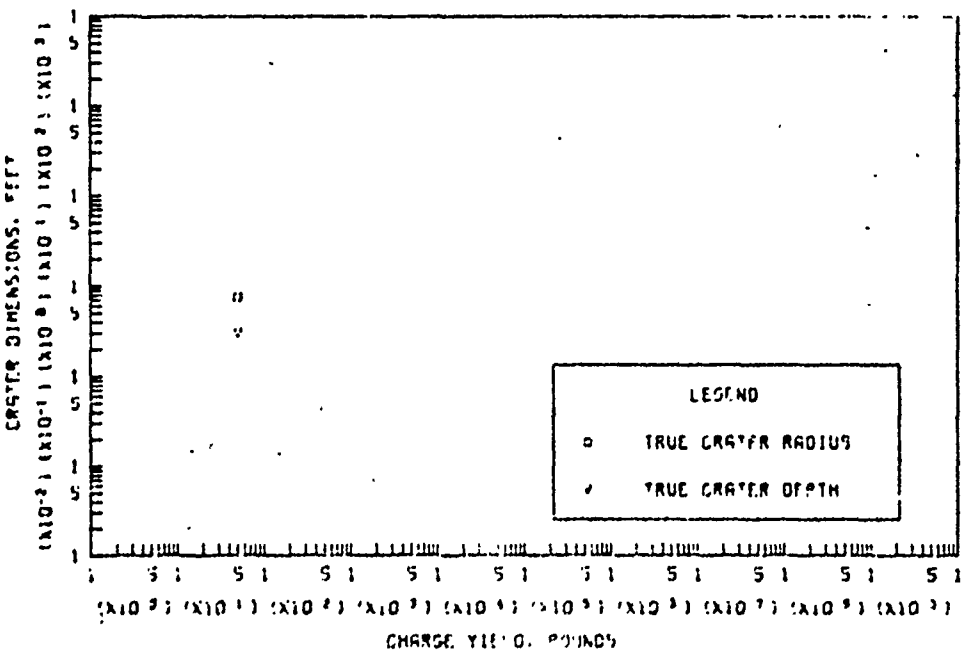

b. TRUE CRATER DIMENSIONS VERSUS CHARGE YIELD

Figure B.18 Dimensions of craters in shale, tuff, and frozen ground for $-0.20 \leq Z < -0.05$ ft/lb$^{1/3}$, Category 5 (sheet 1 of 2).

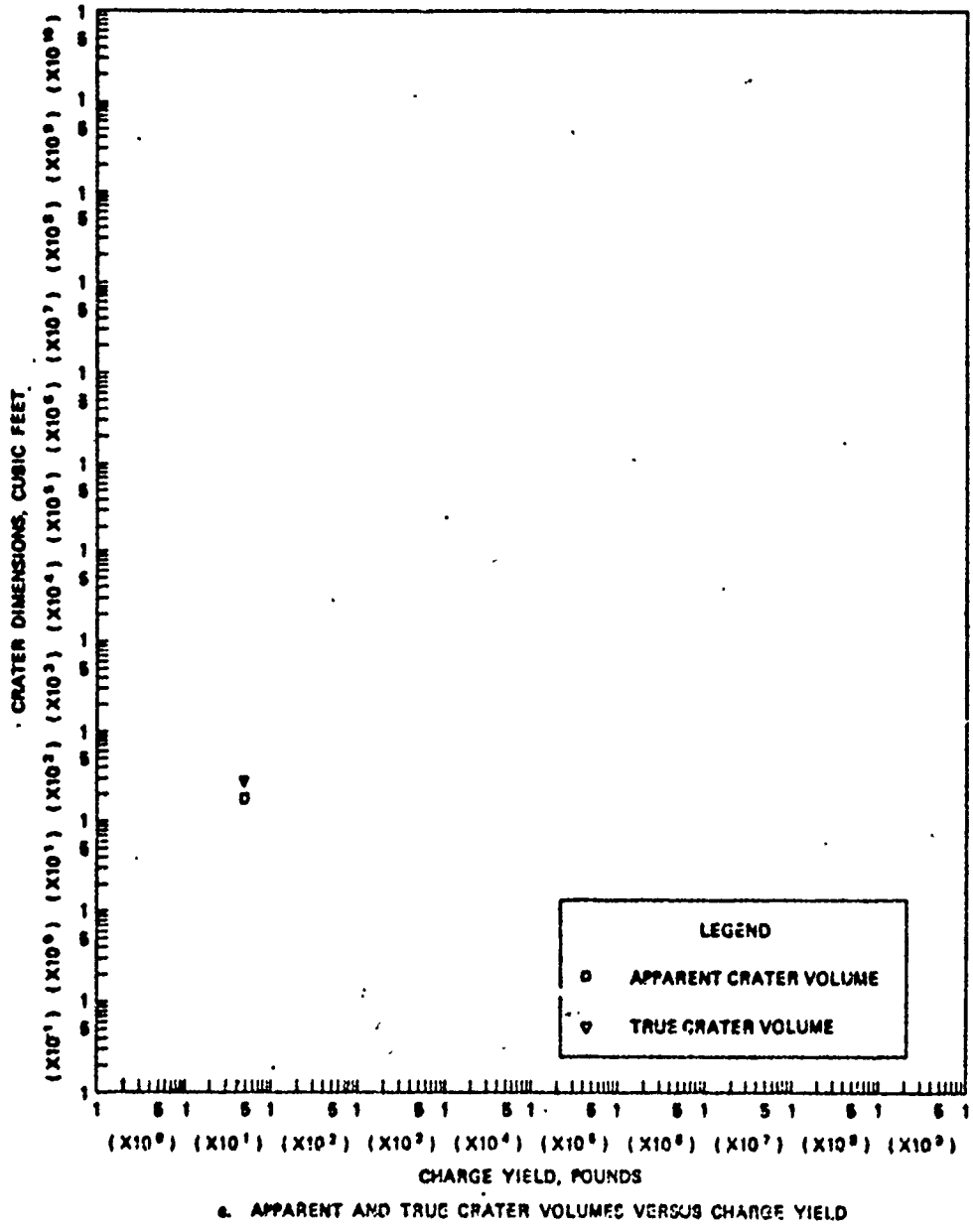

a. APPARENT AND TRUE CRATER VOLUMES VERSUS CHARGE YIELD

Figure B.18 (sheet 2 of 2).

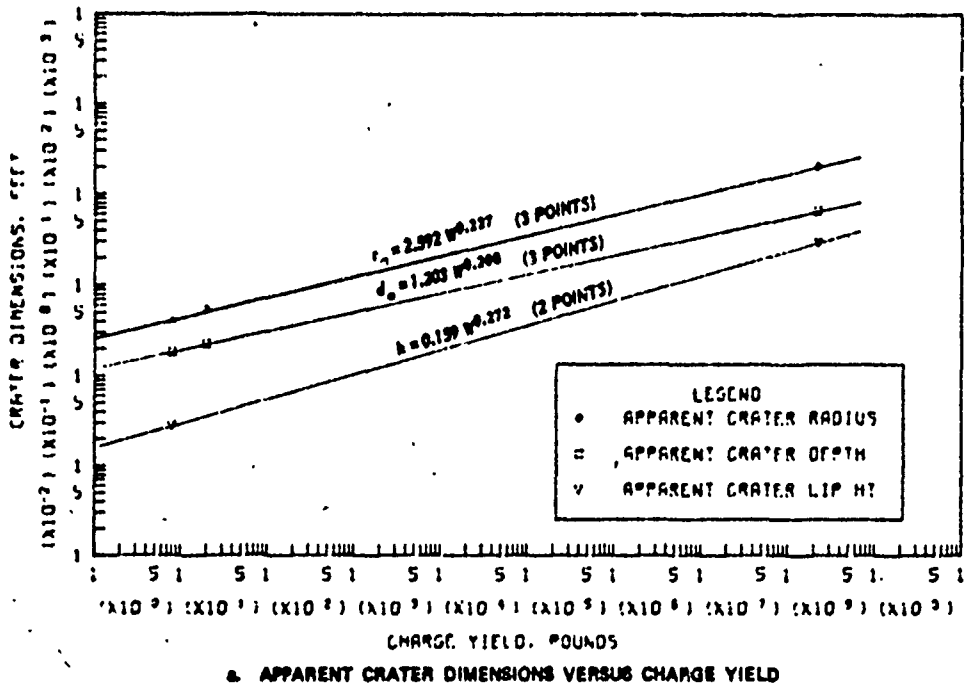

a. APPARENT CRATER DIMENSIONS VERSUS CHARGE YIELD

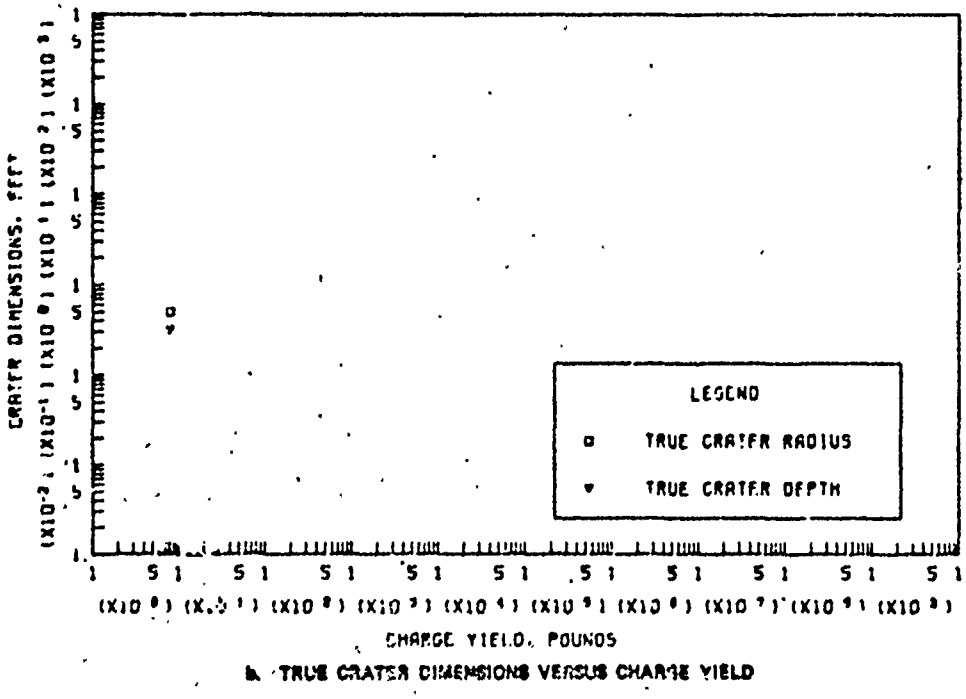

b. TRUE CRATER DIMENSIONS VERSUS CHARGE YIELD

Figure B.19 Dimensions of craters in shale, tuff, and frozen ground for $-0.50 \leq \beta < -0.20$ ft/lb$^{1/3}$, Category 6 (sheet 1 of 2).

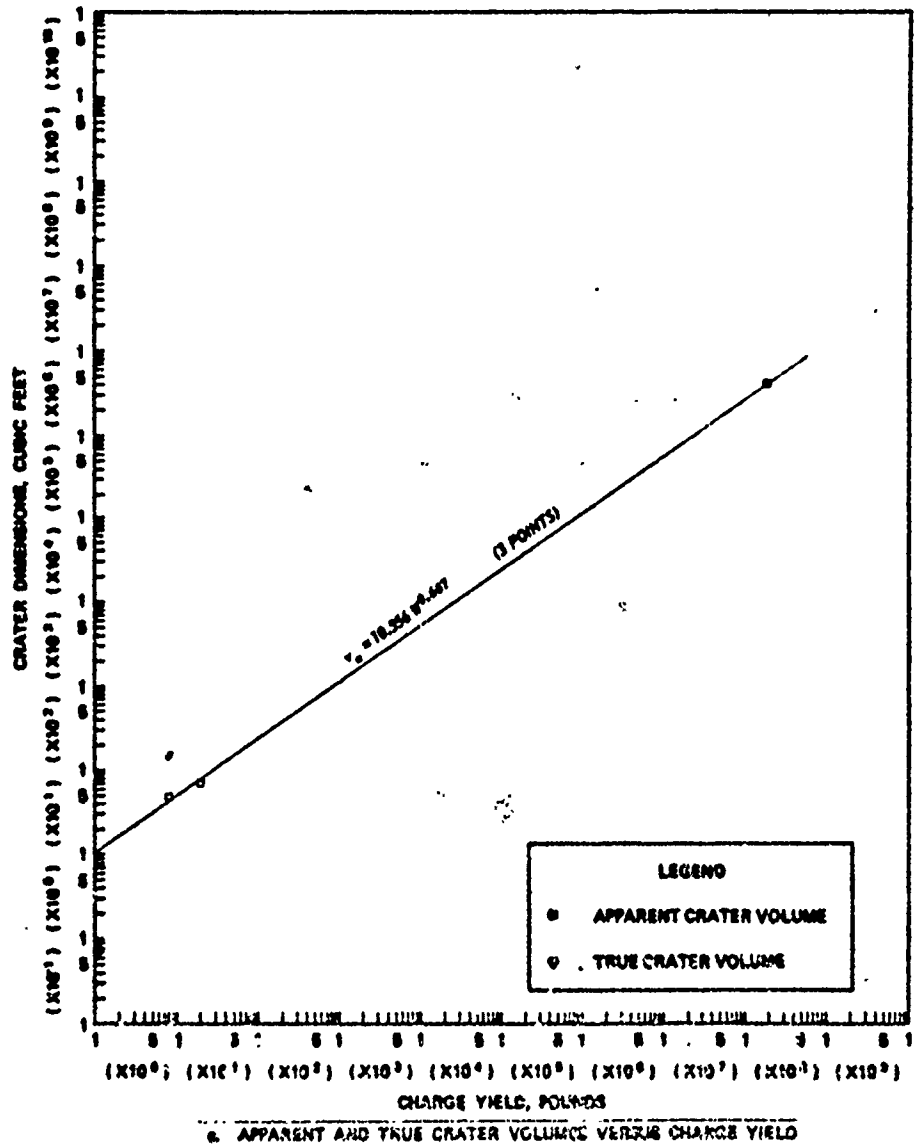

a. APPARENT AND TRUE CRATER VOLUMES VERSUS CHARGE YIELD

Figure B.19 (sheet 2 of 2).

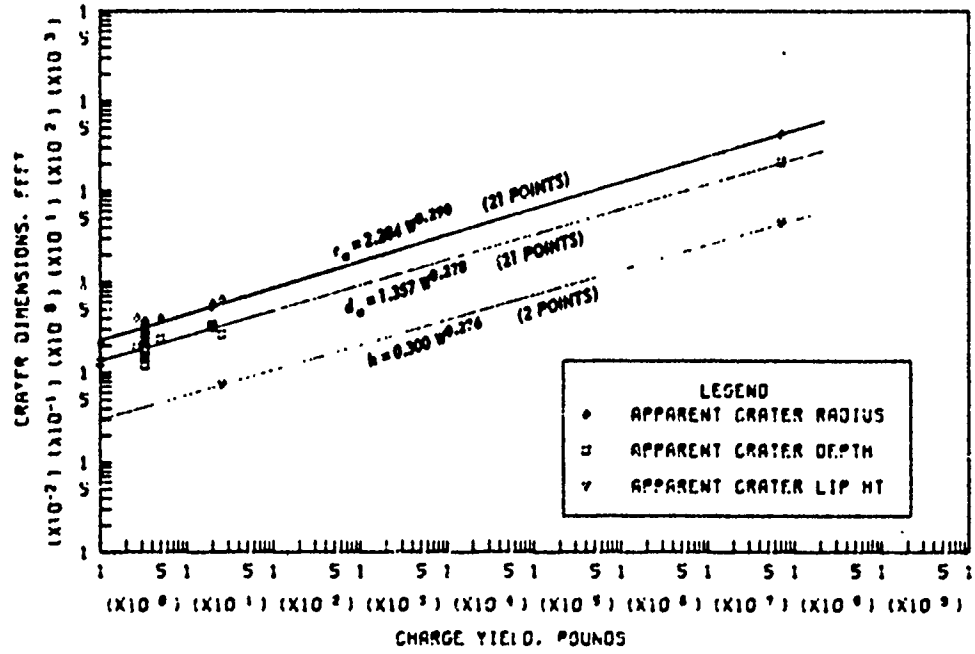

a. APPARENT CRATER DIMENSIONS VERSUS CHARGE YIELD

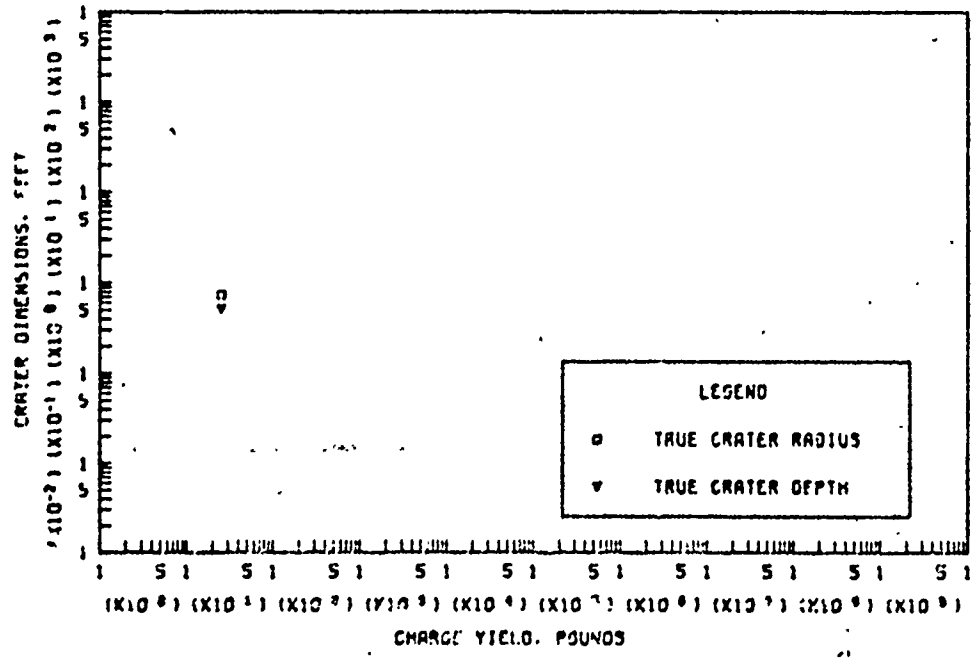

b. TRUE CRATER DIMENSIONS VERSUS CHARGE YIELD

Figure B.20 Dimensions of craters in shale, tuff, and frozen ground for $-0.90 \leq Z < -0.50$ ft/lb$^{1/3}$, Category 7 (sheet 1 of 2).

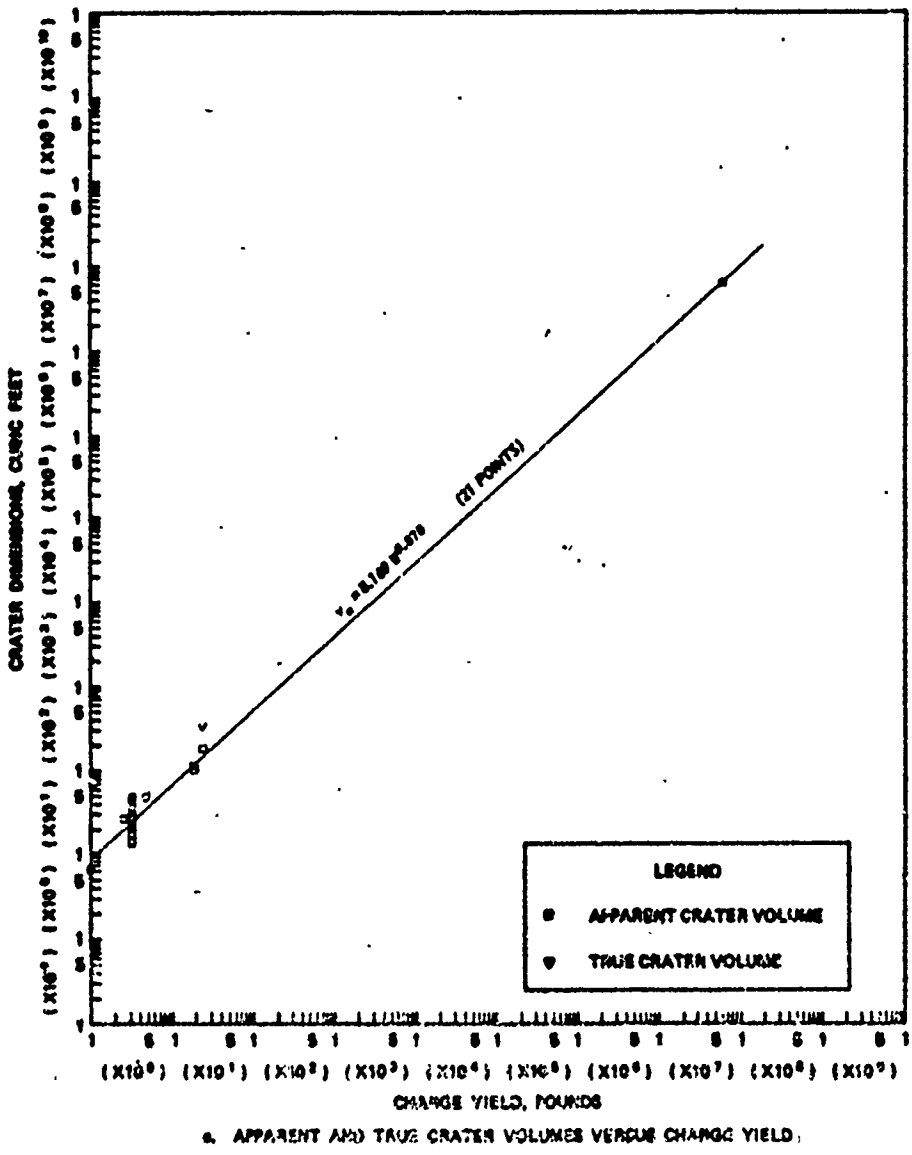

a. APPARENT AND TRUE CRATER VOLUMES VERSUS CHARGE YIELD.

Figure B.20 (sheet 2 of 2).

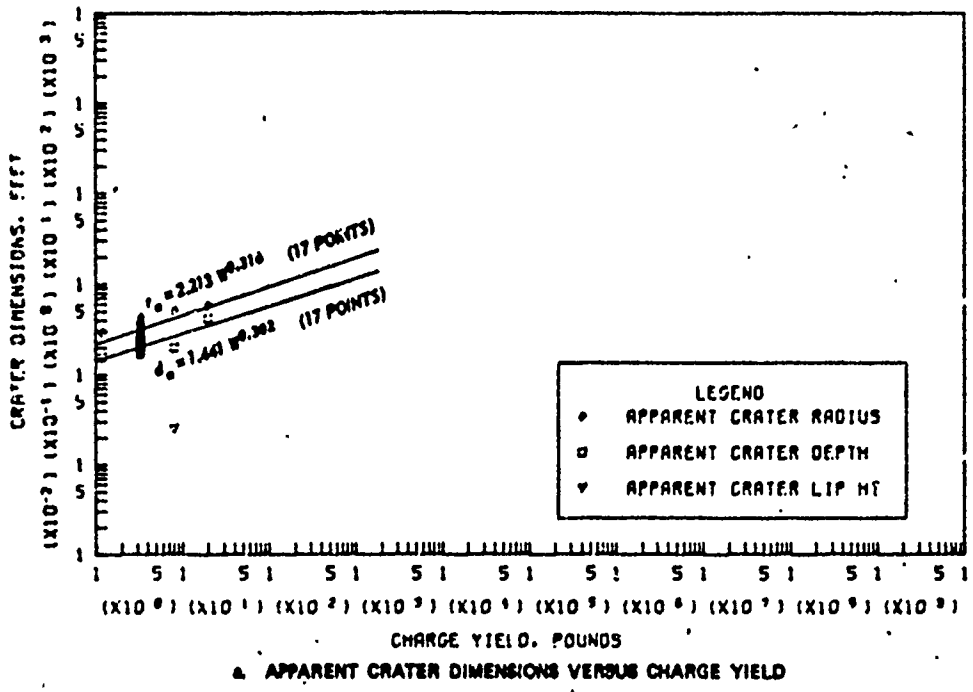

a. APPARENT CRATER DIMENSIONS VERSUS CHARGE YIELD

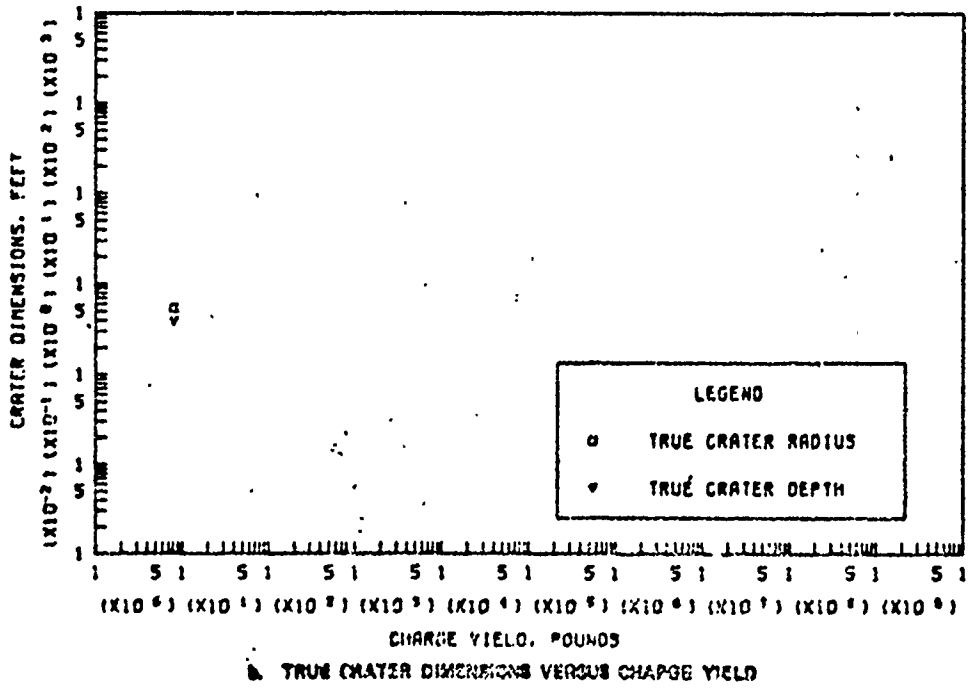

b. TRUE CRATER DIMENSIONS VERSUS CHARGE YIELD

Figure B.21 Dimensions of craters in shale, tuff, and frozen ground for $-1.10 \leq Z < -0.90$ ft/lb$^{1/3}$, Category 8 (sheet 1 of 2)

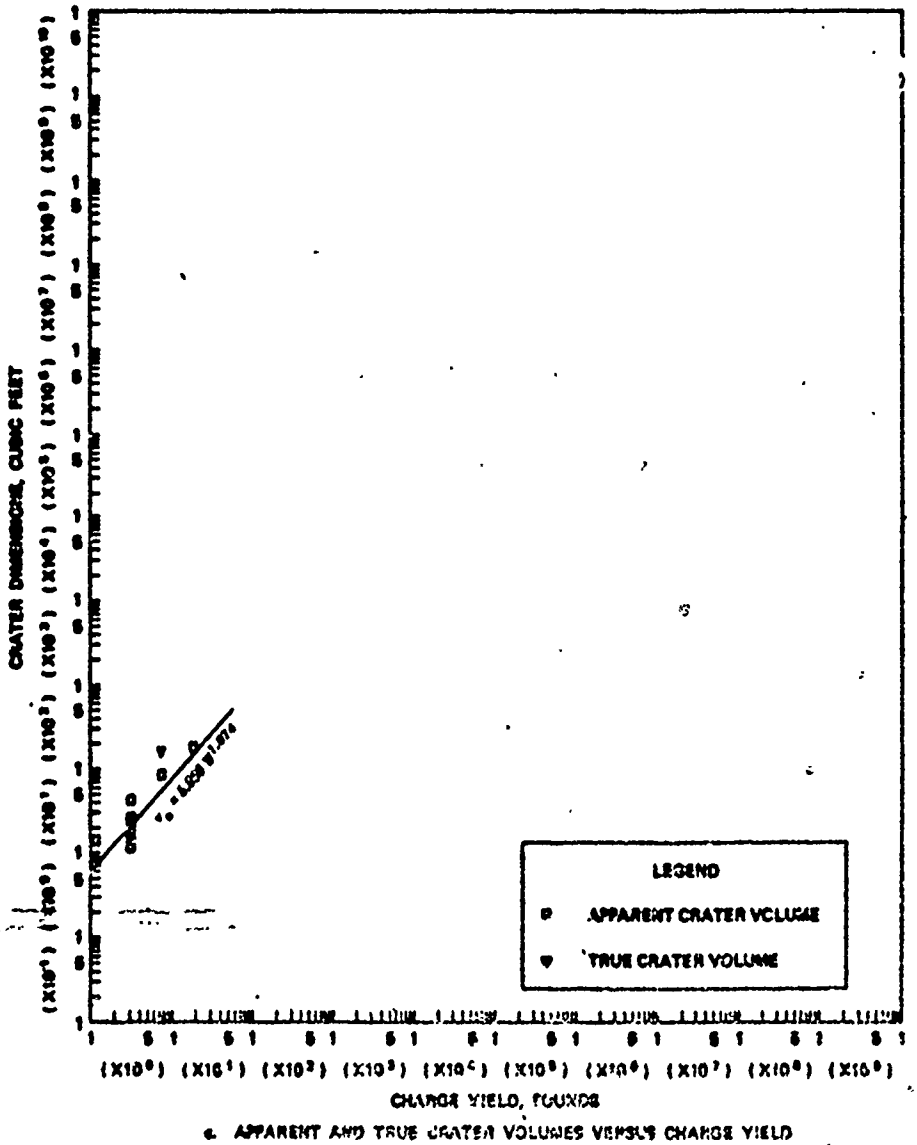

c. APPARENT AND TRUE CRATER VOLUMES VERSUS CHARGE YIELD

Figure 3.21 (sheet 2 of 2).

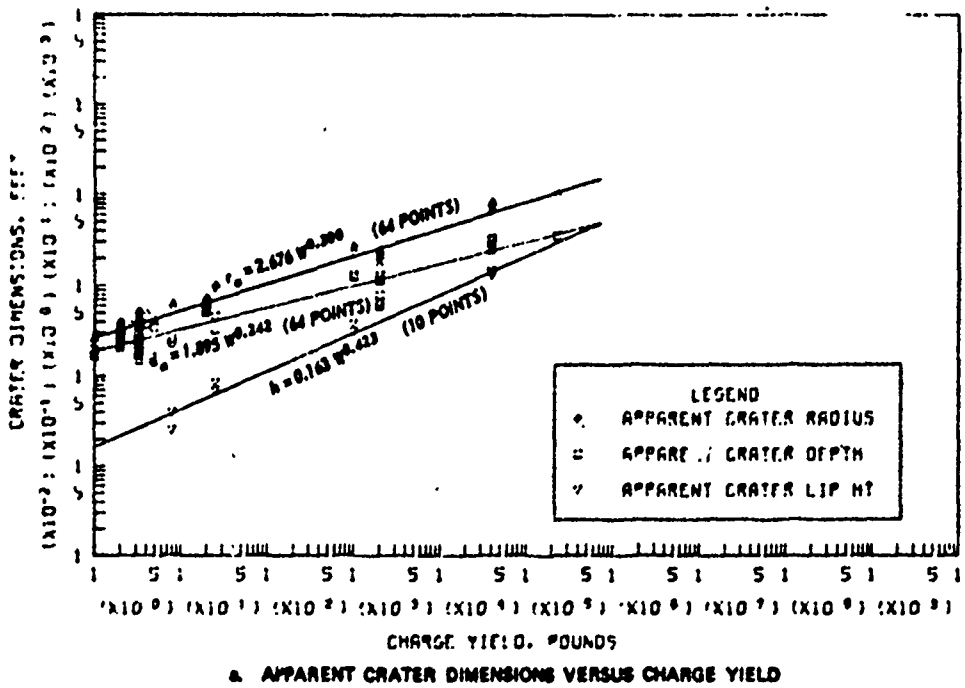

a. APPARENT CRATER DIMENSIONS VERSUS CHARGE YIELD

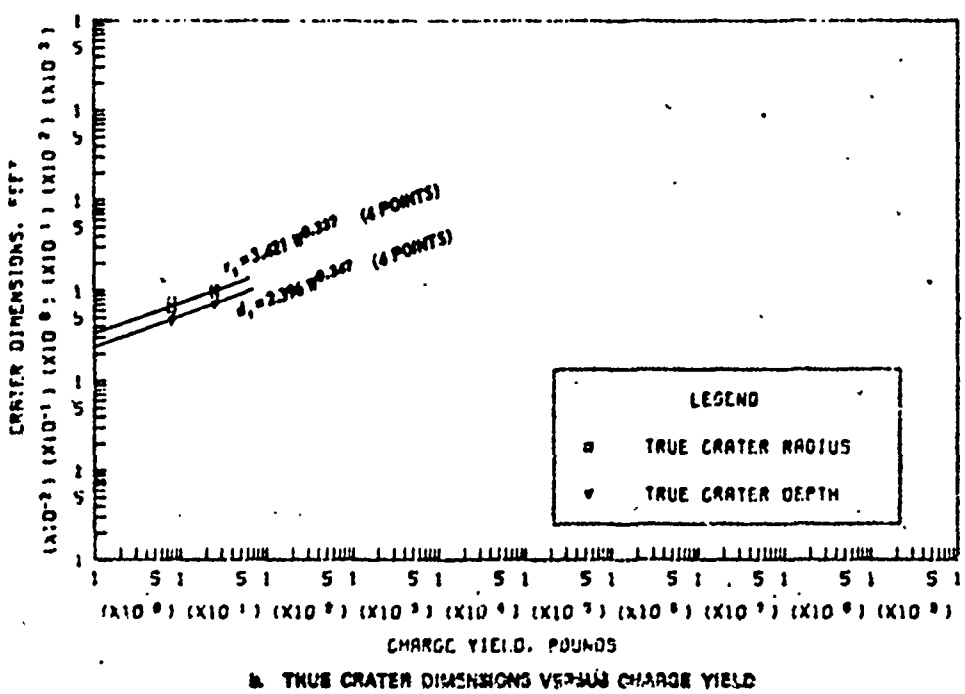

b. TRUE CRATER DIMENSIONS VERSUS CHARGE YIELD

Figure B.22 Dimensions of craters in shale, tuff, and frozen ground for $-2.00 \leq Z < -1.10$ ft/lb$^{1/3}$, Category 9 (sheet 1 of 2).

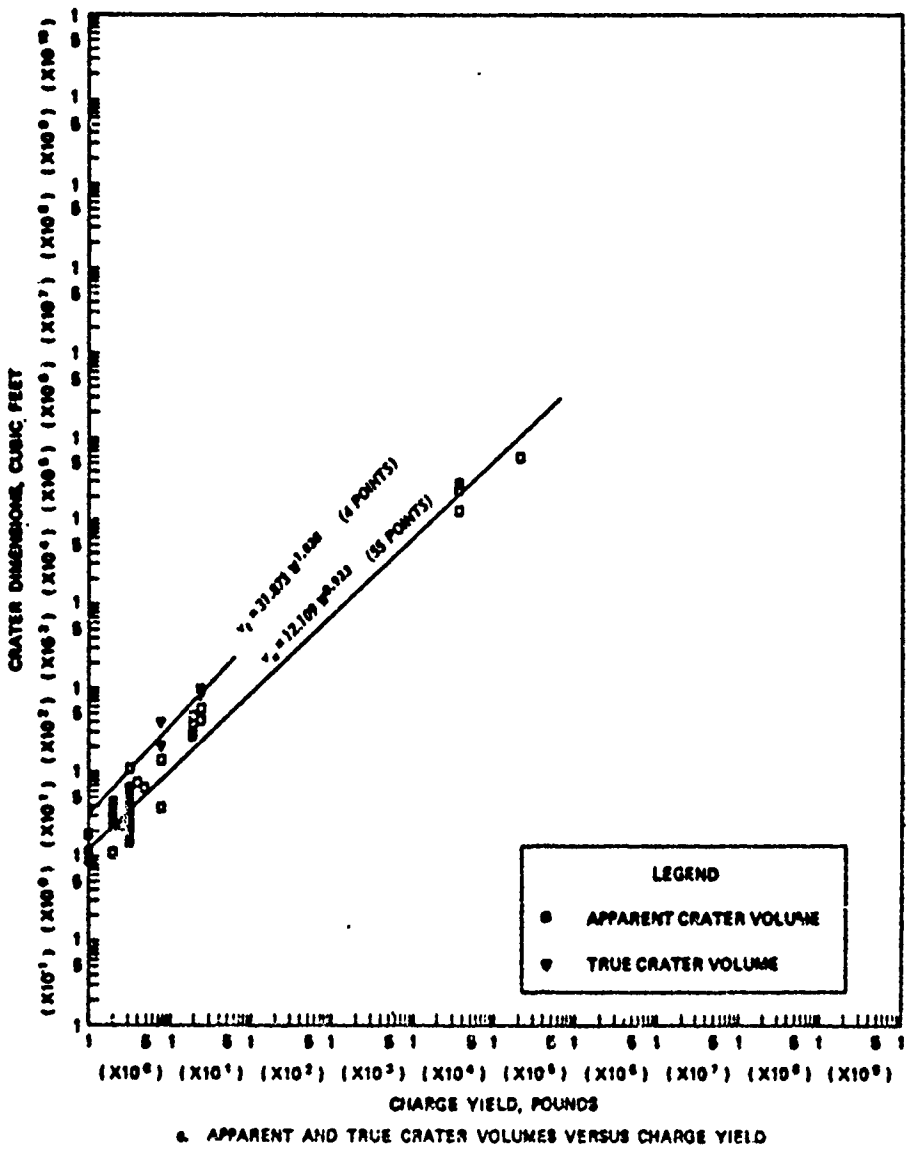

a. APPARENT AND TRUE CRATER VOLUMES VERSUS CHARGE YIELD

Figure B.22 (sheet 2 of 2).

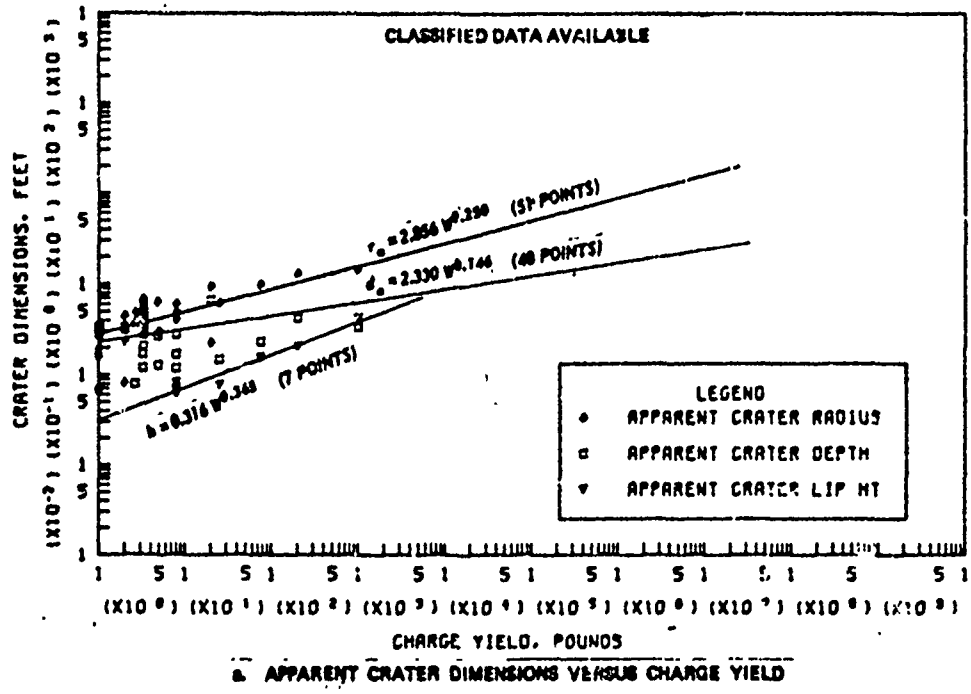

a. APPARENT CRATER DIMENSIONS VERSUS CHARGE YIELD

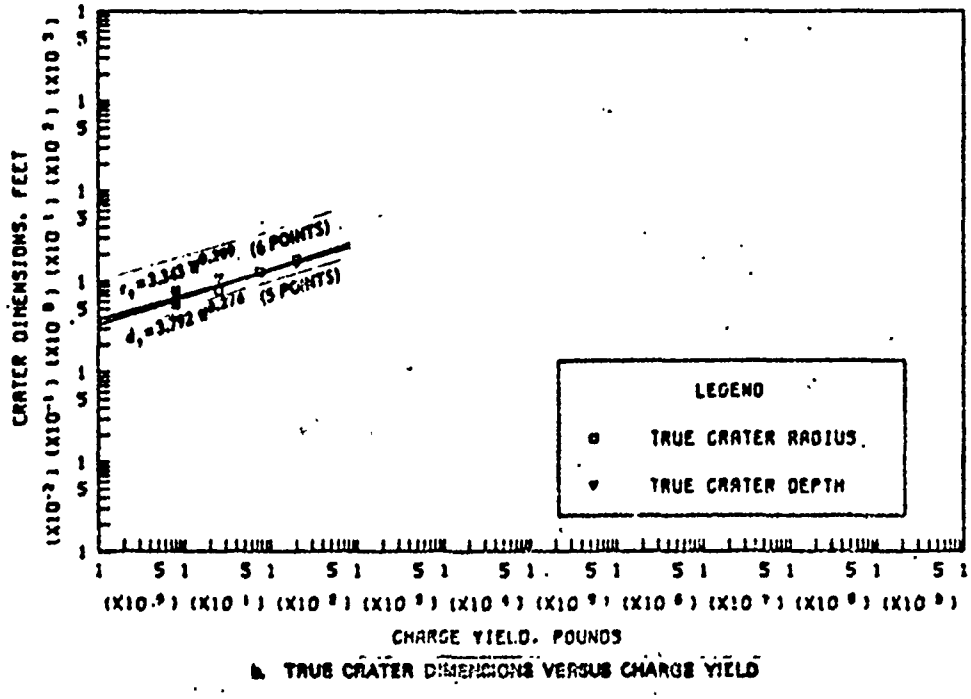

b. TRUE CRATER DIMENSIONS VERSUS CHARGE YIELD

Figure B.23 Dimensions of craters in shale, tuff, and frozen ground for $Z < -2.00$ ft/lb$^{1/3}$, Category 10 (sheet 1 of 2).

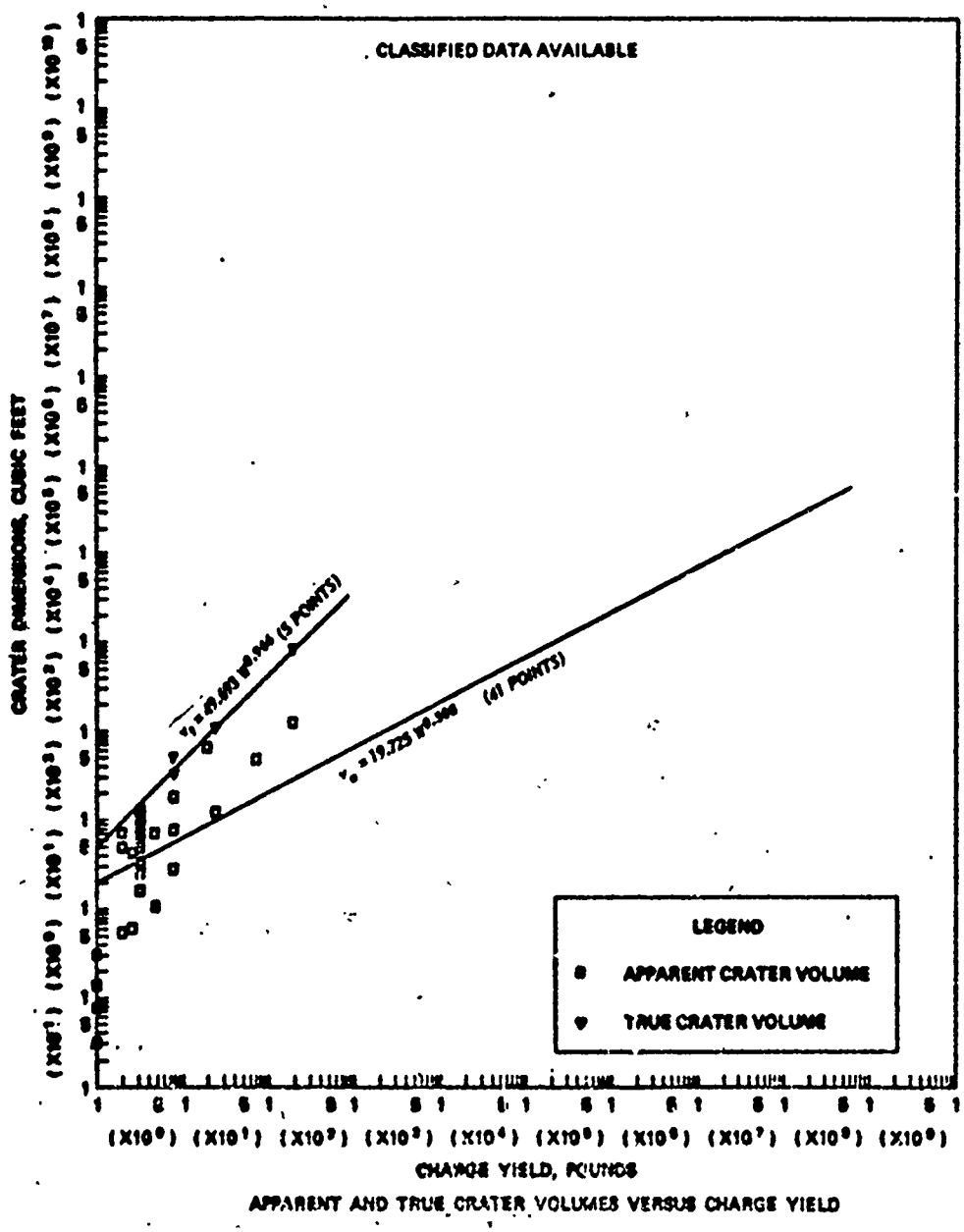

APPARENT AND TRUE CRATER VOLUMES VERSUS CHARGE YIELD

Figure B.23 (sheet 2 of 2).

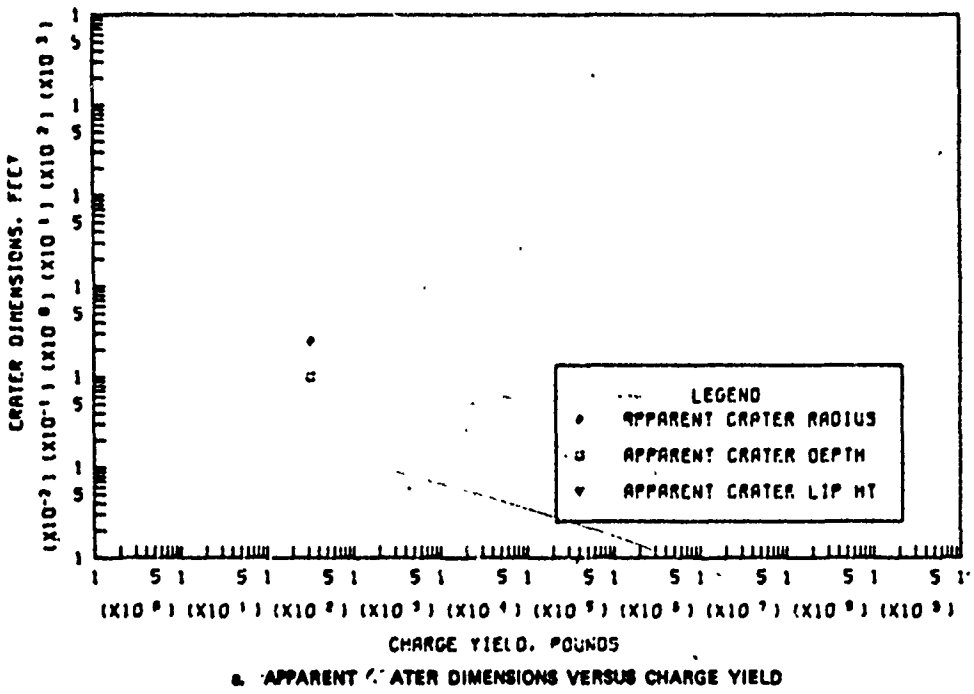

a. APPARENT CRATER DIMENSIONS VERSUS CHARGE YIELD

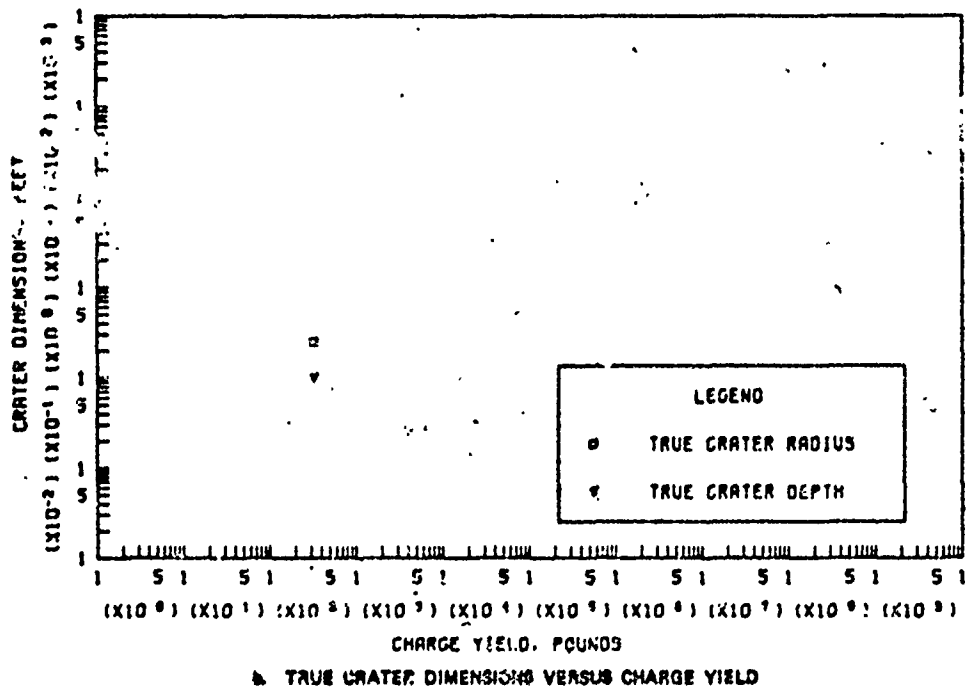

b. TRUE CRATER DIMENSIONS VERSUS CHARGE YIELD

Figure B.24 Dimensions of craters in dry clay for $0.50 \leq Z$ ft/lb$^{1/3}$, Category 1 (sheet 1 of 2).

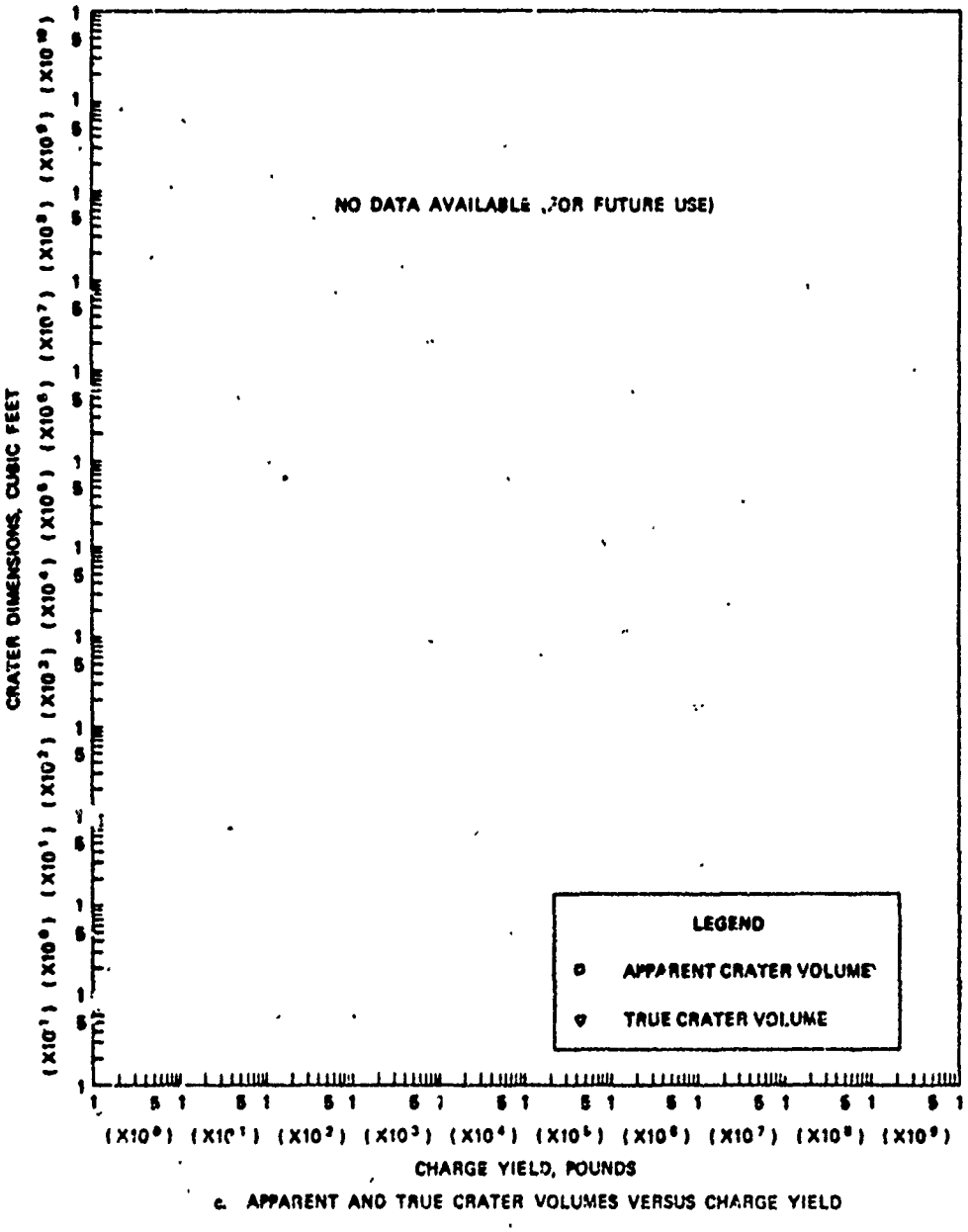

e. APPARENT AND TRUE CRATER VOLUMES VERSUS CHARGE YIELD

Figure B.24 (sheet 2 of 2).

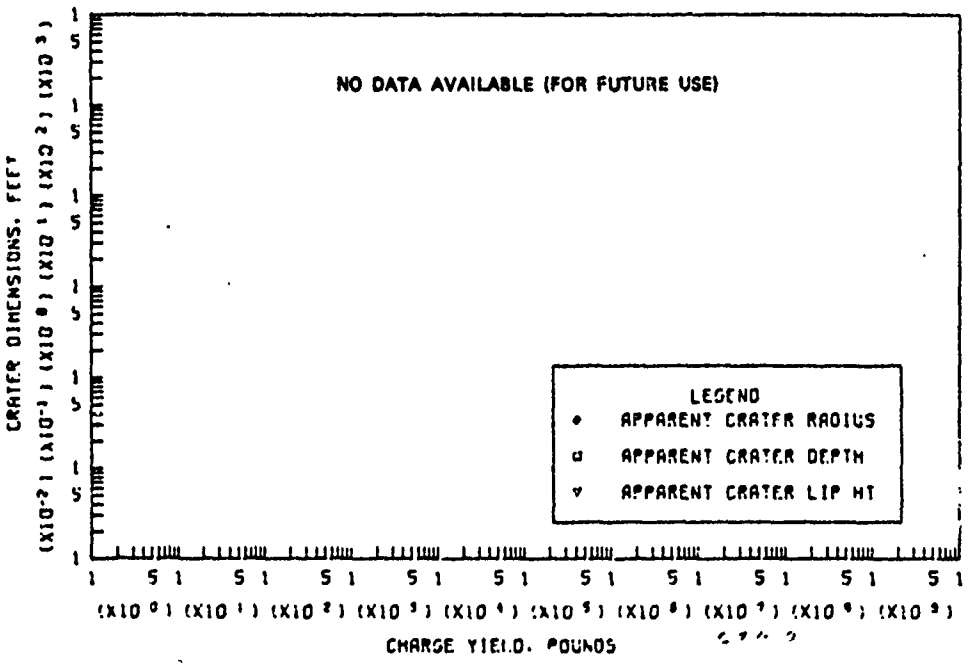

a. APPARENT CRATER DIMENSIONS VERSUS CHARGE YIELD

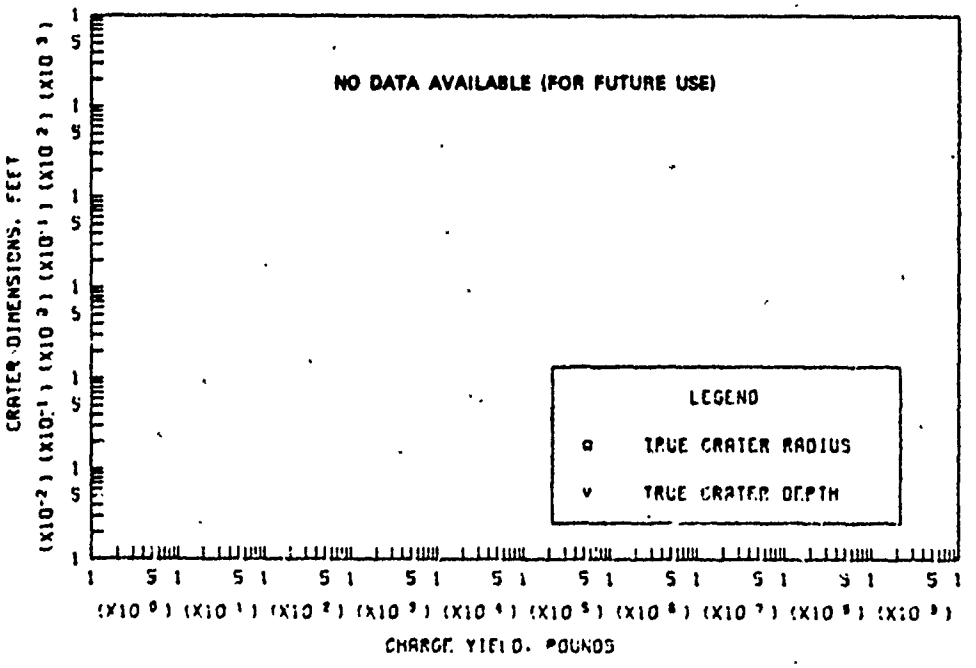

b. TRUE CRATER DIMENSIONS VERSUS CHARGE YIELD

Figure B.25 Dimensions of craters in dry clay for $0.20 \leq Z < 0.50$ ft/lb$^{1/3}$, Category 2 (sheet 1 of 2).

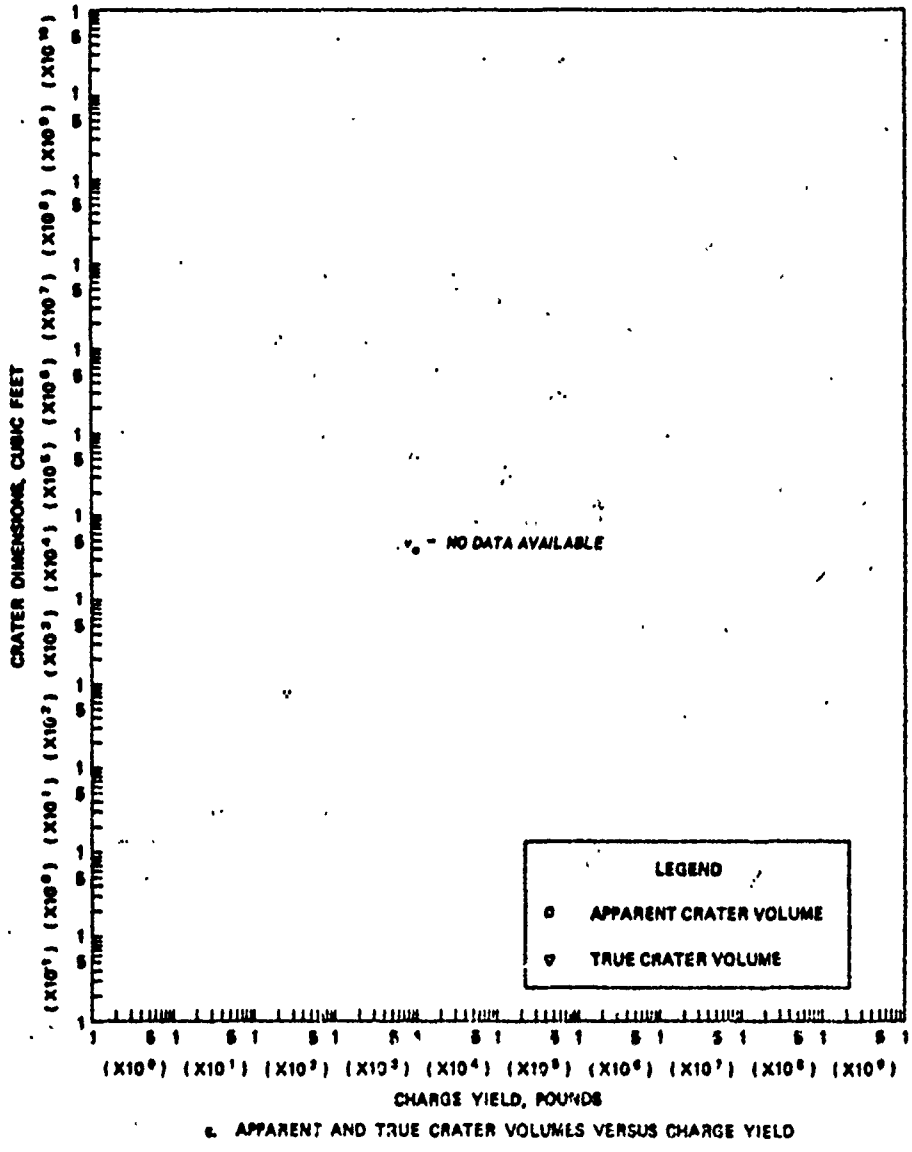

e. APPARENT AND TRUE CRATER VOLUMES VERSUS CHARGE YIELD

Figure B.25 (sheet 2 of 2).

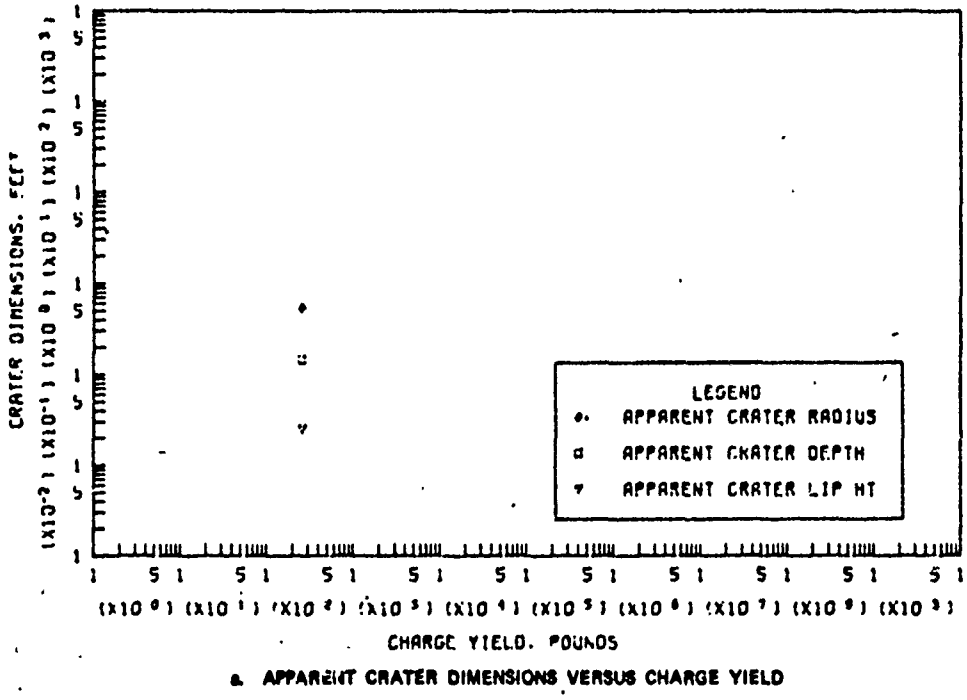

a. APPARENT CRATER DIMENSIONS VERSUS CHARGE YIELD

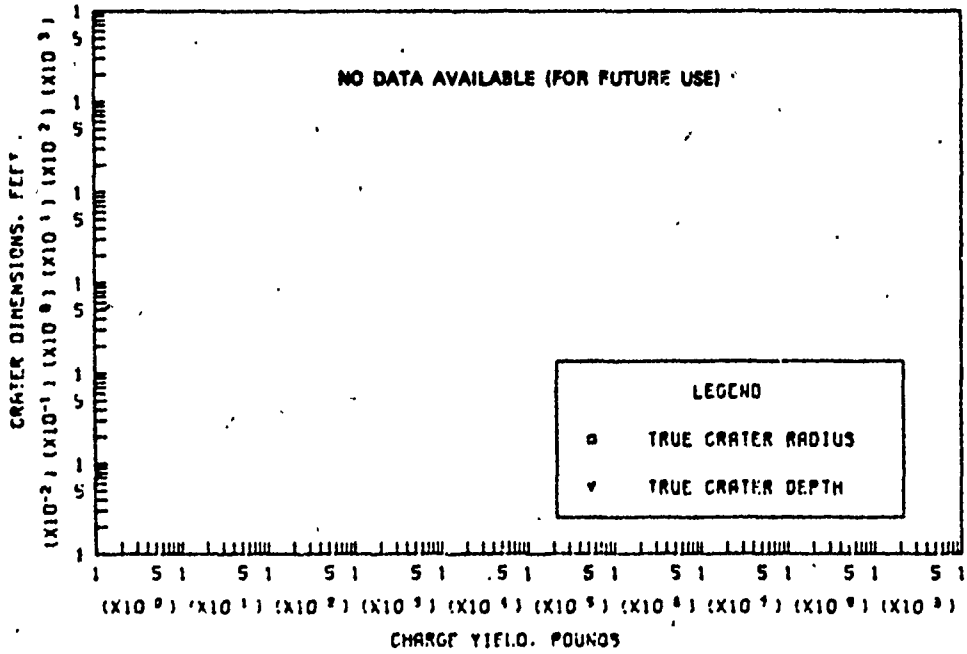

b. TRUE CRATER DIMENSIONS VERSUS CHARGE YIELD

Figure B.26 Dimensions of craters in dry clay for $0.05 \leq Z < 0.20$ ft/lb$^{1/3}$, Category 3 (sheet 1 of 2).

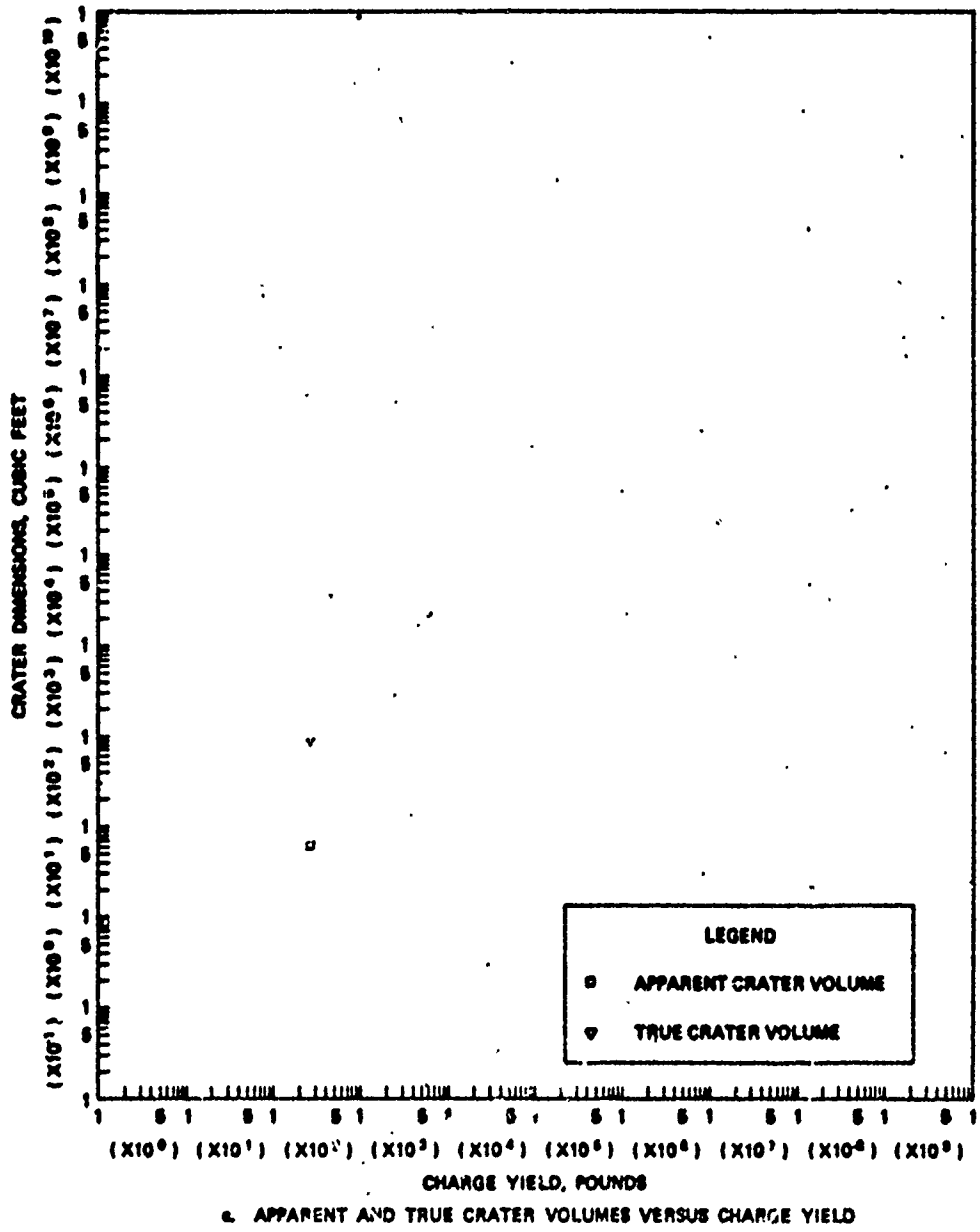

a. APPARENT AND TRUE CRATER VOLUMES VERSUS CHARGE YIELD

Figure B.26 (sheet 2 of 2).

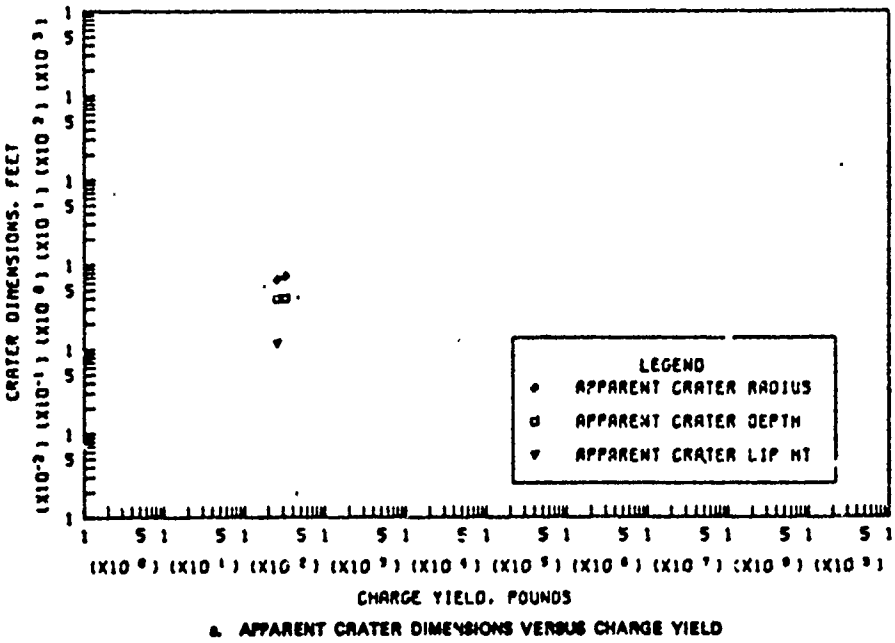

a. APPARENT CRATER DIMENSIONS VERSUS CHARGE YIELD

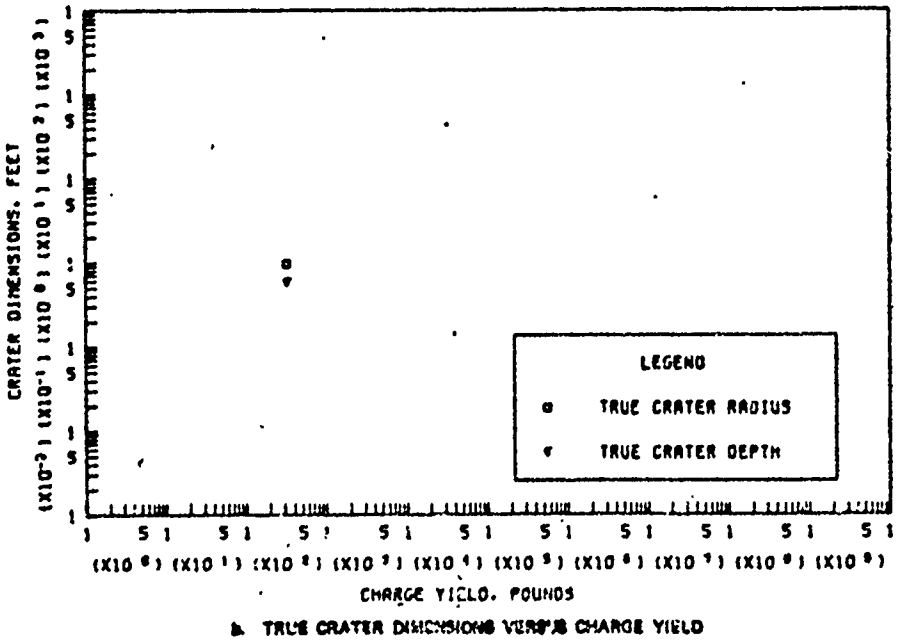

b. TRUE CRATER DIMENSIONS VERSUS CHARGE YIELD

Figure B.27 Dimensions of craters in dry clay for $-0.05 \leq Z < 0.05$ ft/lb$^{1/3}$, Category 4 (sheet 1 of 2).

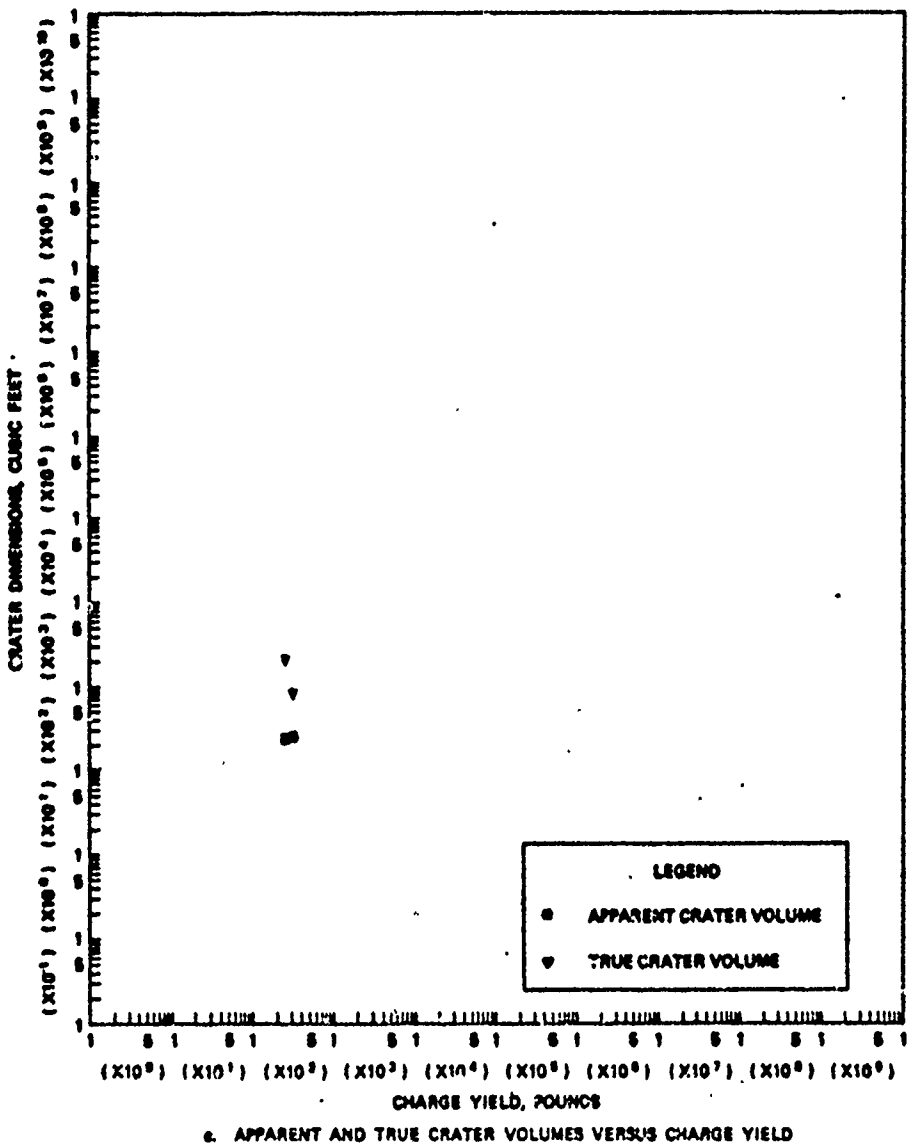

e. APPARENT AND TRUE CRATER VOLUMES VERSUS CHARGE YIELD

Figure B.27 (sheet 2 of 2).

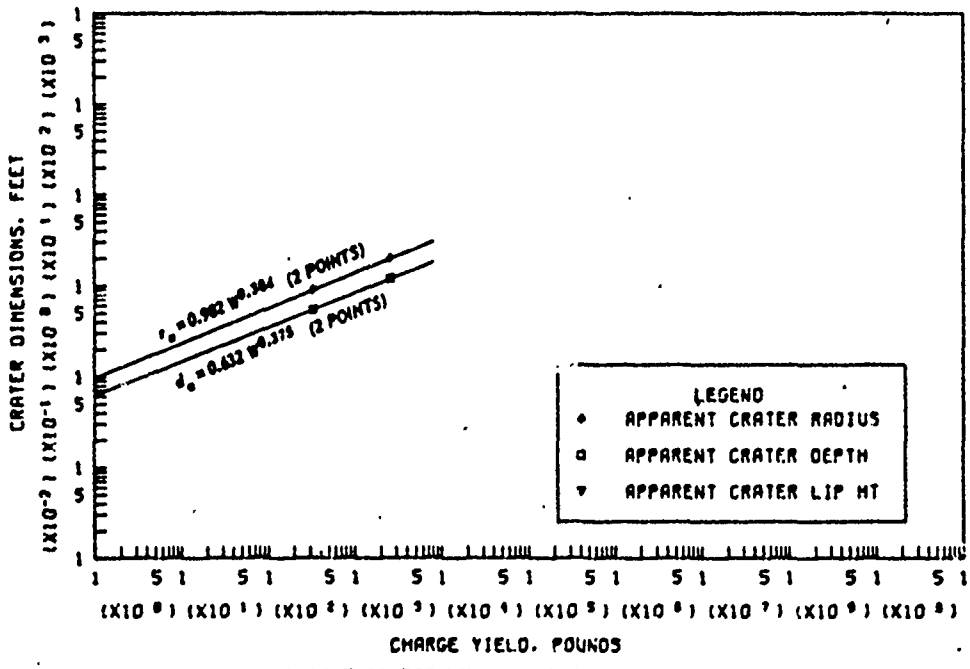

a. APPARENT CRATER DIMENSIONS VERSUS CHARGE YIELD

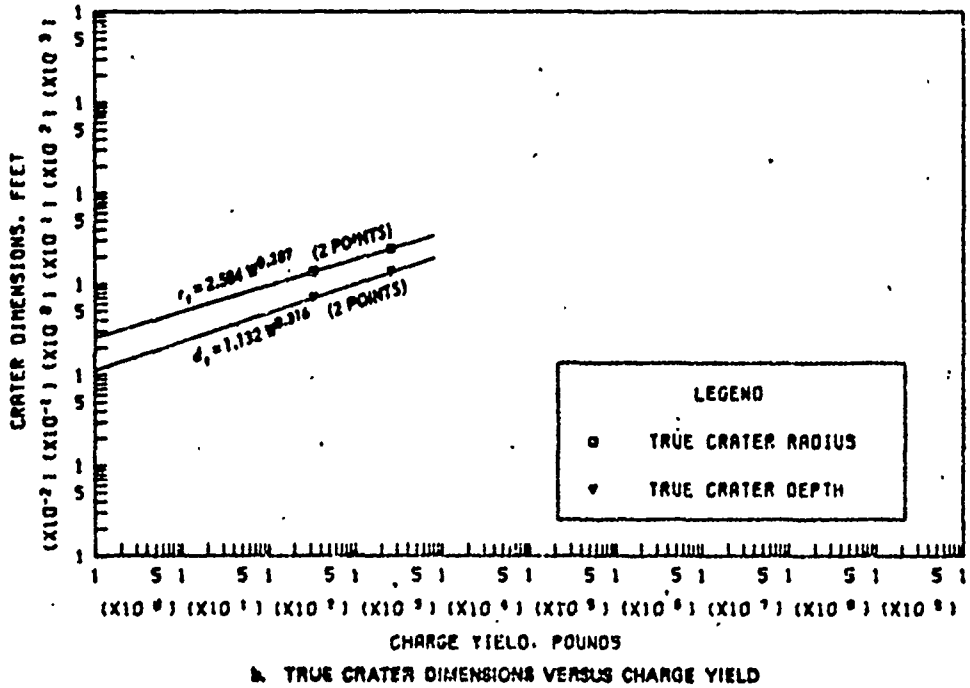

b. TRUE CRATER DIMENSIONS VERSUS CHARGE YIELD

Figure B.28 Dimensions of craters in dry clay for $-0.20 \leq Z < -0.05$ ft/lb$^{1/3}$, Category 5 (sheet 1 of 2).

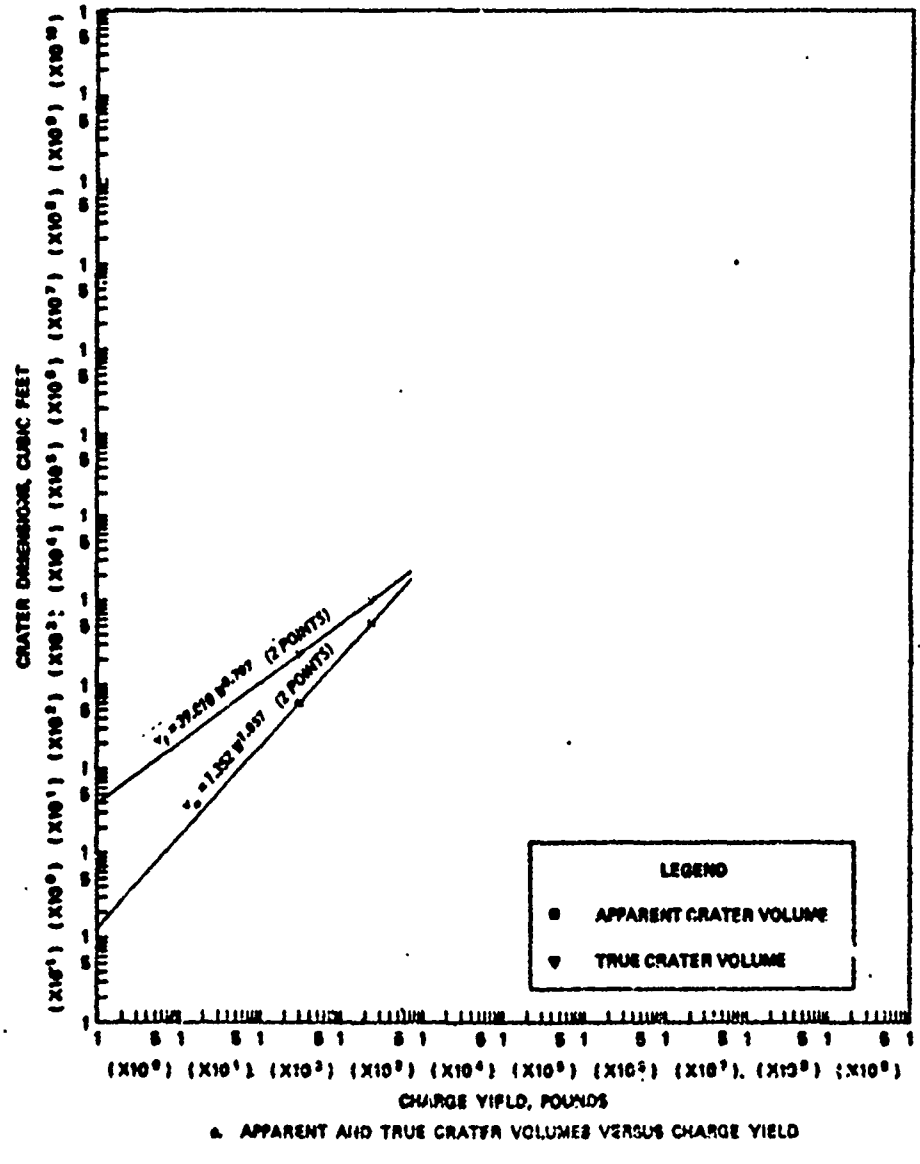

a. APPARENT AND TRUE CRATER VOLUMES VERSUS CHARGE YIELD

Figure B.28 (sheet 2 of 2).

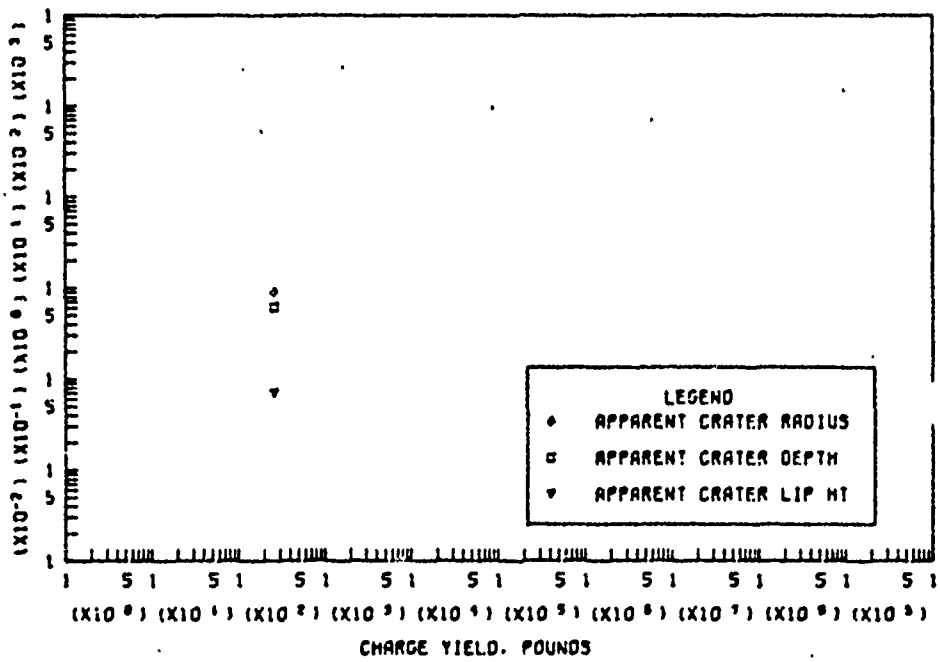

a. APPARENT CRATER DIMENSIONS VERSUS CHARGE YIELD

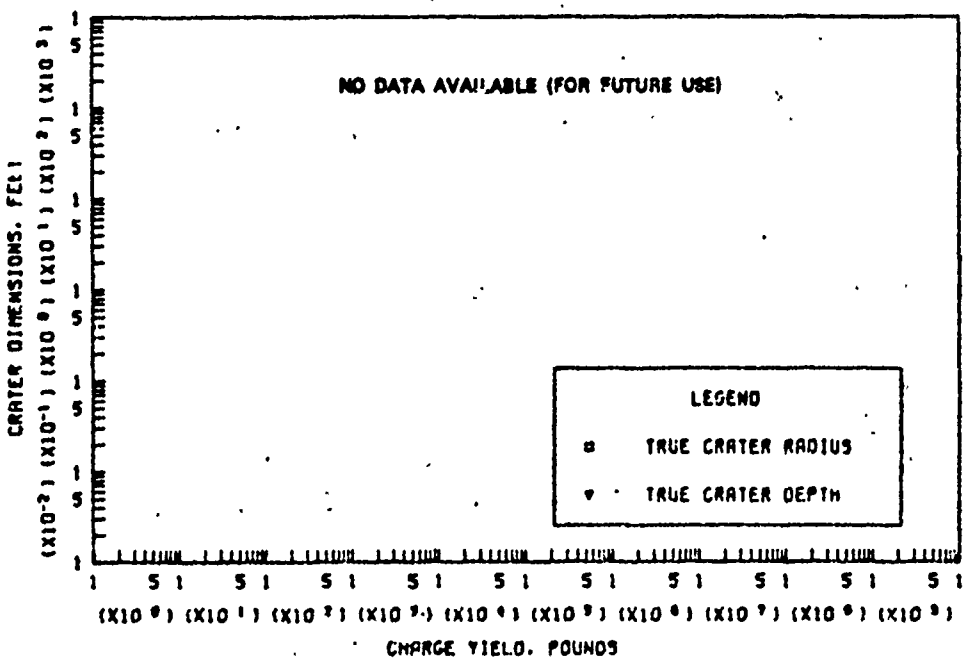

b. TRUE CRATER DIMENSIONS VERSUS CHARGE YIELD

Figure B.29 Dimensions of craters in dry clay for $-0.50 \leq Z < -0.20$ ft/lb$^{1/3}$, Category 6 (sheet 1 of 2).

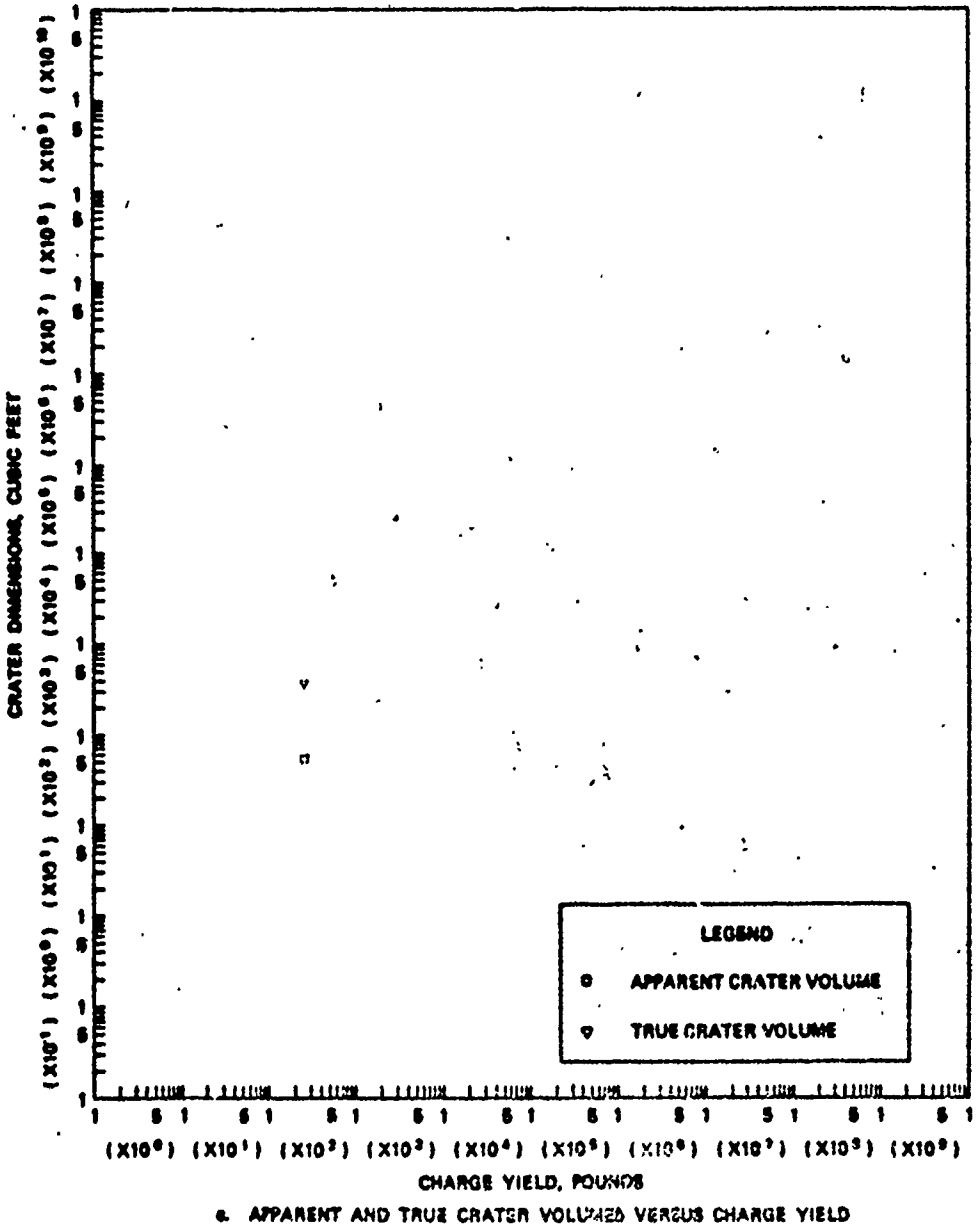

a. APPARENT AND TRUE CRATER VOLUMES VERSUS CHARGE YIELD

Figure B.29 (sheet 2 of 2).

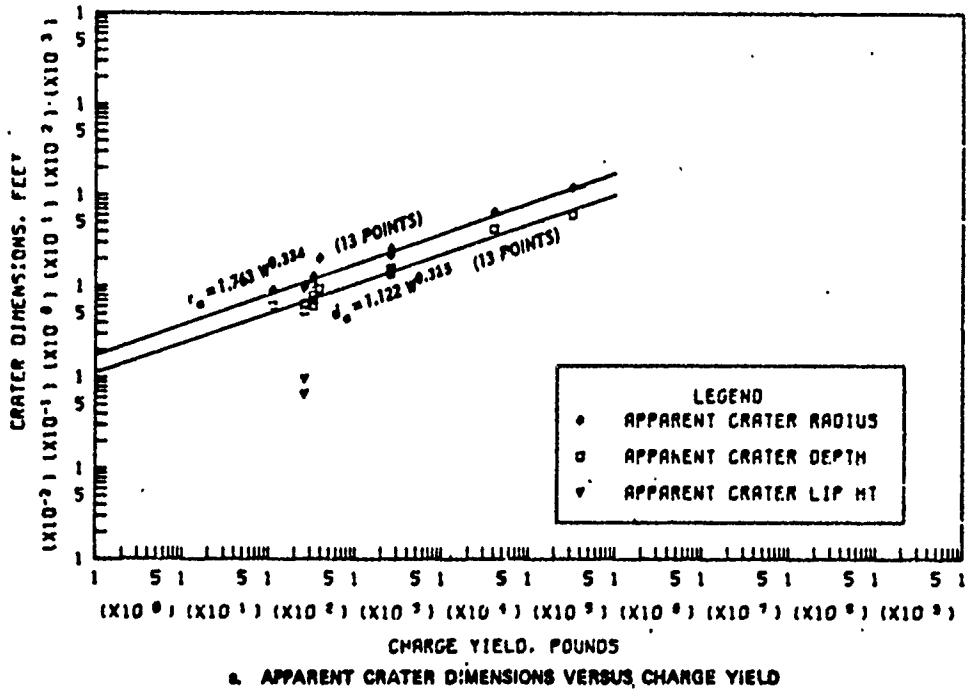

a. APPARENT CRATER DIMENSIONS VERSUS CHARGE YIELD

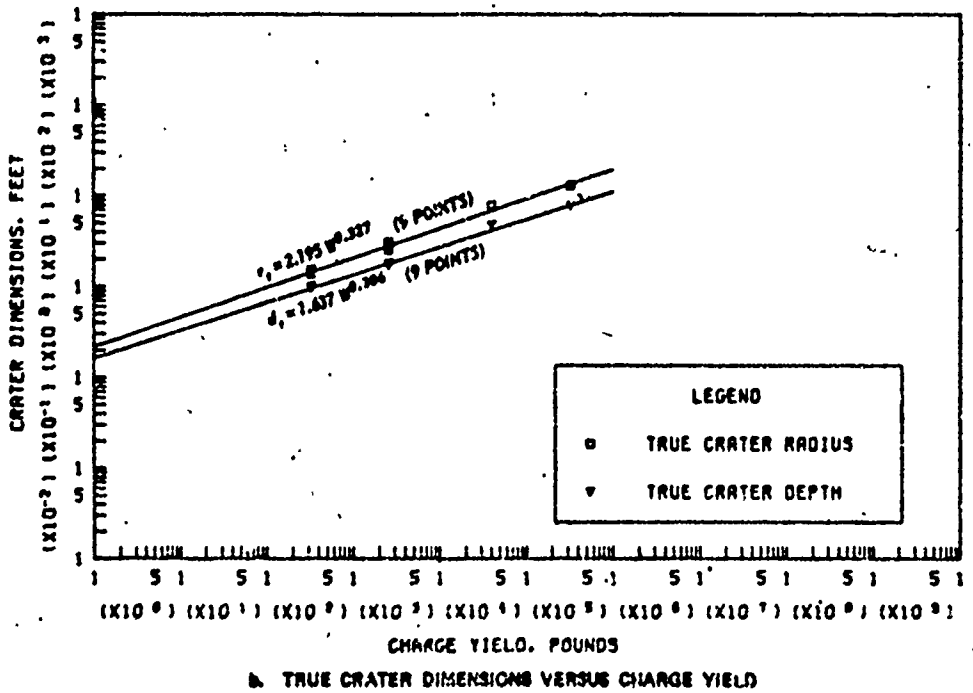

b. TRUE CRATER DIMENSIONS VERSUS CHARGE YIELD

Figure B.30 Dimensions of craters in dry clay for $-0.90 \leq Z < -0.50$ ft/lb$^{1/3}$, Category 7 (sheet 1 of 2).

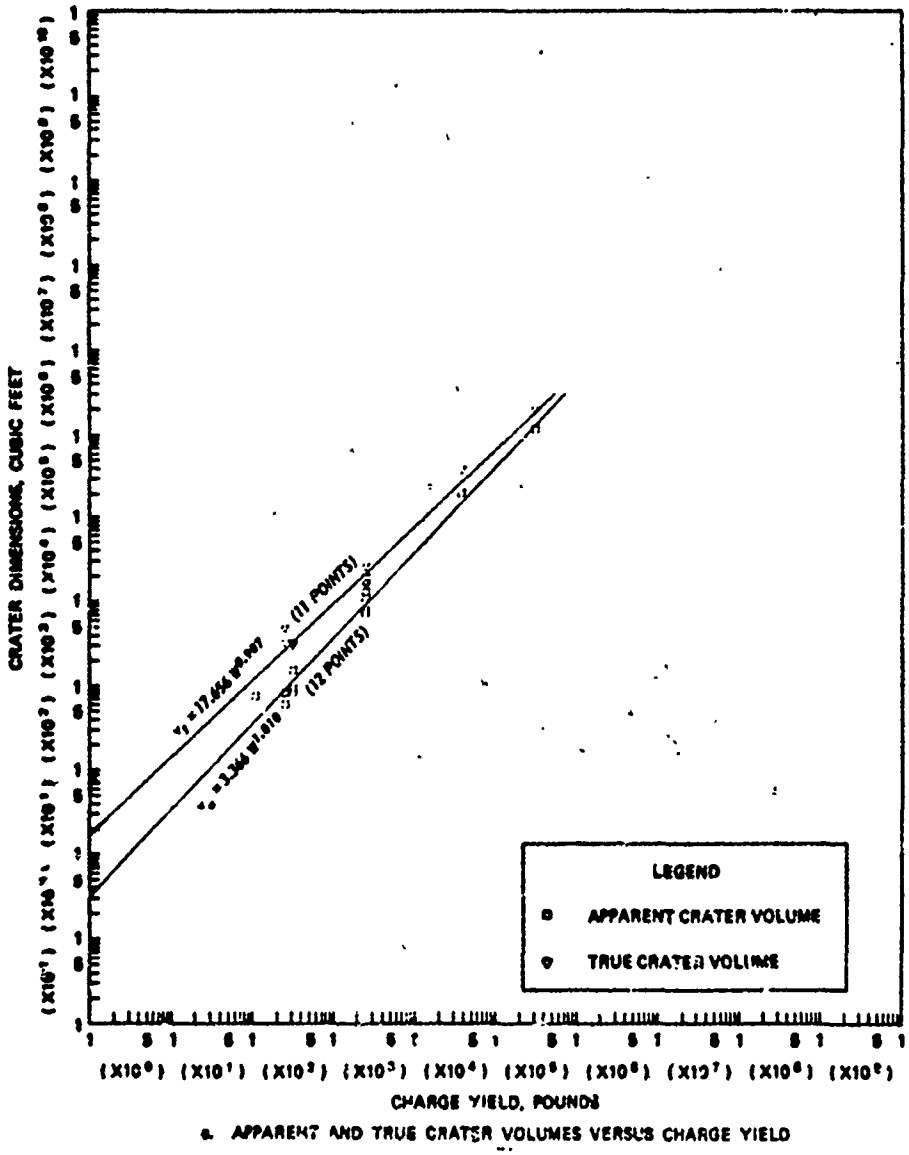

a. APPARENT AND TRUE CRATER VOLUMES VERSUS CHARGE YIELD

Figure B.30 (sheet 2 of 2).

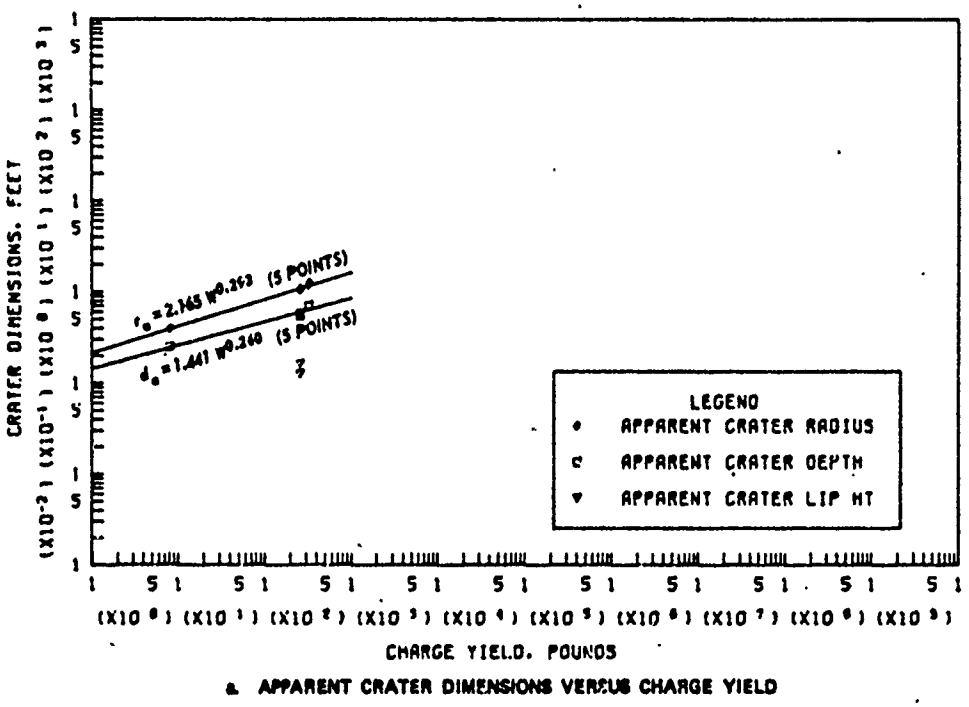

a. APPARENT CRATER DIMENSIONS VERSUS CHARGE YIELD

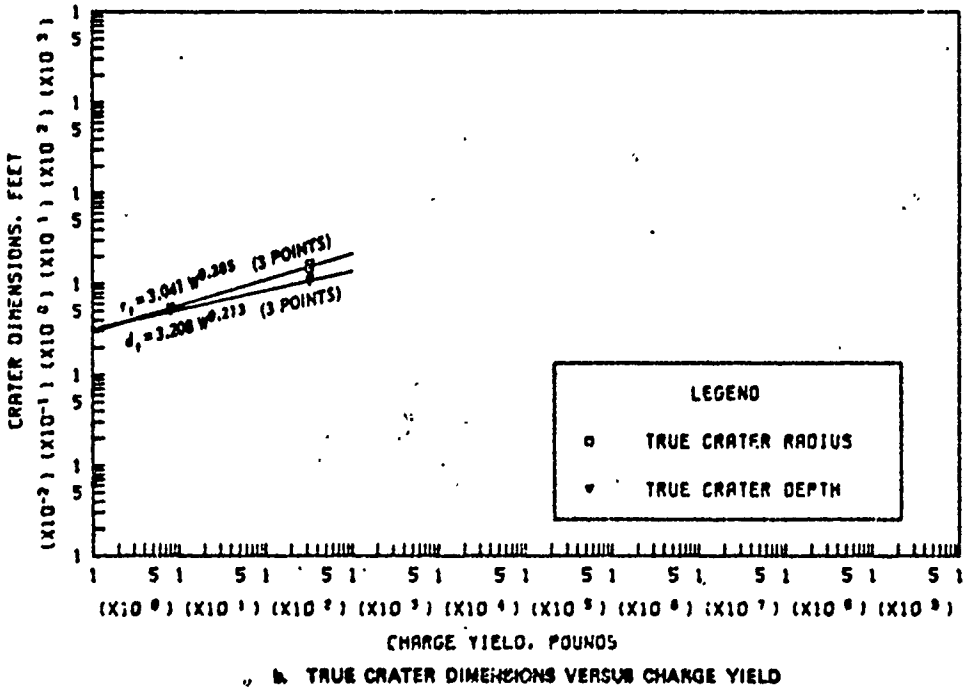

b. TRUE CRATER DIMENSIONS VERSUS CHARGE YIELD

Figure B.31 Dimensions of craters in dry clay for $-1.10 \leq Z < -0.90$ ft/lb$^{1/3}$, Category 8 (sheet 1 of 2).

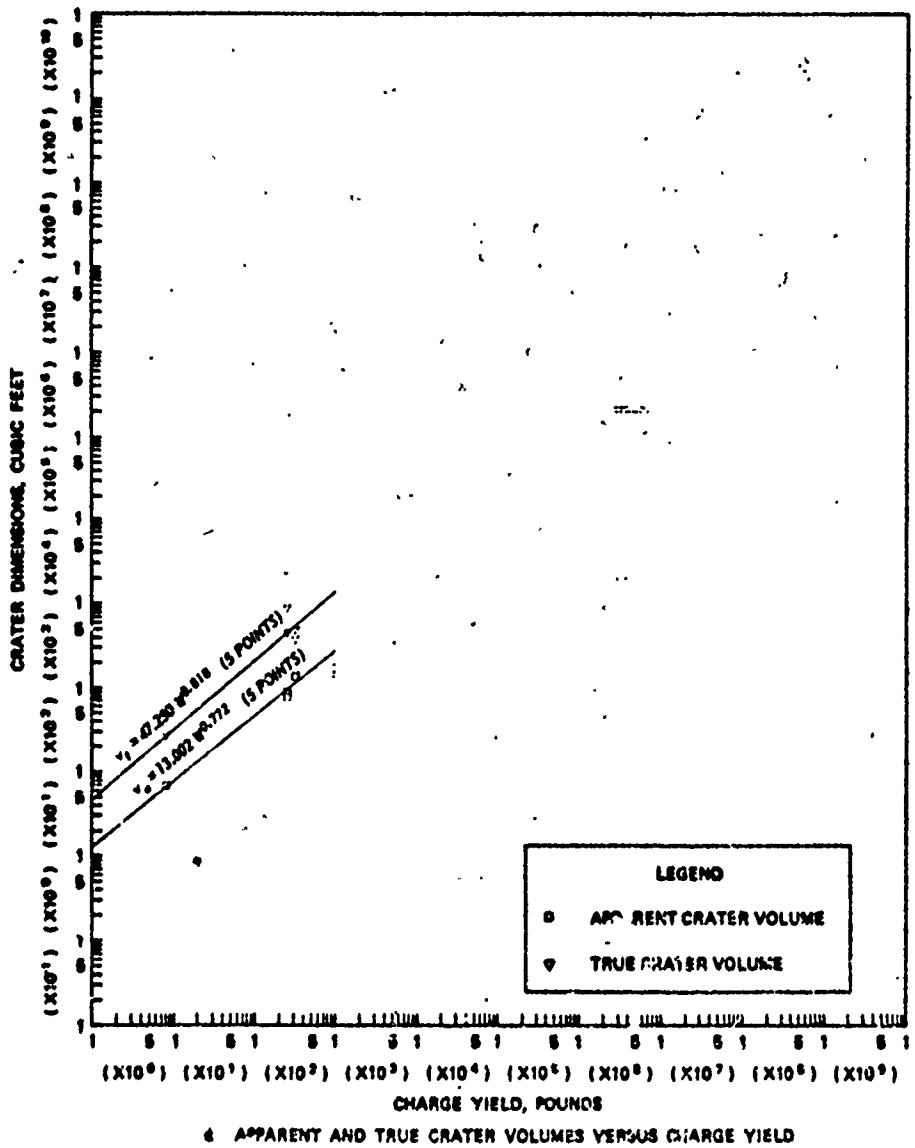

4 APPARENT AND TRUE CRATER VOLUMES VERSUS CHARGE YIELD

Figure B.31 (sheet 2 of 2).

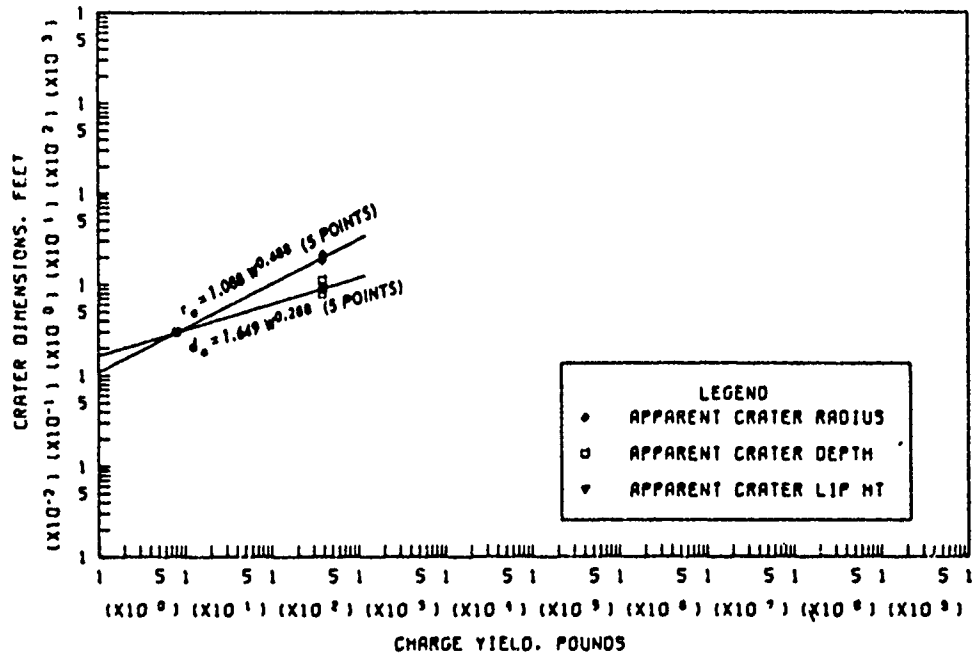

a. APPARENT CRATER DIMENSIONS VERSUS CHARGE YIELD

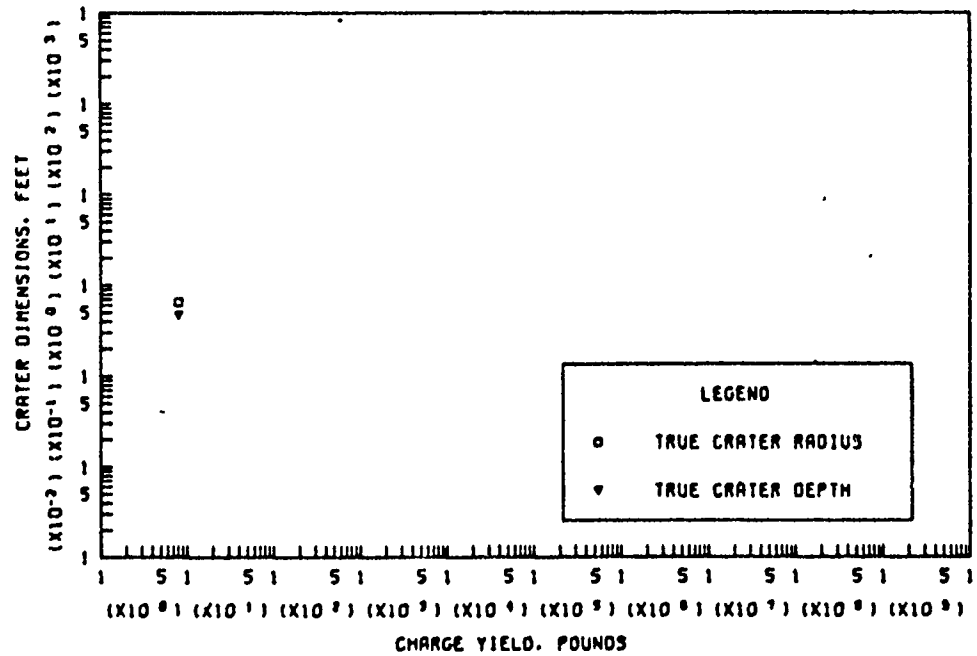

b. TRUE CRATER DIMENSIONS VERSUS CHARGE YIELD

Figure B.32 Dimensions of craters in dry clay for $-2.00 \leq Z < -1.10$ $f_s/lb^{1/3}$, Category 9 (sheet 1 of 2).

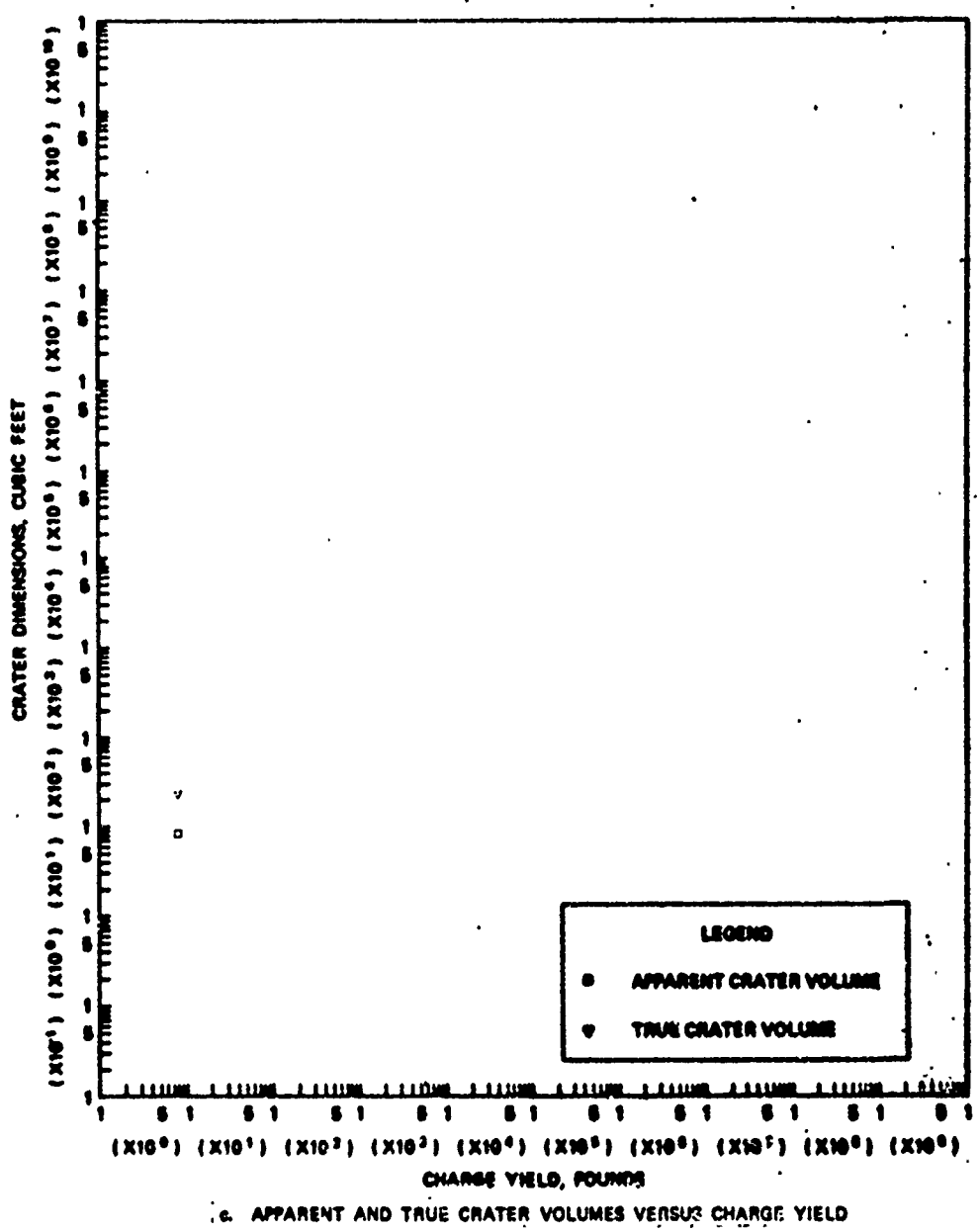

c. APPARENT AND TRUE CRATER VOLUMES VERSUS CHARGE YIELD

Figure B.32 (sheet 2 of 2).

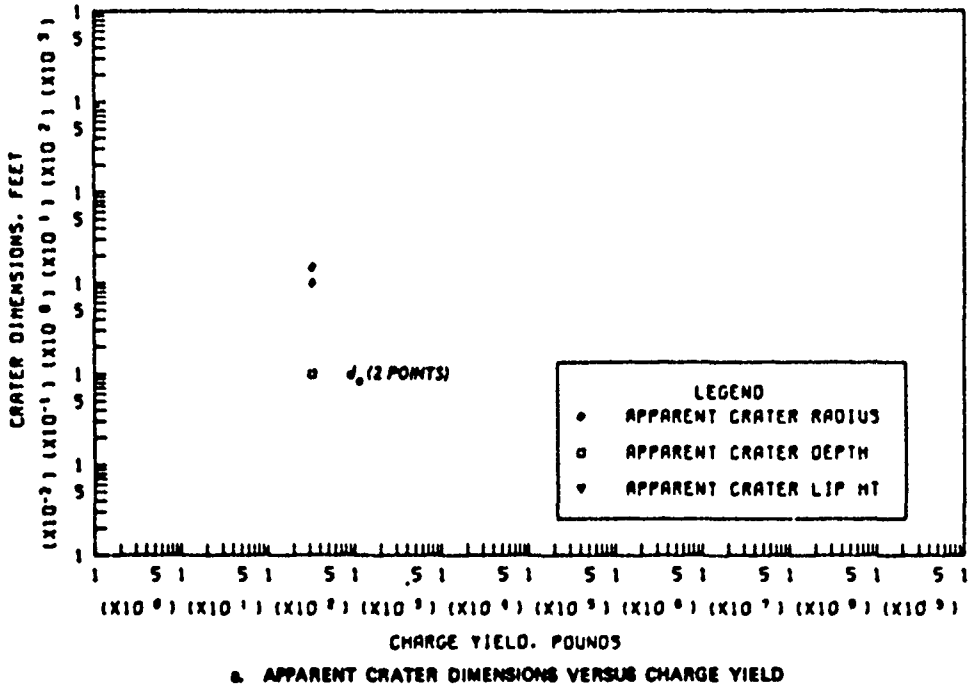

a. APPARENT CRATER DIMENSIONS VERSUS CHARGE YIELD

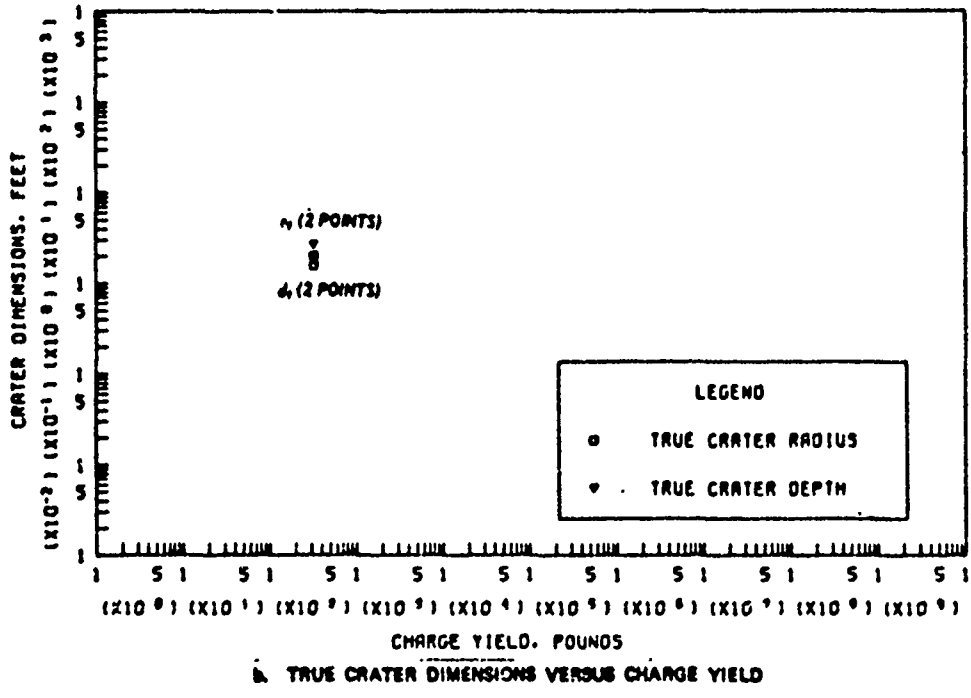

b. TRUE CRATER DIMENSIONS VERSUS CHARGE YIELD

Figure B.33 Dimensions of craters in dry clay for $Z < -2.00$ ft/lb$^{1/3}$, Category 10 (sheet 1 of 2).

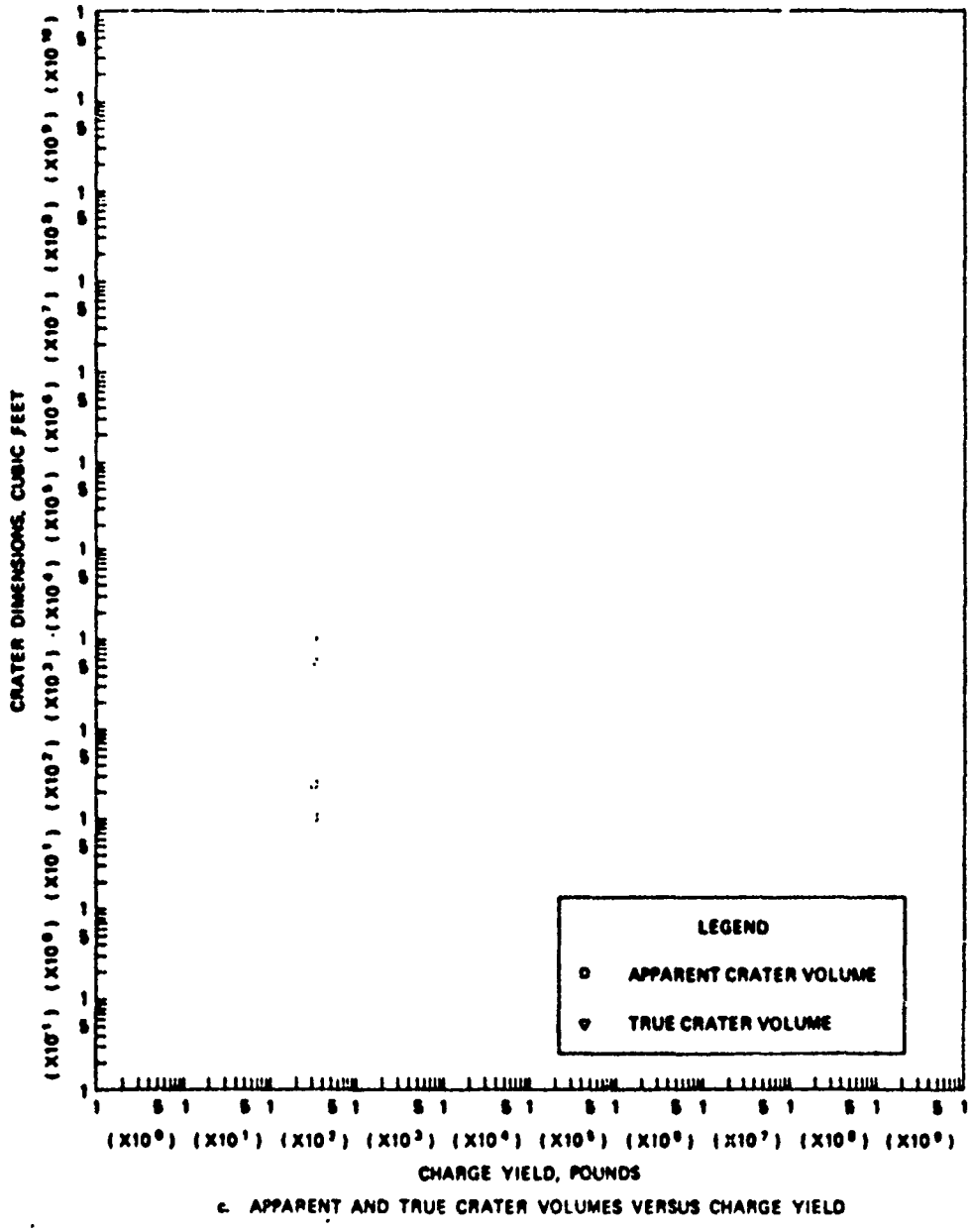

c. APPARENT AND TRUE CRATER VOLUMES VERSUS CHARGE YIELD

Figure B.33 (sheet 2 of 2).

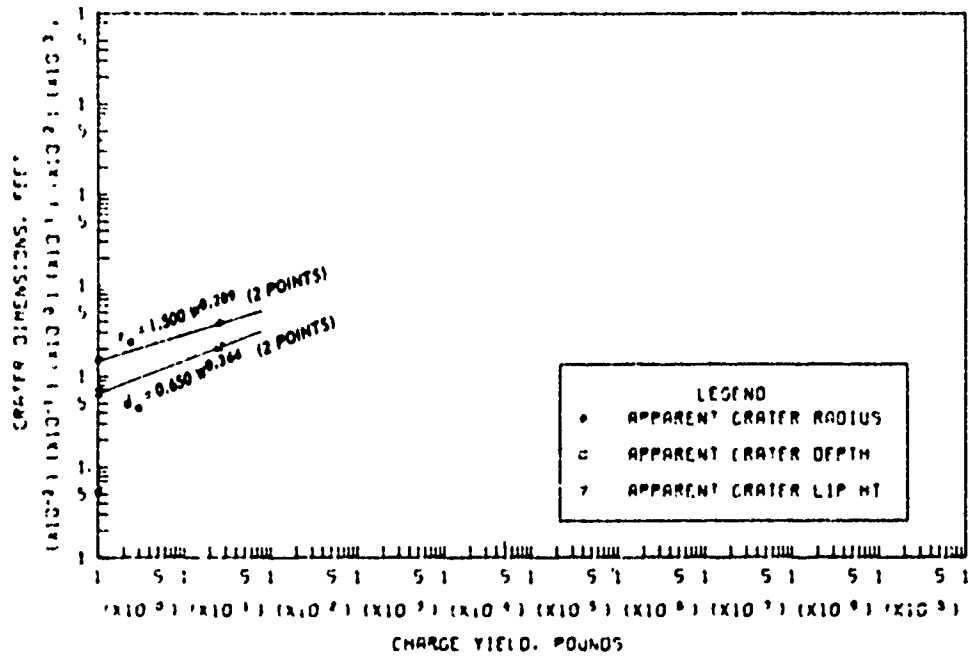

a. APPARENT CRATER DIMENSIONS VERSUS CHARGE YIELD

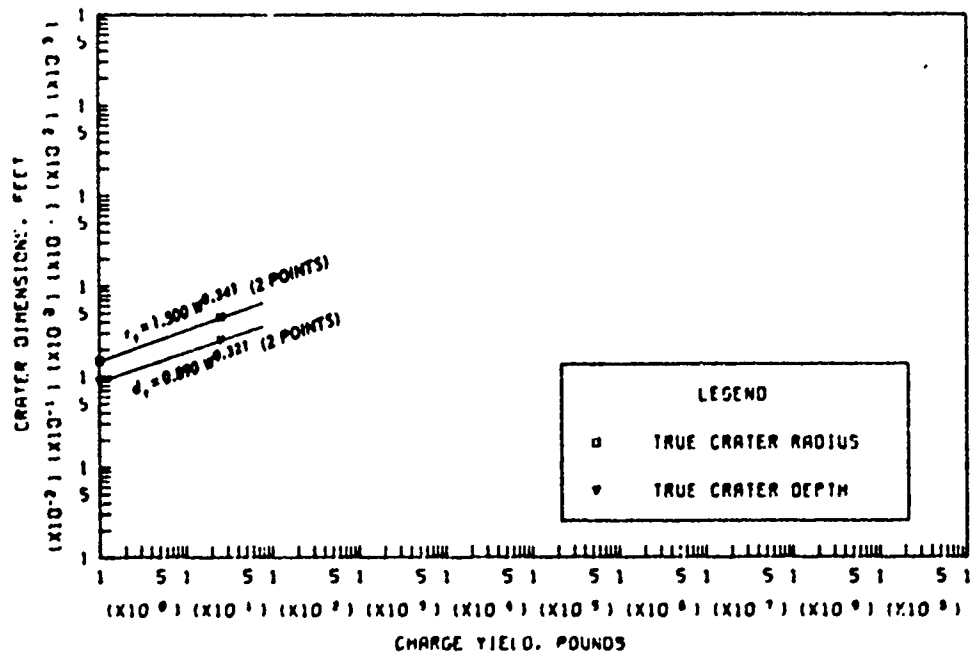

b. TRUE CRATER DIMENSIONS VERSUS CHARGE YIELD

Figure B.74 Dimensions of craters in moist clay for $-0.05 \leq Z < 0.05$ ft/lb$^{1/3}$, Category 4 (sheet 1 of 2).

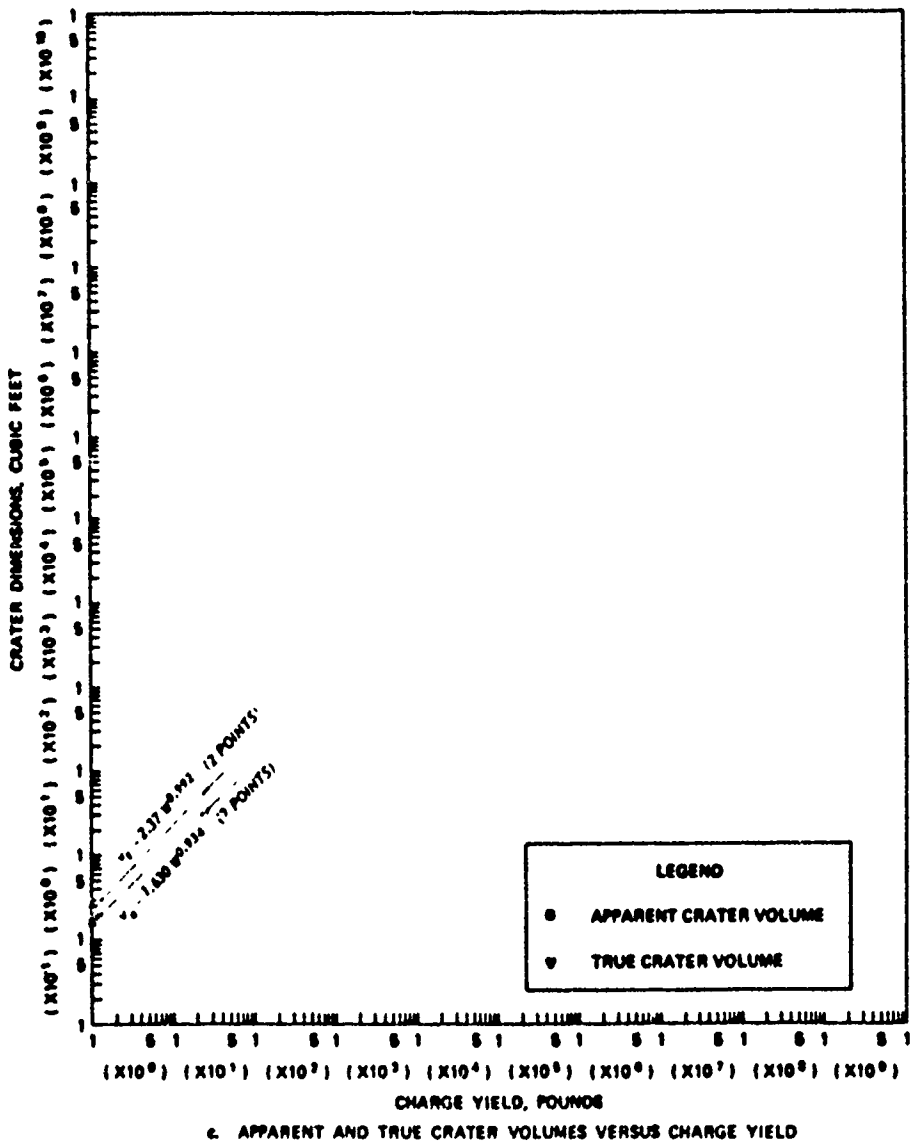

c. APPARENT AND TRUE CRATER VOLUMES VERSUS CHARGE YIELD

Figure B.34 (sheet 2 of 2).

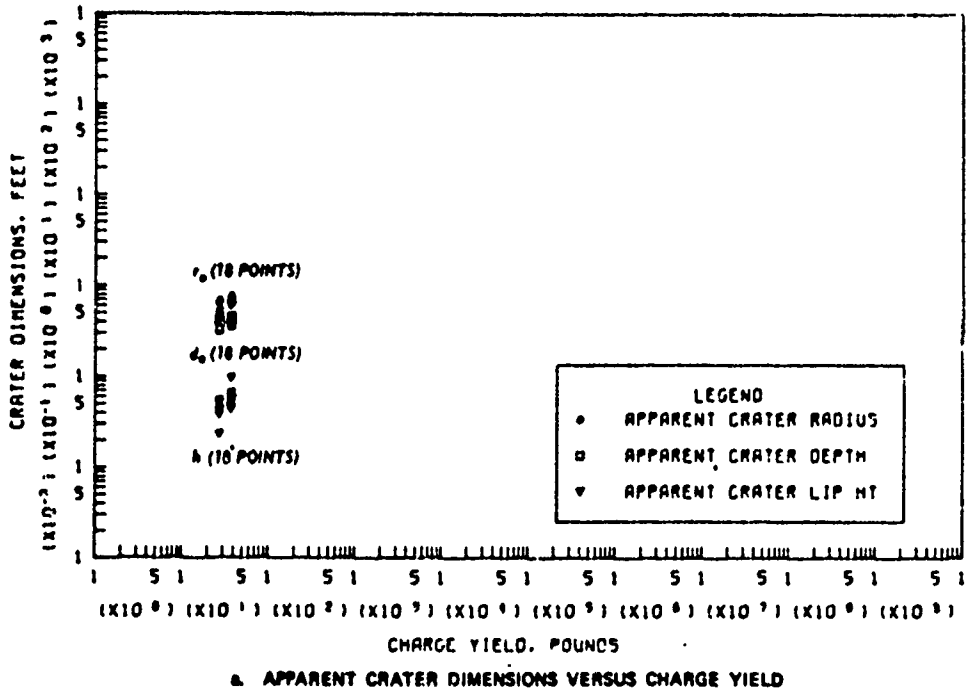

a. APPARENT CRATER DIMENSIONS VERSUS CHARGE YIELD

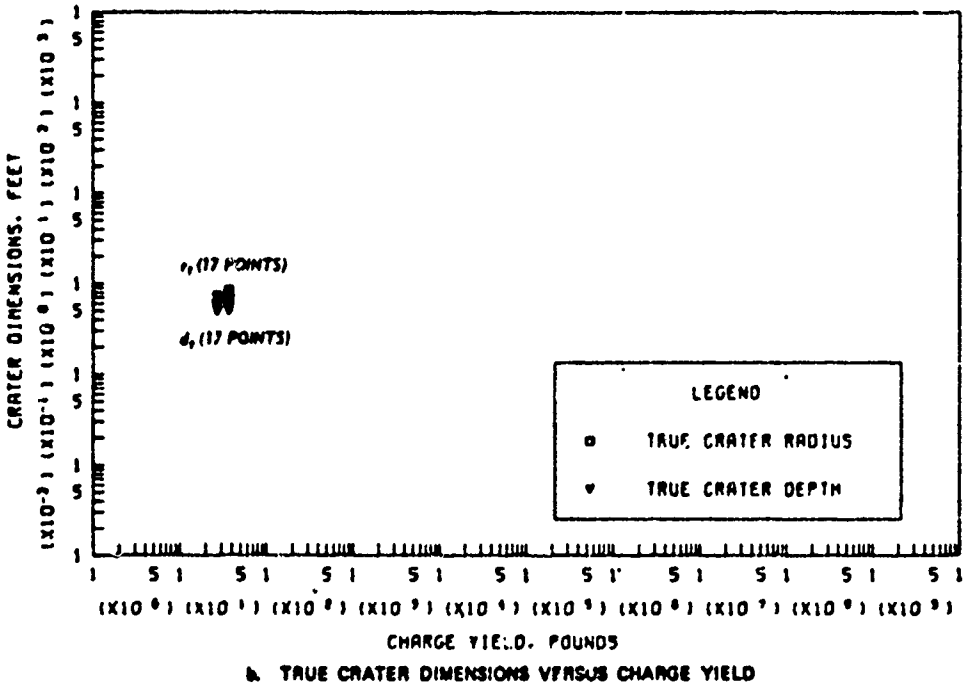

b. TRUE CRATER DIMENSIONS VERSUS CHARGE YIELD

Figure B.35 Dimensions of craters in moist clay for $-0.50 \leq Z < -0.20$ ft/lb$^{1/3}$, Category 6 (sheet 1 of 2).

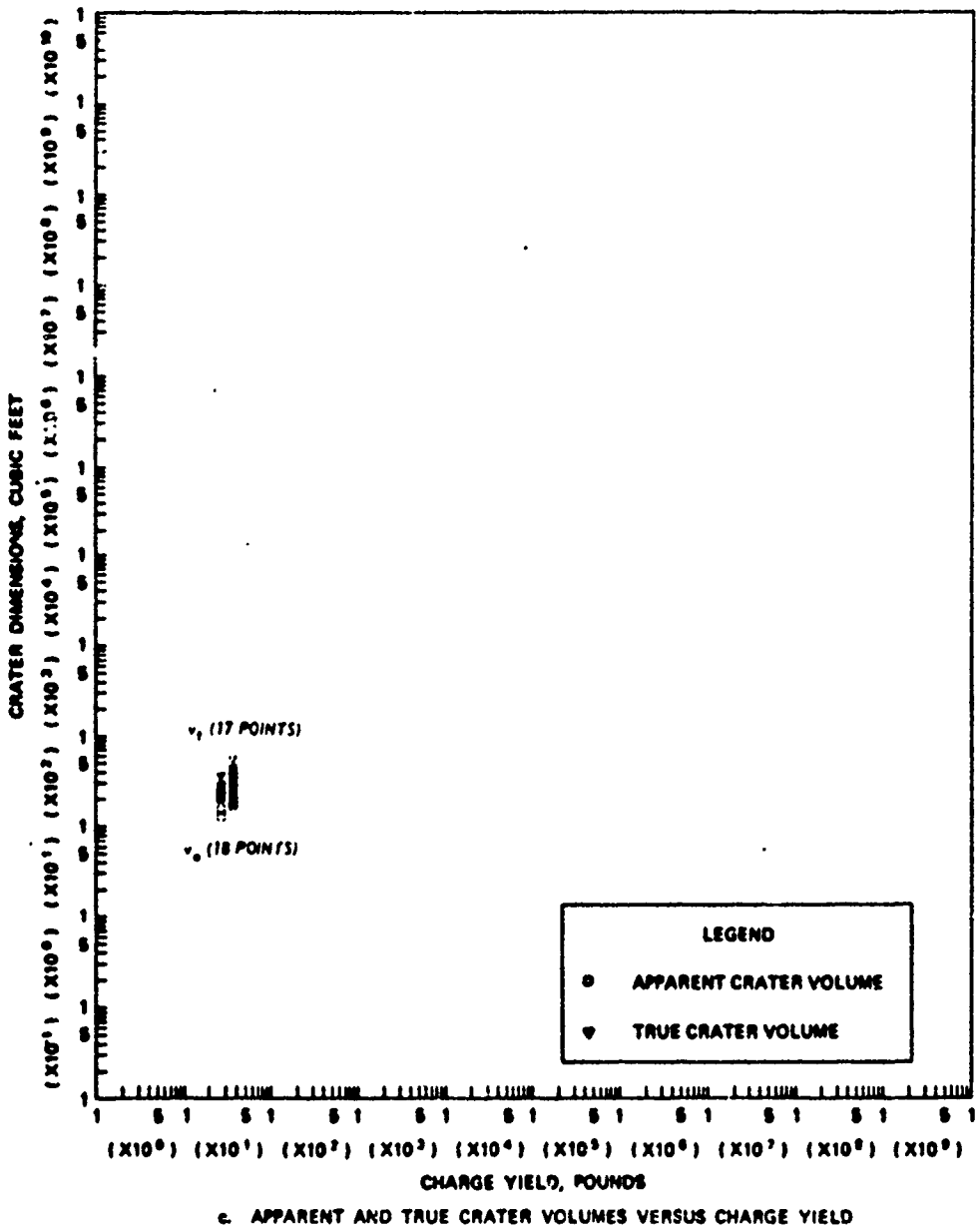

c. APPARENT AND TRUE CRATER VOLUMES VERSUS CHARGE YIELD

Figure B.35 (sheet 2 of 2).

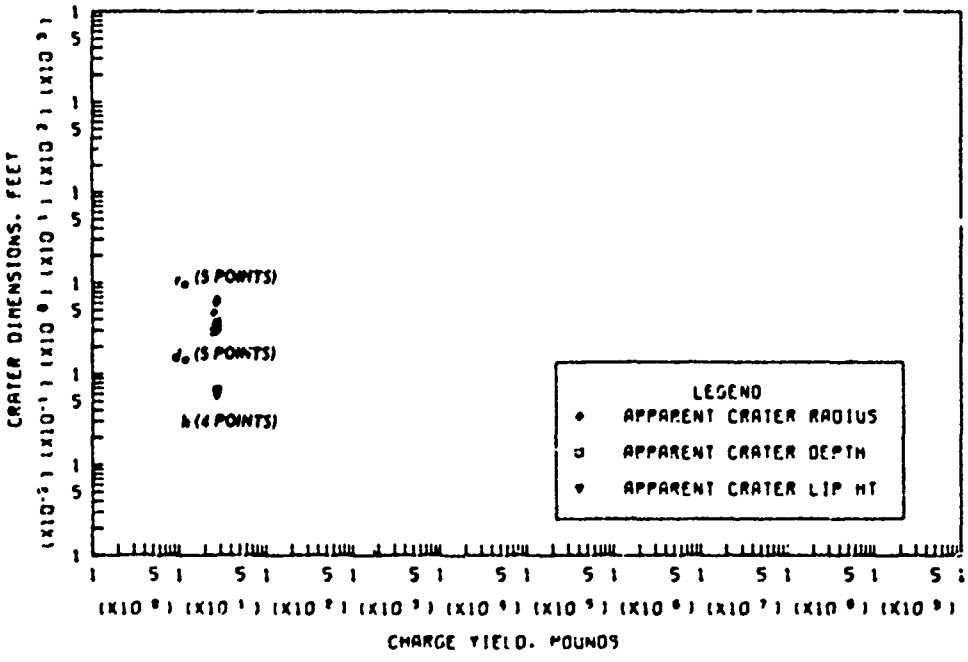

a. APPARENT CRATER DIMENSIONS VERSUS CHARGE YIELD

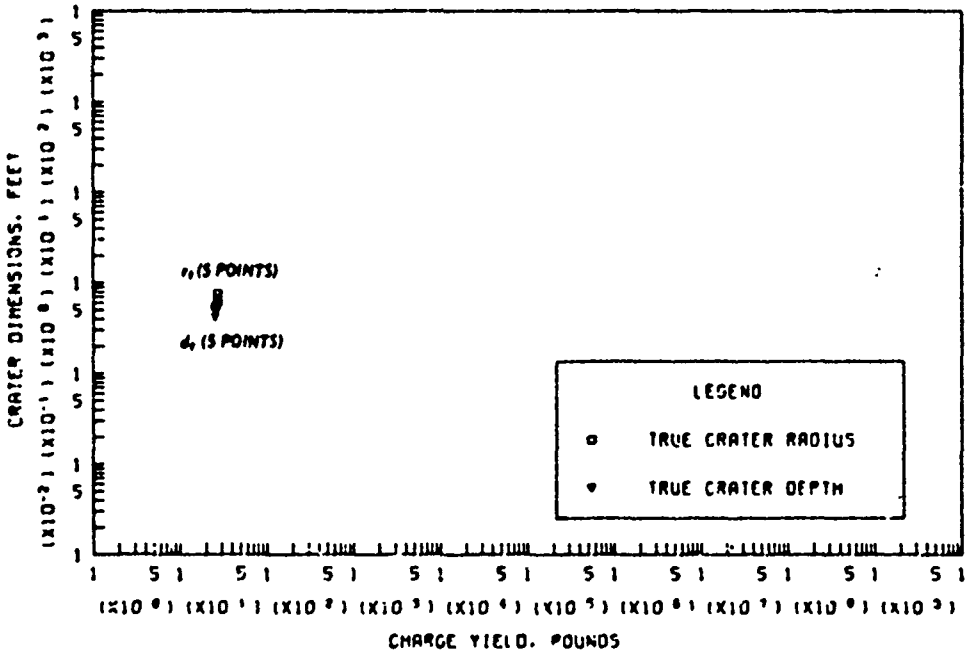

b. TRUE CRATER DIMENSIONS VERSUS CHARGE YIELD

Figure B.36 Dimensions of craters in moist clay for $-0.90 \leq Z < -0.50$ ft/lb$^{1/3}$, Category 7 (sheet 1 of 2).

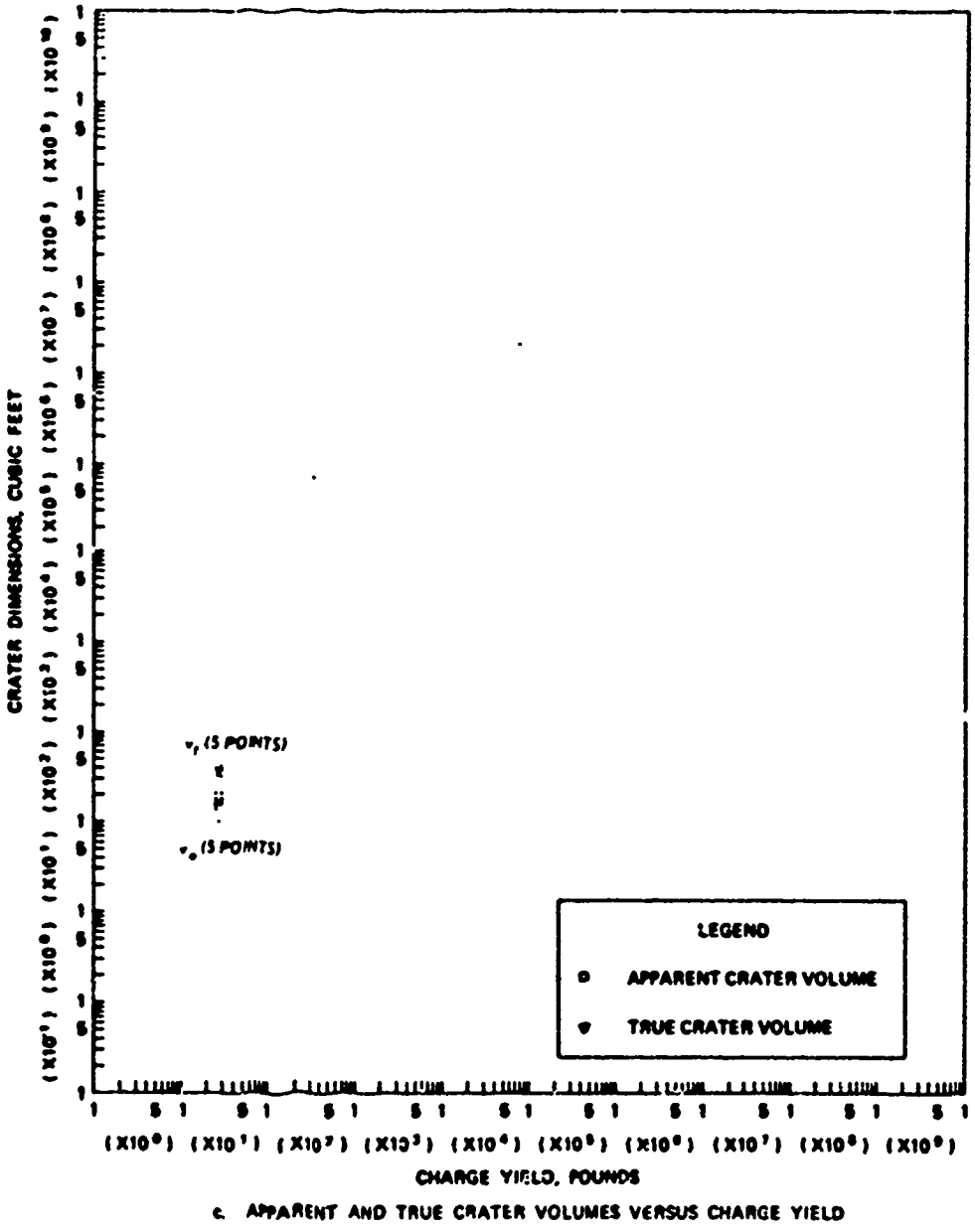

c. APPARENT AND TRUE CRATER VOLUMES VERSUS CHARGE YIELD

Figure B.36 (sheet 2 of 2).

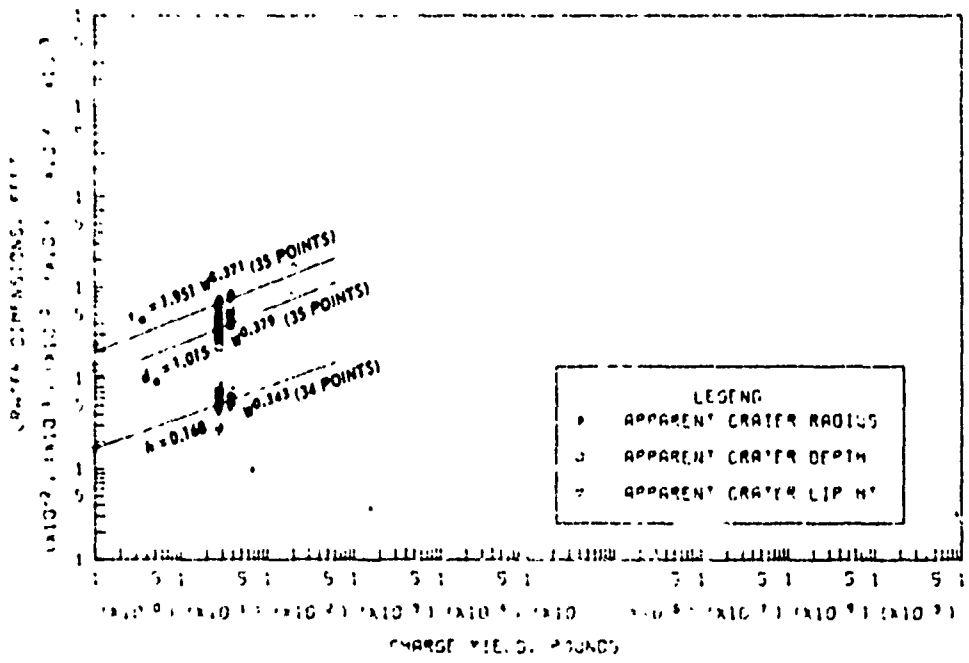

a. APPARENT CRATER DIMENSIONS VERSUS CHARGE YIELD

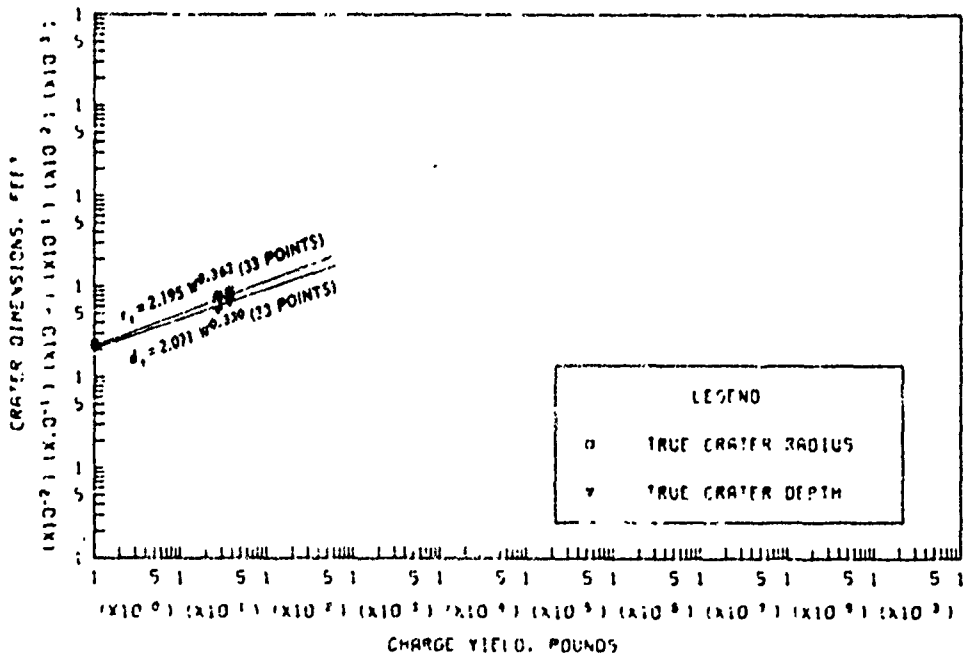

b. TRUE CRATER DIMENSIONS VERSUS CHARGE YIELD

Figure B.37 Dimensions of craters in moist clay for $-1.10 \leq Z < -0.90$ ft/lb$^{1/3}$, Category 8 (sheet 1 of 2).

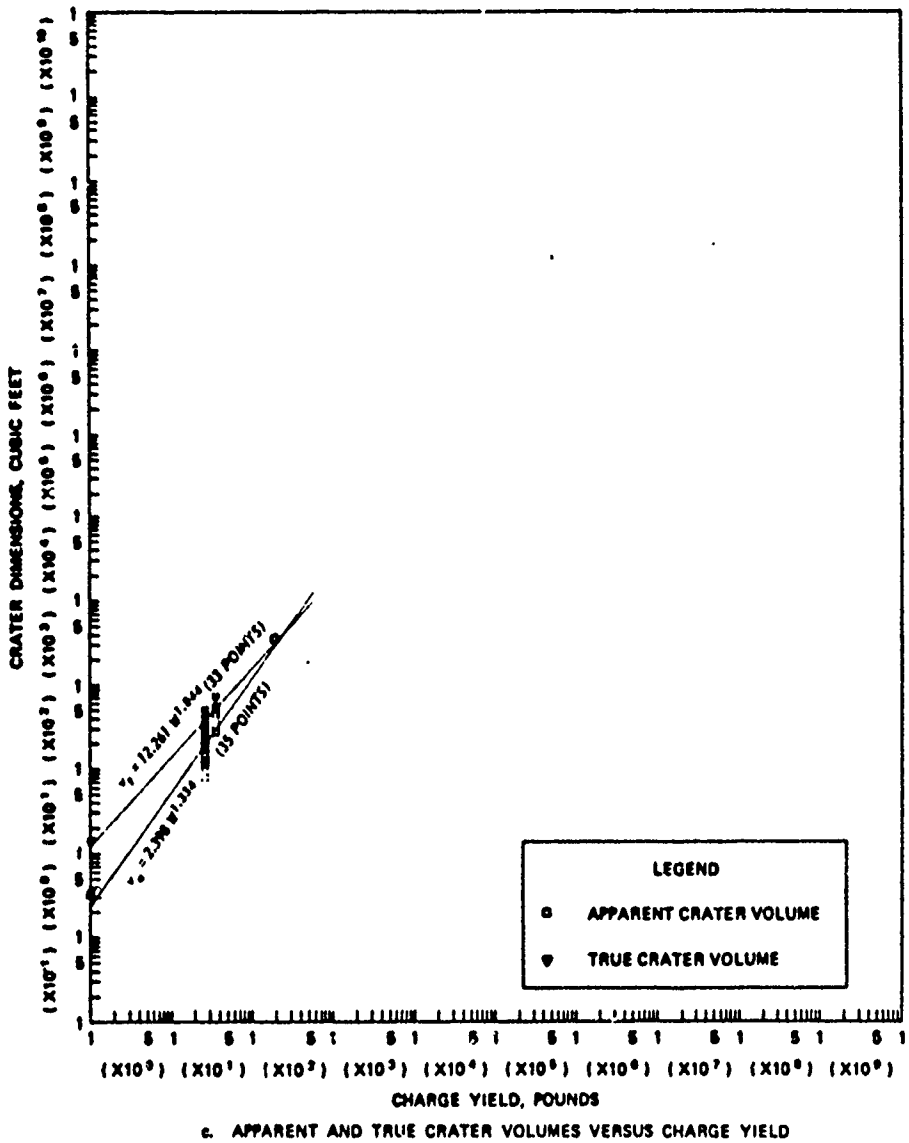

c. APPARENT AND TRUE CRATER VOLUMES VERSUS CHARGE YIELD

Figure b.37 (sheet 2 of 2).

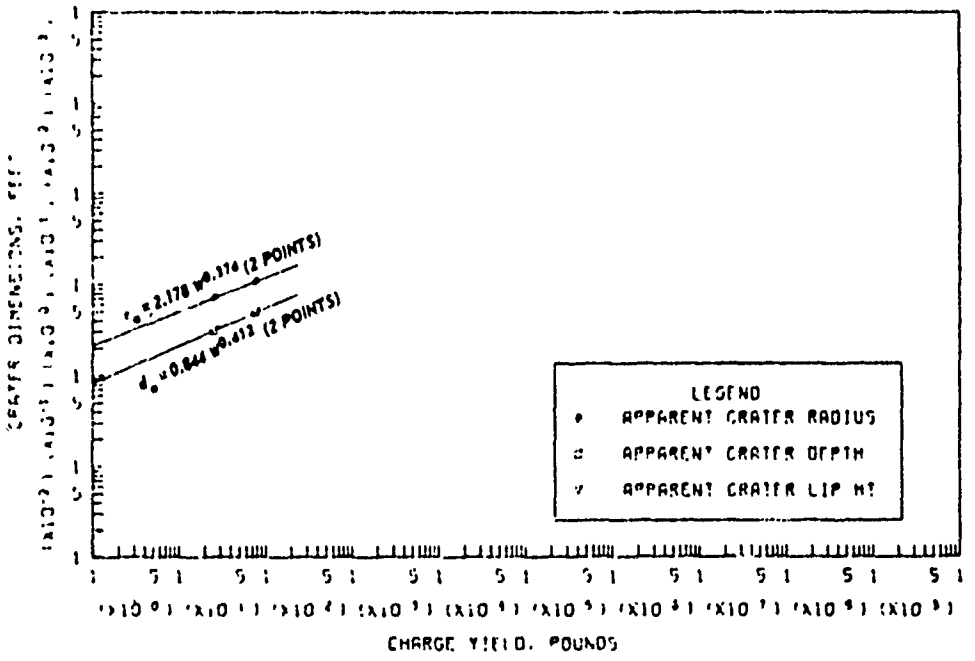

a. APPARENT CRATER DIMENSIONS VERSUS CHARGE YIELD

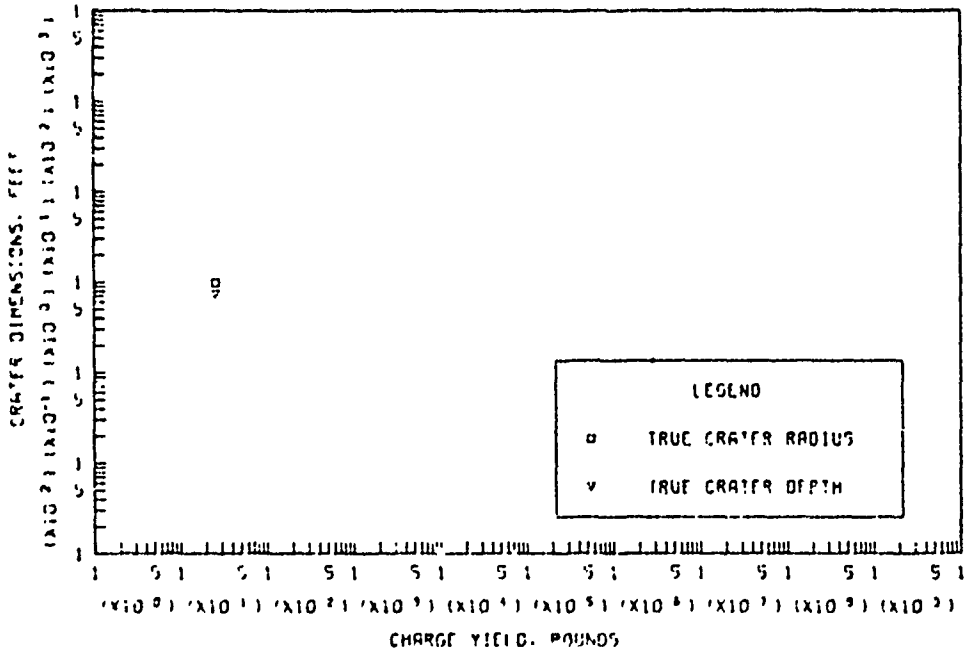

b. TRUE CRATER DIMENSIONS VERSUS CHARGE YIELD

Figure B.38 Dimensions of craters in moist clay for $-2.00 \leq Z < -1.10$ ft/lb$^{1/3}$, Category 9 (sheet 1 of 2)

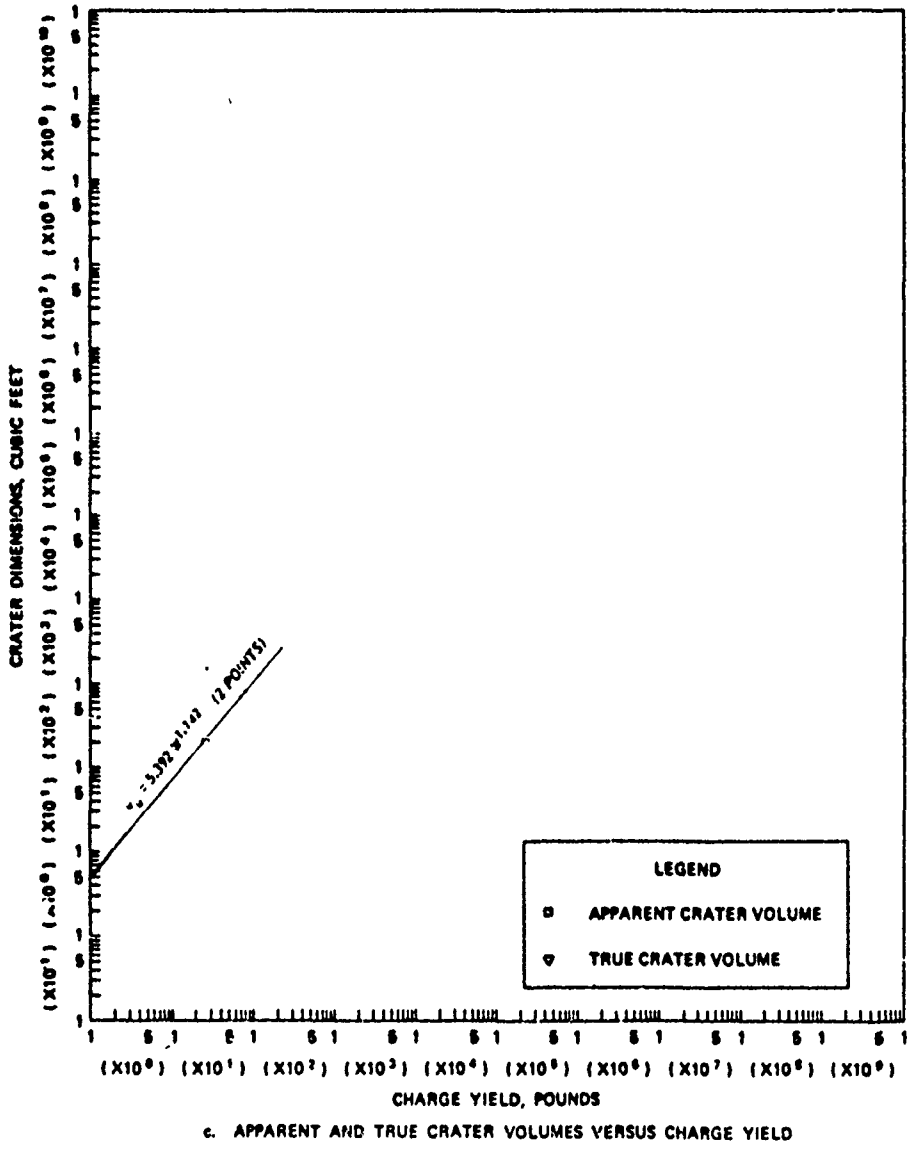

c. APPARENT AND TRUE CRATER VOLUMES VERSUS CHARGE YIELD

Figure B.38 (sheet 2 of 2).

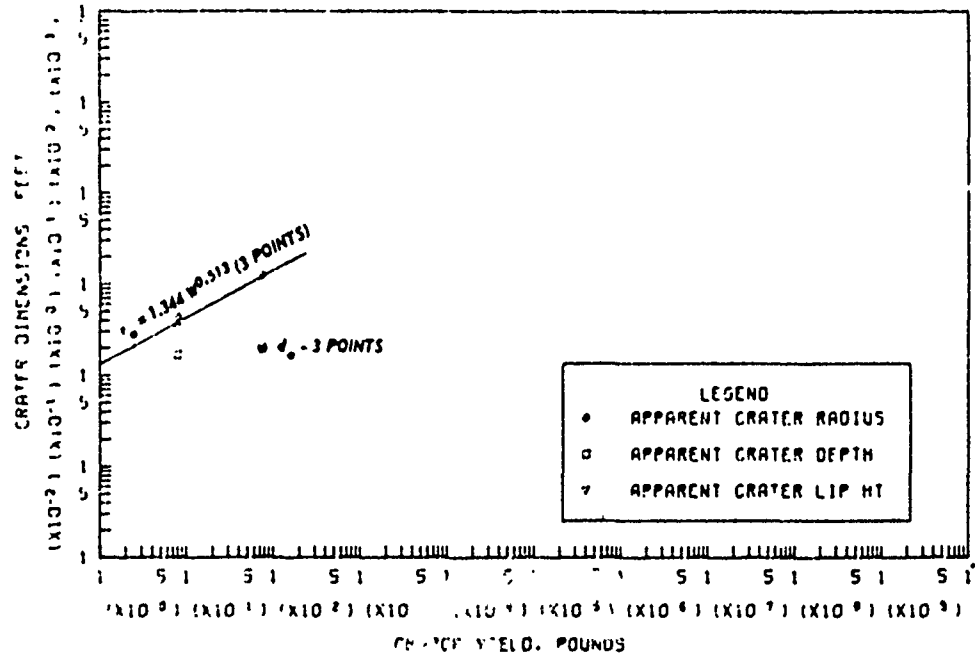

a. APPARENT CRATER DIMENSIONS VERSUS CHARGE YIELD

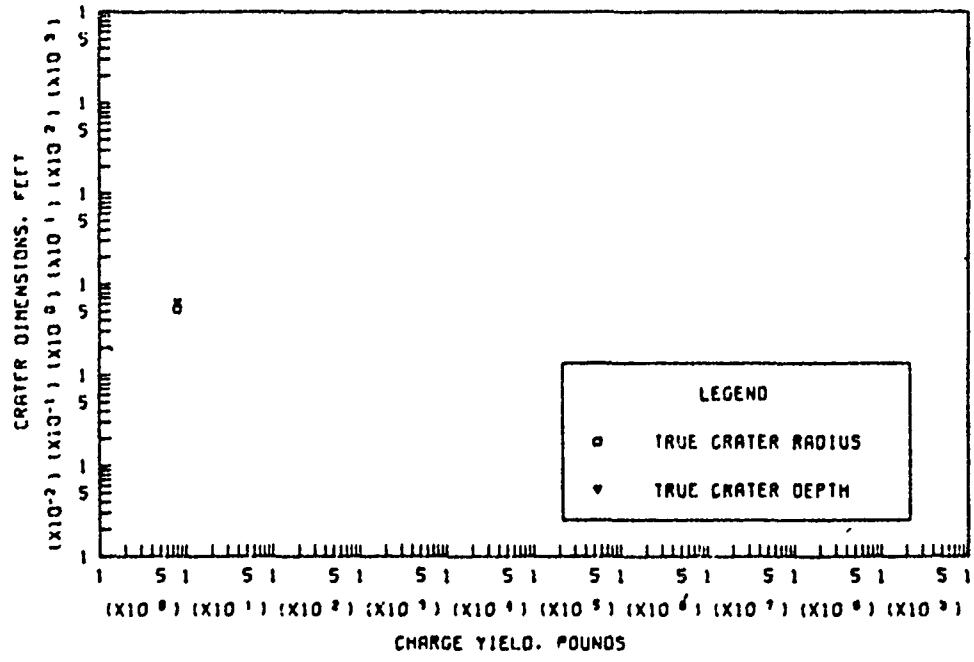

b. TRUE CRATER DIMENSIONS VERSUS CHARGE YIELD

Figure B.39 Dimensions of craters in moist clay for $Z < -2.00$ ft/lb$^{1/3}$, Category 10 (sheet 1 of 2).

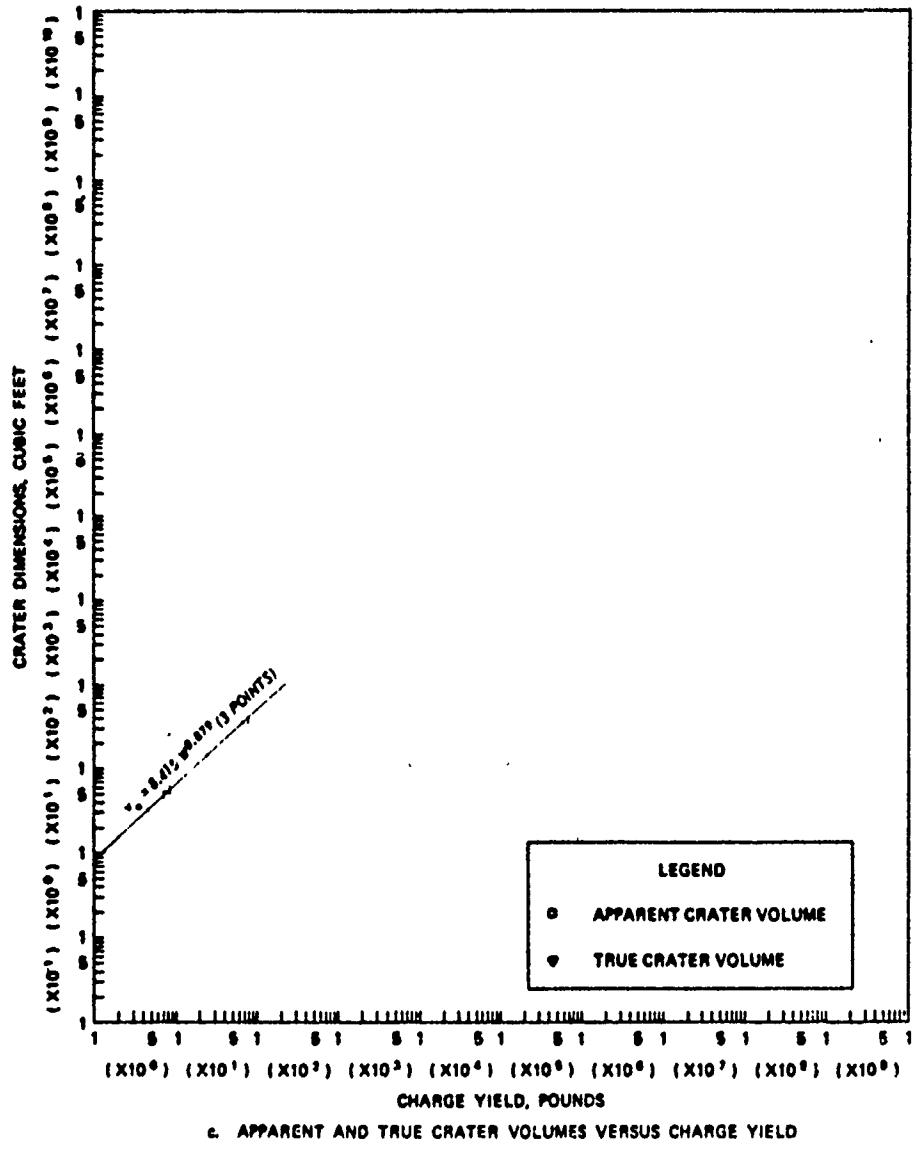

c. APPARENT AND TRUE CRATER VOLUMES VERSUS CHARGE YIELD

Figure B.39 (sheet 2 of 2).

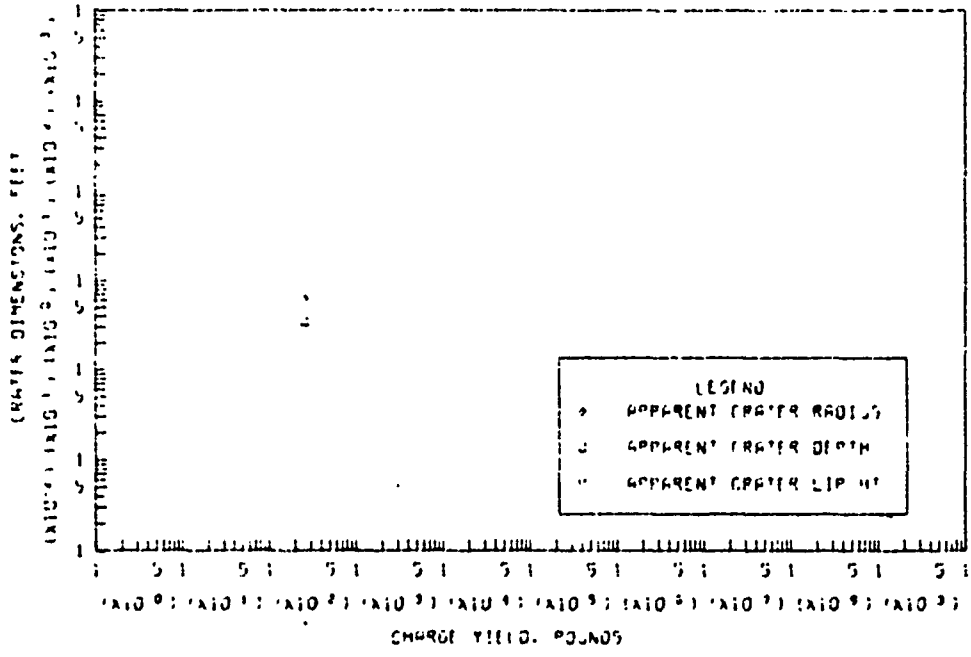

a. APPARENT CRATER DIMENSIONS VERSUS CHARGE YIELD

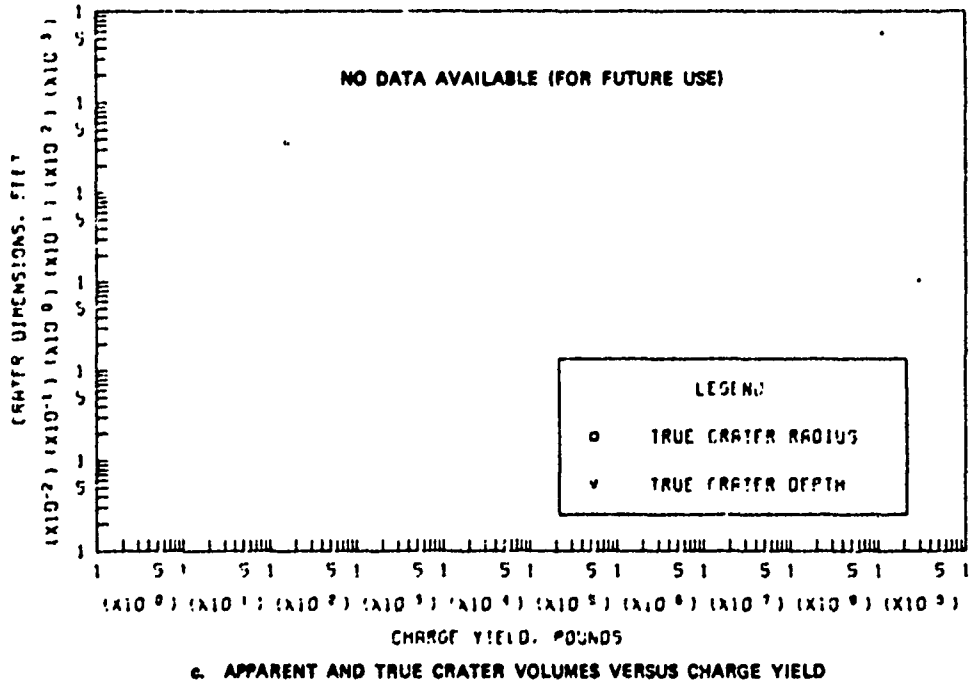

c. APPARENT AND TRUE CRATER VOLUMES VERSUS CHARGE YIELD

Figure B.40 Dimensions of craters in wet clay for $0.05 \leq Z < 0.20$ ft/lb$^{1/3}$, Category 3 (sheet 1 of 2).

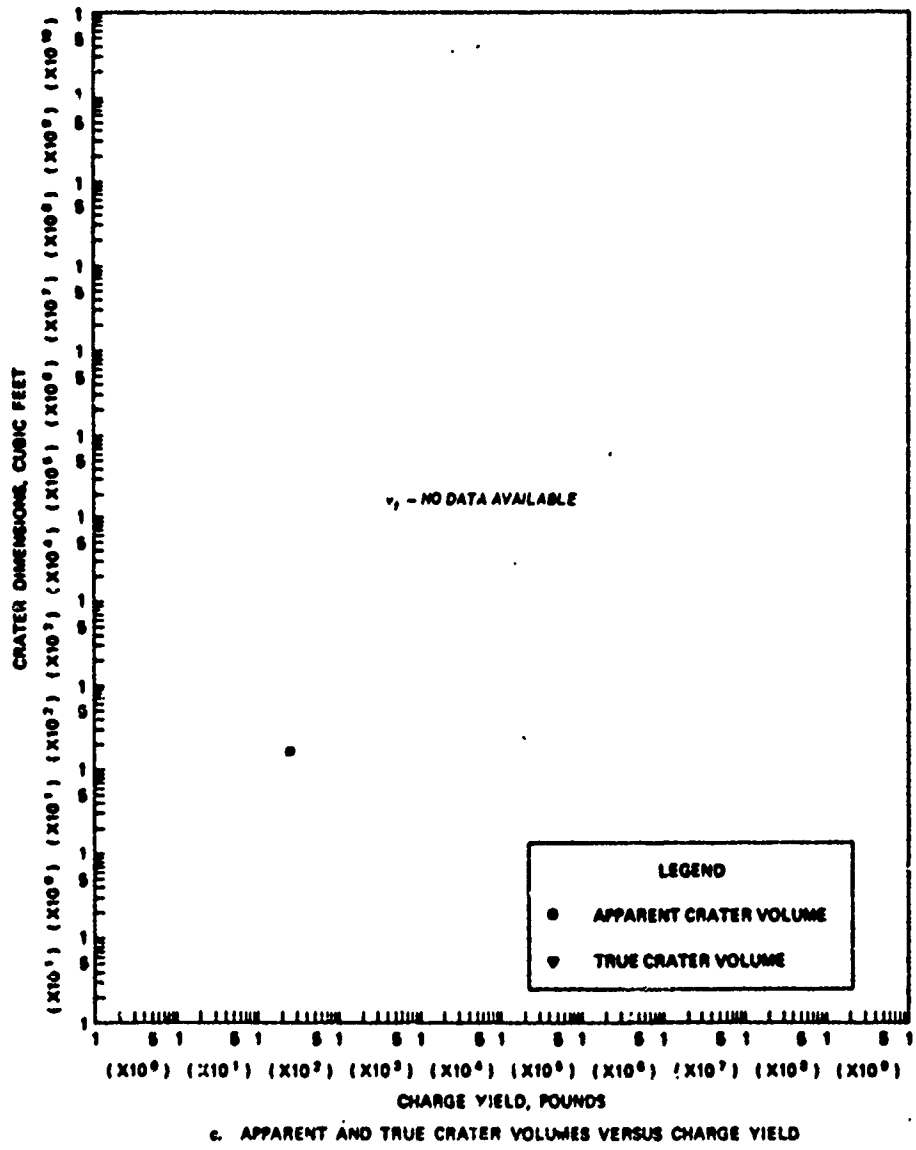

c. APPARENT AND TRUE CRATER VOLUMES VERSUS CHARGE YIELD

Figure B.40 (sheet 2 of 2).

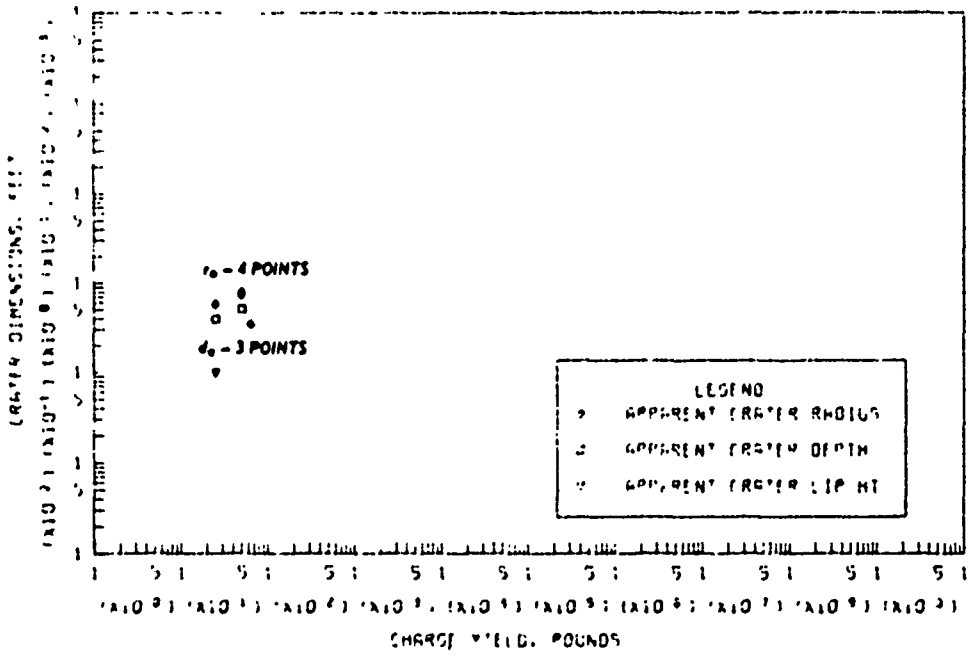

a. APPARENT CRATER DIMENSIONS VERSUS CHARGE YIELD

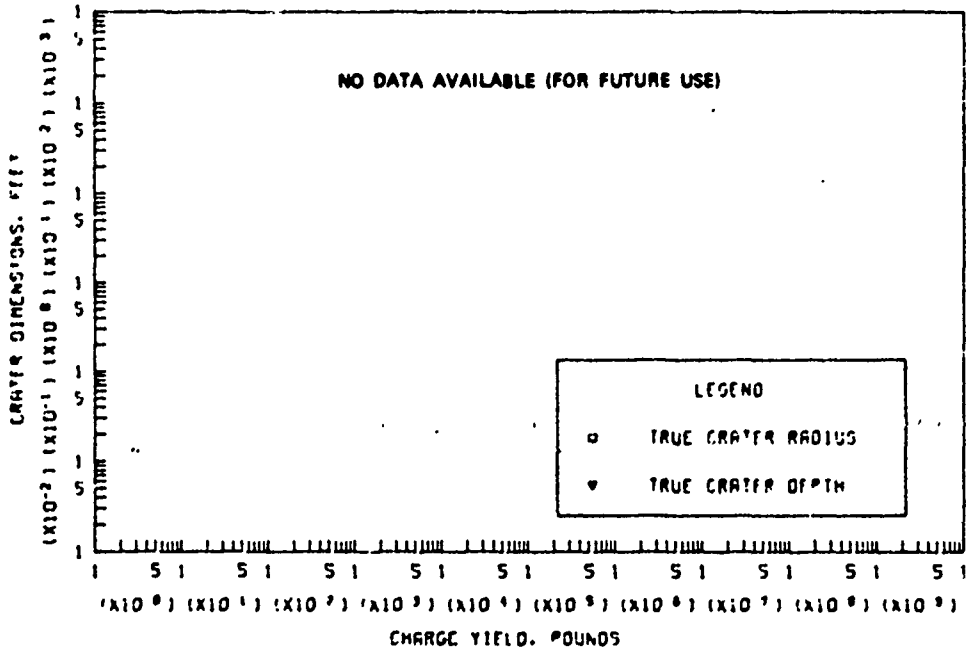

b. TRUE CRATER DIMENSIONS VERSUS CHARGE YIELD

Figure B.41 Dimensions of craters in wet clay for $-0.05 \leq Z < 0.05$ ft/lb$^{1/3}$, Category 4 (sheet 1 of 2).

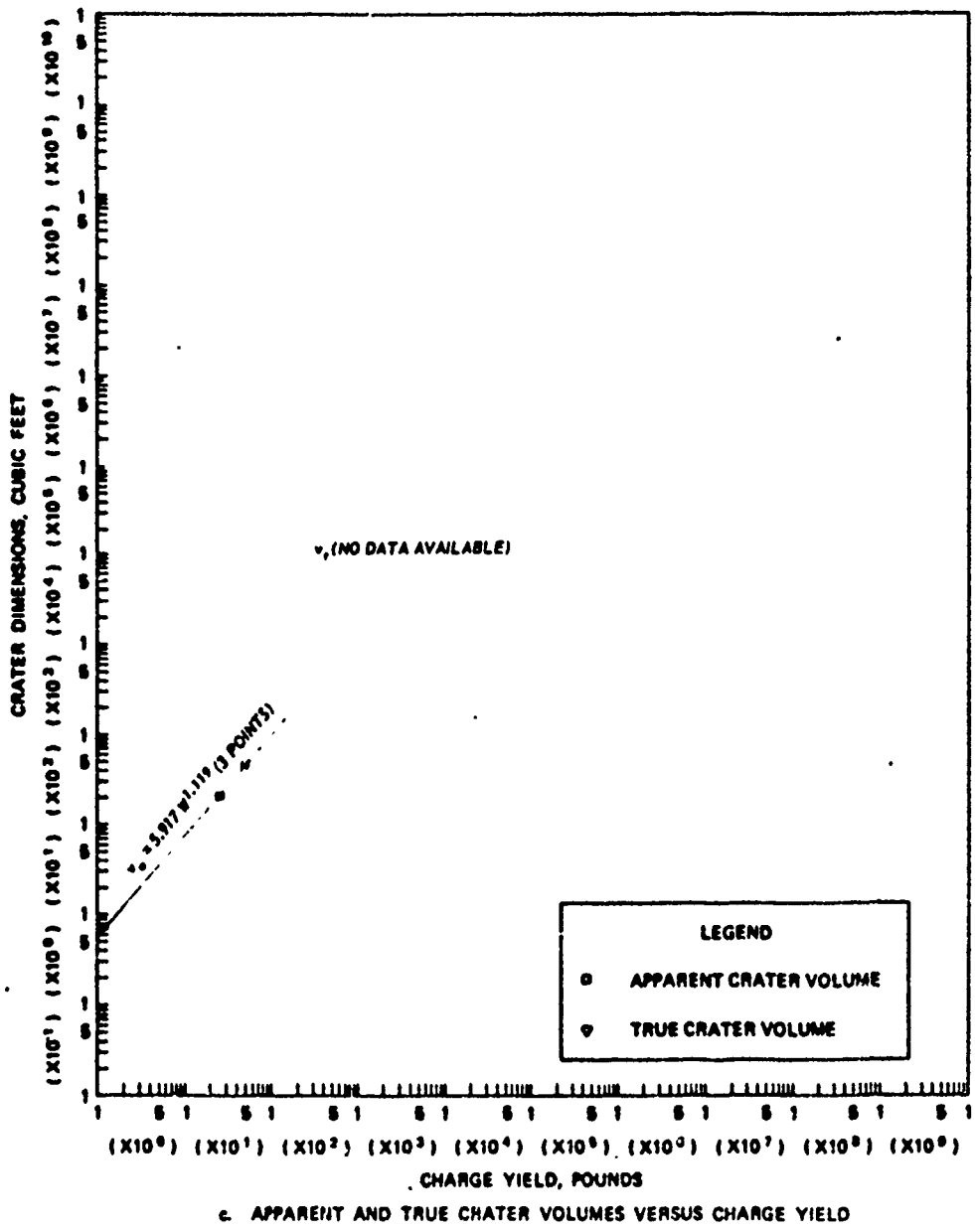

c. APPARENT AND TRUE CHATER VOLUMES VERSUS CHARGE YIELD

Figure B.41 (sheet 2 of 2).

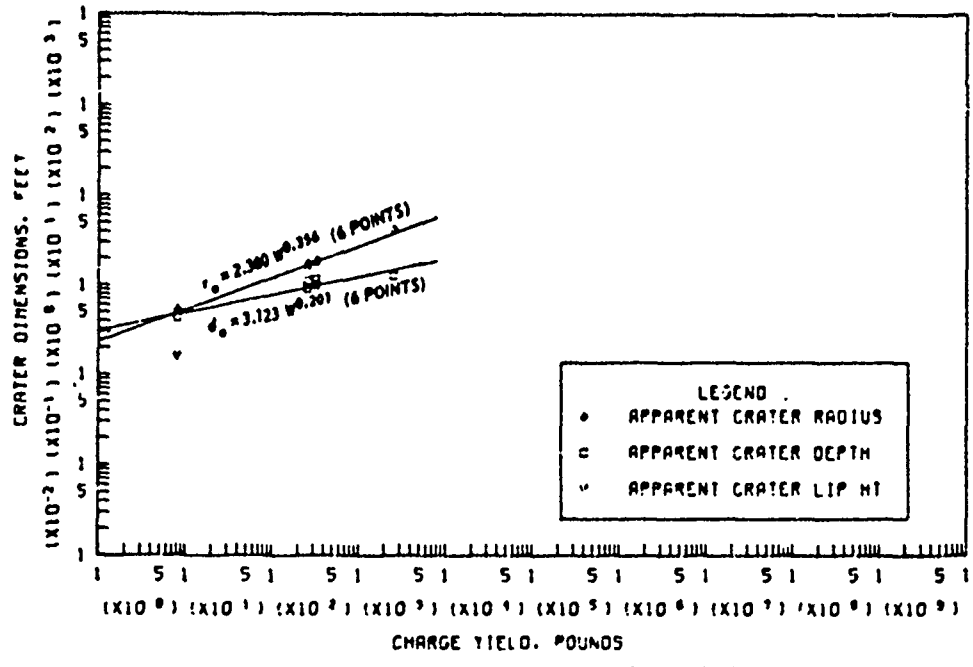

a. APPARENT CRATER DIMENSIONS VERSUS CHARGE YIELD

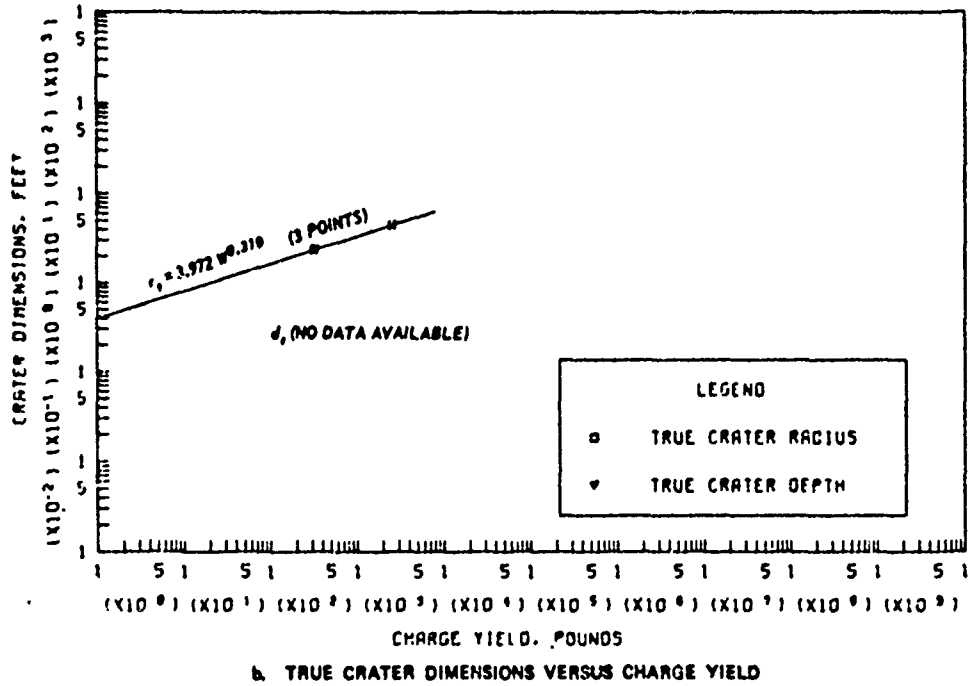

b. TRUE CRATER DIMENSIONS VERSUS CHARGE YIELD

Figure B.42 Dimensions of craters in wet clay for $-0.50 \leq Z < -0.20$ ft/lb$^{1/3}$, Category 6 (sheet 1 of 2).

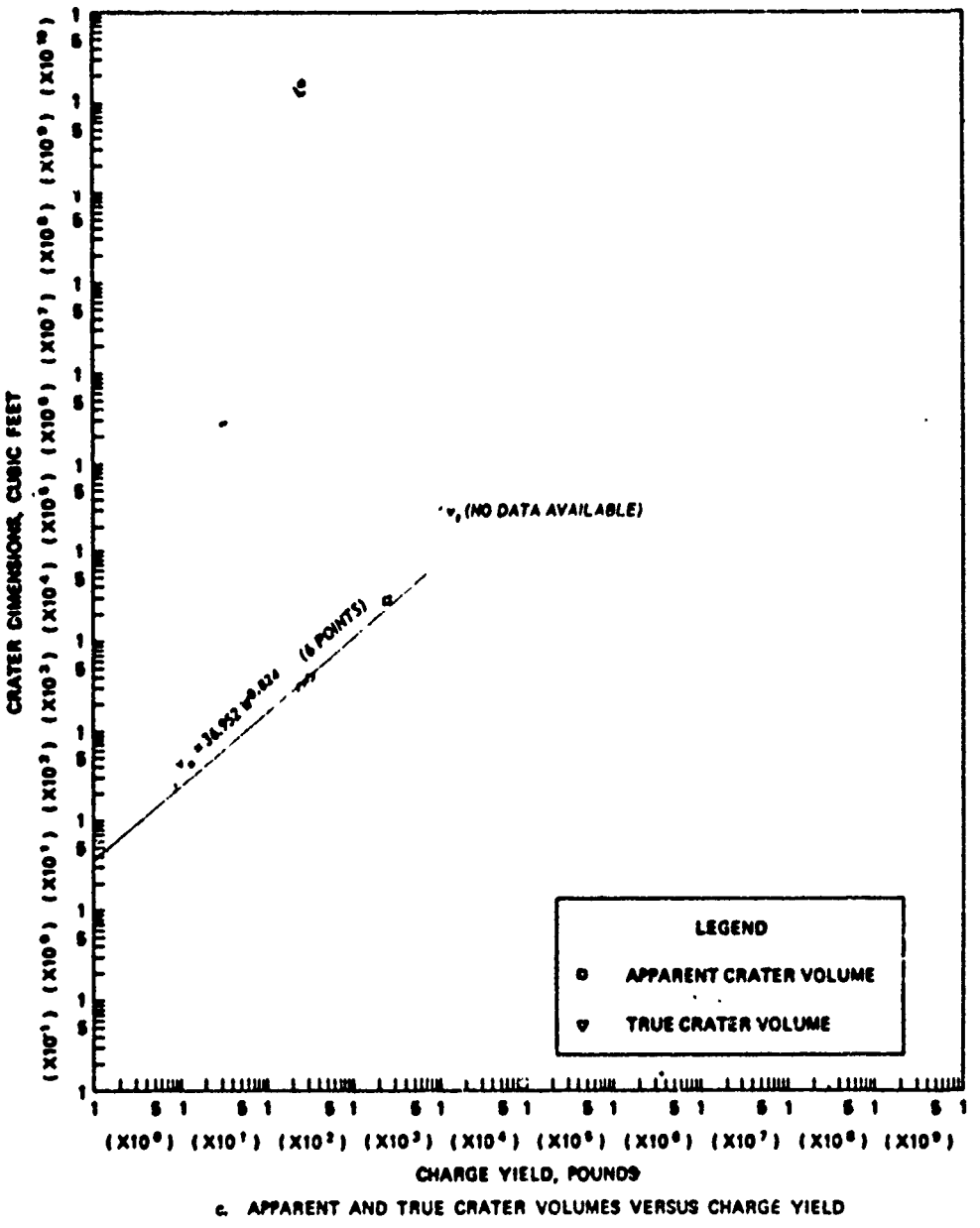

c. APPARENT AND TRUE CRATER VOLUMES VERSUS CHARGE YIELD

Figure B.42 (sheet 2 of 2).

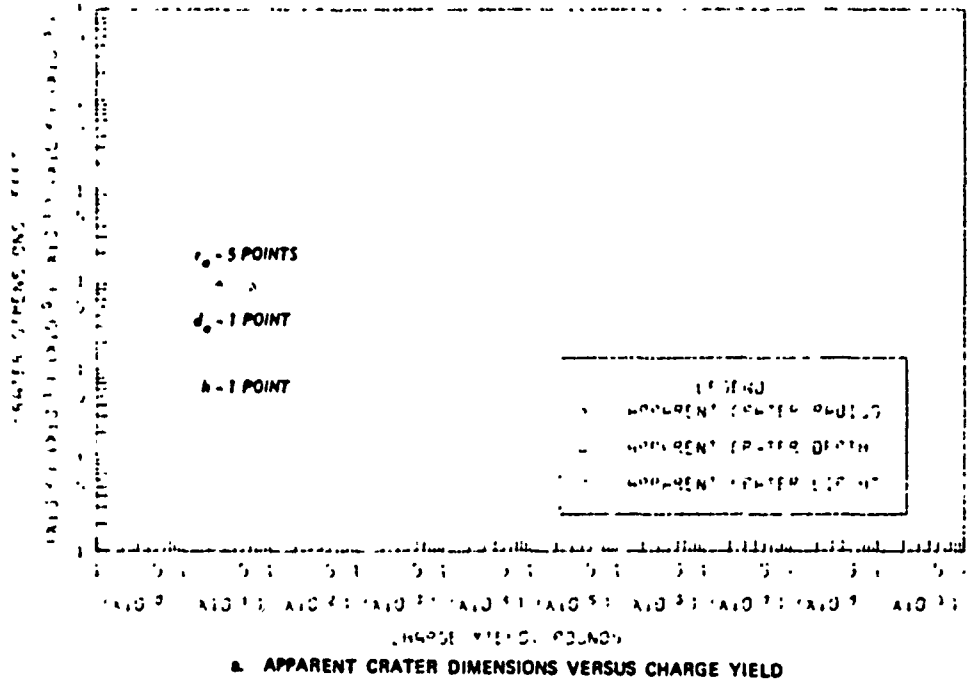

a. APPARENT CRATER DIMENSIONS VERSUS CHARGE YIELD

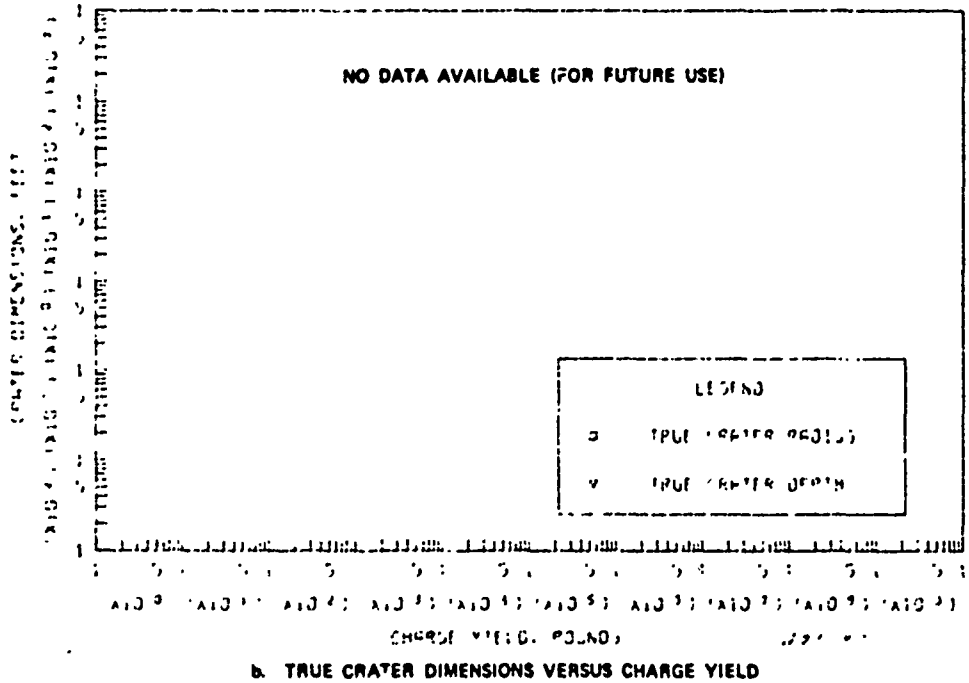

b. TRUE CRATER DIMENSIONS VERSUS CHARGE YIELD

Figure B.43 Dimensions of craters in wet clay for $-0.90 \leq Z < -0.50$ ft/lb$^{1/3}$, Category 7 (sheet 1 of 2).

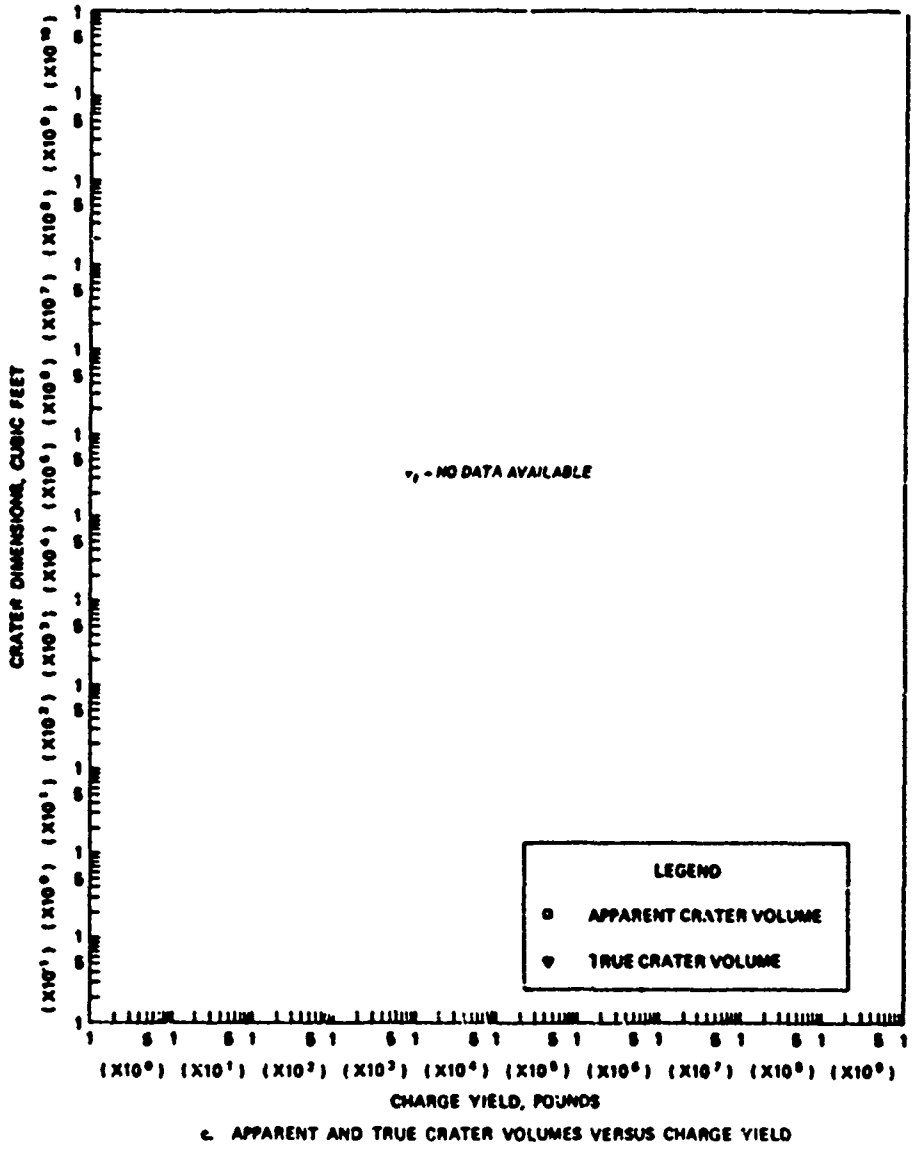

c. APPARENT AND TRUE CRATER VOLUMES VERSUS CHARGE YIELD

Figure B.43 (sheet 2 of 2).

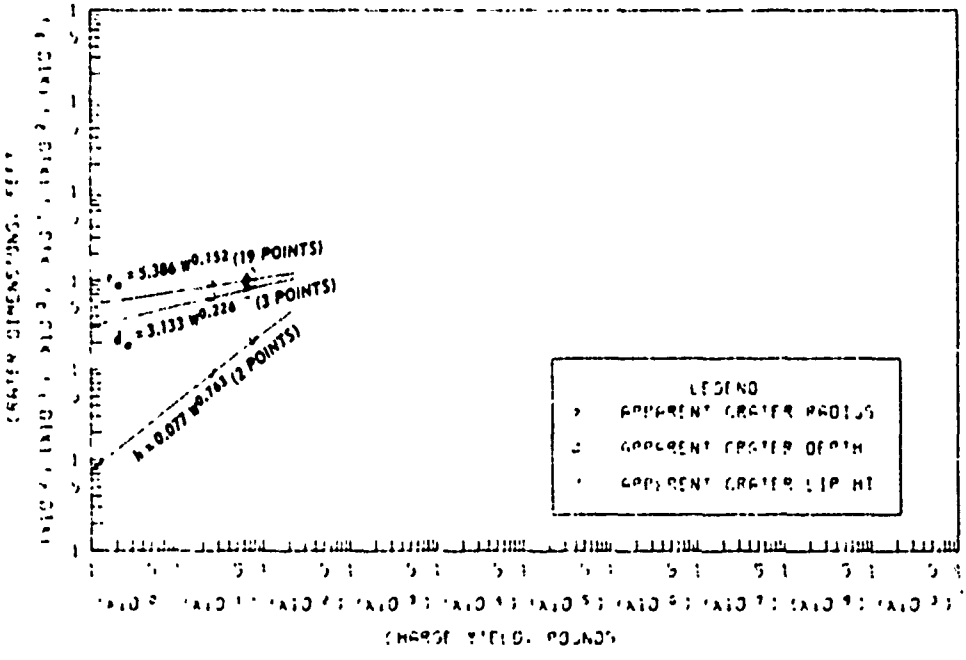

a. APPARENT CRATER DIMENSIONS VERSUS CHARGE YIELD

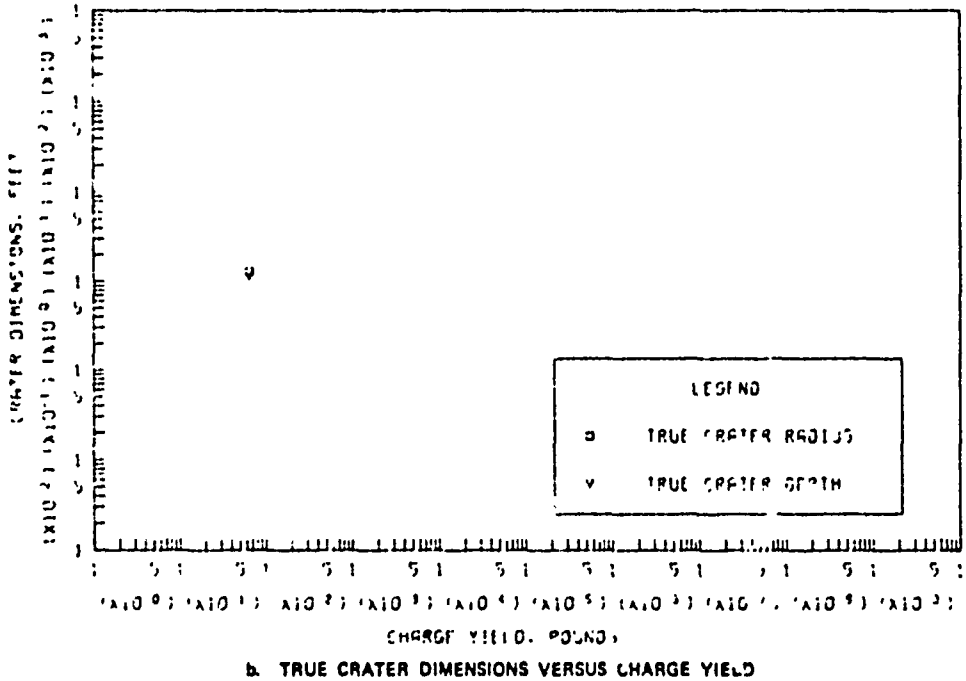

b. TRUE CRATER DIMENSIONS VERSUS CHARGE YIELD

Figure B.44 Dimensions of craters in wet clay for $-1.10 \leq Z < -0.90$ ft/lb$^{1/3}$, Category 8 (sheet 1 of 2).

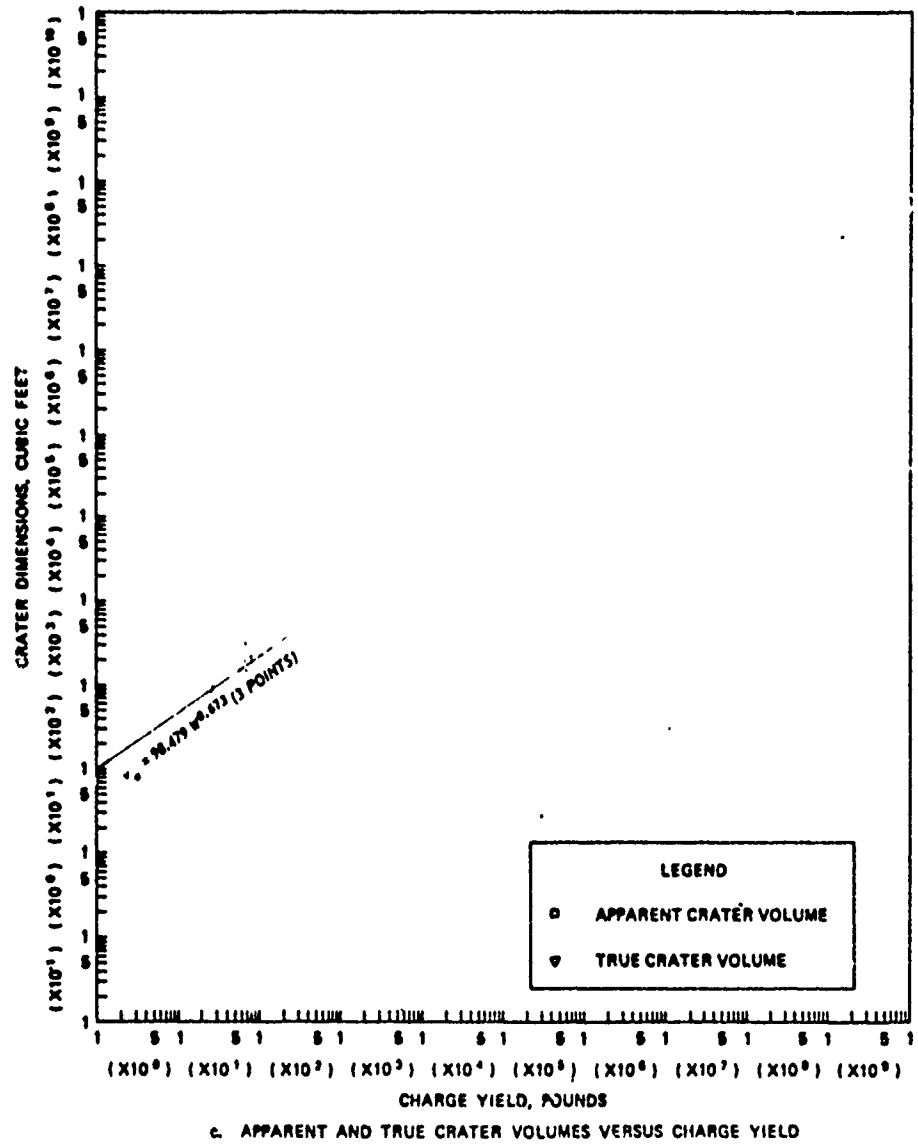

c. APPARENT AND TRUE CRATER VOLUMES VERSUS CHARGE YIELD

Figure B.44 (sheet 2 of 2).

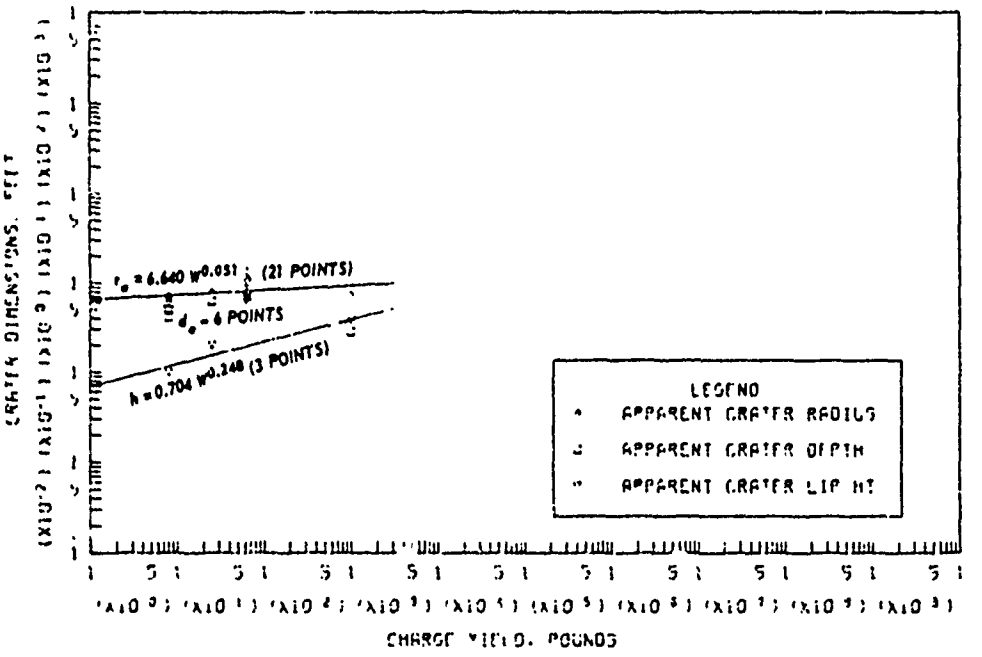

a. APPARENT CRATER DIMENSIONS VERSUS CHARGE YIELD

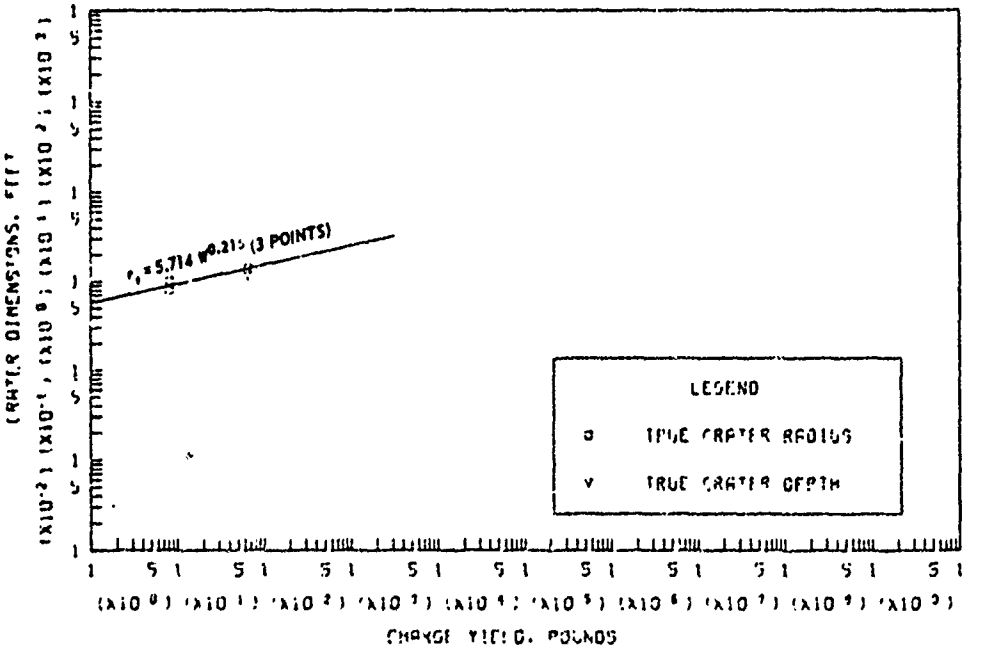

b. TRUE CRATER DIMENSIONS VERSUS CHARGE YIELD

Figure B.45 Dimensions of craters in wet clay for $-2.00 \leq Z < -1.10$ ft/lb$^{1/3}$, Category 9 (sheet 1 of 2).

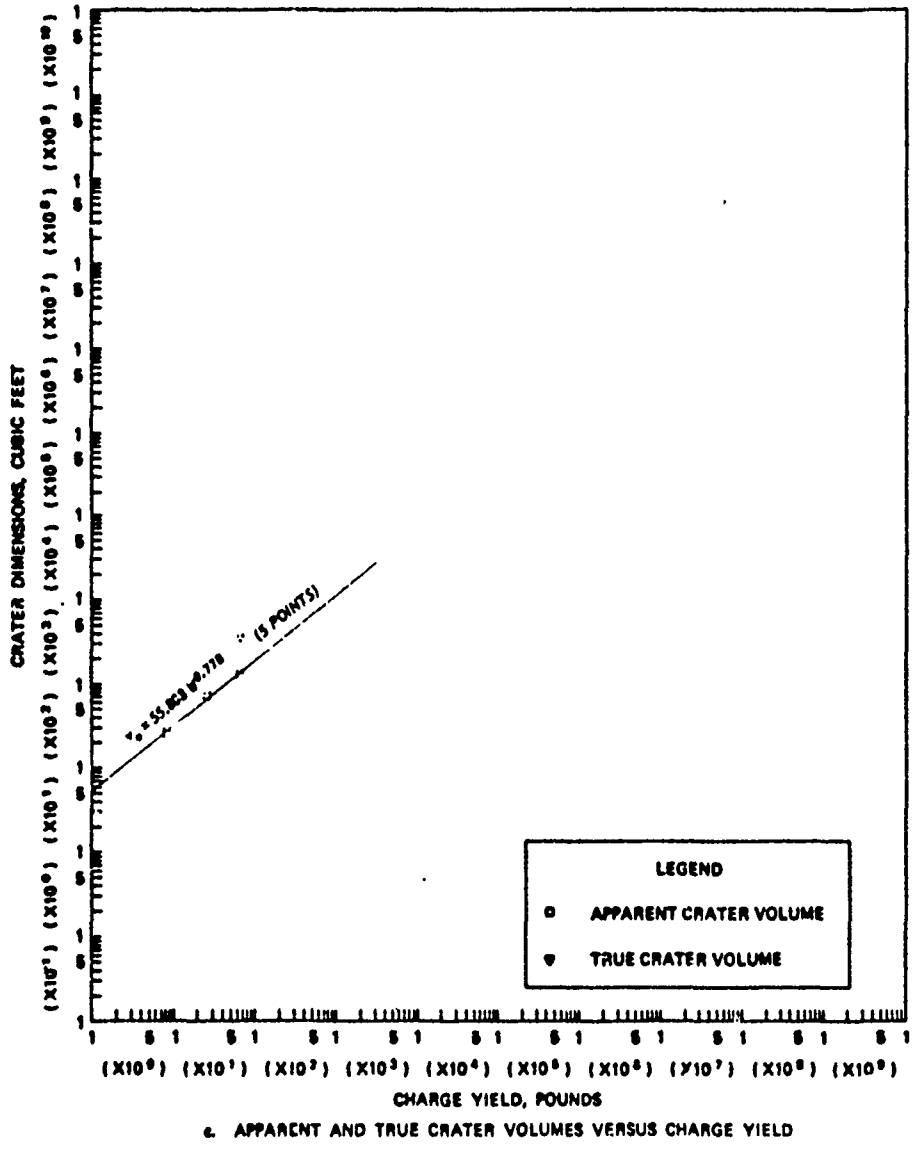

c. APPARENT AND TRUE CRATER VOLUMES VERSUS CHARGE YIELD

Figure B.45 (sheet 2 of 2).

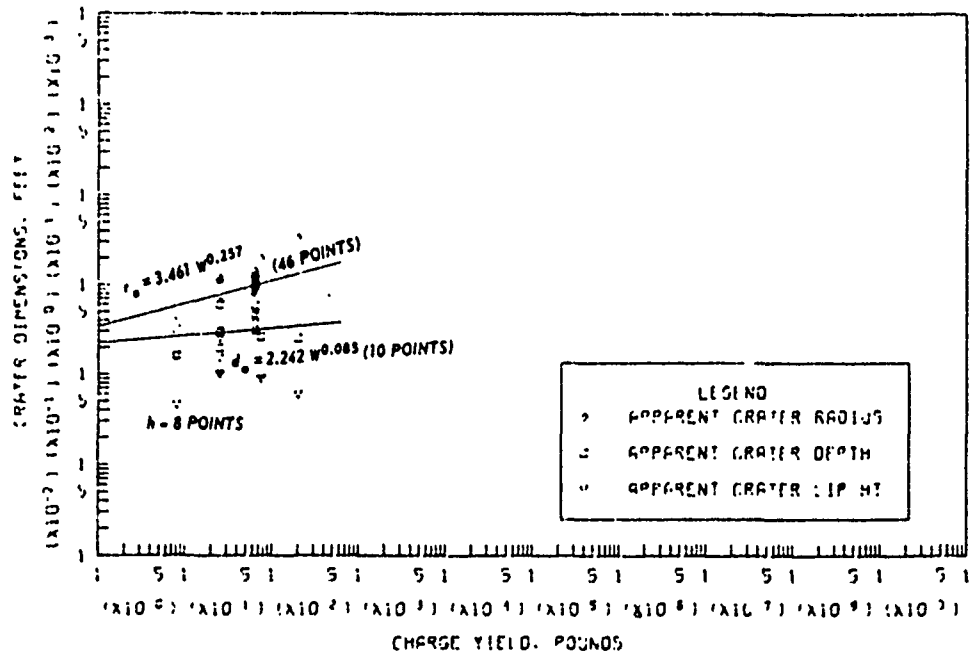

a. APPARENT CRATER DIMENSIONS VERSUS CHARGE YIELD

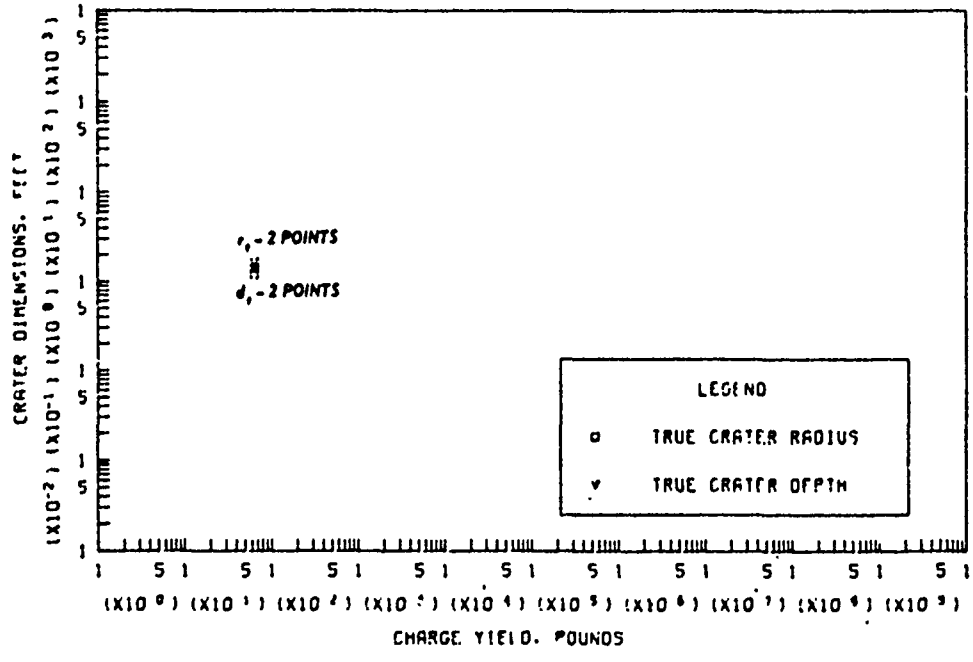

b. TRUE CRATER DIMENSIONS VERSUS CHARGE YIELD

Figure B.46 Dimensions of craters in wet clay for $Z < -2.00$ ft/lb$^{1/3}$, Category 10 (sheet 1 of 2).

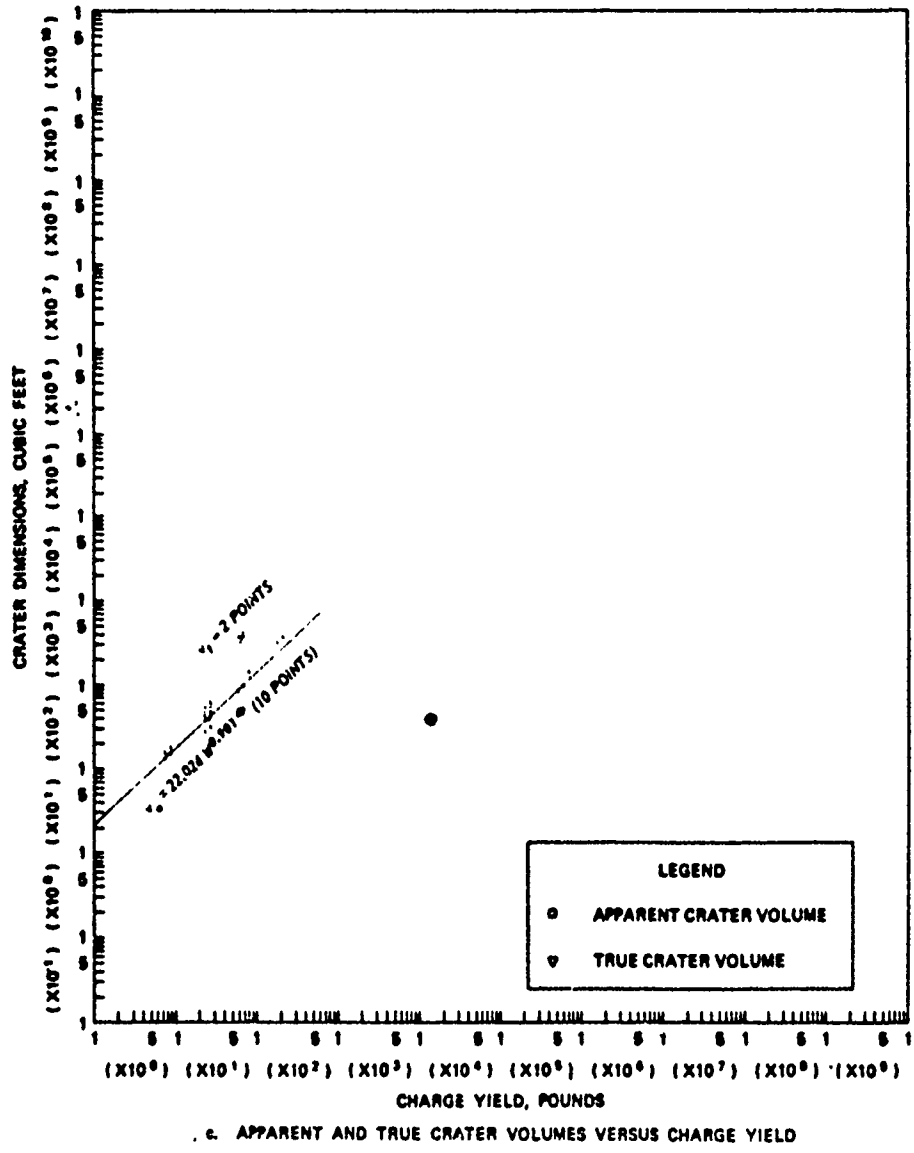

c. APPARENT AND TRUE CRATER VOLUMES VERSUS CHARGE YIELD

Figure B.46 (sheet 2 of 2).

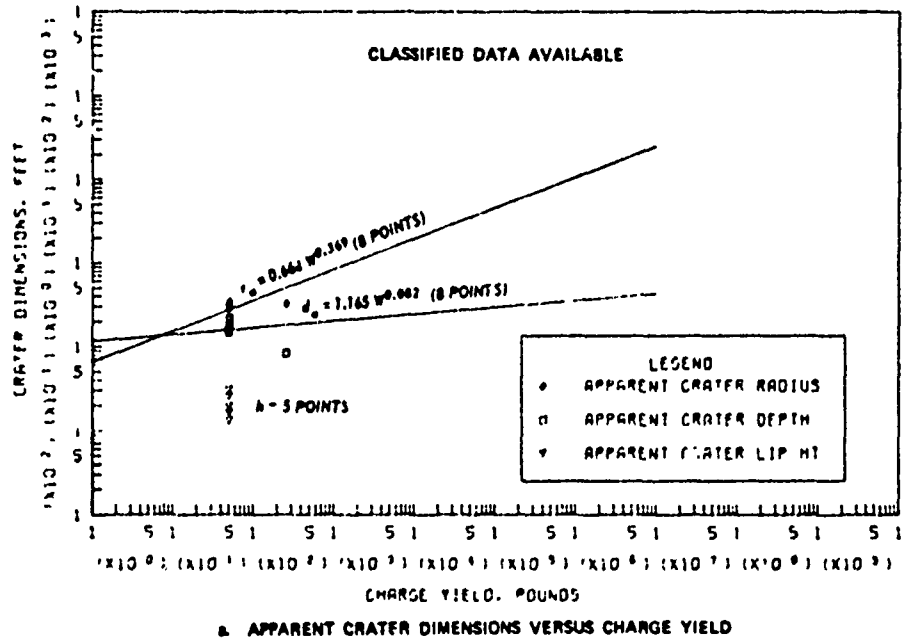

a. APPARENT CRATER DIMENSIONS VERSUS CHARGE YIELD

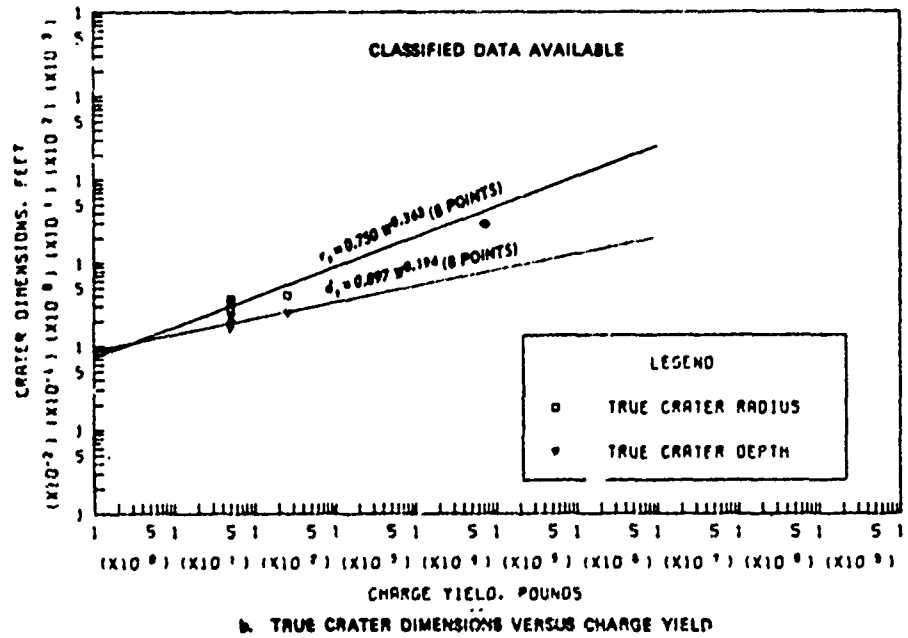

b. TRUE CRATER DIMENSIONS VERSUS CHARGE YIELD

Figure B.47 Dimensions of craters in moist loess and moist lacustrine silt for $0.05 \leq Z < 0.20$ ft/lb$^{1/3}$, Category 3 (sheet 1 of 2).

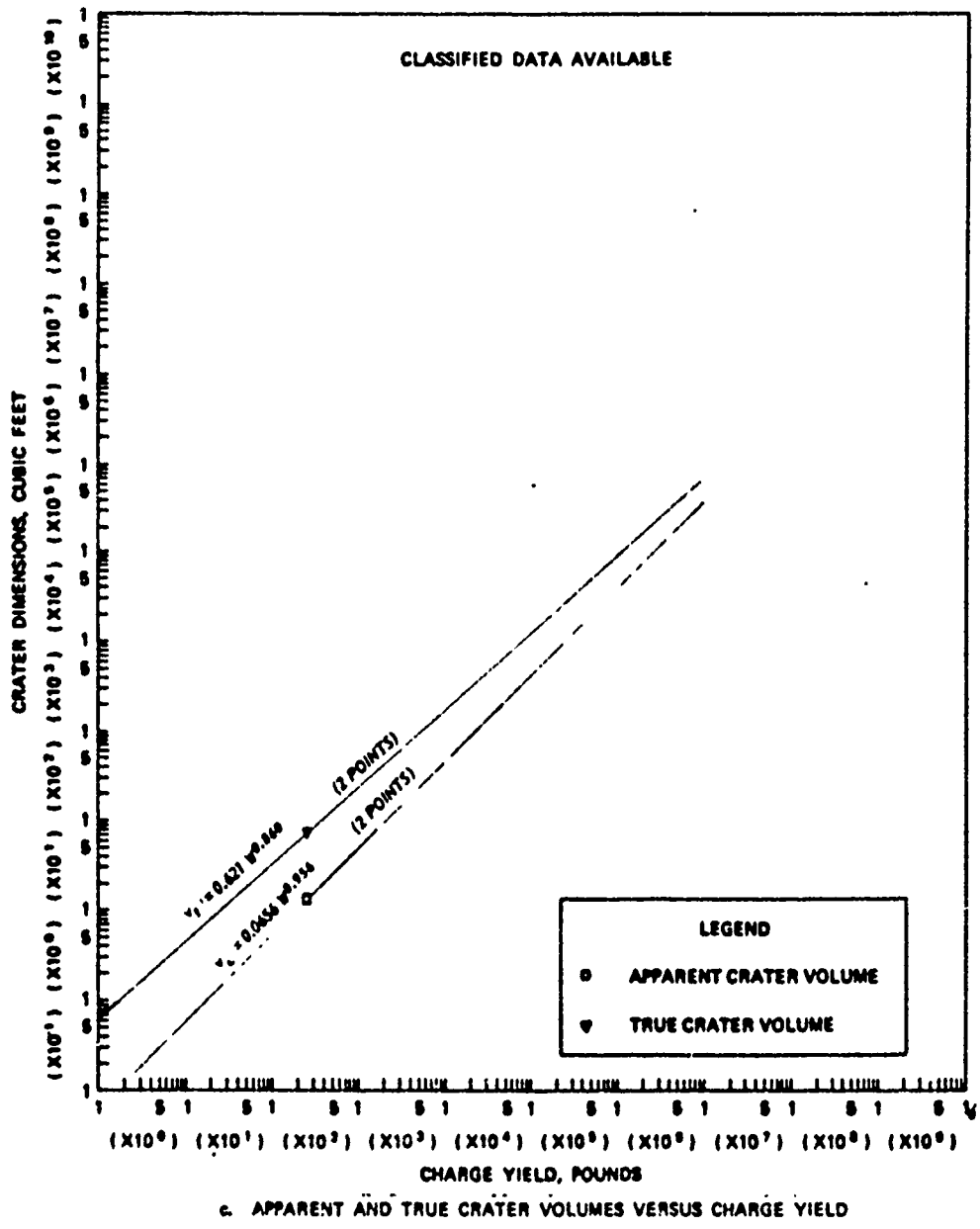

c. APPARENT AND TRUE CRATER VOLUMES VERSUS CHARGE YIELD

Figure B.47 (sheet 2 of 2).

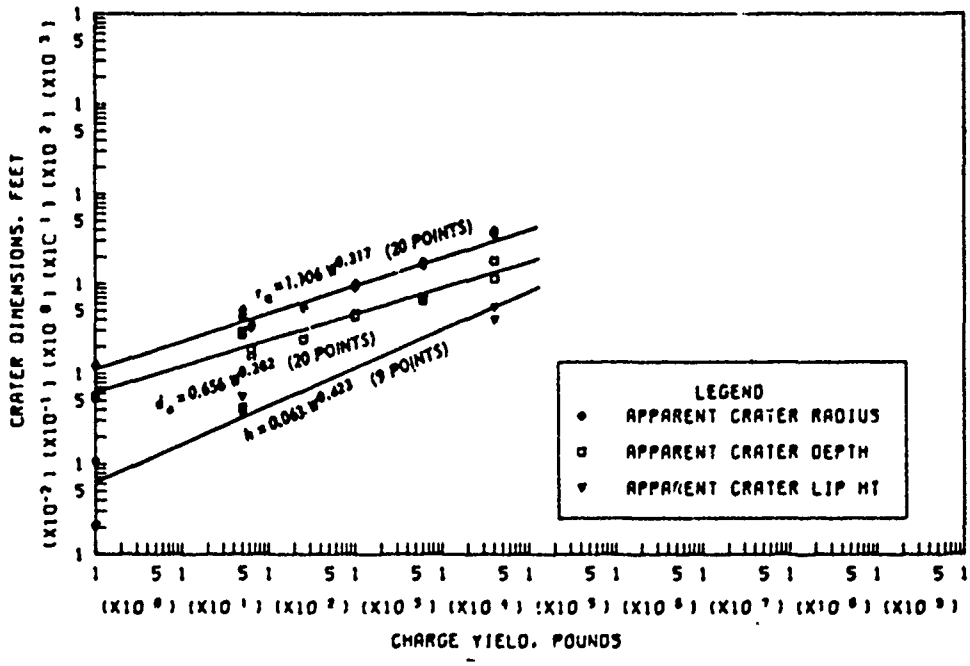

a. APPARENT CRATER DIMENSIONS VERSUS CHARGE YIELD

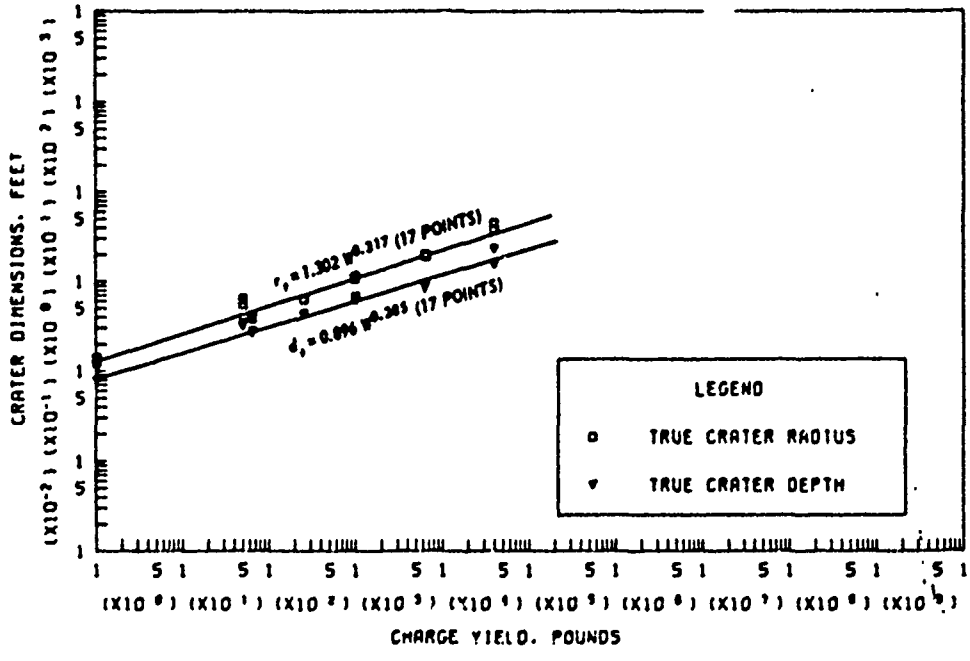

b. TRUE CRATER DIMENSIONS VERSUS CHARGE YIELD

Figure B.48 Dimensions of craters in moist loess and moist lacustrine silt for $-0.05 \leq Z < 0.05$ ft/lb$^{1/3}$, Category 4 (sheet 1 of 2)

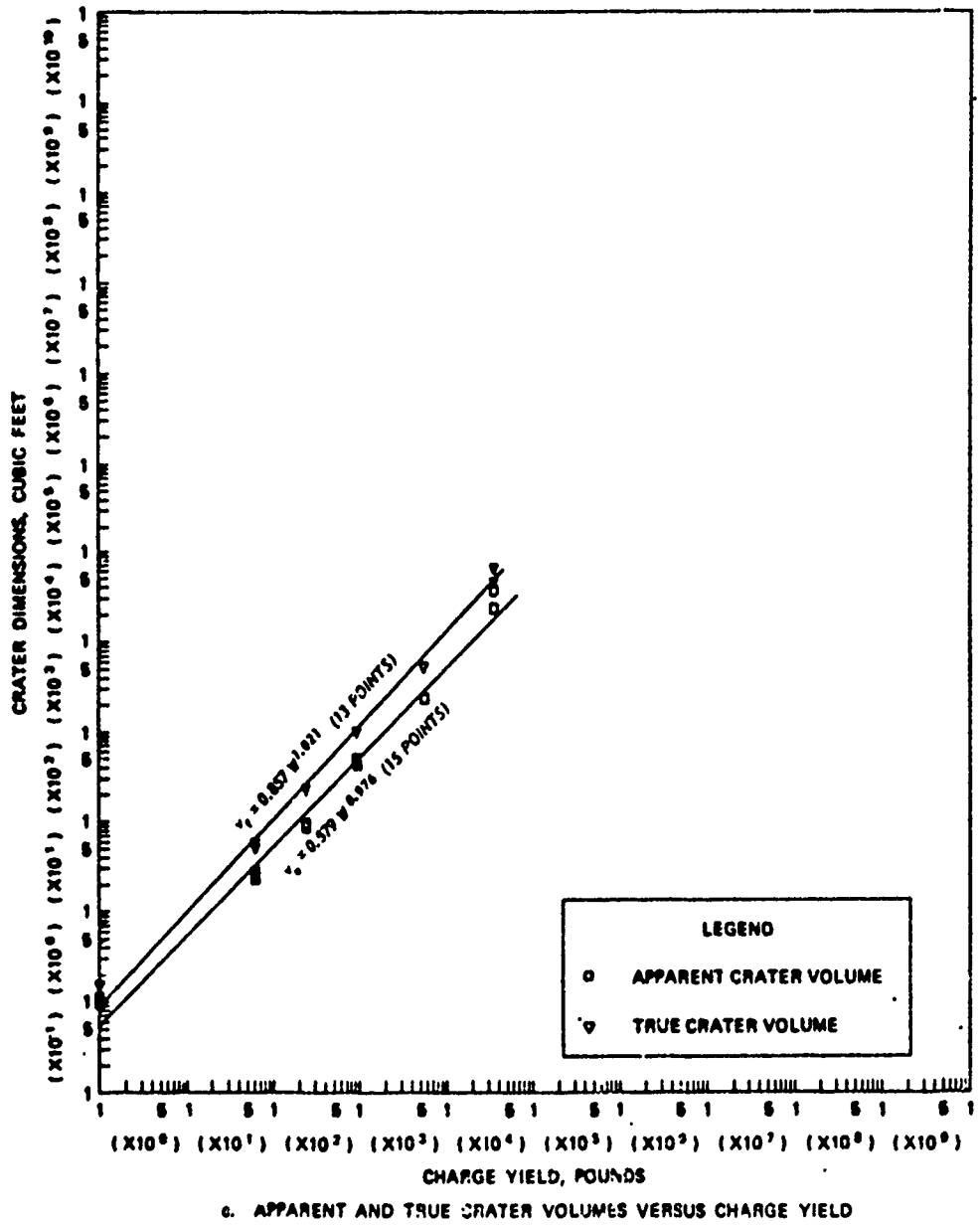

c. APPARENT AND TRUE CRATER VOLUMES VERSUS CHARGE YIELD

Figure B.48 (sheet 2 of 2).

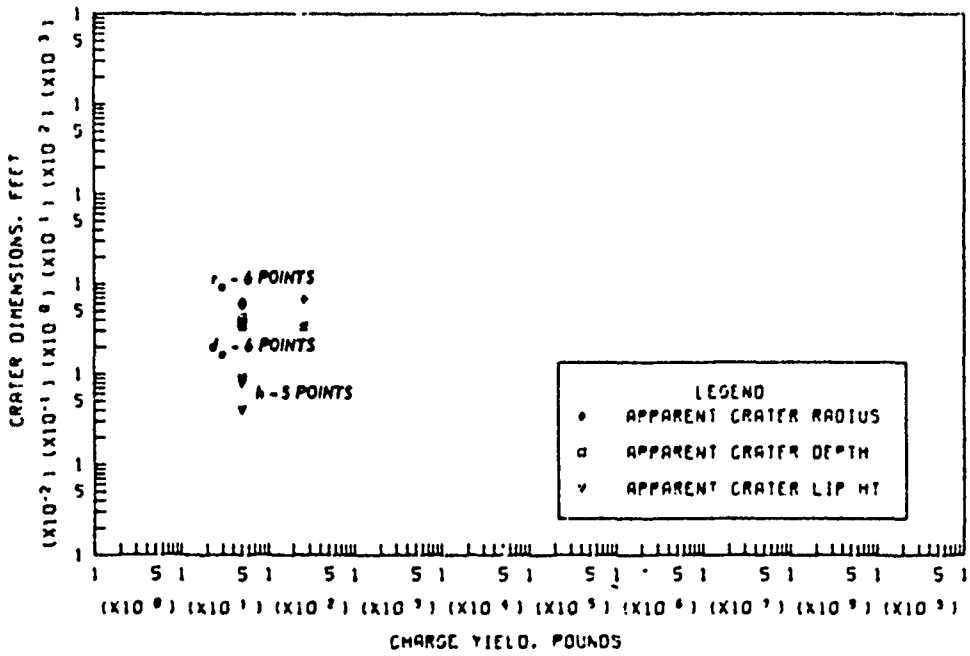

a. APPARENT CRATER DIMENSIONS VERSUS CHARGE YIELD

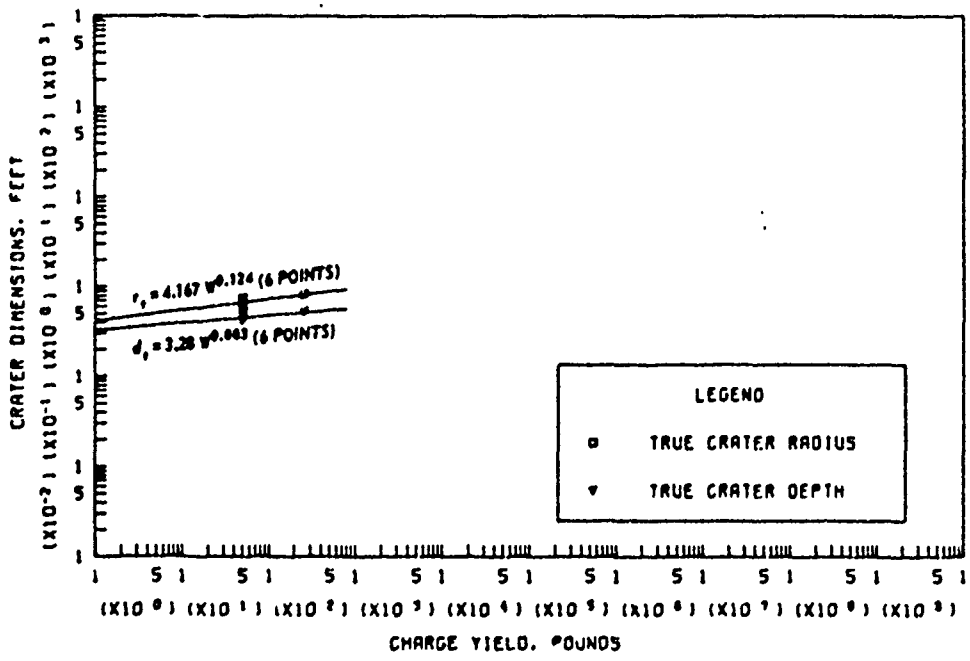

b. TRUE CRATER DIMENSIONS VERSUS CHARGE YIELD

Figure B.49 Dimensions of craters in moist loess and moist lacustrine silt for $-0.20 \leq Z < -0.05$ ft/lb$^{1/3}$, Category 5 (sheet 1 of 2).

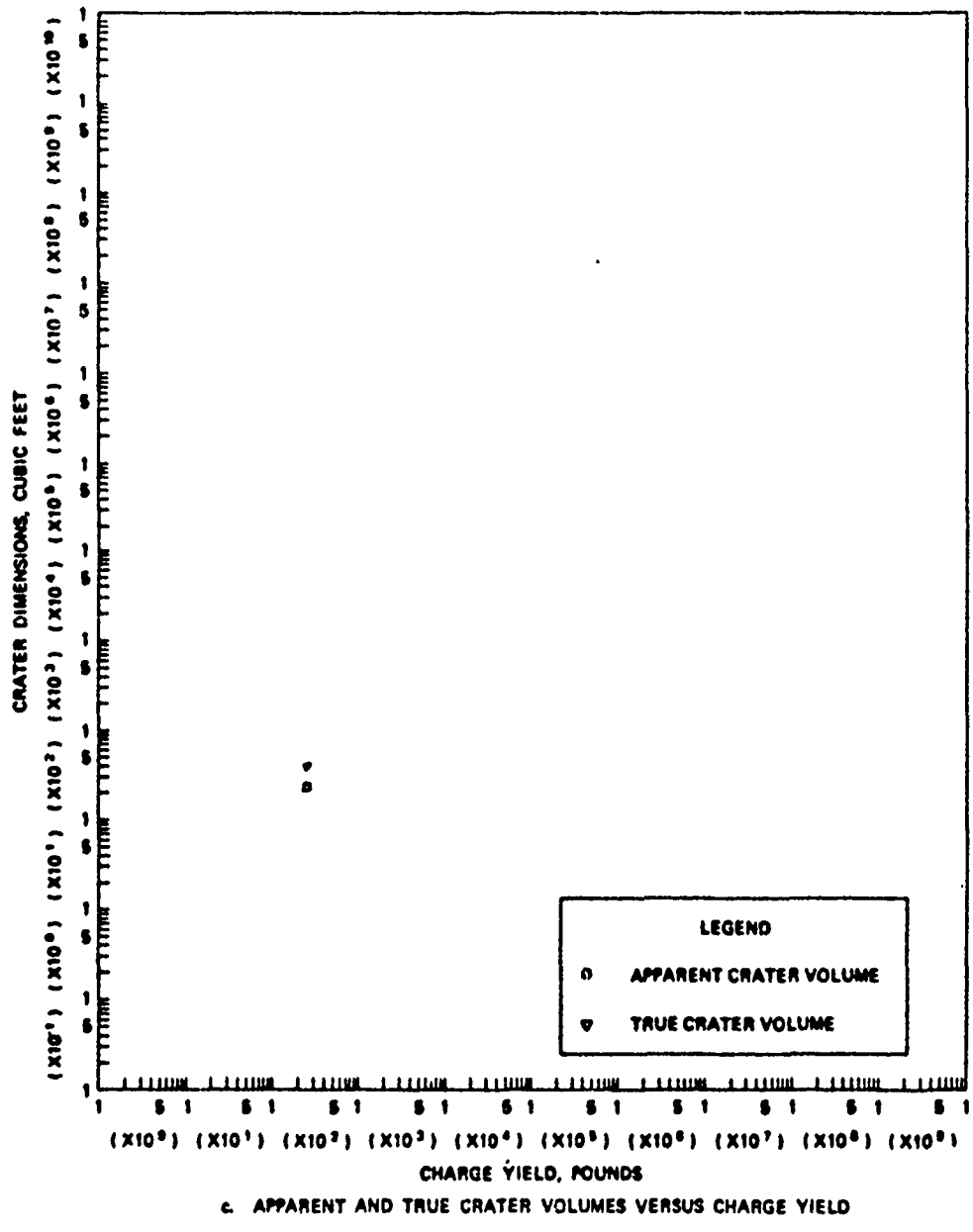

c. APPARENT AND TRUE CRATER VOLUMES VERSUS CHARGE YIELD

Figure B.49 (sheet 2 of 2).

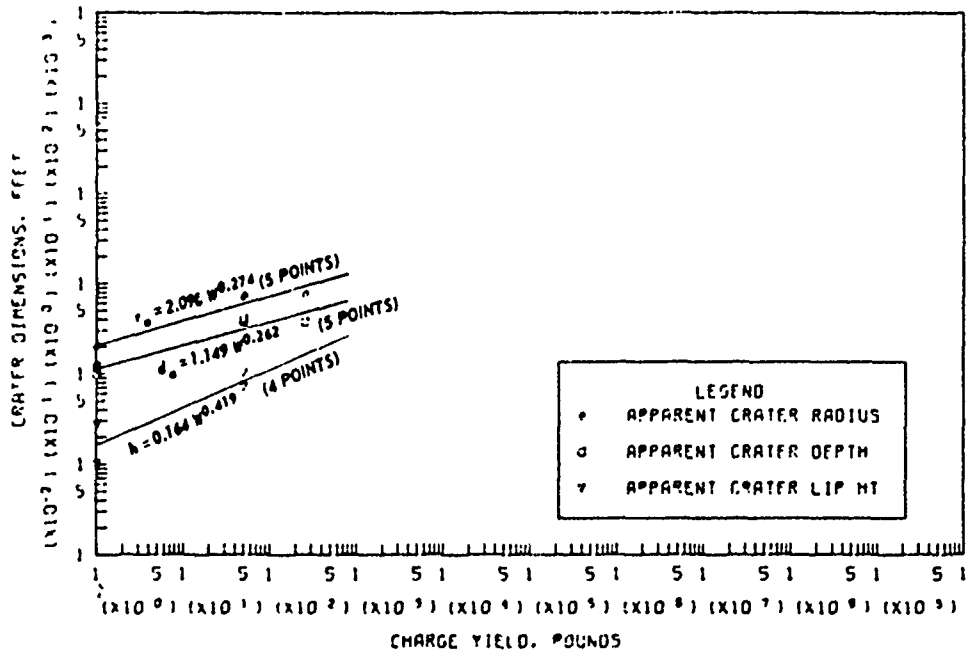

a. APPARENT CRATER DIMENSIONS VERSUS CHARGE YIELD

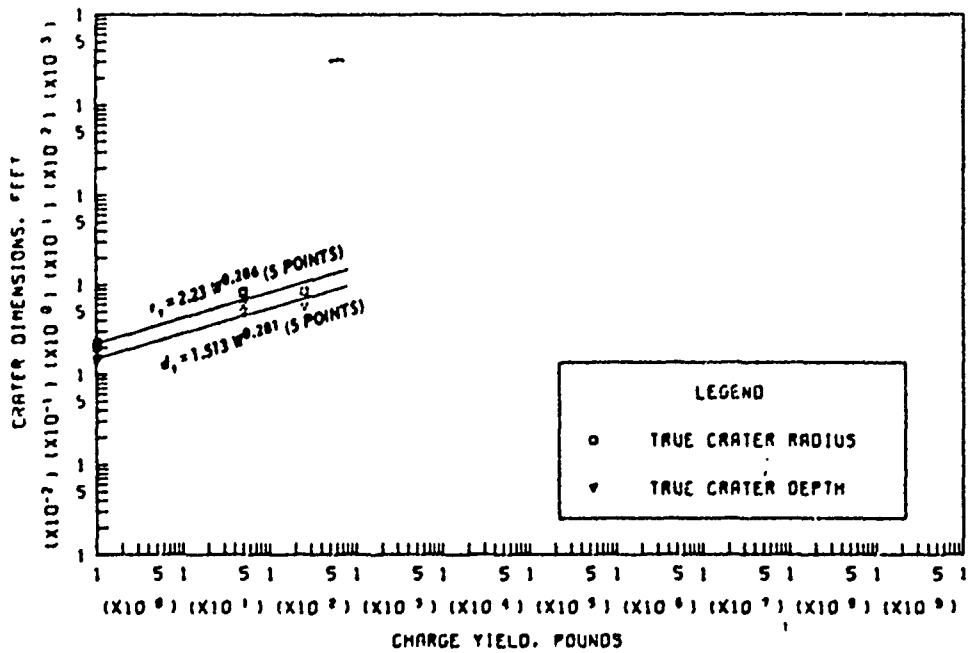

b. TRUE CRATER DIMENSIONS VERSUS CHARGE YIELD

Figure B.50 Dimensions of craters in moist loess and moist lacustrine silt for $-0.50 \leq Z < -0.20$ ft/lb$^{1/3}$, Category 6 (sheet 1 of 2).

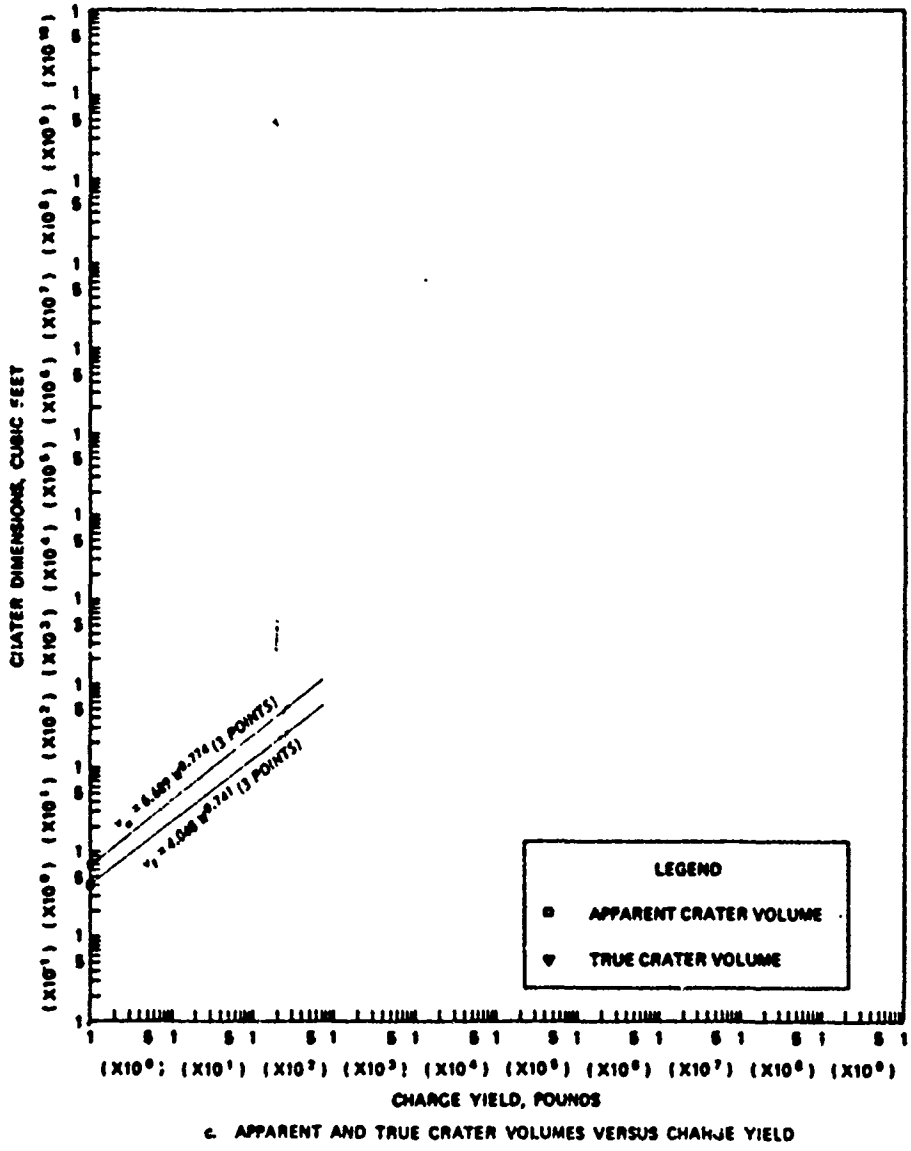

c. APPARENT AND TRUE CRATER VOLUMES VERSUS CHARGE YIELD

Figure B.50 (sheet 2 of 2).

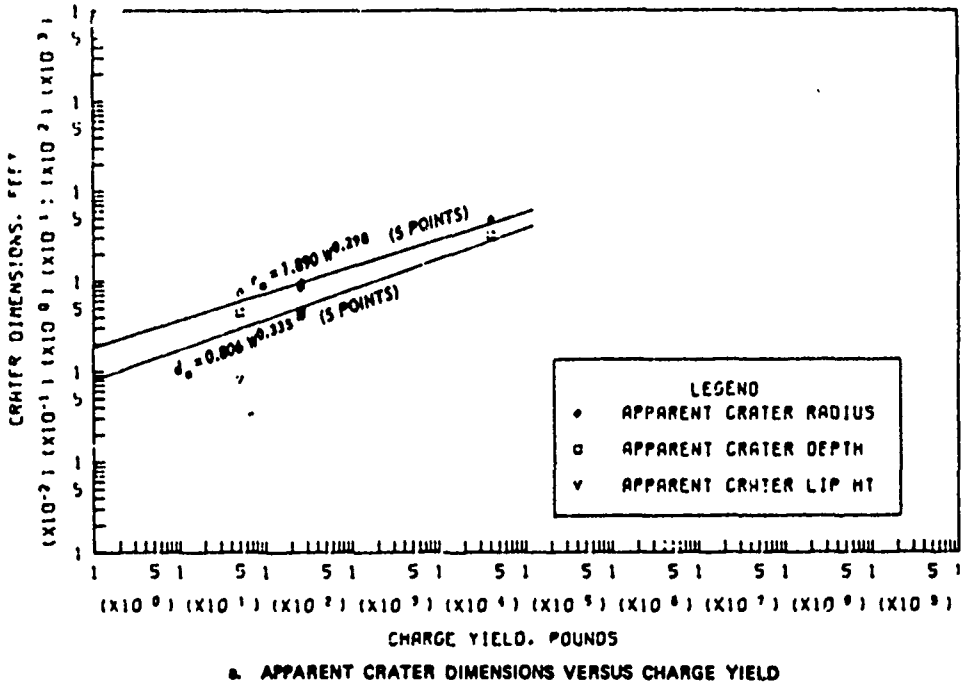

a. APPARENT CRATER DIMENSIONS VERSUS CHARGE YIELD

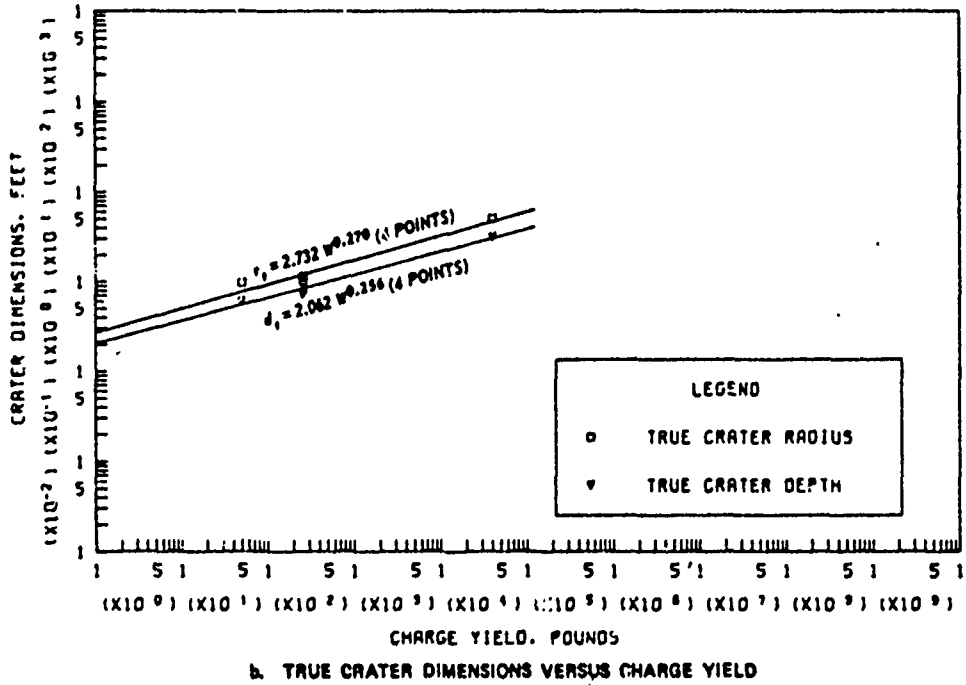

b. TRUE CRATER DIMENSIONS VERSUS CHARGE YIELD

Figure B.51 Dimensions of craters in moist loess and moist lacustrine silt for $-0.90 \leq Z < -0.50$ ft/lb$^{1/3}$, Category 7 (sheet 1 of 2).

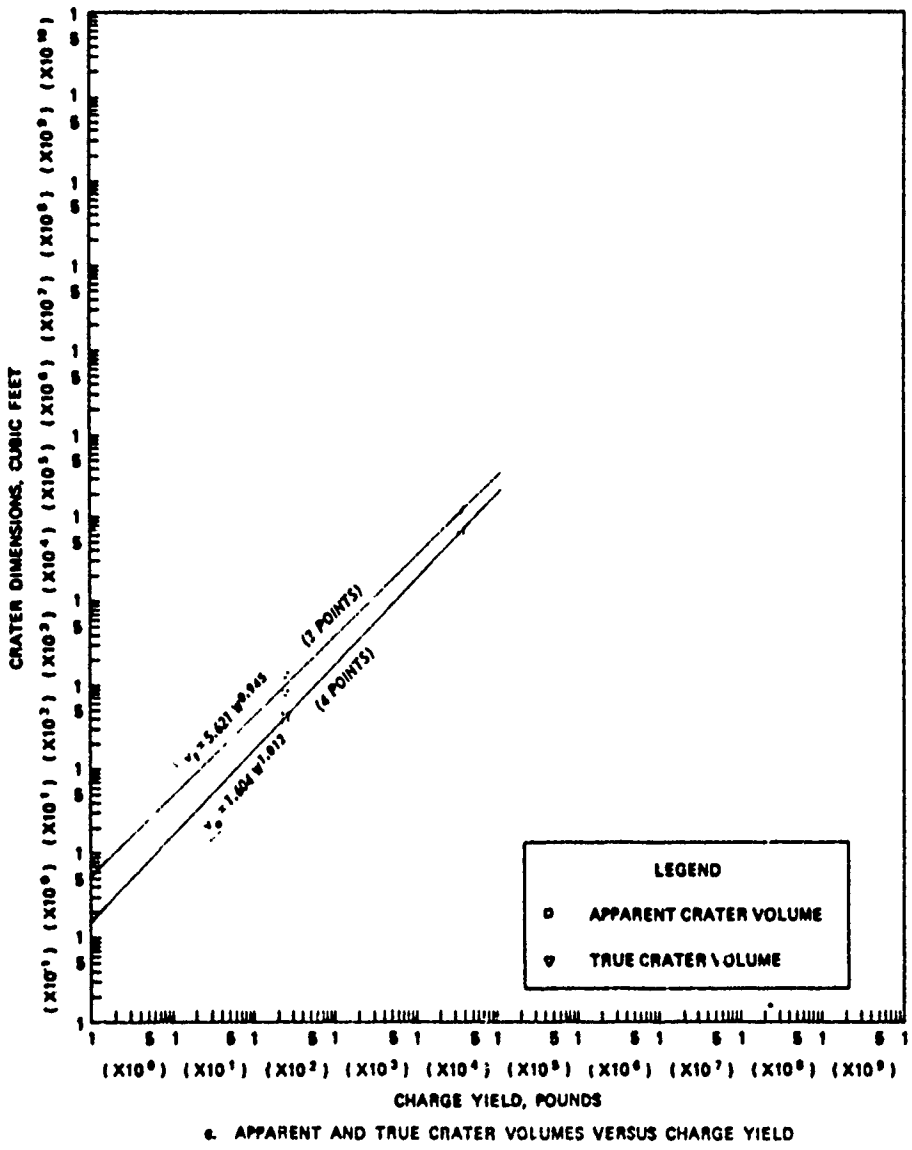

e. APPARENT AND TRUE CRATER VOLUMES VERSUS CHARGE YIELD

Figure B.51 (sheet 2 of 2).

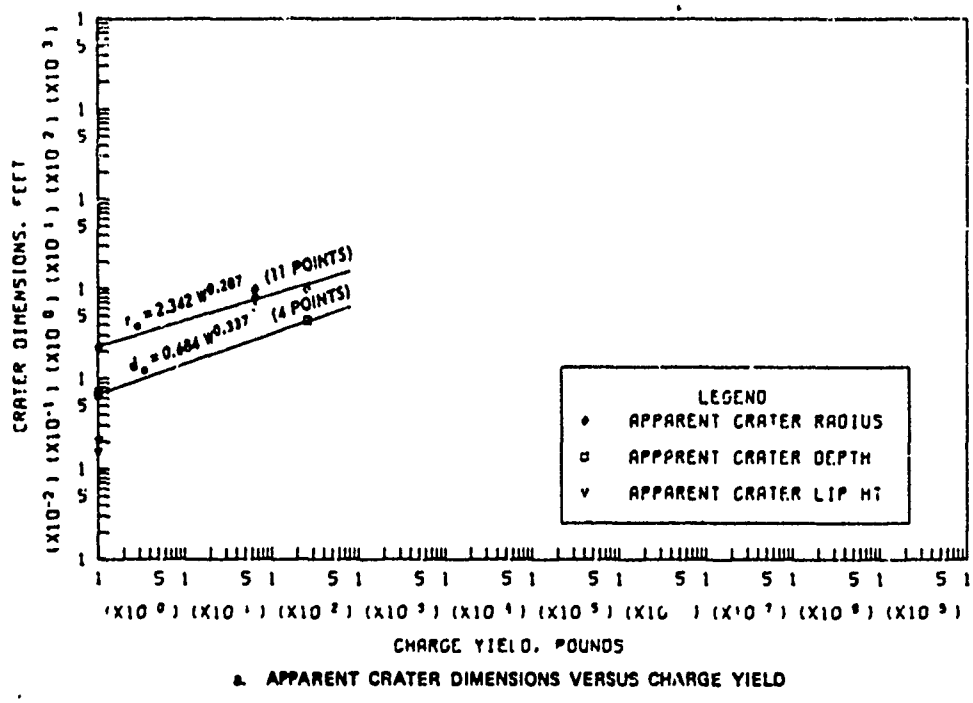

a. APPARENT CRATER DIMENSIONS VERSUS CHARGE YIELD

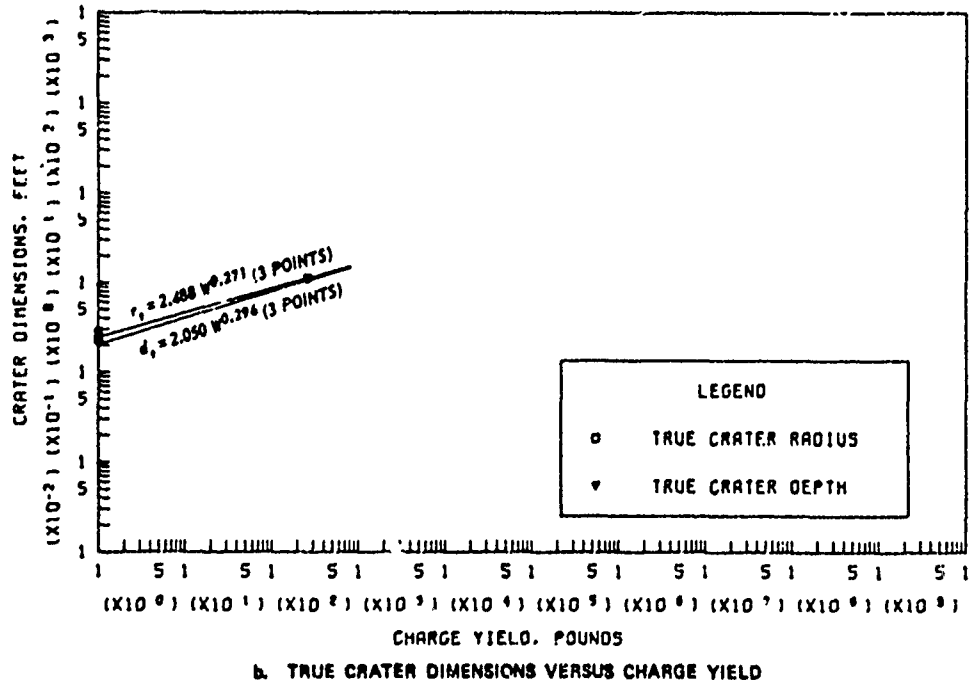

b. TRUE CRATER DIMENSIONS VERSUS CHARGE YIELD

Figure B.52 Dimensions of craters in moist loess and moist lacustrine silt for $-1.10 \leq Z < -0.90$ ft/lb$^{1/3}$, Category 8 (sheet 1 of 2).

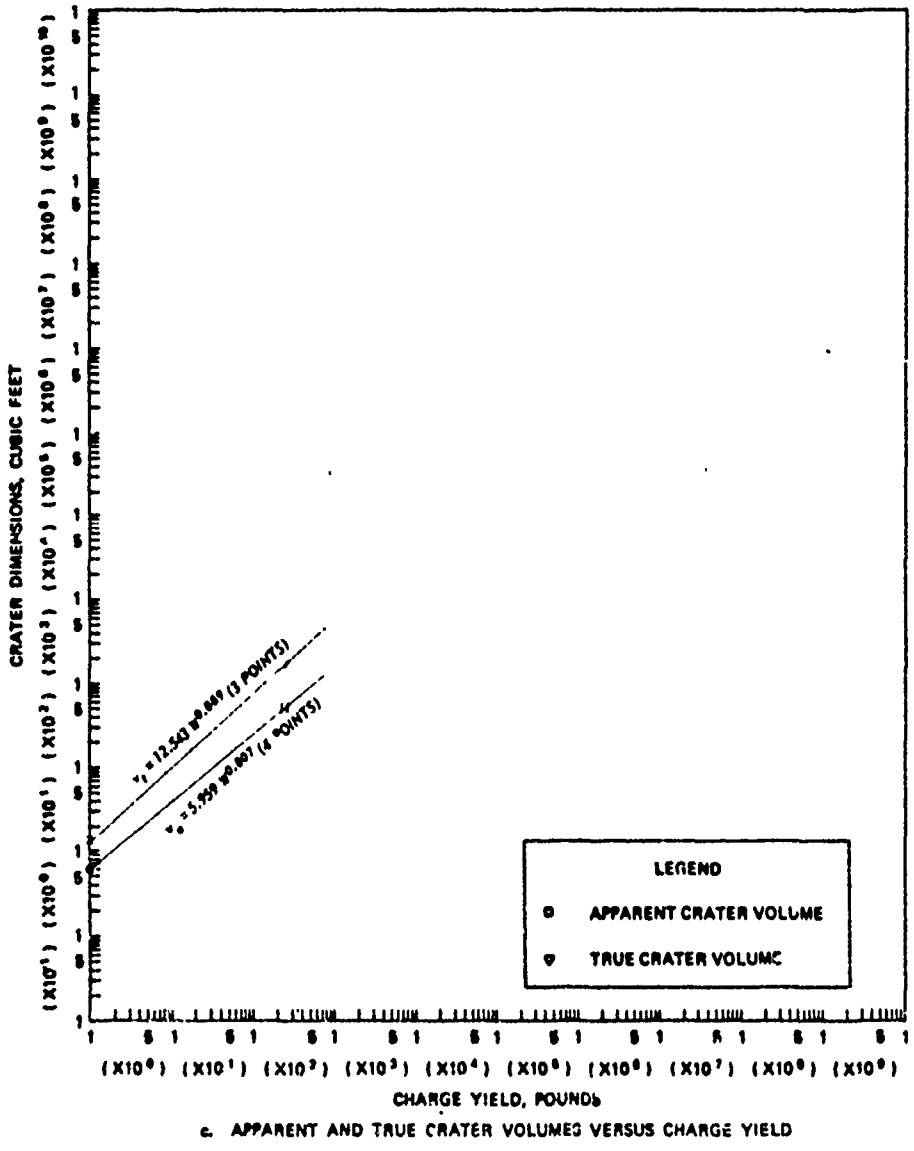

c. APPARENT AND TRUE CRATER VOLUMES VERSUS CHARGE YIELD

Figure B.52 (sheet 2 of 2).

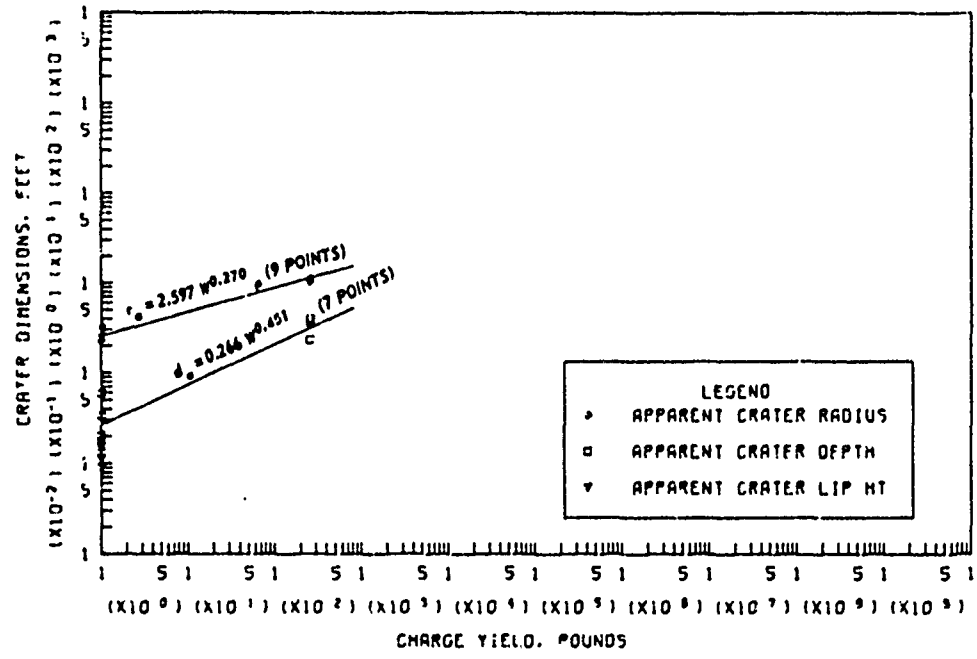

a. APPARENT CRATER DIMENSIONS VERSUS CHARGE YIELD

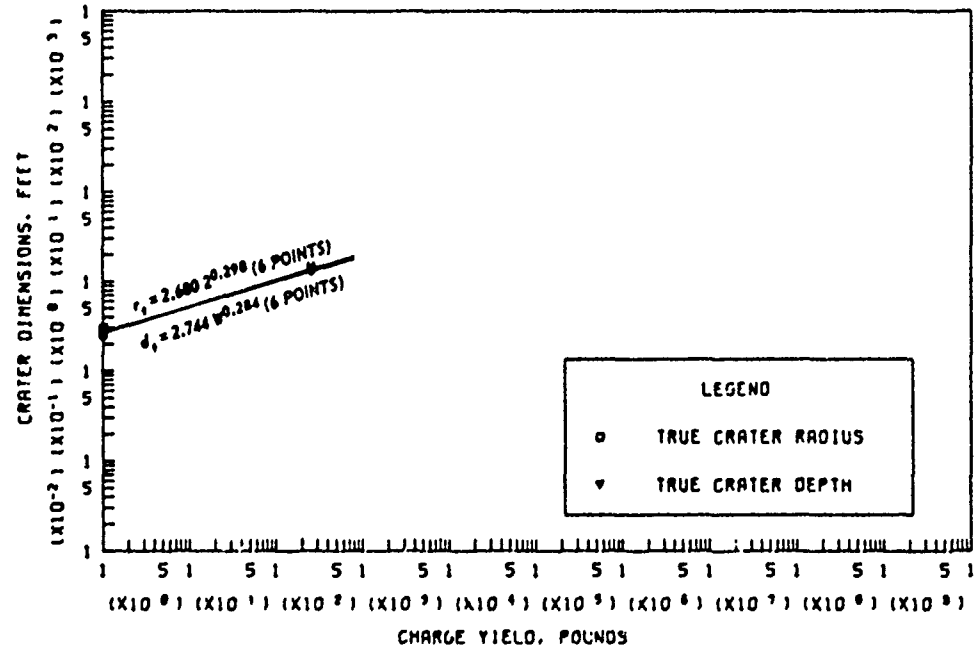

b. TRUE CRATER DIMENSIONS VERSUS CHARGE YIELD

Figure B.53 Dimensions of craters in moist loess and moist lacustrine silt for $-2.00 \leq Z < -1.10$ ft/lb$^{1/3}$, Category 9 (sheet 1 of 2).

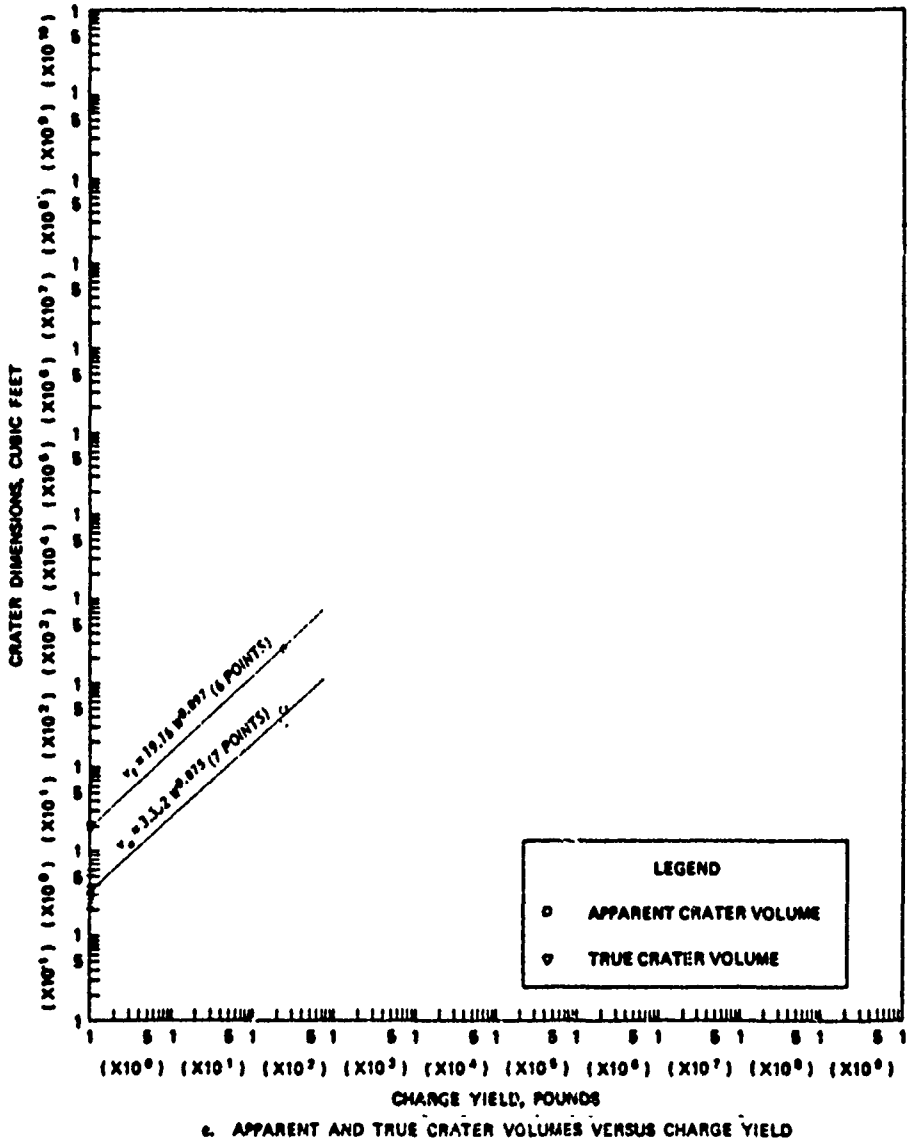

e. APPARENT AND TRUE CRATER VOLUMES VERSUS CHARGE YIELD

Figure B.53 (sheet 2 of 2).

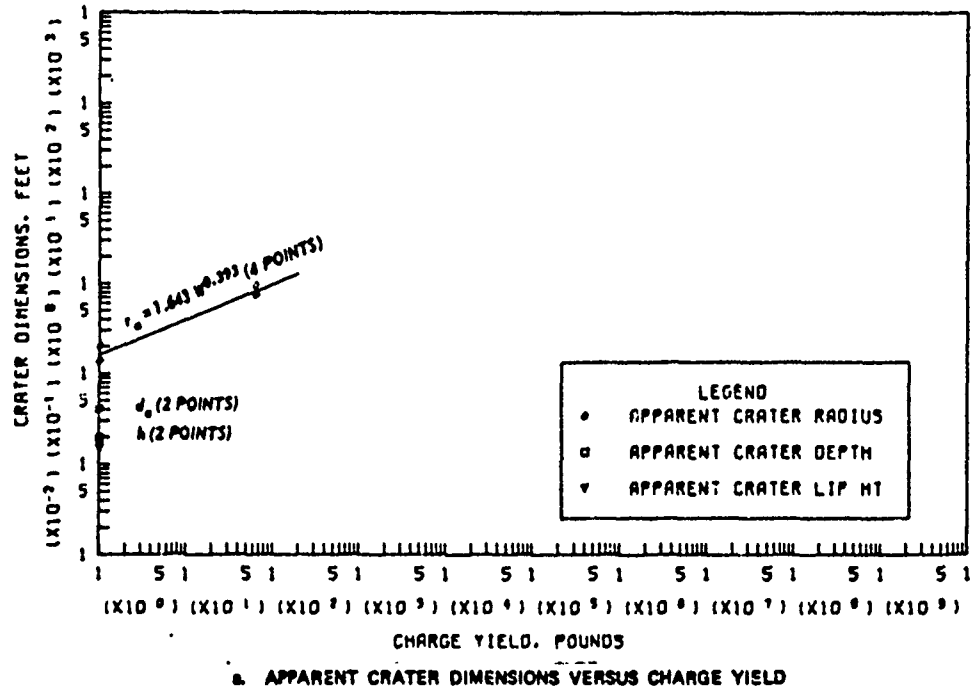

a. APPARENT CRATER DIMENSIONS VERSUS CHARGE YIELD

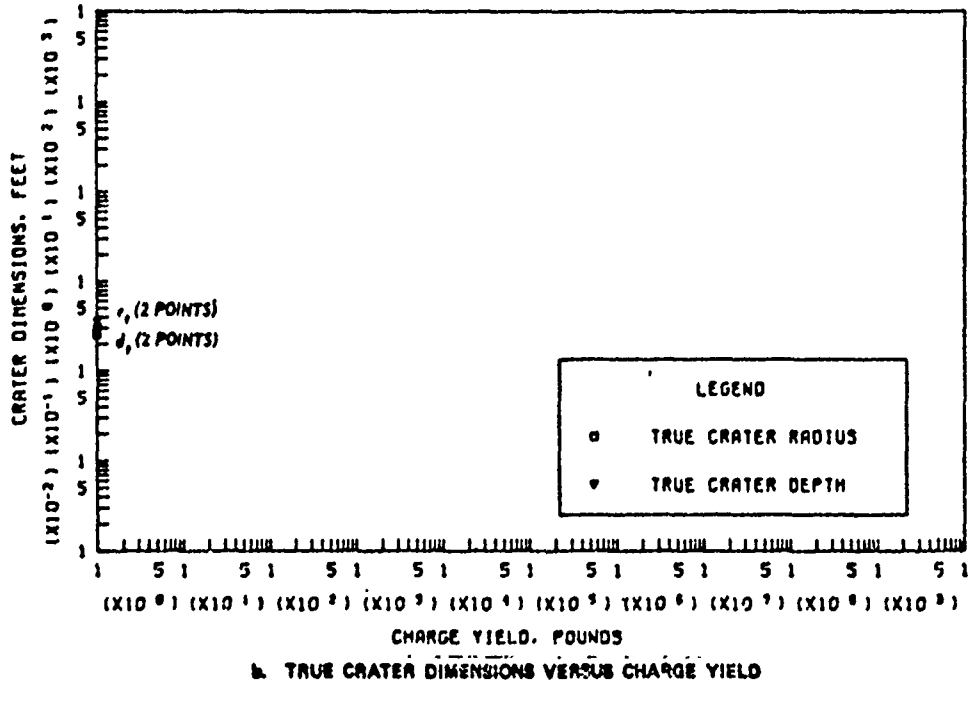

b. TRUE CRATER DIMENSIONS VERSUS CHARGE YIELD

Figure B.54 Dimensions of craters in moist loess and moist lacustrine silt for $Z < -2.00$ ft/lb$^{1/3}$, Category 10 (sheet 1 of 2).

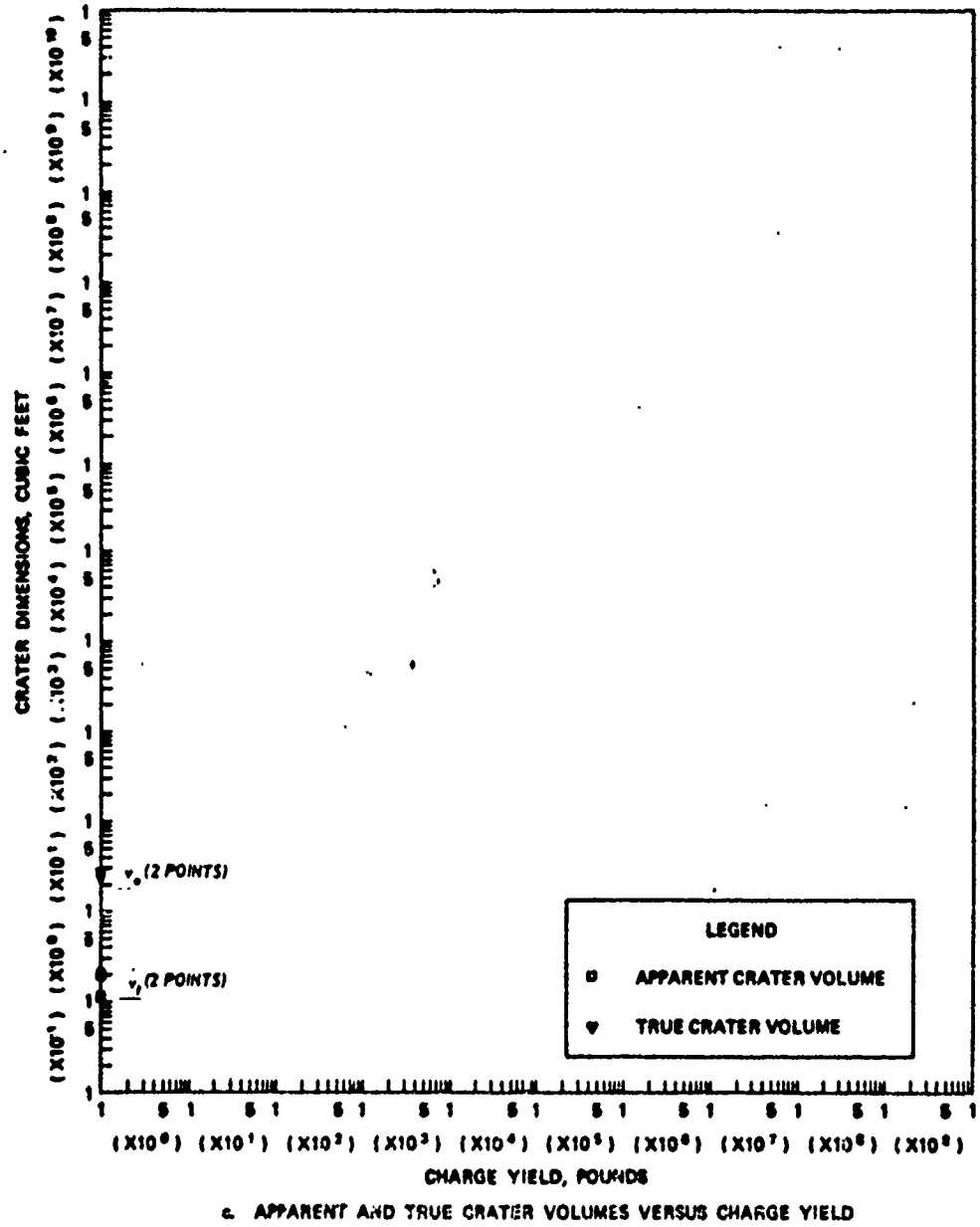

a. APPARENT AND TRUE CRATER VOLUMES VERSUS CHARGE YIELD

Figure B.54 (sheet 2 of 2).

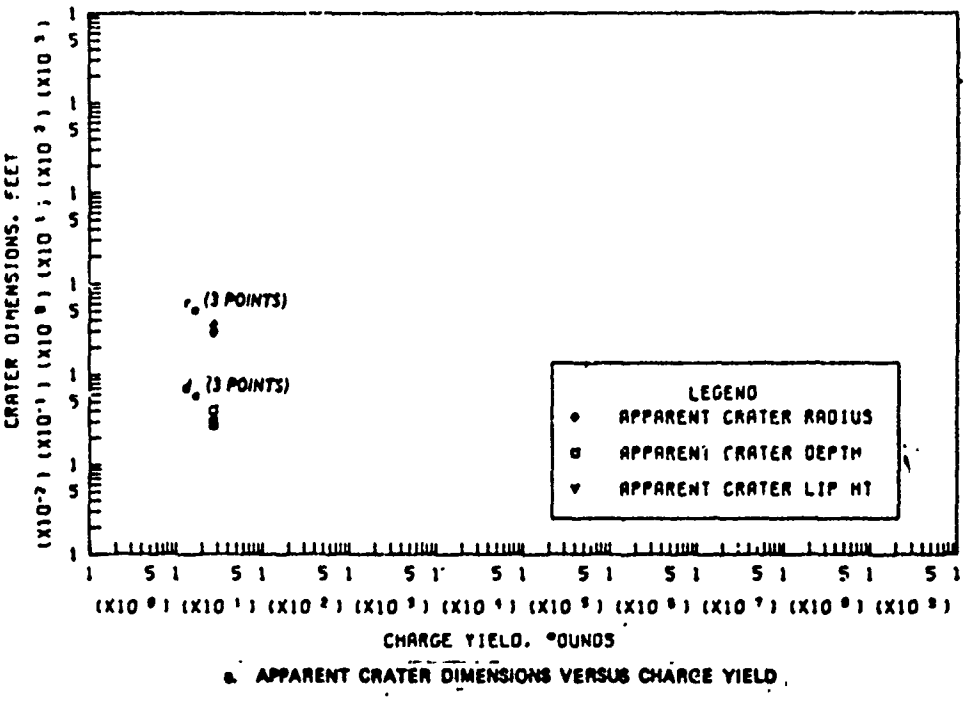

a. APPARENT CRATER DIMENSIONS VERSUS CHARGE YIELD

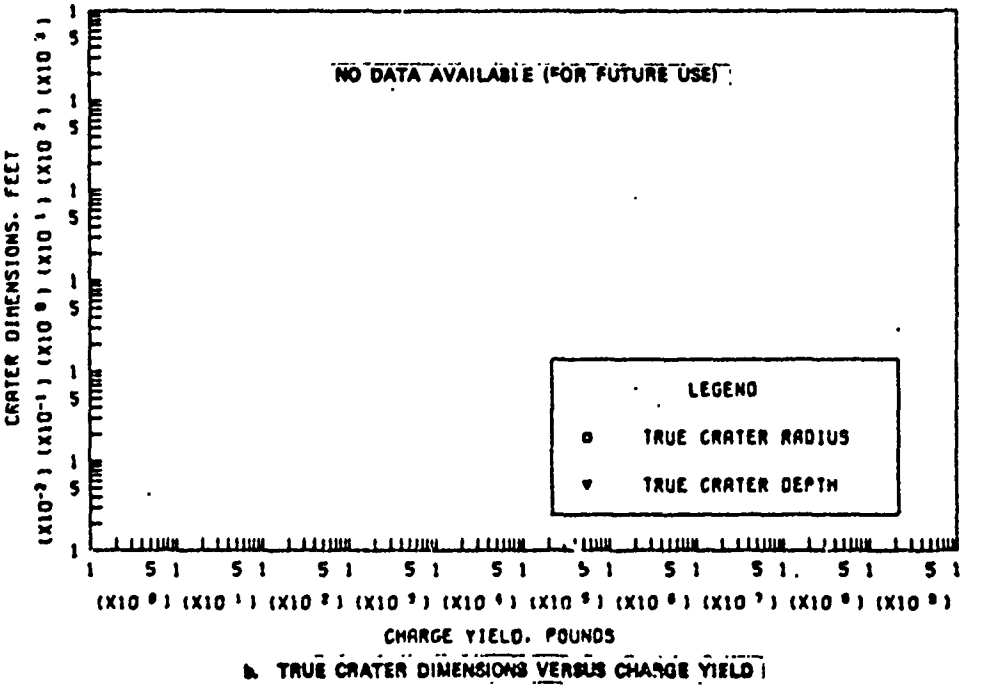

b. TRUE CRATER DIMENSIONS VERSUS CHARGE YIELD

Figure B.55 Dimensions of craters in moist silty clay for $0.50 \leq Z$ ft/lb$^{1/3}$, Category 1 (sheet 1 of 2).

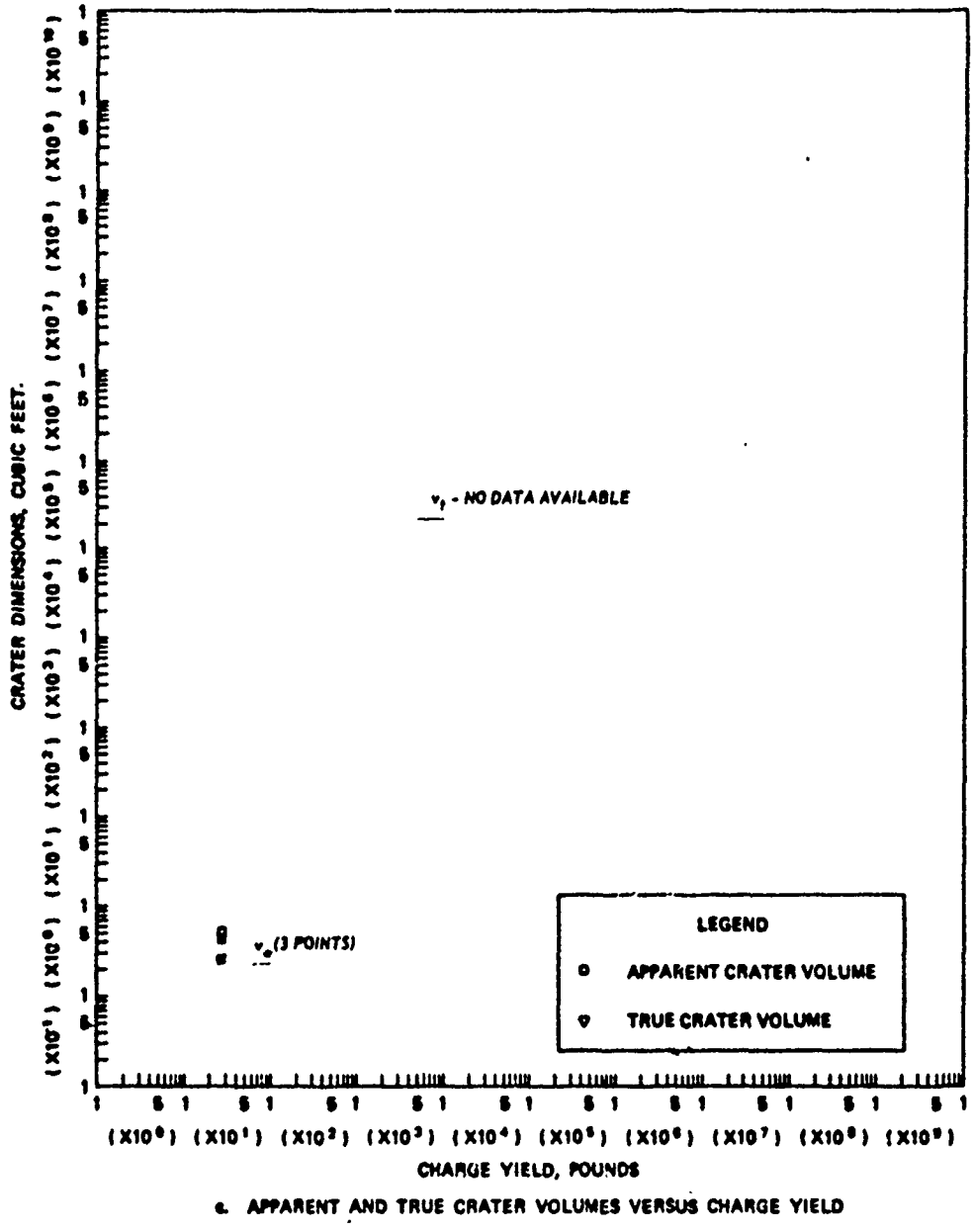

e. APPARENT AND TRUE CRATER VOLUMES VERSUS CHARGE YIELD

Figure B.55 (sheet 2 of 2).

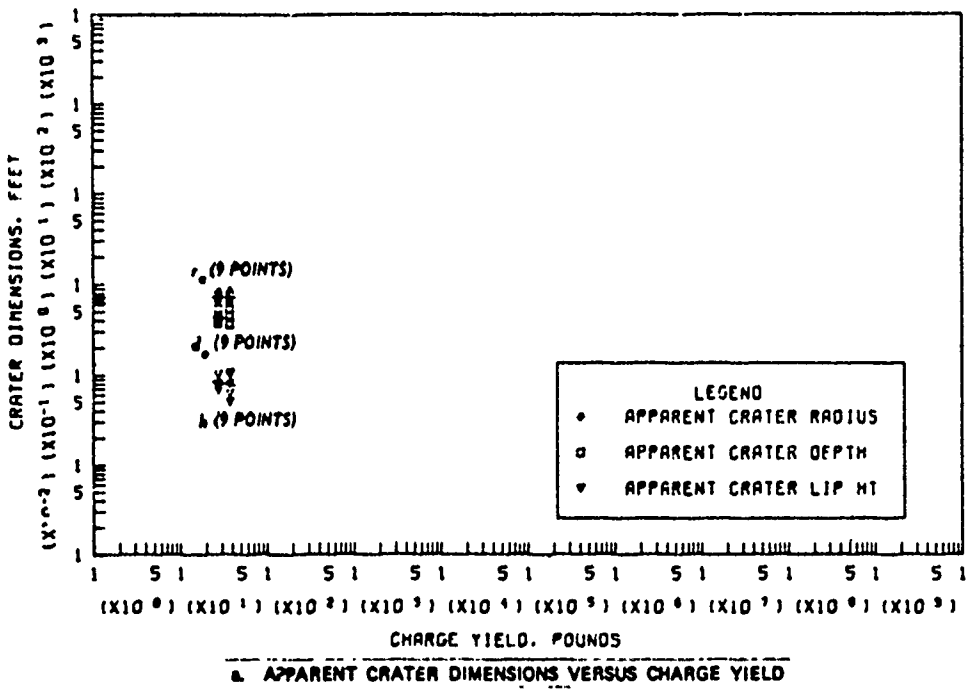

a. APPARENT CRATER DIMENSIONS VERSUS CHARGE YIELD

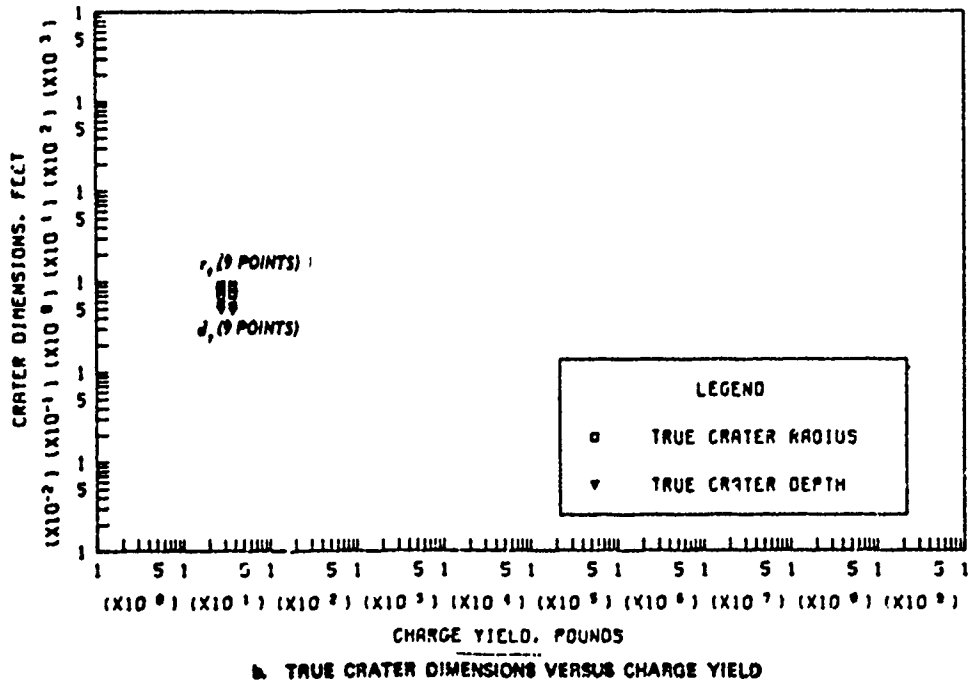

b. TRUE CRATER DIMENSIONS VERSUS CHARGE YIELD

Figure B.56 Dimensions of craters in moist silty clay for $-0.50 \leq Z < -0.20$ ft/lb$^{1/3}$, Category 6 (sheet 1 of 2).

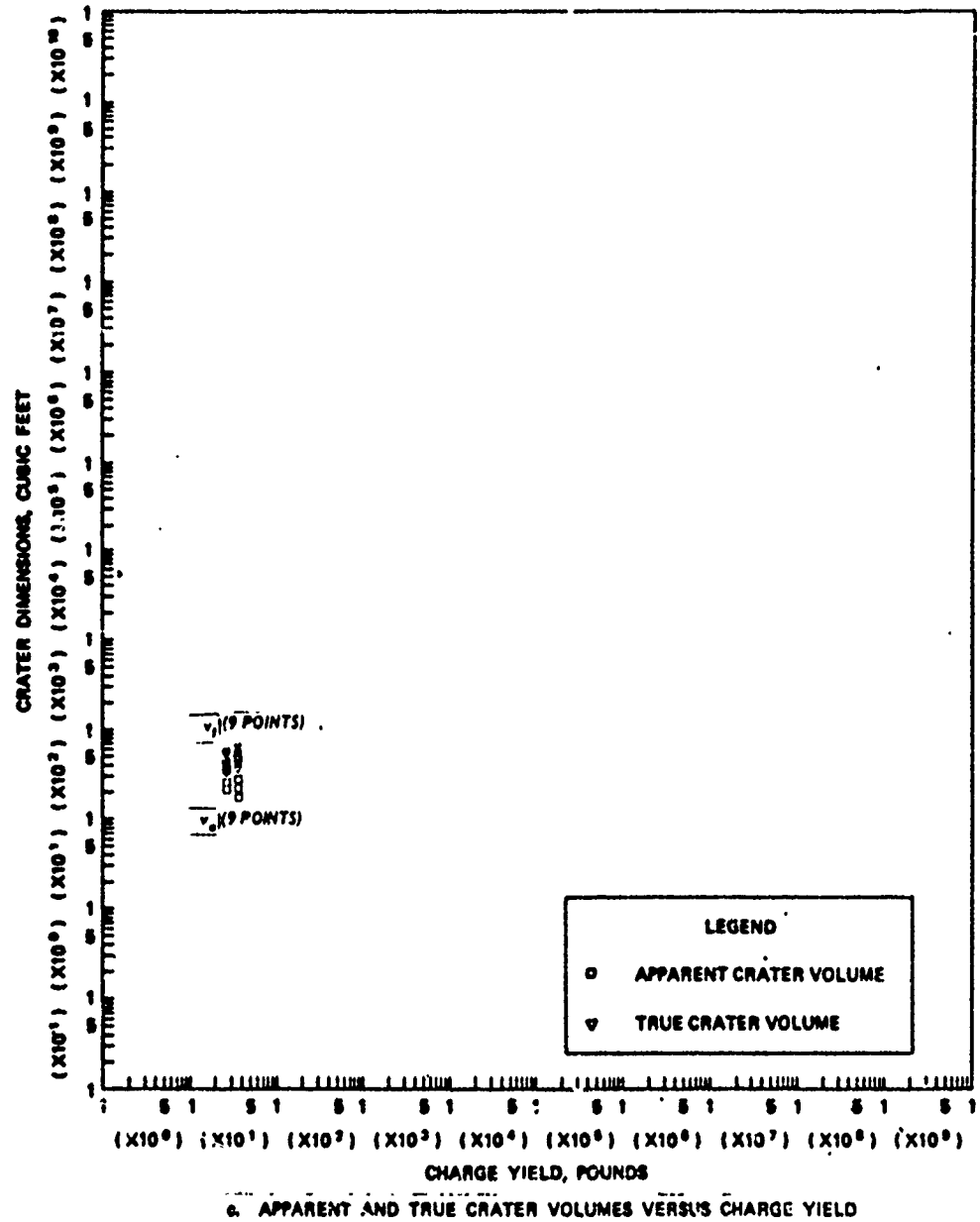

c. APPARENT AND TRUE CRATER VOLUMES VERSUS CHARGE YIELD

Figure B.56 (sheet 2 of 2).

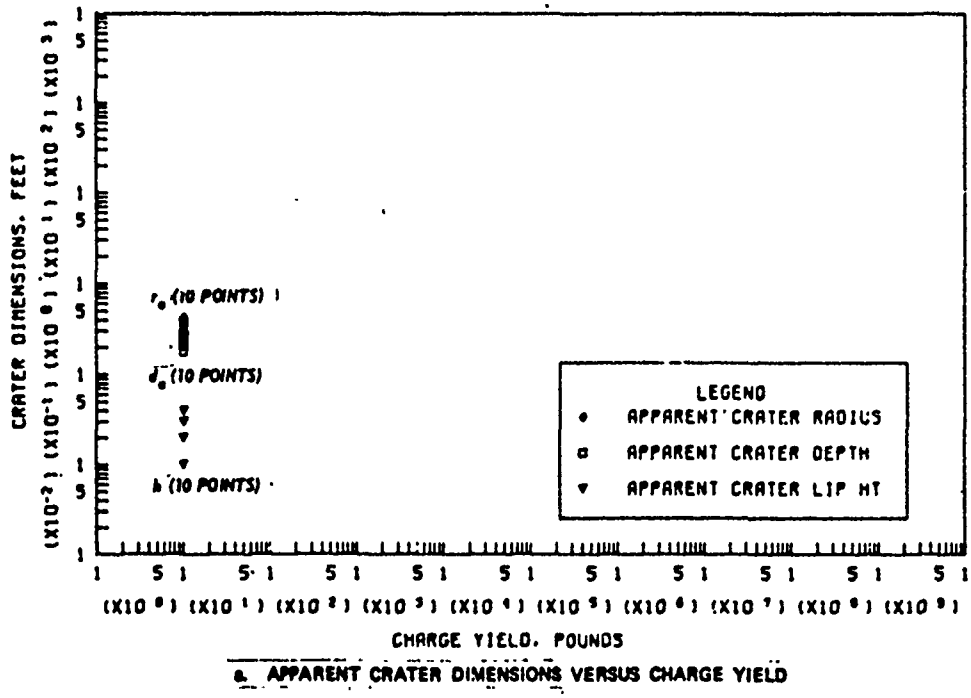

a. APPARENT CRATER DIMENSIONS VERSUS CHARGE YIELD

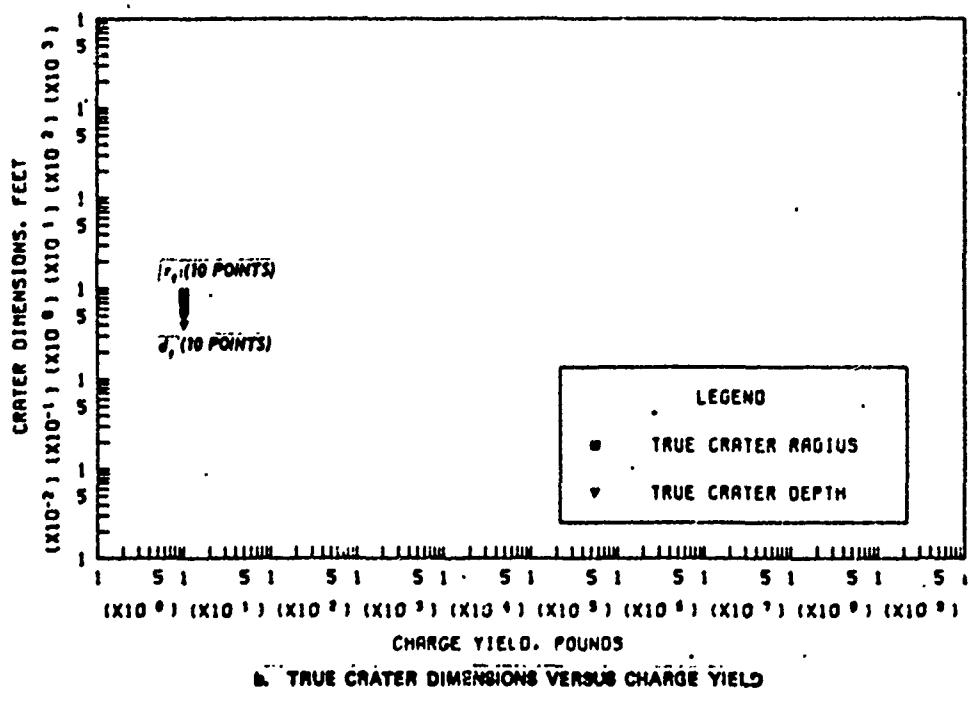

b. TRUE CRATER DIMENSIONS VERSUS CHARGE YIELD

Figure B.57 Dimensions of craters in moist silty clay for $-0.90 \leq Z < -0.50$ ft/lb$^{1/3}$, Category 7 (sheet 1 of 2).

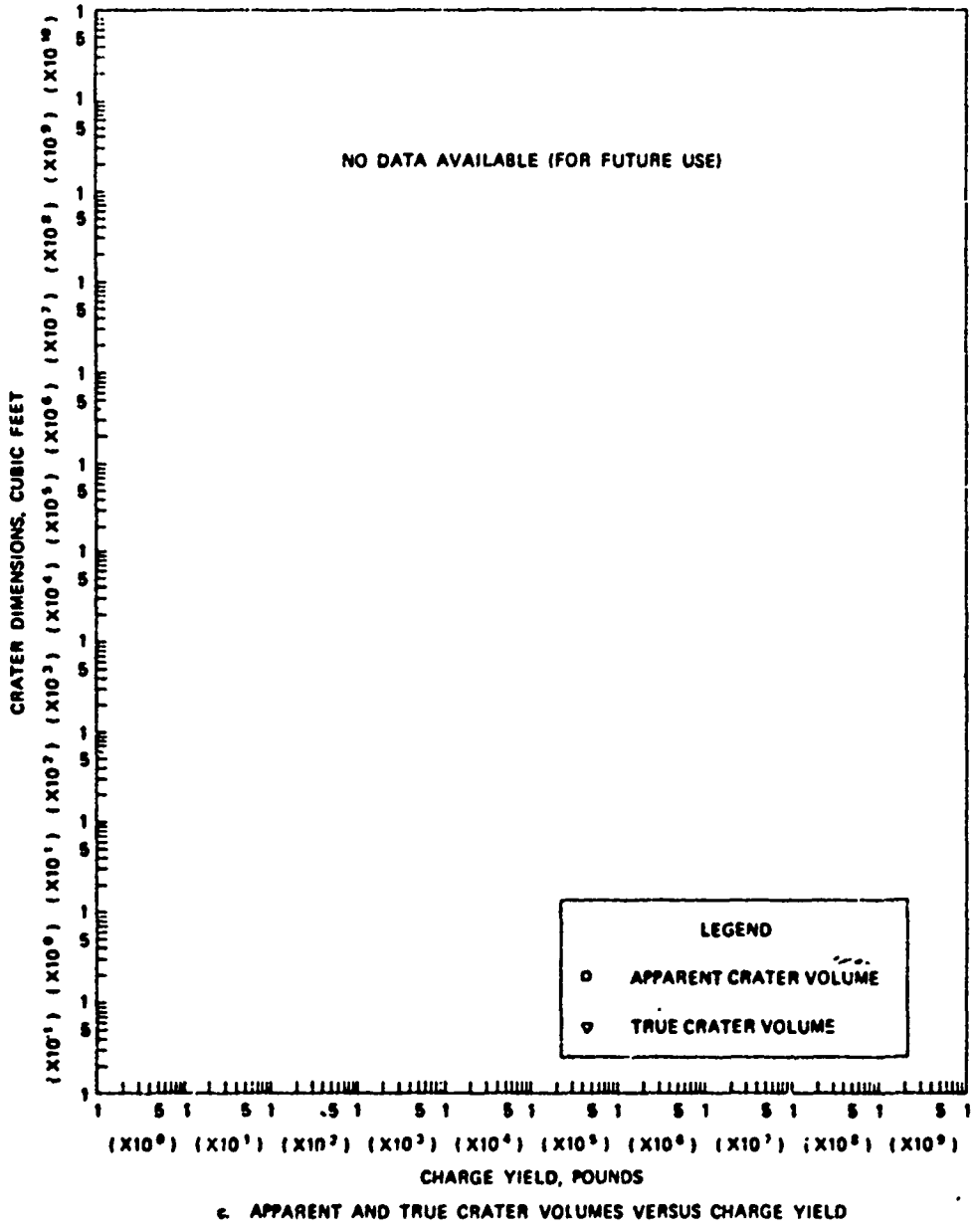

c. APPARENT AND TRUE CRATER VOLUMES VERSUS CHARGE YIELD

Figure B.57 (sheet 2 of 2).

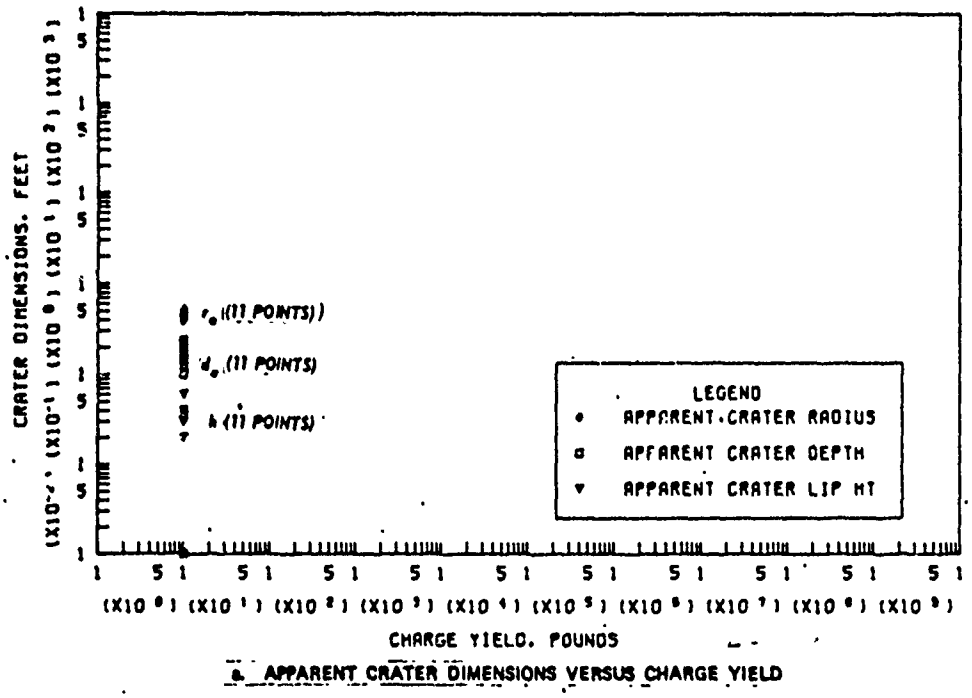

a. APPARENT CRATER DIMENSIONS VERSUS CHARGE YIELD

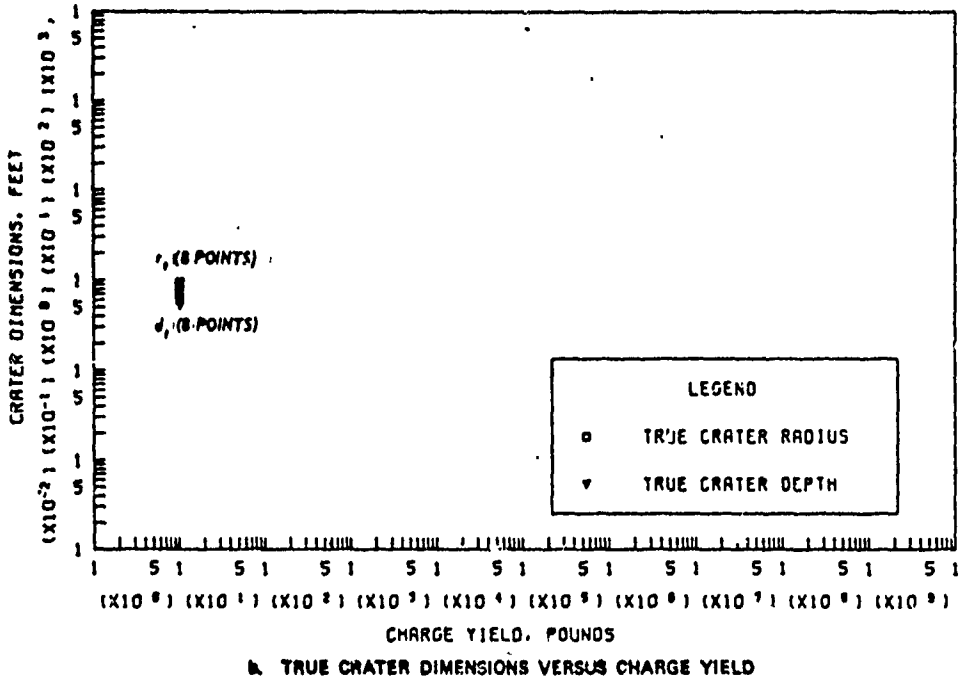

b. TRUE CRATER DIMENSIONS VERSUS CHARGE YIELD

Figure B.58 Dimensions of craters in moist silty clay for $-2.00 \leq Z < -1.10$ ft/lb$^{1/3}$, Category 9 (sheet 1 of 2).

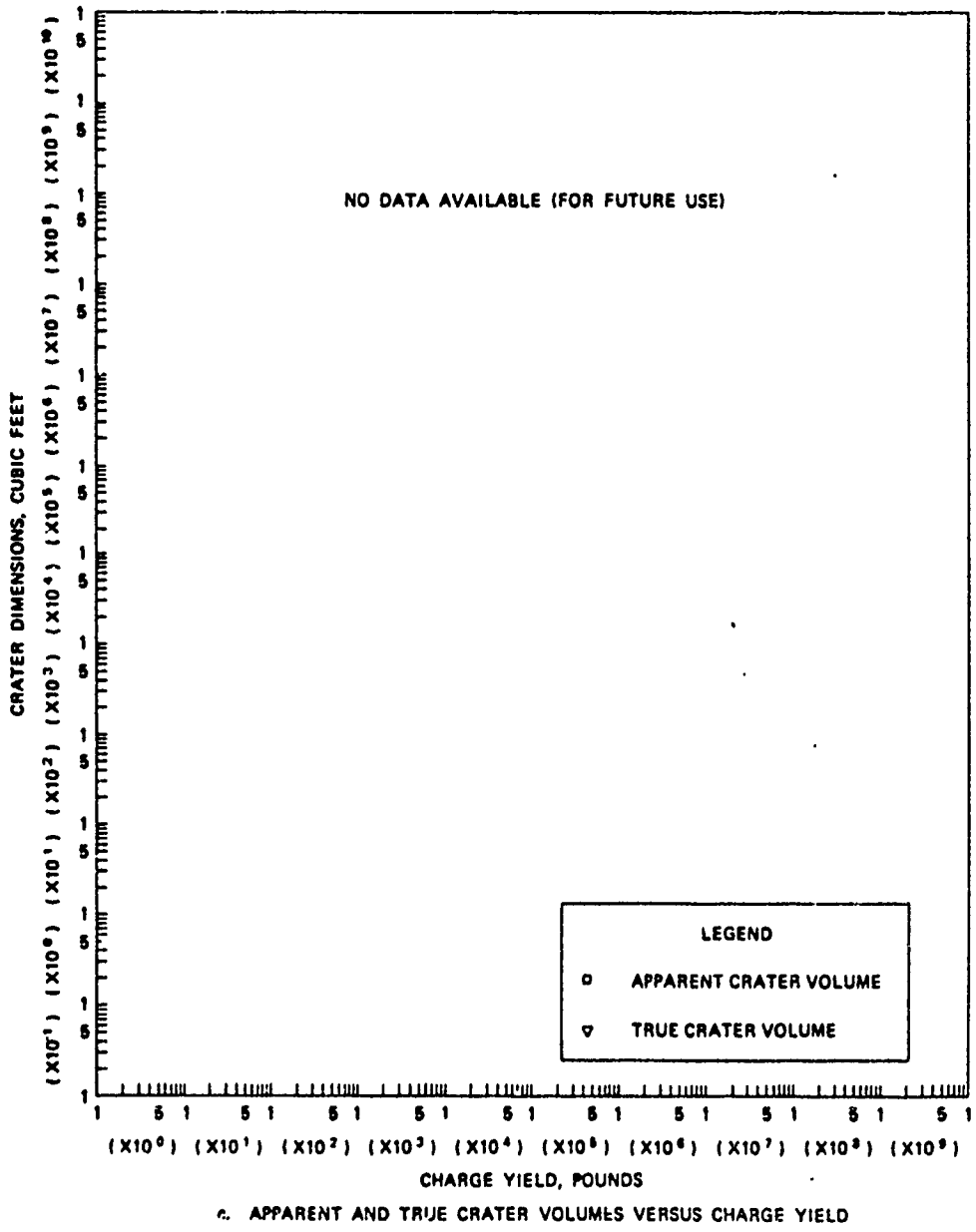

c. APPARENT AND TRUE CRATER VOLUMES VERSUS CHARGE YIELD

Figure B.58 (sheet 2 of 2).

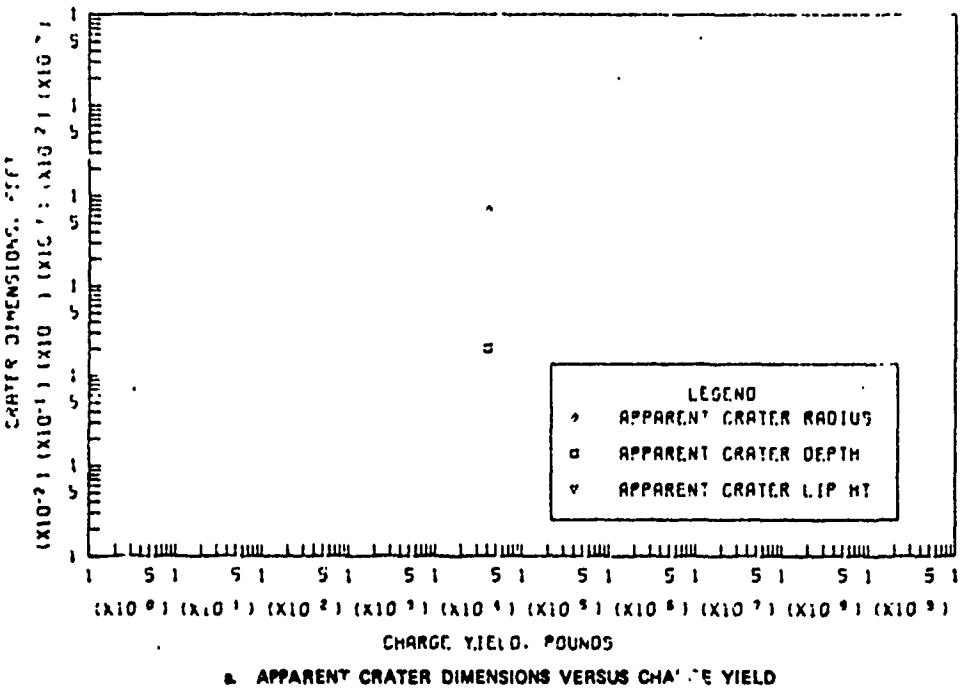

a. APPARENT CRATER DIMENSIONS VERSUS CHARGE YIELD

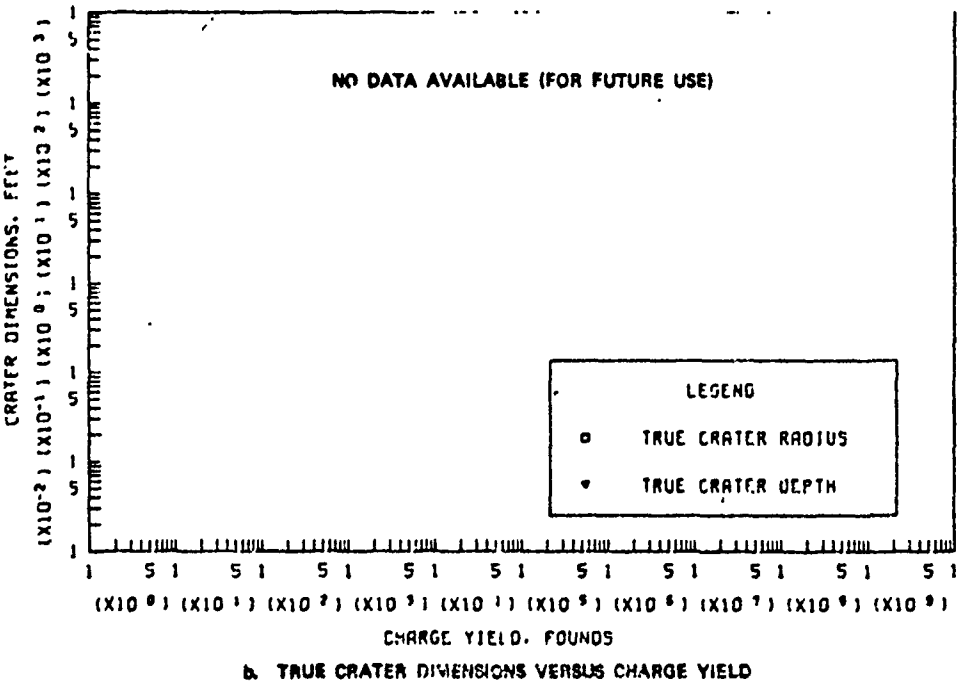

b. TRUE CRATER DIMENSIONS VERSUS CHARGE YIELD

Figure B.59 Dimensions of craters in dry-to-moist sandy silty clay for $0.50 \leq Z$ ft/lb$^{1/3}$, Category 1 (sheet 1 of 2).

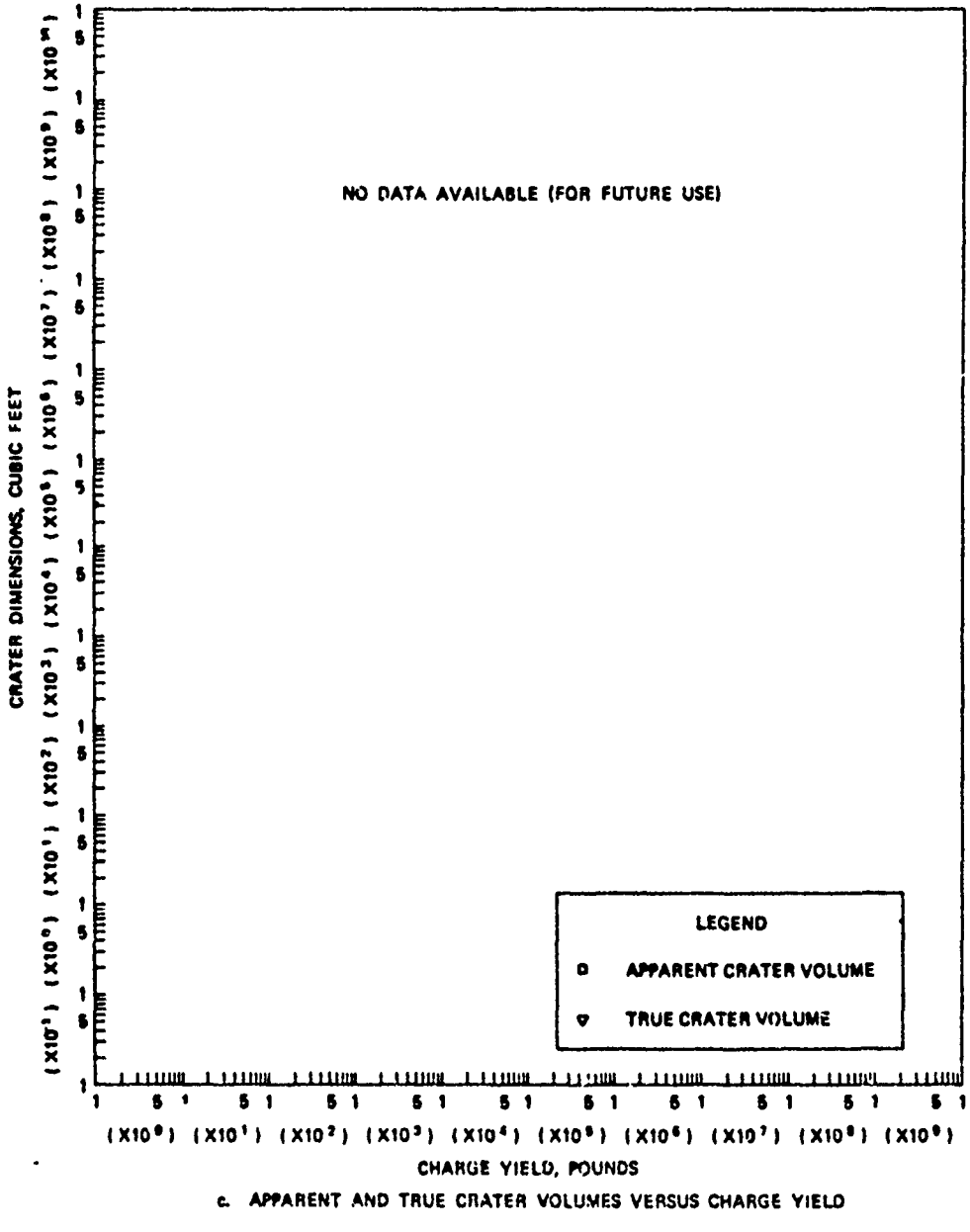

c. APPARENT AND TRUE CRATER VOLUMES VERSUS CHARGE YIELD

Figure B.59 (sheet 2 of 2).

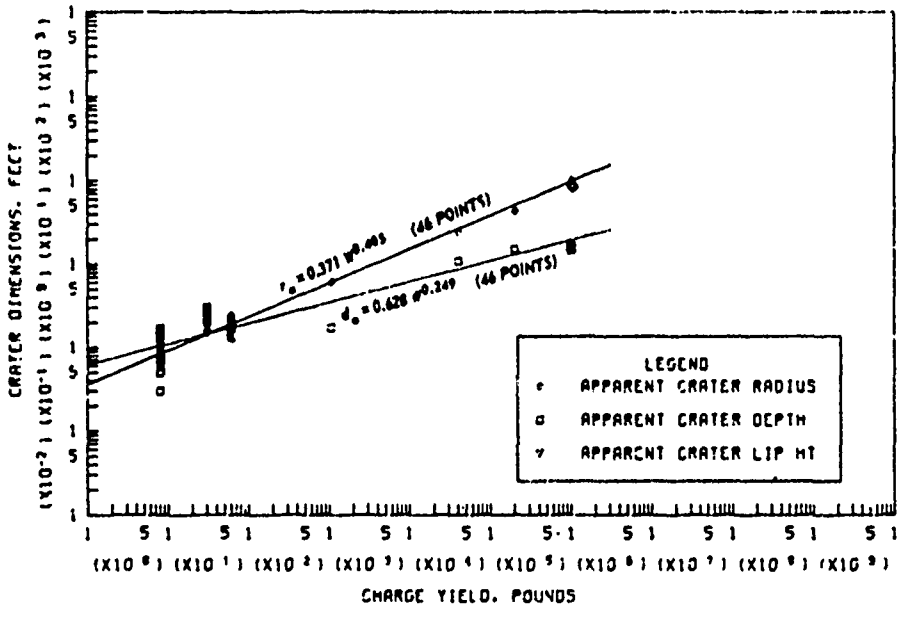

a. APPARENT CRATER DIMENSIONS VERSUS CHARGE YIELD

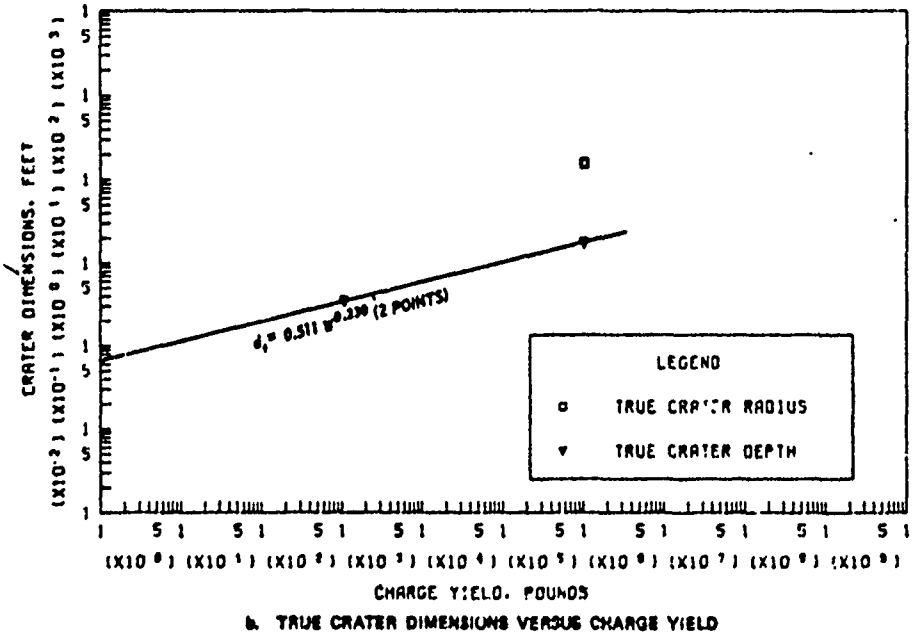

b. TRUE CRATER DIMENSIONS VERSUS CHARGE YIELD

Figure B.60 Dimensions of craters in dry-to-moist sandy silty clay for $0.05 \leq Z < 0.20$ ft/lb$^{1/3}$, Category 3 (sheet 1 of 2).

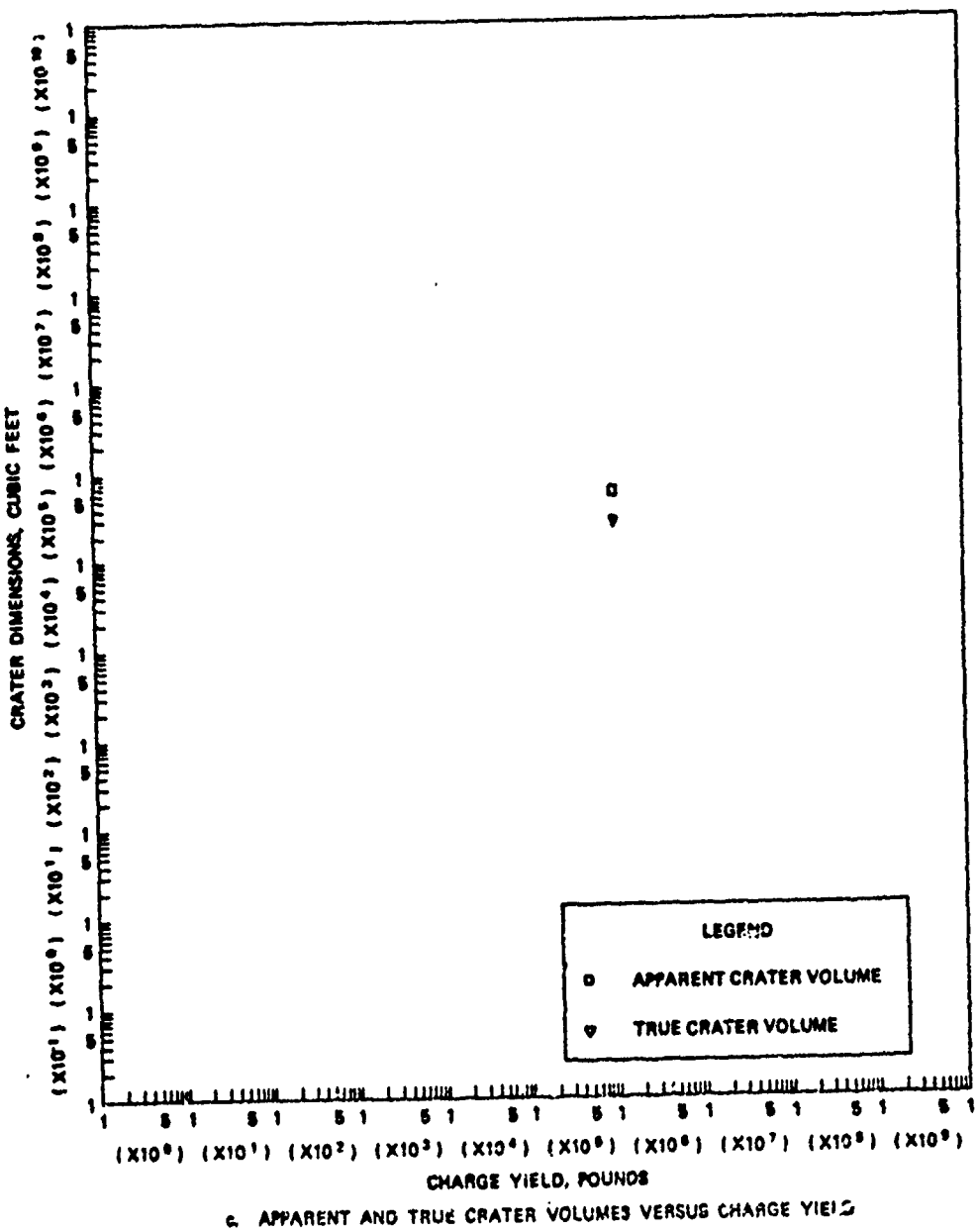

c. APPARENT AND TRUE CRATER VOLUMES VERSUS CHARGE YIELD

Figure B.60 (sheet 2 of 2).

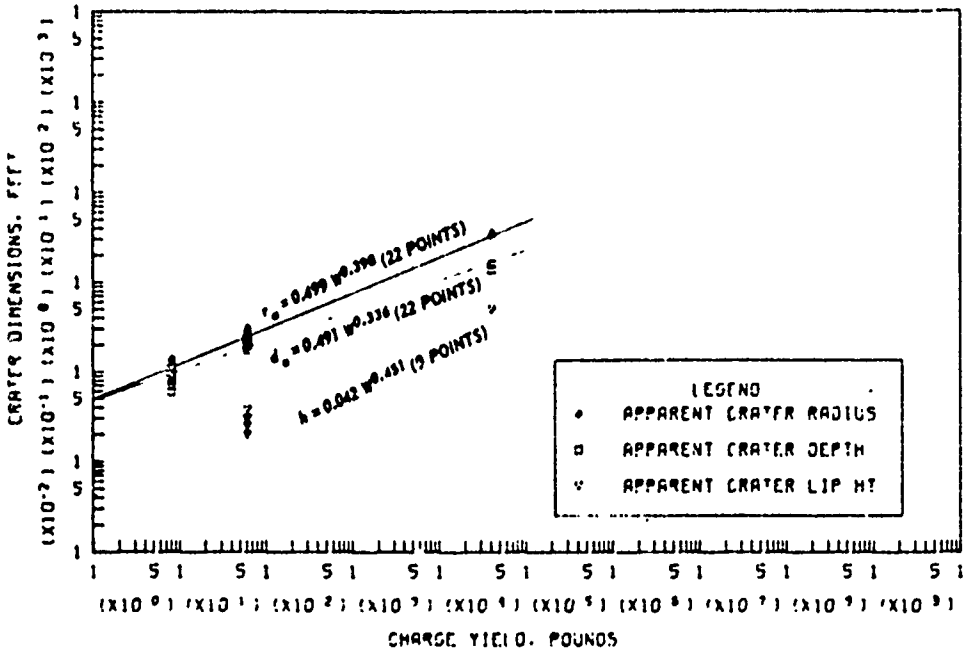

a. APPARENT CRATER DIMENSIONS VERSUS CHARGE YIELD

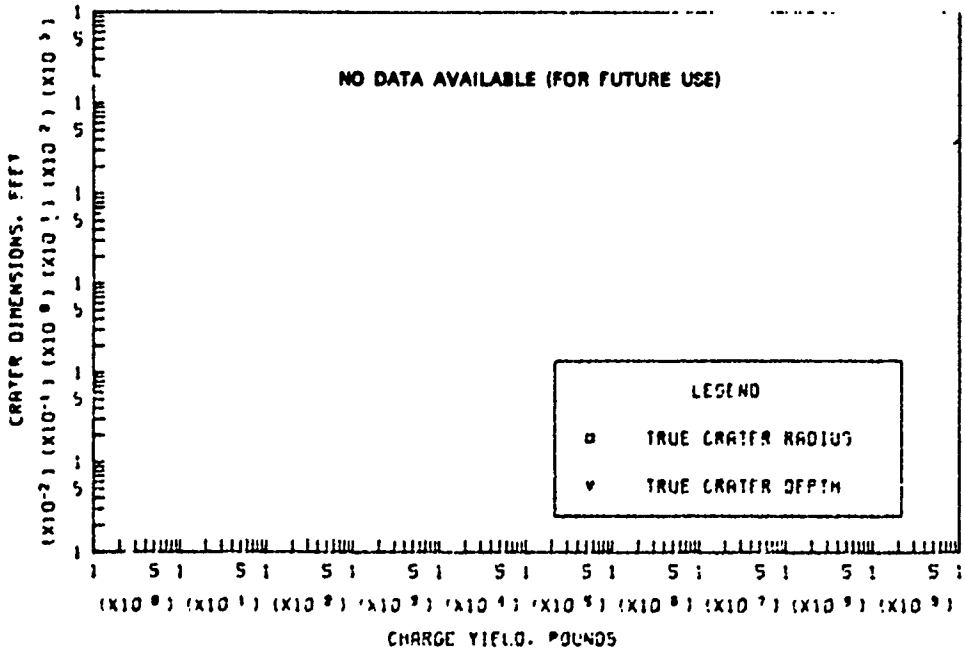

b. TRUE CRATER DIMENSIONS VERSUS CHARGE YIELD

Figure B.61 Dimensions of craters in dry-to-moist sandy silty clay for $-0.05 \leq Z < 0.05$ ft/lb$^{1/3}$, Category 4 (sheet 1 of 2).

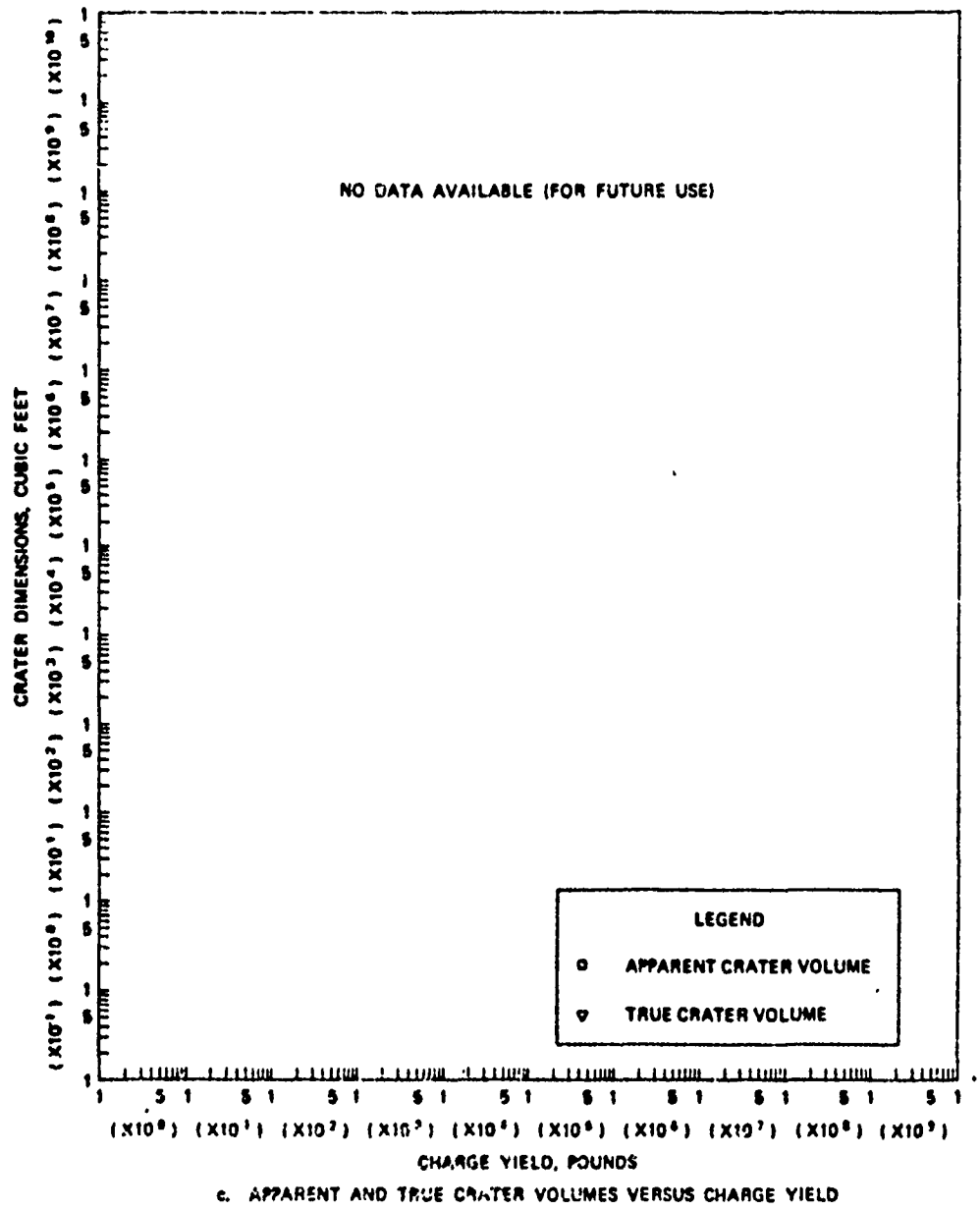

c. APPARENT AND TRUE CRATER VOLUMES VERSUS CHARGE YIELD

Figure B.61 (sheet 2 of 2).

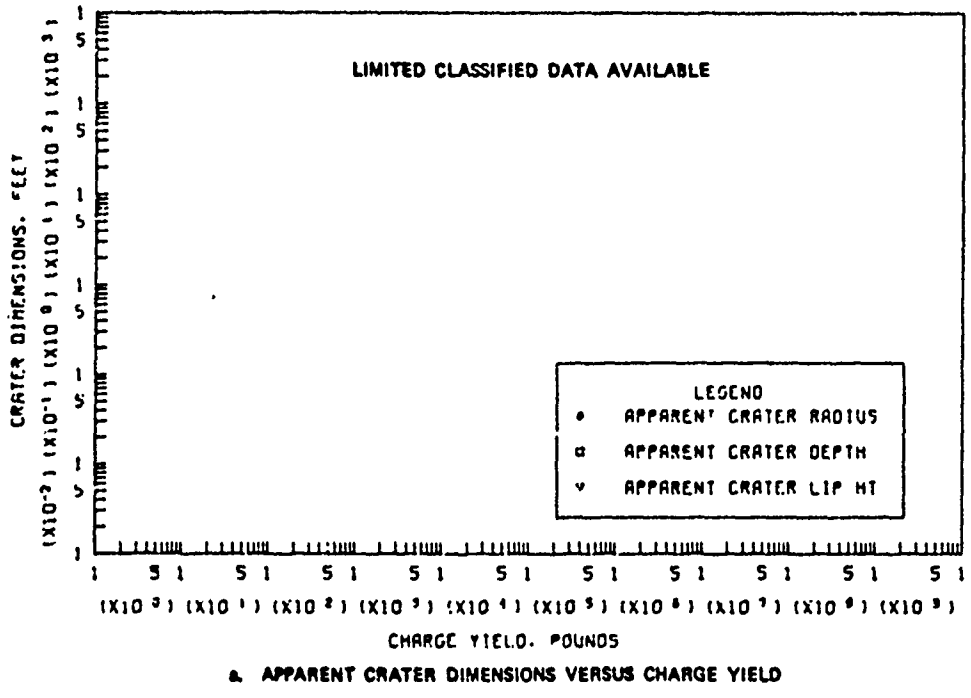

a. APPARENT CRATER DIMENSIONS VERSUS CHARGE YIELD

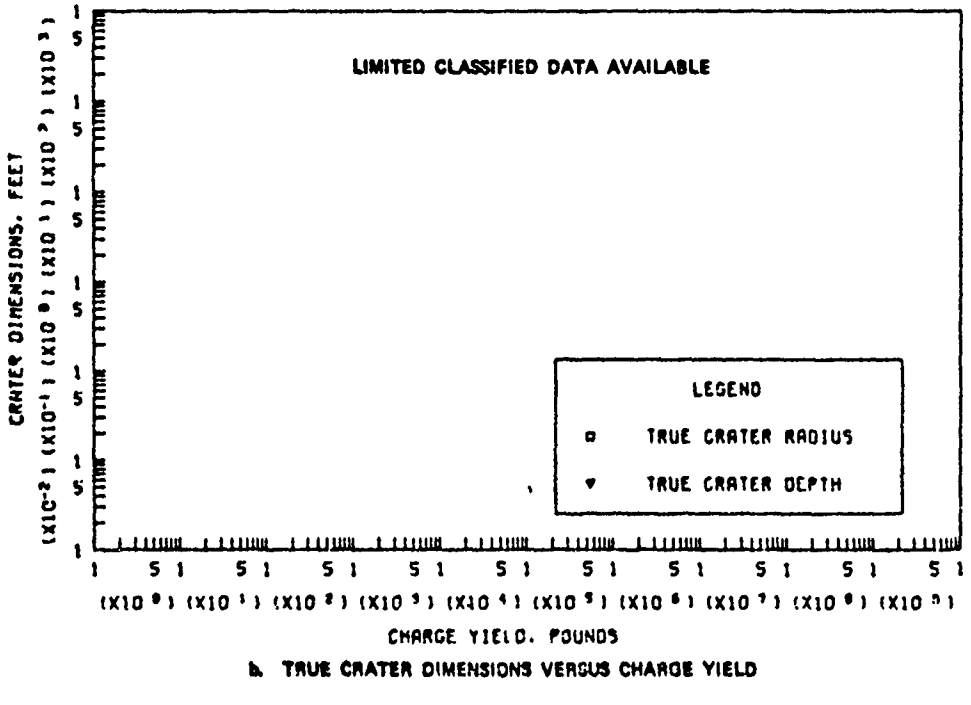

b. TRUE CRATER DIMENSIONS VERSUS CHARGE YIELD

Figure B.62 Dimensions of craters in desert alluvium for $0.05 \leq Z < 0.20$ ft/lb$^{1/3}$, Category 3 (sheet 1 of 2).

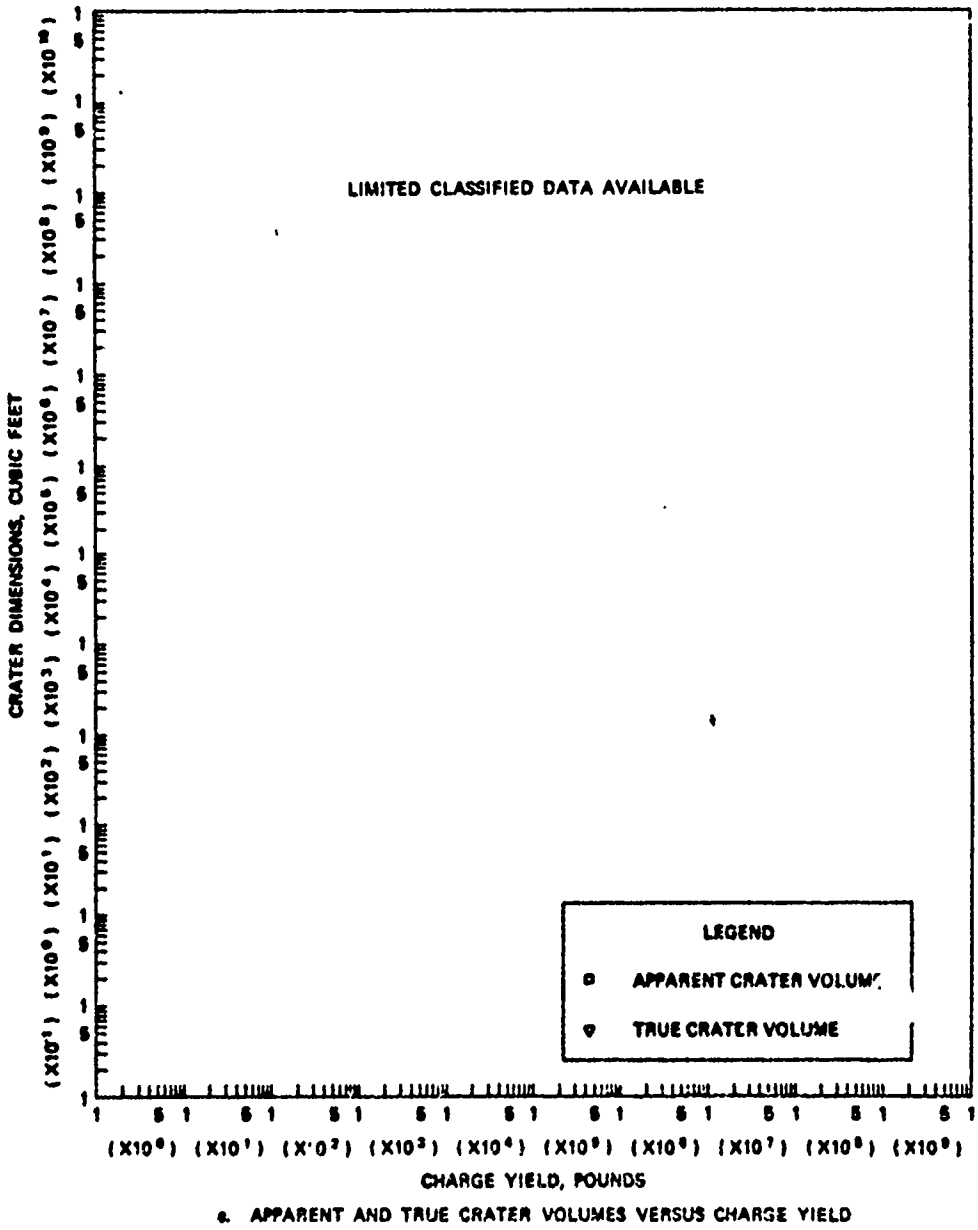

a. APPARENT AND TRUE CRATER VOLUMES VERSUS CHARGE YIELD

Figure B.62 (sheet 2 of 2).

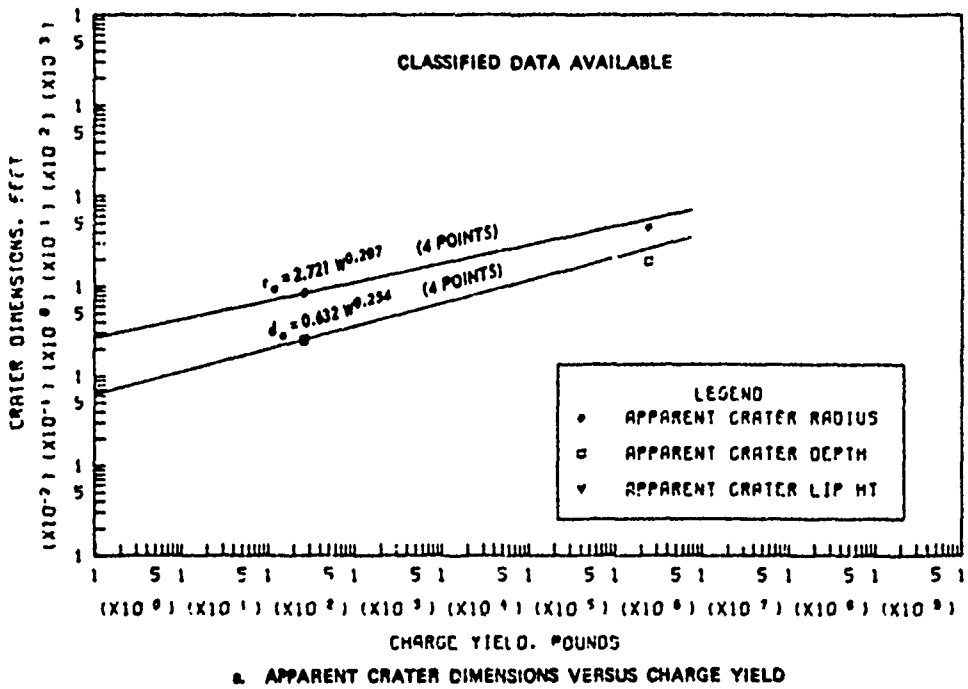

a. APPARENT CRATER DIMENSIONS VERSUS CHARGE YIELD

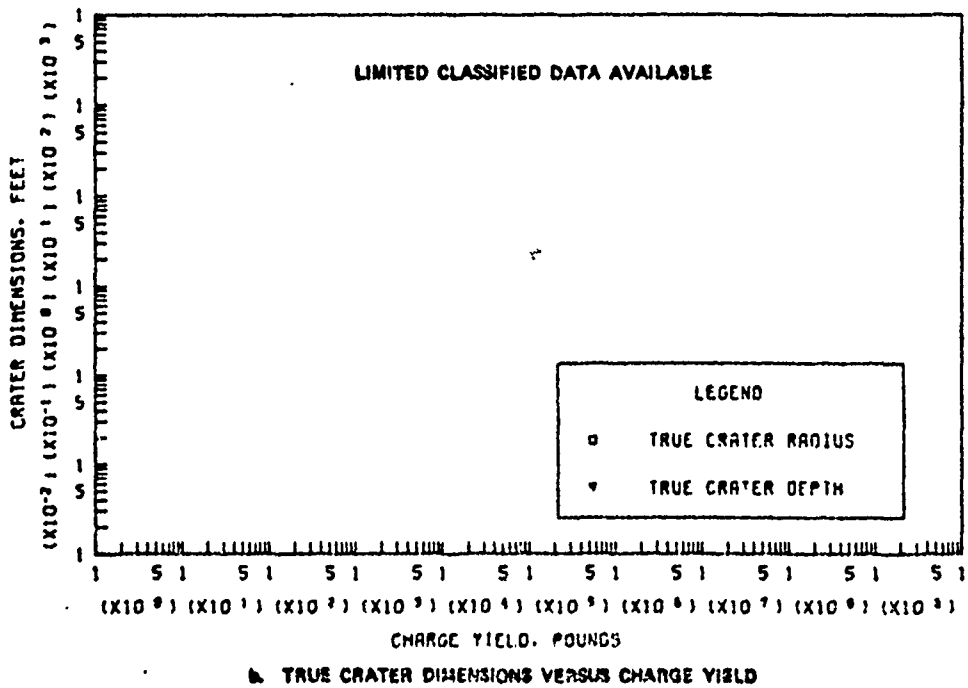

b. TRUE CRATER DIMENSIONS VERSUS CHARGE YIELD

Figure B.63 Dimensions of craters in desert alluvium for $-0.05 \leq Z < 0.05$ ft/lb$^{1/3}$, Category 4 (sheet 1 of 2).

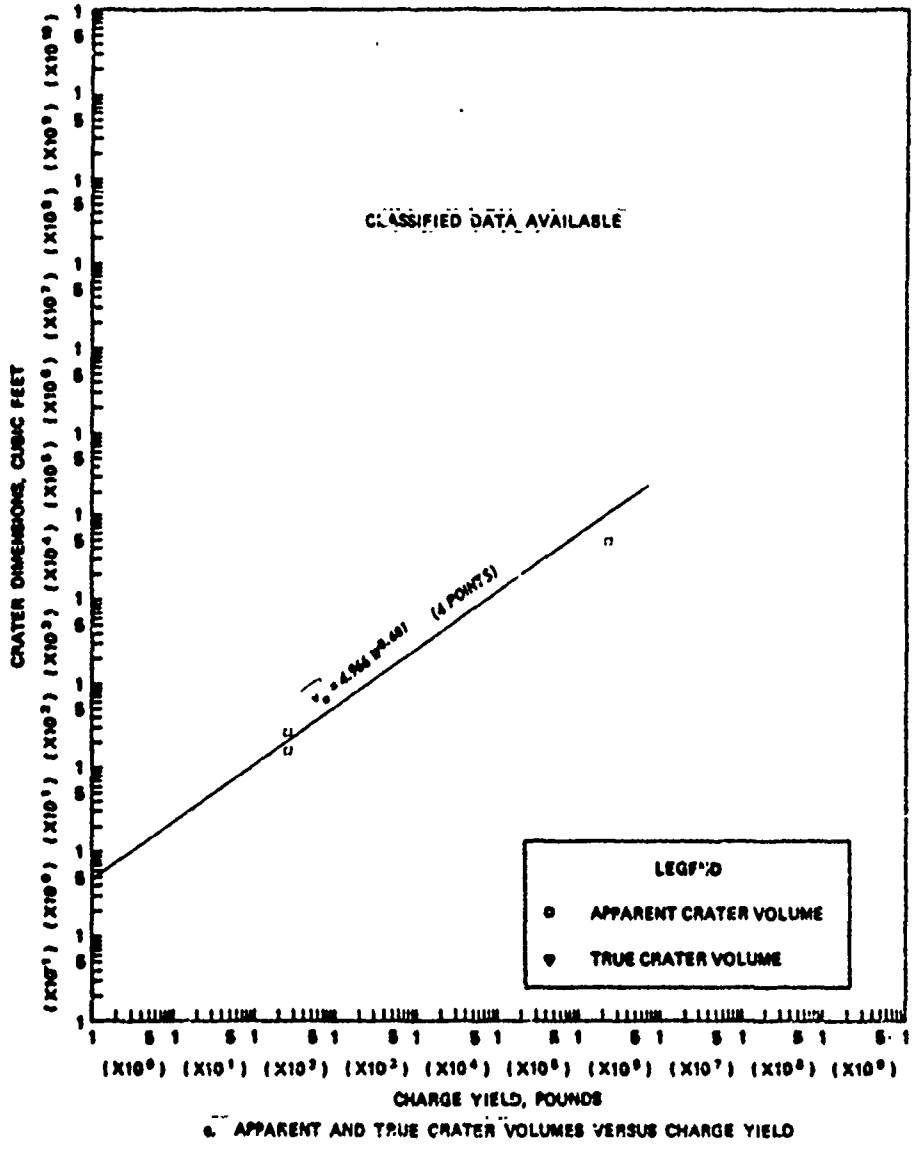

a. APPARENT AND TRUE CRATER VOLUMES VERSUS CHARGE YIELD

Figure B.63 (sheet 2 of 2).

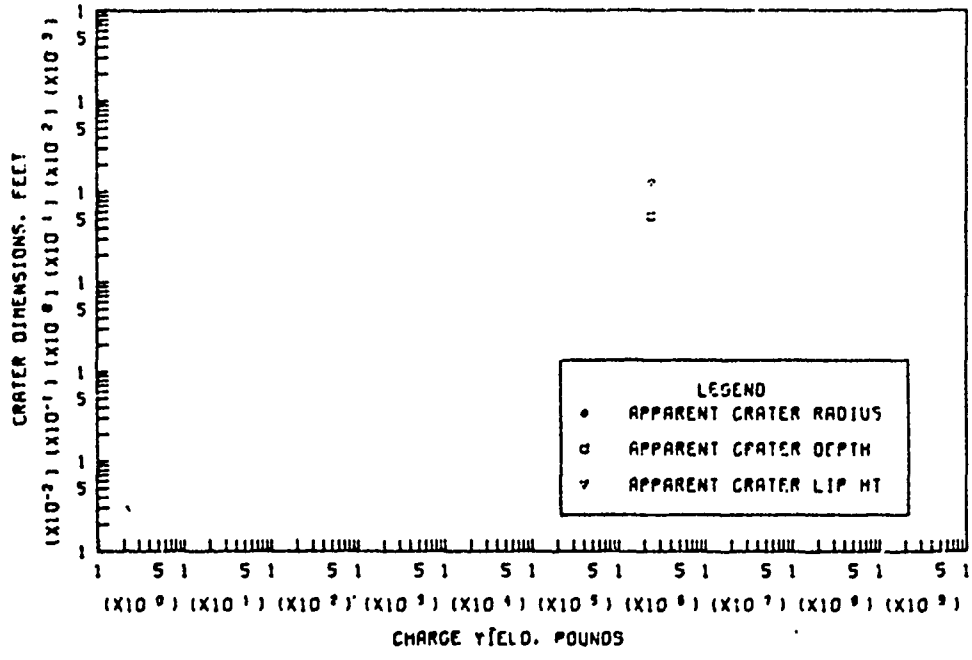

a. APPARENT CRATER DIMENSIONS VERSUS CHARGE YIELD

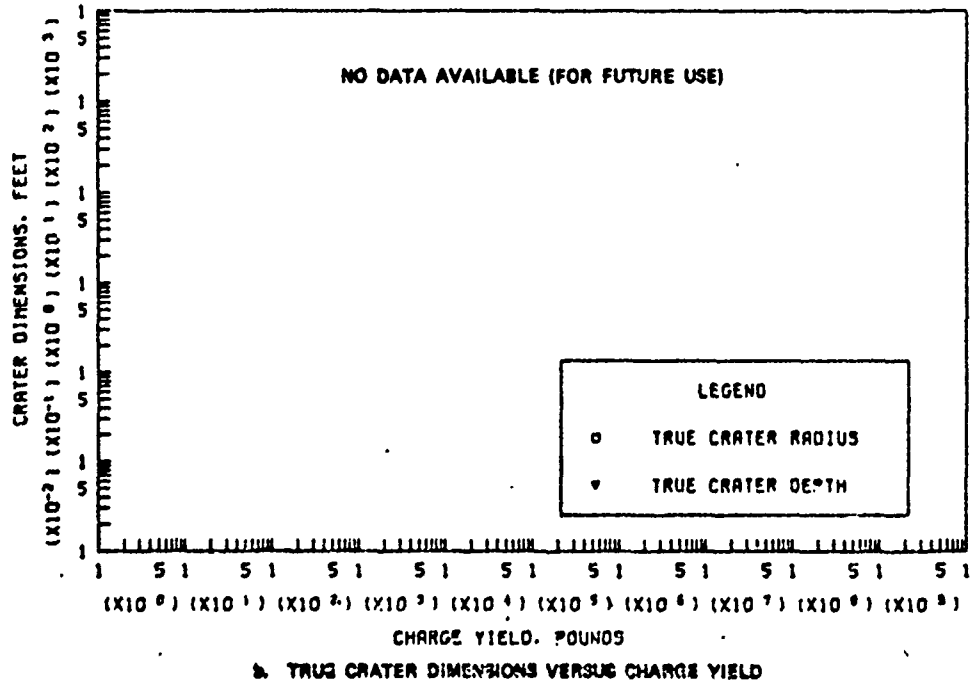

b. TRUE CRATER DIMENSIONS VERSUS CHARGE YIELD

Figure B.64 Dimensions of craters in desert alluvium for $-0.20 \leq Z < -0.05$ ft/lb$^{1/3}$, Category 5 (sheet 1 of 2).

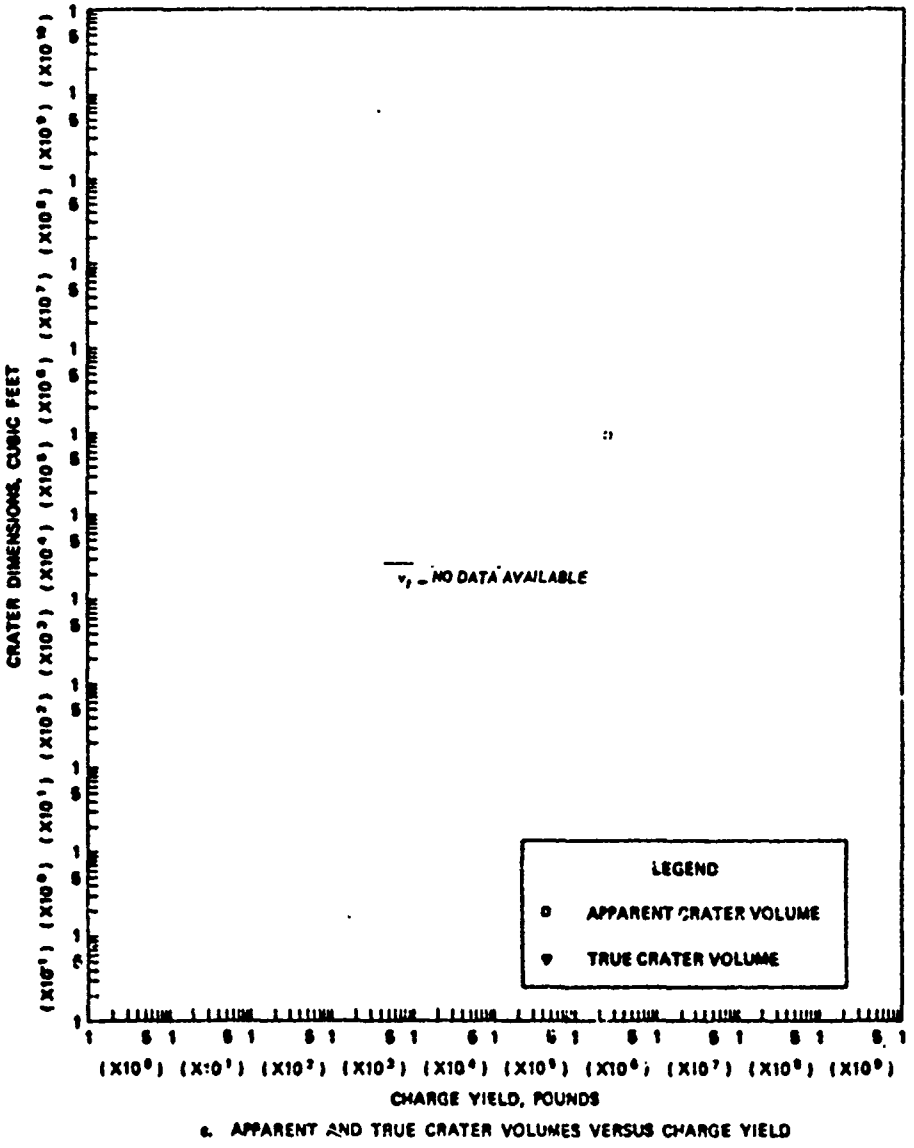

c. APPARENT AND TRUE CRATER VOLUMES VERSUS CHARGE YIELD

Figure B.64 (sheet 2 of 2).

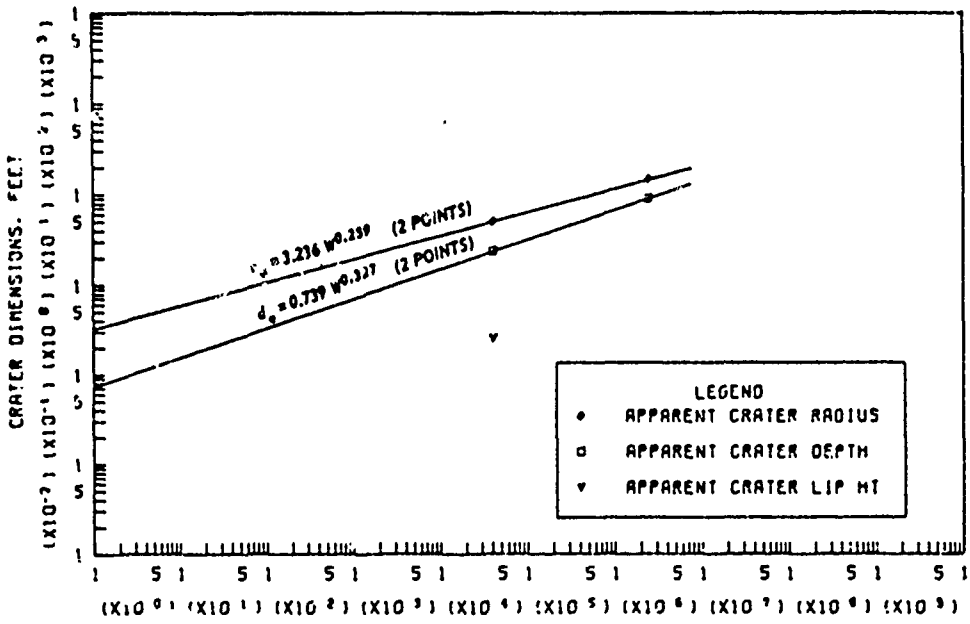

a. APPARENT CRATER DIMENSIONS VERSUS CHARGE YIELD

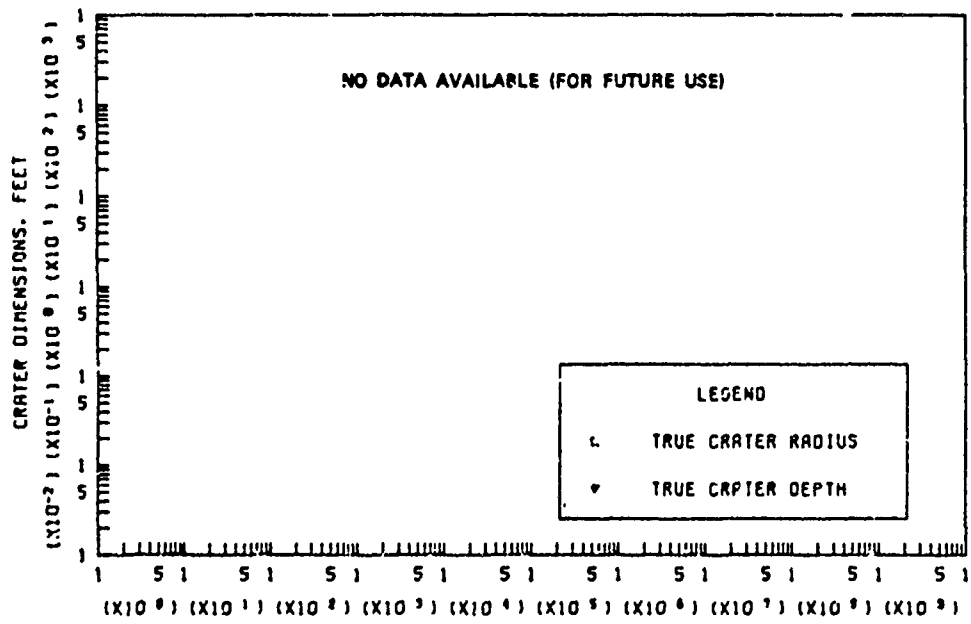

b. TRUE CRATER DIMENSIONS VERSUS CHARGE YIELD

Figure B.65 Dimensions of craters in desert alluvium for $-0.90 \leq Z < -0.50$ ft/lb$^{1/3}$, Category 7 (sheet 1 of 2).

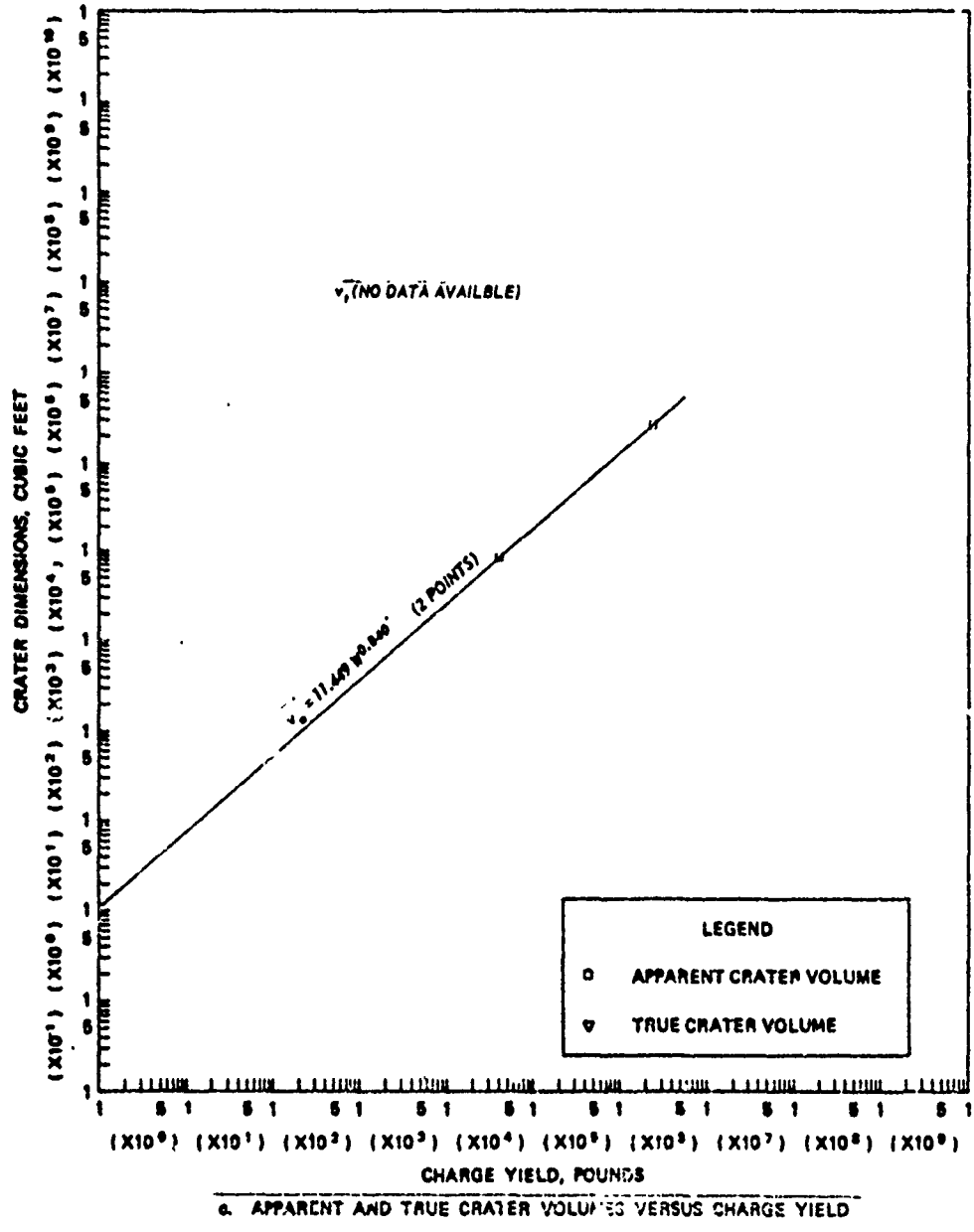

a. APPARENT AND TRUE CRATER VOLUMES VERSUS CHARGE YIELD

Figure B.65 (sheet 2 of 2).

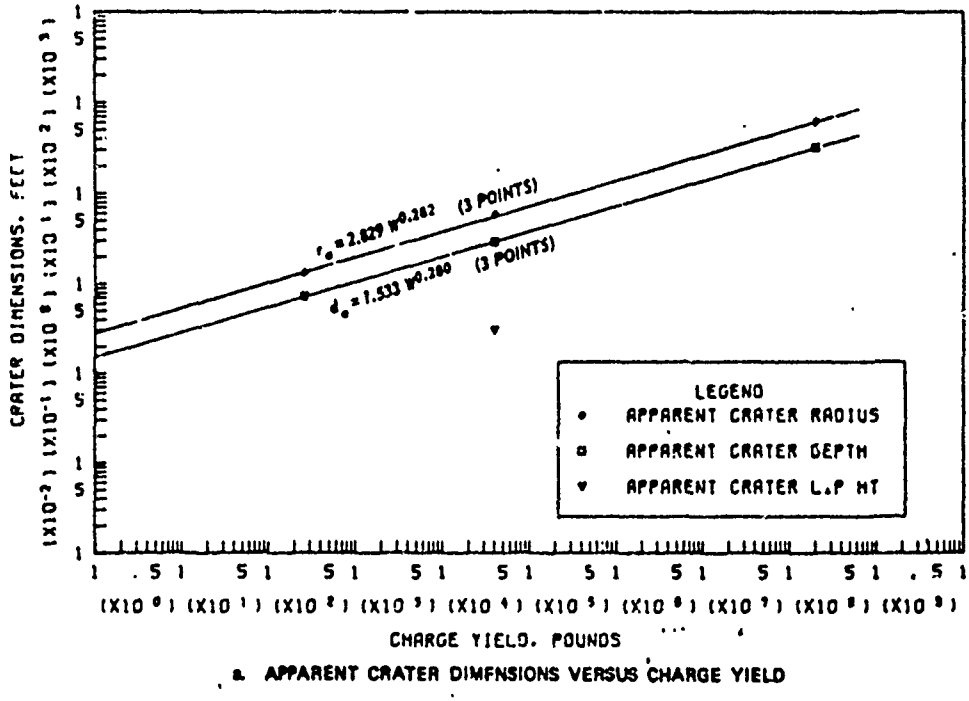

a. APPARENT CRATER DIMENSIONS VERSUS CHARGE YIELD

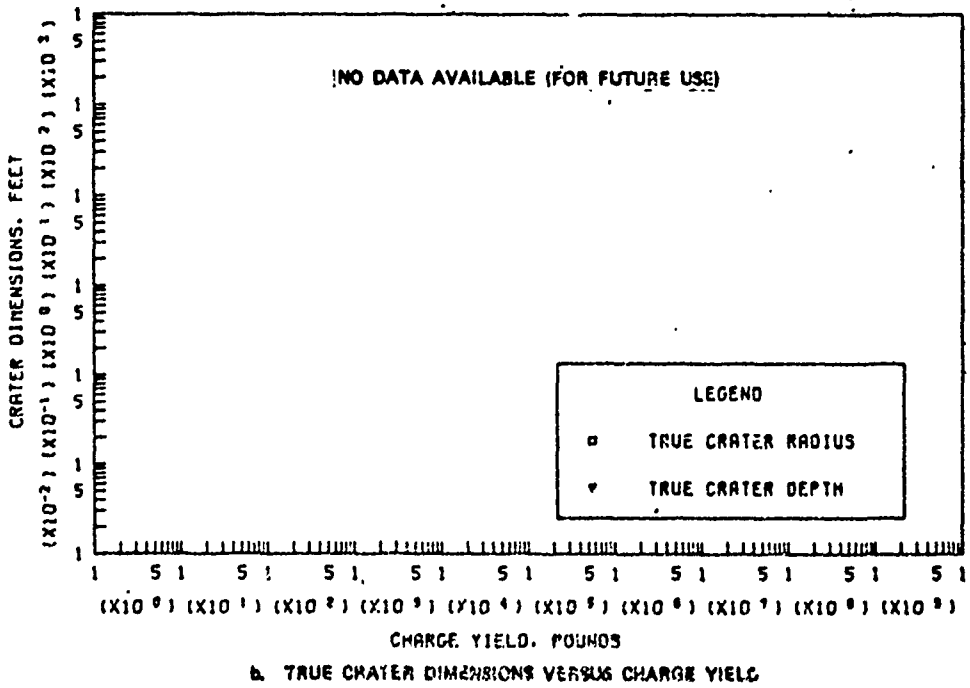

b. TRUE CRATER DIMENSIONS VERSUS CHARGE YIELD

Figure B.66 Dimensions of craters in desert alluvium for $-1.10 \leq Z < -0.90$ ft/lb$^{1/3}$, Category 8 (sheet 1 of 2).

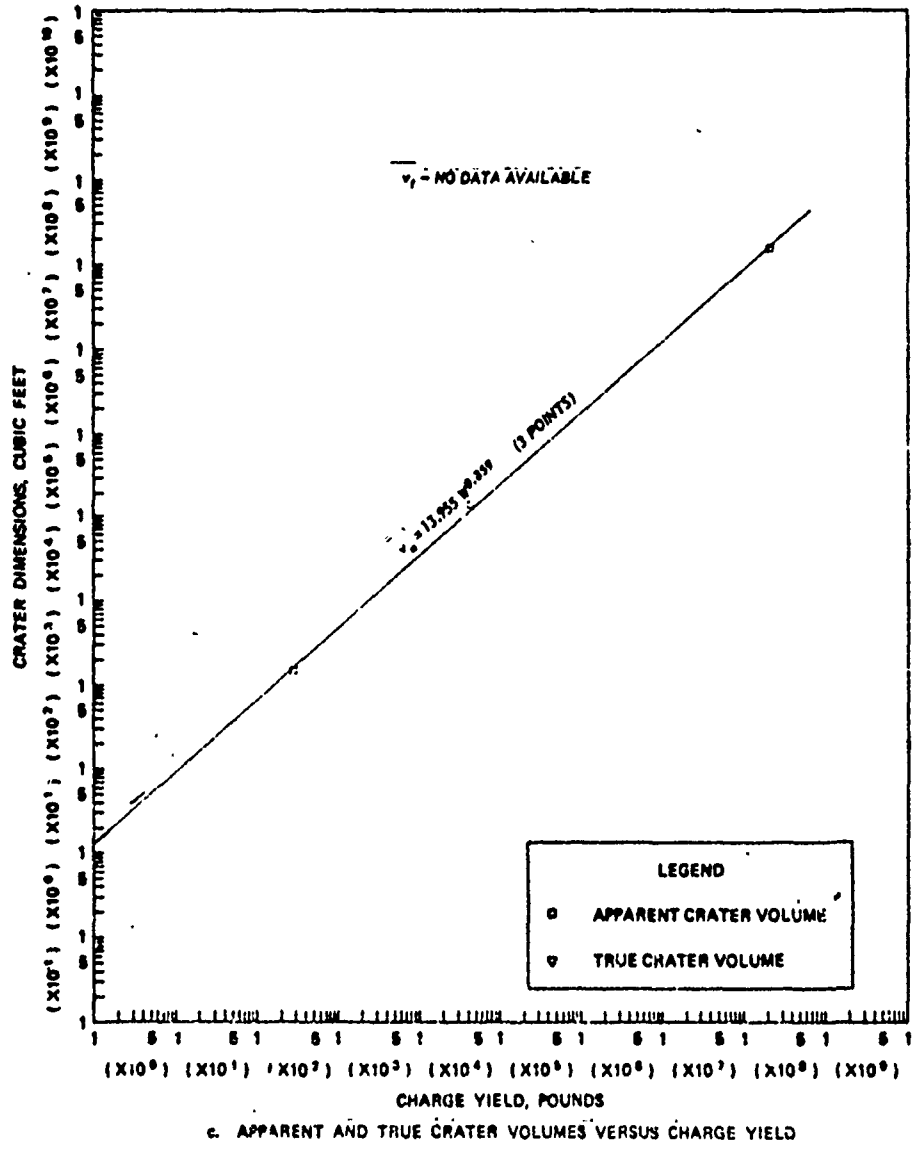

c. APPARENT AND TRUE CRATER VOLUMES VERSUS CHARGE YIELD

Figure B.66 (sheet 2 of 2).

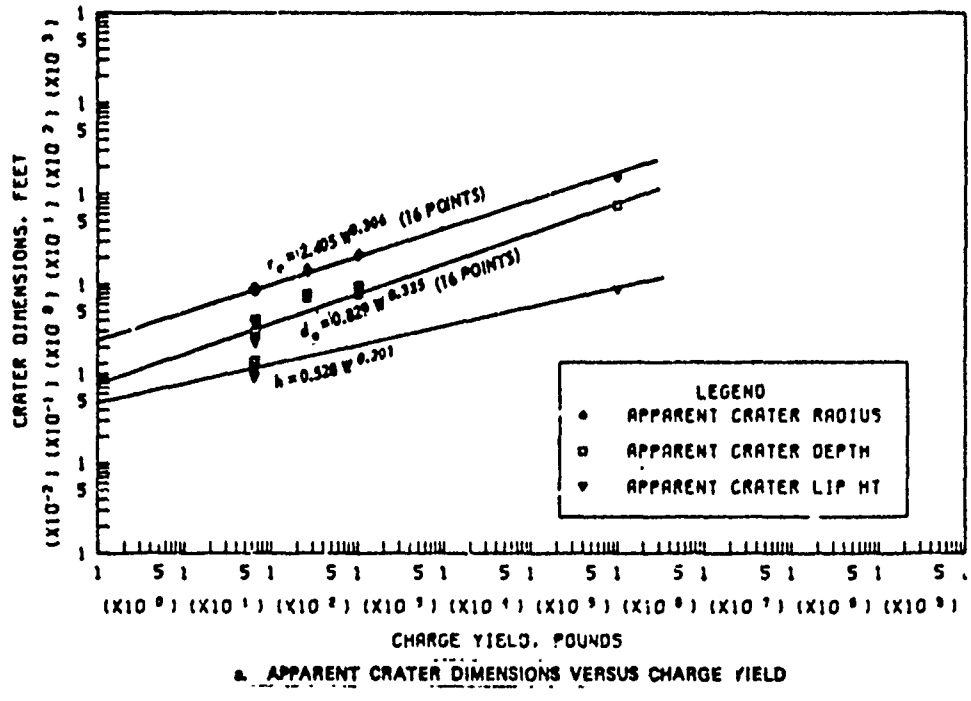

a. APPARENT CRATER DIMENSIONS VERSUS CHARGE YIELD

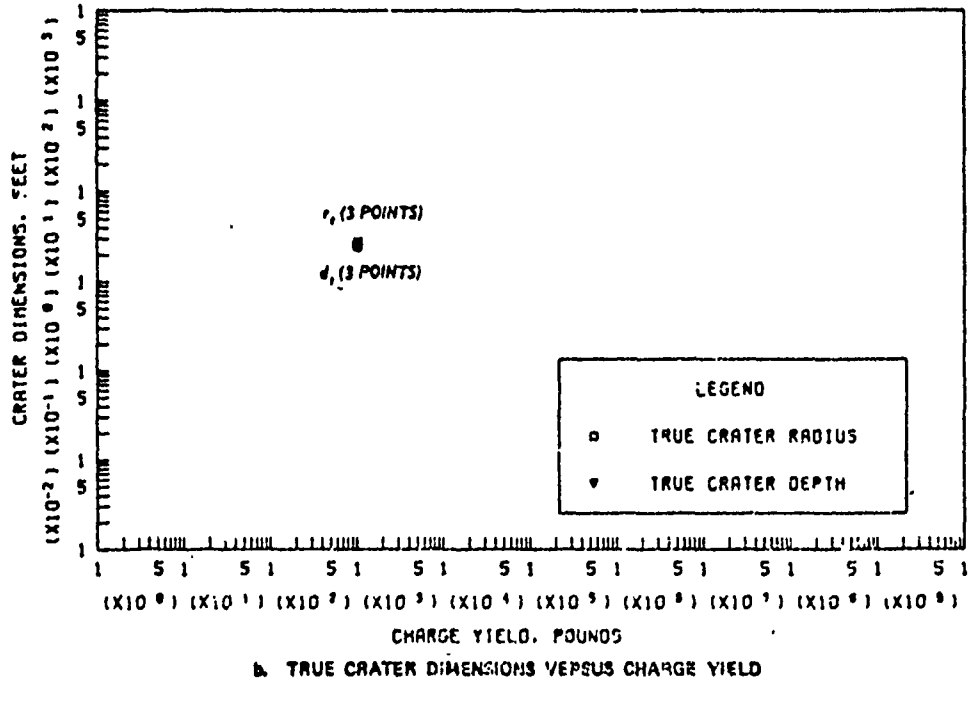

b. TRUE CRATER DIMENSIONS VERSUS CHARGE YIELD

Figure B.67 Dimensions of craters in desert alluvium for $-2.00 \leq Z < -1.10$ ft/lb$^{1/3}$, Category 9 (sheet 1 of 2).

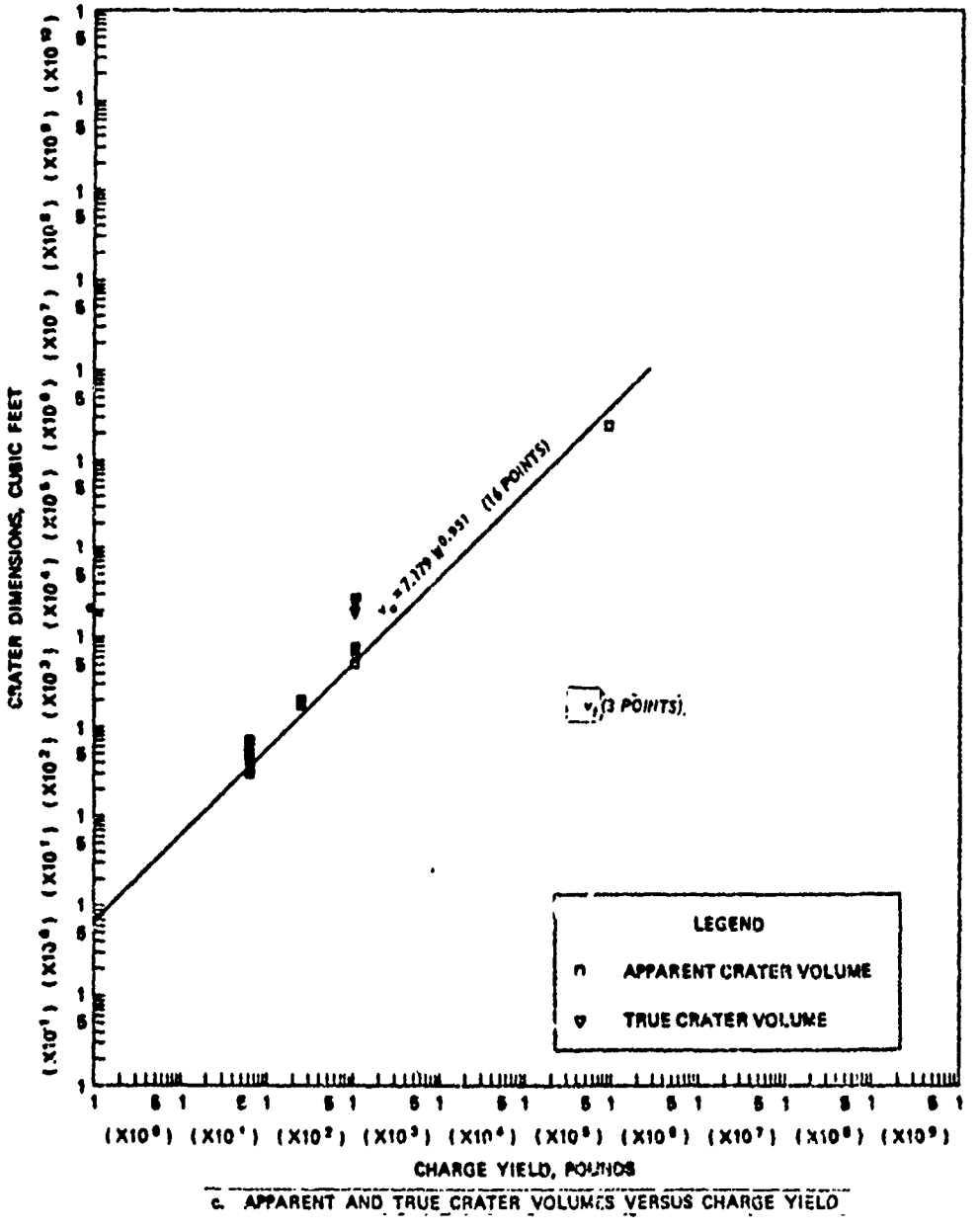

c. APPARENT AND TRUE CRATER VOLUMES VERSUS CHARGE YIELD

Figure B.67 (sheet 2 of 2).

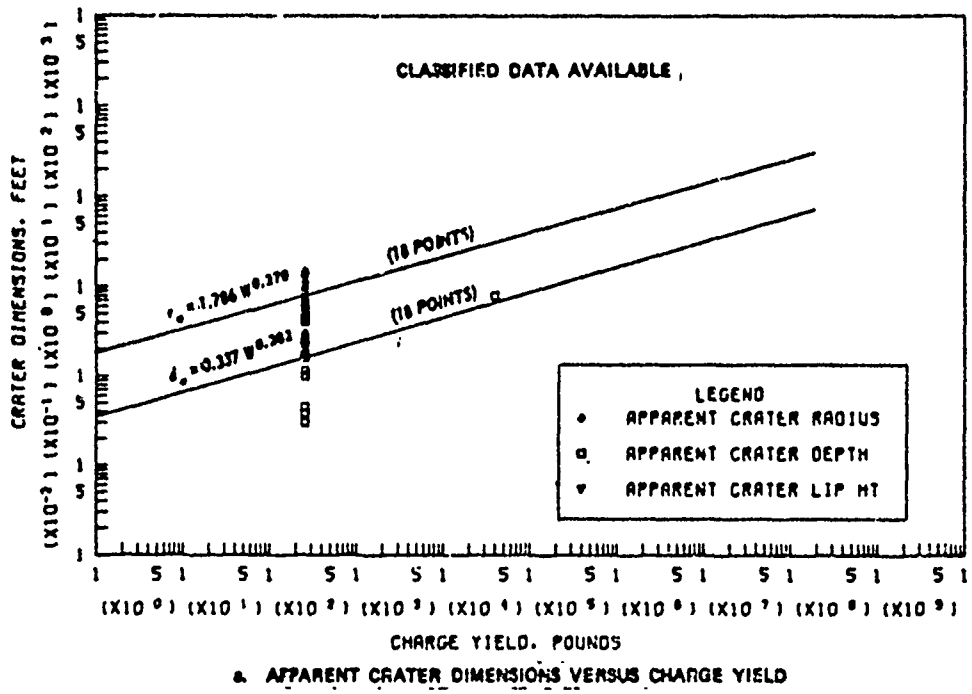

a. APPARENT CRATER DIMENSIONS VERSUS CHARGE YIELD

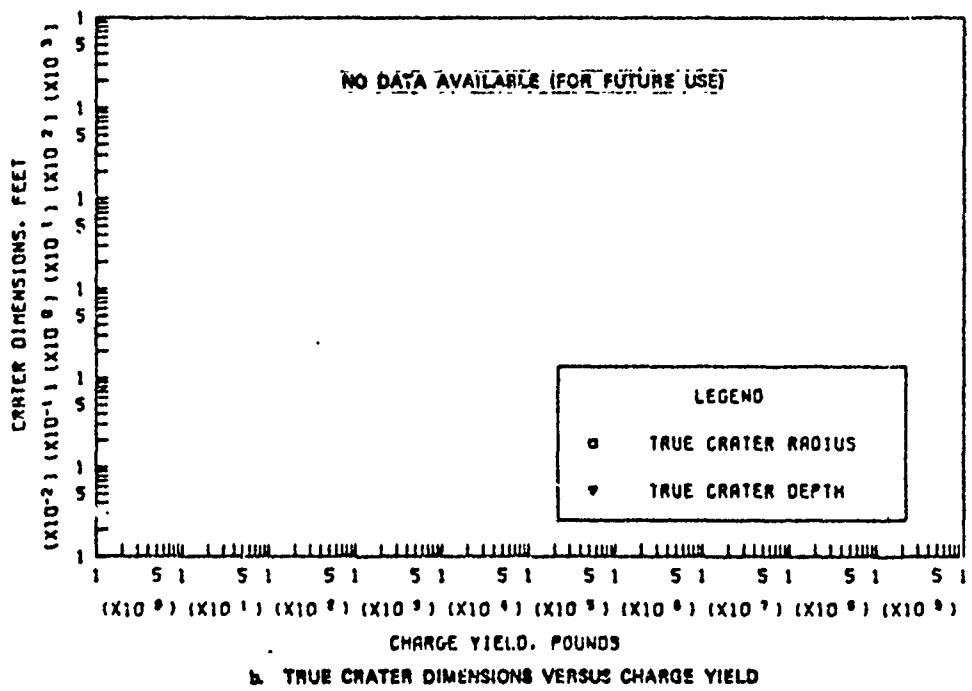

b. TRUE CRATER DIMENSIONS VERSUS CHARGE YIELD

Figure B.68 Dimensions of craters in desert alluvium for $Z \leq -2.00$ ft/lb$^{1/3}$, Category 10 (sheet 1 of 2).

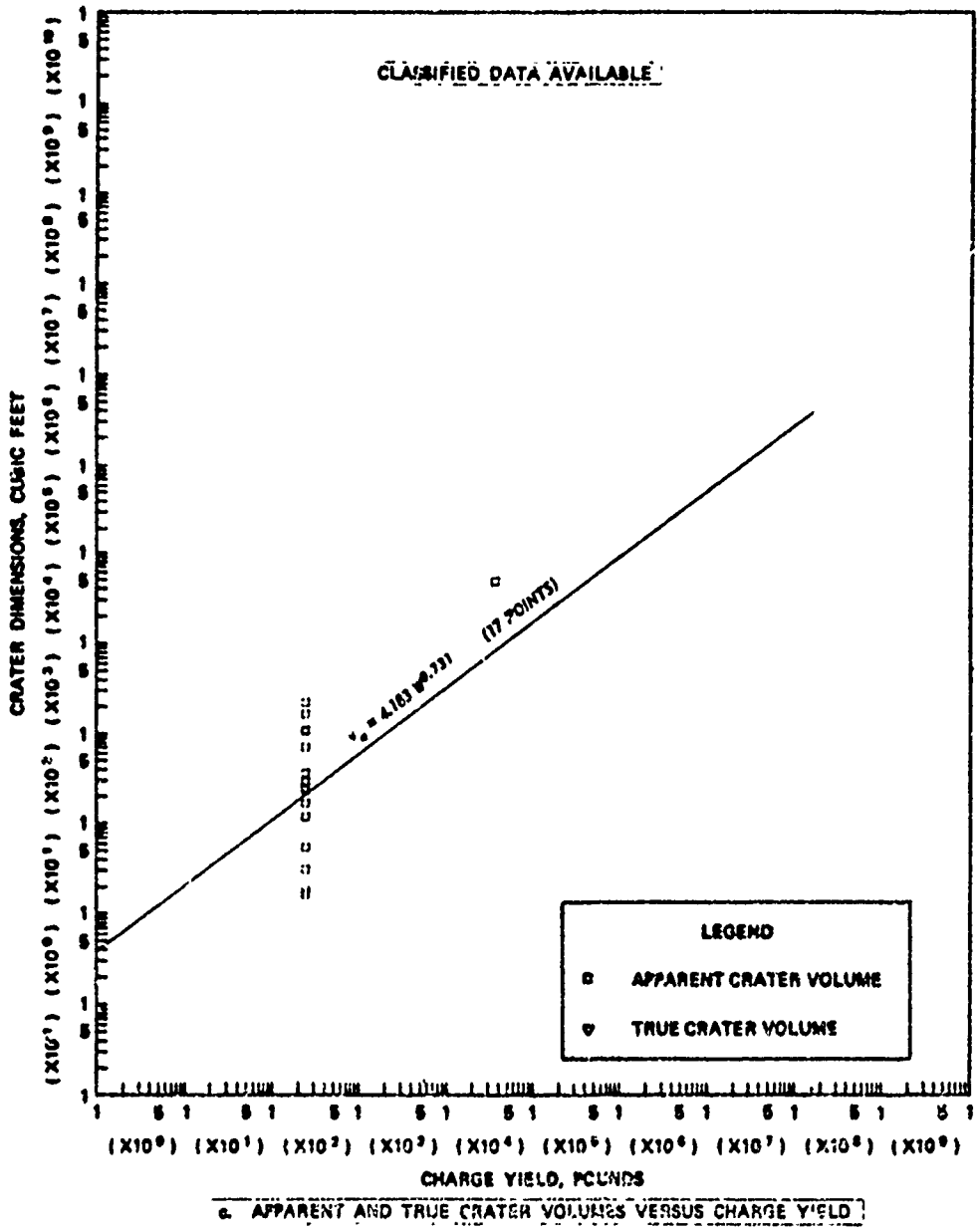

a. APPARENT AND TRUE CRATER VOLUMES VERSUS CHARGE YIELD

Figure B.68 (sheet 2 of 2).

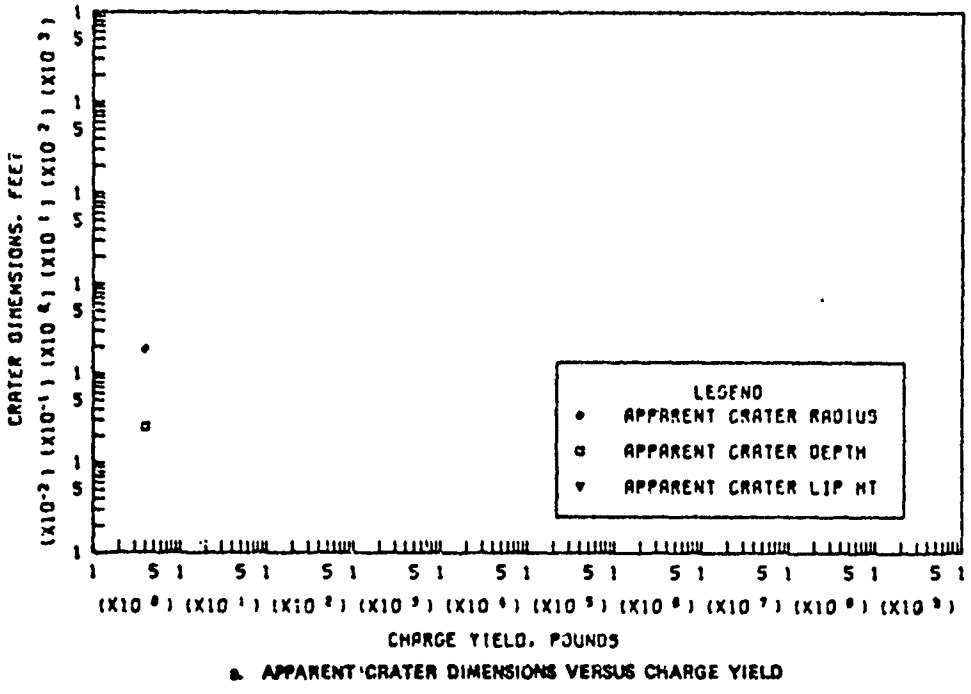

a. APPARENT CRATER DIMENSIONS VERSUS CHARGE YIELD

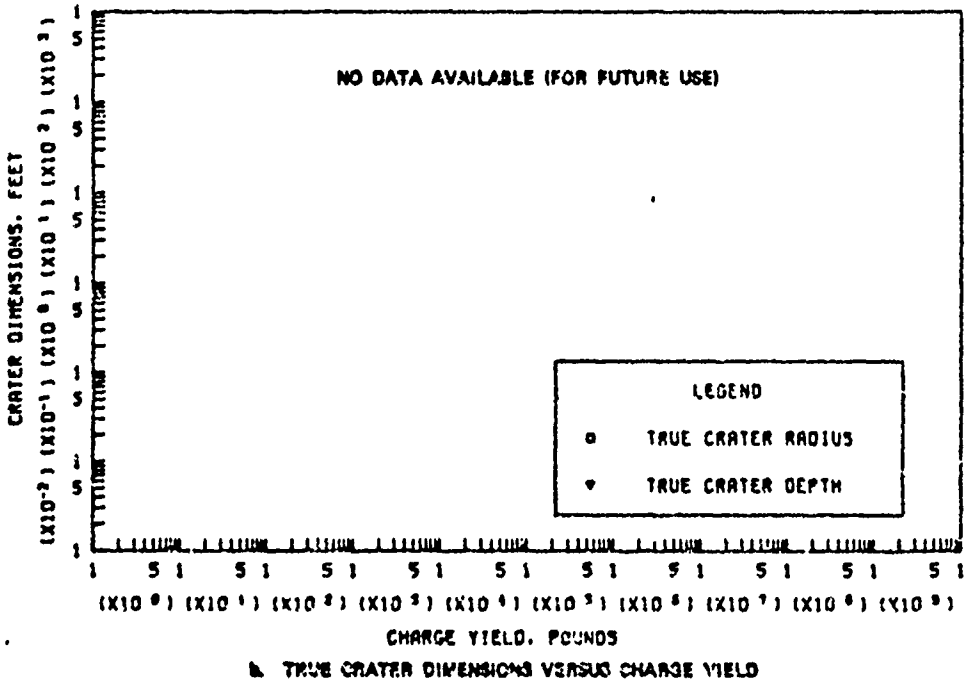

b. TRUE CRATER DIMENSIONS VERSUS CHARGE YIELD

Figure B.69 Dimensions of craters in moist sandy silt for $0.20 \leq Z < 0.50$ ft/lb$^{1/3}$, Category 2 (sheet 1 of 2).

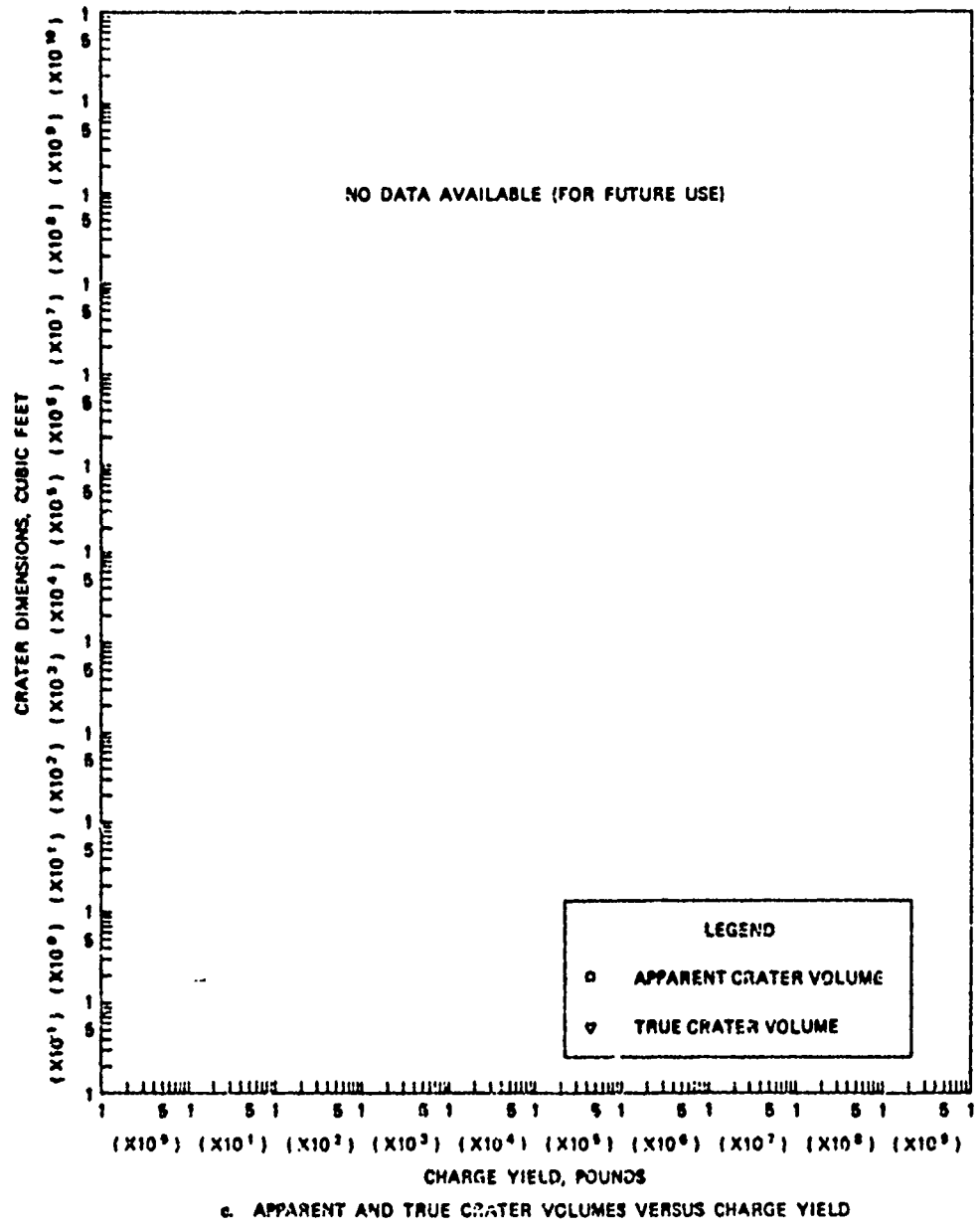

c. APPARENT AND TRUE CRATER VOLUMES VERSUS CHARGE YIELD

Figure B.69 (sheet 2 of 2).

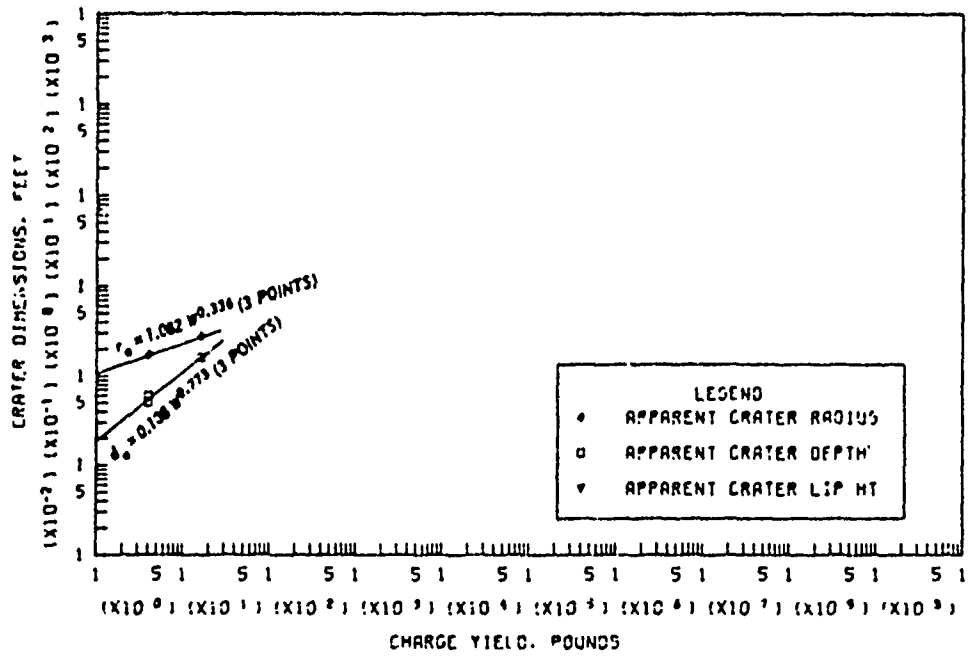

a. APPARENT CRATER DIMENSIONS VERSUS CHARGE YIELD

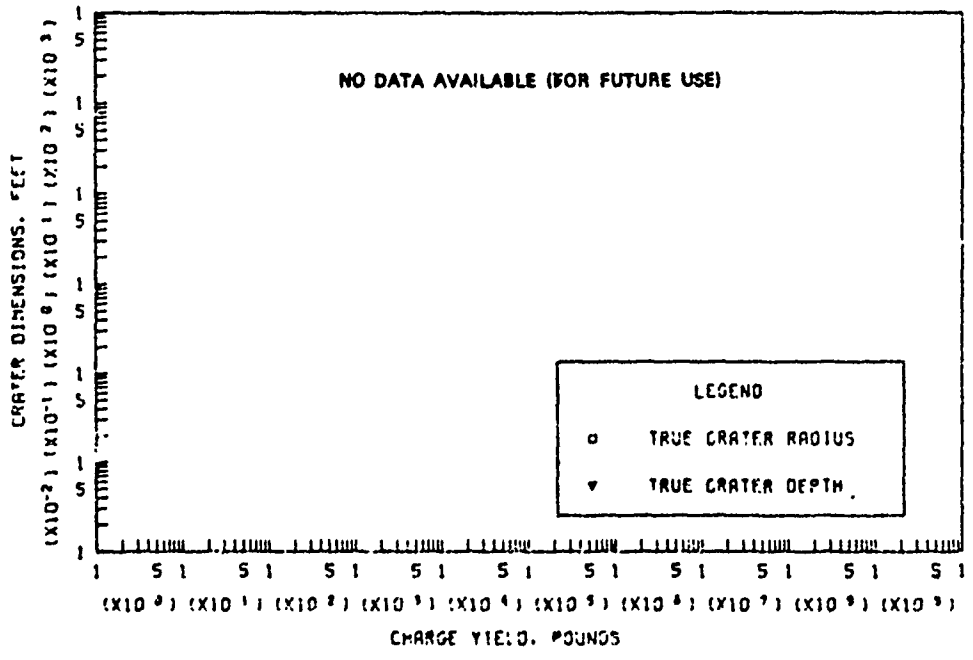

b. TRUE CRATER DIMENSIONS VERSUS CHARGE YIELD

Figure B.70 Dimensions of craters in moist sandy silt for $0.05 \leq Z < 0.20$ ft/lb$^{1/3}$, Category 3 (sheet 1 of 2).

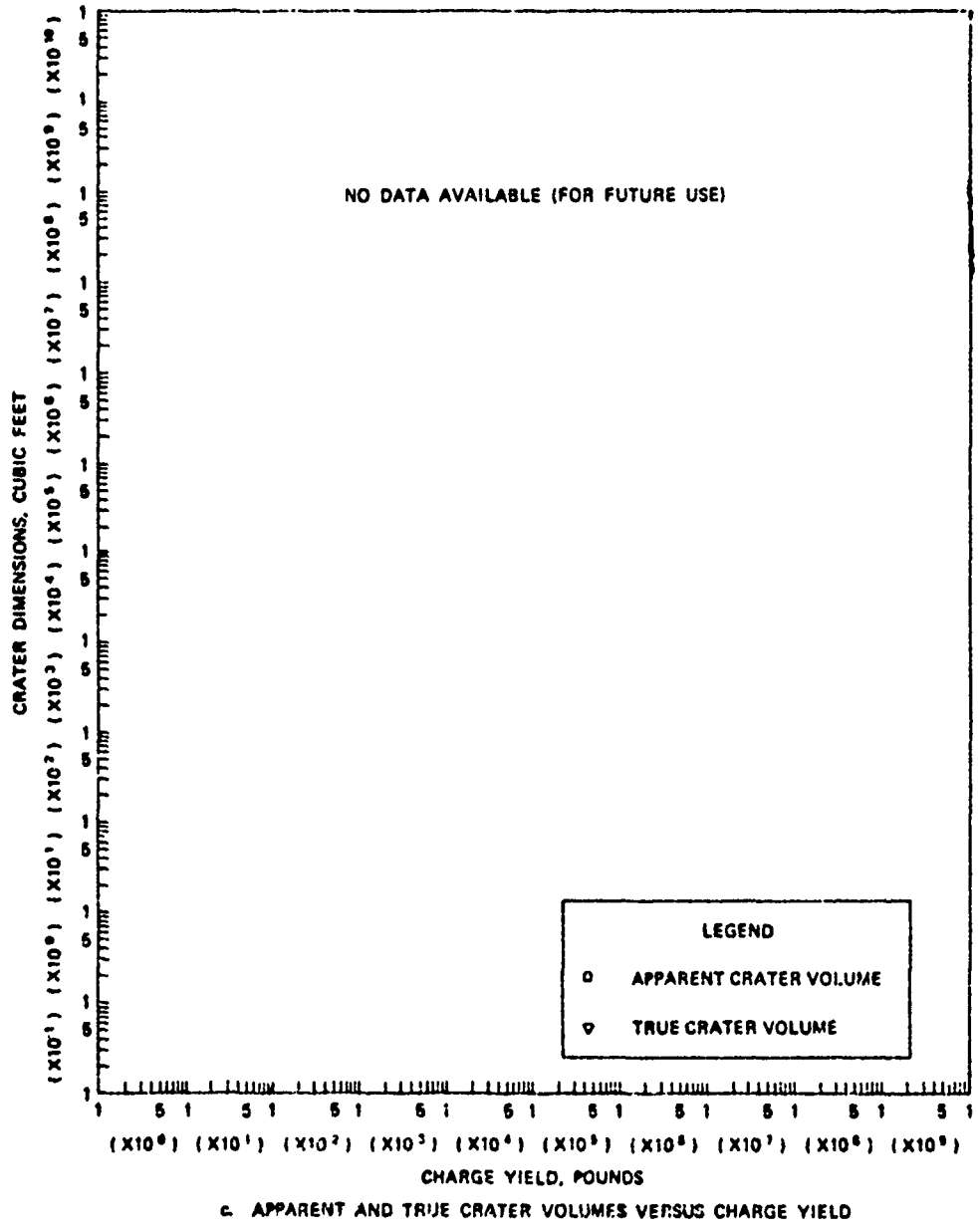

c. APPARENT AND TRUE CRATER VOLUMES VERSUS CHARGE YIELD

Figure B.70 (sheet 2 of 2).

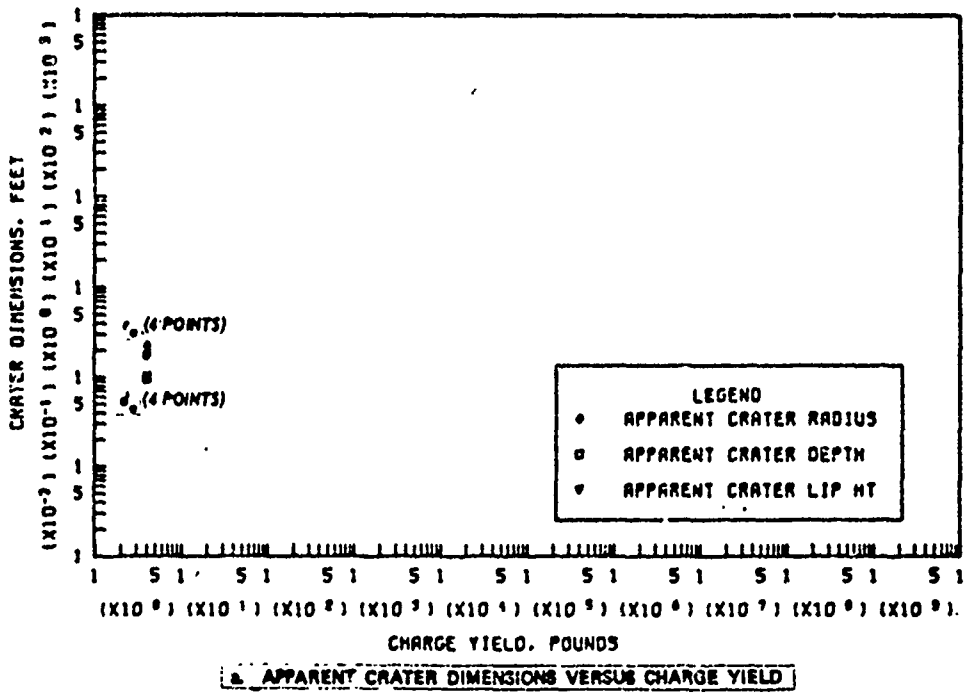

a. APPARENT CRATER DIMENSIONS VERSUS CHARGE YIELD

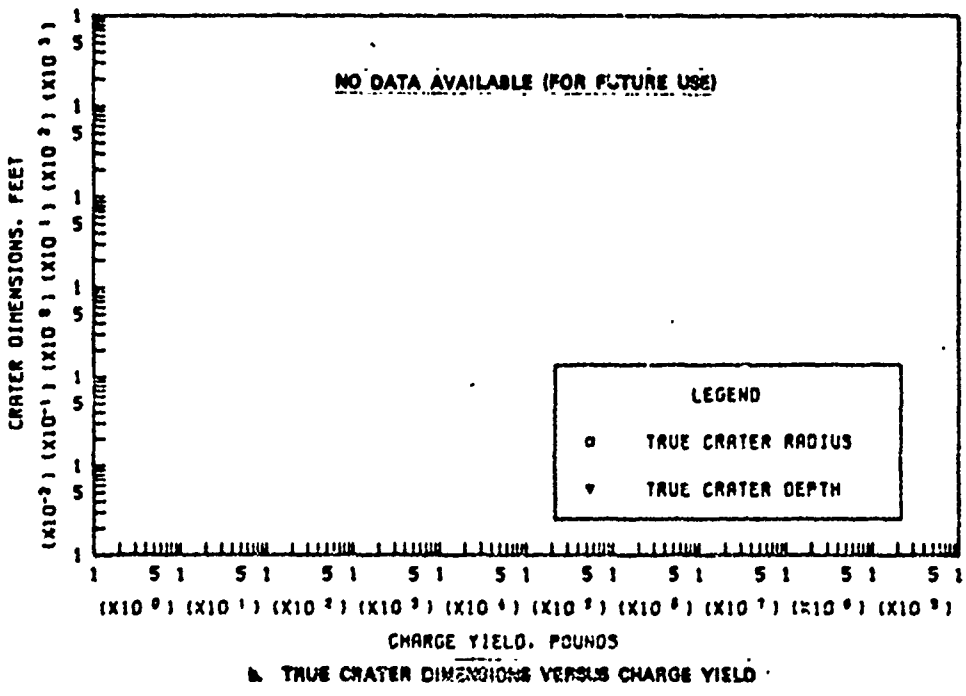

b. TRUE CRATER DIMENSIONS VERSUS CHARGE YIELD

Figure B.71 Dimensions of craters in moist sandy silt for $-0.05 \leq Z < 0.05$ ft/lb$^{1/3}$, Category 4 (sheet 1 of 2).

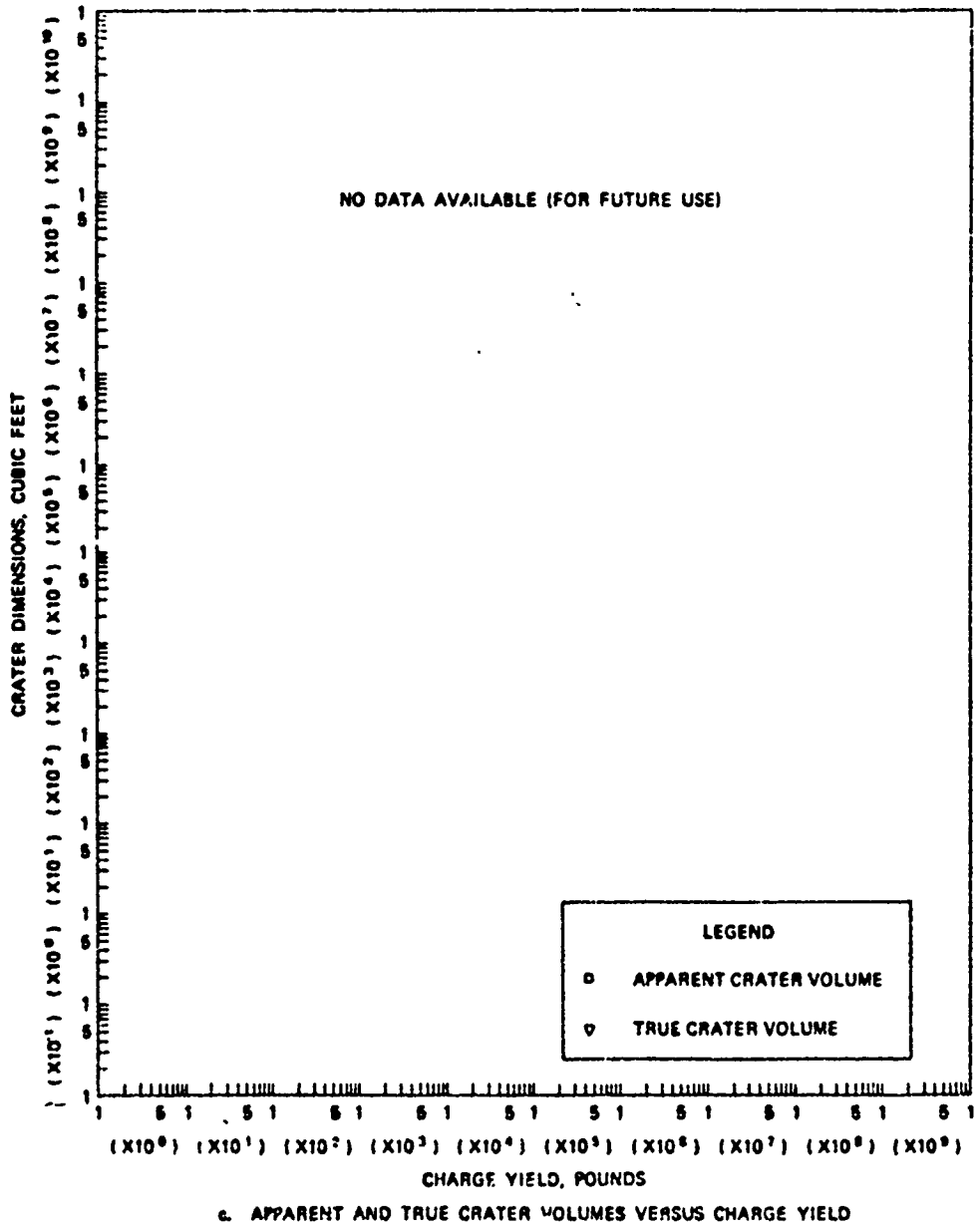

c. APPARENT AND TRUE CRATER VOLUMES VERSUS CHARGE YIELD

Figure B.71 (sheet 2 of 2).

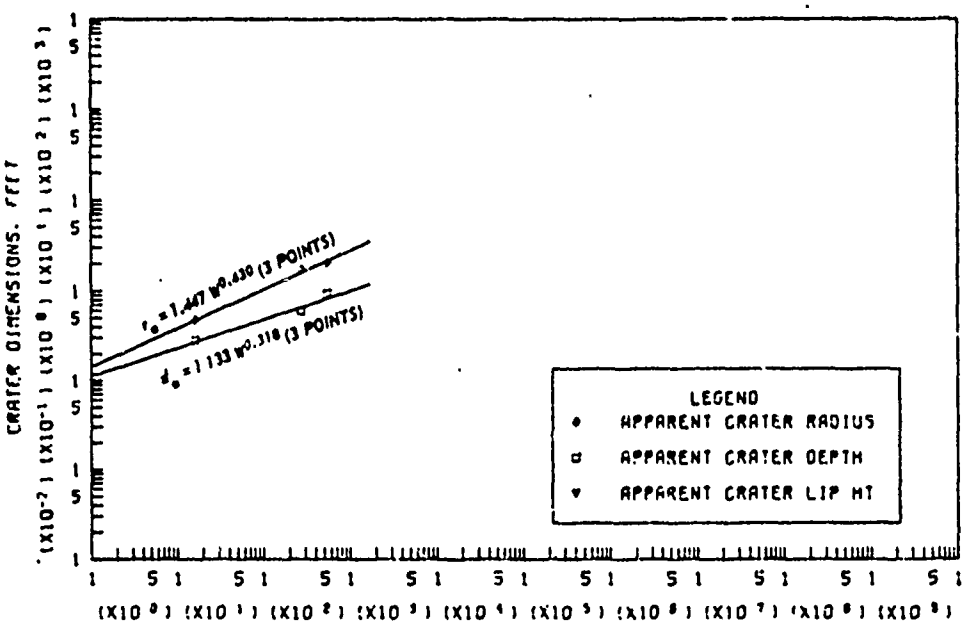

a. APPARENT CRATER DIMENSIONS VERSUS CHARGE YIELD

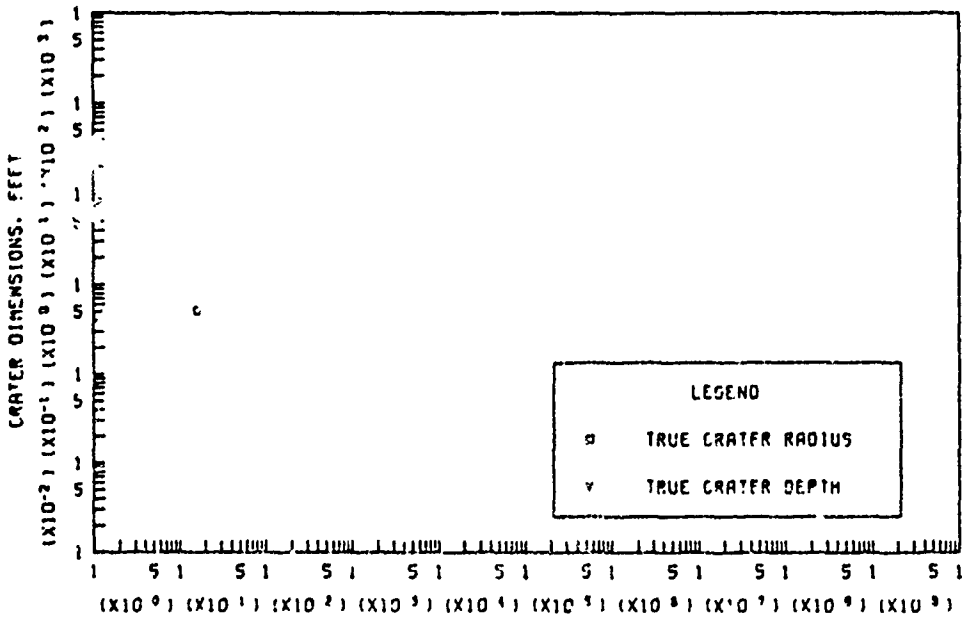

b. TRUE CRATER DIMENSIONS VERSUS CHARGE YIELD

Figure B.72 Dimensions of craters in moist sandy silt for $-0.90 \leq Z < -0.50$ ft/lb$^{1/3}$, Category 7 (sheet 1 of 2).

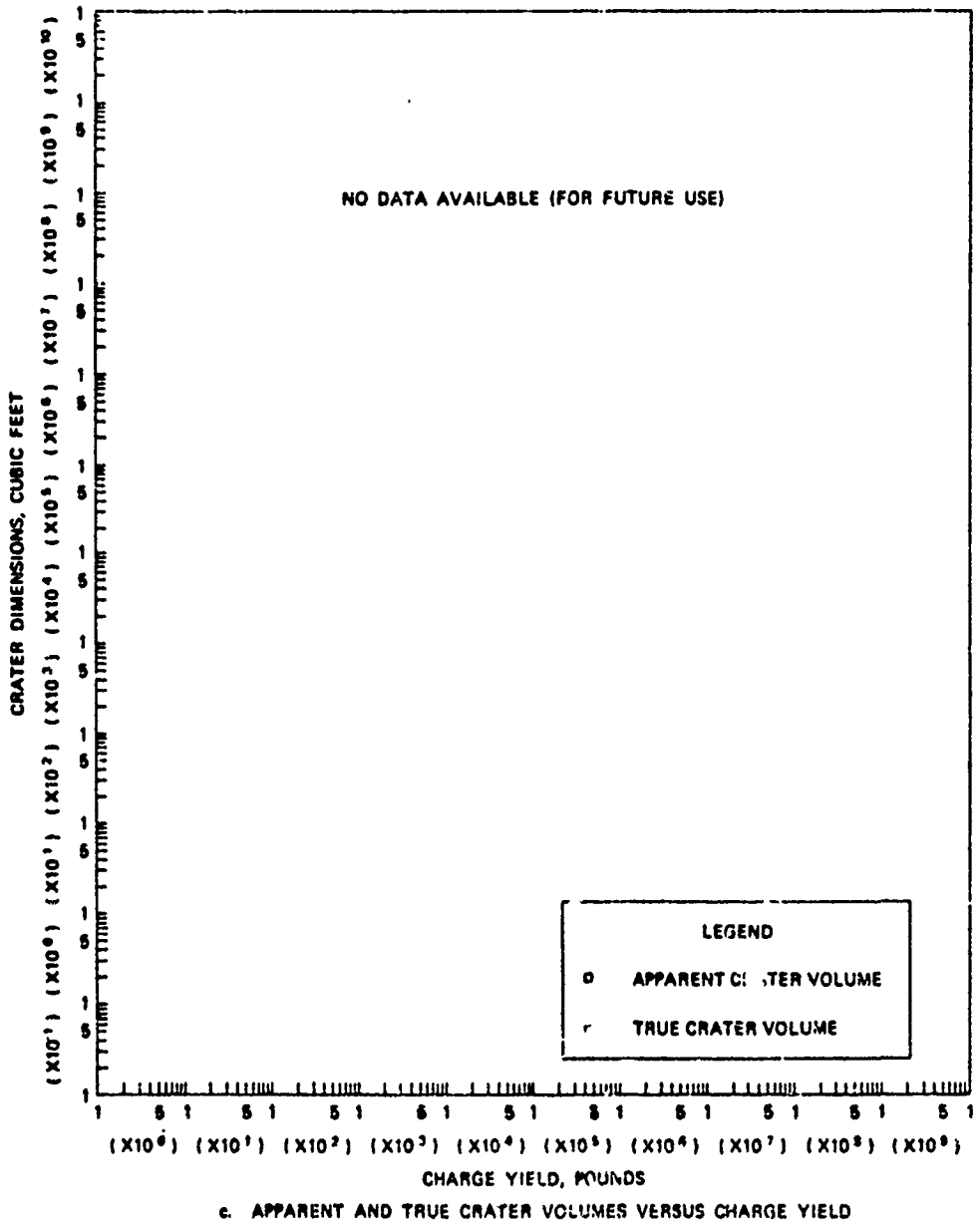

c. APPARENT AND TRUE CRATER VOLUMES VERSUS CHARGE YIELD

Figure B.72 (sheet 2 of 2).

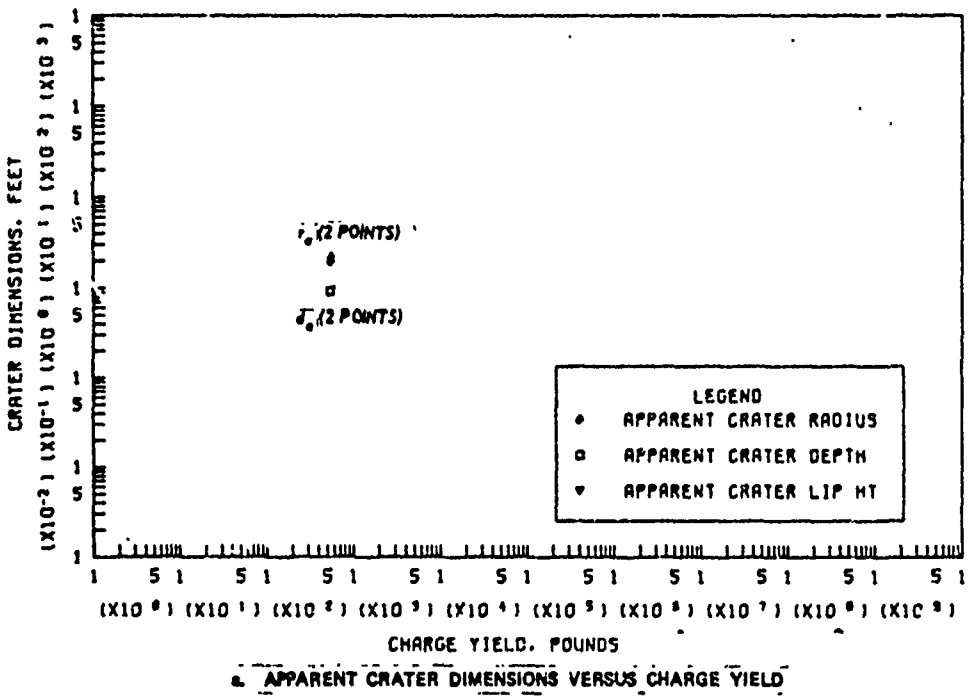

a. APPARENT CRATER DIMENSIONS VERSUS CHARGE YIELD

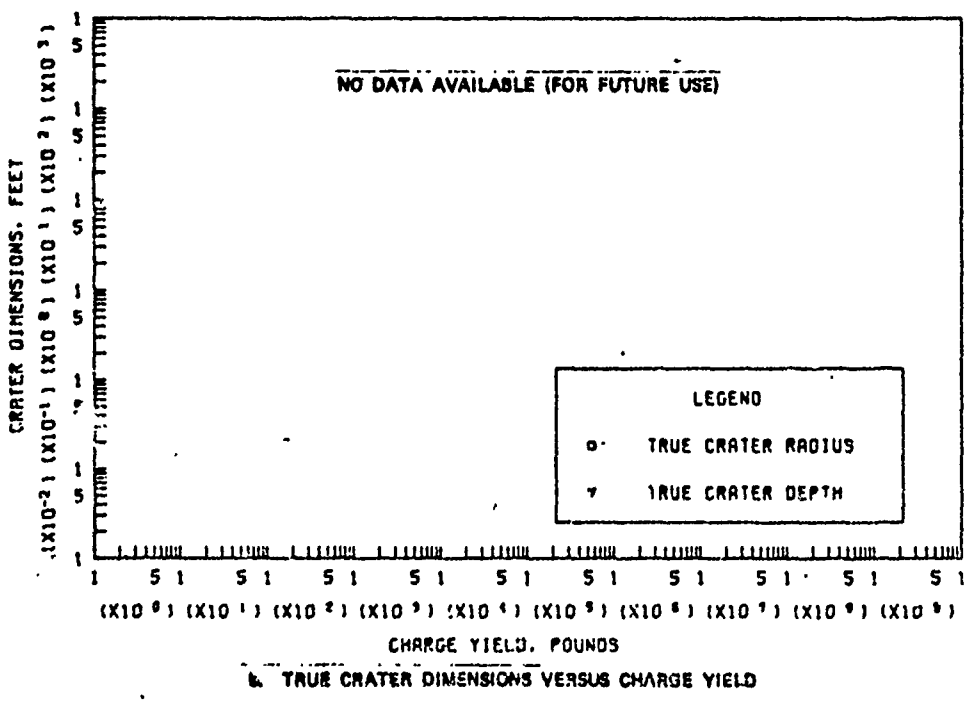

b. TRUE CRATER DIMENSIONS VERSUS CHARGE YIELD

Figure B.73 Dimensions of craters in moist sandy silt for $-1.10 \leq Z < -0.90$ ft/lb$^{1/3}$, Category 8 (sheet 1 of 2).

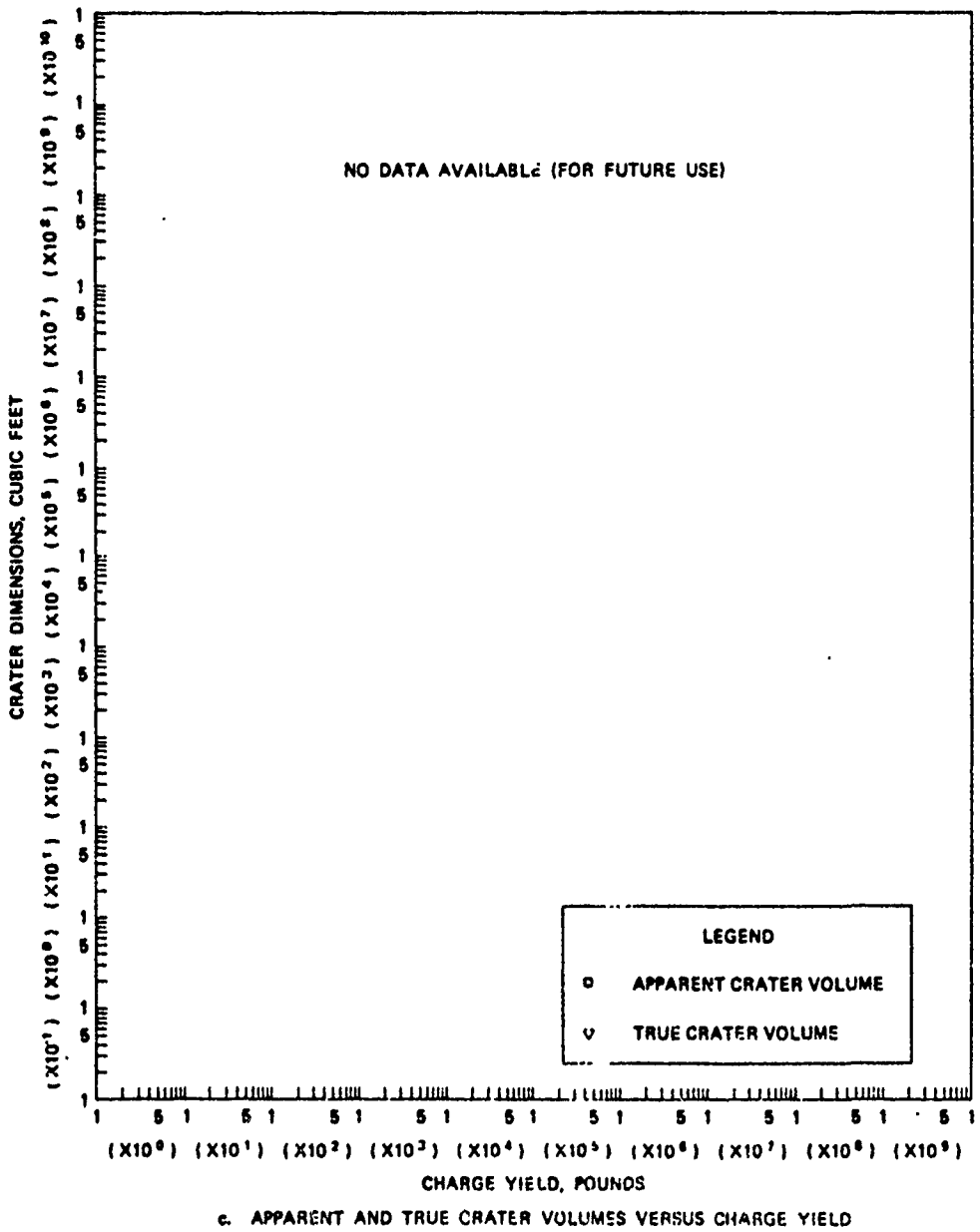

c. APPARENT AND TRUE CRATER VOLUMES VERSUS CHARGE YIELD

Figure B.73 (sheet 2 of 2).

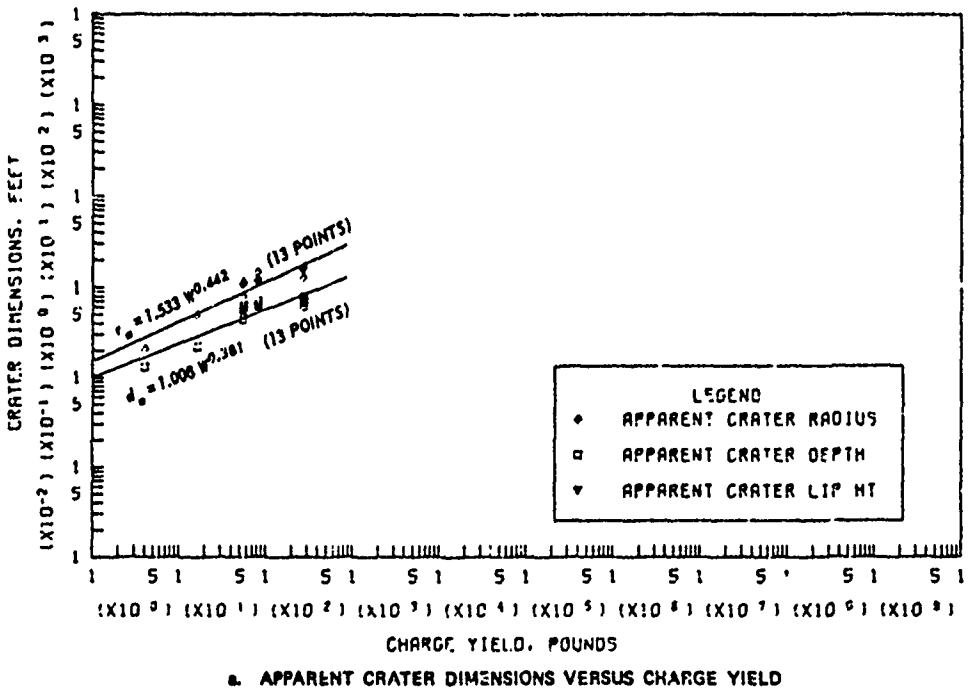

a. APPARENT CRATER DIMENSIONS VERSUS CHARGE YIELD

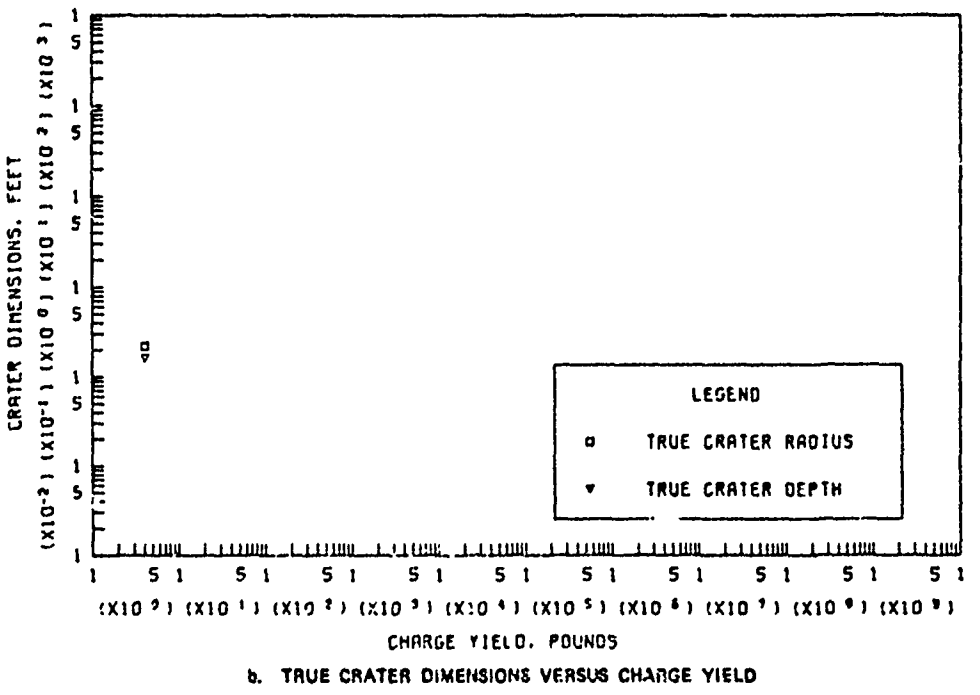

b. TRUE CRATER DIMENSIONS VERSUS CHARGE YIELD

Figure B.74 Dimensions of craters in moist sandy silt for $-2.00 \leq Z < -1.10$ ft/lb$^{1/3}$, Category 9 (sheet 1 of 2).

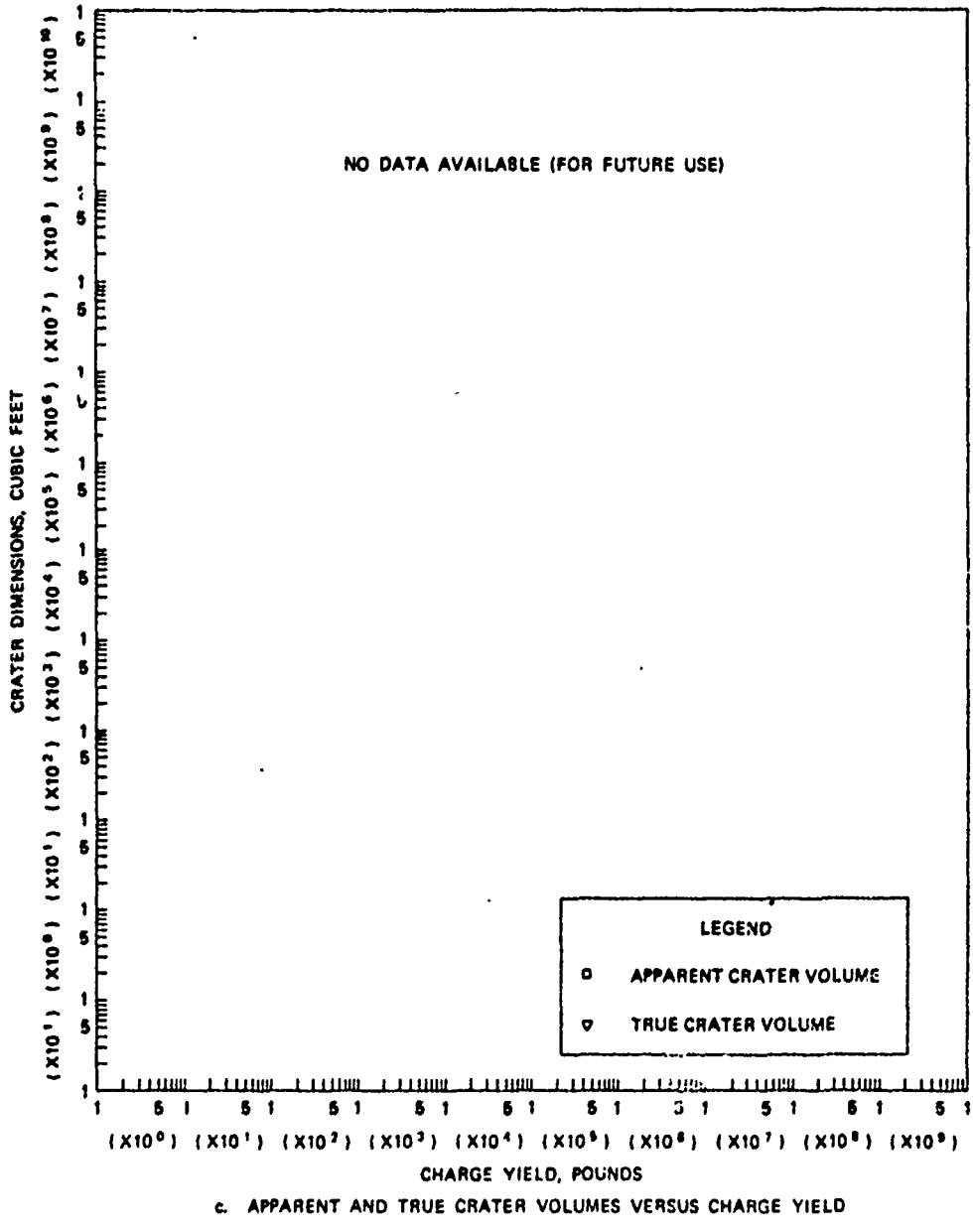

c. APPARENT AND TRUE CRATER VOLUMES VERSUS CHARGE YIELD

Figure B.74 (sheet 2 of 2).

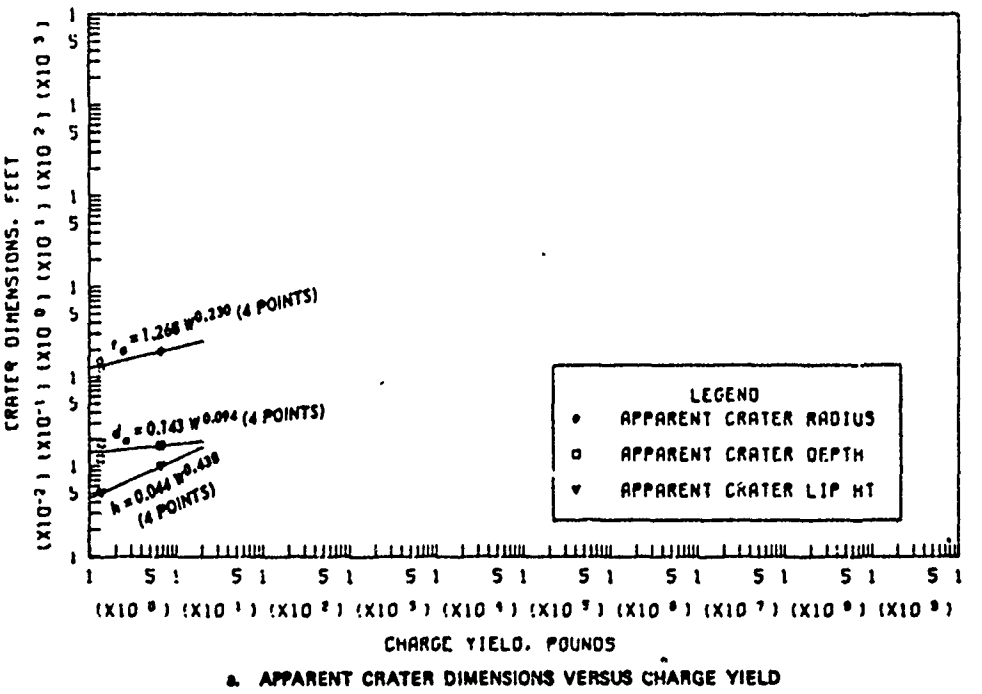

a. APPARENT CRATER DIMENSIONS VERSUS CHARGE YIELD

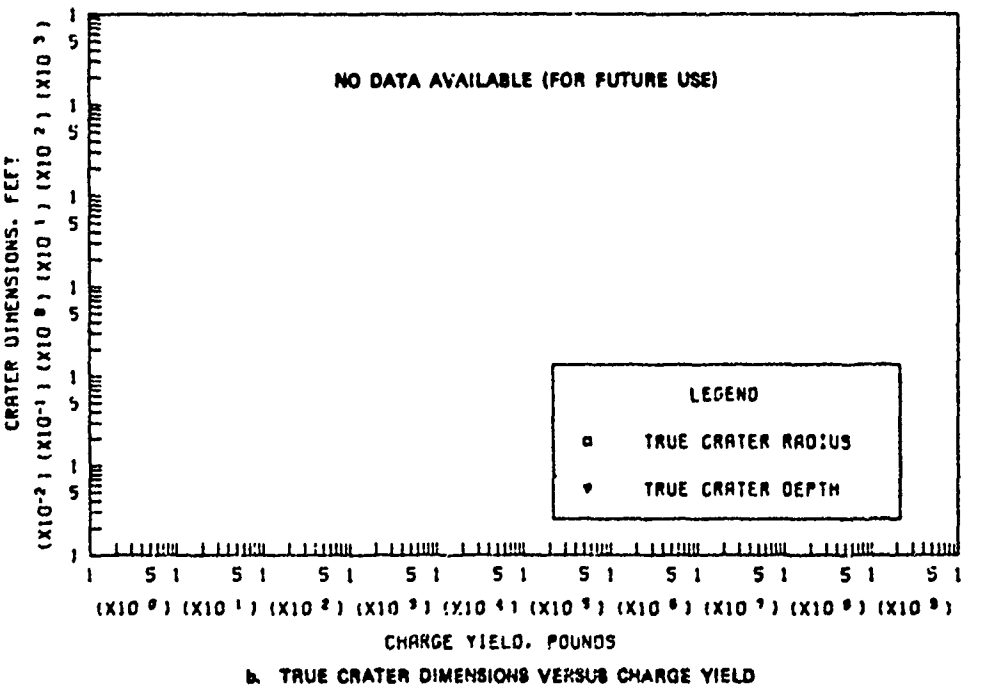

b. TRUE CRATER DIMENSIONS VERSUS CHARGE YIELD

Figure B.75 Dimensions of craters in dry-to-moist sand for $0.50 < Z$ ft/lb$^{1/3}$, Category 1 (sheet 1 of 2).

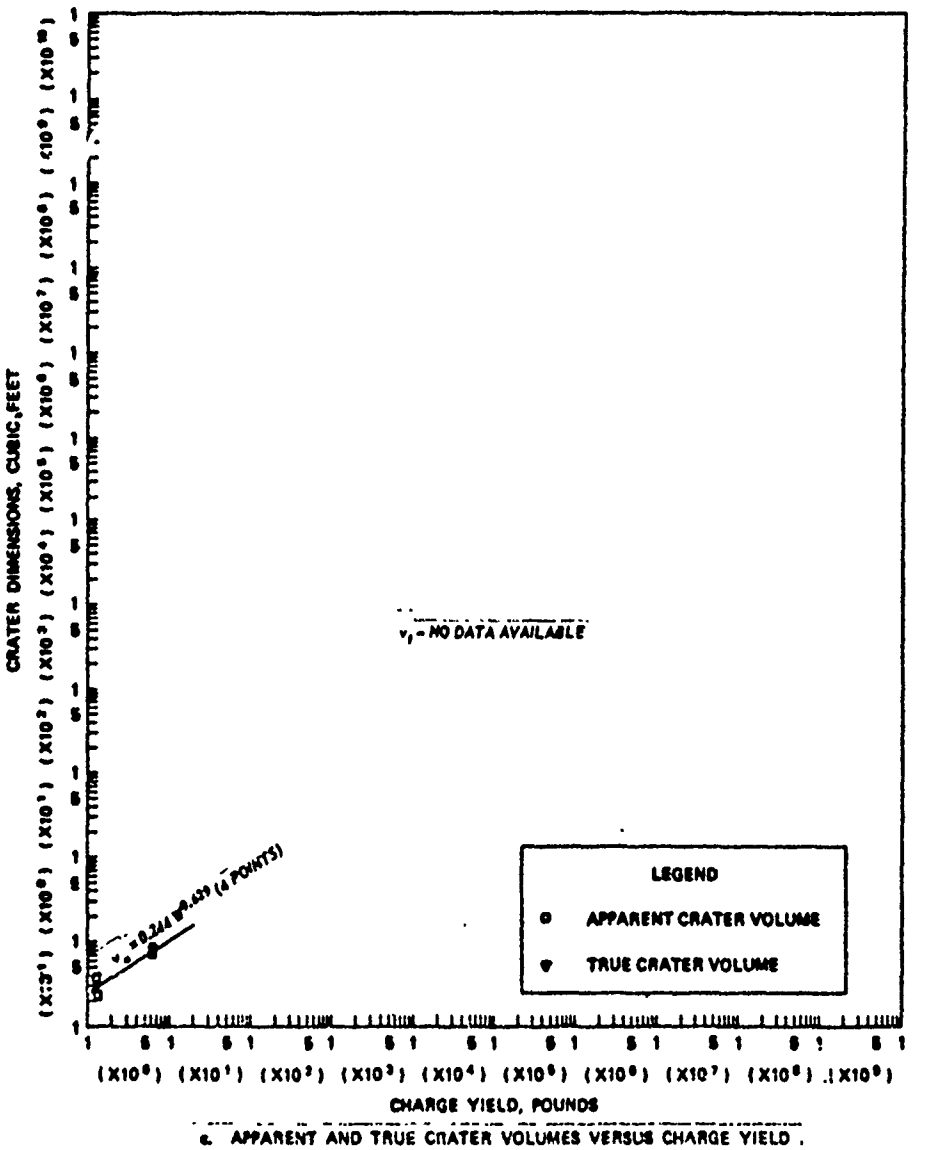

c. APPARENT AND TRUE CRATER VOLUMES VERSUS CHARGE YIELD.

Figure B.75 (sheet 2 of 2).

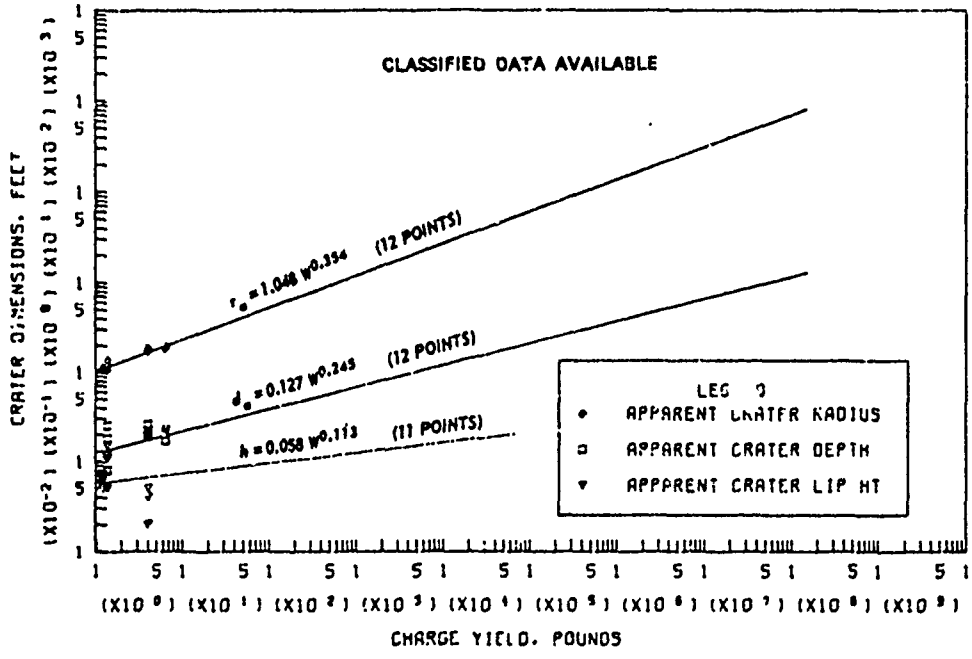

a. APPARENT CRATER DIMENSIONS VERSUS CHARGE YIELD

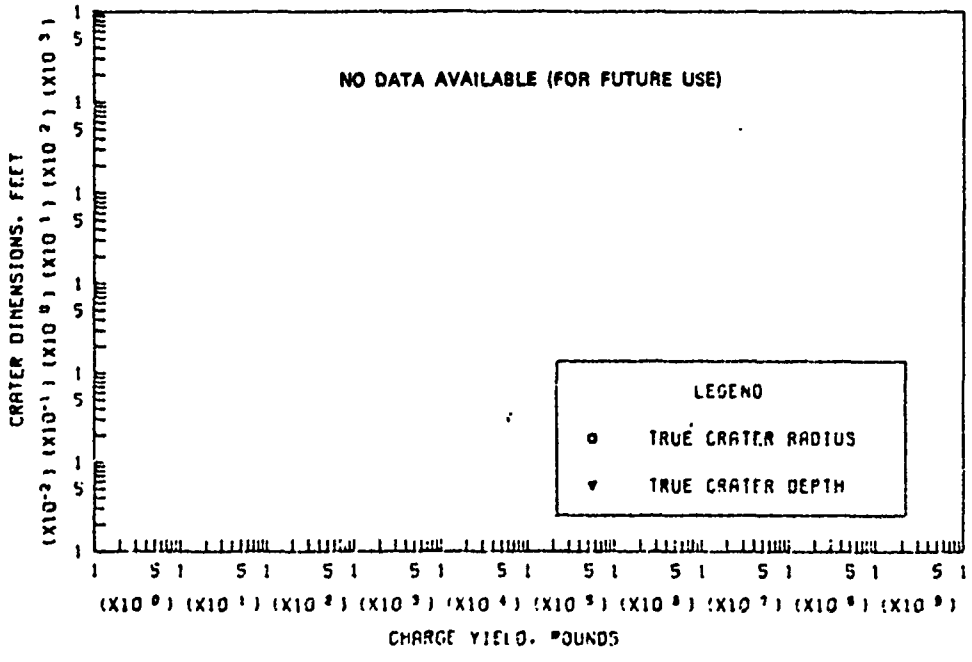

b. TRUE CRATER DIMENSIONS VERSUS CHARGE YIELD

Figure B.76 Dimensions of craters in dry-to-moist sand for $0.20 \leq Z < 0.50$ ft/lb$^{1/3}$, Category 2 (sheet 1 of 2).

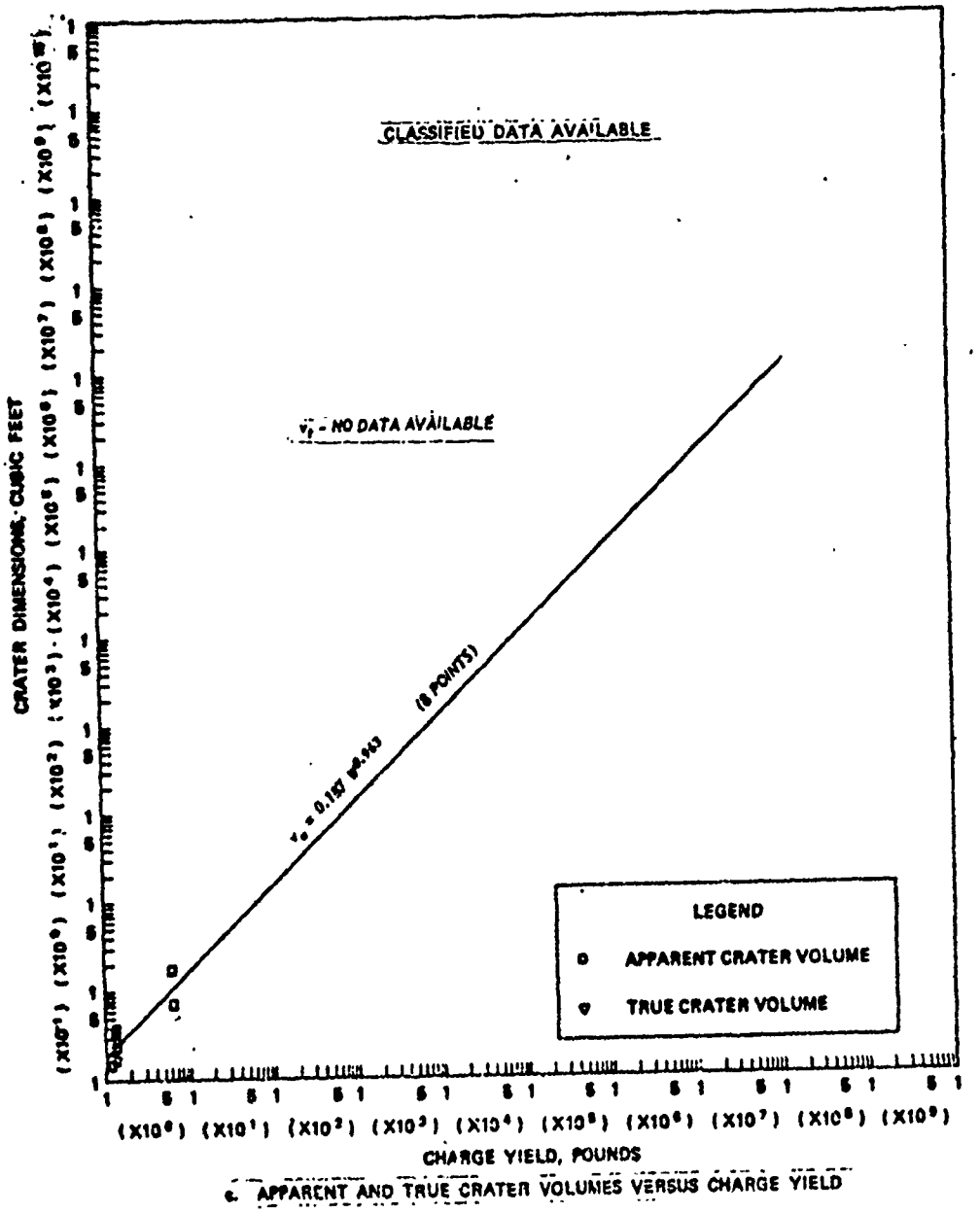

c. APPARENT AND TRUE CRATER VOLUMES VERSUS CHARGE YIELD

Figure B.76 (sheet 2 of 2).

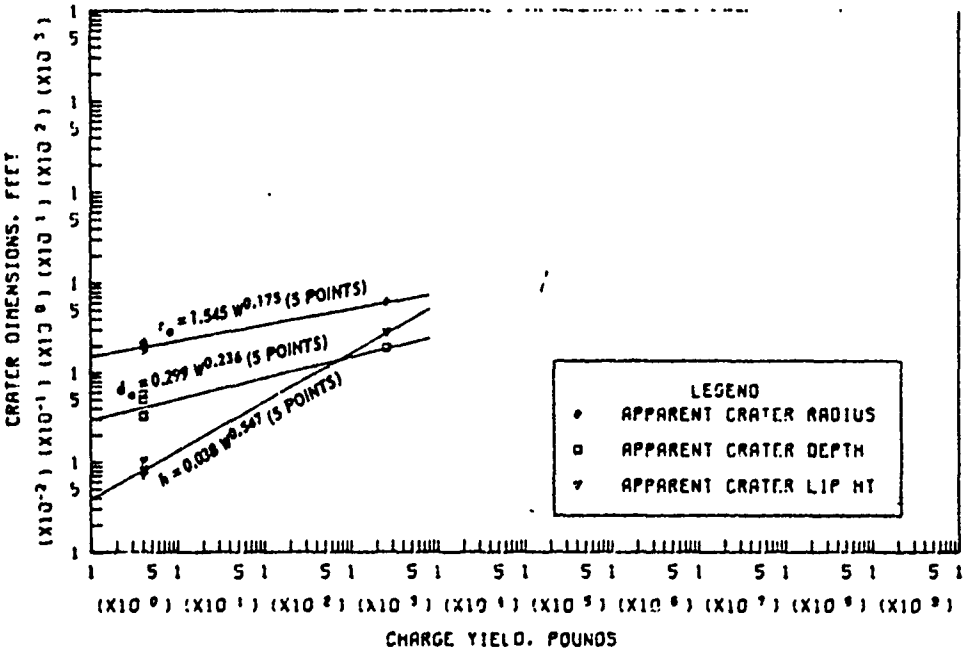

a. APPARENT CRATER DIMENSIONS VERSUS CHARGE YIELD

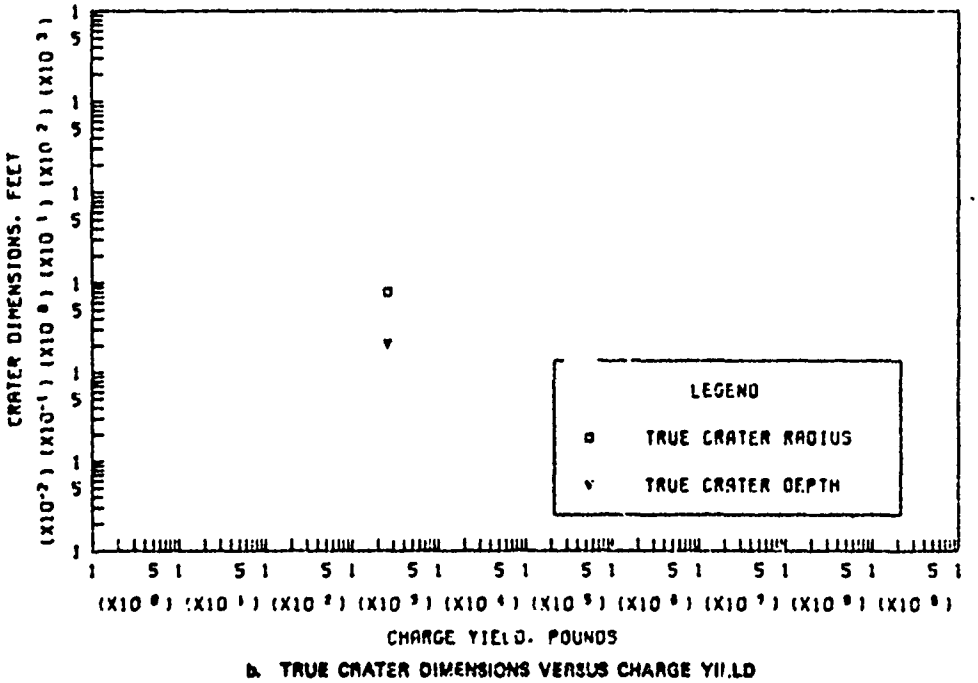

b. TRUE CRATER DIMENSIONS VERSUS CHARGE YIELD

Figure B.77 Dimensions of craters in dry-to-moist sand for $0.05 \leq Z < 0.20$ ft/lb$^{1/3}$, Category 3 (sheet 1 of 2).

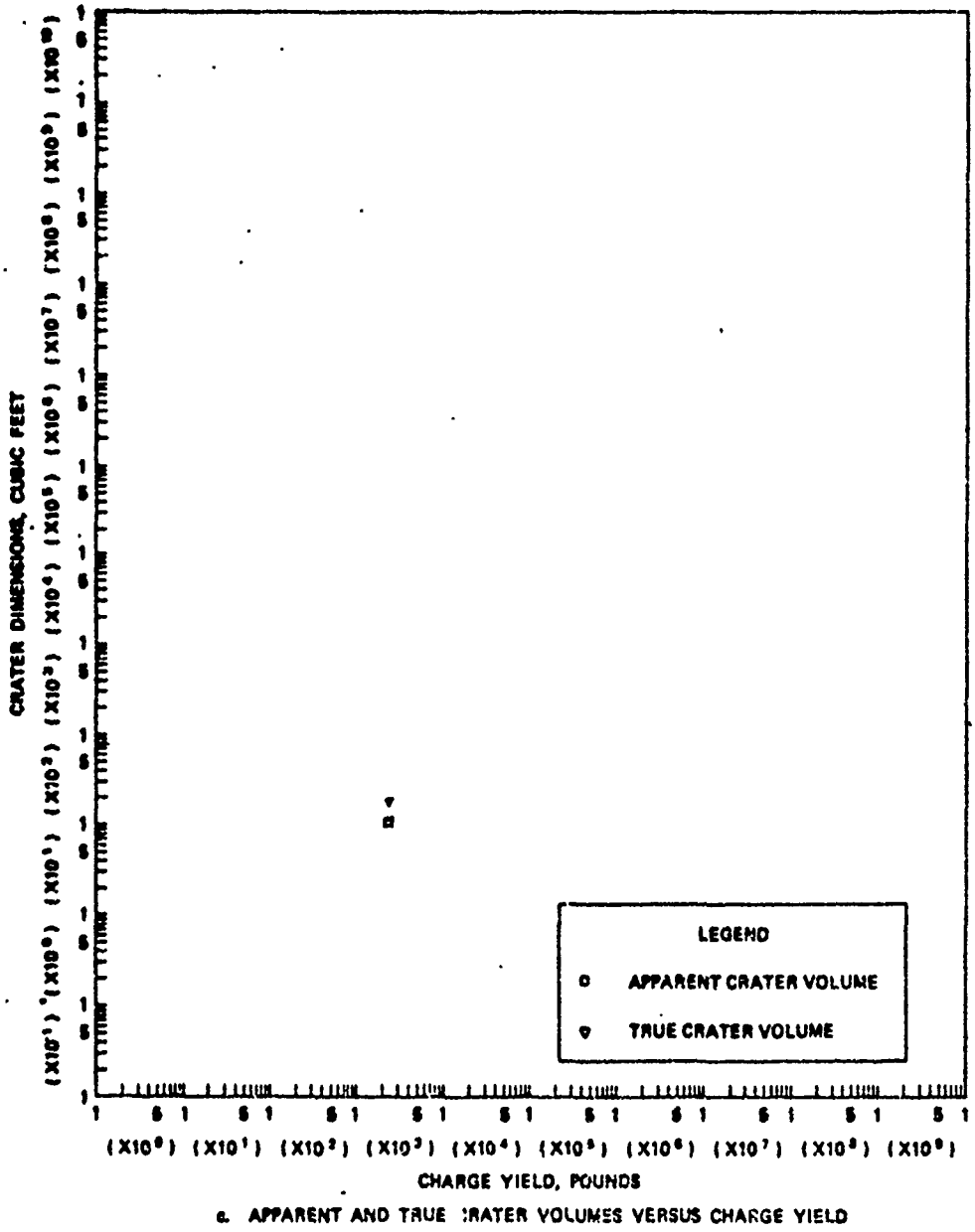

a. APPARENT AND TRUE CRATER VOLUMES VERSUS CHARGE YIELD

Figure B.77 (sheet 2 of 2).

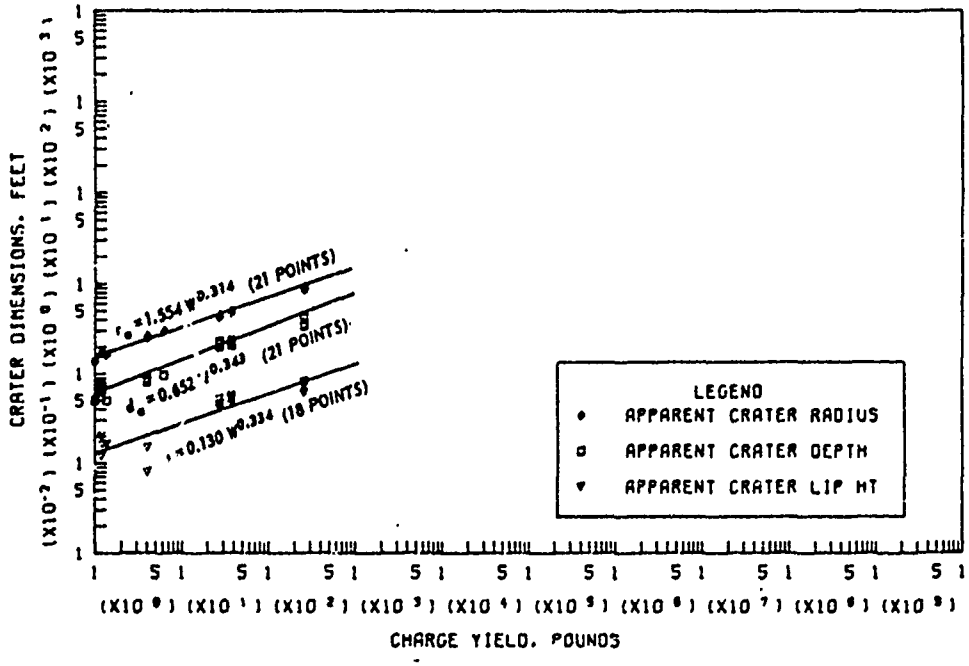

a. APPARENT CRATER DIMENSIONS VERSUS CHARGE YIELD

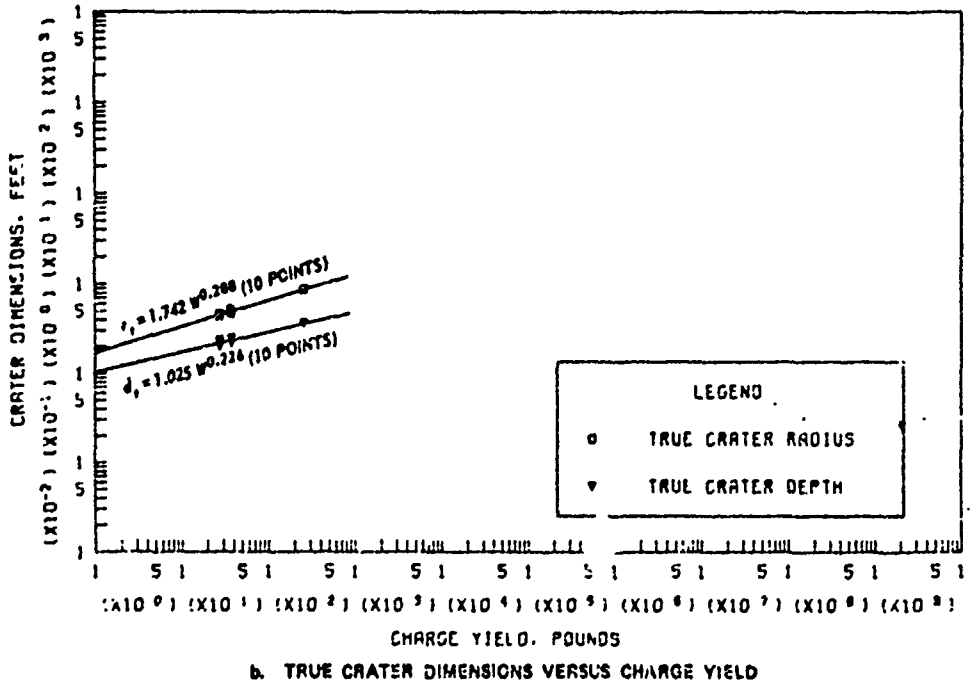

b. TRUE CRATER DIMENSIONS VERSUS CHARGE YIELD

Figure B.78 Dimensions of craters in dry-to-moist sand for $-0.05 \leq Z < 0.05$ ft/lb$^{1/3}$, Category 4 (sheet 1 of 2).

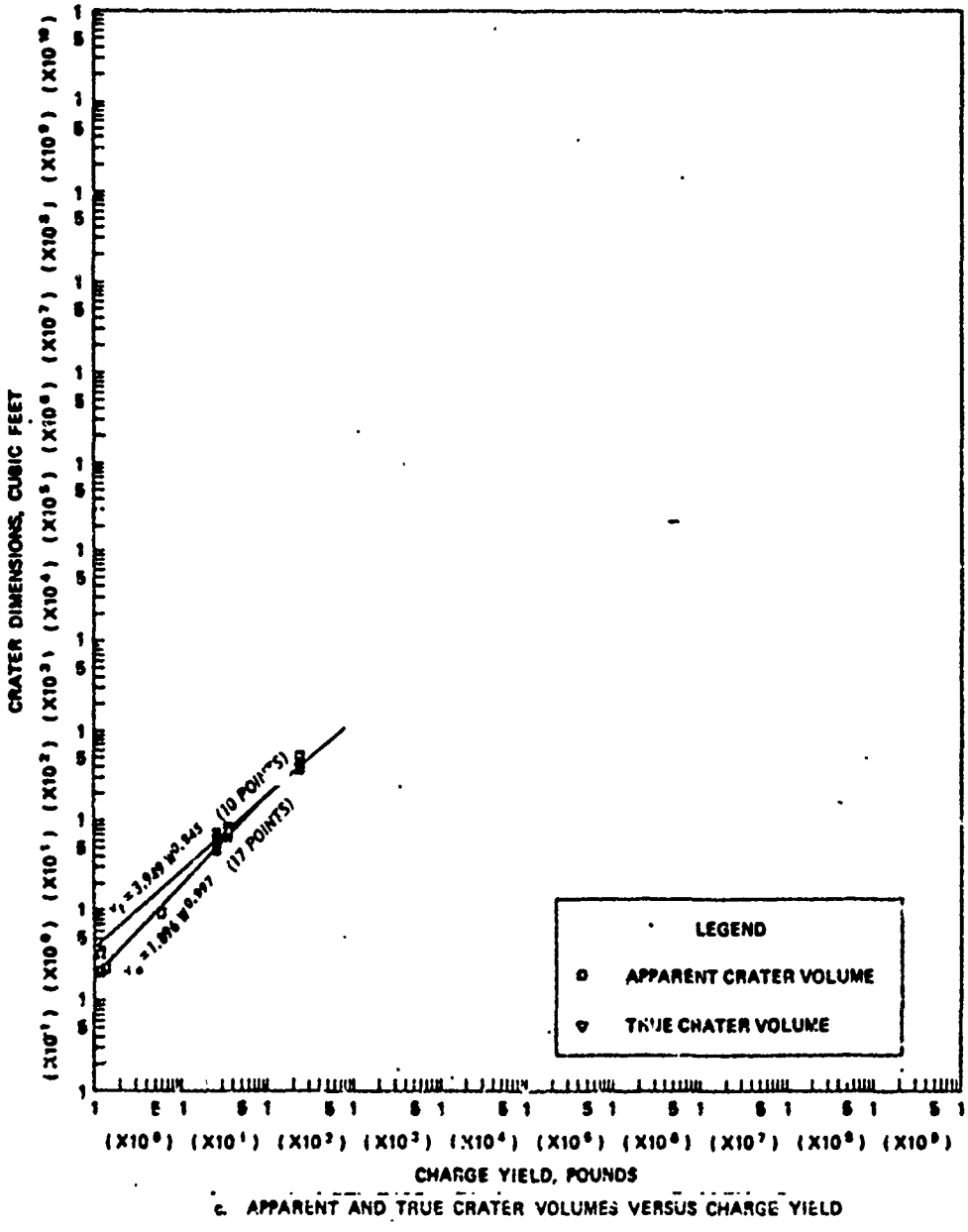

c. APPARENT AND TRUE CRATER VOLUMES VERSUS CHARGE YIELD

Figure 3.78 (sheet 2 of 2).

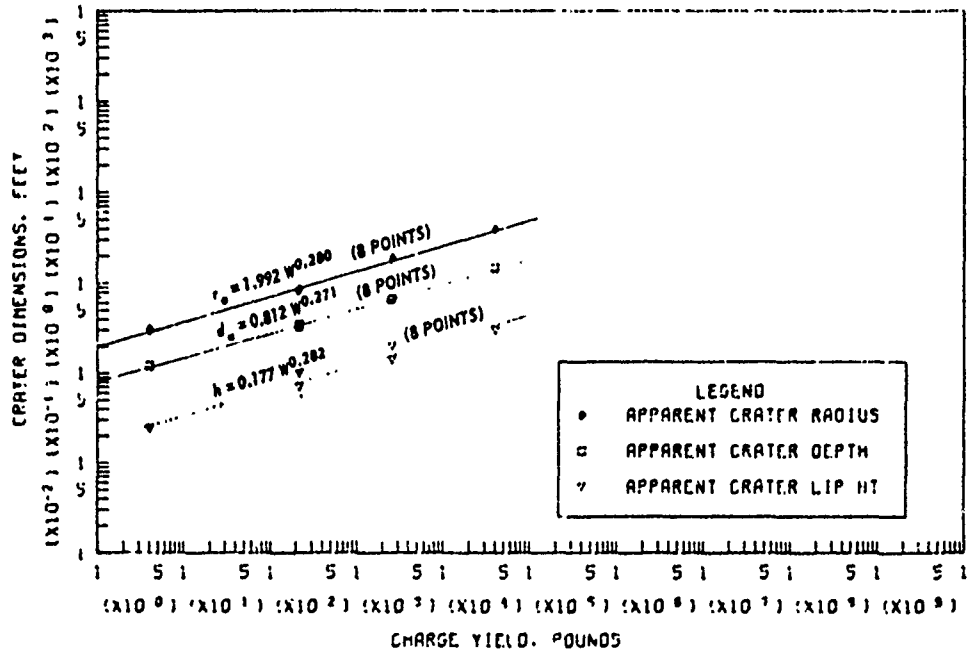

a. APPARENT CRATER DIMENSIONS VERSUS CHARGE YIELD

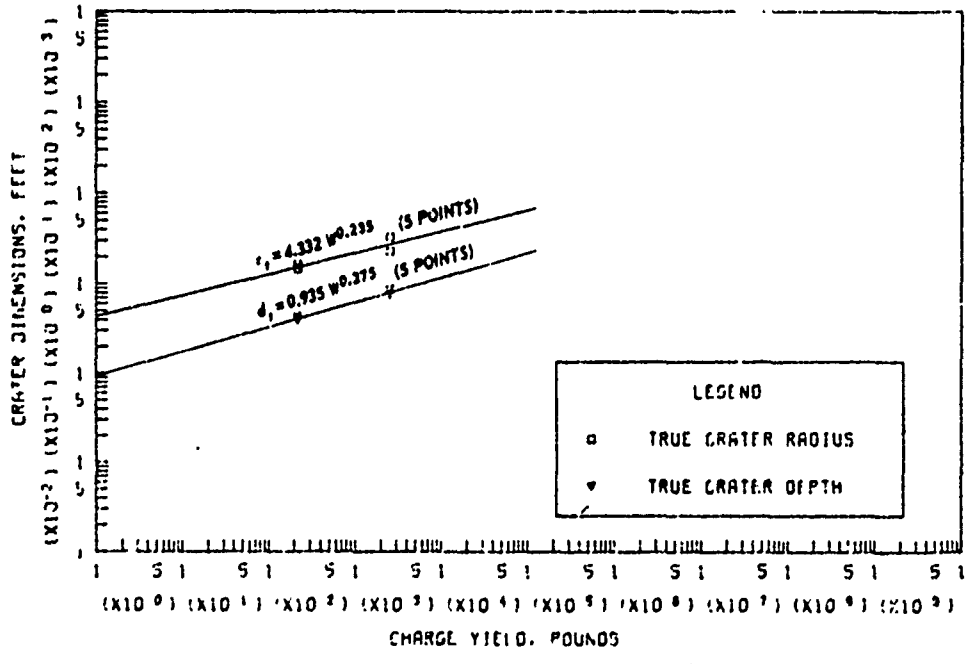

b. TRUE CRATER DIMENSIONS VERSUS CHARGE YIELD

Figure B.79 Dimensions of craters in dry-to-moist sand for $-0.20 \leq Z < -0.05$ ft/lb$^{1/3}$, Category 5 (sheet 1 of 2).

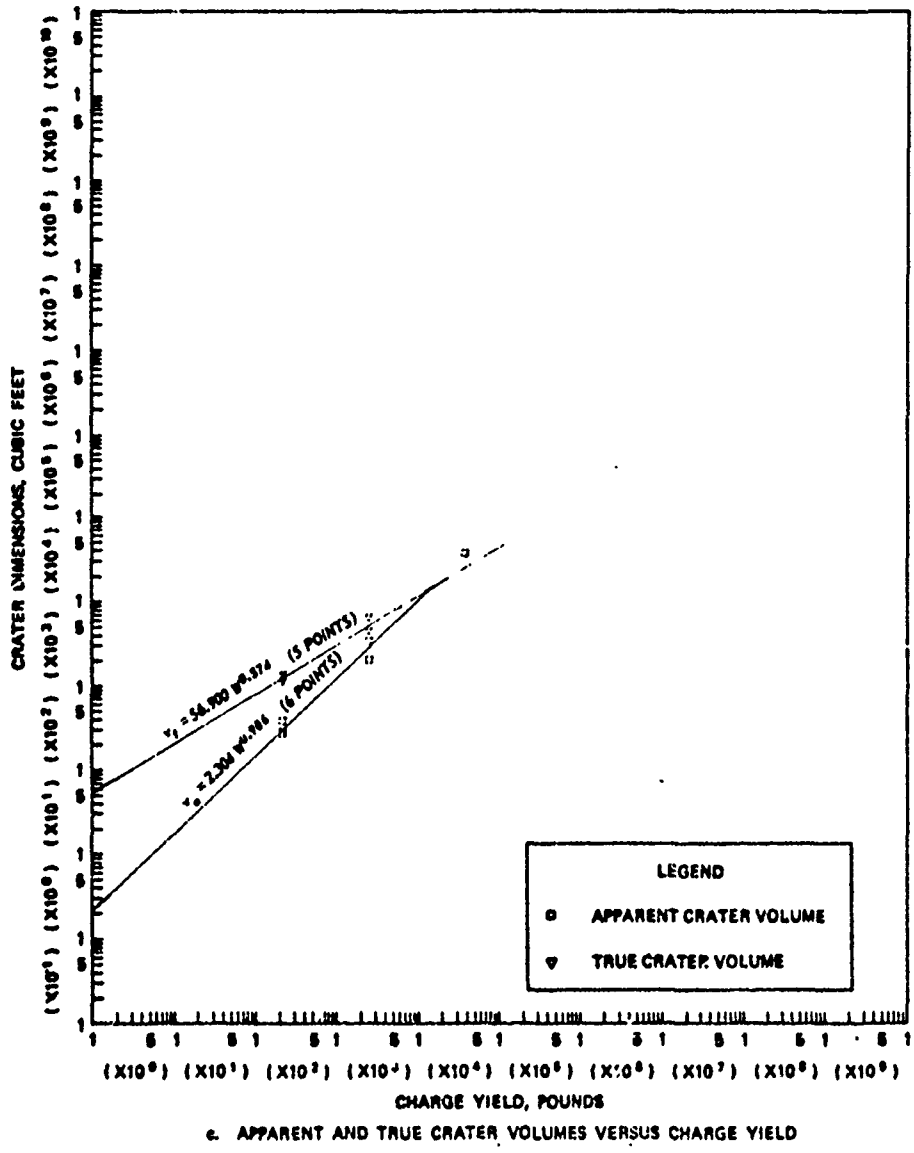

c. APPARENT AND TRUE CRATER VOLUMES VERSUS CHARGE YIELD

Figure B.79 (sheet 2 of 2).

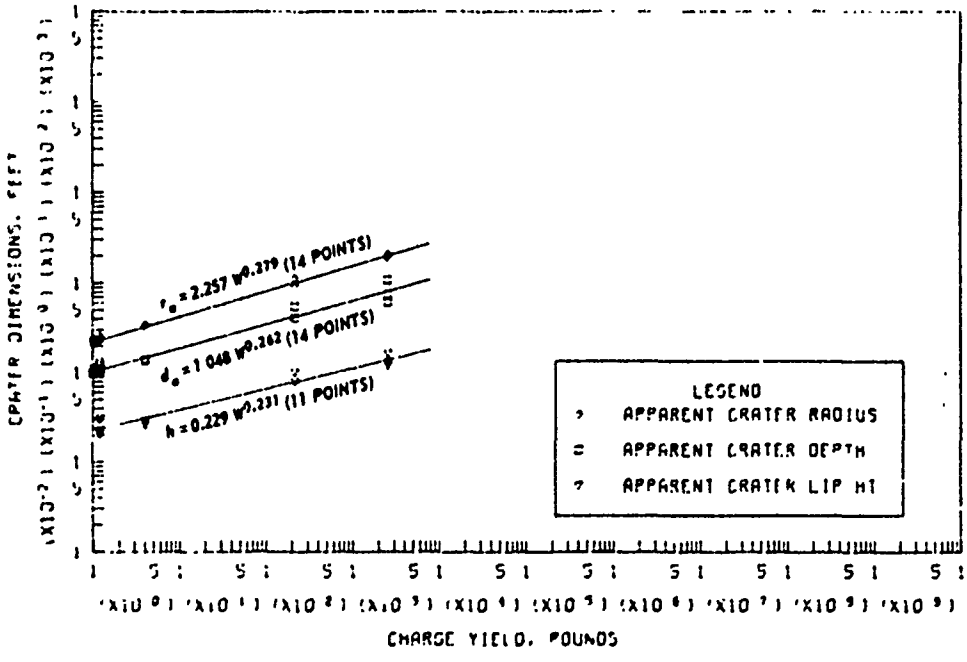

a. APPARENT CRATER DIMENSIONS VERSUS CHARGE YIELD

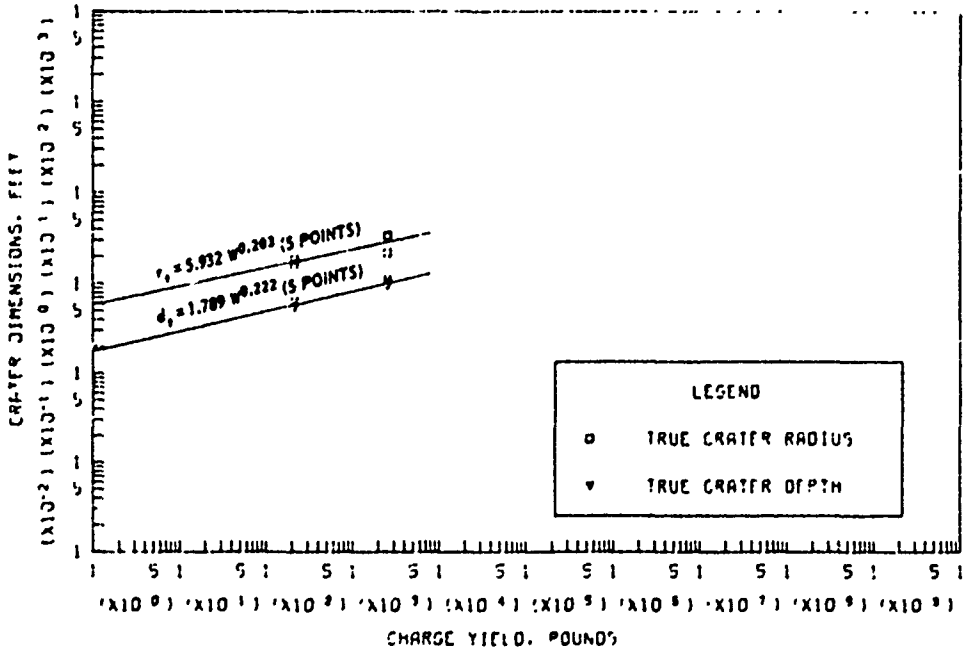

b. TRUE CRATER DIMENSIONS VERSUS CHARGE YIELD

Figure B.80 Dimensions of craters in dry-to-moist sand for $-0.50 \leq Z < -0.20$ ft/lb$^{1/3}$, Category 6 (sheet 1 of 2).

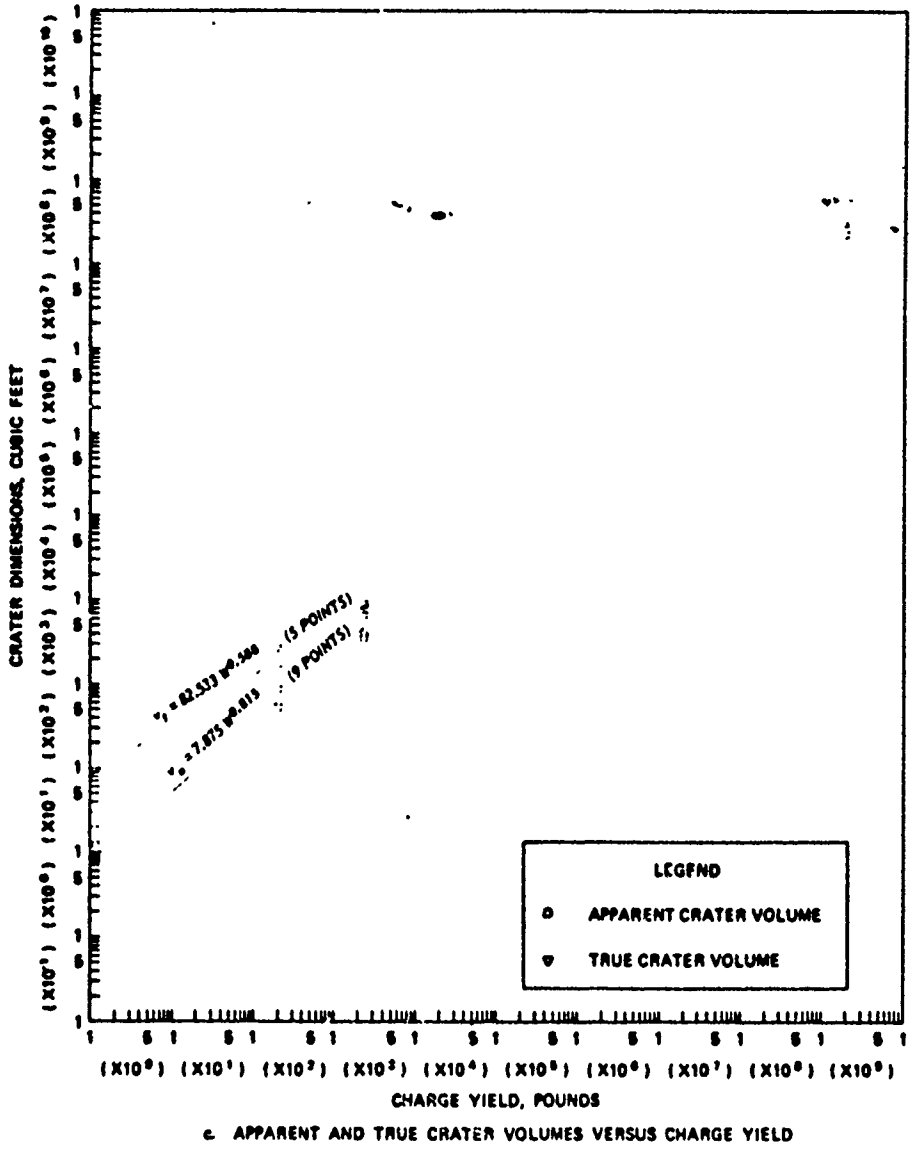

c. APPARENT AND TRUE CRATER VOLUMES VERSUS CHARGE YIELD

Figure B.80 (sheet 2 of 2).

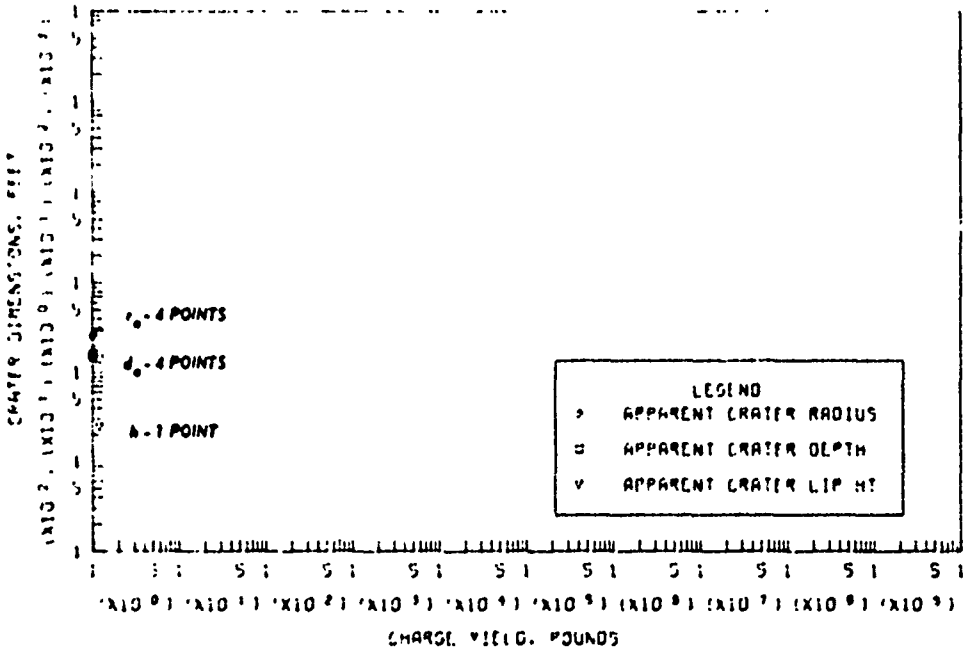

a. APPARENT CRATER DIMENSIONS VERSUS CHARGE YIELD

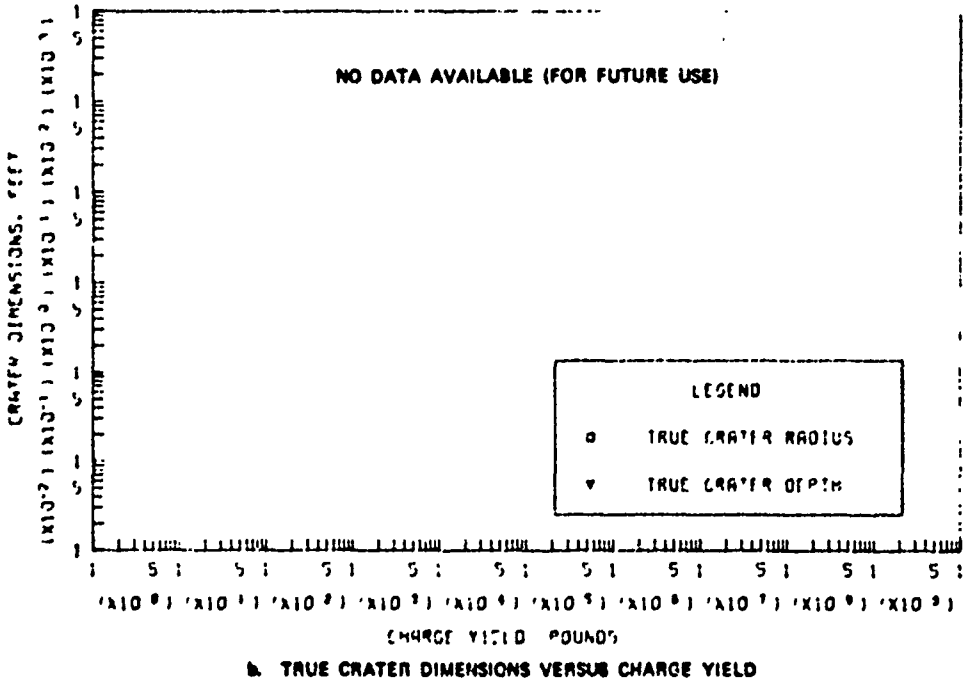

b. TRUE CRATER DIMENSIONS VERSUS CHARGE YIELD

Figure B.81 Dimensions of craters in dry-to-moist sand for $-1.10 \leq Z < -0.90$ ft/lb$^{1/3}$, Category 8 (sheet 1 of 2).

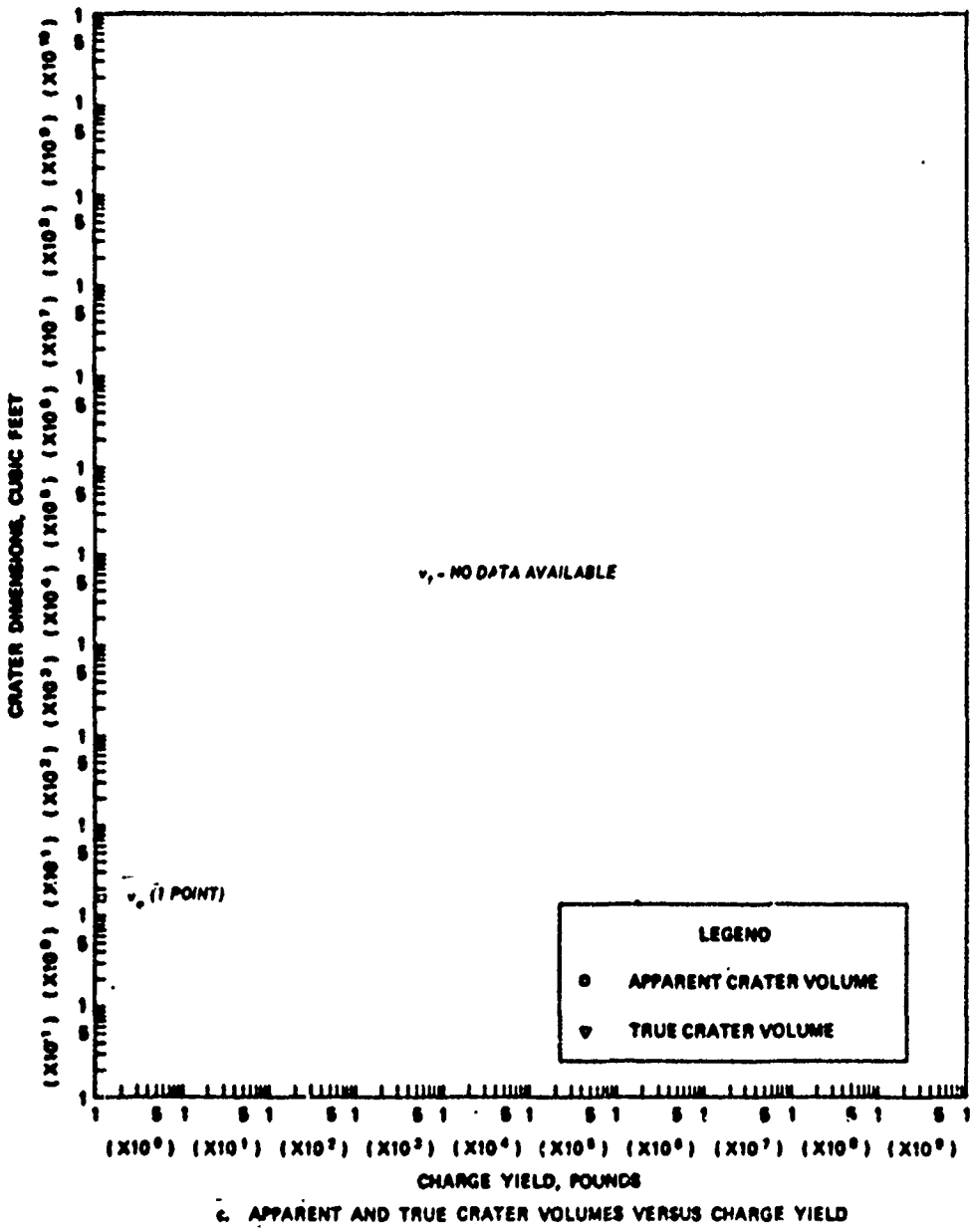

c. APPARENT AND TRUE CRATER VOLUMES VERSUS CHARGE YIELD

Figure B.81 (sheet 2 of 2).

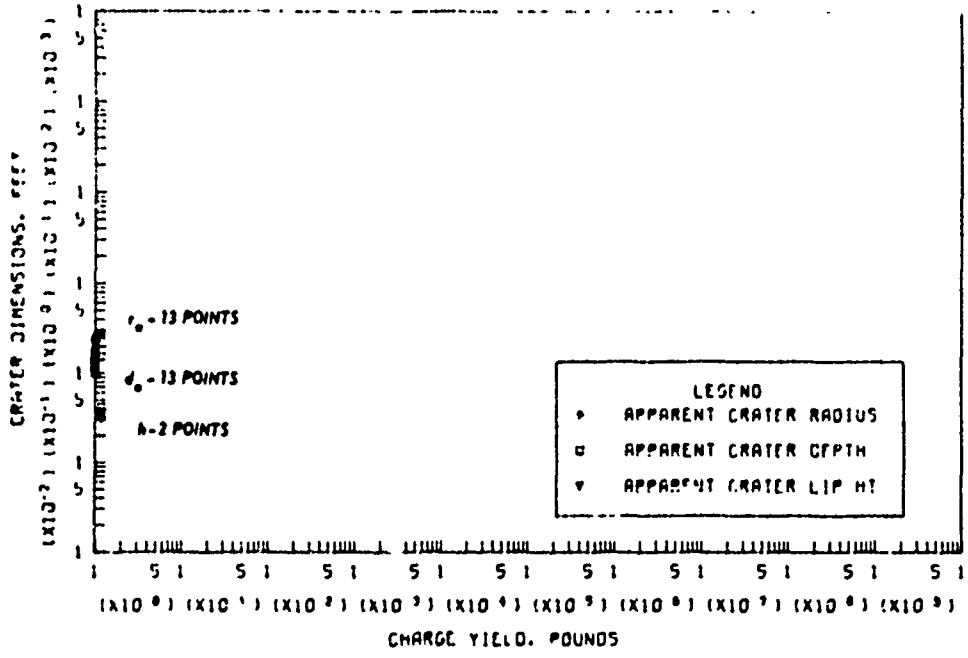

a. APPARENT CRATER DIMENSIONS VERSUS CHARGE YIELD

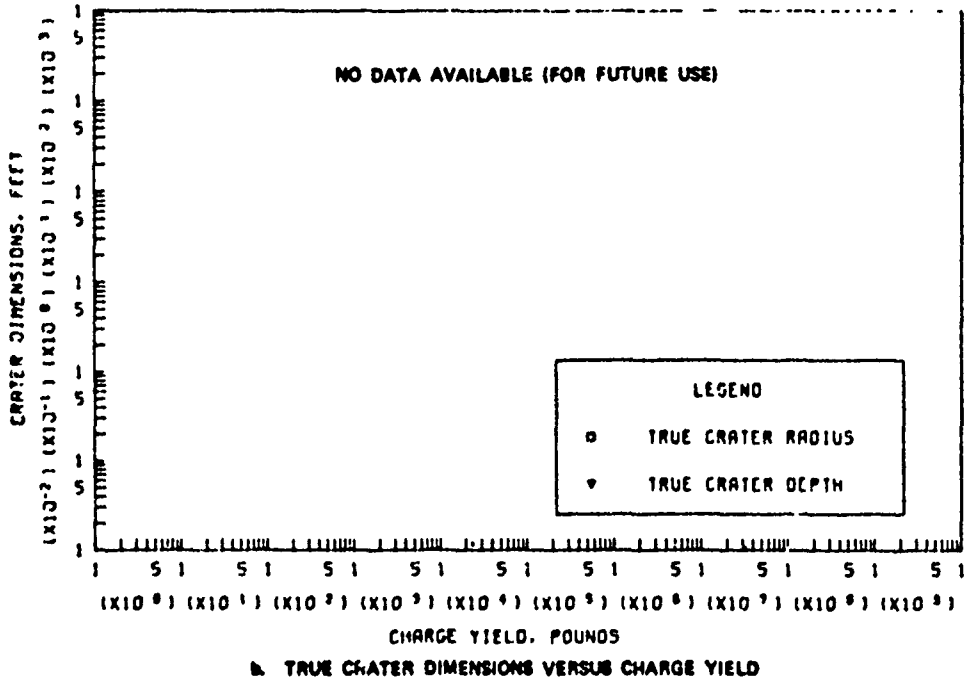

b. TRUE CRATER DIMENSIONS VERSUS CHARGE YIELD

Figure B.82 Dimensions of craters in dry-to-moist sand for $-2.00 \leq Z < -1.10$ ft/lb$^{1/3}$, Category 9 (sheet 1 of 2).

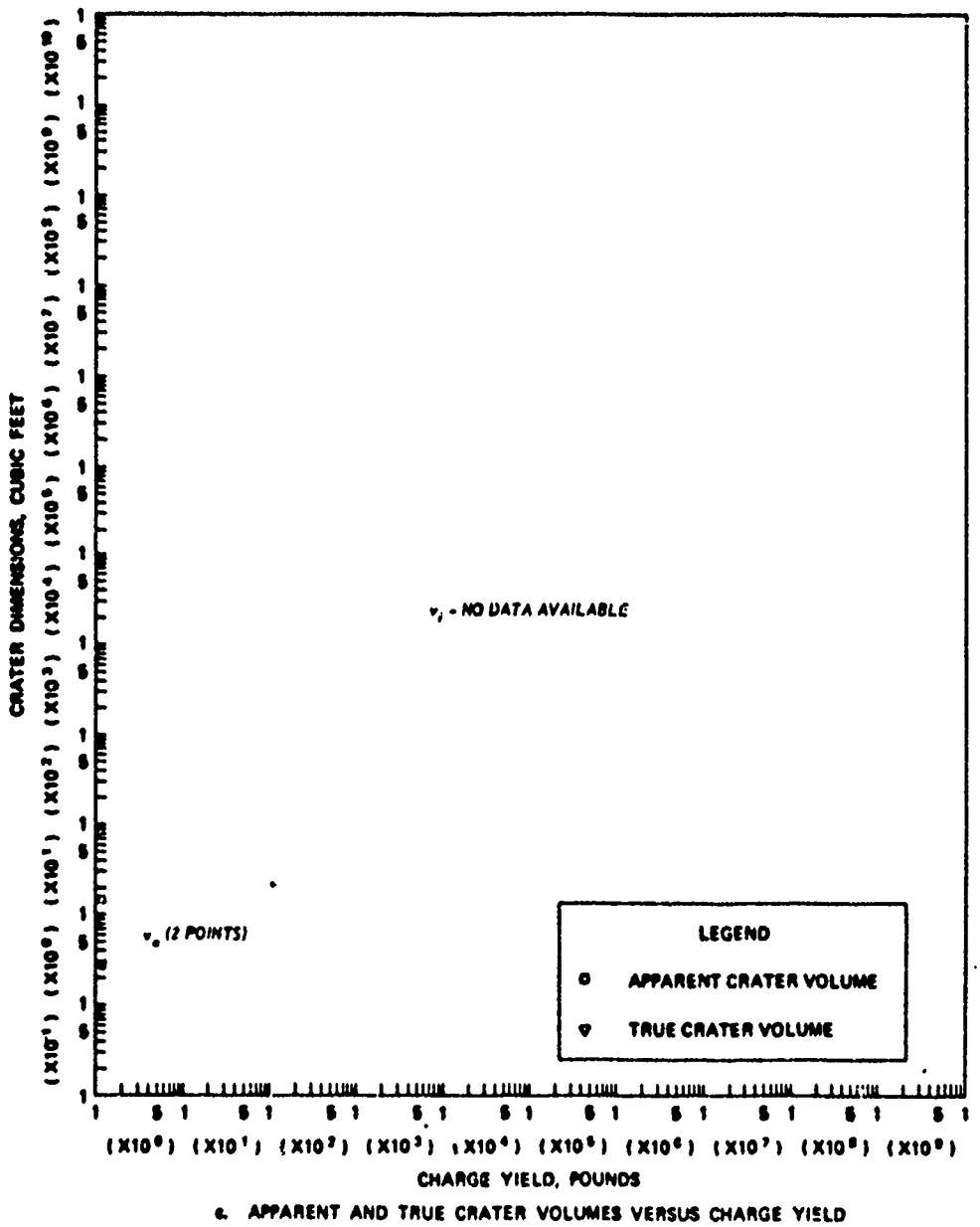

a. APPARENT AND TRUE CRATER VOLUMES VERSUS CHARGE YIELD

Figure B.82 (sheet 2 of 2).

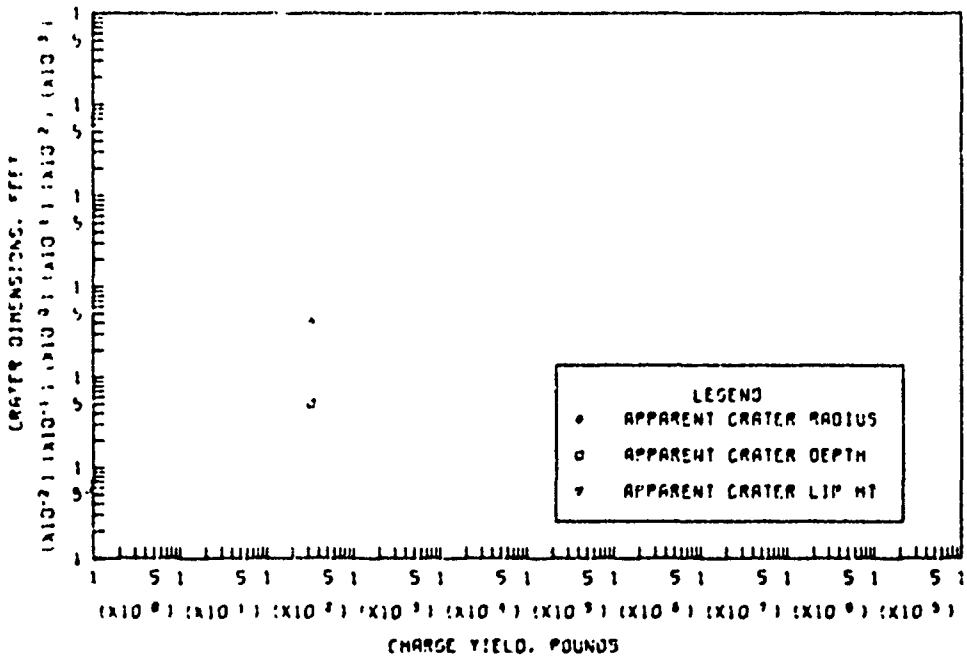

a. APPARENT CRATER DIMENSIONS VERSUS CHARGE YIELD

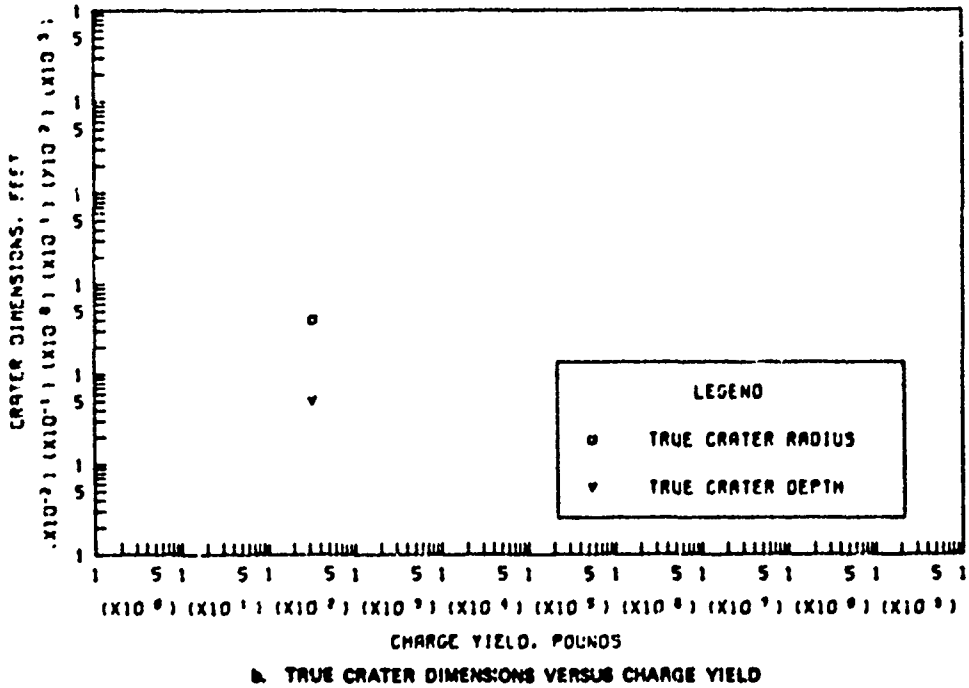

b. TRUE CRATER DIMENSIONS VERSUS CHARGE YIELD

Figure B.83 Dimensions of craters in wet sand for $0.50 < Z$ ft/lb$^{1/3}$, Category 1 (sheet 1 of 2).

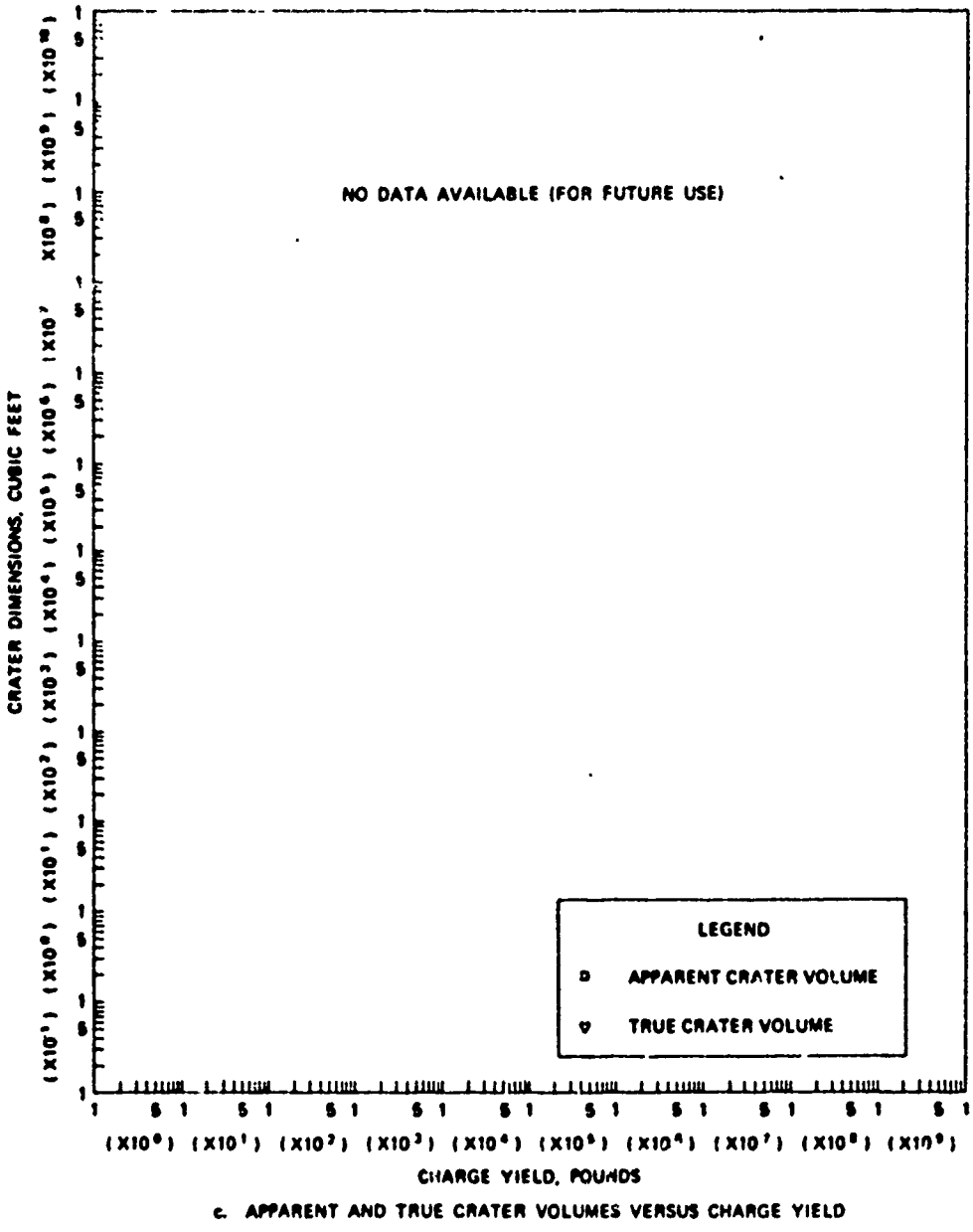

c. APPARENT AND TRUE CRATER VOLUMES VERSUS CHARGE YIELD

Figure B.83 (sheet 2 of 2).

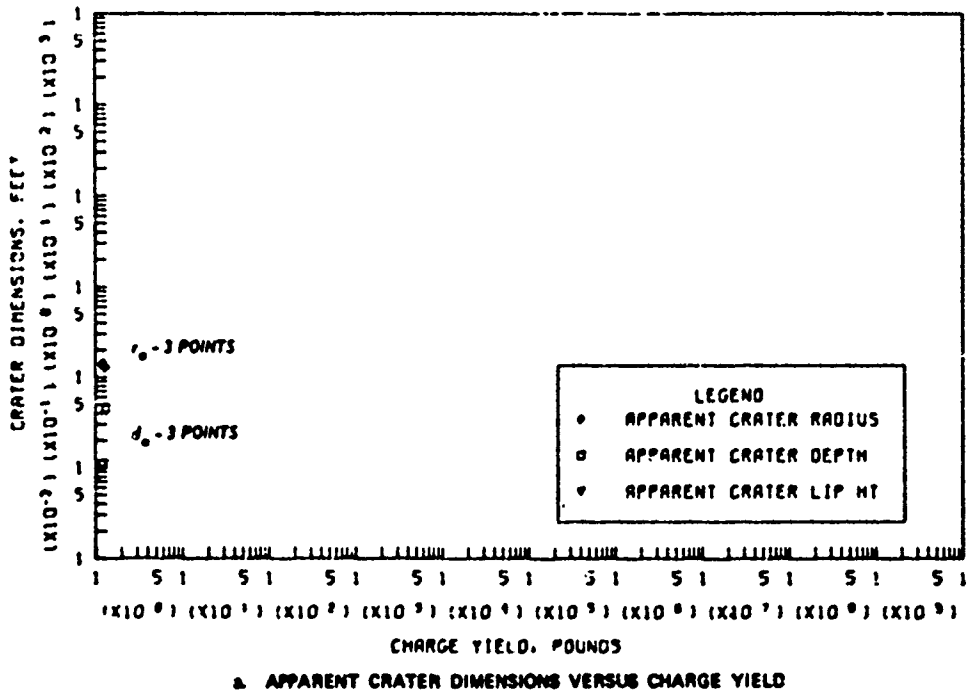

a. APPARENT CRATER DIMENSIONS VERSUS CHARGE YIELD

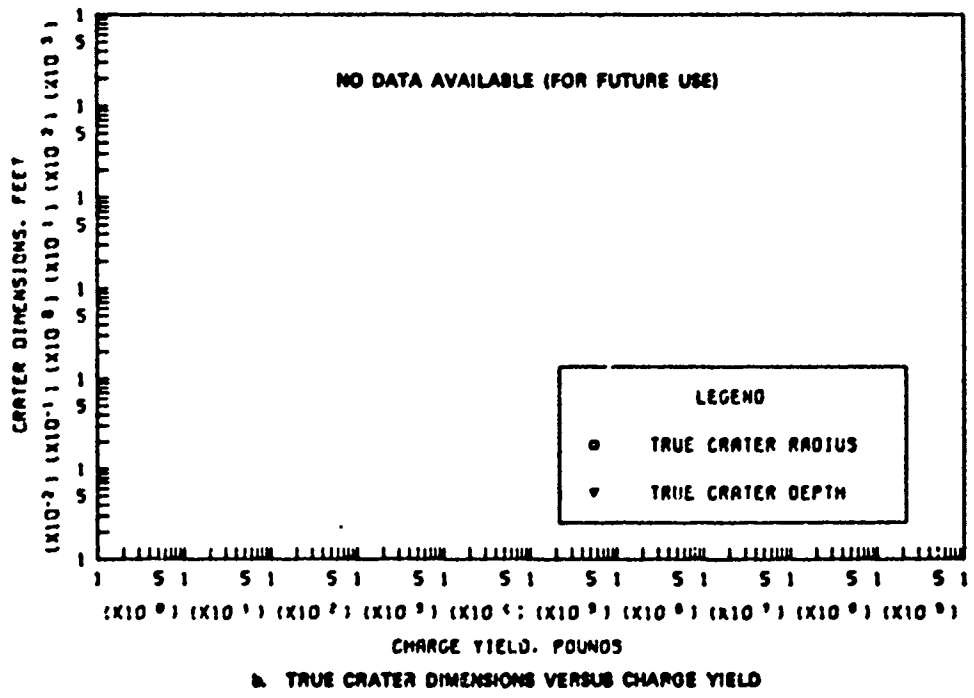

b. TRUE CRATER DIMENSIONS VERSUS CHARGE YIELD

Figure B.84 Dimensions of craters in wet sand for $0.20 \leq Z < 0.50$ ft/lb$^{1/3}$, Category 2 (sheet 1 of 2).

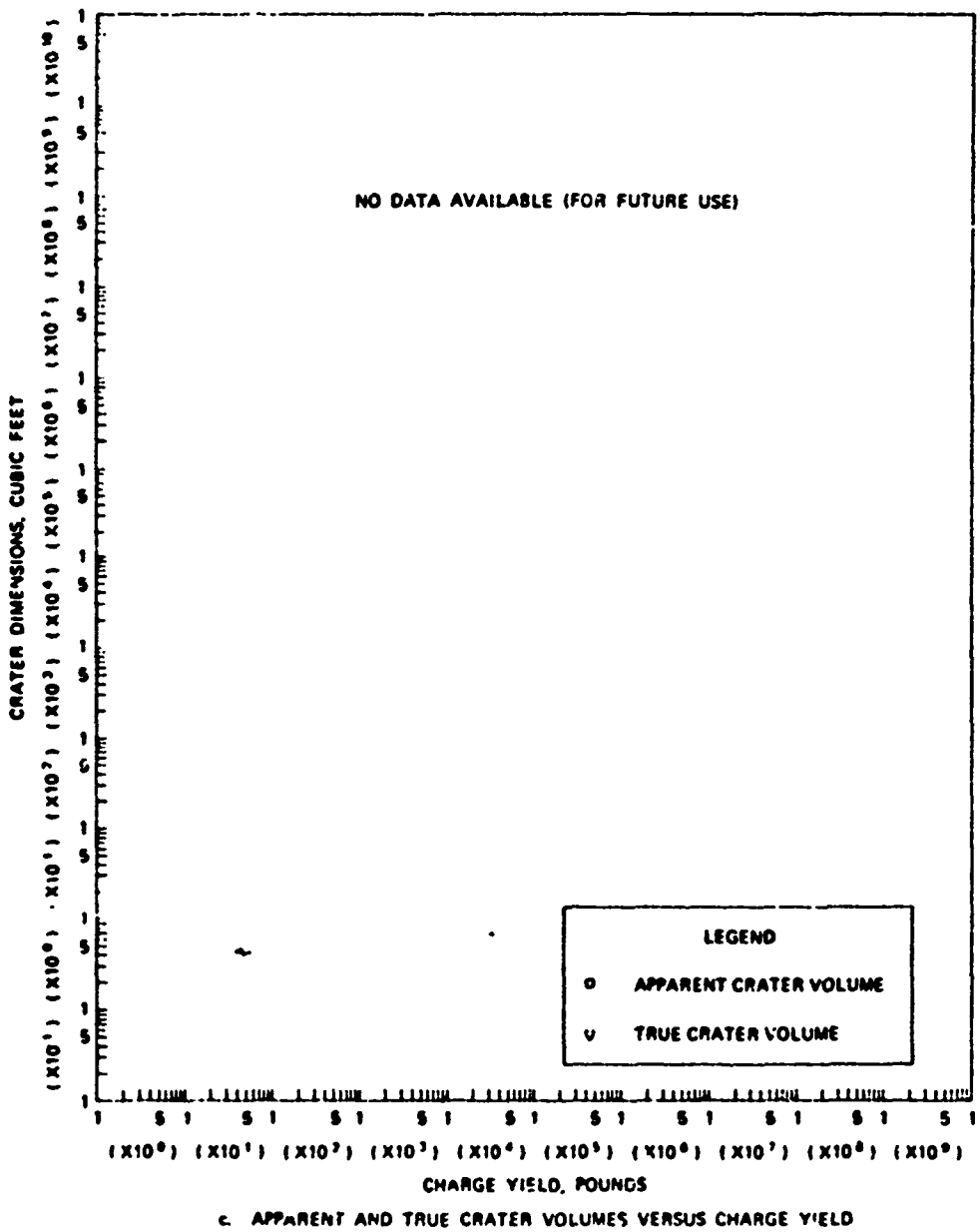

c. APPARENT AND TRUE CRATER VOLUMES VERSUS CHARGE YIELD

Figure B.84 (sheet 2 of 2).

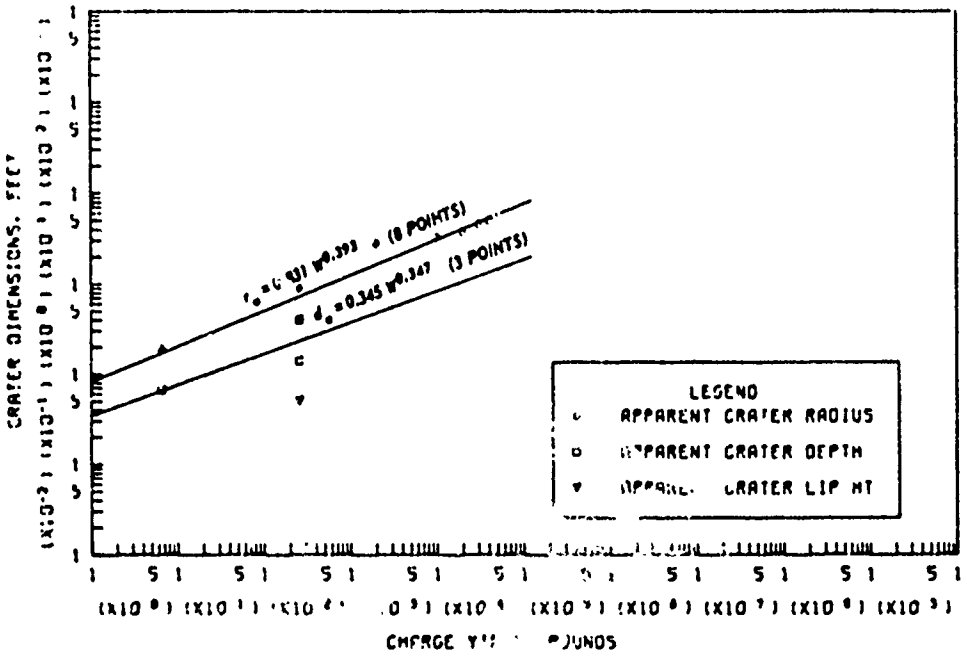

a. APPARENT CRATER DIMENSIONS VERSUS CHARGE YIELD

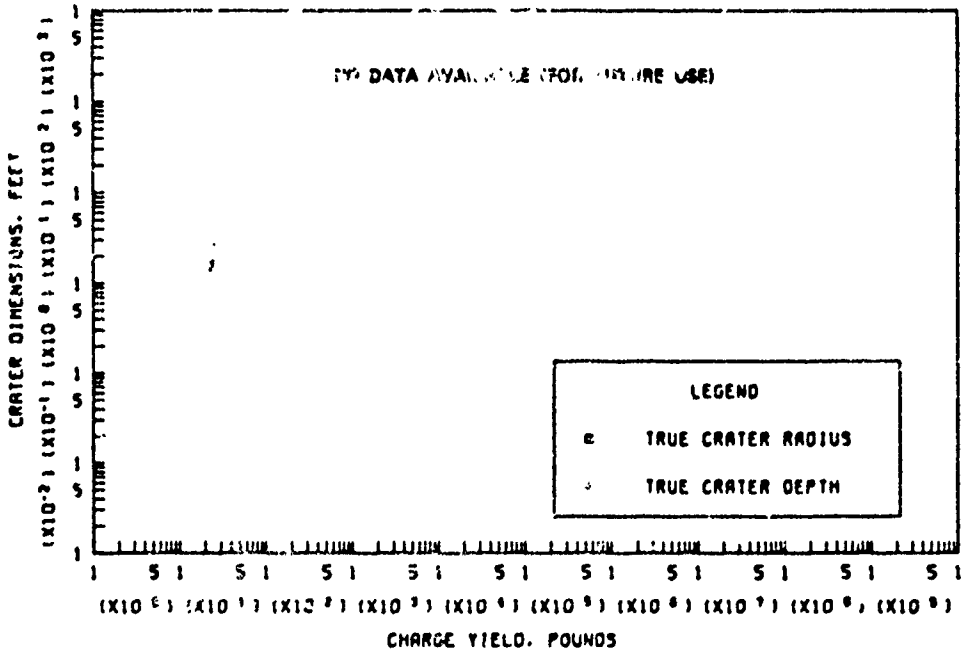

b. TRUE CRATER DIMENSIONS VERSUS CHARGE YIELD

Figure B.85 Dimensions of craters in wet sand for $0.05 \leq Z < 0.20$ ft/lb$^{1/3}$, Category 3 (sheet 1 of 2).

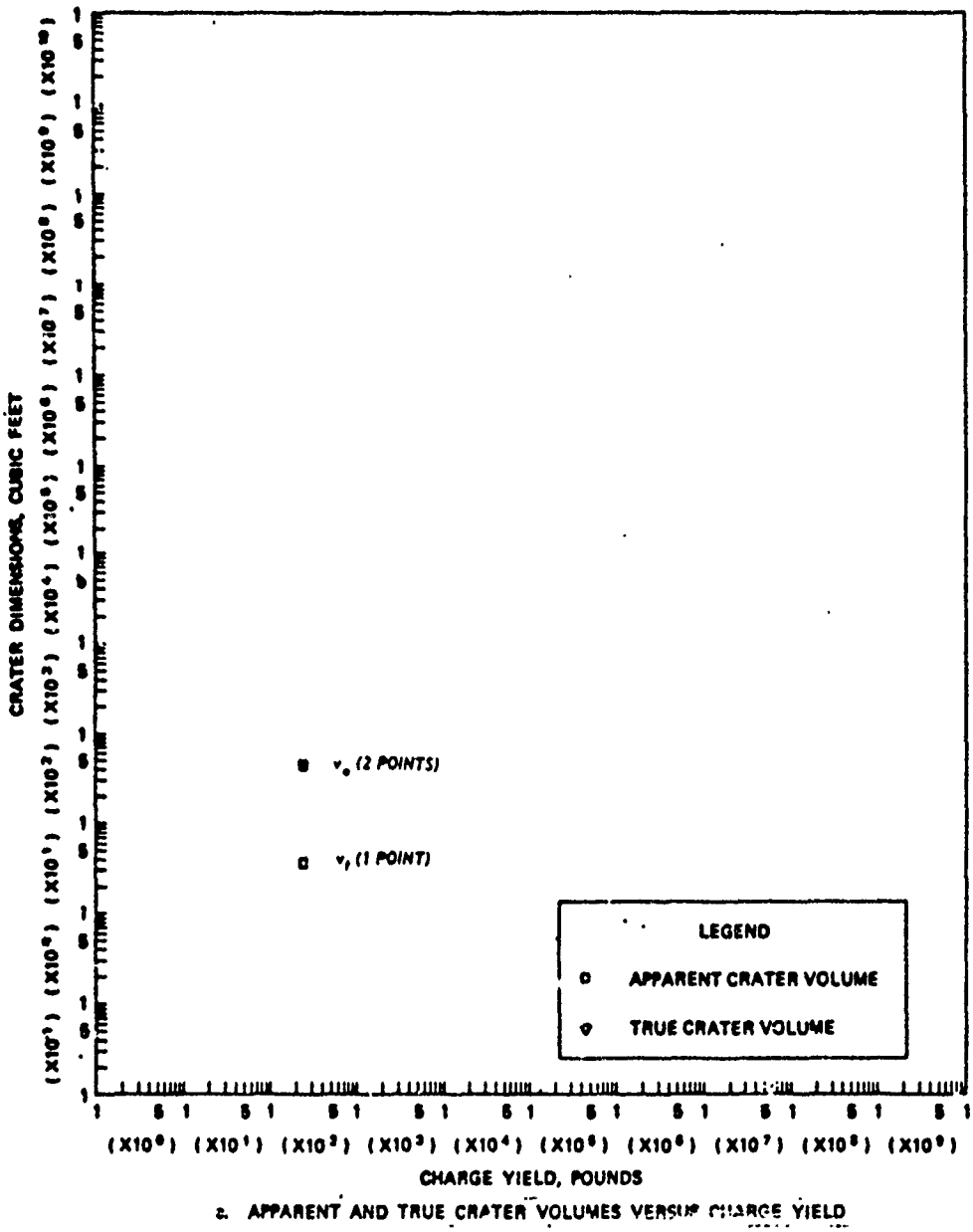

a. APPARENT AND TRUE CRATER VOLUMES VERSUS CHARGE YIELD

Figure B.85 (sheet 2 of 2).

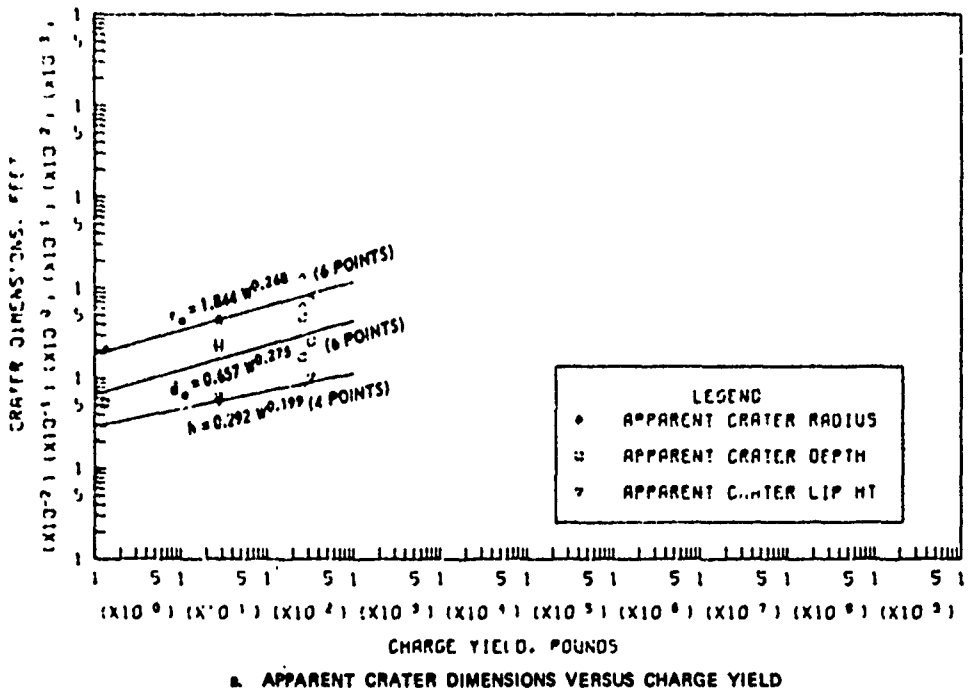

a. APPARENT CRATER DIMENSIONS VERSUS CHARGE YIELD

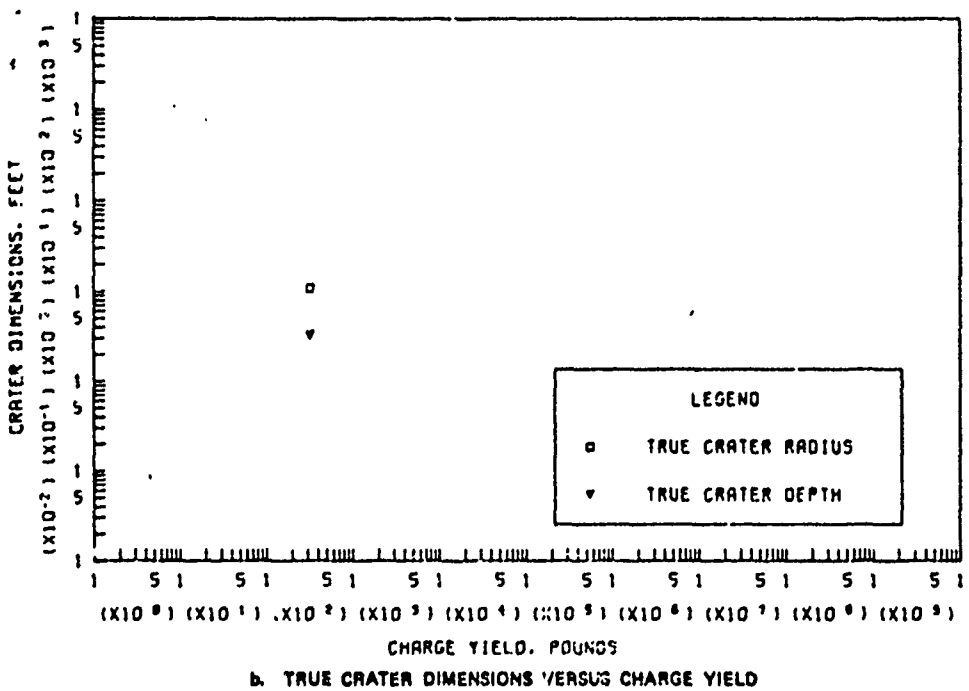

b. TRUE CRATER DIMENSIONS VERSUS CHARGE YIELD

Figure B.86 Dimensions of craters in wet sand for $-0.05 \leq Z < 0.05$ ft/lb$^{1/3}$, Category 4 (sheet 1 of 2).

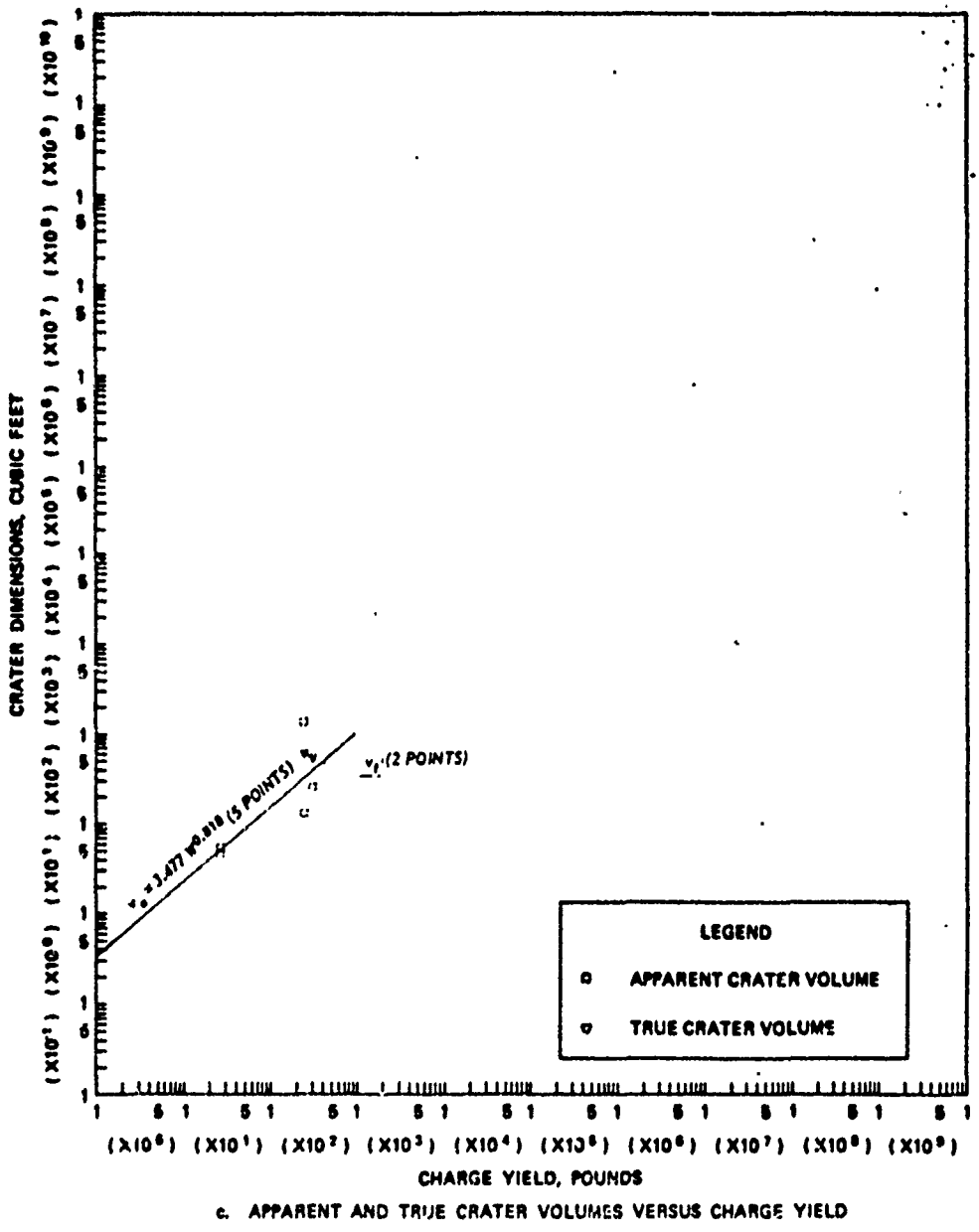

c. APPARENT AND TRUE CRATER VOLUMES VERSUS CHARGE YIELD

Figure B.86 (sheet 2 of 2).

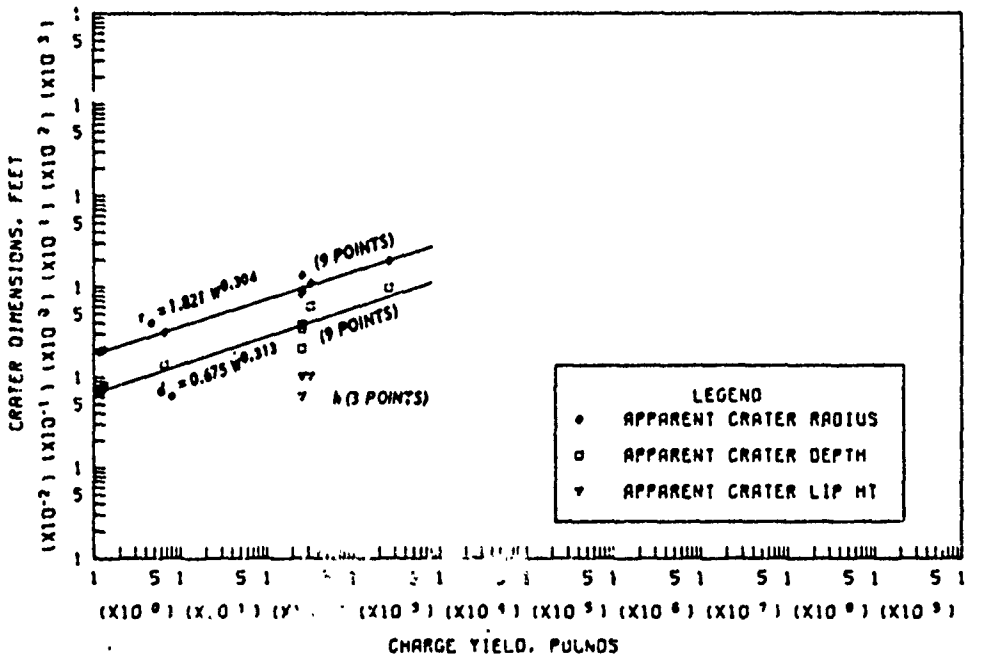

a. APPARENT CRATER DIMENSIONS VERSUS CHARGE YIELD

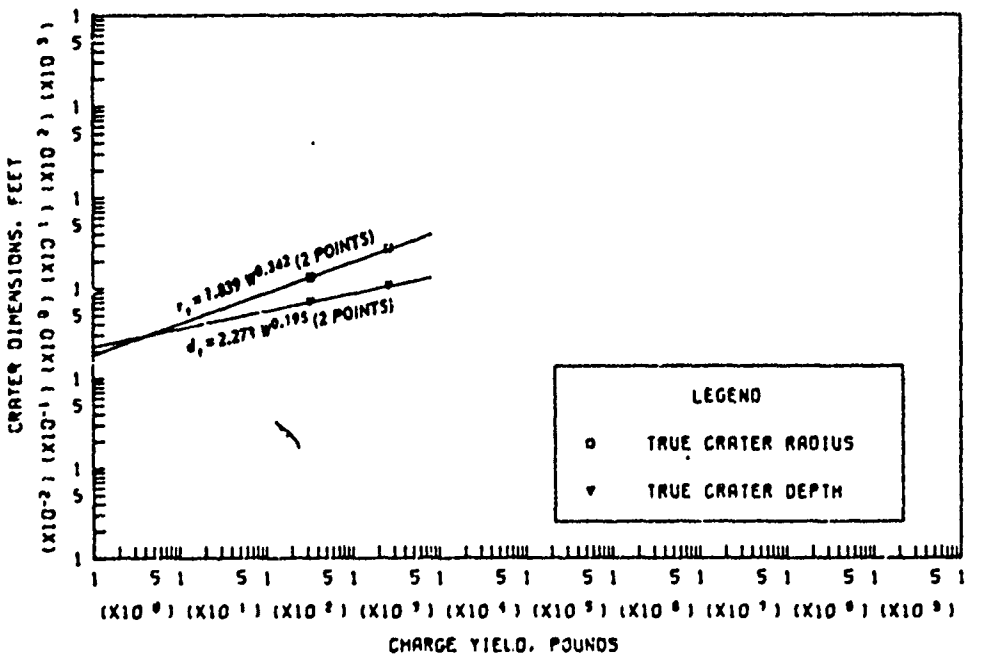

b. TRUE CRATER DIMENSIONS VERSUS CHARGE YIELD

Figure B.87 Dimensions of craters in wet sand for $-0.20 \leq Z < -0.05$ ft/lb$^{1/3}$, Category 5 (sheet 1 of 2).

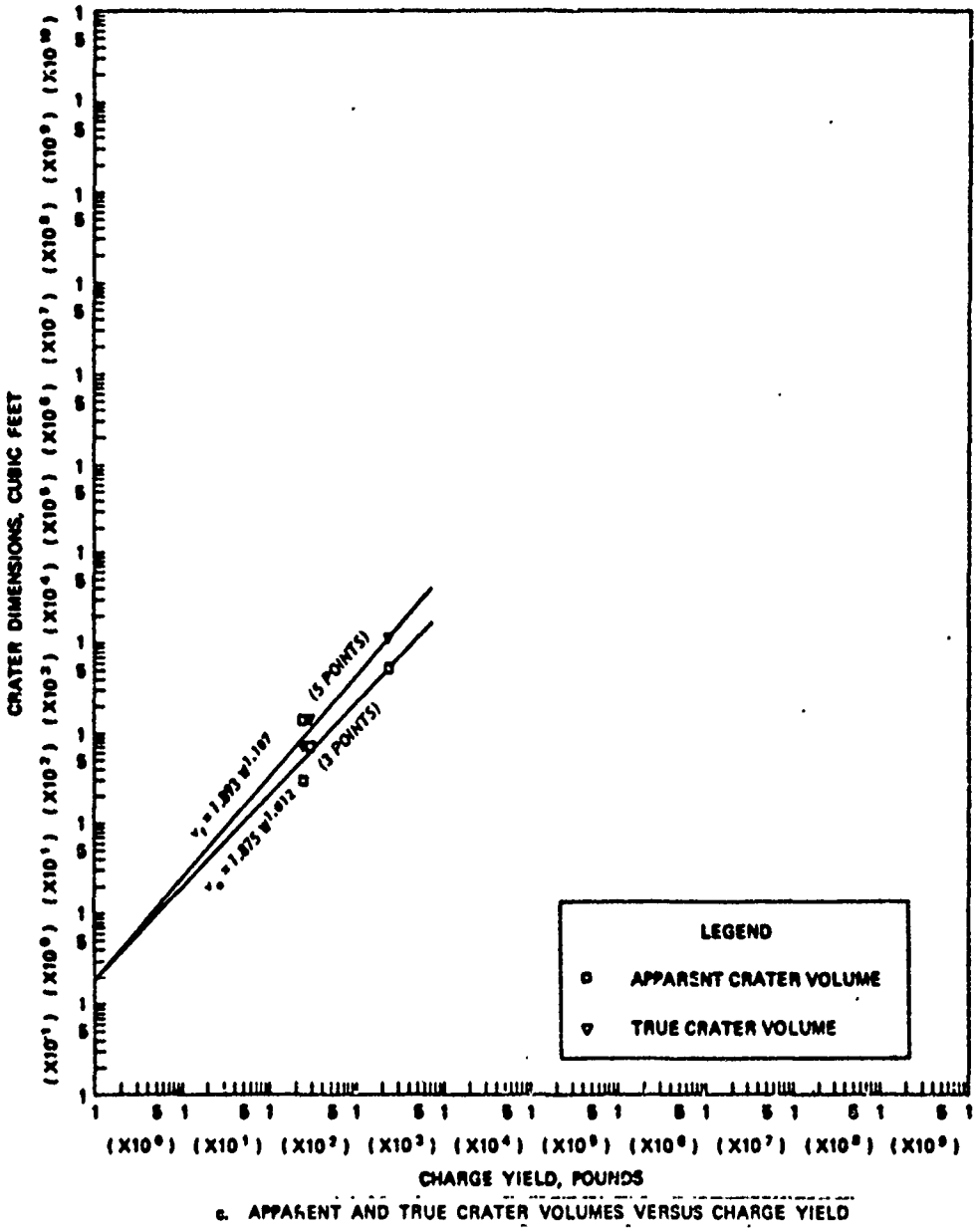

c. APPARENT AND TRUE CRATER VOLUMES VERSUS CHARGE YIELD

Figure B.87 (sheet 2 of 2).

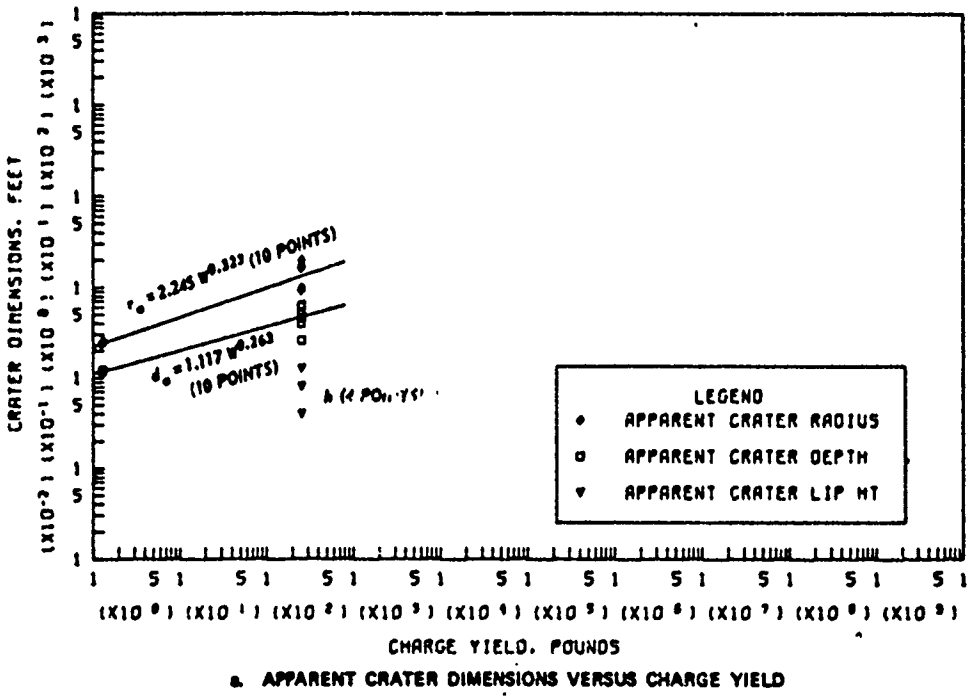

a. APPARENT CRATER DIMENSIONS VERSUS CHARGE YIELD

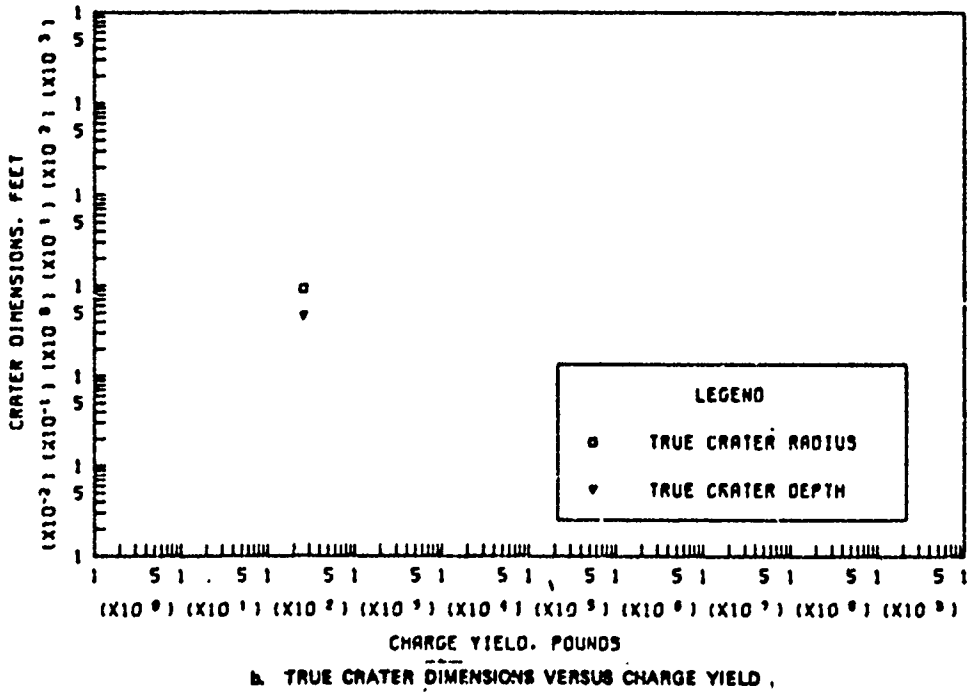

b. TRUE CRATER DIMENSIONS VERSUS CHARGE YIELD

Figure B.88 Dimensions of craters in wet sand for $-0.50 \leq Z < -0.20$ ft/lb$^{1/3}$, Category 6 (sheet 1 of 2).

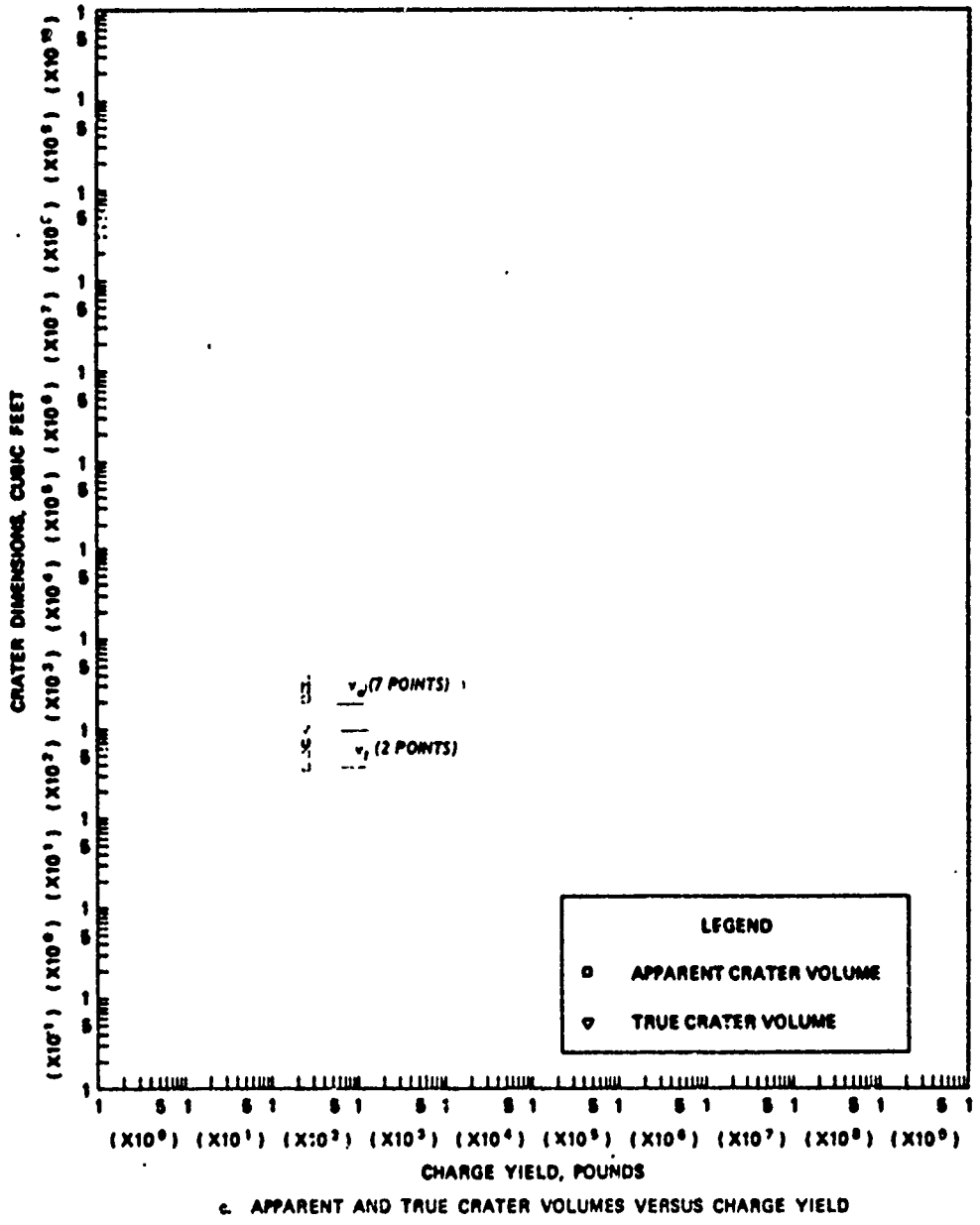

c. APPARENT AND TRUE CRATER VOLUMES VERSUS CHARGE YIELD

Figure B.88 (sheet 2 of 2).

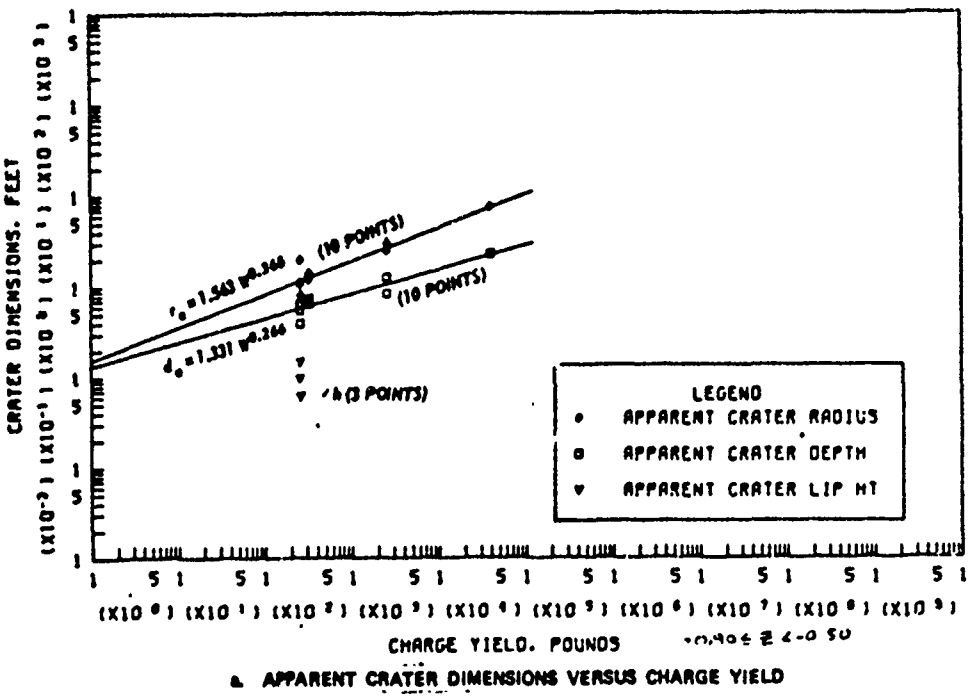

a. APPARENT CRATER DIMENSIONS VERSUS CHARGE YIELD

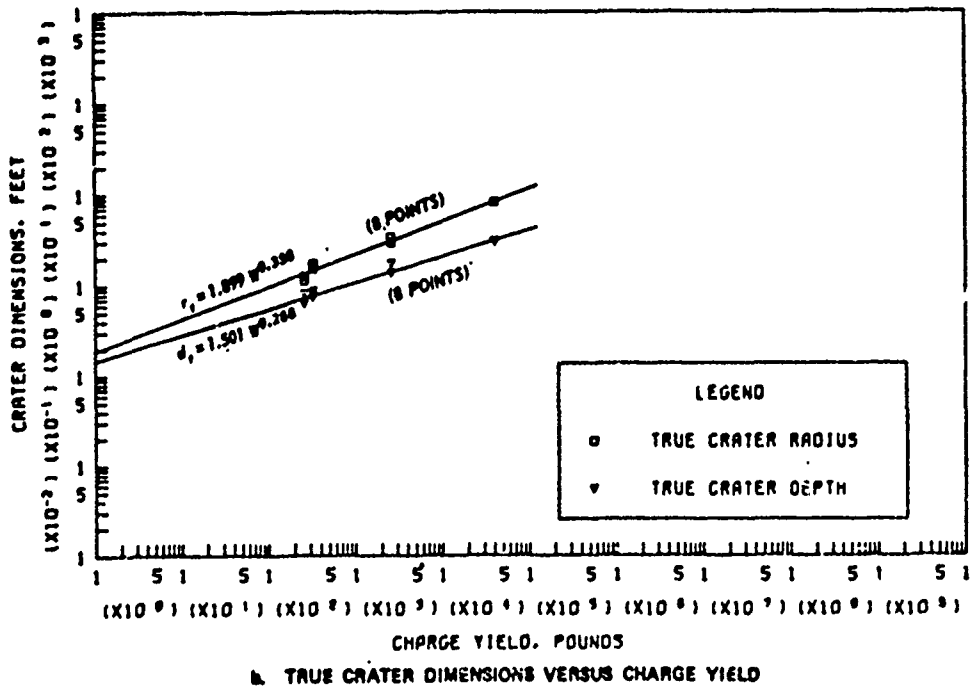

b. TRUE CRATER DIMENSIONS VERSUS CHARGE YIELD

Figure B.89 Dimensions of craters in wet sand for $-0.90 \leq Z < -0.50$ ft/lb$^{1/3}$, Category 7 (sheet 1 of 2).

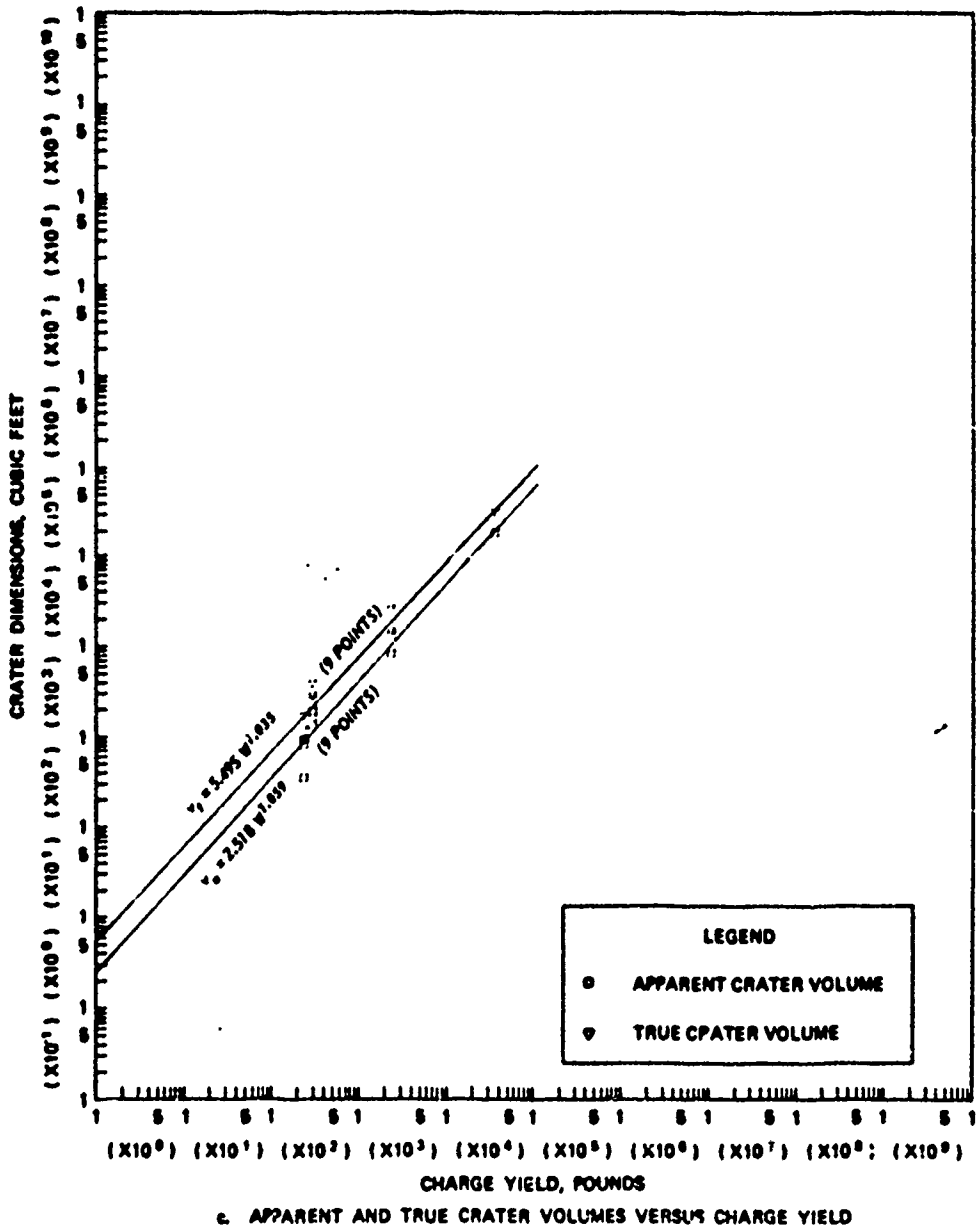

e. APPARENT AND TRUE CRATER VOLUMES VERSUS CHARGE YIELD

Figure B.89 (sheet 2 of 2).

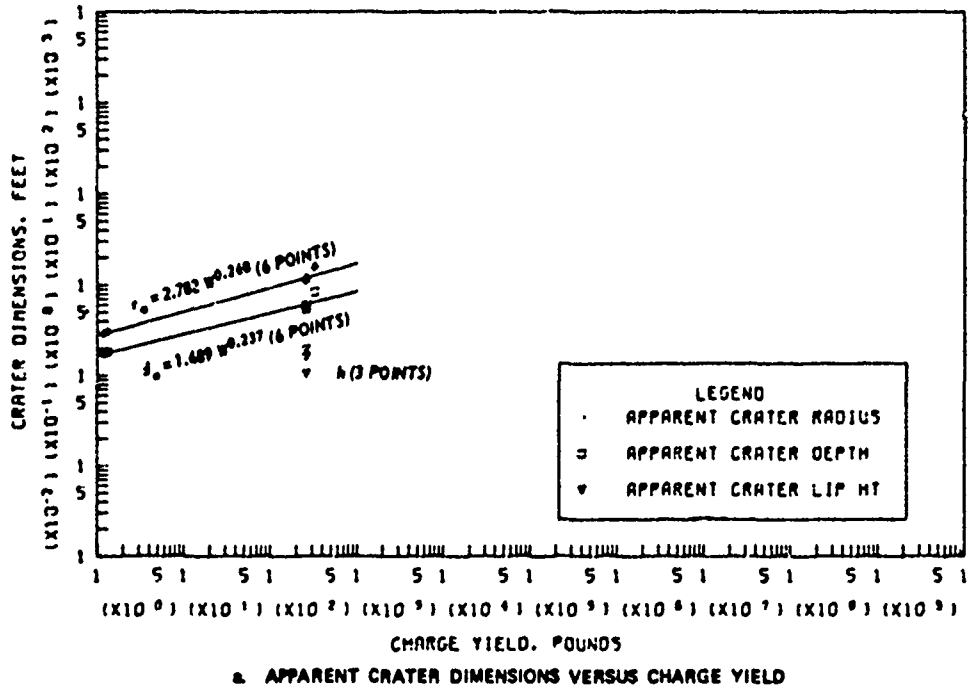

a. APPARENT CRATER DIMENSIONS VERSUS CHARGE YIELD

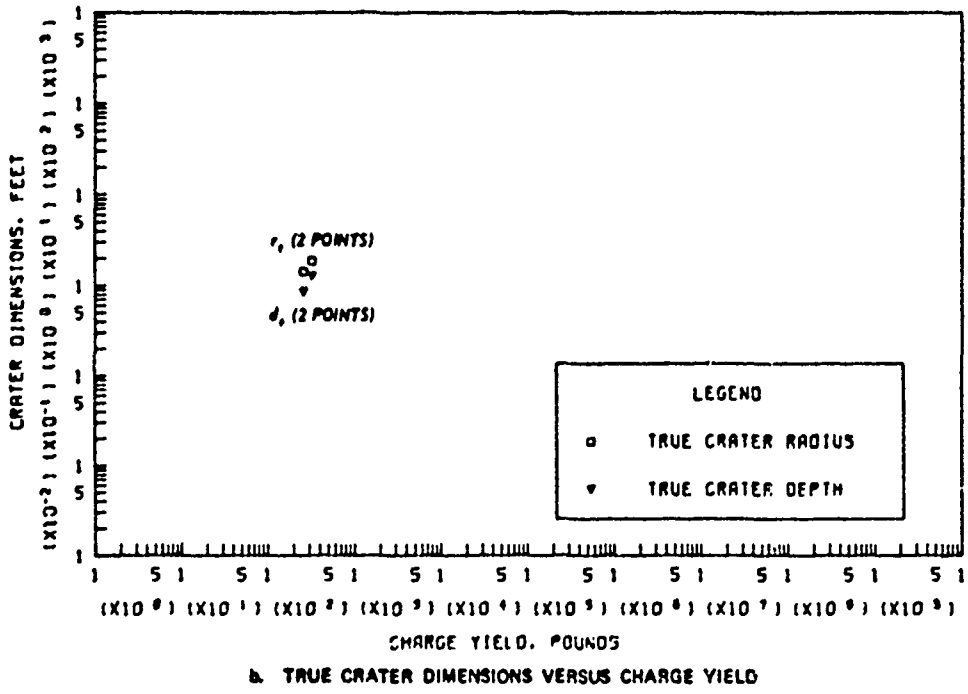

b. TRUE CRATER DIMENSIONS VERSUS CHARGE YIELD

Figure B.90 Dimensions of craters in wet sand for $-1.10 \leq Z < -0.90$ ft/lb$^{1/3}$, Category 8 (sheet 1 of 2).

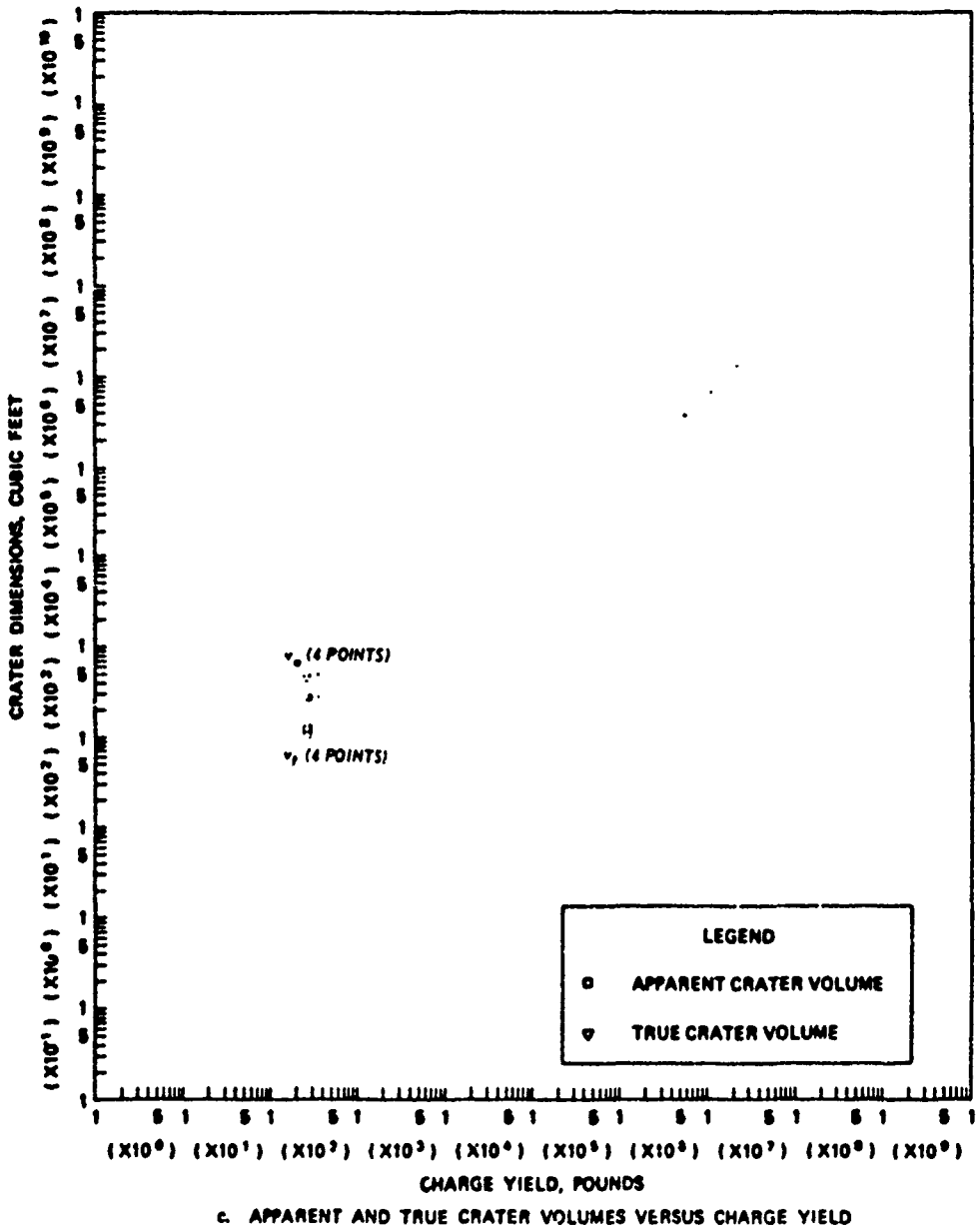

c. APPARENT AND TRUE CRATER VOLUMES VERSUS CHARGE YIELD

Figure B.90 (sheet 2 of 2).

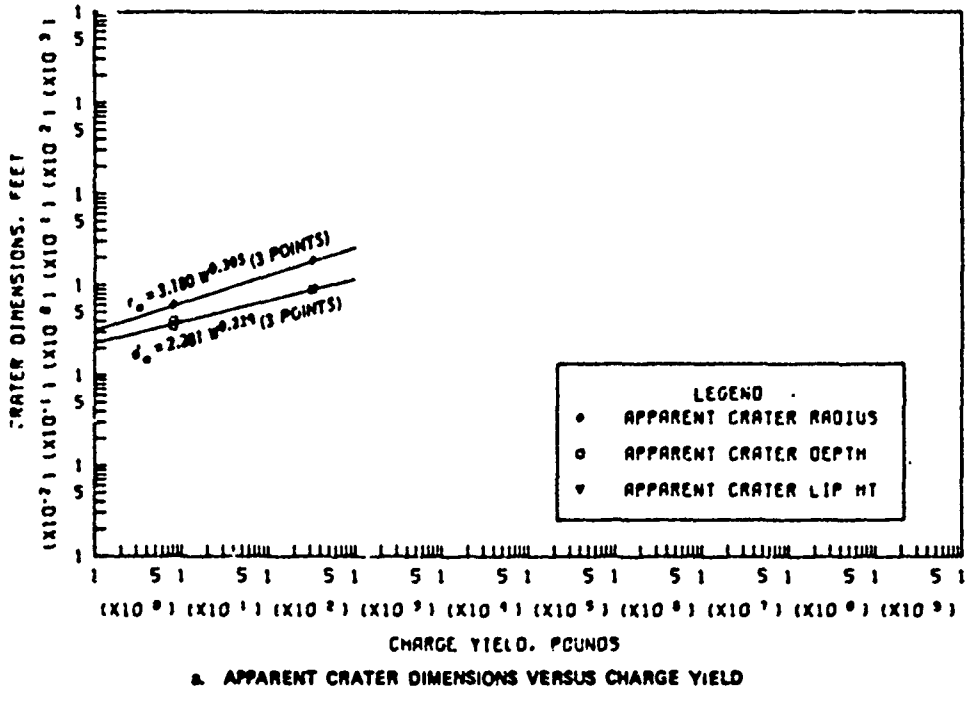

a. APPARENT CRATER DIMENSIONS VERSUS CHARGE YIELD

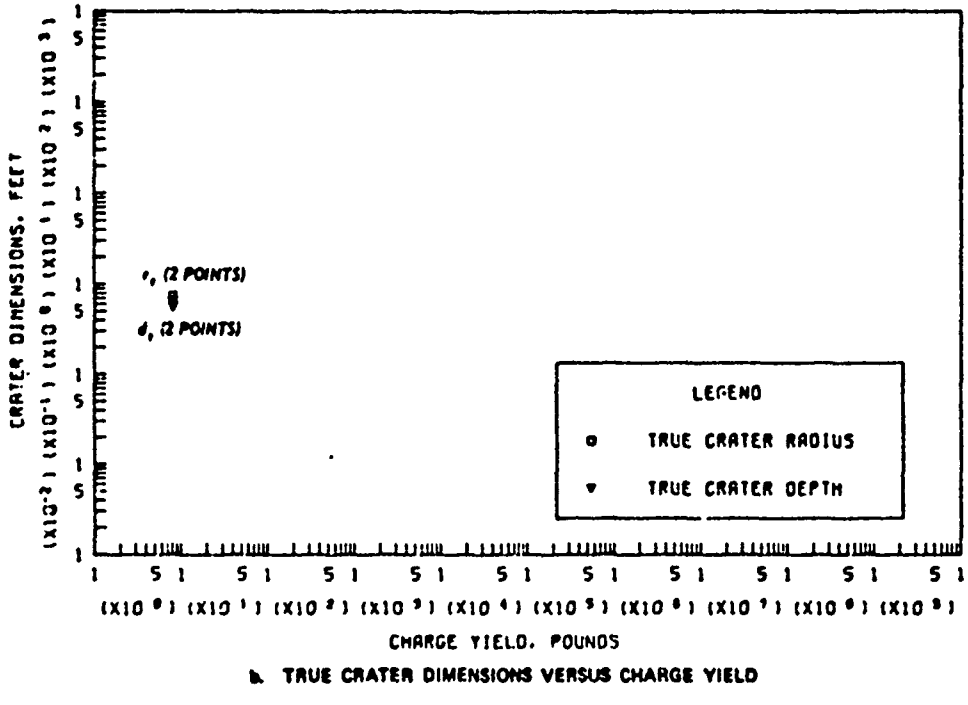

b. TRUE CRATER DIMENSIONS VERSUS CHARGE YIELD

Figure B.91 Dimensions of craters in wet sand for $-2.00 \leq Z < -1.10$ ft/lb$^{1/3}$, Category 9 (sheet 1 of 2).

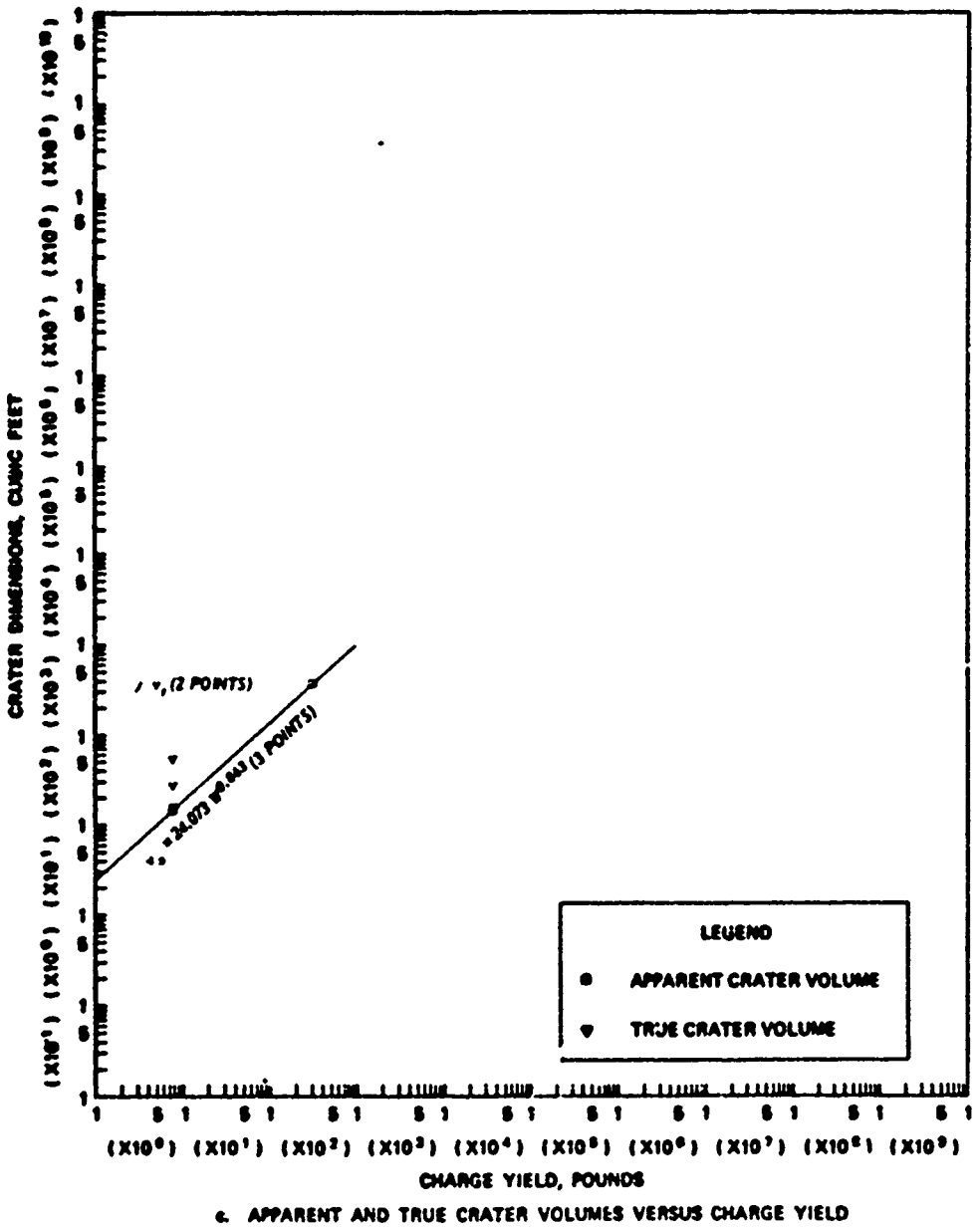

c. APPARENT AND TRUE CRATER VOLUMES VERSUS CHARGE YIELD

Figure B.91 (sheet 2 of 2).

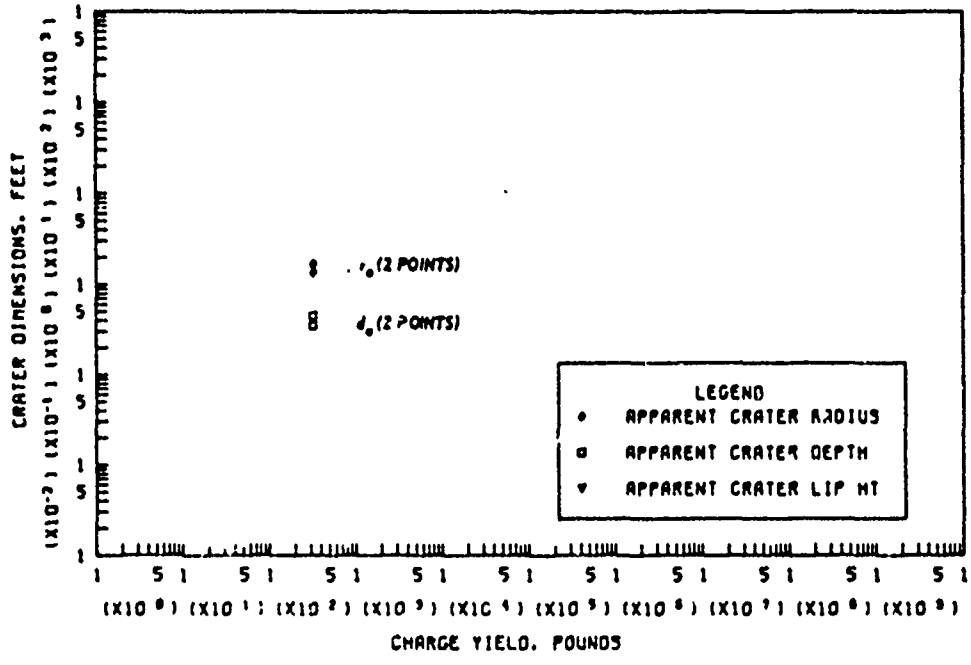

a. APPARENT CRATER DIMENSIONS VERSUS CHARGE YIELD

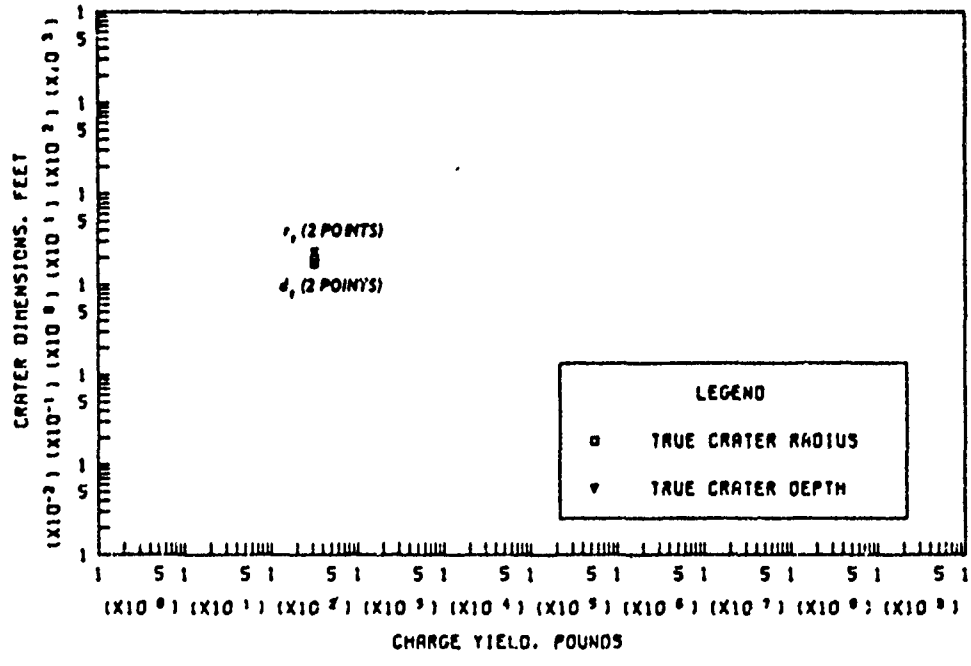

b. TRUE CRATER DIMENSIONS VERSUS CHARGE YIELD

Figure B.92 Dimensions of craters in wet sand for $Z < -2.00$ ft/lb$^{1/3}$, Category 10 (sheet 1 of 2).

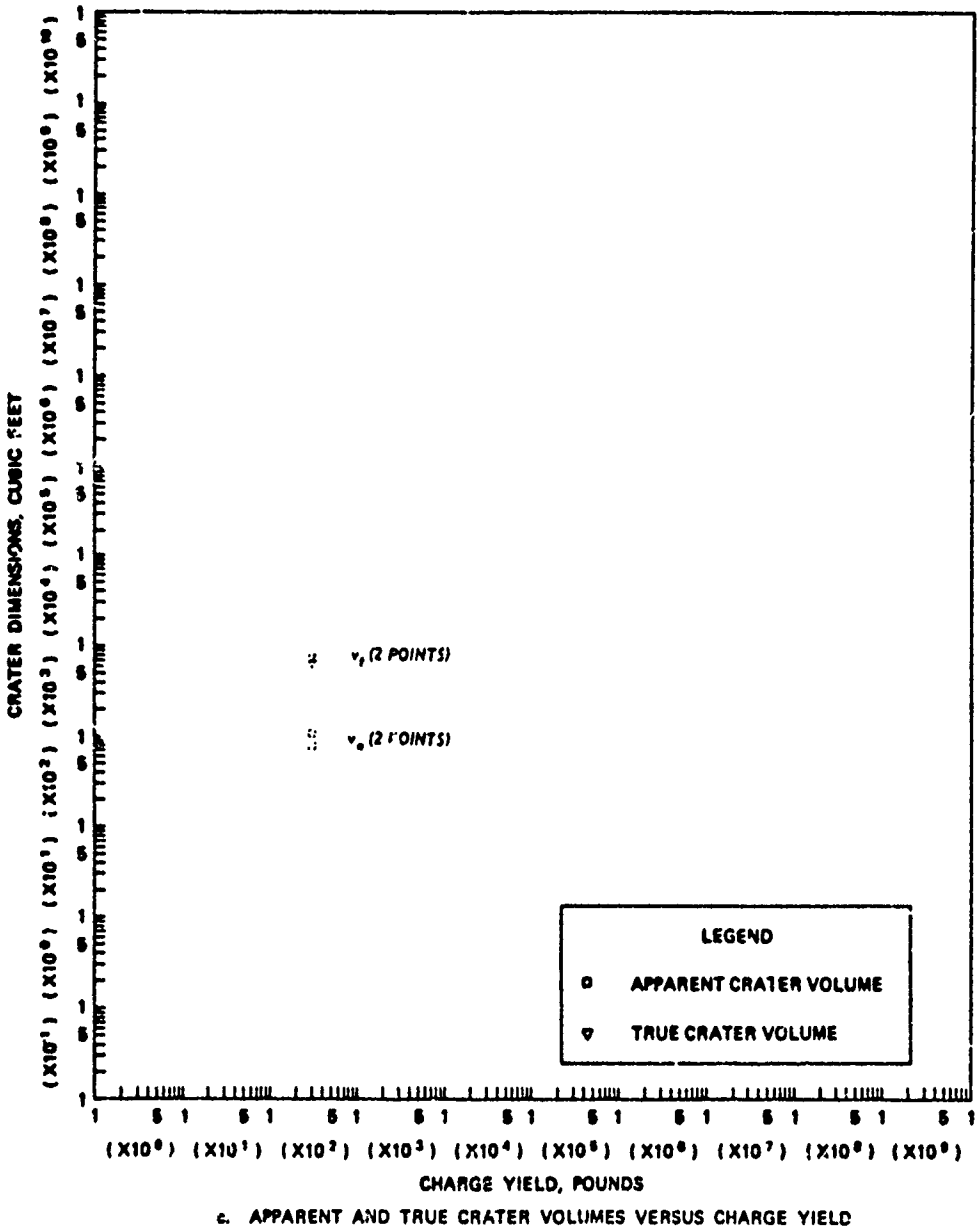

c. APPARENT AND TRUE CRATER VOLUMES VERSUS CHARGE YIELD

Figure B.92 (sheet 2 of 2).

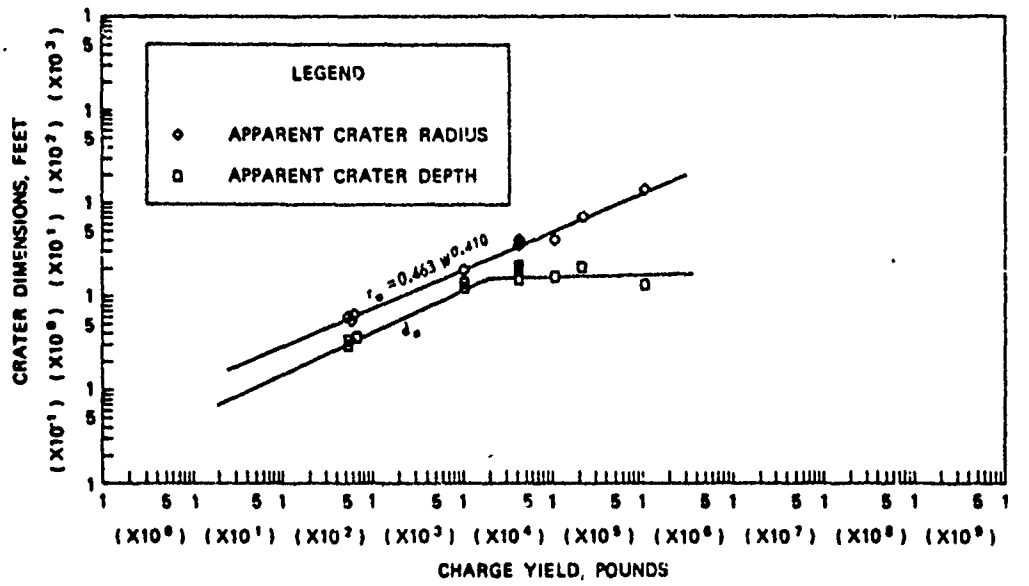

Figure B.93 Apparent crater radius and depth versus charge yield for hemispherical charges in sandy silty clay. Both curves are based upon 15 data points. The depth curve is approximated; for yields up to about 10,000 pounds, its equation is $0.20\ W^{0.45}$.

APPENDIX C

BIBLIOGRAPHY

This appendix contains a listing, generally in the order of introduction in the text, of reference material which was drawn upon most heavily to obtain crater data or to prepare the synopsis of cratering research in Chapter 2 or the discussions in Chapters 5, 6, and 7. It is divided into general fields of cratering subjects, and it will be noted that a few entries appear more than once in this appendix or appear both here and in the list of specific references.

BOMB/SHELL CRATERS

1. F. W. Anderson; "Crater Dimensions from Experimental Data"; FWE-18, September 1942 (TIS Issuance Date, October 1954); United States Atomic Energy Commission, Oak Ridge, Tennessee; Confidential.

2. U. S. Army Engineer Waterways Experiment Station, CE; "Simulated Artillery and Mortar Shell Tests 1967"; (unpublished); Conducted at Fort Benning, Georgia, 1967; Vicksburg, Mississippi; Unclassified.

3. B. B. Hoot; "Portable Bunker Tests and Evaluation"; Technical Report N-71-6, June 1971; "Appendix B: Crater Analysis of Live- and Static-Fire Tests", Pages 65-82; U. S. Army Engineer Waterways Experiment Station, CE, Vicksburg, Mississippi; Unclassified.

4. U. Fano; "Weight of Material Required to Fill Bomb Craters (Model Experiments)"; Report No. 488, September 1944; Ballistic Research Laboratories, Aberdeen Proving Ground, Maryland; Unclassified.

CRATERING BY HE SPHERES

5. T. J. Flanagan; "Project Air Vent, Crater Studies"; SC-RR-64-1704, April 1966; Sandia Corporation, Albuquerque, New Mexico; Unclassified.

6. U. S. Army Engineer Waterways Experiment Station, CE; "Ammonium Nitrate Cratering Tests"; (unpublished); Vicksburg, Mississippi; Unclassified.

7. L. J. Vortman and others; "Project Buckboard, 20-Ton and 1/2-Ton High Explosive Cratering Experiments in Basalt Rock"; SC-4675(RR), August 1962; Sandia Corporation, Albuquerque, New Mexico; Unclassified.

8. B. R. Redpath; "Project Trinidad: Explosive Excavation Tests in Sandstone and Shale"; Technical Report E-71-1, January 1973; U. S. Army Engineer Waterways Experiment Station, CE, Explosive Excavation Research Laboratory, Livermore, California; Unclassified.

9. C. V. Fulmer; "Cratering Characteristics of Wet and Dry Sand"; D2-90683-1, October 1965; The Boeing Company, Seattle, Washington; Unclassified.

10. R. Shnider; "Compilation of Crater Data from Surface and Underground Explosions"; Technical Report No. USNRDL-TR-212, March 1958; U. S. Naval Radiological Defense Laboratory, San Francisco, California; Unclassified.

11. U. S. Army Engineer Waterways Experiment Station, CE; "Cratering Effects of Surface and Buried HE Charges in Loess and Clay"; Technical Report No. 2-482, June 1958; Vicksburg, Mississippi; Unclassified.

12. L. J. Vortman; "Cratering Experiments with Large High Explosive Charges"; Geophysics, Volume XXVIII, No. 3, June 1963; Sandia Corporation, Albuquerque, New Mexico; Unclassified.

13. D. Conant and J. Swineford; "Cratering in Sand from Spherical Charges"; Report No. 669, May 1953; Ballistic Research Laboratories, Aberdeen, Maryland; Unclassified.

14. R. A. Sager; "Craters Formed by Small Explosions in Dry Sand"; Miscellaneous Paper No. 2-524, September 1962; U. S. Army Engineer Waterways Experiment Station, CE, Vicksburg, Mississippi; Unclassified.

15. C. A. Rappleyea; "Crater, Ejecta, and Air-Blast Studies from Five High-Explosive Charges in a Horizontal Square Array"; SC-RR-66-480, April 1967; Sandia Corporation, Albuquerque, New Mexico; Unclassified.

16. G. H. S. Jones, N. Spackman, and F. H. Winfield; "Cratering by Ground Burst TNT at Suffield Experimental Station, Ralston, Alberta"; Suffield Technical Paper No. 158, October 1959; Defence Research Establishment, Suffield, Alberta, Canada; Unclassified.

17. U. S. Army Engineer Waterways Experiment Station, CE; "Cratering from High Explosive Charges"; Technical Report No. 2-547; Vicksburg, Mississippi; Unclassified.

a. R. A. Sager, C. W. Denzel, and W. B. Tiffany; "Compendium of Crater Data"; Report No. 1, May 1960.

b. J. N. Strange, C. W. Denzel, and T. I. McLane; "Analysis of Crater Data"; Report No. 2, June 1961.

18. L. J. Vortman; "Craters from an Individually Detonated Multiple Charge Array"; SC-RR-67-727, November 1967; Sandia Laboratories, Albuquerque, New Mexico; Unclassified.

19. L. J. Vortman; "Craters from Surface Explosions and Scaling Laws"; Journal of Geophysical Research, July 1968; Volume 73, No. 14, Pages 4621-4636; American Geophysical Union, Richmond, Virginia; Unclassified.

20. U. S. Special Engineering Division, The Panama Canal; "Crater Tests in Basalt"; ICS Memorandum 284-P, April 1948; Canal Zone; Unclassified.

21. U. S. Special Engineering Division, The Panama Canal; "Crater Tests in Cucaracha and Culebra Formations"; ICS Memorandum 283-P, April 1948; Canal Zone; Unclassified.

22. U. S. Special Engineering Division, The Panama Canal; "Crater Tests in Gatun Sandstone"; ICS Memorandum 285-P, May 1948; Canal Zone; Unclassified.

23. U. S. Special Engineering Division, The Panama Canal; "Crater Tests in Marine Muck"; ICS Memorandum 286-P, May 1948; Canal Zone; Unclassified.

24. U. S. Special Engineering Division, The Panama Canal; "Crater Tests in Residual Clay"; ICS Memorandum 287-P, May 1948; Canal Zone; Unclassified.

25. U. S. Special Engineering Division, The Panama Canal; "Crater and Slope Tests with Explosives"; ICS Memorandum 282-P, June 1948; Canal Zone; Unclassified.

26. A. D. Rooke, Jr., J. W. Meyer, and J. A. Conway; "Dial Pack: Crater and Ejecta Measurements from a Surface-Tangent Detonation on a Layered Medium"; Miscellaneous Paper N-72-9, December 1972; U. S. Army Engineer Waterways Experiment Station, CE, Vicksburg, Mississippi; Unclassified.

27. A. D. Rooke, Jr., and others; "Participation in Operation Distant Plain, Apparent Crater and Ejecta Measurements"; Miscellaneous Paper No. 1-901, May 1967; U. S. Army Engineer Waterways Experiment Station, CE, Vicksburg, Mississippi; Unclassified.

28. L. K. Davis and others; "Participation in Operation Distant Plain, Project 3.01: Apparent Crater and Ejecta Measurements, Events 6A, 6, and 1A"; Miscellaneous Paper N-71-1, January 1971; U. S. Army Engineer Waterways Experiment Station, CE, Vicksburg, Mississippi; Unclassified.

29. U. S. Army Engineer Waterways Experiment Station, CE; "Effects of a Soil-Rock Interface on Cratering"; Technical Report No. 2-478, May 1958; Vicksburg, Mississippi; Unclassified.

30. C. W. Lampson; "Effects of Underground Explosions, IV, Influence of Variations of Soil Type and Depths of Charge and Gauge"; Report No. 6304 (NDRC A-359), February 1946; U. S. Office of Scientific Research and Development, Washington, D. C.; Restricted.

31. B. F. Murphey; "Explosion Craters in Desert Alluvium"; March 1961; Sandia Corporation, Albuquerque, New Mexico; Unclassified.

32. L. J. Vortman; "Explosive Cratering Experiments"; SCR-406, May 1961; Sandia Corporation, Albuquerque, New Mexico; Unclassified.

33. A. D. Rooke, Jr., and L. K. Davis; "Ferris Wheel Series, Flat Top Event, Project 1.9, Crater Measurements"; POR-3008 (WT-3008), August 1966; Defense Atomic Support Agency, Washington, D. C.; Unclassified

34. B. F. Murphey; "High Explosive Crater Studies: Tuff"; SC-4574(RR), April 1961; Sandia Corporation, Albuquerque, New Mexico; Unclassified.

35. L. J. Vortman; "High Explosive Craters in Tuff and Basalt"; March 1961; Sandia Corporation, Albuquerque, New Mexico; Unclassified.

36. B. F. Murphey; "High Explosive Crater Studies: Desert Alluvium"; SC-4614(RR), May 1961; Sandia Corporation, Albuquerque, New Mexico; Unclassified.

37. L. J. Vortman; "Jangle True Crater Measurements"; SC-RR-64-19, February 1964; Sandia Corporation, Albuquerque, New Mexico; Unclassified.

38. D. C. Campbell; "Operation Jangle, Project 1(9)-3, Some HE Tests and Observations on Craters and Base Surges"; WT-410, November 1951; Armed Forces Special Weapons Project, Washington D. C.; Unclassified.

39. E. B. Doll and V. Salmon; "Operation Jangle, Project 1(9)-1, Scaled HE Tests"; AFSWP-123, December 1952; Stanford Research Institute, Menlo Park, California; Secret.

40. J. A. Bishop and F. E. Lowance; "Operation Jangle, Project 4.2, Cratering and Missile Phenomena, Physical Characteristics of Crater and Lip"; WT-399 (in WT-375), May 1952; U. S. Naval Civil Engineering Research and Evaluation Laboratory, Port Hueneme, California; Unclassified.

41. L. K. Davis; "Mine Shaft Series, Subtask N123, Calibration Cratering Series"; Technical Report N-70-4, February 1970; U. S. Army Engineer Waterways Experiment Station, CE, Vicksburg, Mississippi; Unclassified.

42. L. K. Davis; "Mine Shaft Series, Events Mine Under and Mine Ore, Subtask N121, Crater Investigations"; Technical Report N-70-8, March 1970; U. S. Army Engineer Waterways Experiment Station, CE, Vicksburg, Mississippi; Unclassified.

43. L. K. Davis and B. L. Carnes; "Operation Mine Shaft, Cratering Effects of a 100-Ton Detonation on Granite"; Miscellaneous Paper N-72-1, February 1972; U. S. Army Engineer Waterways Experiment Station, CE, Vicksburg, Mississippi; Unclassified.

44. R. B. Vaile, Jr.; "Small Explosion Tests, Phase I of Project Mole"; AFSWP 288, December 1952; Stanford Research Institute, Stanford, California; Unclassified.

45. D. C. Sachs and L. M. Swift; "Small Explosion Tests, Project Mole"; AFSWP 291, Volumes I and II, December 1955; Stanford Research Institute, Menlo Park, California; Unclassified.

46. F. F. Videon; "Project Palanquin, Studies of the Apparent Crater"; PNE-904, July 1966; U. S. Army Engineer Nuclear Cratering Group, Lawrence Radiation Laboratory, Livermore, California; Unclassified.

47. G. H. S. Jones and others; "Operation Prairie Flat, Crater and Ejecta Study"; POR-2115 (TW-2115), December 1970; Defence Research Establishment, Suffield, Ralston, Alberta, Canada; Unclassified.

48. R. W. Harlan; "Project Pre-Gondola I, Crater Studies: Crater Measurements"; PNE-1107, Part I, May 1967; U. S. Army Engineer Nuclear Cratering Group, Lawrence Radiation Laboratory, Livermore, California; Unclassified.

49. G. W. Christopher and J. E. Lattery; "Project Pre-Gondola I, Crater Studies: Surface Motion"; PNE-1107, Part II, February 1969; U. S. Army Engineer Nuclear Cratering Group, Lawrence Radiation Laboratory, Livermore, California; Unclassified.

50. R. H. Benfer; "Project Pre-Schooner II, Apparent Crater Studies"; PNE-508, May 1967; U. S. Army Engineer Nuclear Cratering Group, Lawrence Radiation Laboratory, Livermore, California; Unclassified.

51. W. C. Day, editor; "Project Pre-Gondola II, Summary Report"; PNE-1112, February 1971; U. S. Army Engineer Nuclear Cratering Group, Lawrence Radiation Laboratory, Livermore, California; Unclassified.

52. J. L. Spruill and R. A. Paul; "Project Pre-Schooner, Crater Measurements"; PNE-502F, March 1965; U. S. Army Engineer Nuclear Cratering Group, Lawrence Radiation Laboratory, Livermore, California; Unclassified.

53. "Railroad Vulnerability Program"; TM-21, August 1958; Case Institute of Technology, Cleveland, Ohio; Unclassified.

54. R. W. Henny; "Schooner Observations and Early Results"; Technical Report No. AFWL-TR-69-133, October 1969; Air Force Weapons Laboratory, Kirtland Air Force Base, New Mexico; Unclassified.

55. W. R. Perrett and others, "Project Scooter"; SC-4602(RR), October 1963; Sandia Corporation, Albuquerque, New Mexico; Unclassified.

56. L. J. Vortman and others; "Project Stagecoach, 20-Ton HE Cratering Experiments in Desert Alluvium"; SC-4595(RR), May 1962; Sandia Corporation, Albuquerque, New Mexico; Unclassified.

57. R. F. Bourque; "Summary of Explosive Cratering Performance Tests Conducted at Site 300 During 1969"; NCG/TM 69-11, July 1970; U. S. Army Engineer Nuclear Cratering Group, Lawrence Radiation Laboratory, Livermore, California; Unclassified.

58. "Underground Explosion Test Program, Granite and Limestone"; Technical Report No. 4, Volume I, August 1952; Engineering Research Associates, Arlington, Virginia; Unclassified.

59. "Underground Explosion Test Program, Sandstone"; Technical Report No. 5, Volume I, February 1953; Engineering Research Associates, Arlington, Virginia; Unclassified.

60. "Underground Explosive Test Program, Soil"; Final Report, Volume I, August 1952; Engineering Research Associates, Arlington, Virginia; Unclassified.

61. "Undergrcund Explosion Test Program, Series I and Series II Experiments"; December 1948; Colorado School of Mines, Golden, Colorado; Unclassified.

62. "Investigation of Charge Shape"; (unpublished); Tests conducted at Fort Churchill, February-March 1957; U. S. Army Snow Ice and Permafrost Research Establishment, Wilmette, Illinois; Unclassified.

63. W. W. Johnson and D. L. Nelson; "Project Zulu II - Phase I, Single-Charge Calibration Series"; Technical Report No. 3, November 1968; U. S. Army Engineer Nuclear Cratering Group, Lawrence Radiation Laboratory, Livermore, California; Unclassified.

CRATERING BY HE HEMISPHERES

64. C. H. H. Diehl, G. H. S. Jones, and J. E. Krohn; "Cratering and Displacement Data for Three Surface Burst TNT Trials at SES (1963)"; Suffield Technical Paper No. 301, March 1965; Defence Research Establishment, Suffield, Ralston, Alberta, Canada; Unclassified.

65. C. H. H. Diehl, R. C. Wyld, and J. E. Krohn; "Cratering, Ejecta, and Displacement Data for a 40,000 Lb TNT Surface Burst Charge (1963)"; Suffield Technical Paper No. 300, November 1964; Defence Research Establishment, Suffield, Ralston, Alberta, Canada; Unclassified.

66. G. H. S. Jones, N. Spackman, and F. H. Winfield; "Cratering by Ground Burst TNT at Suffield Experimental Station, Ralston, Alberta"; Suffield Technical Paper No. 158, October 1959; Defence Research Establishment, Suffield, Alberta, Canada; Unclassified.

67. J. N. Strange and J. M. Pinkston, Jr.; "Crater Measurements from a 100-Ton Surface Explosion"; Miscellaneous Paper No. 2-529, October 1962; U. S. Army Engineer Waterways Experiment Station, CE, Vicksburg, Mississippi; Unclassified.

68. J. N. Strange and R. A. Sager; "Crater Measurements from a Twenty-Ton Surface Explosion"; Miscellaneous Paper No. 2-490, June 1962; U. S. Army Engineer Waterways Experiment Station, CE, Vicksburg, Mississippi; Unclassified.

69. J. N. Strange, W. L. Wallace, and W. E. Strohm; "Crater and Permanent Displacement Measurements from a Five-Ton Surface Explosion, U. S. Project 1.6, Canadian HE Test Program, 1959"; Miscellaneous Paper No. 2-424, April 1961; U. S. Army Engineer Waterways Experiment Station, CE, Vicksburg, Mississippi; Unclassified.

70. C. V. Fulmer; "Cratering in Sand with One-Pound Hemispheres"; D2-84111-1, February 1966; The Boeing Company, Seattle, Washington; Unclassified.

71. L. J. Vortman; "Dimensions of a Crater from a 500-Ton TNT Hemisphere Detonated on Rock"; SC-RR-65-277, July 1965; Sandia Corporation, Albuquerque, New Mexico; Unclassified.

72. G. H. S. Jones and J. E. Krohn; "Ground Displacement near the Detonation of a 40,000 Lb Hemisphere of TNT"; Suffield Technical Paper No. 213, December 1960; Defence Research Establishment, Suffield, Ralston, Alberta, Canada; Unclassified.

73. G. H. S. Jones and J. E. Krohn; "Permanent and Transient Displacement Due to Five-Ton Surface Bursts"; Suffield Technical Paper No. 178, March 1960; Defence Research Establishment, Suffield, Ralston, Alberta, Canada; Unclassified.

74. C. H. H. Diehl and G. H. S. Jones; "The Snowball Crater Profile and Ejecta Pattern"; Suffield Technical Note No. 188, May 1967; Defence Research Establishment, Suffield, Ralston, Alberta, Canada; Unclassified.

75. A. D. Rooke, Jr., and others; "Operation Snow Ball, Project 3.1, Crater Measurements and Earth Media Determinations; The Apparent and True Craters"; Miscellaneous Paper No. 1-987, April 1968; U. S. Army Engineer Waterways Experiment Station, CE, Vicksburg, Mississippi; Unclassified.

76. R. H. Carlson and W. A. Roberts; "Local Distribution of Material Ejected by Surface Explosions: White Tribe Interim Report"; D2-6955-2, August 1961; The Boeing Company, Seattle, Washington; Unclassified.

CRATERING BY NUCLEAR EXPLOSIONS

77. W. J. Christensen; "Cratering from Atomic Weapons"; AFSWP-514, June 1956; Headquarters, Armed Forces Special Weapons Project, Washington, D. C.; Confidential.

78. H. L. Brode and R. L. Bjork; "Cratering from a Megaton Surface Burst"; RM-2600, June 1960; Rand Corporation, Santa Monica, California; Unclassified.

79. M. D. Nordyke, "Project Danny Boy, Crater Studies"; ITR-1816, August 1962; Lawrence Radiation Laboratory, Livermore, California; Unclassified.

80. J. L. Gaylord; "Operation Ivy, Photographic Crater Survey"; WT-618, November 1952; Lookout Mountain Laboratory, Los Angeles, California; Unclassified.

81. A. D. Rooke, Jr., and J. N. Strange; "Crater Measurements, Project 1.9, Operation Sun Beam, Shot Johnie Boy"; POR-2284 (WT-2284), April 1965; Defense Atomic Support Agency, Washington, D. C.; Secret-Formerly Restricted Data.

82. A. V. Shelton, M. D. Nordyke, and R. H. Goeckermann; "The Neptune Event, A Nuclear Explosive Cratering Experiment"; UCRL-5766, April 1960; Lawrence Radiation Laboratory, Livermore, California; Unclassified.

83. L. J. Circeo, Jr., and M. D. Nordyke; "Nuclear Cratering Experience at the Pacific Proving Grounds"; UCRL-12172, November 1964; Lawrence Radiation Laboratory, Livermore, California; Unclassified.

84. M. D. Nordyke and M. M. Williamson; "Project Sedan, The Sedan Event"; PNE-242F, August 1965; Lawrence Radiation Laboratory, Livermore, California; Unclassified.

85. A. D. Rooke, Jr., L. K. Davis, and J. N. Strange; "Project 1.9, Operation Sun Beam, Shot Small Boy, Crater Measurements"; POR-2208 (WT-2208), March 1965; U. S. Army Engineer Waterways Experiment Station, CE, Vicksburg, Mississippi; Secret.

86. M. A. Chaszeyka; "Studies of Surface and Underground Nuclear Explosions (Analysis and Correlations of Nuclear and High Explosive Detonations with Regard to Cratering), Phase Report VII"; ARF Project 4195, February 1961; Armour Research Foundation of the Illinois Institute of Technology, Chicago, Illinois; Unclassified.

87. J. G. Lewis; "Operation Teapot, Project 1.6, Crater Measurements"; WT-1105, July 1958; Armed Forces Special Weapons Project, Sandia Base, Albuquerque, New Mexico; Unclassified.

88. U. S. Army Engineer Waterways Experiment Station, CE; "Project Trinity"; (unpublished); Vicksburg, Mississippi; Unclassified.

88a. R. B. Vaile; "Operation Castle, Project 3.2, Crater Survey"; WT-920, June 1955; Stanford Research Institute, Menlo Park, California; Secret.

USSR CRATERING EXPERIENCE

89. A. N. Dashkov; "Formation of an Excavation by a 1009-Ton Throw-Out Blast"; UCRL-Trans-10138, October 1967; Lawrence Radiation Laboratory, Livermore California; Unclassified.

90. O. L. Kedrovskiy; "Prospective Applications of Underground Nuclear Explosions in the National Economy of the USSR"; UCRL-Trans-10477, July 1970; Lawrence Radiation Laboratory, Livermore, California; Unclassified.

91. G. C. Werth; "The Soviet Program on Nuclear Explosives for the National Economy"; UCRL-72573, November 1970; Lawrence Radiation Laboratory, Livermore, California; Unclassified.

EJECTA MEASUREMENTS FROM HE SPHERES

92. R. H. Carlson and G. D. Jones; "Project Air Vent, Ejecta Distribution Studies"; D2-90575, November 1964; The Boeing Company, Seattle, Washington; Unclassified.

93. J. Wisotski; "Analysis of In-Flight Ejecta from Photography of a 100-Ton TNT Detonation on Granite"; DRI-2538, May 1970; Denver Research Institute, Denver, Colorado; Unclassified.

94. L. J. Vortman and others; "Project Buckboard, 20-Ton and 1/2-Ton High Explosive Cratering Experiments in Basalt Rock"; SC-4675(RR), August 1962, Sandia Corporation, Albuquerque, New Mexico; Unclassified.

95. C. A. Rappleyea; "Crater, Ejecta, and Air-Blast Studies from Five High-Explosive Charges in a Horizontal Square Array"; SC-RR-66-480, April 1967; Sandia Corporation, Albuquerque, New Mexico; Unclassified.

96. E. B. Ahlers; "Crater Ejecta Studies, Air Vent, Phase I"; IITRI-Proj M6072, May 1965; IIT Research Institute, Chicago, Illinois; Unclassified.

97. D. I. Fienstein; "Debris Distribution"; IITRI-Proj M6066, March 1966; IIT Research Institute, Chicago, Illinois; Unclassified.

98. J. W. Meyer; "Event Dial Pack, Project 3.01, Crater and Ejecta Studies"; (unpublished); U. S. Army Engineer Waterways Experiment Station, CE, Vicksburg, Mississippi; Unclassified.

99. A. D. Rooke, Jr., and others; "Participation in Operation Distant Plain, Apparent Crater and Ejecta Measurements"; Miscellaneous Paper No. 1-901, May 1967; U. S. Army Engineer Waterways Experiment Station, CE, Vicksburg, Mississippi; Unclassified.

100. R. W. Henny and R. H. Carlson; "Distribution of Natural Missiles Resulting from Cratering Explosions in Hard Rock"; (unpublished); October 1966; The Boeing Company, Seattle, Washington; Unclassified.

101. A. E. Sherwood; "The Effect of Air Drag on Particles Ejected During Explosive Cratering"; UCRL-14974, June 1966; Lawrence Radiation Laboratory, Livermore, California; Unclassified.

102. R. H. Carlson, D. M. Young, and G. D. Jones; "Ejecta Distribution from Cratering Events in Soil and Rock"; WL-TR-64-111, February 1965; Air Force Weapons Laboratory, Kirtland Air Force Base, New Mexico; Secret.

103. W. A. Roberts and T. P. Day; "Ejecta Missile Environment"; D2-125515-1, February 1968; The Boeing Company, Seattle, Washington; Secret.

104. R. H. Carlson and R. T. Newell; "Ejecta from Single-Charge Cratering Explosions: Volume I"; SC-RR-69-1, June 1970; Sandia Corporation, Albuquerque, New Mexico; Unclassified.

105. M. V. Anthony and others; "Ferris Wheel Series, Flat Top Event, Ejecta Distribution from Flat Top I Event, Project 1.5b"; POR-3007 (WT-3007), October 1965; The Boeing Company, Seattle, Washington; Unclassified.

106. E. B. Ahlers and C. A. Miller; "Crater Ejecta Studies, Project 1.5a, Flat Top Event"; POR-3006 (WT-3006), November 1966; IIT Research Institute, Chicago, Illinois; Unclassified.

107. J. A. Bishop and F. E. Lowance; "Operation Jangle, Project 4.2, and Missile Phenomena, Physical Characteristics of Crater and Lip"; WT-399 (in WT-375), May 1952; U. S. Naval Civil Engineering Research and Evaluation Laboratory, Port Hueneme, California; Unclassified.

108. L. J. Vortman; "Maximum Missile Ranges from Surface and Buried Explosions"; SC-RR-67-616, September 1967; Sandia Corporation, Albuquerque, New Mexico; Unclassified.

109. J. Wisotski; "Technical Photography of a 100-Ton TNT Detonation on Granite, Mineral Rock Event"; DRI-2543, June 1970; Denver Research Institute, Denver, Colorado; Unclassified.

110. J. W. Meyer and A. D. Rooke, Jr.; "Mine Shaft Series, Events Mine Under and Mine Ore Ejecta Studies"; Miscellaneous Paper N-69-2, September 1969; U. S. Army Engineer Waterways Experiment Station, CE, Vicksburg, Mississippi; Unclassified

111. R. W. Henny and R. H. Carlson; "Natural Missile Distributions for High Explosive Craters in Hard Rock; Multiple Threat Cratering Experiment"; Technical Report No. AFWL-TR-67-8, Volume III, June 1970; Air Force Weapons Laboratory, Kirtland Air Force Base, New Mexico; Unclassified.

112. W. C. Day, editor; "Project Pre-Gondola II, Summary Report"; PNE-1112, February 1971; U. S. Army Engineer Nuclear Cratering Group, Lawrence Radiation Laboratory, Livermore, California; Unclassified.

113. S. B. Mellsen; "Correlation of Drag Measurements in Operation Prairie Flat with Known Steady Flow Values"; Suffield Memorandum No. 12/69, April 1969; Defence Research Establishment, Suffield, Ralston, Alberta, Canada; Unclassified.

114. S. B. Mellsen; "Development of the Free Flight Method for the Measurement of Drag on Cylinders in Operation Prairie Flat"; Suffield Memorandum No. 119/68, January 1969; Defence Research Establishment, Suffield, Ralston, Alberta, Canada; Unclassified.

115. R. H. Carlson and W. A. Roberts; "Rayed Debris Distribution Systems Associated with Explosion Craters"; D2-09151, March 1962; The Boeing Company, Seattle, Washington; Unclassified.

116. W. A. Roberts and E. N. York; "Outer Crater Lip Debris Ejected by Scooter - A Buried High Explosive Cratering Shot"; D2-90086, April 1962; The Boeing Company, Seattle, Washington; Unclassified.

117. B. D. Anderson; "A Simple Technique to Determine the Size Distribution of Crater Fallback and Ejecta"; Technical Report No. 18, March 1970; U. S. Army Engineer Nuclear Cratering Group, Lawrence Radiation Laboratory, Livermore, California; Unclassified.

118. W. A. Roberts and J. A. Blaylock; "Distribution of Debris Ejected by the Stagecoach Series of High Explosive Cratering Bursts"; D2-6955-1, October 1961; The Boeing Company, Seattle, Washington; Unclassified.

EJECTA MEASUREMENTS FROM HE HEMISPHERES

119. R. H. Carlson and W. A. Roberts; "Ejecta Study of 100-Ton Suffield Explosive Cratering Shot"; D2-90203, September 1962; The Boeing Company, Seattle, Washington; Unclassified.

120. R. H. Carlson and W. A. Roberts; "Local Distribution of Material Ejected by Surface Explosions: White Tribe Interim Report"; D2-6955-2, August 1961; The Boeing Company, Seattle, Washington; Unclassified.

121. K. Kaplan; "Techniques for Preventing Damage from Ejecta Missiles for a Test with a 500 Ton Hemispherical Charge"; Report No. 655-81, December 1965; Defense Atomic Support Agency, Washington, D. C.; Unclassified.

EJECTA MEASUREMENTS FROM NUCLEAR EXPLOSIONS

122. L. K. Davis and A. D. Rooke, Jr.; "Danny Boy Event, Project 1.6, Mass Distribution Measurements of Crater Ejecta and Dust; Volumetric Equalities of the Crater"; Miscellaneous Paper No. 1-754, Appendix B, December 1965; U. S. Army Engineer Waterways Experiment Station, CE, Vicksburg, Mississippi; Unclassified.

123. E. B. Ahlers; "Danny Boy Event, Project 1.5, Throwout Study of an Underground Nuclear Detonation"· POR-1814 (WT-1814), February 1964; Armour Research Foundation of the Illinois Institute of Technology, Chicago, Illinois; Official Use Only.

124. A. D. Rooke, Jr., and L. K. Davis; "Danny Boy Event, Project 1.6, Mass Distribution Measurements of Crater Ejecta and Dust"; POR-1815 (WT-1815), February 1964; U. S. Army Engineer Waterways Experiment Station, CE, Vicksburg, Mississippi; Official Use only.

125. G. P. Ganong and W. A. Roberts; "The Effect of the Nuclear Environment on Crater Ejecta Trajectories for Surface Bursts"; Technical Report No. AFWL-TR-68-125, October 1968; Air Force Weapons Laboratory, Kirtland Air Force Base, New Mexico; Unclassified.

126. W. B. Wright, Jr.; "Fragment Size Distributions of Debris"; Memo RM-5698-DASA, June 1969; The Rand Corporation, Santa Monica, California; Secret.

127. D. T. Hove and J. L. Farr; "An Investigation of the Effects of Debris Size Distribution on the Depth of Debris Around a Nuclear Crater"; DASA-2515, April 1970; Defense Atomic Support Agency, Washington, D. C.; Confidential.

128. A. D. Rooke, Jr., G. B. Clark, and J. N. Strange; "Operation Sun Beam, Shot Johnie Boy, Project 1.5, Mass Distribution Measurements"; POR-2282 (WT-2282), February 1965; Defense Atomic Support Agency, Washington, D. C.; Confidential.

129. G. L. Kruchko; "Operation Sun Beam, Shot Little Feller II, Project 1.5, Debris Throwout"; POR-2262 (WT-2262), April 1965; Defense Atomic Support Agency, Washington, D. C.; Confidential.

130. D. E. Stroberger; "Nuclear Weapon Ejecta Parameters"; D2-125955-1, November 1968; The Boeing Company, Seattle, Washington; Secret.

131. J. Allen; "Project Sedan, Radioactive Pellet Trajectory Study"; PNE-218F, July 1965; Lawrence Radiation Laboratory, Livermore, California; Unclassified.

132. R. H. Carlson and W. A. Roberts; "Project Sedan, Mass Distribution and Throwout Studies"; PNE-217F, August 1963; The Boeing Company, Seattle, Washington; Unclassified.

133. W. A. Roberts, R. H. Carlson, and G. L. Keister; "Ejecta Studies, Sedan Event"; D2-90296, December 1962; The Boeing Company, Seattle, Washington; Unclassified.

HE MULTIPLE-CHARGE ARRAYS

134. L. J. Vortman; "Crater Formed by Detonating a Row of Charges Beneath a Ridge"; SC-RR-68-449, September 1968; Sandia Corporation, Albuquerque, New Mexico; Unclassified.

135. V. A. Harris; "Craters Formed by Row Charges in the Vertical Face of a 90-Degree Wedge"; SC-RR-66-477, November 1966; Sandia Corporation, Albuquerque, New Mexico; Unclassified.

136. L. J. Vortman; "Craters from Rows of Charges Detonated One at a Time in Permuted Sequences"; SC-RR-70-525, September 1970; Sandia Corporation, Albuquerque, New Mexico; Unclassified.

137. L. J. Vortman; "Craters from Row Charges Interrupted by a Dud"; SC-RR-67-3, February 1967; Sandia Corporation, Albuquerque, New Mexico; Unclassified.

138. L. J. Vortman; "Craters from Short-Row Charges and Their Interaction with Pre-Existing Craters"; SC-RR-66-324, July 1966; Sandia Corporation, Albuquerque, New Mexico; Unclassified.

139. L. J. Vortman; "Craters from a Single Row of Charges Buried Beneath the Craters from Parallel Rows of Charges"; SC-RR-65-478, October 1965; Sandia Corporation, Albuquerque, New Mexico; Unclassified.

140. L. J. Vortman; "Dimensions of Craters Produced by Simultaneous Detonation of Two Parallel Rows of Charges"; SC-RR-70-492, September 1970; Sandia Corporation, Albuquerque, New Mexico; Unclassified.

141. J. L. Spruill; "Project Dugout, Apparent Crater Studies"; PNE-601F, March 1965; U. S. Army Engineer Nuclear Cratering Group, Lawrence Radiation Laboratory, Livermore, California; Unclassified.

142. L. J. Vortman and L. N. Schofield; "The Effect of Row Charge Spacing and Depth on Crater Dimensions"; SC-4730(RR), November 1963; Sandia Corporation, Albuquerque, New Mexico; Unclassified.

143. V. A. Harris; "Explosion Craters with Flat Slopes in Alluvium Using Two-Pass Triple Rows"; SC-RR-69-158, September 1969; Sandia Corporation, Albuquerque, New Mexico; Unclassified.

144. A. D. Rooke, Jr., and L. K. Davis; "Project Pre-Buggy, Emplacement and Firing of High-Explosive Charges and Crater Measurements"; Miscellaneous Paper No. 1-663, February 1965; U. S. Army Engineer Waterways Experiment Station, CE, Vicksburg, Mississippi; Unclassified.

145. J. L. Spruill and F. F. Videon; "Project Pre-Buggy II, Studies of the Pre-Buggy II Apparent Craters"; PNE-315F, June 1965; U. S. Army Engineer Nuclear Cratering Group, Lawrence Radiation Laboratory, Livermore, California; Unclassified.

146. U. S. Army Engineer Nuclear Cratering Group, Lawrence Radiation Laboratory; "Summary of Raw Data Pre-Buggy II Chemical Explosive Experiments"; August 1963; Livermore, California; Unclassified.

147. J. P. Cress; "NCG Pre-Gondola III Sixty-Four Pound TNT Flat-Slope Experiments Conducted at Fort Peck, Montana"; NCG/TM 68-10, July 1968; U. S. Army Engineer Nuclear Cratering Group, Lawrence Radiation Laboratory, Livermore, California; Unclassified.

148. M. K. Kurtz, Jr., and W. C. Day; "A Report of the Scope and Preliminary Results of Project Pre-Gondola II, Row Charge Cratering Experiment"; NCG/TM 67-9, August 1967; U. S. Army Engineer Nuclear Cratering Group, Lawrence Radiation Laboratory, Livermore, California; Unclassified.

149. J. P. Cress and others; "Project Pre-Gondola III, Phase I, Summary Report"; PNE-1114, April 1970; U. S. Army Engineer Nuclear Cratering Group, Lawrence Radiation Laboratory, Livermore, California; Unclassified.

150. L. J. Vortman and L. N. Schofield; "Row-Charge Craters Through Terrain with a Single Elevation Change (A Contribution to the Plowshare Program)"; SC-4922(RR), July 1963; Sandia Corporation, Albuquerque, New Mexico; Unclassified.

151. L. J. Vortman; "A Scale-Model Experiment of the Crater Produced Through Terrain of Randomly Varying Elevation by Row Charges"; SC-4735(RR), November 1962; Sandia Corporation, Albuquerque, New Mexico; Unclassified.

152. L. J. Vortman; "A Small-Scale Investigation of Excavation with Parallel Rows of Explosions"; SC-RR-66-416, Part II, October 1966; Sandia Corporation, Albuquerque, New Mexico; Unclassified.

153. L. J. Vortman; "A Small-Scale Investigation of the Possibility of Constructing Low-Relief Earth-Fill Dams Using Nuclear Explosives"; SC-RR-65-41, February 1965; Sandia Corporation, Albuquerque, New Mexico; Unclassified.

154. L. J. Vortman; "A Small-Scale Investigation of Excavation with Parallel Rows of Explosions"; SC-RR-65-303, September 1965; Sandia Corporation, Albuquerque, New Mexico; Unclassified.

155. L. J. Vortman and others; "Project Stagecoach, 20-Ton HE Cratering Experiments in Desert Alluvium"; SC-4595(RR), May 1962; Sandia Corporation, Albuquerque, New Mexico; Unclassified.

156. M. A. Novak; "Project ZULU II, Laboratory-Scale Row-Charge Cratering Series"; Technical Report No. 5, November 1968; U. S. Army Engineer Nuclear Cratering Group, Lawrence Radiation Laboratory, Livermore, California; Unclassified.

NE ROW-CHARGE MEASUREMENTS

157. U. S. Army Engineer Nuclear Cratering Group, Lawrence Radiation Laboratory; "Buggy Crater Measurements"; (extract from unpublished report); Livermore, California; Unclassified.

158. L. J. Vortman; "Construction of a Sea-Level, Transisthmian Canal Using Nuclear Explosives"; SC-4929(RR), February 1964; Sandia Corporation, Albuquerque, New Mexico; Unclassified.

159. G. W. Johnson; "Excavation with Nuclear Explosives"; UCRL-5917, November 1960; Lawrence Radiation Laboratory, Livermore, California; Unclassified.

STEMMING

160. R. T. Allen; "The Effect of Stemming on Crater Formation at Shallow Depths of Burial"; DASA-2184, October 1968; Defense Atomic Support Agency, Washington, D. C.; Secret.

161. H. L. Knudson and others; "Effects of Stemming on High-Explosive Cratering"; Miscellaneous Paper N-72-6, May 1972; U. S. Army Engineer Waterways Experiment Station, CE, Vicksburg, Mississippi; Unclassified.

162. U. S. Army Engineer Waterways Experiment Station, CE; "Effects of Stemming on Underground Explosions"; Technical Report No. 2-438, January 1957; Vicksburg, Mississippi; Unclassified.

163. D. L. Martin and W. J. Hinze; "Energy Partition of Underground Explosions"; AFSWP-789, March 1958; U. S. Army Engineer Research and Development Laboratories, Fort Belvoir, Virginia; Unclassified.

164. H. Firstenberg; "An Investigation of the Stemming Effects on Underground Nuclear Explosives"; NUS-346, April 1967; U. S. Army Engineer Research and Development Laboratories, Fort Belvoir, Virginia; Unclassified.

165. U. S. Army Engineer Waterways Experiment Station, CE; "Stemming Effects for Certain HE Charges"; Miscellaneous Paper No. 2-192, March 1957; Vicksburg, Mississippi; Unclassified.

166. U. S. Army Engineer Waterways Experiment Station, CE; "Study of Energy Partitioning for Partially Confined Explosives"; Technical Memorandum No. 2-422, November 1955; Vicksburg, Mississippi; Unclassified.

WATER-TABLE EFFECTS

167. L. K. Davis; "Effects of a Near-Surface Water Table on Crater Dimensions"; Miscellaneous Paper No. 1-939. October 1967; U. S. Army Engineer Waterways Experiment Station, CE, Vicksburg, Mississippi; Unclassified.

UNDERWATER CRATERING

168. L. K. Davis and A. D. Rooke, Jr.; "High-Explosive Cratering Experiments in Shallow Water"; Miscellaneous Paper No. 1-946, December 1968; U. S. Army Engineer Waterways Experiment Station, CE, Vicksburg, Mississippi; Unclassified.

169. U. S. Naval Weapons Laboratory; "Shallow Underwater Explosion Tests"; October 1962; Dahlgren, Virginia; Unclassified.

170. J. E. Eldridge and P. M. Fye; "Underwater Craters Formed by Explosions on the Sea Floor"; Report No. 6244 (NDRC A-366), November 1945; U. S. Office of Scientific Research and Development, Washington, D. C.; Unclassified.

171. J. N. Strange; "Underwater Cratering"; Miscellaneous Paper No. 1-598, September 1963; U. S. Army Engineer Waterways Experiment Station, CE, Vicksburg, Mississippi; Confidential.

REPEATED EXPLOSIONS ALONG A COMMON VERTICAL AXIS

172. J. N. Strange and A. D. Rooke, Jr.; "Craters Resulting from Repeated Explosions Along a Common Vertical Axis"; Technical Report No. 1-665, November 1964; U. S. Army Engineer Waterways Experiment Station, CE, Vicksburg, Mississippi; Unclassified.

173. L. J. Vortman; "Craters from Repeated Direct Hits at the Same Aiming Point"; SC-4760(RR), January 1963; Sandia Corporation, Albuquerque, New Mexico; Unclassified.

174. T. E. O'Brien and others; "Multiple Threat Cratering Experiment, Volume I, Successive Cratering in Hard Rock"; Technical Report No. AFWL-TR-67-8, April 1967; Air Force Weapons Laboratory, Kirtland Air Force Base, New Mexico; Unclassified.

175. B. Bennett; "Successive Cratering Shots Along the Same Vertical Axis"; D2-90454, November 1963; The Boeing Company, Seattle, Washington; Unclassified.

CRATERING IN ICE AND SNOW

176. R. A. Sager; "Cratering Data for 1960 Greenland Test Series of High-Explosive Charges in Snow"; (unpublished); U. S. Army Engineer Waterways Experiment Station, CE, Vicksburg, Mississippi; Unclassified.

177. J. A. Conway and J. W. Meyer; "Cratering in Greenland Icecap Snow"; Miscellaneous Paper N-70-6, July 1970; U. S. Army Engineer Waterways Experiment Station, CE, Vicksburg, Mississippi; Unclassified.

178. C. W. Livingston; "Fort Churchill Blast Tests, Blasts in Frozen Glacial Till"; Volume II, September 1956; U. S. Army Snow, Ice and Permafrost Research Establishment, CE, Wilmette, Illinois; Unclassified.

179. U. S. Army Engineer Waterways Experiment Station, CE; "Explosions in Ice"; (unpublished); Tests Conducted in Greenland in 1957; Vicksburg, Mississippi; Unclassified.

180. C. W. Livingston; "Explosions in Snow"; TR 86, May 1968; U. S. Army Cold Regions Research and Engineering Laboratory, Hanover, New Hampshire; Unclassified.

APPENDIX D

COMPUTER PROGRAM FOR CRATER DATA

This appendix contains an annotated listing (Table D.1) of the computer program developed to sort, analyze, and plot the crater data in Appendixes A and B. The program is shown in this form in the hope that it may be more understandable to the layman, while at the same time providing sufficient information from which a similar program could be constructed if desired.

Note that the program is essentially in two parts--a main program and a plotting subroutine. The computer language is FORTRAN[1] IV; the program was run on a GE-400 Series computer at the WES. Plotting was accomplished on a CalComp Plotter.

---

[1] Formula translation.

BEST AVAILABLE COPY

TABLE D.1 COMPUTER PROGRAM FOR CRATER DATA

Explanation	Card No.	Statement
Control Cards		$ NOLABEL
		$ BCDIN
		$ BCDOUT
	1	DIMENSION IBUF(1600)
	2	DIMENSION WORDS(13),CY(200),HOB(200),RA(200),DA(200),HL(200)
	3	DIMENSION VA(200),HT(200),DT(200),VT(200),Z(200)
	4	DIMENSION P(7),SUMY(7),SXY(7),CO(7),SX2(7),SUMX(7),
	5	DIMENSION IBEN(200)
	6	COMMON X(75),Y1(75),Y2(75),Y3(75),Y4(75),Y5(75),Y6(75),Y7(75),NO,F
	7	COMMON YS(7),YL(7),EX(7),IB(75)
	8	CALL PLOTS(IBUF(1),1600,3)
	9	REWIND 3
	10	CALL PLOT(0.,-10.,-3)
	11	CALL PLOT(5.,3.,-3)
	12	PRINT 417
	13	417 FORMAT(1H1,61X,14HBENNY L CARNES//53X,32HNUCLEAR WEAPONS EFFECTS D 1IVISION//57X,23HCRATER DATA COMPILATION)
Read in Data	14	53 CONTINUE
	15	READ 1, (WORDS(I),I=1,13),N
	16	1 FORMAT(12A6,4X,I4)
	17	IF(N.GT.0) GO TO 51
	18	IF(N.LT.0) GO TO 52
	19	GO TO 53
	20	51 DO 101 I=1,N
	21	READ 2, CY(I),HOB(I),RA(I)
	22	2 FORMAT(15X,E15.5,15X,F10.1,5X,F10.1)
	23	READ 3, DA(I),HL(I),VA(I),HT(I),DT(I),VT(I),IBEN(I)
	24	3 FORMAT(2F5.1,2F10.1,F5.1,F10.1,10X,I5)
	25	Z(I)=HOB(I)/CY(I)**(1.0/3.0)
	26	101 CONTINUE
	27	PRINT 418, (WORDS(IJ),IJ=1,I2)
	28	418 FORMAT(1H1,29X,12A6/)
	29	PRINT 402
	30	402 FORMAT(1H ,36X,3HDIM,2X,3HTOT,3X,5HCOEFF,7X,3HEXP, 6X,2HX1,7X,2HY1 1,9X,2HX2,10X,2HY2)
Begin to Separate into HOB Categories	31	NO=0
	32	DO 102 J=1,10
	33	NO=0
	34	FIT=0.
	35	F=0.
	36	DO 228 L=1,7
	37	M(L)=0
	38	SUMY(L)=0.
	39	SXY(L)=0.
	40	SUMX(L)=0.
	41	SX2(L)=0.
	42	228 CONTINUE
	43	PRINT 407, J
	44	407 FORMAT(1H ,51X, 31HSCALED HEIGHT OF BURST CATEGORY,I3)
	45	DO 103 I=1,N
	46	IF(Z(I).GE.0.9.AND.J.EQ.1) GO TO 202
	47	IF(Z(I).LT.0.9.AND.Z(I).GE.0.2.AND.J.EQ.2) GO TO 202
	48	IF(Z(I).LT.0.2.AND.Z(I).GE.0.05.AND.J.EQ.3) GO TO 202
	49	IF(Z(I).LT.0.05.AND.Z(I).GE.-0.05.AND.J.EQ.4) GO TO 202

(Continued)

BEST AVAILABLE COPY

TABLE D.1 (CONTINUED)

Explanation	Card No.		Statement
Finish Separation into ROD Categories and Begin Calculations on Least-Squares Fit Curves	50		IF(Z(I).LT.-0.05.AND.Z(I).GE.-0.2.AND.J.EQ.5) GO TO 202
	51		IF(Z(I).LT.-0.2.AND.Z(I).GE.-0.5.AND.J.EQ.6) GO TO 202
	52		IF(Z(I).LT.-0.5.AND.Z(I).GE.-0.9.AND.J.EQ.7) GO TO 202
	53		IF(Z(I).LT.-0.9.AND.Z(I).GE.-1.1.AND.J.EQ.8) GO TO 202
	54		IF(Z(I).LT.-1.1.AND.Z(I).GE.-2.0.AND.J.EQ.9) GO TO 202
	55		IF(Z(I).LT.-2.0.AND.J.EQ.10) GO TO 202
	56		GO TO 201
	57	202	NO=NO+1
	58		IF(RA(I).EQ.0.) GO TO 211
	59		M(1)=M(1)+1
	60		SUMY(1)=SUMY(1)+ALOG(RA(I))
	61		SXY(1)=SXY(1)+ALOG(CY(I))*ALOG(RA(I))
	62		SUMX(1)=SUMX(1)+ALOG(CY(I))
	63		SX2(1)=SX2(1)+ALOG(CY(I))*ALOG(CY(I))
	64	211	IF(DA(I).EQ.0.) GO TO 212
	65		M(2)=M(2)+1
	66		SUMY(2)=SUMY(2)+ALOG(DA(I))
	67		SXY(2)=SXY(2)+ALOG(CY(I))*ALOG(DA(I))
	68		SUMX(2)=SUMX(2)+ALOG(CY(I))
	69		SX2(2)=SX2(2)+ALOG(CY(I))*ALOG(CY(I))
	70	212	IF(HL(I).EQ.0.) GO TO 213
	71		M(3)=M(3)+1
	72		SUMY(3)=SUMY(3)+ALOG(HL(I))
	73		SXY(3)=SXY(3)+ALOG(CY(I))*ALOG(HL(I))
	74		SUMX(3)=SUMX(3)+ALOG(CY(I))
	75		SX2(3)=SX2(3)+ALOG(CY(I))*ALOG(CY(I))
	76	213	IF(RT(I).EQ.0.) GO TO 214
	77		M(4)=M(4)+1
	78		SUMY(4)=SUMY(4)+ALOG(RT(I))
	79		SXY(4)=SXY(4)+ALOG(CY(I))*ALOG(RT(I))
	80		SUMX(4)=SUMX(4)+ALOG(CY(I))
	81		SX2(4)=SX2(4)+ALOG(CY(I))*ALOG(CY(I))
	82	214	IF(DT(I).EQ.0.) GO TO 215
	83		M(5)=M(5)+1
	84		SUMY(5)=SUMY(5)+ALOG(DT(I))
	85		SXY(5)=SXY(5)+ALOG(CY(I))*ALOG(DT(I))
	86		SUMX(5)=SUMX(5)+ALOG(CY(I))
	87		SX2(5)=SX2(5)+ALOG(CY(I))*ALOG(CY(I))
	88	215	IF(VA(I).EQ.0.) GO TO 216
	89		M(6)=M(6)+1
	90		SUMY(6)=SUMY(6)+ALOG(VA(I))
	91		SXY(6)=SXY(6)+ALOG(CY(I))*ALOG(VA(I))
	92		SUMX(6)=SUMX(6)+ALOG(CY(I))
	93		SX2(6)=SX2(6)+ALOG(CY(I))*ALOG(CY(I))
	94	216	IF(VT(I).EQ.0.) GO TO 217
	95		M(7)=M(7)+1
	96		SUMY(7)=SUMY(7)+ALOG(VT(I))
	97		SXY(7)=SXY(7)+ALOG(CY(I))*ALOG(VT(I))
	98		SUMX(7)=SUMX(7)+ALOG(CY(I))
	99		SX2(7)=SX2(7)+ALOG(CY(I))*ALOG(CY(I))
	100	217	CONTINUE
	101		IF(HL(I).EQ.0.0) HL(I)=0.001
	102		Y3(NO)=ALOG10(HL(I))+2.0
	103		Y3(NO)=Y3(NO)+0.75

(Continued)

(2 of 7 Sheets)

BEST AVAILABLE COPY

TABLE D.1 (CONTINUED)

Explanation	Card No.	Statement
Finish Least-Squares Fit Calculations and Begin Preparing Data for Plotting	104	IF(VT(I).EQ.0.0) VT(I)=0.001
	105	Y7(NO)=ALOG10(VT(I))+1.0
	106	Y7(NO)=Y7(NO)+0.75
	107	IF(DT(I).EQ.0.0) DT(I)=0.001
	108	Y5(NO)=ALOG10(DT(I))+2.0
	109	Y5.NO)=Y5(NO)+0.75
	110	IF(RT(I).EQ.0.0) RT(I)=0.001
	111	Y4(NO)=ALOG10(RT(I))+2.0
	112	Y4(NO)=Y4(NO)+0.75
	113	IF(VA(I).EQ.0.0) VA(I)=0.001
	114	Y6(NO)=ALOG10(VA(I))+1.0
	115	Y6(NO)=Y6(NO)+0.75
	116	IF(DA(I).EQ.0.0) DA(I)=0.001
	117	Y2(NO)=ALOG10(DA(I))+2.0
	118	Y2(NO)=Y2(NO)+0.75
	119	IF(RA(I).EQ.0.0) RA(I)=0.001
	120	Y1(NO)=ALOG10(RA(I))+2.0
	121	Y1(NO)=Y1(NO)+0.75
	122	IB(NO)=IBEN(I)
	123	X(NO)=ALOG10(CY(I))
	124	X(NO)=X(NO)+0.75
	125	IF(X(NO).GT.F) F=X(NO)
	126	IF(X(NO).LT.FIT) FIT=X(NO)
	127	BENT=F-FIT
	128	201 IF(I.LT.N) GO TO 103
	129	IF(NO.EQ.0) GO TO 103
	130	F=F+0.375
	131	M=EXP10(F/0.75)
	132	DO 218 K=1,7
	133	IF(M(K).LT.2) GO TO 406
	134	IF(BENT.LT.0.37 GO TO 406
	135	EN=M(K)
	136	B=EN*SXY(K)
	137	C=EN*SX2(K)
	138	D=SUMX(K)*SUMY(K)
	139	E=SUMX(K)*SUMX(K)
	140	FF=B-D
	141	G=C-E
	142	IF(G.LT.0.000001) EX(K)=0.0
	143	IF(G.LT.0.00001) GO TO 410
	144	EX(K)=FF/G
	145	410 H=(SUMY(K)-EX(K)*SUMX(K))/EN
	146	CO(K)=EXP(H)
	147	YS(K)=CO(K)*(1.0)**EX(K)
	148	YL(K)=CO(K)*H**EX(K)
	149	GO TO 405
	150	406 YS(K)=0.001
	151	YL(K)=0.001
	152	CO(K)=0.
	153	EX(K)=0.
	154	405 CONTINUE
	155	MO=MO+1
	156	IF(MO.GT.44) GO TO 401
	157	403 CONTINUE

(Continued)

(3 of 7 Sheets)

BEST AVAILABLE COPY

TABLE D.1 (CONTINUED)

Explanation	Card No.	Statement
Call Plotting Subroutine Print Out Least-Square Fit Data	158	PRINT 219, CO(K),EX(K)
	159	219 FORMAT(1H+,43X,F10.4,F10.5)
	160	GO TO 404
	161	401 CONTINUE
	162	PRINT 418, (WORDS(IJ),IJ=1,12)
	163	PRINT 402
	164	MO=0
	165	GO TO 403
	166	404 CONTINUE
	167	X1=1.0
	168	PRINT 227, K,M(K),X1,YS(K),M,YL(K)
	169	227 FORMAT(1H ,33X,215,20X,F7.1,F10.1,F13.1,F10.1)
	170	IF(YS(K).EQ.0.) YS(K)=0.001
	171	IF(YL(K).EQ.0.) YL(K)=0.001
	172	IF (K.GT.5) GO TO 500
	173	YS(K)=ALOG10(YS(K))+2.0
	174	YS(K)=YS(K)+0.75
	175	YL(K)=ALOG10(YL(K))+2.0
	176	YL(K)=YL(K)+0.75
	177	GO TO 218
	178	500 CONTINUE
	179	YS(K)=(ALOG10(YS(K))+1.0)+0.75
	180	YL(K)=(ALOG10(YL(K))+1.0)+0.75
	181	218 CONTINUE
	182	412 CONTINUE
	183	CALL CHATER
Control Cards	184	411 CONTINUE
	185	103 CONTINUE
	186	102 CONTINUE
	187	GO TO 93
	188	52 CONTINUE
	189	CALL PLOT(15.,0.,999)
	190	REWIND 3
	191	END

* * * * *

CONTINUE WITH SUBROUTINES

(Continued)

(4 of 7 Sheets)

BEST AVAILABLE COPY

TABLE D.1 (CONTINUED)

Explanation	Card No.	Statement
Control Cards	1	SUBROUTINE CRATER
	2	REAL LEG,IDENT
	3	COMMON X(75),Y1(75),Y2(75),Y3(75),Y4(75),Y5(75),Y6(75),Y7(75),NO,F
	4	COMMON YS(7),YL(7),EX(7),IB(75)
	5	DIMENSION XLBL(3),YLBL(4),LEG(2),IDENT(3)
	6	YLBL(1)= 8HCRATER D
	7	YLBL(2)= 8HIMENSION
	8	YLBL(3)= 6HS, FEET
	9	YLBL(4)= 8H
	10	XLBL(1)= 8HCHARGE Y
	11	XLBL(2)= 8HIELD, PO
	12	XLBL(3)= 8HUNDS
	13	T=0.75
	14	CALL LGAXIS(0.,0.,YLBL,-24,.1, T,6,1,.01,1,2,1)
Draw First Set of Axes	15	CALL PLOT(0.,4.5,3)
	16	CALL PLOT(7.5,4.5,2)
	17	CALL PLOT(7.5,0.,2)
	18	CALL LGAXIS(0.,0.,XLBL,-24,.1, T, 10,0,1,,1,2,1)
	19	CALL PLOT(4.,0.3,3)
	20	CALL PLOT(4.,1.6,2)
	21	CALL PLOT(7.,1.6,2)
	22	CALL PLOT(7.,0.3,2)
	23	CALL PLOT(4.,0.3,2)
	24	IDENT(1)=8HAPPARENT
	25	IDENT(2)=8H CRATER
	26	IDENT(3)=8HRADIUS
	27	LEG(1)=6HLEGEND
	28	CALL SYMBOL(5.2,1.3,0.1,LEG,0.,6)
	29	CALL SYMBOL(4.6,1.1,0.1,IDENT,0.,24)
	30	IDENT(2)=8H CRATER
	31	IDENT(3)=8HDEPTH
	32	CALL SYMBOL(4.6,0.8,0.1,IDENT,0.,24)
	33	IDENT(2)=8H CRATER
	34	IDENT(3)=8HLIP HT
	35	CALL SYMBOL(4.6,0.5,0.1,IDENT,0.,24)
	36	CALL POINT(4.2,1.15,.1,.06)
	37	CALL POINT(4.2,0.85,2,.06)
	38	CALL POINT(4.2,0.55,3,.06)
Plot Points and Begin to Draw Least-Squares Curves	39	DO 301 I=1,NO
	40	IF(Y1(I).LT.0.) GO TO 311
	41	IF(IB(I).GT.0) GO TO 311
	42	CALL POINT(X(I),Y1(I),1,.06)
	43	311 IF(Y2(I).LT.0.) GO TO 312
	44	IF(IB(I).GT.0) GO TO 312
	45	CALL POINT(X(I),Y2(I),2,.06)
	46	312 IF(Y3(I).LT.0.) GO TO 301
	47	IF(IB(I).GT.0) GO TO 301
	48	CALL POINT(X(I),Y3(I),3,.06)
	49	301 CONTINUE
	50	IF(YS(1).LT.0.0) GO TO 220
	51	IF(EX(1).GT.1.5) GO TO 220
	52	IF(EX(1).EQ.0.) GO TO 220
	53	CALL PLOT(0.,YS(1),3)
	54	CALL PLOT(F,YL(1),2)

(Continued)

BEST AVAILABLE COPY

TABLE D.1 (CONTINUED)

Explanation	Card No.	Statement
Finish Drawing Least-Squares Curves	55	220 CONTINUE
	56	IF(YS(2).LT.0.0) GO TO 221
	57	IF(EX(2).GT.1.5) GO TO 221
	58	IF(EX(2).EQ.0.) GO TO 221
	59	CALL PLOT(0.,YS(2),3)
	60	CALL PLOT(F,YL(2),2)
	61	221 CONTINUE
	62	IF(YS(3).LT.0.0) GO TO 222
	63	IF(EX(3).GT.1.5) GO TO 222
	64	IF(EX(3).EQ.0.) GO TO 222
	65	CALL PLOT(0.,YS(3),3)
	66	CALL PLOT(F,YL(3),2)
	67	222 CONTINUE
Draw Second Set of Axes	68	CALL PLOT(0.,8.,-3)
	69	CALL LGAXIS(0.,0.,YLBL,-24,.1, Y,6.1,.01,1.2,1)
	70	CALL PLOT(0.,4.5,3)
	71	CALL PLOT(7.5,4.5,2)
	72	CALL PLOT(7.5,0.,2)
	73	CALL LGAXIS(0.,0.,XLBL,-24,.1, Y, 10.0,1.,1.2,1)
	74	CALL PLOT(4.,0.3,3)
	75	CALL PLOT(4.,1.6,2)
	76	CALL PLOT(7.,1.6,2)
	77	CALL PLOT(7.,0.3,2)
	78	CALL PLOT(4.,0.3,2)
	79	CALL SYMBOL(5.2,1.3,0.1,LEG,0.,6)
	80	IDENT(1)=8HTRUE CRA
	81	IDENT(2)=8HTER RADI
	82	IDENT(3)=8HUS
	83	CALL SYMBOL(4.6,0.9,0.1,IDENT,0.,24)
	84	IDENT(2)=8HTER DEPT
	85	IDENT(3)=8HH
	86	CALL SYMBOL(4.8,0.5,0.1,IDENT,0.,24)
Plot Points and Draw Least-Squares Curves	87	CALL POINT(4.3,0.95,.2,.06)
	88	CALL POINT(4.3,0.55,3,.06)
	89	DO 302 I=1,NO
	90	IF(Y4(I).LT.0.) GO TO 313
	91	IF(IB(I).GT.0) GO TO 313
	92	CALL POINT(X(I),Y4(I),2,.06)
	93	313 IF(Y5(I).LT.0.) GO TO 302
	94	IF(IB(I).GT.0) GO TO 302
	95	CALL POINT(X(I),Y5(I),3,.06)
	96	302 CONTINUE
	97	IF(YS(4).LT.0.0) GO TO 223
	98	IF(EX(4).GT.1.5) GO TO 223
	99	IF(EX(4).EQ.0.) GO TO 223
	100	CALL PLOT(0.,YS(4),3)
	101	CALL PLOT(F,YL(4),2)
	102	223 CONTINUE
	103	IF(YS(5).LT.0.0) GO TO 226
	104	IF(EX(5).GT.1.5) GO TO 226
	105	IF(EX(5).EQ.0.) GO TO 226
	106	CALL PLOT(0.,YS(5),3)
	107	CALL PLOT(F,YL(5),2)
	108	226 CONTINUE

(Continued)

BEST AVAILABLE COPY

TABLE D.1 (CONCLUDED)

Explanation	Card No.	Statement
	109	YLBL(3)= 8HS, CUBIC
	110	YLBL(4)= 8H FEET
	111	CALL PLOT(0.,8.,-3)
	112	CALL LGAXIS(0.,0.,YLBL,+32,.1, 7,6,1,0,1,1,2,1)
	113	CALL PLOT(0.,4.5,3)
	114	CALL PLOT(7.5,4.5,2)
	115	CALL PLOT(7.5,0.,2)
Draw Third Set of Axes	116	CALL LGAXIS(0.,0.,XLBL,-24,.1, 7, 10,0,1,,1,2,1)
	117	CALL PLOT(4.,0.3,3)
	118	CALL PLOT(4.,1.6,2)
	119	CALL PLOT(7.,1.6,2)
	120	CALL PLOT(7.,0.3,2)
	121	CALL PLOT(4.,0.3,2)
	122	CALL SYMBOL(5.2,1.3,0.1,LEG,0.,6)
	123	IDENT(1)=8HAPPARENT
	124	IDENT(2)=8H CRATER
	125	IDENT(3)=8HVOLUME
	126	CALL SYMBOL(4.6,0.9,0.1,IDENT,0.,24)
	127	IDENT(1)=8HTRUE CRA
	128	IDENT(2)=8HTER VOLU
	129	IDENT(3)=8HME
	130	CALL SYMBOL(4.6,0.5,0.1,IDENT,0.,24)
	131	CALL POINT(4.2,0.95,2,.06)
	132	CALL POINT(4,2,0.55,3,.06)
	133	DO 303 I=1,NO
	134	IF(Y6(I).LT.0.) GO TO 314
	135	IF(IB(I).GT.0) GO TO 314
	136	CALL POINT(X(I),Y6(I),2,.06)
	137	314 IF(Y7(I).LT.0.) GO TO 303
Plot Points and Draw Least-Squares Curves	138	IF(IB(I).GT.0) GO TO 303
	139	CALL POINT(X(I),Y7(I),3,.06)
	140	303 CONTINUE
	141	IF(YS(0).LT.0.0) GO TO 224
	142	IF(EX(6).GT.1.5) GO TO 224
	143	IF(EX(6).EQ.0.) GO TO 224
	144	CALL PLOT(0.,YS(6),3)
	145	CALL PLOT(F,YL(6),2)
	146	224 CONTINUE
	147	IF(YS(7).LT.0.0) GO TO 225
	148	IF(EX(7).GT.1.5) GO TO 225
	149	IF(EX(7).EQ.0.) GO TO 225
	150	CALL PLOT(0.,YS(7),3)
	151	CALL PLOT(F,YL(7),2)
	152	225 CONTINUE
Control Cards	153	CALL PLOT(12.,-30.,-3)
	154	CALL PLOT(0.,3.,-3)
	155	RETURN
	156	END

(7 of 7 Sheets)

REFERENCES

1. R. A. Sager, C. W. Denzel, and W. B. Tiffany; "Cratering from High Explosive Charges, Compendium of Crater Data"; Technical Report No. 2-547, Report 1, May 1960; U. S. Army Engineer Waterways Experiment Station, CE, Vicksburg, Mississippi; Unclassified.

2. J. N. Strange, C. W. Denzel, and T. I. McLane; "Cratering from High Explosive Charges, Analysis of Crater Data"; Technical Report No. 2-547, Report 2, June 1961; U. S. Army Engineer Waterways Experiment Station, CE, Vicksburg, Mississippi; Unclassified.

3. G. C. Werth; "The Soviet Program on Nuclear Explosives for the National Economy"; UCRL-72573, November 1970; Lawrence Radiation Laboratory, Livermore, California; Unclassified.

4. R. H. Carlson and W. A. Roberts; "Project Sedan, Mass Distribution and Throwout Studies"; PNE-217F, August 1963; The Boeing Company, Seattle, Washington; Unclassified.

5. A. J. Chabai; "Scaling Dimensions of Craters Produced by Buried Explosions"; SC-RR-65-70, February 1965; Sandia Corporation, Albuquerque, New Mexico; Unclassified.

6. R. H. Carlson; "Crater Scaling as a Function of Charge Burst Depth"; D180-10100-1, February 1970; The Boeing Company, Seattle, Washington; Unclassified.

7. L. J. Vortman; "Maximum Missile Ranges from Surface and Buried Explosions"; SC-RR-67-616, September 1967; Sandia Corporation, Albuquerque, New Mexico; Unclassified.

8. H. L. Knudson, J. W. Meyer, S. B. Price, and A. D. Rooke, Jr.; "Effects of Stemming on High-Explosive Cratering"; Miscellaneous Paper N-72-6, May 1972; U. S. Army Engineer Waterways Experiment Station, CE, Vicksburg, Mississippi; Unclassified.

9. L. K. Davis and A. D. Rooke, Jr.; "High Explosive Cratering Experiments in Shallow Water"; Miscellaneous Paper No. 1-946, December 1968; U. S. Army Engineer Waterways Experiment Station, CE, Vicksburg, Mississippi; Unclassified.

10. A. D. Rooke, Jr., and L. K. Davis; "Project Pre-Buggy, Emplacement and Firing of High-Explosive Charges and Crater Measurements"; Miscellaneous Paper No. 1-663, February 1965; U. S. Army Engineer Waterways Experiment Station, CE, Vicksburg, Mississippi; Unclassified.

11. G. H. Higgins and T. R. Butkovich; "Effect of Water Content, Yield, Medium, and Depth of Burst on Cavity Radii"; UCRL-50203, February 1967; Lawrence Radiation Laboratory, Livermore, California; Unclassified.

12. B. R. Redpath; "A Concept of Row Crater Enhancement"; Proceedings of Symposium on Engineering with Nuclear Explosives, Las Vegas, Nevada, January 1970; CONF-700101, Vol. 2; American Nuclear Society; Unclassified.

DISTRIBUTION LIST FOR TECHNICAL REPORT N-74-1

Address	No. of Copies
Army	
Commander, U. S. Army Materiel Command Washington, D. C. 20315 ATTN: AMCRD-BN	1
Defense Civil Prepardness Agency Washington, D. C. 20301 ATTN: Mr. George Sisson (RE-SR)	1
Commander, U. S. Army Combat Development Command Institute of Nuclear Studies Fort Bliss, Tex. 79916	1
Director, U. S. Army Ballistic Research Laboratories Aberdeen Proving Ground, Md. 21005	
ATTN: Mr. J. Keefer	1
Mr. J. Meszaros	1
Commander, U. S. Army Mobility Equipment R&D Center Fort Belvoir, Va. 22060	
ATTN: Mr. R. Medding	1
Mr. E. Leland	1
Safeguard System Command P. O. Box 1500, Huntsville, Ala. 35807 ATTN: Mr. Henry Solomonson, SSC-DH	1
Director, Explosive Excavation Research Laboratory, U. S. Army Engineer Waterways Experiment Station P. O. Box 808, Livermore, Calif. 94550	1
Commander/Director, U. S. Army Cold Regions Research and Engineering Laboratories, P. O. Box 282, Hanover, N. H. 03755	
ATTN: Mr. Ted Vogel	1
Mr. North Smith	1
Chief of Engineers, Department of the Army Washington, D. C. 20314	
ATTN: DAEN-MER-M/LTC D. Hughes	1
DAEN-MCN-X, Mr. George O. Fellers	1
DAEN-MCE-D, Mr. M. L. Martin	1
DAEN-CWE-G, Mr. G. W. Prescott	1
DAEN-FD, Mr. C. F. Corns	1
Division Engineer, U. S. Army Engineer Division, Huntsville P. O. Box 1600, West Station, Huntsville, Ala. 35807 ATTN: Mr. Michael Dembo, HNDED-R	1

Address	No. of Copies
Army (Continued)	
Director, U. S. Army Construction Engineering Research Laboratory, P. O. Box 4005, Champaign, Ill. 61820 ATTN: Library	1
U. S. Army Research Office, Arlington, Va. 22209 ATTN: Mr. Merrill Kreipke	1
U. S. Army Advanced Ballistic Missile Defense Agency 1320 Wilson Blvd & Ft. Meyer Drive, Arlington, Va. 22209 ATTN: Mr. Archie Gold	2
Division Engineer, U. S. Army Engineer Division, Missouri River, P. O. Box 103, Downtown Station, Omaha, Nebr. 68101 ATTN: Mr. E. G. Erikson	1
Safeguard Systems Manager, Safeguard Systems Office 1320 Wilson Blvd., Arlington, Va. 22209 ATTN: Dr. John Shea	1
Chief of Research and Development, Department of the Army Washington, D. C. 20310 ATTN: Dr. Valentine E. Zadnik	1
Navy	
Commander, U. S. Naval Ordnance Laboratory, Silver Spring, Md. 20910 ATTN: Mr. J. Petes Dr. L. Rudin	 1 1
Commanding Office and Director, U. S. Naval Civil Engineering Laboratory, Port Hueneme, Calif. 93041 ATTN: Dr. W. A. Shaw Mr. J. R. Allgood	 1
Air Force	
Commander, Air Force Weapons Laboratory Kirtland Air Force Base, N. Mex. 87117 ATTN: WLIL Dr. M. A. Plamondon Mr. R. W. Henney	 2 1 1
Space and Missile Systems Organization, AF Unit Post Office Los Angeles, Calif. 90045	3
Headquarters, USAF, ATTN: AFRDQSN, Washington, D. C. 20330	1
Commander, Field Command, Defense Nuclear Agency Kirtland Air Force Base, N. Mex. 87115 ATTN: FCDT-B FCSD-C	 15 1

Address	No. of Copies
AEC	
U. S. Atomic Energy Commission ATTN: Assistant General Manager for Military Application Washington, D. C. 20545	3
Division of Technical Information Extension, U. S. Atomic Energy Commission, P. O. Box 12, Oak Ridge, Tenn. 37830	2
Director, Lawrence Radiation Laboratory Box 808, Livermore, Calif. 94550 ATTN: Technical Library	10
Director, Los Alamos Scientific Laboratory, P. O. Box 1663 Los Alamos, N. Mex. 87544 ATTN: Document Control	2
Sandia Laboratories, P. O. Box 5800, Sandia Base, N. Mex. 87115	
ATTN: Document Library	6
Mr. Luke Vortman	1
Dr. M. L. Merritt	1
	1
Other Government	
Center of Astrogeology, 601 East Cedar Ave. Flagstaff, Ariz. 86001 ATTN: Dr. David Roddy	1
U. S. Bureau of Mines, Denver Federal Center, Bldg. 20 Denver, Colo. 80225	
ATTN: Dr. L. A. Obert	1
Mr. Wilbur Duvall	1
Mr. Harry Nicholls	1
Commander, White Sands Missile Range White Sands Missile Range, N. Mex. 88002 ATTN: STEWS-TE-NT, Mr. J. Gorman	1
DOD	
Assistant to the Secretary of Defense (Atomic Energy) Washington, D. C. 20305 ATTN: LTC Luther B. Aull III	1
Director, Defense Nuclear Agency, Washington, D. C. 20305	
ATTN: APSI	1
APTL	1
SPSS	5

Address	No. of Copies
DOD (Continued)	
Defense Documentation Center, Cameron Station Bldg. 5, Alexandria, Va. 22314 ATTN: Mr. Meyer Kahn	2
Director, Weapons Systems Evaluation Group Washington, D. C. 20305	1
Director, Advanced Research Projects Agency, The Pentagon Washington, D. C. 20315 ATTN: Dr. Stan Ruby (NMRO-RM, 3D170)	1
Chairman, Department of Defense Explosives Safety Board Room GB-270, Forrestal Bldg., Washington, D. C. 20314	1
Director, Defense Intelligence Agency, Department of Defense Washington, D. C. 20310	
ATTN: DIAAP-8B, Mr. A. W. Holt	1
DIAST-3	1
Director of Defense Research and Engineering Washington, D. C. 20301	
ATTN: Assistant Director (Strategic Weapons)	1
Assistant Director (Nuclear Programs)	2
DOD Contractors	
Physics International Company, 2700 Merced St. San Leandro, Calif. 94557	
ATTN: Mr. F. M. Sauer	1
Mr. Joe Kochly	1
Dr. C. Godfrey	1
Mr. T. F. Stubbs	1
TRW Systems, Inc., One Space Park, Redondo Beach, Calif. 90278 ATTN: Mr. F. Galbraith	1
General Electric Company, TEMPO, 816 State St. Santa Barbaram Calif. 93101 ATTN: Mr. Warren Chan (DASIAC)	1
The Boeing Company, P. O. Box 3707, Seattle, Wash. 98124	
ATTN: Mr. G. D. Jones	1
Mr. H. Leistner	1
Kaman Aircraft Corporation, Nuclear Division 1700 Garden of the Gods Road, Colorado Springs, Colo. 80907	
ATTN: Mr. D. Sachs	1
Mr. Dale Seacrist	1

Address	No. of Pages
DOD Contractors (Continued)	
University of Denver, Colorado Seminary, Denver Research Institute, University Park, Denver, Colo. 80210 ATTN: Mr. J. Wisotski	1
Chief Superintendent, Defence Research Establishment, Suffield Ralston, Alberta, Canada	2
IIT Research Institute, 10 West 35th St., Chicago, Ill. 60616 ATTN: Dr. Eliot Raisen Dr. Ted Schiffman	 1 1
Aerospace Corporation, P. O. Box 95085 Los Angeles, Calif. 90045 ATTN: Dr. Mason Watson	
TRW Systems Group, 600 E. Mill St., Bldg. 527, Room 710 San Bernardino, Calif. 92402 ATTN: Mr. Fred Pieper Mr. J. Carpenter Dr. Lieberman	 1 1 1
Agbabian Associates, 250 N. Nash St. El Segundo, Calif. 90245 ATTN: Dr. Jim Workman	 2
Applied Theory, Inc., 1010 Westwood Blvd. Los Angeles, Calif. 90024 ATTN: Dr. J. G. Trulio	1
Director, Institute for Defense Analysis, 400 Army-Navy Dr. Arlington, Va. 22202 ATTN: Technical Information Office	2
The Rand Corporation 1700 Main St., Santa Monica, Calif. 90406 ATTN: Library Dr. A. L. Latter Mr. W. B. Wright Dr. C. C. Mow	 1 1 1 1
R&D Associates, P. O. Box 3580, Santa Monica, Calif. 90403 ATTN: Dr. Harold L. Brode	1
Systems, Science, and Software, P. O. Box 1620 La Jolla, Calif. 92037 ATTN: Document Control	1
Weidlinger Associates, Consulting Engineers, 110 East 59th St. New York, N. Y. 10022 ATTN: Dr. M. L. Baron	1

Address	No. of Pages
DOD Contractors (Continued)	
Southwest Research Institute 8500 Culebra Road, San Antonia, Tex. 78228 ATTN: Dr. Robert C. DeHart	1
Dr. Olen A. Nance South Lakeview Drive Baton Rouge, La. 70810	1

345-946

Unclassified
Security Classification

DOCUMENT CONTROL DATA - R & D

(Security classification of title, body of abstract and indexing annotation must be entered when the overall report is classified)

1. ORIGINATING ACTIVITY (Corporate author) U. S. Army Engineer Waterways Experiment Station Vicksburg, Mississippi	2a. REPORT SECURITY CLASSIFICATION Unclassified 2b. GROUP

6

CRATERING BY EXPLOSIONS: A COMPENDIUM AND AN ANALYSIS.

9

Final report, Jan 70-Apr 71,

Allen D. Rooke, Jr.,
Benny L. Carnes
Landon K. Davis

12 343p.

7a. TOTAL NO. OF PAGES ~~[illegible]~~	7b. NO. OF REFS 192
8a. CONTRACT OR GRANT NO. b. PROJECT NO. 4A062118A880 Task 04 c. d.	9a. ORIGINATOR'S REPORT NUMBER(S) Technical Report N-74-1 14 WES-TR-N-74-1 9b. OTHER REPORT NO. (Any other report)

16 17

10. DISTRIBUTION STATEMENT
Distribution limited to U. S. Government agencies only; test and evaluation; January 1974. Other requests for this document must be referred to U. S. Army Engineer Waterways Experiment Station.

11. SUPPLEMENTARY NOTES	12. SPONSORING MILITARY ACTIVITY Office, Chief of Engineers, U. S. Army Washington, D. C.

13. ABSTRACT

Cratering programs and data resulting from numerous single-charge explosion tests are summarized and compiled in tabular form. Analyses are performed on these data to provide means of predicting basic cratering parameters. Prediction equations are developed from least-squares, straight-line plots, and are presented in graphical form. Means of updating these tabulations and analyses on a regular basis by automatic data processing are discussed. Data are grouped so as to account for the factors which primarily affect crater size and shape: yield, burst geometry, and cratered medium. The influence of other conditions, such as soil moisture, layered media, etc., is also considered. Emphasis is on single-charge, dry-land experiments, which best permit isolation of the factors contributing to the basic parameters. However, effects of environmental influences, unusual charge geometries, and other factors significantly affecting craters are also briefly considered. Similarly, basic ejecta phenomena are included. Trends in crater dimensions are shown by means of graphs normalized to charge sizes commensurable to large chemical and small nuclear yields. Scaling as a prediction tool is discussed.

DD FORM 1 NOV 65 1473 REPLACES DD FORM 1473, 1 JAN 64, WHICH IS OBSOLETE FOR ANY USE.

Unclassified
Security Classification

038100

13. KEY WORDS	LINK A		LINK B		LINK C	
	ROLE	WT	ROLE	WT	ROLE	WT
Cratering						
Explosions						

In accordance with ER 70-2-3, paragraph 6c(1)(b), dated 15 February 1973, a facsimile catalog card in Library of Congress format is reproduced below.

Rooke, Allen D

Cratering by explosions: a compendium and an analysis, by A. D. Rooke, Jr., B. L. Carnes [and] L. K. Davis. Vicksburg, U. S. Army Engineer Waterways Experiment Station, 1974.

348 p. illus. 27 cm. (U. S. Waterways Experiment Station. Technical report M-74-1)

Sponsored by Office, Chief of Engineers, U. S. Army

Project 4A062118A380, Task 04.

Bibliography: p. 315-330.

1. Cratering. 2. Explosions. I. Carnes, Benny L., joint author. II. Davis, Landon K., joint author. III. U. S. Army. Corps of Engineers. (Series: U. S. Waterways Experiment Station, Vicksburg, Miss. Technical report M-74-1)

TA7.W34 no.M-74-1